UNCLASSIFIED

AD. **295 794**

Reproduced
by the

ARMED SERVICES TECHNICAL INFORMATION AGENCY
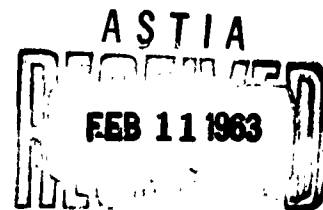ARLINGTON HALL STATION
ARLINGTON 12, VIRGINIA

UNCLASSIFIED

ELECTRON PARAMAGNETIC RESONANCE

By

S. A. Al'tshuler and B. M. Kozyrev

UNEDITED ROUGH DRAFT TRANSLATION

ELECTRON PARAMAGNETIC RESONANCE

BY: S. A. Al'tshuler and B. M. Kozyrev

English Pages: 469

S

S. A. Al'tshuler and B. M. Kozyrev

ELEKTRONNYY PARAMAGNITNYY REZONANS

FTD-TT-62-1086/1+2

NOTE

The electron paramagnetic resonance, discovered in 1944 by the Soviet physicist Ye.K. Zavoyskiy, is now one of the most fruitful physical research methods. Its use has yielded valuable data in the field of solid state physics, magnetism, semiconductor physics, and nuclear physics. In radio, this method has been the basis for the development of a new type of amplifier with exceedingly low internal noise level. Electron paramagnetic resonance is widely used in modern chemistry, and its study in biological objects has also begun.

The book contains a complete survey of research in the field of electron paramagnetic resonance. The most detailed treatment has been given to the theoretical and experimental results pertaining to ionic crystals. It is intended for senior and graduate students as well as for scientists working in physics, radio, chemistry, and biology.

TABLE OF CONTENTS

FOREWORD

Electron paramagnetic resonance, discovered in 1944 by Ye.K. Zavoyskiy, has become one of the most powerful physical research methods. The applications of electron paramagnetic resonance cover a very wide field. In ionic crystals it permits a determination of the magnetic-center energy-level structure, of the minor details of the crystal-lattice structure, and of the parameters characterizing the magnetization kinetics; the study of crystal-lattice imperfections is particularly interesting. In liquid salt solutions, electron paramagnetic resonance makes it possible to investigate the construction of the solvate shells. Interesting data have been obtained on the properties of conduction electrons in metals and semiconductors. For nuclear physics, paramagnetic resonance is a valuable method for the determination of nuclear moments and is one of the most effective means of nuclear polarization.

The paramagnetic resonance method is particularly fruitful in chemistry. It made possible the first detection of free radicals in amounts down to 10^{-10}-10^{-13} mole. A promising start toward a study of paramagnetic resonance in biological objects has also been made.

Paramagnetic resonance has recently found a very important application in radio, for the design of a new type of a low-noise amplifier.

All this has made paramagnetic resonance of great interest at present not only to physicists but also to chemists, biologists, and radio engineers.

This book is the first attempt to provide as complete a survey as

- 1 -

possible of the research made in electron paramagnetic resonance. To limit the size of the book the authors had to forego in most cases detailed derivations or detailed descriptions of experimental methods which incidentally have already been described to a considerable extent in the available Russian-language literature. Theoretical and experimental results pertaining to ionic crystals have been dealt with in greatest detail, since such crystals are most thoroughly investigated by paramagnetic resonance methods.

The book covers all the basic literature on electron paramagnetic resonance up to about 1959. The authors have attempted here to summarize all the most important theoretical results and the experimental data that are the most trustworthy.

Chapter I was written by both authors, Chapters II, IV, VII, and §§5.5, 5.7 of Chapter V were written by B.M Kozyrev; Chapters III, VI, VIII, and §§5.1-5.4, 5.6, 5.8, 5.9, and 5.10 of Chapter V were written by S.A. Al'tshuler.

In conclusion, the authors express their deep gratitude to Ye.K. Zavoyskiy for valuable discussions concerning many problems considered in this book. They are also most grateful to R.Sh. Nigmatullin for reviewing the manuscript of Chapter II, to V.B. Shteynshleyger for reviewing the portion of the book devoted to paramagnetic amplifiers, and to N.G. Koloskova for appreciable help in the compilation of the tables.

S.A. Al'tshuler, B.M. Kozyrev

Kazan', 15 July 1959.

PRINCIPAL NOTATION

A — hyperfine magnetic interaction constant;

$\underline{a}$ — spin-Hamiltonian constant;

a_0 — Bohr radius;

B — hyperfine magnetic interaction constant;

$\underline{c}$ — velocity of light;

$D,\ E$ — spin-Hamiltonian constants;

$\underline{e}$ — electron charge;

e_{eff} — effective charge;

F — spin-Hamiltonian constant;

$\underline{g}$ — spectroscopic splitting factor;

g_0 — Lande factor;

$g_x,\ g_y,\ g_z$ — principal values of g-tensor;

g_N — nuclear g-factor;

$g(\nu)$ — function of the paramagnetic resonance absorption line shape;

H_0 — intensity of static magnetic field;

H_r — amplitude of oscillating magnetic field;

H_{kr} — electron energy in the crystal electric field;

$h \equiv 2\pi\hbar$ — Planck's constant;

I — nuclear-spin quantum number;

J — electron shell total momentum quantum number;

$J,\ J_{1k}$ — exchange integral;

$\underline{k}$ — Boltzmann's constant;

L — electron shell orbital momentum quantum number;

M — momentum projection quantum number;

- 3 -

M_k — $\underline{k}$th moment of resonance line;

M — number of ions per unit cell;

M_m — number of magnetically nonequivalent ions per unit cell;

m_e — electron mass;

N_0 — number of paramagnetic centers per cubic centimeter;

N_k — number of paramagnetic centers at the $\underline{k}$ level per cubic centimeter;

$\underline{n}$ — population difference between two neighboring spin sublevels;

n_0 — population difference between two neighboring spin sublevels in equilibrium state;

P — hyperfine quadrupole interaction constant;

P — radio-frequency field power absorbed per cubic centimeter of the paramagnetic material;

$P_{MM'}$ — probability of system transition from the level M to the level M' under the influence of the oscillating magnetic field;

Q — quality factor;

$\underline{q}$ — quadrupole moment of the nucleus;

q_{1k} — saturation factor;

R — equilibrium distance from the center to the vertex of the octahedral complex;

S — electron spin quantum number;

S' — effective spin;

T — absolute temperature;

T_1 — longitudinal paramagnetic relaxation time;

T_2 — transverse paramagnetic relaxation time;

T_{21} — cross-relaxation time;

$\underline{v}$ — average velocity of sound;

Z — nuclear charge;

β_0 — Bohr magneton;

β_N — nuclear magneton;

γ — gyromagnetic ratio;

$\Delta\nu$ — width of paramagnetic resonance line, in cycles per second;

ΔH — line width in oersteds;

θ — Debye temperature;

χ_0 — static paramagnetic susceptibility;

χ — complex paramagnetic susceptibility;

χ' — real part of χ;

χ'' — imaginary part of χ;

μ — magnetic moment of the particle;

ν — frequency of oscillating magnetic field;

ν_0 — Larmor precession frequency;

ρ — density of the substance;

σ — ultrasonic absorption coefficient;

τ — spin-lattice relaxation time;

τ' — spin-spin relaxation time.

Chapter I

INTRODUCTION

§1.1. Elementary Magnetic Resonance

Many modern methods used to investigate properties of particles with nonzero magnetic moments are based on a phenomenon which can be called elementary magnetic resonance. The use of this method has enabled Rabi to propose his well-known method of determining nuclear moments [1], Alvarez and Bloch [2] to measure the magnetic moment of the neutron, Detch [3] to determine the fine structure of the ground level of positronium, Kastler [4] to discover a new optical effect, etc. The same phenomenon serves as the basis for paramagnetic resonance and a few other related effects which occur in substances that contain particles with nonzero magnetic moments.

The nature of elementary magnetic resonance can be explained with the aid of simple classical concepts. Let a particle having a magnetic moment $\vec{\mu}$ be placed in a magnetic field with intensity $\vec{H}_0$. Then the moment $\vec{\mu}$ will precess about $\vec{H}_0$ with Larmor frequency $v_0 = g_0 e H_0 / 4\pi m_0 c$, where g_0 is the Lande factor, which takes on the values 2 and 1 for particles with pure spin and pure orbital electron magnetism, respectively.

Let us assume that a weak magnetic field $\vec{H}_1$ is applied perpendicular to the field $\vec{H}_0$ (Fig. 1.1) and rotates about $\vec{H}_0$ with frequency v. If $v = v_0$, then the additional rotating moment produced by the field $\vec{H}_1$ is always so directed as to make the magnetic moment $\vec{\mu}$ try to occupy a position in the equatorial plane. The result is a rapid change in the orientation of the moment $\vec{\mu}$.

- 6 -
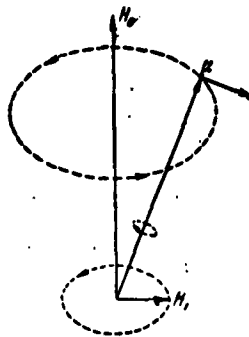
Fig. 1.1. Elementary magnetic
resonance.

If the frequencies v and v_0 differ noticeably from each other,
then the effect of the field $\vec{H_1}$ is negligible, since the motion it in-
duces in the moment $\vec{\mu}$ rapidly goes out of phase with its precession.
For the same reason, the effect of the field will also be small if $v =$
$= v_0$, but the direction of rotation of $\vec{H_1}$ is opposed to that of the
precession. As a result of the latter fact, the rotating field is re-
placed in practice by an oscillating one, which can be regarded as the
superposition of two fields of equal magnitude but rotating in oppo-
site directions at the same frequency.

It is natural to raise the question of the extent to which the
magnitude of the resonance effect depends on the accuracy with which
the frequencies v and v_0 coincide. The sharpness of the magnetic reso-
nance will be the greater, the smaller the ratio H_1/H_0.

Let us proceed to analyze the quantum relations in elementary mag-
netic resonance. Give the particle mechanical and magnetic moments, the
maximum components of which in the direction of $\vec{H_0}$ will be denoted by
$J\hbar$ and μ, respectively. As is well known, $\mu = g_0\beta J$, and consequently
$2J + 1$ equidistant energy levels* will arise in the magnetic field $\vec{H_0}$,
namely:

$$E_M = g_0\beta H_0 M,$$

(1.1)

where M is the magnetic quantum number, $J \geq M \geq -J$.

- 7 -

An alternating magnetic field $\vec{H}_r \cos 2\pi\nu t$ can induce magnetic dipole transitions between neighboring energy levels ($\Delta M = \pm 1$), provided this field is perpendicular to $\vec{H}_0$* and if the following resonance condition is satisfied:

$$E_M - E_{M-1} = g_0 \beta H_0 = h\nu. \qquad (1.2)$$

This is identical to the classical condition $\nu = \nu_0$.

The alternating field will induce transitions from the lower energy levels to the upper ones and vice versa with equal probability. The probabilities of these nonadiabatic transitions were calculated by Guttinger [5], Majorana [6], and Rabi [1].

It can be readily calculated with the aid of (1.2) that the Larmor precession frequency lies within the radio or microwave bands for all the magnetic-field intensities encountered in modern experiments. This is a very important practical fact, for it makes it possible to use the highly sensitive and very convenient radio equipment for experiments based on elementary magnetic resonance.

§1.2. Paramagnetic Resonance

We now proceed from an examination of an isolated magnetic particle to macroscopic bodies, which contain many such particles. We shall call such bodies paramagnetic regardless of the magnitude of the diamagnetic component of the over-all magnetic moment of the substance. The behavior of a paramagnet in a magnetic field depends essentially on the interactions of the paramagnetic particles with one another and with the surrounding diamagnetic particles. These interactions will contribute to the establishment of a thermodynamic equilibrium, if the latter is disturbed for some reason or another. Therefore, in a static magnetic field $\vec{H}_0$ in which an equilibrium state has been attained and the distribution laws of classical statistics are applicable, the populations of the individual energy levels are determined by the Boltz-

mann factor $e^{-g_0 \beta H_0 M/kT}$. The populations of the lower energy levels are larger than those of the upper levels, and therefore, if an alternating magnetic field at resonant frequency is turned on, the number of absorption events induced by this field exceeds the number of forced emission events; consequently, the substance will absorb energy from the radio frequency field. Thus, two opposing processes take place in the paramagnet: the radio frequency field equalizes the populations of the different magnetic levels, while the internal interactions tend to restore the Boltzmann distribution, by converting the absorbed radio-frequency field energy into heat.

The ultimate result is a stationary state in which the populations of the magnetic levels stop varying and the radio frequency energy is uniformly absorbed by the paramagnet. If at the same time the intensity of the alternating magnetic field is very large, then the populations of the different magnetic levels will become equalized in the stationary state, after which the absorbed energy will no longer increase with increasing power of the radio frequency field (the so-called saturation sets in).

We see that the effect of resonant paramagnetic absorption is very tightly linked with processes that determine the kinetics of magnetization of paramagnets, or in other words, with paramagnetic relaxation. A very fruitful suggestion in the theory of paramagnetic relaxation was that of Casimir and du Pre [7, 8], namely that the magnetization of the paramagnet be regarded as a two-stage process consisting of the establishment of equilibrium within the "spin system," or the system of magnetic moments of all the paramagnetic particles, followed by energy exchange between the spin system and the "lattice," to which all the remaining degrees of freedom of the paramagnet belong. Of course, this consideration is possible if the interactions inside the

spin system (spin-spin interactions) are much stronger than the inter-actions between the spin system and the lattice (spin-lattice interac-tions).

Unless ultra-low temperatures are considered, the lattice tempera-ture can be regarded as invariant, since the specific heat of the lat-tice greatly exceeds the specific heat of the spin system. The lattice therefore acts like a thermostat in which the spin-system is immersed. The spin system can also be assigned a certain temperature which gen-erally differs from that of the lattice. The establishment of equilib-rium between the spin system and the lattice can be regarded as an ex-change of energy between these systems, leading to an equalization of their temperatures. The speed of this process can be characterized by the spin-lattice relaxation time, which we denote by τ. The spin-lat-tice relaxation mechanisms of different substances may differ greatly from one another. Therefore the quantity τ, in addition to having a strong dependence on the temperature of the paramagnet, is also char-acterized by variations over a wide range on going from one substance to another.

The rate at which equilibrium is established within the spin sys-tem can be characterized by the spin-spin relaxation time τ'. Obviously, the very possibility of separating the paramagnet into a spin system and a lattice implies that $\tau' \ll \tau$. Unlike the time τ, the value of τ' depends very little on the lattice temperature. We note still another difference between the spin-spin and spin-lattice relaxations. Equi-librium is established within the spin system by energy exchange be-tween different parts of the system, while the total energy of the spin system remains constant. On the contrary, spin-lattice relaxation is connected with a change in the energy of the spin system.

In his phenomenological theory of paramagnetic resonance, Bloch

- 10 -

[9] introduced two relaxation times, longitudinal T_1 and transverse T_2. Assume that the paramagnet is placed in a static field $\vec{H}_0$; then the time T_1 characterizes the rate at which equilibrium is established if the magnitude of the field $\vec{H}_0$ is instantaneously changed, while its direction is maintained constant; the time T_2 determines the relaxation if the direction of the field $\vec{H}_0$ is changed instantaneously while its absolute value remains constant. The time T_1 characterizes the balancing process associated with the change in the spin-system energy, and can therefore be identified with the spin-lattice relaxation time τ. The time T_2 characterizes the speed of a relaxation process in which the spin-system energy is constant; it can be identified with the time τ'. However, the times τ and τ' are not always identical with T_1 and T_2, since the concept of longitudinal and transverse relaxation times T_1 and T_2 can always be introduced, whereas the times τ and τ' are meaningful only when $\tau \gg \tau'$. We do not consider here at all whether the two parameters T_1 and T_2 suffice to describe the complicated process of paramagnetic relaxation. We shall see below that in some cases a large number of parameters must be introduced (see Chapter V).

The internal interactions in the paramagnet not only cause it to absorb energy from the radio frequency field, but also broaden the paramagnetic resonance lines. Whereas for an isolated particle the sharpness of the magnetic resonance depends on the ratio H_1/H_0, for a paramagnet the sharpness of resonance and the associated absorption-line width are determined by the spin-spin and spin-lattice interactions, provided there is no saturation. Let us assume that the spin-spin interactions are much stronger than the spin-lattice ones. We take two neighboring magnetic particles. Assuming them isolated, in first approximation, we can ascribe to each particle a system of energy levels (1.1). Let the levels of the two particles have magnetic quantum num-

bers M_1 and M_2, respectively. The spin-spin interactions give rise to a certain probability A' that the particles will exchange energy after 1 second; if the first particle makes in this case a transition to a level with magnetic quantum number $M_1 + 1$, then the second goes to the level $M_2 - 1$. The spin-spin relaxation time τ' will have an order of $1/A'$; this time, as we shall show, determines the lifetime of the particles at a definite magnetic energy level, and consequently the width of the absorption line, due to the spin-spin interactions, can be estimated to be $1/\tau'$.

If spin-lattice interactions dominate, then the concept of the time τ' becomes meaningless, but the spin-lattice relaxation time τ can be introduced if we consider the probability that an individual paramagnetic particle will go over under the influence of thermal agitation from one magnetic energy level to another. If this probability per second is A, then $\tau \sim 1/A$ and the width of the absorption line will have an order of magnitude $1/\tau$. In general, we can estimate the width of the absorption line to be $1/\tau + 1/\tau'$. No rigorous general relation can be given between the width and the relaxation times, since the width depends heavily on the shape of the absorption line.

It follows from what we know concerning the temperature dependence of the relaxation times, that if the resonant paramagnetic absorption line width is determined by spin-lattice interactions, it will decrease rapidly with decrease in temperature; on the other hand, if the decisive role is played by spin-spin interactions, the temperature dependence of the width will be quite weak.

The internal interactions in the paramagnet determine also the position and number of the paramagnetic resonant absorption lines. If the form of the energy spectrum resulting under the action of the field H_0 were to be independent of the internal interactions, the sys-

tem of energy levels would be determined as before by Formula (1.1) if in addition the selection rules for transitions between these levels under the influence of the alternating magnetic field were to be conserved, then there would exist only one absorption line, the position of which for a specified intensity H_0 would be determined by the magnitude of the Lande factor g_0. Actually, however, whereas in many para-
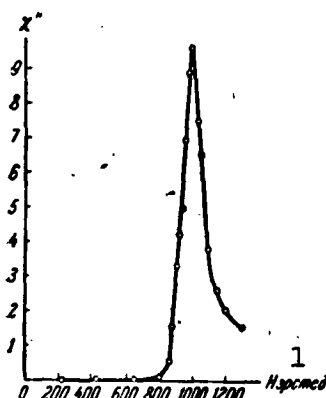
Fig. 1.2. Plot of paramagnetic resonance absorption in $CrCl_3$ for $\lambda = 10.87$ cm, $T = 298^\circ K$ (Ye.K. Zavoyskiy, Sov. phys. 10, 197, 1946). 1) H, oersteds.
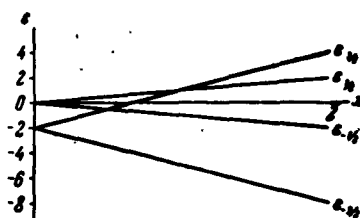
Fig. 1.3. Splitting of the ground level of the Cr^{3+} ion in a trigonal crystal field and in a magnetic field H_0 applied parallel to the trigonal axis.

magnets the system of equidistant magnetic energy levels is conserved, the g factor deviates from its value for the free particle, owing to internal interactions. Figure 1.2 shows a plot of paramagnetic reso-
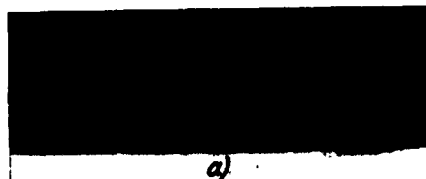
Fig. 1.4. Photographs of the fine structure of the spectrum of Cr^{3+} in Al_2O_3.
a) $\vec{H}_0$ parallel to the crystal trigonal axis; b) $\vec{H}_0$ perpendicular to the crystal trigonal axis.

nance absorption in chromium chloride; the absorption maximum corresponds, as can be readily calculated with the aid of (1.2), to a factor $g \approx 2$, whereas for the ground state $^4F_{3/2}$ of the free Cr^{3+} ion, the Lande factor has a value 2/5. The absorption curve of Fig. 1.2 represents the energy absorbed by the paramagnet per second from the radio frequency field, as a function of the intensity H_0 of the static magnetic field, for in the overwhelming majority of cases the experiments are carried out at fixed frequency v and variable fields H_0.

In condensed media, as pointed out by Kittel [10], the g factor, which determines the splitting of the energy levels in a magnetic field, does not coincide with the factor that yields the gyromagnetic ratio, the latter factor being obtained by measuring the magnetomechanical effects. We shall therefore follow Kittel and call the g factor obtained from experiments on paramagnetic resonance the "spectroscopic splitting factor."

In many paramagnets, particularly those whose magnetism is not purely spin, the system of Zeeman levels ceases to be equidistant. Con-

sequently, several absorption lines arise in place of one, and one observes, as is customarily stated, the fine structure of the paramagnetic resonance spectrum. In single crystals, the form of the spectrum can depend strongly on their orientation relative to the field $\vec{H}_0$. By way of an example, Fig. 1.3 shows the splitting of the ground level of a Cr^{3+} ion contained in an Al_2O_3 crystal, as a function of the intensity of the magnetic field $\vec{H}_0$ applied parallel to the trigonal axis of the crystal. In this figure $\varepsilon = E_M/D$, $x = g\beta H_0/D$, and 2D is the initial splitting. Figure 1.4 shows photographs of the fine structure of the paramagnetic resonance spectrum for two different crystal orientations, with the trigonal axis parallel and perpendicular to the field H_0.

It is seen from Fig. 1.3 that in the absence of the fields H_0 the splitting of the ground level of the paramagnetic particles lies in the radio-frequency region. Thus, resonance absorption of energy from a radio frequency field can occur in many cases under the influence of magnetic dipole transitions between sublevels that exist in the absence of a static magnetic field.

We note finally that the internal interactions change the selection roles. For example, transitions become possible between Zeeman levels that are not neighboring, and for a paramagnet in which these levels are equidistant this causes the appearance, in addition to the principal absorption line corresponding to the Larmor frequency v_0, of satellites at frequencies $2v_0$, $3v_0$, etc.

The form of the paramagnetic resonance spectrum depends on the presence of magnetic moments in the nuclei of the paramagnetic atoms (molecules). The magnetic moments of the nucleus and of the electron shell interact with each other and with the static magnetic field H_0 to produce a new system of energy levels for the paramagnet; an important factor here is whether the field H_0 is strong enough to break
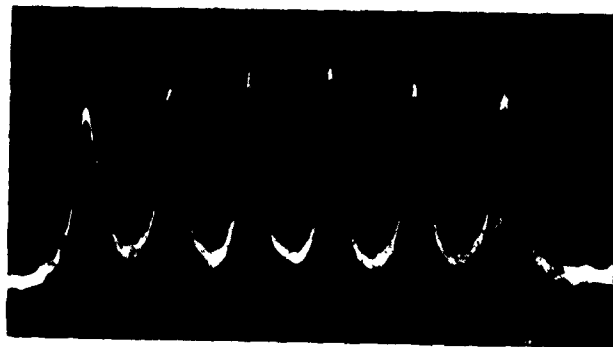
Fig. 1.5a. Hyperfine structure of the spectrum of Mn^{2+} in an aqueous solution of $MnCl_2$ at $\nu = 9345$ Mc.
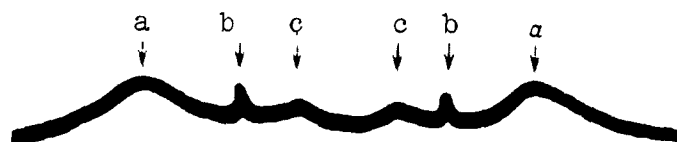
Fig. 1.5b. Effect of nuclear spin on the spectrum of Mn^{2+} in an aqueous solution of $MnCl_2$ at $\nu = 147$ Mc. a) $^{55}Mn^{2+}$ $(g = 1)$; b) free radical $(g = 2)$; c) Fe^{3+} impurities in the ampoule glass $(g \approx 4)$.
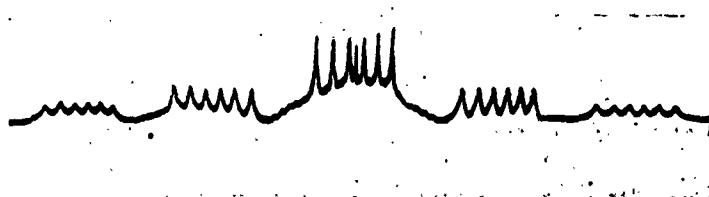
Fig. 1.6. Fine and hyperfine structures of the spectrum of Mn^{2+} in manganese apatite at $\nu \approx 10^{10}$ cps; each of the five fine-structure lines is split into six hyperfine components. (The narrow line in the center of the third group is due to the free radical.)

the bond between the electron and nuclear moments, or whether the field H_0 is so weak that this bond remains unchanged. In the former case,

the position of the paramagnetic resonance absorption lines due to the magnetic moments of the electron shells of the atoms (molecules) is conserved, but a hyperfine structure appears, in that each line breaks up into several components, the number of which depends on the nuclear spin. In the latter case, the picture of the spectrum is completely changed, since the g factors that determine the positions of the absorption lines assume entirely different values.

Figure 1.5a shows the absorption spectrum observed in an aqueous solution of $MnCl_2$ at $v = 9345$ Mc in strong fields H_0, ranging from 2900 to 3400 oersteds. The center of the spectrum corresponds to $g = 2.000$; this g factor would determine the position of the absorption line were it not split by the presence of the magnetic moment of the manganese nucleus. Figure 1.5b shows an absorption spectrum consisting of one line and observed in the same solution of $MnCl_2$ at 147 Mc in weak fields H_0, ranging from −175 to +175 oersted. The absorption maximum corresponds here to a value of g which is practically exactly equal to 1. Thus, the interaction with the nucleus in weak fields reduces the g factor by one-half in our case. **Figure 1.6** shows a typical fine and hyperfine structure of the spectrum of Mn^{2+}, observed in an apatite single crystal.

A few other phenomena are closely related with paramagnetic resonance absorption. It is easy to conclude that the effect of an alternating magnetic field on a paramagnet under the conditions of resonance should be to change its magnetization. The result is the appearance of a strong dependence of paramagnetic susceptibility on the frequency v; if v is found equal to v_0, the dispersion of susceptibility becomes anomalous. The rotation of the plane of polarization of the radio waves and other magnetooptical phenomena also become anomalous, provided that the experimental conditions are such that the magnetic vector of the wave is perpendicular to the applied static magnetic field and that the frequencies v and v_0 are close to each other.

We have considered different aspects of the paramagnetic resonance effect, and we can now define it in general terms.

Paramagnetic resonance is an aggregate of phenomena, connected with quantum transitions occurring between energy levels of macroscopic systems under the influence of an alternating magnetic field of resonant frequency.

We refer in this definition to an aggregate of phenomena, for along with paramagnetic resonance absorption, there is observed also paramagnetic resonance dispersion, paramagnetic resonance rotation, etc. In addition, we emphasize here that the phenomena are observed in macroscopic systems, where spin-spin, spin-lattice and similar interactions take place, which distinguishes paramagnetic resonance from the resonance experiments made by Rabi with molecular beams and by Alvarez and Bloch with neutron beams, etc.

Finally, whereas Debye dispersion and absorption of electromagnetic waves in dielectrics occur as a result of electric dipole transitions due to the electric component of the wave, the phenomena which were are studying are due to magnetic dipole transitions, which are excited by an alternating magnetic field.

In the overwhelming majority of cases, paramagnetic resonance is investigated by superimposing on the paramagnet two magnetic fields, a strong static field and a weak alternating one. However, we have seen with Cr^{3+} as an example that magnetic dipole transitions are possible under the influence of a radio frequency field even in the absence of a static magnetic field. The phenomena connected with transitions of this type are also naturally ascribed to paramagnetic resonance.

The great difference in the magnitude of magnetic moments of the electrons and the nuclei makes it natural to distinguish between electron and nuclear paramagnetic resonance, although both the experimental research methods and the theory of both effects have much in common. One should include in nuclear paramagnetic resonance also nuclear quad-

rupole resonance, a phenomenon due to magnetic dipole transitions occurring in the absence of an external static magnetic field between energy levels arising as a result of interaction between nuclear quadrupole moments and the electric field inside condensed media.

§1.3. Magnitude of the Effect

We proceed to establish certain quantitative relationships. Let the ground level of a magnetic particle be split under the influence of an external magnetic field and internal forces into η sublevels, to which we shall assign the quantum numbers M and M'. According to the quantum theory of radiation, the probability that the oscillating magnetic field H_r cos $2\eta vt$ will cause a transition within one second from the level M to the level M' is

$$p_{MM'} = \frac{8\pi^2}{h^2} |<M|\mu_x|M'>|^2 \rho_v,$$ (1.3)

where $<M|\mu_x|M'>$ is the matrix element of the projection of the magnetic moment of the particle along the direction of the alternating magnetic field, and ρ_v is the mean spectral density of electromagnetic energy, for which we can use in our case the expression

$$\rho_v = \frac{H_r^2}{8\pi} g(v).$$ (1.4)

We have introduced here a form factor, which takes account of the fact that the absorption line is not infinitesimally narrow but has an appreciable width. The function $g(v)$ reproduces the absorption line shape and is normalized so that

$$\int_0^\infty g(v)\,dv = 1.$$ (1.5)

If the temperature of the paramagnet is sufficiently high to make $E_M - E_{M'} = hv \ll kT$, then for a volume of 1 cm^3, containing N_0 magnetic particles, the difference in the populations of the pair of levels M and M' will be

$$N_M - N_{M'} = \frac{N_0}{\eta} \frac{hv}{kT}.$$ (1.6)

- 19 -

With the aid of (1.3), (1.4), and (1.6) we obtain the following expression for the power absorbed by a unit volume of the paramagnet in transitions from the level M to the level M':

$$P_{MM'} = (N_M - N_{M'}) \, p_{MM'} \cdot h\nu =$$
$$= \pi^2 \frac{N_0}{\psi kT} |<M|\mu_x|M'>|^2 H_r^2 \nu^2 g(\nu). \qquad (1.7)$$

To obtain the total power P absorbed as a result of transitions between all the sublevels, it is necessary to sum over all the possible values of M and M'. Since the static paramagnetic susceptibility is [11]:

$$\chi_0 = \frac{2N_0}{\psi kT} \sum_{M>M'} |<M|\mu_x|M'>|^2, \qquad (1.8)$$

we get

$$P = \frac{\pi^2}{2} \chi_0 H_r^2 \nu^2 g(\nu). \qquad (1.9)$$

The total power is of interest if the matrix elements $<M|\mu_x|M'> \neq 0$ for those pairs of levels which are spaced by equal intervals, for in this case transitions between different level pairs produce one and the same absorption line.

The Q of the resonant circuit loaded by the paramagnet can be determined from the expression

$$\frac{1}{Q} = \frac{\left(\frac{P}{\nu}\right)}{2\pi (H_r^2/8\pi)} = 2\pi^2 \chi_0 \nu g(\nu). \qquad (1.10)$$

Maximum absorption, which occurs at a frequency $\nu = \nu_0$, can be related with the width $\Delta\nu$, for if we write

$$g(\nu_0) = \frac{q}{\Delta\nu}, \qquad (1.11)$$

then we see from (1.5) that $q \approx 1$. The exact value of $\underline{q}$ depends on the absorption line shape; if the line has a Gaussian shape, then $q = 0.939$; if it has a Lorentz shape, then $q = 0.636$ (see §1.4).

Formula (1.7) is valid if the field H_r is regarded as being suffi-

ciently small so as not to disturb the equilibrium distribution of the
particles over the energy levels. With increasing intensity of the
radio frequency radiation, these disturbances can occur and can lead
to saturation. Let us establish a quantitative criterion for the ex-
istence of this effect. We consider the simplest case of paramagnetic
particles, having only two energy sublevels. The population excess in
the lower sublevel above that in the upper sublevel will be denoted by
$\underline{n}$; let $n = n_0$ in the equilibrium state. From the definition of the
spin-lattice relaxation time we can conclude that in the absence of a
radio frequency field the transition to the equilibrium state will be
determined by the equation

$$\frac{dn}{dt} = -\frac{n-n_0}{\tau}.$$ (1.12)

In the presence of a radio frequency field, the equation for $\underline{n}$ becomes

$$\frac{dn}{dt} = -\frac{n-n_0}{\tau} - 2n p_{MM'}.$$ (1.13)

After the stationary mode is established, we have

$$\frac{n}{n_0} = [1 + 2\tau p_{MM'}]^{-1}.$$ (1.14)

If the energy level in the magnetic field is split into two sub-
levels, it can always be related to an effective spin $S' = 1/2$ and to
a spectroscopic splitting factor $\underline{g}$, the calculation of which will be
described in Chapter III. We can therefore put

$$< M|\mu_x|M' > = < -\tfrac{1}{2}|g\beta S'_x|+\tfrac{1}{2} > = g\beta.$$ (1.15)

Substituting (1.3) in (1.14) and using (1.4), (1.11), and (1.15) we
obtain

$$\frac{n}{n_0} = \left[1 + \frac{2\pi^2 g\xi^{*\beta^2}\tau H_1^2}{h^2(\Delta\nu)}\right]^{-1}.$$ (1.16)

In the equilibrium state we have $n/n_0 = 1$, and this ratio tends to
zero as saturation sets in. The quantity $q_n = n/n_0$ is called the satura-

tion factor. If the Larmor precession frequency in a field of intensity H_r is designated by $\nu_r = g\beta H_r/h$, then the saturation criterion is the following condition:

$$\nu_r^2 > \Delta\nu\frac{1}{\tau},$$ (1.17)

§1.4. Paramagnetic Resonance as a Branch of the Theory of Magnetism

The contemporary state of the theory of paramagnetism is characterized by a changeover from investigation of the magnetic properties of matter under static conditions to phenomena observed in alternating magnetic fields. Modern theory of dynamic paramagnetism is developing along three trends: 1) adiabatic demagnetization; 2) paramagnetic relaxation, and 3) paramagnetic resonance.

The connection between these trends is so close, that some authors [12] believe, for example, paramagnetic resonance to be part of the theory of paramagnetic relaxation, whereas others [13], to the contrary, regard paramagnetic relaxation as paramagnetic resonance due to transitions at zero frequency. This close relation permits a general theoretical analysis of many problems pertaining to all three trends, and acquiring mutually complementary information on different physical constants, such as the magnetic specific heat of substances, relaxation times, etc.

Whereas in the study of the behavior of substances in a constant magnetic field the main characteristic is the static susceptibility χ_0, on going over to dynamic phenomena the susceptibility is best regarded as a complex quantity, $\chi = \chi' - i\chi''$. The magnetization component that varies in phase with the field is determined by the dynamic susceptibility χ', while the energy absorbed by the paramagnet from the alternating field is determined by the coefficient χ''. The task of the theory of paramagnetic absorption and dispersion is to establish the

- 22 -

dependence of the coefficients χ'' and χ' on the frequency of the alternating field and on the intensity of the applied static field. The general connection between the coefficients χ' and χ'' is given by the Kramers-Kronig relationships [14]

$$\chi'(v) = \frac{2}{\pi}\int\limits_0^\infty \frac{v_1\chi''(v_1)}{v_1^2-v^2}\,dv_1 + \text{const,} \qquad \chi''(v) = -\frac{2}{\pi}\int\limits_0^\infty \frac{v\chi'(v_1)}{v_1^2-v^2}\,dv_1. \qquad (1.18)$$

Dispersion formulas in closed form were obtained only for gases [15]. Naturally, for condensed systems, with their rather complicated internal interactions, a simple solution can hardly be obtained for this problem. It becomes necessary therefore to use approximate formulas. A comparison of (1.18) with $v = 0$ with (1.5) gives the connection between χ'' and the line shape function $g(v)$:

$$\chi''(v) = \frac{\pi}{2}\,v\chi_0\,g(v). \qquad (1.19)$$

In comparisons with experiment, $g(v)$ is usually described either by means of a Gaussian function, such as

$$g(v) = \frac{1}{\sqrt{2\pi}\,\sigma}\left\{e^{-\frac{(v-v_0)^2}{2\sigma^2}} + e^{-\frac{(v+v_0)^2}{2\sigma^2}}\right\} = g_1(v) + g_2(v), \qquad (1.20)$$

or by a Lorentz function

$$g(v) = \frac{\Delta v}{2\pi}\left\{\frac{1}{(v-v_0)^2+\frac{1}{4}\Delta v^2} + \frac{1}{(v+v_0)^2+\frac{1}{4}\Delta v^2}\right\} = g_1(v) + g_2(v). \qquad (1.21)$$

Here $v_0 = g\beta H_0/h$, $\sigma = \Delta v/2\sqrt{2\ln 2}$, and Δv is the absorption line at high frequencies. The second terms in the right members of (1.20) and (1.21) vanish when $v \gg \Delta v$; the need for introducing these terms is determined by the parity of the absorption effect relative to the field H_0 [16].

Experiments on electron paramagnetic resonance are carried out by investigating the dependences of χ' and χ'' on the magnitude of the

- 23 -
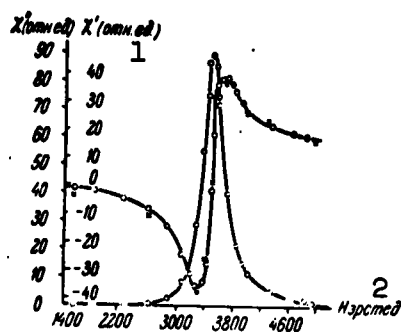
Fig. 1.7. Curves showing paramagnetic resonance absorption and susceptibility dispersion in $MnSO_4$ for $\nu = 9620$ Mc (B.M. Kozyrev, S.G. Salikhov, Yu.Ya. Shamonin, ZhETF 22, 56, 1952). 1) Relative units; 2) H, oersteds.
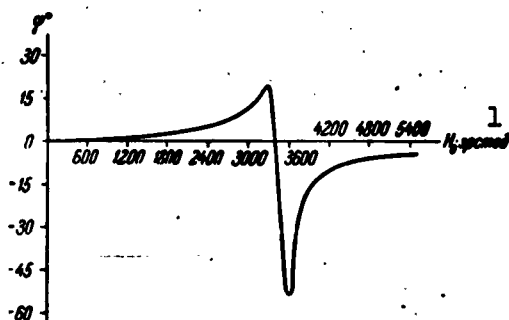
Fig. 1.8. Curves of paramagnetic resonance rotation in $CuSO_4 \cdot 5H_2O$ (N.N. Neprimerov, Izv. AN SSSR, ser. fiz., 18, 368, 1954). 1) H_0, oersteds.

field H_0 with $\nu = $ const. Therefore the Kramers-Kronig relations should be modified into [16]:

$$\left. \begin{aligned} \chi_0 - \chi'(H_0) &= \frac{1}{\pi} \int_0^\infty \frac{F(H_0+H)-F(H_0-H)}{H} \, dH, \\ F(H_0) &= \frac{1}{\pi} \int_0^\infty \frac{\chi'(H_0+H)-\chi'(H_0-H)}{H} \, dH, \end{aligned} \right\} \qquad (1.22)$$

where we put $F(H_0) = \chi''(H_0) - \pi\nu\chi_0 g_2(\nu)$; $g_2(\nu)$ is a monotonically decreasing function, so that its specific expression is immaterial. Paramagnetic resonance is investigated in most cases by measuring $\chi''(H_0)$.

- 24 -

Paramagnetic dispersion under resonant conditions was first observed by Zavoyskiy [17] in the salt $MnSO_4$; further measurements of $\chi'(H_0)$ are described in references [18]. Figure 1.7 shows typical paramagnetic resonance absorption and dispersion curves.

Paramagnetic resonance can be observed not only by measuring χ' and χ'', but also by studying the rotation of the plane of polarization of microwaves in paramagnets, induced by a static magnetic field. Many workers have considered the theory of this effect [19] and have made suitable measurements [20]. A typical $\varphi(H_0)$ curve is shown in Fig. 1.8.

The angle of rotation φ of the plane of polarization and the paramagnetic absorption are related by the simple integral equation [21]

$$\varphi = \frac{4\pi \nu \sqrt{\varepsilon}}{c} \int\limits_0^\infty \frac{\chi''(H_0+H) - \chi''(H_0-H)}{H} dH. \qquad (1.23)$$

Here ε is the dielectric constant of the paramagnet.

The integral relations (1.22) and (1.23) enable us to monitor the correctness of the form of the experimentally obtained paramagnetic-resonance curves. Recently, research was initiated also on other analogs of magnetooptical phenomena in the microwave region under magnetic resonance conditions, such as the Cotton-Mouton effect [22].

The aggregate of the results obtained with the aid of paramagnetic resonance provides important characteristics of various substances. It is sufficient to mention the determination of the magnetic and mechanical moments of atoms, molecules, or atomic nuclei, the times of paramagnetic relaxation, etc.

§1.5. Paramagnetic Resonance and Spectroscopy

Paramagnetic resonance is a component part of spectroscopy, since it makes it possible to determine the position of energy levels of magnetic particles. It is of interest to consider the features of para-

magnetic resonance as compared with spectroscopy at optical frequencies.

1. We note first that the range of frequencies used in magnetic-resonance experiments lies between 10^6 and 10^{11} cps. The use of these frequencies, which lie beyond the infrared portion of the spectrum, enables us to investigate with great accuracy energy-level splitting, which is inaccessible or practically inaccessible to optical methods.

2. At radio frequencies the probability of spontaneous transitions is very small, since it is proportional to ν^3. It is therefore necessary to deal only with forced absorption or emission in the study of paramagnetic resonance.

3. Whereas optical spectra are due in the overwhelming majority of cases to electrical dipole transitions between the energy levels, paramagnetic resonance absorption lines arise exclusively as a result of magnetic dipole transitions. Consequently, the Einstein coefficients for induced absorption and emission are approximately 4 orders of magnitude lower in the case of paramagnetic resonance.

4. In view of the foregoing, the effect of paramagnetic resonance is a very fine one; it can be detected not alone by virtue of the high sensitivity of the radio detection methods employed, but because of the tremendous number of photons that come into play. Thus, 1 milliwatt of power corresponds to n $\approx 10^{20}$ photons of frequency 10^{10} cps per second.

5. From the uncertain relations between the numbers of photons and the phase of the electromagnetic wave it follows that in our case, in view of the large value of n, the phase will be determined with very great accuracy. A consequence of this is the possibility of considering the electromagnetic field in radio spectroscopy as being a classical quantity.

6. At optical frequencies the line width is always very small com-

pared with the fundamental frequency. In investigations of paramagnetic resonance, the relation between these quantities becomes entirely different, since the interactions that bring about the broadening of the lines can have the same order of magnitude as the energy splittings, which determine the resonant frequencies. Therefore the width of paramagnetic resonance lines is frequently comparable with the fundamental frequency and can be measured with great accuracy. This uncovers great possibilities for the investigation of different types of interactions in paramagnets, by analyzing the shapes and widths of paramagnetic resonance lines and the character of their dependence on different factors.

7. The most important factors that determine the line width are magnetic dipole interactions, exchange forces, local electric fields produced by the surrounding magnetic particles, and finally thermal motion; the natural line width of radio frequency spectra is quite negligible.

8. Unlike conditions prevailing in optical experiments, the radiation used in radio spectroscopy is so monochromatic, that the generated bandwidth turns out to be incomparably narrower than the absorption line width.

9. Paramagnetic resonance spectra are investigated not by measuring the frequency of the incident radiation, but by measuring the natural frequencies of absorbing systems. This measurement is carried out by varying the static magnetic field.

§1.6. History of the Discovery of Paramagnetic Resonance

Paramagnetic resonance was discovered by Ye.K. Zavoyskiy [23] in 1944, in Kazan'; his first experiments pertained to resonant absorption in salts of ions of the iron group. Zavoyskiy's discovery was preceded by certain theoretical assumptions concerning the nature of the

- 27 -

expected effect. Following the well-known experiments by Stern and Gerlach on spatial quantization, Einstein and Ehrenfest [24] advanced several ideas on quantum transitions between magnetic sublevels of atoms under the influence of equilibrium radiation. On the basis of these ideas, Dorfman suggested in 1923 the possibility of resonant absorption of electromagnetic waves by paramagnets, and called this phenomenon the photomagnetic effect [25].

In 1932, I. Waller [26] published at Pauli's suggestion a fundamental paper containing a quantum theory of paramagnetic relaxation in solids. This paper served as the basis for further development of the theory of dynamic phenomena in paramagnets, particularly paramagnetic resonance.

In the middle thirties, Gorter and his co-workers [8] started a systematic study of the absorption and dispersion of radio frequency electromagnetic waves by paramagnets at $10^6-3\cdot10^7$ cps in the presence of static magnetic fields. However, Gorter's attempts at observing paramagnetic resonance were not fruitful [27] in view of shortcomings in the procedure and of the insufficiently high frequencies employed.

Zavoyskiy [23] developed new highly sensitive methods for the investigation of paramagnetic resonance: in place of determining the amount of heat released by the paramagnet, as did Gorter, he started to measure the attenuation of the high-frequency field energy as a result of absorption. To obtain fully resolvable paramagnetic resonance absorption lines, he expanded the range of frequencies employed to $3\cdot10^9$ cps. He not only succeeded in discovering paramagnetic resonance, but investigated many of its regularities, and also greatly extended the region in which paramagnetic relaxation was investigated.

The first theoretical interpretation of Zavoyskiy's experiments was suggested by Ya. I. Frenkel' [28].

A natural continuation of the study of paramagnetic resonance due, to magnetic moments of electrons was the discovery of an analogous effect in atomic nuclei, made by Purcell [29] and Bloch [30] and their co-workers two years after the publication of Zavoyskiy's papers. Finally, in 1950, paramagnetic resonance due to transitions between quadrupole energy levels of nuclei in crystals in the absence of an external magnetic field was discovered by Dehmelt and Kruger [31].

A tremendous number of investigations based on this method have been reported in recent years, in connection with the great progress made in microwave techniques, on the one hand, and the observed rather valuable applications of the paramagnetic resonance method to the solution of certain problems in solid state physics, atomic physics, chemistry, and engineering on the other.

REFERENCES TO CHAPTER I

1. Rabi J.J., Phys. Rev. 51, 652, 1937.

2. Alvarez Z.W., Bloch F., Phys. Rev. 57, 111, 1940.

3. Detch M., Phys. Rev. 84, 601, 1951; 85, 1047, 1951.

4. Kastler A.J., J. Phys. Radium 11, 255, 1950; Physica 17, 191, 1957.

5. Guttinger P., Zs. f. Phys. (J. Phys.) 73, 169, 1931.

6. Majorana E., Nuovo Cimento 9, 43, 1932.

7. Casimir H.B.G., du Pre F.K., Physica 5, 507, 1938.

8. Gorter K., Paramagnitnaya relaksatsiya (Paramagnetic relaxation), IL (Foreign Literature Press), Moscow, 1949.

9. Bloch F., Phys. Rev. 70, 460, 1946.

10. Kittel C., Phys. Rev. 76, 743, 1949.

11. Van Vleck J.H., The theory of electric and magnetic susceptibilities, Oxford, 1932.

12. Shaposhnikov I.G., Doctor's dissertation, Moscow, FIAN (Physics Institute, Academy of Sciences), 1949.

13. Gorter K., UFN (Progress in the Physical Sciences) 53, 545, 1954.

14. Kramers H.A., Atti Congr. Fis., Como, 545, 1927; Kronig R., J. Opt. Soc. Amer. 12, 547, 1926.

15. Van Vleck J.H., Weisskopf V.F., Rev. Mod. Phys. 17, 227, 1945; Frölich H., Nature L. 157, 478, 1948.

16. Al'tshuler S.A., ZhETF (J. Experimental and Theoretical Physics), 20, 1047, 1950.

17. Zavoyskiy Ye.K., ZhETF 17, 155, 1947.

18. Kozyrev B.M., Salikhov S.G., Shamonin Yu.Ya., ZhETF 22, 56, 1952; Romanov I.M., Uch. zap. KGU (Scientific Notes of the Kiev State University) 113, 187, 1953; Neprimerov N.N., Izv. AN SSSR, ser. fiz. (Bull. Acad. Sci. USSR, Physics Series) 18, 360, 1954.

19. Kastler A.J., Compt. Rend. 228, 1640, 1949; Tsirul'nikova L.M., Shaposhnikov I.G., Izv. AN SSSR, ser. fiz. 20, 125, 1956; Shekun L.Ya., Izv. AN SSSR, ser. fiz. 20, 1265, 1956.

20. Wilson M.C., Hull G.F., Phys. Rev. 74, 711, 1948; Neprimerov N.N., Izv. AN SSSR, ser. fiz. 18, 368, 1954.

21. Shekun L.Ya., Izv. AN SSSR, ser. fiz. 20, 1262, 1956.

22. Battaglia A., Gozzini A., Polacco E., Nuovo Cimento 10, 1205, 1953; Hedvig P., Acta Phys. Hung. 6, 489, 1957.

23. Zavoyskiy Ye.K., Doctors's dissertation, Moscow, FIAN, 1944; J. Phys. USSR 9, 245, 1945.

24. Einstein A., Ehrenfest P., Zs. f. Phys. 11, 31, 1922.

25. Dorfman Ya.G., Zs. f. Phys. 17, 98, 1923.

26. Waller I., Zs. f. Phys. 79, 370, 1932.

27. Gorter C.J., Physica 3, 995, 1936; 9, 591, 1942; Deikstra Z.F., Thesis, Amsterdam, 1943.

28. Frenkel' Ya.I., ZhETF 15, 409, 1945.

29. Purcell E.M., Pound R.V., Torrey N.S., Phys. Rev. 69, 37, 1946.

30. Bloch F., Hansen W.W., Paccard N., Phys. Rev. 69, 127, 1946.

31. Dehmelt H.G., Krüger H., Naturwiss. (Natural Sciences) 37, 111, 1950; Zs. f. Phys. 129, 401, 1951.

Manu-script Page No.	[Footnotes]
7	If the magnetic moment of the particle has both spin and or-bital components, we assume that the field H_0 is incapable of disturbing the spin-orbit coupling.
8	If the magnetic particle is not isolated but is located, for example, in a crystal lattice, then in some cases resonant transitions are possible if the alternating and static mag-netic fields are parallel (see Chapter III).

Chapter II

MEASUREMENT METHODS

§2.1. Microwave Spectroscopes

Modern procedures for the measurement of paramagnetic resonance are based on the determination of the change in some parameter of an oscillating system containing a paramagnet; these changes may be due to paramagnetic absorption, dispersion of the susceptibility, or rotation of the plane of polarization in the investigated substance.

Methods of this type were first developed by Zavoyskiy both for the frequency range 10^7-10^8 cps [1], and for higher frequencies, on the order of 10^9 cps [2], approaching the microwave band.

The experiments made prior to the discovery of paramagnetic resonance by Gorter and his school [3], aimed at determining the non-resonant paramagnetic losses at frequencies up to 10^7 cps, were carried out by calorimetric determination of the heat released in the paramagnet. The heat was determined from the rate at which the specimen was heated by losses occurring in it. This method, in view of its low sensitivity and the difficulty in separating paramagnetic absorption from other types of losses (dielectric losses, losses due to electric conductivity) could not be used to investigate paramagnetic resonance. On the other hand, the procedure of measuring the dynamic susceptibility χ', used by Gorter, although one of the indirect electrical methods, was suitable only for very low frequencies. Thus, it was Zavoyskiy himself who laid the groundwork for modern methods of magnetic radio spectroscopy.

Different measurement techniques, of course, are used for the microwave band ($\nu \approx 10^{10}$ cps), on the one hand, and for the radio band ($\nu \approx 10^6$-10^9 cps) on the other. This has caused some authors to distinguish between radio frequency and microwave magnetic spectroscopy. Such a distinction is, however, little justified, since the nature of the investigated phenomena is the same in both cases.

Let us first discuss the methods used in the microwave band. Each microwave magnetic spectroscope consists of the following main parts: 1) a microwave generator with stabilized frequency and stabilized power supply, with provision for monitoring the frequency and the power; 2) an absorbing cell, made in the form of a cylindrical or rectangular resonant cavity; 3) a detector; 4) an amplifying and recording unit, and 5) a source of constant magnetic field. In most cases there is, in addition, 6) a unit for modulating the constant magnetic field (see, for example, Fig. 2.2).

A resonant cavity containing a sample of the investigated substance is placed between the poles of an electromagnet in such a way that the static and microwave magnetic fields acting on the substance are mutually perpendicular. The sample is located in such a place in the cavity, where the microwave magnetic field is maximal and the electric field is minimal (in order to attenuate the nonmagnetic losses). During the course of the measurements, the frequency of the microwave generator exciting the electromagnetic oscillations in the cavity is maintained constant while the intensity of the static magnetic field is varied. This experimental procedure is made necessary by the fact that a study of the dependence of the paramagnetic absorption coefficient on the frequency of the microwave field at $H_0 = $ const would introduce additional experimental difficulties, connected with the change in the generator power with changing frequency of the radiation pro-

duced by the generator.

There are two types of microwave magnetic spectrometers. In the first the paramagnetic resonance absorption is investigated by determining the change in the power passing through the resonant cavity containing the substance (transmitted-wave method), and in the second it is determined from the change in the power reflected from the cavity with the specimen (reflected-wave method).

The transmitted-wave method was first experimentally employed by Cummerow, Holliday, and Moore [4], who showed that the coefficient of paramagnetic absorption can be determined by measuring the power at the output of the cavity resonator.

The second method permits the paramagnetic absorption coefficient to be determined from the coefficient of reflection from the cavity containing the investigated substance. Whitmer, Weidner, Hsiang, and Weiss [5] constructed a microwave magnetic spectroscope operating on the balanced-T bridge method using a dual tee. Measurement of the power P resulting from the unbalancing of the bridge by the paramagnetic losses, makes it possible to determine the reflection coefficient γ, which is connected with the dynamic susceptibility of the paramagnet:

$$P \sim \gamma^3 = \text{const} \, (\chi'^3 + \chi''^3).$$
(2.1)

Both the transmitted-wave and the reflected-wave methods are used in modern spectroscopes.

Before we proceed to consider individual specific installations, which differ essentially in the methods used to indicate the transmitted or reflected power, let us dwell on a few factors that determine the sensitivity of a magnetic spectroscope. By virtue of (1.9) and (1.19), the paramagnet specimen placed in an oscillating magnetic field $H_r \cos 2\pi \nu t$ absorbs a power $P = \pi \nu \chi'' H_r^2$. On the other hand, the power absorbed by the cavity itself can be expressed by $P_0 = (1/Q_0) \nu H_r^2 V/4$,

- 34 -

where Q_0 is the unloaded Q of the cavity and V is its effective volume. Therefore the ratio of the power absorbed by the investigated specimen to the power dissipated by the cavity itself is

$$\frac{P}{P_\bullet} = \frac{4\pi\chi''Q_\bullet}{V}. \qquad (2.2)$$

We see therefore that the apparatus has maximum sensitivity for the measurement of the coefficient of paramagnetic absorption χ'' when the unloaded Q of the resonant cavity is largest and when the cavity volume is smallest.
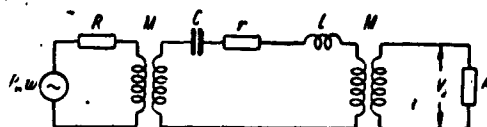
Fig. 2.1. Equivalent circuit used in the determination of the sensitivity of a microwave spectroscope.

For a specimen containing paramagnetic particles with spin S = $= 1/2$, the absorption coefficient will be $\chi'' \approx \chi_0 v/\Delta v$, where χ_0 is the static magnetic susceptibility of the specimen, v the frequency of the oscillating magnetic field, and Δv the width of the resonance absorption line, expressed in frequency units. When S = 1/2 and g = 2, the static magnetic susceptibility of one mole of substance is $\chi_0 = 0.38/T$. If the wavelength of the microwave generator is $\lambda \approx 3$ cm, and the width of the paramagnetic resonance line is on the order of 1 oersted,* that is, $\sim 10^{-4}$ cm^{-1}, then $\chi''_{mole} \approx 4$ at room temperat re. Consequently, in order for the Q of the cavity to decrease to about one half of the loaded value Q_0, we must place in the case of $Q_0 \approx 5000$ approximately 10^{-5} mole of our paramagnet in the cavity, if we assume that the effective volume is $V \approx 2-3$ cm^3.

To estimate the limiting sensitivity of the spectroscope we can,

following Bleany and Stevens [6], consider an equivalent circuit, in which the resonant cavity is represented by a tuned network with resistance $\underline{r}$ (Fig. 2.1). The microwave radiation is fed to the tuned network through a self-inductance M from a generator with power P_1 and internal resistance R. The radiation is detected by a receiver, the resistance of which is also R. If the generator has an angular frequency ω and is exactly tuned to the frequency of the resonant network, then the voltage on the indicator is

$$V_2 = \frac{(r' R P_1)^{\frac{1}{2}}}{r + r'},$$

where $r' = 2\omega^2 M^2/R$.

Assume that the paramagnetic absorption has changed the quantity $\underline{r}$ by an amount δr; then the change in voltage will be

$$\delta V_2 = \frac{r'(R P_1)^{\frac{1}{2}} \delta r}{(r + r')^2}.$$

Since r' depends on the coupling with the resonant network, we can tune the latter by changing the coupling (that is, the value of M). The sensitivity will be maximal when the voltage δV_2 reaches a maximum, which occurs when $r = r'$. Let us express δV_2 in terms of the power P_2 entering the receiver. We have $\delta V_2 = \delta r(R P_2)^{1/2}/(r + r')$. This expression shows that the fraction change $\delta V_2/(R P_2)^{1/2}$ is equal to $\delta r/(r + r')$. Although P_2 increases with increasing coupling, on the other hand Q decreases with the load. At the maximum, the change of the indicator voltage, due to the paramagnetic absorption, will be

$$\delta V_2 = (R P_1)^{\frac{1}{2}} \frac{\delta r}{4 r}.$$

If the receiver has a noise figure N and a bandwidth df, then the output signal will be equal to the noise at the output, provided the condition $\delta V_2 = (N k T df R)^{1/2}$ is satisfied.

- 36 -

On the other hand, $\delta r/r$ is the ratio of the power absorbed by the specimen to the power dissipated by the cavity, which as we have seen is equal to $4\pi\chi''Q_0/V$; thus, the minimum value of χ'' that can be detected by the apparatus satisfies the condition

$$\chi''_{min} = \frac{V}{\pi Q_0} \left(\frac{NkTdf}{P_1}\right)^{\frac{1}{2}}. \qquad (2.3)$$

If we assume as before that $Q_0 = 5000$ and $\lambda = 3$ cm, then for $N = 10$, $df = 1$ cps, a generator power of 40 milliwatts, and $V = 2\text{-}3$ cm^3, the theoretical minimum value χ''_{min} will be $\sim 10^{-12}$ at room temperature. For an absorption line width $\sim 10^{-4}$ cm^{-1}, this should correspond to a possibility of detecting a signal against a noise background from about $2.5\cdot 10^{-13}$ mole of paramagnetic particles with $S = 1/2$ (at 300°K). The sensitivity actually attained in the apparatus is as a rule much lower than this figure and depends greatly on many factors, particularly on the method used to measure the signal in the apparatus.

Depending on the method used to indicate the microwave paramagnetic resonance spectra, the existing spectroscopes can be subdivided into several groups: 1) direct current indication; 2) detection followed by low-frequency amplification; 3) double modulation; and 4) the superheterodyne method. Very recent papers [7] report the use of the spin-echo method for the investigation of vary narrow electron paramagnetic resonance lines; this method was previously used only for nuclear paramagnetic resonance.

The first method is easiest to realize, but in view of its low sensitivity it was used only during the first stages in the development of magnetic radio spectroscopy, when the work was limited to investigations of relatively crude effects, occurring in nondilute paramagnets with broad and intense absorption lines. In this method, the microwave signal was rectified after passing through the measurement

cavity (or after being reflected from it) and was fed through a compensation network to a sensitive galvanometer. The paramagnetic absorption curve was plotted "point by point," with the galvanometer deflections, which were proportional to the power flowing through the detector, being noted for different values of the constant magnetic field intensity H_0. For each value of H_0 the cavity was first tuned to the generator frequency.

To proceed to an investigation of the narrower and weaker absorption lines, observed in dilute paramagnets, it is necessary to use methods that yield greater sensitivity and permit the spectral pattern to be displayed on an oscilloscope or recorded on a chart.

A method satisfying these requirements employs modulation of the static field H_0 by a magnetic field of audio frequency; such modulation was first used by Zavoyskiy [1] in 1944, in work carried out in the radio frequency range. If the amplitude of the modulating field H, for a specified intensity of the static magnetic field, encompasses the region of paramagnetic resonance, then a suitable modulation should take place in the power passing through the cavity (or reflected from it). This power modulation can be amplified and fed to an oscilloscope, the horizontal sweep of which is synchronized with the modulation field. During each period of modulation, the field will go through the resonant values of H_0 twice; consequently the portion of the spectrum encompassed by the modulation amplitude (or the entire spectrum, if the amplitude is sufficiently large) will be displayed on the oscilloscope screen in the form of a double picture, symmetrical with respect to the center, representing the dependence $\chi''(H_0)$. This method of investigating paramagnetic resonance is essentially convenient for an initial determination of paramagnetic spectra; a study of the details of these spectra is more conveniently carried out by using a modulation

- 38 -

amplitude which is quite small compared with the width of the investigated line. In this case as we gradually pass through H_0 in the resonant region, we obtain a curve showing the dependence of the derivative $d\chi''/dH_0$ on H_0; it is usually recorded automatically on a chart.
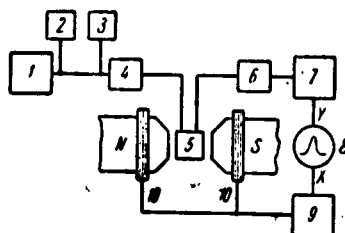
Fig. 2.2. Microwave spectroscope with low-frequency modulation of the magnetic field (transmitted-wave method). 1) Microwave generator; 2) frequency control; 3) power control; 4) attenuator; 5) resonant cavity with the substance; 6) crystal detector; 7) low-frequency amplifier; 8) oscilloscope; 9) phase shifter; 10) modulating coils.
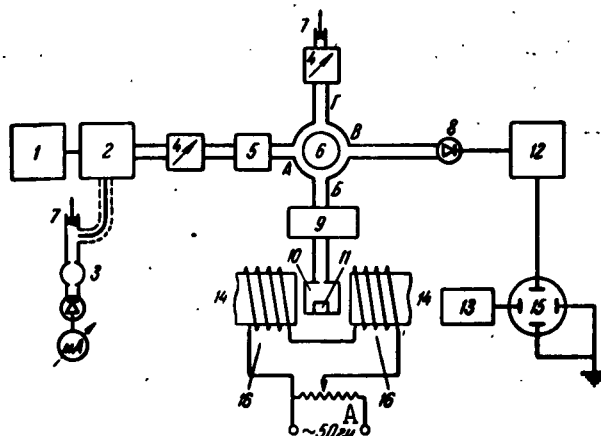
Fig. 2.3. Microwave spectroscope with low-frequency modulation of the magnetic field (reflected-wave method) [8]. 1) Stabilized power supply; 2) klystron oscillator; 3) wave meter; 4) attenuator; 5) phase shifter; 6) hybrid ring; 7) plunger; 8) crystal detector; 9) loop; 10) cavity; 11) specimen; 12) low-frequency amplifier; 13) sweep; 14) electromagnet; 15) oscilloscope; 16) modulating coils. A) cps.

- 39 -

A block diagram of a microwave spectroscope with low-frequency modulation of the magnetic field and with a transmission-type resonant cavity is shown in Fig. 2.2.

Apparatus using the same field modulation but based on the re-flected-wave method has been described by Manenkov and Prokhorov [8]. It is shown in Fig. 2.3.

The main factor limiting the sensitivity of spectroscopes of this type is the low-frequency noise of the crystal detector. To avoid this noise and thus increase the sensitivity, Beringer and Castle [9] con-structed a spectroscope in which a bolometer was used as a detector. The latter can detect power on the order of a milliwatt without appre-ciable low-frequency noise. The Beringer and Castle apparatus uses the transmitted-wave method. The microwave generator is frequency stabil-ized; the narrow-band phase-sensitive amplifier is controlled by a 30 cps frequency, which is used to modulate the field H_0. The experimen-tally estimated sensitivity of this spectroscope does not differ greatly from the theoretically attainable value. A block diagram of the Beringer and Castle spectroscope is shown in Fig. 2.4. This spec-troscope was constructed to investigate very weak paramagnetic reso-nance lines, observed in rarefied gases.

Another method of increasing the sensitivity of radio spectro-scopes was first used to measure paramagnetic resonance by Smaller and Jasaytis [10]. It consists of using double modulation of the magnetic field. The Buckmaster and Scovil spectroscope, built on this principle [11], is no less sensitive than a spectroscope with a bolometer. The double modulation principle consists in the following. The spectral density of the crystal-detector noise is inversely proportional to the frequency (at least in the interval 1-$24 \cdot 10^9$ cps). Therefore, if in addition to modulating at an audio frequency v_1 with high amplitude

the magnetic field is modulated additionally at a frequency ν_2, sufficiently high to cause the fraction of the low-frequency noise in excess of the thermal noise in the crystal detector to be negligibly small, and if amplification at frequency ν_2 is introduced, then the sensitivity (compared with the amplification at the low frequency) should increase greatly. We note that the amplitude of the high-frequency modulation method does not exceed half the width of the investigated spectral line [12].

Buckmaster and Scovil used in their spectroscope a cylindrical cavity, operating in the H_{111} mode; the source of microwave power is a generator operating at $\lambda = 1.2$ cm. The first-modulation frequency is $\nu_1 = 60$ cps, while that of the second modulation is $\nu_2 = 462.5$ kcs. A block diagram of this spectroscope is shown in Fig. 2.5. The microwave power is fed from the reflex klystron to a transmission-type cavity to a diode crystal detector. Connected ahead of the cavity are devices to control and monitor the received microwave power and to measure the wavelength. The video signal obtained at the output of the crystal detector passes through an amplifier tuned to 462 kcs with gain 10^6 and bandwidth 8 kcs; the amplification is to a level at which the signal can be detected linearly. Either an ordinary linear or a phase-sensitive detector can be used, the output of the detector being fed to an oscilloscope. In the former case the oscillogram represents the modulus of the derivative of the line shape, and in the latter the derivative itself. The time sweep voltage of the oscilloscope is obtained from a phase shifter fed by the power source of the low-frequency modulation of the magnetic field (Helmholtz coils). If narrow-band amplification is used, the superposition of a magnetic field of frequency ν_1 is replaced by a slow and linear variation of the field H_0.

The most difficult to attain is the high-frequency modulation,

- 41 -

Fig. 2.4. Microwave spectro-
scope using a bolometer [9].
1) Microwave stabilized oscil-
lator; 2) cavity; 3) bolometer;
4) DC bridge; 5) 30 cps amp-
lifier with high gain; 6) syn-
chronous amplifier; 7) 30 cps
generator; 8) 30 cps power amp-
lifier; 9) galvanometer with
large time constant; 10) modu-
lation coils.

Fig. 2.5. Microwave spectro-
scope with dual field modula-
tion [11]. 1) Stabilized os-
cillator; 2) resonant cavity
with substance; 3) detector;
4) amplifier for the frequen-
cies $v_2 + \Delta v$; 5) linear detec-
tor; 6) amplifier for v_1; 7)
oscilloscopes; 8) phase-sensi-
tive detector; 9) phase
shifter for v_2; 10) modulation
coils for v_2; 11) modulation
coils for v_1; 12) phase
shifter for v_1; 13) frequency
control; 14) power control.

for it is necessary for this purpose to introduce a radio frequency

magnetic field inside the resonant cavity. For this purpose the reso-

nant cavity is frequently slotted in a plane passing through its axis. If the width of the slot is small compared with the wavelength λ, then the Q of the cavity is changed little. The radio frequency field can be produced effectively only by modulation current flowing over the internal surface of the cavity. Such a current can be made sufficiently large to ensure a radio frequency magnetic field with amplitude up to 50 oersted at the location of the investigated substance.

An experimental estimate of the sensitivity of the Buckmaster and Scovil spectroscope operating with amplification at 462 kcs and an amplifier bandwidth of 8 kcs has shown that 10^{-11} of a mole of free radical with a line width 3.5 oersted at $290^\circ K$ produces a signal/noise ratio of 2/1 for the modulus of the derivative of the line shape. Calculation has shown that using amplification on a very narrow band (1 cps) the maximum sensitivity should be on the order of 10^{-13} mole of free radical at $290^\circ K$.

The dual modulation principle is used also in the microwave magnetic spectroscope of Semenov and Bubnov [13]. The high and low modulation frequencies are 975 kcs and 50 cps, respectively. The depth of the low-frequency modulation is on the order of 300 oersted. The spectrometer is equipped with an automatic frequency control for the klystron oscillator against the operating cavity. A voltage of ~15 mv is fed to the klystron repeller from the automatic frequency control oscillator (630 kcs). This voltage frequency-modulates the microwave oscillations produced by the klystron. If the klystron frequency deviates from that of the cavity, the microwave oscillations are amplitude-modulated. The phase of this "automatic frequency control signal" is determined by the sign of the frequency deviation, and the amplitude is proportional to the magnitude of this deviation. After detection of the microwave oscillations, the control signal is amplified by

- 43 -

a tuned amplifier (630 kcs, gain ~10^5) and is fed to a phase-sensitive detector, from which it is applied to the klystron repeller. The end result is that the klystron frequency is set at the resonant frequency of the cavity containing the investigated substance.

Because of the device just described, the microwave spectroscope of Semenov and Bubnov has rather high operating stability. It is therefore most suitable for investigations of the course of chemical reactions. If an oscilloscope is used for registration, its sensitivity corresponds to ~$4 \cdot 10^{-10}$ mole of diphenylpicrylhydrazyl and ~$8 \cdot 10^{-12}$ mole of the same substance if slow chart recording is used. A block diagram of the spectroscope is shown in Fig. 2.6.

The superheterodyne measurement method was first used for the study of paramagnetic resonance by England and Schneider [14]. It is based on the use of a balanced T bridge (or hybrid ring), to which power is applied from a measuring klystron of frequency f_1 and from an auxiliary klystron of frequency f_2. The frequency difference $f_1 - f_2$ is made equal to several times ten megacycles. This is the intermediate frequency used to amplify the signal resulting from the unbalance of the bridge upon occurrence of paramagnetic absorption. The low-frequency noise of the crystal detector is thus made negligibly small. However, with increasing $f_1 - f_2$, the noise of the intermediate-frequency amplifier increases. Taking both factors into account, the theoretical optimum of $f_1 - f_2$ lies close to 30 megacycles [15].

An example of a block diagram of a spectroscope with superheterodyne detection [16] is shown in Fig. 2.7.

If there is no paramagnetic absorption, there should be no signal in the fourth arm of the bridge provided the tuning and the balancing are exact. Absorption produces an unbalance by changing the reflection coefficient and causes the power in klystron 1 to begin to flow in the

- 44 -
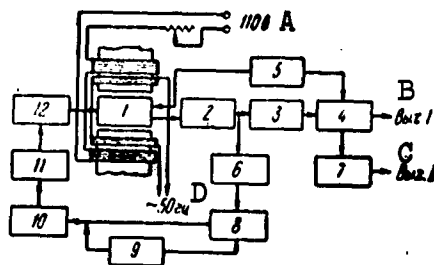
Fig. 2.6. Microwave spectroscope with dual modulation and with automatic frequency control [13]. 1) Cavity with specimen; 2) microwave crystal detector; 3) amplifier ($\nu = 975$ kcs); 4) synchronous detector ($\nu = 975$ kcs); 5) high frequency oscillator ($\nu = 975$ kcs); 6) automatic frequency control amplifier ($\nu = 630$ kcs); 7) DC amplifier; 8) phase sensitive detector for automatic frequency control; 9) automatic frequency control generator ($\nu = 630$ kcs); 10) klystron oscillator ($\lambda = 3.2$ cm); 11) ferrite decoupler; 12) variable attenuator. A) 110 v; B) out I; C) out II; D) cps.

fourth arm and to mix in the crystal mixer with the power from the auxiliary klystron, thus producing an intermediate frequency signal which is fed to the amplifier.

It must be borne in mind that the power δP reflected in the fourth arm is not equal to the absorbed power ΔP, but is only a fraction of the latter; according to Gordy [17]

$$\frac{\delta P}{\Delta P} = \frac{\Delta P}{P};$$

where P is the total power in the cavity.

The different types of microwave magnetic spectroscopes, which we have discussed briefly, make it possible to study with great accuracy the position of the paramagnetic resonance line, and with a somewhat lesser accuracy the line shape.

The accuracy with which the line position is determined depends

- 45 -
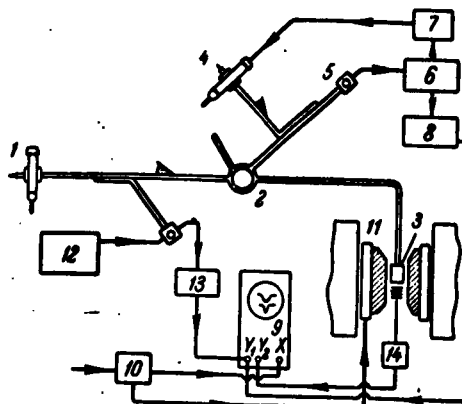
Fig. 2.7. Microwave spectro-
scope operating on the super-
heterodyne principle [16]. 1)
Klystron; 2) hybrid ring (or
T-bridge; 3) resonant cavity;
4) local heterodyne; 5) mixer;
6) intermediate frequency amp-
lifier; 7) automatic frequency
control; 8) video amplifier;
9) oscilloscope; 10) phase
shifter; 11) modulation coils;
12) frequency multiplier; 13)
receiver; 14) proton flux
meter.
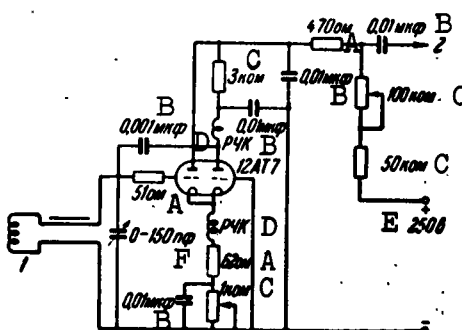
Fig. 2.8. Proton flux meter
[18]. 1) Coil with specimen in
magnetic field; 2) to amplifier
and oscilloscope; RFC) radio
frequency coils. A) ohm; B) μf;
C) kohm; D) RFC; E) 250 v; F)
μμf.

essentially on the accuracy with which the intensity of the constant

magnetic field H_0 is measured at resonance, since the measurement of

the resonant frequency ν can frequently be made without large errors.

The determination of the intensity of the magnetic field reduces as a rule likewise to a measurement of a certain frequency, namely the frequency of proton paramagnetic resonance, observed at a given magnetic field. Flux meters constructed on the proton-resonance principle are presently used in all cases where precision measurement of the magnetic field is required. One of the methods of using proton resonance for the determination of the paramagnetic resonance line position is illustrated in Fig. 2.7. The frequency of the proton flux meter is varied until the positions of the maxima of the electron and proton resonances, observed on the screen of a double-beam oscilloscope, occur at one and the same abscissa. One of the possible proton flux meter circuits [18] is shown in Fig. 2.8.

Understandably, the narrower the line and the higher the frequency at which the paramagnetic resonance is measured, the more accurately can the line position be determined. For lines with $\Delta H \approx 1$ oersted and at frequencies corresponding to the millimeter band, the accuracy with which the effective g factor is determined reaches hundredths of a percent. On the other hand, in nondilute paramagnetic salts with broad lines, the effective g factor can be determined only with accuracy not higher than several tenths of a percent, and usually even with lower accuracy.

The study of the paramagnetic resonance line shape is a more difficult problem. Because paramagnetic absorption (χ'') is always accompanied by dispersion of the magnetic susceptibility (χ'), the observed $\chi''(H_0)$ line should generally speaking always be deformed to some degree or another as a result of the χ' admixture. It is easy to show, however [8], that the influence of the dispersion on the line shape can be neglected provided the following two conditions are satisfied: 1) the natural frequency of the cavity is strictly equal to the frequency

of the microwave oscillator under the conditions of paramagnetic resonance, and 2) the amount of paramagnetic substance chosen for the measurement is sufficiently small to make the paramagnetic losses in the specimen small compared with the over-all losses in the cavity.

Several special methods were also developed to separate the $\chi''(H_0)$ or $\chi'(H_0)$ effect in pure form [19-21]. These methods are important if condition 2) cannot be satisfied for one reason or another.

A procedure for the measurement of the paramagnetic rotation of the plane of polarization is developed in [22].

For lack of space we shall not stop to describe individual units and parts of the apparatus used in microwave spectroscopes. This description can be found in the books by Gordy, Smith, and Trambarulo [23], Strandberg [24], Ingram [16], and also in the specialized radio literature.

We confine ourselves here merely to a description of devices used in low-temperature and high-temperature measurements of paramagnetic resonance.

The first extensive investigations of paramagnetic resonance spectra at liquid hydrogen or helium temperatures were set up by Bleaney and his co-workers in Oxford [16]. To work at $\lambda = 1.25$ cm and at liquid nitrogen and liquid hydrogen temperatures they used a special type of cylindrical cavity with inside diameter 12 mm and height from 6 to 11 mm, with the input and output coupling apertures made in the upper cover of the cavity, for easier placement of the latter in a Dewar flask. The investigated crystal was mounted on a small platform, covering a third aperture located in the center of the same top cover of the cavity. This platform was secured to a long thin-walled tube made of silver, so that the crystal could be rotated in a chosen plane through any angle relative to the external magnetic field. Wave guides

- 48 -

supplying microwave power to the cavity were made of thin-wall silver,* with inside dimensions 2.5x6 mm, and filled with distyrene almost to the upper uncooled end, where they gradually taper down. A section through such a cavity is shown in Fig. 2.9. Similar devices are used also for other wavelengths.
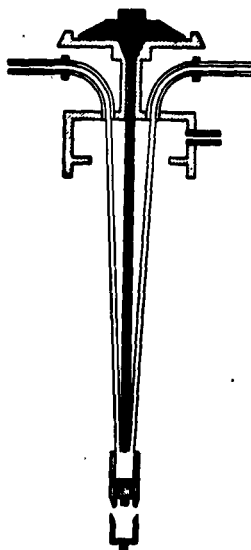
Fig. 2.9. Cavity for measure-
ments at low temperatures on a
wavelength of 1.25 cm [16].
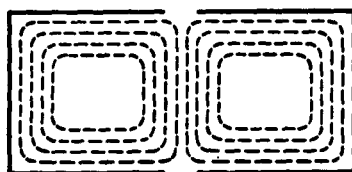
Fig. 2.10. Cavity with aper-
tures for measurements at low
temperatures.

In addition to the foregoing measurement method, others are also used at low temperatures. In particular, the use of a rectangular cavity operating on the H_{012} mode or a cylindrical one on the H_{011} mode offers great advantages. The distribution of the magnetic force lines of the microwave field in such cavities is shown in Fig. 2.10. An aper-

ture is cut in the narrow wall of the cavity (or in the end of the cylinder), and a vessel made of foamed plastic containing the investigated substance is inserted in this aperture [13]. If the required conditions regarding the position and dimensions of the aperture are satisfied, the presence of this aperture does not influence greatly the Q of the cavity, and consequently the sensitivity of the apparatus. Of course, the necessary condition for any measurement with a Dewar flask or with a foamed-plastic vessel, placed inside a cavity, is high stability of the spectroscope, so that the boiling of the cooled liquid does not cause any distortion in the observed spectrum. Such a procedure makes it possible to make measurements at both low and high temperatures [25]. Investigations at high temperatures can also be carried out with the aid of a special heater described in [26].

It must be mentioned that in some cases (for example, in the investigation of relaxation time by the method of paramagnetic resonance line saturation) it becomes necessary to use high amplitudes of the microwave magnetic field. It is customary to use pulse techniques for this purpose [27, 28].

§2.2. Methods of Measurements in the Radio Frequency Band

Two types of methods are used at present to measure $\chi''(H)$ in the radio frequency band: one can be called the method of reaction on the generator, and the other is based on the determination of the change in Q of a resonant circuit (or a cavity) resulting from the paramagnetic losses.

As already mentioned, Gorter's first investigations of nonresonant paramagnetic absorption, observed at low frequencies, were carried out by a direct calorimetric method. The inconvenience of this method, and the fact that it cannot be employed at higher frequencies, have induced Zavoyskiy to go over to indirect electric methods of de-

termining the paramagnetic losses. He developed the method of reaction on the generator [1, 2], which is widely used at present to study both electron and nuclear paramagnetic resonance [29, 30].

When working in the radio frequency band, the investigated substance is usually placed not in a resonant cavity, but in a self-inductance coil, comprising part of the tank circuit of an electronic self-oscillator or inductively coupled to the latter. The Zavoyskiy radio frequency measurement procedure is based on the fact that a change in the active power load ΔW of the generator producing the electromagnetic oscillations causes, if certain conditions are satisfied, a proportional change in the grid current, ΔI_g, or in the anode current, ΔI_a, of the generator. ΔW should be proportional to ΔI_g or ΔI_a if the power dissipated by the substance as a result of paramagnetic absorption is small compared with the over-all losses in the tank circuit.

Work with magnetic spectrographs in the radio frequency band becomes much more convenient, and their sensitivity is greatly increased, if the constant magnetic field is modulated by a low-frequency field. This modulation, to which we already referred in the preceding section, was first used by Zavoyskiy precisely for the radio frequency band.

The simplest schematic diagram of a setup operating by the Zavoyskiy method is shown in Fig. 2.11.

To measure the absolute values of the paramagnetic absorption in the radio frequency band, a very simple method was used in [31]. This method consisted of determining the change in the Q of the tank-circuit inductance coil with the aid of a somewhat modified Q meter. These changes in the Q are proportional to the value of χ'':

$$\Delta Q = - 4\pi\eta\chi''Q^2,$$

where η is the filling factor of the coil. Similar setups were proposed earlier for the measurement of nuclear magnetic resonance [30].

- 51 -
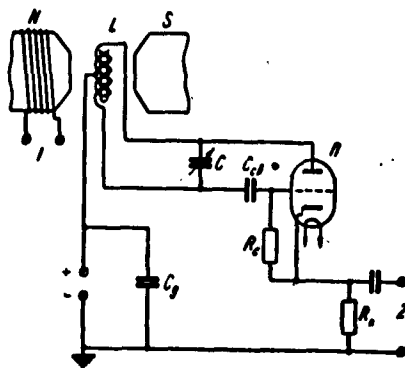
Fig. 2.11. Block diagram of a radio spectroscope operating by the method of reaction on the generator [1]. 1) Modulation winding of the electromagnet; 2) to low-frequency amplifier.

Radio spectroscopes in which the absorbing cell is the tank circuit inductance coil have advantages in that it is more convenient to place the investigated substance in the high frequency field and it is easier to carry out the measurements at either low or high temperatures. However, the low Q of the coils makes such setups not always sufficiently sensitive. Therefore in some cases when particularly high sensitivity is required, the inductance coil of the radio spectroscope is replaced by a high Q cavity. A spectroscope of this type was constructed by Feher and Kip [32] to measure paramagnetic resonance in metals. A block diagram of this spectroscope is shown in Fig. 2.12. The use of a synchronous detector has resulted in this apparatus in a further improvement in the signal/noise ratio.

To conclude this chapter, let us dwell briefly on the sources of constant magnetic field used in the investigation of paramagnetic resonance. In experiments carried out in the microwave band, where the resonant values of H_0 usually range from 3000 oersteds upwards the only suitable sources capable of producing such fields are electromagnets. Inasmuch as paramagnetic resonance lines are in the majority of cases

- 52 -

tens and sometimes even hundreds of oersteds wide, no stringent re-
quirements are imposed on the homogeneity of the magnetic field. In
individual cases, however, very narrow lines can also be observed, on
the order of tenths of an oersted. For such measurements electromag-
nets such as employed in nuclear magnetic resonance are used, with
suitable stabilization [29].
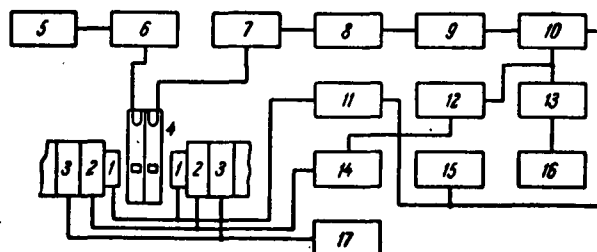
Fig. 2.12. Block diagram of a radio spectro-
scope operating on the principle of measur-
ing Q with a phase-sensitive detector [32].
1) Modulation coils used to produce a sinus-
oidal magnetic field; 2) modulation coils
used to obtain a slowly varying magnetic
field; 3) coils used to obtain a constant
magnetic field; 4) high-Q cavity (Q = 1000-
1500); 5) high-frequency generator; 6,7)
matching transformers; 8) vacuum tube de-
tector; 9) narrow band amplifier; 10) syn-
chronous detector; 11) amplifier to supply
the coils; 12) oscilloscope with DC ampli-
fier; 13) amplifier for automatic recorder;
14) sawtooth voltage generator; 15) generator
for sinusoidal reference voltage; 16) auto-
matic recorder; 17) power supply for coils 3.

In measurements of electron paramagnetic resonance at radio fre-
quencies it is possible to produce the constant magnetic field not
only with electromagnets but also with Helmholtz coils, since the re-
quired field intensity is not large in this case. A determination of
the positions of the paramagnetic resonance lines in the radio fre-
quency band is carried out either by measuring the resonant field in-
tensity H_0 with a proton flux meter or by means of a standard substance,
such as diphenylpicrylhydrazyl, for which the value of the g factor is

known with sufficient accuracy.

REFERENCES (Chapter II)

1. Zavoyskiy, Ye.K., Doctor's dissertation, Moscow, FIAN [Physics Institute Acad. Sci.], 1944; ZhETF [J. Exp. Theor. Phys.], 16, 603, 1946.

2. Zavoyskiy, Ye.K., J. Phys. USSR 9, 245, 1945.

3. Gorter, K., Paramagnitnaya relaksatsiya [Paramagnetic Relaxation], IL [Foreign Literature Press], 1949.

4. Cummerow, R.L., Holliday, D., Moore, G.E., Phys. Rev. 72, 1233, 1947.

5. Whitmer, C.A., Weidner, R.T., Hsiang, J.S., Weiss, P.R., Phys. Rev. 74, 1478, 1948.

6. Bleaney, B., Stevens, K.W.H., Rep. Progr. Phys. 16, 108, 1953.

7. Blume, R.J., Phys. Rev. 109, 1867, 1958; Gordon, J.P., Bowers, K.D., Phys. Rev. Letters 1, 368, 1959.

8. Manenkov, A.A. and Prokhorov, A.M., Radiotekhn. i elektronika [Radio Engineering and Electronics] 1, 469, 1956.

9. Beringer, R., Castle, J.G., Jr., Phys. Rev. 78, 581, 1950.

10. Smaller, B., Jasaytis, E.L., Rev. Sci. Instr. 24, 337, 1953.

11. Buckmaster, H.A., Scovil, H.E.D., Canad. J. Phys. 34, 711, 1956.

12. Smaller, B., Phys. Rev. 83, 812, 1951.

13. Semenov, A.G. and Bubnov, N.N., Pribory i tekhn. eksp. [Instruments and the Technique of Experiment], No. 1, 92, 1959.

14. England, T.S., Schneider, E.E., Nature 166, 437, 1950.

15. Strum, P.D., Proc. Inst. Radio Eng. 41, 875, 1953.

16. Ingram, D.J.E., Spectroscopy at radio and microwave frequencies, London, 1955.

17. Gordy, W., Rev. Mod. Phys. 20, 668, 1948.

18. Pound, R.V., Knight, W.D., Rev. Sci. Inst. 21, 219, 1950.

19. Weidner, R.T., Whitmer, C.A., Rev. Sci. Instr. 23, 75, 1952.

20. Hirshon, J.M., Fraenkel, C.K., Rev. Sci. Instr. 26, 34, 1955.

21. Ruter, C., Lacroix, R., Extermann, C.R., Onde Electr. [The Electric Wave] 35, 338, 1955.

22. Neprimerov, N.N., Izv. AN SSSR, ser. fiz. [Bull. Acad. Sci. USSR, Physics Series] 18, 360, 1954.

23. Gordi, V., Smit, B. and Trambarulo, P., Radiospektroskopiya [Radio Spectroscopy], Gostekhizdat [State Publishing House for Theoretical and Technical Literature], 1955.

24. Strendberg, V., Radiospektroskopiya, IL, 1956.

25. Avvakumov, V.I., Garif'yanov, N.S., Kozyrev, B.M. and Tishkov, P.G., ZhETF 37, 1564, 1959.

26. Bickford, L.R., Jr., Phys. Rev. 78, 449, 1950.

27. Bloembergen, N., Wang, S., Phys. Rev. 93, 72, 1954.

28. Nigmatullin, R.Sh. and Valishev, R.M., Doklad na soveshchanii po paramagnitnomu rezonansu [Report to the Conference on Paramagnetic Resonance], Kazan', 1959.

29. Endryu, E., Yadernyy magnitnyy rezonans [Nuclear Magnetic Resonance], Moscow, IL, 1957.

30. Grivet, P. (editor), La Resonance paramagnetique nucleaire [Nuclear Paramagnetic Resonance], Paris, 1955.

31. Tishkov, P.G., ZhETF 36, 1337, 1959.

32. Feher, G., Kip, A.F., Phys. Rev. 98, 337, 1955.

Manuscript Page No.	[Footnotes]
35	A line width of this order is usually observed in free radicals.
49	Alloys of low heat conductivity (melchior, stainless steel, etc.) are presently used most frequently for this purpose.

[List of Transliterated Symbols]

46	РЧК = RChK = radiochastotnyye katushki = radio-frequency coils
52	с = s = setochnyy = grid
52	к = k = kontur = tank circuit
52	св = sv = [svyazi = coupling]
52	П = P = [not identified]

Chapter 3
THEORY OF SPECTRA OF IONIC CRYSTALS

§3.1. Introduction

The most widely investigated among the various classes of paramagnets are ionic crystals. Paramagnetic properties are possessed by ionic crystals containing transition group elements, for only the atoms of these elements retain unfilled electron shells during the crystal formation process.

To construct a theory for the energy structure of ionic paramagnetic crystals it is necessary first of all to take into account the interactions of the electrons with one another and with the nucleus within each ion, and then take into account the electrostatic, magnetic, and exchange interactions between the different ions, and finally the effect of the external magnetic field. Magnetic and exchange forces produce narrow quasi-continuous energy bands, for these forces are small in substances with not too high a magnetic concentration, and the number of possible orientations of the moments of the magnetic particles of the crystal relative to one another is tremendous. As a result, the magnetic and exchange interactions do not influence as a rule the form of the paramagnetic resonance spectrum* and cause only a broadening of individual lines. We shall therefore dwell on these interactions in Chapter 5, which is devoted to the absorption line shape.

We shall take an approximate account of the electrostatic interaction between free ions by assuming that each ion is in a certain av-

erage electric field produced by all the surrounding particles. We shall call this the crystalline field for short. The action of the crystalline field is always weaker than the Coulomb interaction between the electrons in the atom. We can therefore use the self consistent field method and speak of the configuration of the electrons forming the unfilled shell of the paramagnetic ion. The electron configurations corresponding to various transition groups are $3d^n$ for the iron group (from Ti to Cu), $4d^n$ for the palladium group (from Zr to Ag), $4f^n$ for the rare earth group (from Ce to Yb), $5d^n$ for the platinum group (from Hf to Au), and $6d5f^n$ for the actinides (from U on).

The self consistent field method does not take full account of the electrostatic interaction between electrons. The calculations, which are usually carried out by the perturbation method, therefore call for a knowledge of the relationship between the unaccounted for part of the electrostatic repulsion between electrons, the magnetic couplings between their spin and orbital moments, and the forces of the crystalline field. Three cases are possible. The crystalline field is called weak if it is unable to break the bond between the orbital and spin moments of the entire unfilled electron shell. The field is assumed average if its action is stronger than the spin-orbit coupling of the electrons, but much weaker than the interaction between individual electrons. Finally, the field is called strong if its action is much stronger than the bond between the electrons of the unfilled shell. The first two cases are realized in hydrated salts of rare-earth elements and the iron-group elements, respectively. A strong field is not encountered in pure form, for if the crystal field becomes considerably stronger than the interaction between individual electrons, then the covalent bond between the paramagnetic atom and its immediate vicinity always begins to assume an appreciable role in

place of the ionic bond. The character of splitting of the energy levels of paramagnetic ions by the crystalline field depends to a great degree on the symmetry of this field. This has enabled Bethe [1] to present a qualitative solution of this problem with the aid of group theory. Tables 3.1 and 3.2 indicate how the electron levels are split for the cases of integral and half-integral momentum quantum number J. The third and following columns show how many energy sublevels are produced in a field of corresponding symmetry, and the numbers in the parentheses denote the degree of degeneracy of these sublevels.

We see from Table 3.2 that in the case of a half-integer spin the energy sublevels always remain at least doubly degenerate. This fact is the consequence of Kramers' general theorem [2], which is of fundamental significance in the theory of paramagnetism. The theorem states that the electric forces are unable to eliminate completely the degeneracy of the energy level of a system containing an odd number of electrons. It follows therefore that paramagnetic resonance can always be observed in paramagnetic ions containing an odd number of electrons, for by eliminating the degeneracy of the ground states, the magnetic field can produce splittings that lie in the radio frequency range. If the number of electrons is even, then all levels may turn out to be simple even in the absence of a magnetic field, and the distance between them may be so large that no practically attainable magnetic fields can bring them close enough together to make resonant absorption of radio frequency radiation possible.

The influence of the crystalline field on the static susceptibility of paramagnetic salts was first considered by Van Vleck [3]. Penney and Schlapp made detailed calculations for several rare-earth salts [4] and iron-group elements [5]. Analogous calculations were made then

TABLE 3.1

J	8)Степень вырождения уровня свободного атома	1)Расщепление в поле				
		2)икосаэдрический симметрии*)	3)кубической симметрии	4)тригональной симметрии	5)тетрагональной симметрии	6)ромбической симметрии
0	1	1 (1)	1 (1)	1 (1)	1 (1)	7)Полное расщепление
1	3	1 (3)	1 (3)	2 = 1 (1) + 1 (2)	2 = 1 (1) + 1 (2)	
2	5	1 (5)	2 = 1 (2) + 1 (3)	3 = 1 (1) + 2 (2)	4 = 3 (1) + 1 (2)	
3	7	2 = 1 (3) + 1 (4)	3 = 1 (1) + 2 (3)	5 = 3 (1) + 2 (2)	5 = 3 (1) + 2 (2)	
4	9	2 = 1 (4) + 1 (5)	4 = 1 (1) + 1 (2) + 2(3)	6 = 3 (1) + 3 (2)	7 = 5 (1) + 2 (2)	
5	11	3 = 2 (3) + 1 (5)	4 = 1 (2) + 3 (3)	7 = 3 (1) + 4 (2)	8 = 5 (1) + 3 (2)	
6	13	4 = 1 (1) + 1 (3) + 1 (4) + 1 (5)	6 = 2 (1) + 1 (2) + 3(3)	9 = 5 (1) + 4 (2)	10 = 7 (1) + 3 (2)	
7	15	4 = 2 (3) + 1 (4) + 1 (5)	6 = 1 (1) + 1 (2) + 4(3)	10 = 5 (1) + 5 (2)	11 = 7 (1) + 4 (2)	
8	17	4 = 1 (3) + 1 (4) + 2 (5)	7 = 1 (1) + 2 (2) + 4(3)	11 = 5 (1) + 6 (2)	13 = 9 (1) + 4 (2)	

*See page 93 concerning icosahedral symmetry in ionic crystals.

1) Splitting in a field of; 2) icosahedral symmetry; 3) cubic symmetry; 4) trigonal symmetry; 5) tetragonal symmetry; 6) rhombic symmetry; 7) total splitting; 8) degree of degeneracy of the level of the free atom.

TABLE 3.2

J	1)Степень вырождения уровня свободного атома	2)Расщепление в поле		
		3)икосаэдрической симметрии	4)кубической симметрии	5)Более низкой симметрии
1/2	2	1 = 1 (2)	1 (2)	1 (2)
3/2	4	1 = 1 (4)	1 (4)	2 (2)
5/2	6	1 = 1 (6)	2 = 1 (2) + 1 (4)	3 (2)
7/2	8	2 = 1 (2) + 1 (6)	3 = 2 (2) + 1 (4)	4 (2)
9/2	10	2 = 1 (4) + 1 (6)	3 = 1 (2) + 2 (4)	5 (2)
11/2	12	3 = 1 (2) + 1 (4) + 1 (6)	4 = 2 (2) + 2 (4)	6 (2)
13/2	14	4 = 2 (2) + 1 (4) + 1 (6)	5 = 3 (2) + 2 (4)	7 (2)
15/2	16	3 = 1 (4) + 2 (6)	5 = 2 (2) + 3 (4)	8 (2)

1) Degree of degeneracy of the level of the free atom; 2) splitting in a field of; 3) icosahedral symmetry; 4) cubic symmetry; 5) lower symmetry.

by other authors [6], but only after experimental material on paramagnetic resonance in ionic crystals was accumulated did it become possible to construct a consistent theory of energy spectra of paramagnetic ions.

§3.2. Matrix Elements of the Crystalline Field

To calculate the effect of the crystalline field on the energy levels of paramagnetic ions by the perturbation method it is necessary first to calculate the energy matrix elements H_{kr} of the electrons of

the unfilled shell in the electric field of the crystal. The energy H_{kr} can be represented in the form

$$\mathscr{H}_{\text{кр}} = \sum_i - e V(x_i, y_i, z_i),$$ (3.1)

where V is the potential of the crystalline field and x_1, y_1, z_1 are the coordinates of the i-th electron of the unfilled shell. Assuming that the electron shells of the paramagnetic atoms and of the particles surrounding it do not overlap and that consequently the potential V satisfies the Laplace equation, we can expand the potential in a series of spherical functions:

$$V = \sum_{n, m} A_n^m r^n Y_n^m(\vartheta, \varphi).$$ (3.2)

This expression can be greatly simplified and only a few terms of the series retained. Only the $\underline{d}$ and $\underline{f}$ shells of the paramagnetic atoms can be unfilled in ionic crystals. In calculating the perturbation matrix H_{kr} with the aid of the d-electron wave functions, the spherical functions with n > 4 give matrix elements equal to zero [7]. Precisely in the same way, the terms of the series (3.2) with n > 6 can be left out in the case of $\underline{f}$ electrons. It is also necessary to discard the terms of the series with odd $\underline{n}$, for the matrix elements of odd-order spherical functions vanish by virtue of the invariance of the electron wave functions under the inversion transformation; account is taken here of the fact that all the crystals investigated to date have a symmetry center. The term with n = 0 yields an inessential additive constant, which can be set equal to zero. Finally, the fact that V is real leads to $A_n^m = (A_n^{-m})^*$. Equation (3.2) can be further simplified by taking into account the symmetry of the crystalline field. We notice that the surface spherical function $Y_n^m(\vartheta, \varphi)$ has axial symmetry if m = 0, tetragonal symmetry if m = ± 4, trigonal symmetry if m = ± 3, hexagonal sym-

metry if m = ±6, and finally rhombic symmetry if m = ±2. It follows therefore that if we denote $A_n^0 r^n Y_n^0(\vartheta, \varphi)$ by U_n^0 and $[A_n^m Y_n^m(\vartheta, \varphi) + A_n^{-m} Y_n^{-m}(\vartheta, \varphi)$ by $U_n^{|m|}$, then the potentials of the fields of different symmetries will have the form:

$$V_{\text{тетр}} = U_0^0 + U_2^0 + U_4^0 + U_6^0 + U_6^4 \quad \text{(tetragonal)}, \tag{3.3a}$$

$$V_{\text{триг}} = U_0^0 + U_2^0 + U_4^0 + U_6^0 + U_6^3 + U_6^6 \quad \text{(trigonal)}, \tag{3.3b}$$

$$V_{\text{гекс}} = U_0^0 + U_2^0 + U_4^0 + U_6^6 \quad \text{(hexagonal)}, \tag{3.3c}$$

$$V_{\text{ромб}} = U_0^0 + U_2^0 + U_2^2 + U_4^0 + U_4^2 + U_4^4 + U_6^0 + U_6^2 + U_6^4 \quad \text{(rhombic)}, \tag{3.3d}$$

$$V_{\text{трикл}} = \sum_{m=0}^{2} U_2^m + \sum_{m=0}^{4} U_4^m + \sum_{m=0}^{6} U_6^m \quad \text{(triclinic)}. \tag{3.3e}$$

For a field of cubic symmetry, if the polar axis (the Z axis) coincides with the fourfold symmetry axis, the potential assumes the form

$$V_{\text{куб}} = A_4 r^4 \left\{ Y_4^0(\theta, \varphi) + \sqrt{\frac{5}{14}} [Y_4^4(\theta, \varphi) + Y_4^{-4}(\theta, \varphi)] \right\} + \\ + A_6 r^6 \left\{ Y_6^0(\theta, \varphi) - \sqrt{\frac{7}{2}} [Y_6^4(\theta, \varphi) + Y_6^{-4}(\theta, \varphi)] \right\}. \tag{3.4a}$$

On the other hand, if the polar axis is parallel to the volume diagonal of the cube and is therefore a threefold symmetry axis, we have

$$V_{\text{куб}} = D_4 r^4 \left\{ Y_4^0(\theta, \varphi) + \sqrt{\frac{10}{7}} [Y_4^3(\theta, \varphi) + Y_4^{-3}(\theta, \varphi)] \right\} + \\ + D_6 r^6 \left\{ Y_6^0(\theta, \varphi) + \frac{1}{8} \sqrt{\frac{70}{3}} [Y_6^3(\theta, \varphi) + Y_6^{-3}(\theta, \varphi)] + \\ + \frac{1}{8} \sqrt{\frac{77}{3}} [Y_6^6(\theta, \varphi) + Y_6^{-6}(\theta, \varphi)] \right\}. \tag{3.4b}$$

The tetragonal field is the sum of an actual field and a cubic field, given by an expression such as (3.4a); in precisely the same manner, a trigonal field can be decomposed into a sum of an actual field and a cubic field given by expression (3.4b).

To continue the calculations it is more convenient to change to Cartesian coordinates. If we denote by V_n^m the following homogeneous polynomials of degree n in the coordinates x, y, and z:

$$V_2^0 = 3z^2 - r^2, \quad V_2^1 = xz, \quad V_2^2 = x^2 - y^2,$$
$$V_4^0 = 35z^4 - 30r^2z^2 + 3r^4, \quad V_4^1 = (7z^2 - 3r^2)xz,$$
$$V_4^2 = (7z^2 - r^2)(x^2 - y^2), \quad V_4^3 = (x^2 - 3y^2)xz,$$
$$V_4^4 = x^4 - 6x^2y^2 + y^4, \quad V_6^0 = 231z^6 - 315r^2z^4 + 105r^4z^2 - 5r^6,$$
$$V_6^1 = 33xz^5 - 30xz^3r^2 + 5r^4xz,$$
$$V_6^2 = 16z^4(x^2 - y^2) - 16(x^4 - y^4)z^2 + x^6 + x^2y^4 - y^2x^4 - y^6,$$
$$V_6^3 = (11z^3 - 3r^2)(x^2 - 3y^2)xz, \quad V_6^4 = (11z^2 - r^2)(x^4 - 6x^2y^2 + y^4),$$
$$V_6^5 = x^5z - 10x^3y^2z + 5xy^4z, \quad V_6^6 = x^6 - 15x^4y^2 + 15x^2y^4 - y^6,$$

(3.5)

then we have $U_n^m = B_n^m V_n^m$, where

$$B_2^0 = \frac{1}{4}\sqrt{\frac{5}{\pi}} A_2^0, \quad B_2^1 = \sqrt{\frac{15}{2\pi}}|A_2^1|, \quad B_2^2 = \frac{1}{2}\sqrt{\frac{15}{2\pi}}|A_2^2|,$$
$$B_4^0 = \frac{3}{16\sqrt{\pi}} A_4^0, \quad B_4^1 = \frac{3}{4}\sqrt{\frac{5}{\pi}}|A_4^1|, \quad B_4^2 = \frac{3}{4}\sqrt{\frac{5}{2\pi}}|A_4^2|,$$
$$B_4^3 = \frac{3}{4}\sqrt{\frac{35}{\pi}}|A_4^3|, \quad B_4^4 = \frac{3}{8}\sqrt{\frac{35}{2\pi}}|A_4^4|, \quad B_6^0 = \frac{1}{32}\sqrt{\frac{13}{\pi}}A_6^0,$$
$$B_6^1 = \frac{1}{8}\sqrt{\frac{13\cdot21}{2\pi}}|A_6^1|, \quad B_6^2 = \frac{1}{32}\sqrt{\frac{13\cdot105}{\pi}}|A_6^2|,$$
$$B_6^3 = \frac{1}{16}\sqrt{\frac{13\cdot105}{\pi}}|A_6^3|, \quad B_6^4 = \frac{3}{32}\sqrt{\frac{13\cdot14}{\pi}}|A_6^4|,$$
$$B_6^5 = \frac{3}{16}\sqrt{\frac{13\cdot77}{\pi}}|A_6^5|, \quad B_6^6 = \frac{1}{32}\sqrt{\frac{13\cdot21\cdot11}{\pi}}|A_6^6|.$$

(3.6)

The potential of the cubic field (3.4a) has in Cartesian coordinates the form

$$V_{xyz} = C_4\left(x^4 + y^4 + z^4 - \frac{3}{5}r^4\right) +$$
$$+ C_6[2(x^6 + y^6 + z^6) - 15(x^4y^2 + y^4x^2 +$$
$$+ z^4x^2 + x^4z^2 + z^4y^2 + y^4z^2) + 180x^2y^2z^2],$$

(3.7)

where
$$C_4 = \frac{15}{4\sqrt{\pi}} A_4^0 = 20B_4^0, \quad C_6 = \frac{1}{4}\sqrt{\frac{13}{\pi}} A_6^0 = 8B_6^0.$$

Now that we have derived analytical expressions for the potential of the crystalline field, let us discuss several general premises concerning the calculation of perturbation matrix elements. Let ψ_M ($M = J, J - 1, J - 2, \ldots, -J$) be the wave functions of the ground state of the free atom under the assumption that the only electron interactions considered are those much larger than H_{kr}. The quantum numbers J and M denote the angular momentum and its projection on the Z axis, respectively, which are conserved in this case. It is easy to show that the matrix elements

$$\langle JM|\sum V_n^m|JM'\rangle \equiv \int \psi_M^* \sum V_n^m \psi_{M'} d\tau$$

- 62 -

vanish if $M \neq m + M'$. In accordance with (3.1), the symbol Σ denotes summation over all the electrons of the unfilled shell.

To find the nonvanishing matrix elements that relate states having the same J, it is customary to use the method of equivalent operators [8], [9]. The totality of the functions Y_n^m ($m = 0, \pm 1, \pm 2, \ldots, \pm n$) forms the basis for the irreducible representation of a rotation group of dimensionality $2n + 1$. Each electron coordinate function ΣV_n^m can be set in correspondence with an equivalent operator, that is, with an analogous function of the angular momentum projection operators $\hat{J}_x$, $\hat{J}_y$, $\hat{J}_z$, which have the same transformation properties. Thus, corresponding to the functions $\Sigma(x^2 - y^2)$ and $\Sigma(3z^2 - r^2)$ are the operators $\hat{J}_x^2 - \hat{J}_y^2$ and $3\hat{J}_z^2 - J(J + 1)$. We note that the determination of the equivalent operators is not complicated by the fact that unlike $\underline{x}$, $\underline{y}$, and $\underline{z}$, the operators J_x, J_y, and J_z do not commute. Therefore to determine the operator equivalent to the expression $x^k y^{\underline{l}} z^m$ it becomes necessary to take the arithmetic mean of $(k + \underline{l} + m)!/k!\underline{l}!m!$ possible operator permutations $\hat{J}_x \ldots \hat{J}_x \hat{J}_y \ldots \hat{J}_y \hat{J}_z$. For example, the function Σxy corresponds to the operator $1/2(J_x J_y + J_y J_x)$.

The matrix elements of the functions ΣV_n^m and of the corresponding equivalent operators coincide, apart from a certain common factor, which is the same for all functions with the same $\underline{n}$.

Thus, the cumbersome direct calculations of the matrix elements of the crystalline field potential can be replaced by simple calculations of matrix elements of polynomials of the second, fourth, and sixth degree in $\hat{J}_x$, $\hat{J}_y$, and $\hat{J}_z$. Direct calculations are nevertheless necessary to determine the common factors α, β, and γ, but for this purpose it is sufficient to calculate only one matrix element ΣV_n^m for each electron configuration and for only one potential function with specified $\underline{n}$.

TABLE 3.3

$$\overline{V_2^0} = \alpha \overline{r^2}\,[3J_z^2 - J(J+1)];$$

$$V_2^1 = \frac{\alpha \overline{r^2}}{2}\,[J_x J_z + J_z J_x] = \frac{\alpha \overline{r^2}}{4}\,\{J_z(J_+ + J_-) + (J_+ + J_-)J_z\};$$

$$V_2^2 = \frac{\alpha \overline{r^2}}{2}\,[J_+^2 + J_-^2];$$

$$V_4^0 = \beta \overline{r^4}\,[35J_z^4 - 30J(J+1)J_z^2 + 25J_z^2 - 6J(J+1) + 3J^2(J+1)^2];$$

$$V_4^1 = \frac{\beta}{4}\,\overline{r^4}\,\{[7J_z^3 - 3J(J+1)J_z - J_z](J_+ + J_-) + (J_+ + J_-)\,[7J_z^3 - 3J(J+1)J_z - J_z]\};$$

$$V_4^2 = \frac{\beta}{4}\,\overline{r^4}\,\{[7J_z^2 - J(J+1) - 5](J_+^2 + J_-^2) + (J_+^2 + J_-^2)\,[7J_z^2 - J(J+1) - 5]\};$$

$$V_4^3 = \frac{\beta}{4}\,\overline{r^4}\,\{J_z(J_+^3 + J_-^3) + (J_+^3 + J_-^3)J_z\};$$

$$V_4^4 = \frac{\beta}{2}\,\overline{r^4}\,(J_+^4 + J_-^4);$$

$$V_6^0 = \gamma \overline{r^6}\,\{231J_z^6 - 315J(J+1)J_z^4 + 735J_z^4 + 105J^2(J+1)^2 J_z^2 - 525J(J+1)J_z^2 + 294J_z^2 - 5J^3(J+1)^3 + 40J^2(J+1)^2 - 60J(J+1)\};$$

$$V_6^1 = \frac{\gamma}{4}\,\overline{r^6}\,\{[33J_z^5 - 30J(J+1)J_z^3 + 15J_z^3 + 5J^2(J+1)^2 J_z - 10J(J+1)J_z + 12J_z](J_+ + J_-) + (J_+ + J_-)\,[33J_z^5 - 30J(J+1)J_z^3 + 15J_z^3 + 5J^2(J+1)^2 J_z - 10J(J+1)J_z + 12J_z]\};$$

$$V_6^2 = \frac{\gamma}{4}\,\overline{r^6}\,\{[33J_z^4 - 18J(J+1)J_z^2 - 123J_z^2 + J^2(J+1)^2 + 10J(J+1) + 102] \times (J_+^2 + J_-^2) + (J_+^2 + J_-^2)\,[33J_z^4 - 18J(J+1)J_z^2 - 123J_z^2 + J^2(J+1)^2 + 10J(J+1) + 102]\};$$

$$V_6^3 = \frac{\gamma}{4}\,\overline{r^6}\,\{[11J_z^3 - 3J(J+1)J_z - 59J_z](J_+^3 + J_-^3) + (J_+^3 + J_-^3) \times [11J_z^3 - 3J(J+1)J_z - 59J_z]\};$$

$$V_6^4 = \frac{\gamma}{4}\,\overline{r^6}\,\{[11J_z^2 - J(J+1) - 38](J_+^4 + J_-^4) + (J_+^4 + J_-^4)[11J_z^2 - J(J+1) - 38]\};$$

$$V_6^5 = \frac{\gamma}{4}\,\overline{r^6}\,\{J_z(J_+^5 + J_-^5) + (J_+^5 + J_-^5)J_z\};$$

$$V_6^6 = \frac{\gamma}{2}\,\overline{r^6}\,\{J_+^6 + J_-^6\}.$$

где $J_+ = J_x + iJ_y$, $J_- = J_x - iJ_y$.

1) Where.

Table 3.3 lists the linearly independent equivalent operators of the polynomials V_n^m of second, fourth, and sixth degree. The sign of the sum in the expressions for ΣV_n^m has been left out everywhere, and $\underline{r}$ stands for the distance between the electron and the nucleus.

The calculation of the matrix elements relating states with different J calls for a separate analysis, for in this case the method of

equivalent operators becomes much more complicated. The results of some calculations are given in §3.6.

In calculating the matrix elements of the functions V_n^m it is useful to bear in mind that

$$\langle J+k, J_z-m |V_n^m| J, J_z\rangle = (-1)^{m+k} \langle J+k, m-J_z |V_n^m| J, -J_z\rangle. \qquad (3.8)$$

§3.3. Iron Group Element Compounds

It is well known from investigations of the static magnetic susceptibility [10] that the effect of the crystalline field is usually much stronger in these substances than the spin-orbit coupling, but is weaker than the forces that determine the principal term of the ion. Consequently the Hamiltonian for the paramagnetic ion of the iron group is best written in the following form:

$$\mathcal{H} = \mathcal{H}^0 + \mathcal{H}_{xp} + \mathcal{H}_{LS} + \mathcal{H}_{ss} + \mathcal{H}_z \qquad (3.9)$$

Here H^0 is the principal part of the Hamiltonian, which includes all the free-atom interactions that are independent of the spin variables. The remaining terms of the Hamiltonian can be regarded as a perturbation, namely

$$\mathcal{H}_{LS} = \lambda \hat{L}\hat{S}$$

is the spin-orbit interaction operator,

$$\mathcal{H}_{ss} = -\rho \left[(\hat{L}\hat{S})^2 + \tfrac{1}{2}(\hat{L}\hat{S}) - \tfrac{1}{3} L(L+1)S(S+1) \right]$$

is the spin-spin interaction operator [11], and

$$\mathcal{H}_z = \beta(\hat{L}+2\hat{S})H_0$$

is the energy of the electrons in the external magnetic field (the Zeeman energy). The splittings caused by the perturbation forces are of the order of:

$$\mathcal{H}_{xp} \approx 10^4 \, cm^{-1}, \quad \mathcal{H}_{LS} \approx 10^2 \, cm^{-1}, \quad \mathcal{H}_{ss} \approx 1 \, cm^{-1}, \quad \mathcal{H}_z \approx 1 \, cm^{-1}.$$

If only the principal Hamiltonian H^0 is considered, then the total orbital momentum L and the spin momentum S will obviously be conserved

quantities. We shall assume that the problem of the possible eigen-states of $\overset{\bullet}{\hat{H}}{}^0$ has been solved by the self-consistent field method. In calculations by the perturbation method we shall start from the ground state $\overset{\bullet}{\hat{H}}{}^0$, characterized by a definite electron configuration and by definite values of L and S. The higher-order approximations, which take into account the influence of the excited terms of $\overset{\bullet}{\hat{H}}{}^0$ will in most cases be unnecessary. Table 3.4 lists the configurations and terms of the ground states of different ions of the iron-group elements.

The calculation of the effect of the perturbations can be broken up into several stages. A comparison of the magnitudes of the perturbing forces shows that it is possible to calculate first the splitting of the 2L + 1-fold orbital level under the influence of the crystalline field $H_{\overset{\bullet}{kr}}$, setting the remaining interaction aside for the time being.

Since we are dealing with $\underline{d}$ electrons, expressions (3.3) and (3.4) for the potentials of the crystalline field can be simplified, leaving out the terms U_n^m with n = 6. The matrix elements of the potential functions V_n^m can be calculated with the aid of the equivalent operators of Table 3.3. It remains to determine the coefficients α and β. For this purpose it is sufficient to calculate one matrix element of some potential function V_n^m with n = 2 and one with n = 4. We choose the functions V_2^0 and V_4^0, because they have only diagonal matrix elements. For what follows it is necessary to express any one of the wave functions of the principal term of the paramagnetic atom in terms of the one-electron $\underline{d}$ functions. This is simplest to do by taking a state with maximum projections of the spin and orbital momenta $\{ \overset{+}{2} \ \overset{+}{1} \ \overset{+}{0} \ .. \}$, which obviously will be characterized by a symmetrical spin function and an antisymmetrical linear combination of the one-electron $\underline{d}$ functions:

- 66 -

TABLE 3.4

1 Ион	2 Конфигу- рация	3 Основной терм	4 λ, см⁻¹	α	β
Ti³⁺	d^1	^2D	154	$-\frac{2}{21}$	$\frac{2}{63}$
V⁴⁺	d^2	^3F	104	$-\frac{2}{105}$	$-\frac{2}{315}$
V³⁺	d^3	^4F	55	$\frac{2}{105}$	$\frac{2}{315}$
Cr³⁺	d^3	^4F	87	$\frac{2}{105}$	$\frac{2}{315}$
Cr²⁺	d^4	^5D	57	$\frac{2}{21}$	$-\frac{2}{63}$
Mn³⁺	d^4	^5D	85	$\frac{2}{21}$	$-\frac{2}{63}$
Mn²⁺	d^5	^6S	—	—	—
Fe³⁺	d^5	^6S	—	—	—
Fe²⁺	d^6	^5D	—100	$-\frac{2}{21}$	$\frac{2}{63}$
Co²⁺	d^7	^4F	—180	$-\frac{2}{105}$	$-\frac{2}{315}$
Ni²⁺	d^8	^3F	—335	$\frac{2}{105}$	$\frac{2}{315}$
Cu²⁺	d^9	^2D	—852	$\frac{2}{21}$	$-\frac{2}{63}$

1) Ion; 2) configuration; 3) principal term; 4) λ, cm⁻¹.

$f_m = R(r)Y_2^m(\vartheta,\varphi)$ with m = 2, 1, ... Thus, we choose from among the 2L + 1 different coordinate functions ψ_M, corresponding to the ground state $\overset{\circ}{H}{}^0$, the function with the maximum magnetic quantum number M. It is easy to verify that if there are less than five d electrons, then

$$\int \psi_M^* \sum V_n^s \psi_M \, d\tau = \int f_2^* V_n^s f_2 \, d\tau + \int f_1^* V_n^s f_1 \, d\tau + \dots \qquad (3.10)$$

The number of the integrals in the right half of the equation is equal to the number of d electrons. If their number exceeds five, the calculation is made for the number of electrons lacking to fill the d shell, and the result is taken with the opposite sign. The values of α and β calculated in this manner are listed in Table 3.4.

In most of the salts investigated the crystalline field can be resolved into two components: a strong field of cubic symmetry and a

- 67 -
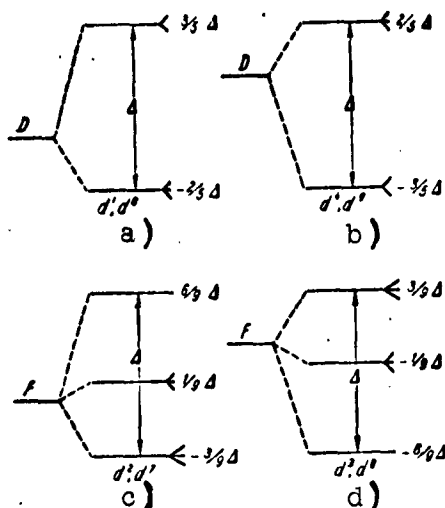
Fig. 3.1. Splitting of the
principal orbital levels of
the ions of the iron group in
a cubic field.

weak field of lower symmetry, for example trigonal or tetragonal. Thus, the energy $\hat{H}_{.kr}$ is represented by the sum $\hat{H}_{.kr} = \hat{K} + \hat{T}$. The cubic field $\hat{K}$ is produced frequently by the six water molecules located at the vertices of the octahedron whose center is occupied by the paramagnetic ion. This field changes little on going from one element in the iron group to another or even from one salt to another. The apparent reason for this is that the dimensions of the octahedron are determined by the diameter of the paramagnetic atom.

The field T has a dual nature: first, it is produced by all the ions of the crystal and has the symmetry of the latter, and second it is due to the deformation of the octahedron resulting from the Jahn-Teller effect. According to the well known theorem of Jahn and Teller [12], the stable state of a nonlinear system of atoms is the one having the least possible degree of degeneracy.

It is necessary to solve first the question of the effect of the cubic field. We see from Table 3.4 that only S, D, and F terms are encountered for the free ions of the iron-group elements. The ions in

- 68 -

the S state will be considered separately. On the other hand, the qualitative picture of the splitting of the D and F terms can be obtained directly from group-theoretical considerations (Table 3.1). The F term splits in a cubic-symmetry field into one singlet and two triplets (Fig. 3.1c and d), while the D term splits into a doublet and a triplet (Fig. 3.1a and b). Calculation by the perturbation method yields the following values of the energies and the corresponding ψ functions [9], calculated for the following two cases:

1) Quantization axis coincides with the trigonal axis of the cube

2) Quantization axis coincides with the tetragonal axis of the cube

$$L = 2$$

$$\frac{3}{5}\Delta \begin{cases} \sqrt{\frac{1}{3}}\,\psi_{-2} - \sqrt{\frac{2}{3}}\,\psi_1 \\ \sqrt{\frac{1}{3}}\,\psi_2 + \sqrt{\frac{2}{3}}\,\psi_{-1} \end{cases} \qquad \begin{cases} \psi_0 \\ \frac{1}{\sqrt{2}}(\psi_2 + \psi_{-2}) \end{cases}$$

$$-\frac{2}{5}\Delta \begin{cases} \psi_0 \\ \sqrt{\frac{2}{3}}\,\psi_{-2} + \sqrt{\frac{1}{3}}\,\psi_1 \\ \sqrt{\frac{2}{3}}\,\psi_2 - \sqrt{\frac{1}{3}}\,\psi_{-1} \end{cases} \qquad \begin{cases} \psi_1 \\ \psi_{-1} \\ \frac{1}{\sqrt{2}}(\psi_2 - \psi_{-2}) \end{cases}$$

$$\Delta = 6\beta\overline{r^4}C_4$$

$$L = 3$$

$$\frac{1}{3}\Delta \begin{cases} \frac{2}{3}\psi_0 + \frac{1}{3}\sqrt{\frac{5}{2}}(\psi_3 - \psi_{-3}) \\ \sqrt{\frac{5}{6}}\,\psi_2 + \sqrt{\frac{1}{6}}\,\psi_{-1} \\ \sqrt{\frac{5}{6}}\,\psi_{-2} - \sqrt{\frac{1}{6}}\,\psi_1 \end{cases} \qquad \begin{cases} \sqrt{\frac{3}{8}}\,\psi_{-1} + \sqrt{\frac{5}{8}}\,\psi_3 \\ \sqrt{\frac{3}{8}}\,\psi_1 + \sqrt{\frac{5}{8}}\,\psi_{-3} \\ \psi_0 \end{cases} \qquad (3.11)$$

$$-\frac{1}{9}\Delta \begin{cases} \frac{1}{\sqrt{2}}(\psi_3 + \psi_{-3}) \\ \sqrt{\frac{1}{6}}\,\psi_2 - \sqrt{\frac{5}{6}}\,\psi_{-1} \\ \sqrt{\frac{1}{6}}\,\psi_{-2} + \sqrt{\frac{5}{6}}\,\psi_1 \end{cases} \qquad \begin{cases} \sqrt{\frac{5}{8}}\,\psi_{-1} - \sqrt{\frac{3}{8}}\,\psi_3 \\ \sqrt{\frac{5}{8}}\,\psi_1 - \sqrt{\frac{3}{8}}\,\psi_{-3} \\ \frac{1}{\sqrt{2}}(\psi_2 + \psi_{-2}) \end{cases}$$

$$-\frac{2}{3}\Delta \begin{cases} \frac{\sqrt{2}}{3}(\psi_3 - \psi_{-3}) - \frac{\sqrt{5}}{3}\psi_0 \end{cases} \qquad \frac{1}{\sqrt{2}}(\psi_2 - \psi_{-2})$$

$$\Delta = 54\beta\overline{r^4}C_4$$

The modulus Δ denotes total splitting in the cubic field.

Gorter [15] considered the ordering of the energy levels produced under the influence of the field of the water-molecule octahedron, in other words, the question of the sign of C_4. It turned out that $C_4 > 0$.

It follows therefore that if the ion contains only one $\underline{d}$ electron, then the lower orbital level will be a triplet and the upper a doublet. The electron configuration d^6 differs from d^1 by an addition of five electrons. Since the term corresponding to the configuration d^5 is ^6S, which is affected by the action of the cubic field only if the higher approximations are taken into account, the same pattern of splitting of the orbital level will occur for both cases, d^1 and d^6 (Fig. 3.1a). The configuration d^9 can be regarded as a filled shell with one hole or with one positive electron. A similar correspondence will exist between the configurations d^6 and d^4. Consequently the level sequence in the case of d^9 and d^4 will be reversed (Fig. 3.1b).

For the configurations forming the F terms, it is easy to conclude that in the case of d^3 and d^8 the lower orbital level will be a singlet (Fig. 3.1d); on the other hand, the configurations d^7 and d^2 correspond to an inverse sequence of levels, and consequently the lower level is a triplet.

Gorter has also shown that in tetrahedral complexes $C_4 < 0$ for the cubic component of the field. Consequently, the sequence of the sublevels will be the inverse of that indicated for ions with octahedral surroundings.

We now proceed to consider the remaining perturbations, which can be written, in accord with (3.9), in the form

$$\mathscr{H}' = T + \lambda)\hat{L}\hat{S}) - \rho\left[(\hat{L}\hat{S})^2 + \tfrac{1}{2}(\hat{L}\hat{S}) - \tfrac{1}{3}L(L+1)S(S+1)\right] + + \beta(\hat{L} + 2\hat{S})H, \qquad (3.12)$$

The experiments are usually made at such temperatures that one can regard as populated those energy levels whose distances from the ground level do not exceed a few hundred cm^{-1}. We can therefore be interested only in the lowest orbital level occurring in a cubic field. It is very important to know whether this level is simple or degenerate.

Let us assume that the lower level is simple. If we take into consideration the electron spin, then (2S + 1)-fold degeneracy appears. The field T, which does not act on the electron spin, can produce only an inessential level shift. In a singlet orbital state, the average momentum L is zero, and consequently the spin-orbit interaction H_{LS} also vanishes in the first approximation. Consequently, it is necessary to take the second approximation into consideration, and this yields for the orbital level splitting values of approximately $\lambda^2/\Delta \approx$ ≈ 1 cm^{-1}, that is, of the same order of magnitude as the Zeeman energy and the spin-spin interaction.

A method for calculating the splittings of the ground state of a magnetic ion was developed in [16, 17] and has found extensive use in experimental investigations of paramagnetic resonance; it is known as the spin-Hamiltonian method. It consists of the following. We go through the usual perturbation theory procedure in two stages. We first calculate the matrix elements $\hat{H}'$ with the aid of the coordinate wave functions, this being possible by virtue of the fact that the unperturbed Hamiltonian is independent of the spin variables. As a result the perturbation energy turns out to be a function of the spin operator $\vec{\hat{S}}$; we shall call this function the spin Hamiltonian.

It is easy to show that the spin Hamiltonian has the form

$$\mathscr{H}_{cn} = D_{ij}\hat{S}_i\hat{S}_j + \beta g_{ij}H_{\phi i}\hat{S}_{i\flat} \tag{3.13}$$

where the tensors D_{ij} and g_{ij} are determined from the formulas

$$\left. \begin{array}{l} D_{ij} = -\lambda^2\Lambda_{ij} - \rho l_{ij}; \quad g_{ij} = 2(\delta_{ij} - \Lambda_{ij}); \\ \Lambda_{ij} = \sum_{n \neq 0} \dfrac{\langle 0|L_i|n\rangle \langle n|L_j|0\rangle}{E_n - E_0}; \\ l_{ij} = \dfrac{1}{2} \langle 0|L_iL_j + L_jL_i|0\rangle - \dfrac{1}{3}L(L+1)\delta_{ij}. \end{array} \right\} \tag{3.14}$$

Here i, j = x, y, z, and E_0 and E_n denote the energies of the ground and excited orbital levels, respectively.

If $\hat{H}_{kr}$ has tetragonal or trigonal symmetry, then the tensors D_{ij} and g_{ij} are characterized by two principal values, corresponding to two directions: parallel and perpendicular to the symmetry axis. Taking the symmetry axis to be the Z axis, we have

$$\mathcal{H}_{cn} = D\left[\hat{S}_z^2 - \tfrac{1}{3}S(S+1)\right] + \beta g_{\|}H_{0z}\hat{S}_z +$$
$$+ \beta g_{\perp}(H_{0x}\hat{S}_x + H_{0y}\hat{S}_y). \qquad (3.15)$$

Deviations from tetragonal symmetry can be taken into account by adding the term $E(\hat{S}_x^2 - \hat{S}_y^2)$ and replacing $g_{\perp}$ by the coefficients g_x and g_y. The part of the spin Hamiltonian proportional to D (and to E) determines the splitting of the orbital level in the absence of an external magnetic field. The terms proportional to H_{0x}, H_{0y}, and H_{0z} indicate that the magnetic moment of the atom in the crystal is anisotropic; deviations of the g factor from the value g = 2 denote that a small fraction of the momentum connected with the orbital motion is added to the spin momentum of the electrons.

The spin-Hamiltonian method makes it possible to describe the spectrum of paramagnetic resonance by means of a small number of constants: D, E, $g_{\|}$, $g_{\perp}$, ... The determination of these constants from the form of the spectrum constitutes the main task of the experiments in paramagnetic resonance. The theoretical problem is to determine these constants on the basis of a definite model of the crystal.

The theory developed here applies primarily to ions whose lower orbital level in a cubic field is a singlet. These include the ions Cr^{3+}, V^{2+}, and Ni^{2+}. The ions Cr^{2+}, Mn^{3+}, and Cu^{2+} should also be included in this group, if the field T has a tetragonal symmetry. In the case of these ions L = 2 and the lower level resulting from the action of the cubic field is an orbital doublet, on which, in accord with (3.11), the spin-orbit coupling H_{LS} has no influence whatever, while a tetragonal field does split it. Thus, the lower orbital level will

again be simple, and its spin degeneracy will as before be $(2S + 1)$-fold.

Let us consider a more general case, when the degeneracy of the lower orbital level in a cubic field makes the matrix elements of the spin-orbit coupling $H_{.LS}$ different from zero even in the first approximation. Now the perturbations caused by the spin-orbit coupling $H_{.LS}$ and by the field T are of the same order of magnitude and should be considered simultaneously. Because of the Jahn-Teller effect, the paramagnetic ion should have minimum degeneracy following the action of these forces. If we apply in addition the Kramers theorem, then we arrive at the following important conclusions: $H_{.LS}$ and the lower-symmetry field T cause complete splitting of the energy levels of paramagnetic ions with an even number of electrons. Now not only the orbital but also the spin levels will be simple. As a rule, the intervals between these levels exceed 1 cm^{-1}, and consequently paramagnetic resonance can be observed only with the aid of radio frequency fields in the millimeter band.

If the paramagnetic ion has an odd number of electrons, then the Kramers double degeneracy is retained. In this case the splitting of the energy level in an external magnetic field can be calculated by introducing an effective spin with value 1/2. The spin Hamiltonian will have the following simple form:

$$\mathscr{H}_{cu} = \beta \{ g_x H_{ox} S'_x + g_y H_{oy} S'_y + g_z H_{oz} S'_z \},' \qquad (3.16)$$

where S'_i are the Pauli matrices. We shall not stop to discuss the connection between the coefficients g_x, g_y, and g_z with λ and with the constants of the crystalline field.

Many investigations have been devoted to a detailed theoretical analysis of the paramagnetic resonance spectra of salts of cobalt [18, 19], nickel [20-22], and copper [23-25]. In particular, many theoretical

investigations have been devoted to chrome alums [26-34], which are extensively used in adiabatic demagnetization.

In order to determine the form of the paramagnetic resonance spectrum, it is necessary to know not only the system of the lower energy levels of the paramagnetic ions, but also the probabilities of the magnetic dipole transitions between these levels. The probability of transition between any two levels M and M' is proportional to the square of the nondiagonal matrix element of the projection of the magnetic moment of the electrons on the direction of the alternating magnetic field $|\langle M \, \mu_{H_1} \, M'\rangle|^2$. These matrix elements are particularly easy to calculate if the spin Hamiltonian has been established. If the position of the alternating magnetic field intensity vector is defined in terms of direction cosines α_1, α_2, and α_3, then we can write for the operator of the component of the magnetic moment:

$$\dot{\mu}_{H_1} = \alpha_1 g_x \beta \hat{S}_x + \alpha_2 g_y \beta \hat{S}_y + \alpha_3 g_z \beta \hat{S}_z. \qquad (3.17)$$

It remains to calculate the matrix elements $\hat{S}_x$, $\hat{S}_y$, and $\hat{S}_z$ with the aid of the spin wave eigenfunctions of the levels M and M'.

§3.4. Paramagnetic Resonance Spectrum of Nickel Ion in an Axial Crystalline Field

We shall examine the general methods used to calculate the paramagnetic spectrum resonance using by way of an example the Ni^{2+} ion in a tetrahedral or trigonal field of a crystal. These calculations pertain, in particular, to the well investigated nickel fluorosilicates, in which the crystalline field has a tetrahedral symmetry. The lower orbital level of Ni^{2+} is a singlet (Fig. 3.1d), and the spectrum can therefore be calculated with the aid of the spin Hamiltonian (3.15), provided that the tetragonal axis is directed along the Z axis.

The nonvanishing matrix elements of the vector $\vec{S}$ can be calculated from the well known formulas (7):

$$\langle M|S_x - iS_y|M+1\rangle = \sqrt{S(S+1) - M(M+1)}, \left.\begin{array}{c}\\\\\end{array}\right\} \qquad (3.18)$$
$$\langle M|S_z|M\rangle = M.$$

In our case $S = 1$, and the nonvanishing elements of $\vec{S}$ assume the following values

$$\left.\begin{array}{l}\langle -1|S_x|0\rangle = \langle 0|S_x|1\rangle = \dfrac{1}{\sqrt{2}}; \\[2mm] \langle -1|S_y|0\rangle = \langle 0|S_y|1\rangle = \dfrac{i}{\sqrt{2}}; \\[2mm] \langle -1|S_z|-1\rangle = -1; \ \langle 1|S_z|1\rangle = 1.\end{array}\right\} \qquad (3.19)$$

We assume first that the static magnetic field H_0 is parallel to the tetragonal axis of the crystal. Then the possible values of the spin-level energies E_i and the corresponding spin wave functions η_i are determined from the equation

$$\mathcal{H}_{cn}\eta_i \equiv (D\hat{S}_z^2 + g_\parallel \beta H_0 \hat{S}_z)\,\eta_i = E_i\eta_i. \qquad (3.20)$$

It is convenient to use the value of D as the energy unit. We therefore introduce the notation

$$\epsilon_i = \frac{E_i}{D}, \quad x_\parallel = \frac{g_\parallel \beta H_0}{D}, \quad x_\perp = \frac{g_\perp \beta H_0}{D}. \qquad (3.21)$$

We denote by η_M the eigenfunction $\hat{S}_z$, corresponding to the eigenvalue M. Since we are using a representation in which the matrix S_z is diagonal, the matrix (3.20) is obviously also diagonal and consequently the eigenvalues of $\hat{H}_{sp}$ and the corresponding eigenfunctions are

$$\epsilon_a = 0, \ \eta_a = \eta_0, \ \epsilon_b = 1 - x_\parallel, \ \eta_b = \eta_{-1}, \ \epsilon_c = x_\parallel + 1, \ \eta_c = \eta_1. \qquad (3.22)$$

With the aid of (3.22), (3.19), and (3.17) we can readily ascertain that the magnetic dipole transitions between the spin levels are possible only under the influence of the alternating magnetic field component perpendicular to the Z axis. According to (3.19) two absorption lines of equal intensity ($\sim\frac{1}{4}g_\perp^2\beta^2$) should occur, corresponding to the transitions $1 \rightarrow 0$ and $0 \rightarrow 1$.

Let us assume now that the magnetic field H_0 is perpendicular to the crystal axis. If we assume the field H_0 to be parallel to the X axis, then the spin Hamiltonian assumes the form

- 75 -

$$\mathscr{H}_{cn} = D\hat{S}_z^2 + g_\perp \beta H_0 \hat{S}_x \qquad (3.23)$$

With the aid of (3.18) we obtain the following secular equation for the determination of the spin energy levels:

$$\begin{vmatrix} 1-\epsilon & \dfrac{x_\perp}{\sqrt{2}} & 0 \\[2mm] \dfrac{x_\perp}{\sqrt{2}} & -\epsilon & \dfrac{x_\perp}{\sqrt{2}} \\[2mm] 0 & \dfrac{x_\perp}{\sqrt{2}} & 1-\epsilon \end{vmatrix} = 0. \qquad (3.24)$$

The solution of this equation yields the following eigenvalues and eigenfunctions:

$$\left. \begin{aligned} \epsilon_a &= \tfrac{1}{2}(1-\xi), & \eta_a &= \frac{x_\perp}{\sqrt{\xi^2+\xi}}\left(\eta_{-1} - \frac{\xi+1}{\sqrt{2}\,x_\perp}\eta_0 + \eta_{+1}\right), \\[1mm] \epsilon_b &= 1, & \eta_b &= \frac{1}{\sqrt{2}}(\eta_{-1} - \eta_1), \\[1mm] \epsilon_c &= \tfrac{1}{2}(1+\xi), & \eta_c &= \frac{x_\perp}{\sqrt{\xi^2-\xi}}\left(\eta_{-1} - \frac{\xi-1}{\sqrt{2}\,x_\perp}\eta_0 + \eta_1\right), \\[1mm] & & \xi &= \sqrt{1+4x_\perp^2}. \end{aligned} \right\} \qquad (3.25)$$

The matrix elements of the components of the vector $\vec{S}$, calculated with the aid of the spin functions (3.25) are

$$\left. \begin{aligned} \langle a|S_x|b\rangle &= \langle b|S_x|c\rangle = 0, & \langle a|S_x|c\rangle &= -\frac{1}{\xi}, \\[1mm] \langle a|S_y|b\rangle &= -i\sqrt{\frac{\xi+1}{2\xi}}, & \langle b|S_y|c\rangle &= i\sqrt{\frac{\xi-1}{2\xi}}, \\[1mm] & \langle a|S_y|c\rangle = 0, & \\[1mm] \langle a|S_z|b\rangle &= -\frac{\sqrt{2}\,x_\perp}{\sqrt{\xi^2+\xi}}, & \langle b|S_z|c\rangle &= -\frac{\sqrt{2}\,x_\perp}{\sqrt{\xi^2-\xi}}, \\[1mm] & \langle a|S_z|c\rangle = 0. & \end{aligned} \right\} \qquad (3.26)$$

It is seen from these formulas that in strong magnetic fields, when $x_\perp \gg 1$, paramagnetic resonance occurs only if the alternating field is perpendicular to the field H_0. In weak and intermediate magnetic fields, the matrix element is $\langle a|S_x|c\rangle \neq 0$ and consequently resonant paramagnetic absorption is possible between the levels a and c, provided the static and alternating magnetic fields are parallel to each other. A scheme of the energy levels and of the possible transitions is shown in Fig. 3.2.
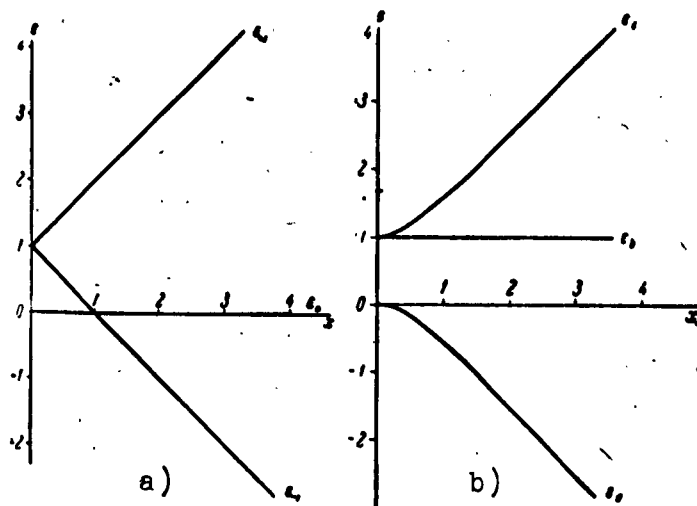
Fig. 3.2. Dependence of the spin energy levels of the Ni^{2+} ion in fluorosilicate on the intensity of the magnetic field H_0. a) H_0 parallel to the tetragonal axis of the crystal; b) H_0 perpendicular to the tetragonal axis.

§3.5. Hyperfine Structure of Paramagnetic Resonance Spectra

The theory of the hyperfine structure of atomic spectra was developed long ago. The novelty in its application to paramagnetic resonance spectra of crystals lies in the need for taking into account the effect of the crystalline field and a few other effects which are of no significance in optical research. The first calculations of the hyperfine structure of paramagnetic resonance spectra, pertaining to copper salts, namely Tutton's salt [35] and the fluorosilicate [36], have disclosed a clear-cut disagreement with the experimental data. The differences between theory and experiment became particularly sharp when, in spite of the theoretical predictions, a hyperfine structure was experimentally established for the paramagnetic absorption lines in the salts of Mn^{2+}.

All these contradictions were eliminated with the aid of the "s-configuration interaction" hypothesis [37]. It is well known [38] that the magnetic interaction of the s electrons with the nucleus is much

stronger than that of the electrons with $\underline{l} \neq 0$. It was assumed that the ground state of the paramagnetic ion contains besides the usually assumed configuration $3d^n$ also a small admixture of configurations containing an unpaired $\underline{s}$ electron. It is most probable that the hyperfine structure is due to the admixture of the configuration $3sp^6d^n4s$ because, first, the transition of the 3s electron to the 4s orbit calls for a small expenditure of energy; second, in this configuration the total orbital and spin angular momenta can assume the same quantum values L and S, resulting from Hund's rule for the ground state of the ion. The $\underline{s}$ configuration interaction takes place in free atoms and depends little on the crystalline field.

A confirmation of the hypothesis of $\underline{s}$ configuration interaction can therefore be the isotropy of the hyperfine structure of the paramagnetic resonance spectrum and the fact that the hyperfine splitting constant is approximately the same for all the investigated salts of Mn^{2+}. It must be noted that the $\underline{s}$ configuration effect is particularly important for salts of the iron-group elements, for in these crystals the orbital magnetism is suppressed (the orbital levels are singlets), which greatly reduces the hyperfine splitting.

The general theory of the hyperfine structure of paramagnetic resonance spectra of iron-group element compounds has been developed in [17]. If the paramagnetic atom has a nuclear spin different from zero, then the following expression is added to the Hamiltonian (3.9)

$$\mathscr{H}_{cn}^{N} = p\left\{ (\hat{L}\hat{I}) + [\xi L(L+1) - k](\hat{S}\hat{I}) - \frac{3}{2}\xi(\hat{L}\hat{S})(\hat{L}\hat{I}) - \frac{3}{2}\xi(\hat{L}\hat{I})(\hat{L}\hat{S}) \right\} + q'\left\{ (\hat{L}\hat{I})^2 + \frac{1}{2}(\hat{L}\hat{I}) \right\} - g_N\beta_N(\hat{H}\hat{I}),$$

(3.27)

where

$$p = \frac{2g_N\beta\beta_N}{r^3}, \quad q' = \frac{\eta^2 q}{2I(2I-1)r^3}, \quad \xi = \frac{(2I+1)-4S}{S(2I-1)(2I+3)(2I-1)},$$
$$\eta = \pm 2S\xi.$$

- 78 -

if I is the nuclear spin, $g_N\beta_N$ is the magnetic moment, and $\underline{q}$ is the quadrupole moment of the nucleus; η has a plus or minus sign depending on whether the first or second half of the $\underline{d}$ shell of the atom is filled. The first term in (3.27) takes into account the interaction between the electrons and the magnetic moment of the nucleus, while the second represents the interaction with the quadrupole nuclear moment and the third the energy of the nucleus in the external magnetic field. The coefficient $\underline{k}$ is introduced to allow for the influence of the s-configuration interaction. A theoretical calculation of $\underline{k}$ is extremely complicated. On the other hand, comparison with the experimental data has disclosed the interesting fact that the coefficient $\underline{k}$ is practically the same for all ions of the iron group.

The transition from (3.27) to the spin Hamiltonian can be carried out by the method described in §3.3. We know that it is necessary to distinguish between two cases, depending on whether the atom is in a simple or degenerate state after the action of the cubic field of the crystals. In the former case the spin Hamiltonian, with account of the interaction between the moments of the nucleus and the electron shell and with the external magnetic field has the form

$$\mathscr{H}_{cn}^N = A_{ij}\hat{S}_i I_j + P_{ij} I_i I_j - g_N\beta_N H_i I_i. \qquad (3.28)$$

If the resultant crystalline field has trigonal or tetragonal symmetry, then

$$\mathscr{H}_{cn}^N = A\hat{S}_z I_z + B(\hat{S}_x I_x + \hat{S}_y I_y) + P\left(I_z^2 - \frac{1}{3}I(I+1)\right) - g_N\beta_N H_i I_i. \qquad (3.29)$$

In the second case, the spin Hamiltonian will have the same form but $\hat{S}$ now stands for the effective spin $\hat{S}'$. We shall not dwell here on the connection of the coefficients A and B with the constants of the crystalline field and the nuclear moments, but it is obvious that the constants of the magnetic hyperfine structure A and B are proportional to $g_N\langle 1/r^3\rangle$, and the quadrupole interaction constant P is proportional to

- 79 -

$q(\text{I}/r^3)$. The intensity of the individual hyperfine components of the paramagnetic resonance spectrum will be determined as before only by the magnitude of the matrix element of the electron magnetic moment (3.17), since the nuclear magnetic moment is very small. Consequently, in the simplest cases when the component of the nuclear angular momentum I_z is conserved, a selection rule $\Delta m = 0$ exists for the magnetic quantum number.

Most theoretical calculations and experimental researches pertain to strong magnetic fields, the action of which on the unpaired electrons of the paramagnetic atoms exceeds greatly the interactions between the latter and the moments of the nucleus. Calculations of hyperfine splitting in weak magnetic fields are more complicated and have been made only for a few particular cases [39].

In order to verify the hypothesis of the s-configuration interaction, an analysis was made in [37] of the experimental data on the optical spectra of neutral atoms and paramagnetic resonance spectra of the ions of the 3d-transition group elements. This analysis confirmed a premise already stated by Fermi [38] that if there are no s electrons in the ground state of the atom, then an appreciable portion of the hyperfine splitting is frequently determined by the unpaired s electrons of the excited levels. A quantitative estimate of the coefficient k was also made [40] with the aid of the Hartres-Fok functions and yielded a value approximately ten times smaller than that observed. The discrepancy between the theory and experiment can be attributed to the fact that the Hartres-Fok method is not suitable for the calculation of the wave functions near the nucleus.

§3.6. Parameters of the Crystalline Field. The Jahn-Teller Effect

Up to now all the calculations of the energy spectra of the paramagnetic ions in crystals were carried out by the "crystalline field"

method. The parameters of the crystalline field A_n^m were determined here as a rule by comparing the theoretical results with the experimental data on paramagnetic resonance, on the temperature dependence of the static paramagnetic susceptibility, on the optical absorption spectra, etc. It would be interesting to make a theoretical estimate of the magnitude of the crystalline field and primarily its principal cubic component. Van Vleck [13] and Polder [6] made a numerical calculation under the assumption that the cubic field is made by six pointlike charges e_{eff} or by six dipoles each with moment μ_e, located at the vertices of an octahedron at a distance R from the center. It follows from this model that the parameter C_4, which was introduced in (3.7), has a value

$$C_4 = -\frac{35}{4}\frac{ee_{eff}}{4R^5}, \quad \text{or} \quad C_4 = \frac{175}{4}\frac{e\mu_e}{R^6}. \tag{3.30}$$

An x-ray structural analysis of alums [41] has shown that R = 2.0 A. To calculate the splitting Δ we must also know the value of $\overline{r^4}$ for the 3d electrons. If we use the 3d hydrogen functions, we obtain

$$\overline{r^2} = 126a_0^2 Z^{-2} = 4{,}40a_0^2, \quad \overline{r^4} = 25{,}515a_0^4 Z^{-4} = 31{,}2a_0^4. \tag{3.31}$$

We have assumed here Z = 5.35, which follows from the experimental value of 43 ev for the ionization potential of Ti^{3+}. If we assume $e_{eff} \approx -e$ or $\mu_e = 2 \cdot 10^{-18}$ CGSE, then the calculated intervals between energy levels in the cubic field are in good agreement with the experimental data. This agreement must nevertheless be regarded as fortuitous, since the model assumed is very crude. Kleiner [42] made more precise calculations for chrome alums, taking into consideration the distribution of the electron cloud in the oxygen ion. The water molecules have their oxygen atoms, which can be regarded as O^- ions, facing the center of the octahedron. The results of the calculations were in complete contradiction to the experimental data, for even the sign of

the parameter C_4 was found to be incorrect. Tanabe and Sugano [43] took account of the covalent bonds between the central ion and the surrounding atoms (see §3.8). Exchange effects cause an inversion of the energy levels and their sequence becomes correct. The absolute value of C_4 turns out here to be about 3/2 times larger than the experimental value.

We have already indicated that only in the first approximation does the crystalline field surrounding a paramagnetic particle have a cubic symmetry in the case of the salts of the iron-group elements. Actually, however, appreciable deviations exist. Superimposed on the strong cubic field is a weak field of lower symmetry, the origin of which is connected with the following three different causes [26].

1. <u>Direct action exerted on the paramagnetic particle by the electric field of the remote particles situated outside the octahedral complex.</u> In alums, for example, this field has a trigonal symmetry and can be represented in the following form:

$$V_{\text{трин}} = (G + 30Hr^2)(xy + yz + zx) - 35H(x^3y + xy^3 + \\ + y^3z + yz^3 + zx^3 + z^3x) + C. \qquad (3.32)$$

Here $\underline{x}$, $\underline{y}$, and $\underline{z}$ are the Cartesian coordinates of the electron and pertain to the principal cubic axes; G and H are constants independent of $\underline{r}$; C is a polynomial with cubic symmetry and therefore immaterial for our purposes. If we introduce the spherical coordinates R_1, α_1, and β_1, which define the position of the charge e_1 relative to the paramagnetic center, then we obtain the following expressions for the constants G and H:

$$\left. \begin{array}{l} G = -\sum e_i e R_i^{-3} \left(\dfrac{3}{2} \cos^2 \alpha_i - \dfrac{1}{2} \right), \\[2mm] H = -\dfrac{1}{63} \sum e_i e R_i^{-5} \left[35 \cos^4 \alpha_i - 30 \cos^2 \alpha_i + 3 + \\[1mm] + 7\sqrt{2} \cos \alpha_i \sin^3 \alpha_i \cos 3\beta_i \right]. \end{array} \right\} \qquad (3.33)$$

Calculations shows that for titanium alums, for example, the splitting of the lower energy level by the field (3.32) is equal to about 350 cm^{-1}.

2. Indirect action of the remote particles. The remote particles cause the octahedral complex to become deformed and distort its cubic field. If we have three pointlike charges a, b, and c, then the direct action of charge a on charge c is stronger than the indirect action due to the motion of charge b under the influence of charge a. In our case, however, the indirect action can exceed the direct action, since the electron clouds of the particles forming the paramagnetic octahedral complex overlap one another. One proof of the significance of the indirect action is the well known fact that the initial splittings of the spin level of iron alums increase when they are magnetically diluted by substituting aluminum ions for the iron ions. In this case the direct effect cannot change appreciably, since the iron and aluminum ions have the same charge, and the radii of these ions are very small compared with the distances between trivalent atoms. On the other hand, the deformation of the octahedron can be greatly influenced by whether the ion at its center is iron or aluminum.

3. The Jahn-Teller effect. This cause of lattice deformation, which leads to a lowering of the symmetry of the crystalline field, is frequently very important. The Jahn-Teller theorem was initially proved for molecules [12] and then extended to include crystals [13, 14]. According to this theorem, the geometrical configuration of nuclei cannot be stable if the electron state of the molecule is degenerate, except in the two following cases: a) the molecule is linear, that is, the nuclei lie on one line; b) the molecule contains an odd number of electrons, and the degeneracy of its electron state is a double Kramers degeneracy, that is, one that cannot be lifted by any change in the electrostatic forces.

The lowering of the symmetry of nuclear configuration, if we exclude the two indicated cases, will lift the degeneracy of the elec-

tron state. It can be proved that the mean energy of different electron states remains constant after the splitting of the energy level. Thus, at least one electron level will lie below the initial one after the deformation of the molecule.

Van Vleck [13] made the transition from the molecule to the crystal by considering the behavior of an octahedral paramagnetic complex in an external trigonal field. The Hamiltonian $\hat{H}$ of the electron state contains as parameters the distances between the centers of the particles (atoms or molecules) forming the complex. An arbitrary displacement of these particles can be described with the aid of 21 normal vibrational coordinates Q_i. Expanding the Hamiltonian in powers of Q_i we get

$$\mathscr{H} = \mathscr{H}_0 + \hat{V}_{триг} + \sum_i \hat{V}_i Q_i. \qquad (3.34)$$

Here $\hat{H}_0$ contains all the interactions that are possible inside the regular octahedral complex and are independent of the electron spin of the paramagnetic ion; $\hat{V}_{trig}$ takes into account the effect of the remote atoms of the crystal lattice. Let W_0 be one of the eigenvalues of $\hat{H}_0$. Connected with the energy W_0 is one of the set of wave functions given in (3.11). By considering the second and third terms of (3.34) as a perturbation, we can set up and solve a secular equation, the solution of which will give in first approximation the correction to the energy W_0. The energy of the entire system is thus a certain function of the displacements Q_i. By solving the system of equations

$$\frac{\partial W}{\partial Q_i} = 0 \qquad (i=1,2,3,\ldots), \qquad (3.35)$$

we can find such displacements Q_i^0 as correspond to a minimum energy W, and consequently, to the most stable configuration of the paramagnetic complex. Van Vleck made detailed calculations for titanium, vanadium,

and chrome (excited state) alums. The Q_1^0 were found to be of the order of 10^{-9} cm. The potential of the low-symmetry crystalline field resulting from the distortion of the octahedral configuration of the water molecules will be a quadratic function of Q_1^0. The splittings of the orbital levels due to this field have been calculated to be on the order of 10^2 cm^{-1}. The potential energy of the $\underline{f}$ electrons of rare-earth atoms in the crystalline field is approximately 100 times smaller than the energy of the $\underline{d}$ electrons of the iron-group atoms. Consequently $Q_1^0 \approx 10^{-11}$ cm in rare-earth crystals, and consequently the level splitting due to the Jahn-Teller effect can have an approximate value $10^2 \cdot (10^{-2})^2 = 10^{-2}$ cm^{-1}. As will be shown below, experiment confirms this conclusion.

The Van Vleck theory was further developed by Pryce and his co-workers [14]. From general considerations, they reached the conclusion that the Jahn-Teller effect pertains not only to degenerate but also to almost-degenerate systems. An interesting example of such almost-degenerate systems are linear triatomic molecules of the type BAB.

In addition, they investigated in detail octahedral complexes which, let us note, are encountered not only in paramagnetic salts, but also in crystals containing F centers, luminescent centers, exciton states, etc. The degeneracy of the electron state of an octahedral paramagnetic complex can be triple or double. If the degeneracy of the energy level is triple, then the deformation of the complex on going to stable nuclear configurations will follow in some cases the (100) axis, and in others the (111) axis. As a result, the complex has either a tetragonal or trigonal symmetry. If the degeneracy is double, the situation is more complicated. The point is that in this case the energy splitting due to the deformation of the complex is proportional to $Q_2^2 + Q_3^2$ if we denote by Q_2 and Q_3 certain normal vibrational coor-

dinates of an octahedron of even type. It is convenient to introduce new variables ρ and α:

$$Q_1 = \rho \sin \alpha, \quad Q_2 = \rho \cos \alpha. \tag{3.36}$$

It is clear that the splitting is independent of α. Thus, there exists an infinite set of configurations corresponding to one and the same value of the energy. If we take anharmonic effects into account, then we find that the most stable configuration is obtained by stretching the octahedron along one of the tetragonal axes.

All these results, as indicated by Abragam and Pryce [36] can explain why copper salts, the crystals of which have trigonal symmetry, have an isotropic g factor and an isotropic and small hyperfine structure constant. In a field of cubic symmetry, the lower orbital level of the copper ion is doubly degenerate and the wave functions belonging to it are, in accord with (3.11), $\varphi_1 = \psi_0$ and $\varphi_2 = (1/2)(\psi_2 + \psi_{-2})$.

Neither spin-orbit interaction nor a field of trigonal symmetry can lift the degeneracy. The only reason for the splitting of the given orbital level is the Jahn-Teller effect. The following wave functions will belong to the energy sublevels:

$$\psi_I = \varphi_1 \cos \alpha + \varphi_2 \sin \alpha, \quad \psi_{II} = \varphi_1 \sin \alpha - \varphi_2 \cos \alpha. \tag{3.37}$$

The principal values of the g tensor, calculated with the aid of these functions, are

$$\left. \begin{aligned}
g_x &= 2 - 2\frac{\lambda}{\Delta}(\cos \alpha - \sqrt{3}\sin \alpha)^2, \\
g_y &= 2 + 2\frac{\lambda}{\Delta}(\cos \alpha + \sqrt{3}\sin \alpha)^2, \\
g_z &= 2 - 8\frac{\lambda}{\Delta}\cos^2 \alpha
\end{aligned} \right\} \tag{3.38}$$

If we average over α, we obtain $\overline{g}_x = \overline{g}_y = \overline{g}_z = 2 - 4(\lambda/\Delta)$. We can explain in similar fashion the isotropy of the hyperfine structure of the paramagnetic resonance spectrum.

- 86 -

§3.7. Salts of Rare-Earth Elements

It is well known that the room-temperature static magnetic susceptibility of rare earth salts can be calculated by assuming that the carriers of the paramagnetism are the three rare earth ions in states determined by Hund's rule [10]. This hypothesis is also confirmed by optical data [44]. We can therefore conclude, first, that deviations from the normal (Russel-Saunders) coupling are small, at least in the ground states, and second, that the action of the crystal field on the paramagnetic ion is weak and not capable of disturbing the spin-orbit coupling. The latter is explained by the following two singularities of rare earth ions.

1. The magnetic properties of the rare earth ions are due to the low-lying 4f-electrons, the mean distance of which to the nucleus is much smaller than that of the 3d electrons. In addition, the external electron shell has a screening effect. The crystalline field therefore causes in the rare earth elements level splittings on the order of 100 cm^{-1}, i.e., about 100 times smaller than in ions of the iron group.

2. Multiple splitting is much larger in rare earth ions than in iron-group ions; it has an order of 10^3-10^4 cm^{-1}.

The spin orbit coupling thus turns out to have a much stronger influence than the crystalline field, and therefore the Hamiltonian for the paramagnetic ion must be written in the form

$$\mathcal{H} = \mathcal{H}^0 + \mathcal{H}_{sp} + \mathcal{H}_z. \qquad (3.39)$$

Here $\hat{H}^0$ is the Hamiltonian of the free ion. In the perturbation-method calculations we shall start from the ground state at $\hat{H}^0$, in which the conserved quantities can be taken to be the total angular momentum J and the orbital and spin momenta L and S. Sometimes higher approximations, which take into account the influence of the excited levels of H^0, are of importance; it is usually sufficient to consider the first

- 87 -

excited multiplet level. The intervals between the ground and first-excited levels are known for many elements from optical and magnetic measurements. For the remaining elements, the multiplet-structure constant can be estimated, in accordance with [45], from the following formula:

$$\lambda = 200 \, (Z - 55) . cм^{-1}. \tag{3.40}$$

Table 3.5 lists the ground state of the rare earth ions, and also the data on the first excited energy levels, known from experiment and obtained with the aid of (3.40).

Let us proceed to examine the splittings of the (2J + 1)-fold level of a free ion in a crystalline field $\hat{H}_{кр}$. Unlike the hydrated salts of the iron group elements, in which the paramagnetic ion is usually surrounded by an octahedron of water molecules which produces a strong electric field of cubic symmetry, in most salts of rare earth elements the paramagnetic ion surrounding produces a field of trigonal symmetry [47]. The energy levels of ions containing an odd number of electrons therefore splits into J + 1/2 doublets (Table 3.2); on the other hand, if the number of electrons is odd, singlets and doublets are obtained (Table 3.1).

For a quantitative calculation it is first necessary to find an expression for the potential of the crystalline field.* In the case of a C_{3v} symmetry (formates) the potential is given by formula (3.3b), in which all six coefficients A_n^m differ from zero. For the somewhat higher symmetry C_{3h} (ethyl sulfates, bromates), we have $A_4^3 = A_6^3 = 0$. The matrix elements $H_{кр}$ necessary for the calculations in the first perturbation-theory approximation can be obtained with the aid of the equivalent operators (Table 3.3); the common factors α, β, and γ for all rare earth ions can be determined with the aid of the ψ functions corresponding to the states with maximum J_z, by changing over from the

- 88 -

TABLE 3.5

Energy Levels of Free Rare Earth Ions

Элемент (X³⁺)	z	Основное состояние	Возбужденное состояние	$E_1 - E_0$ (теорет.) см⁻¹	$E_1 - E_0$ (эксперим.) см⁻¹	Ссылка
Ce	58	$f^1\ {}^2F_{5/2}$	${}^2F_{7/2}$	2 100	2 240	[46]
Pr	59	$f^2\ {}^3H_4$	${}^3H_5$	2 000	—	
Nd	60	$f^3\ {}^4I_{9/2}$	${}^4I_{11/2}$	1 800	—	
Pm	61	$f^4\ {}^5I_4$	${}^5I_5$	1 500	—	
Sm	62	$f^5\ {}^6H_{5/2}$	${}^6H_{7/2}$	980	1 100	[3]
Eu	63	$f^6\ {}^7F_0$	${}^7F_1$	270	300, 340	[3, 47]
Gd	64	$f^7\ {}^8S_{7/2}$				
Tb	65	$f^8\ {}^7F_6$	${}^7F_5$	2 000	—	[46]
Dy	66	$f^9\ {}^6H_{15/2}$	${}^6H_{13/2}$	3 300	—	
Ho	67	$f^{10}\ {}^5I_8$	${}^5I_7$	4 800	5 050	[48]
Er	68	$f^{11}\ {}^4I_{15/2}$	${}^4I_{13/2}$	6 500	8 000	[48]
Tm	69	$f^{12}\ {}^3H_6$	${}^3H_5$	8 400	8 250	[49]
Yb	70	$f^{13}\ {}^2F_{7/2}$	${}^2F_{5/2}$	10 500	10 300	[48]

1) Element; 2) ground state; 3) excited state; 4) theoretical; 5) cm⁻¹; 6) experimental; 7) reference.

J, J_z representation to the L_z, S_z representation and then to the l_z, s_z representation [8].

To calculate the splittings due to $\hat{H}_{kr}$ in the second approximation we must know the matrix elements of $\hat{H}_{kr}$, relating the ground and first-excited states:

$$\langle J+1,\ J_z+m\,|\,V_n^m\,|\,J,\ J_z\rangle.$$

For this purpose, the following formulas were described in [45, 51]:

$$\langle J+1,\quad J_z|\,V_2^0\,|J,\ J_z\rangle = \alpha' \overline{r^2} J_z \sqrt{(J+1)^2 - J_z^2}.$$

$$\langle J+1, J_z|\,V_4^0\,|J,J_z\rangle = \beta' \overline{r^4} J_z\,(7J_z^2 - 3J^2 - 6J + 2)\sqrt{(J+1)^2 - J_z^2}.$$

$$\langle J+1,J_z|\,V_6^0\,|J,J_z\rangle = \gamma' \overline{r^6} J_z\,[33J_z^4 - 5J_z^2(6J^2 + 12J + 15) + 5J^4 + 20J^3 - 5J^2 - 50J + 12]\sqrt{(J+1)^2 - J_z^2}.$$

$$\langle J+1,J_z+3|V_4^3|J,J_z\rangle = -\tfrac{1}{40}\beta'\overline{r^4}(4J_z - J + 5)\sqrt{\tfrac{(J+J_z+4)!(J-J_z)!}{(J+J_z)!(J-J_z-2)!}}.$$

$$\langle J+1,J_z+3|V_6^3|J,J_z\rangle = -\tfrac{1}{28}\gamma'\overline{r^6}[22J_z^2 - 11J_z^2(J-8) - J_z(4J^2 + 41J - 142) + (J-2)(J-7)(J+6)]\sqrt{\tfrac{(J+J_z+4)!(J-J_z)!}{(J+J_z)!(J-J_z-2)!}}.$$

$$\langle J+1,J_z+6|V_6^6|J,J_z\rangle = -\tfrac{1}{14}\gamma'\overline{r^6}\sqrt{\tfrac{(J+J_z+7)!(J-J_z)!}{(J+J_z)!(J-J_z-5)!}}.$$

The coefficients α, β, γ and α', β', γ' are listed in Table 3.6.

The values of α, β, and γ can also be calculated with the aid of the Racah coefficients [52].

After solving the secular equation and thus determining the energy levels of the ion in the crystalline field and the corresponding wave functions, it is necessary to proceed to calculate the splittings of these levels by the external magnetic field. We know that $\hat{H}_{kr}$ gives rise either to doublets (ions with odd number of electrons) or to doublets with singlets (ions with even number of electrons). Since the intervals between the energy levels in the crystalline field are somewhat larger than the Zeeman splittings in ordinary magnetic fields, we shall consider the action of the magnetic field on each level separately. Since the spin-lattice interaction in salts of rare earth elements is very strong at room temperature (see §5.3), the experiments must be carried out at temperatures that are so low that only the lowest level is populated in practice.* It is clear that paramagnetic resonance can be observed if this level is not a singlet. The wave functions of the lower doublet are used to calculate the perturbation matrix elements $\hat{H}_Z = \beta \vec{H}_0 (\vec{L} + 2\vec{S})$ by means of the following formulas:

$$\langle J,\ldots|\hat{L} + 2\hat{S}|J,\ldots\rangle = g_0 \langle J\ldots|\hat{J}|J\ldots\rangle, \tag{3.41}$$

where g_0 is the Lande effect for the free ion and

$$\left. \begin{aligned} \langle J+1, J_z|\hat{L}_z + 2\hat{S}_z|J, J_z\rangle &= g'\sqrt{(J+1)^2 - J_z^2}, \\ \langle J+1, J_z \pm 1|\hat{L}_x + 2\hat{S}_x|J, J_z\rangle &= \langle J+1, J_z \pm \\ \pm 1|\pm i(\hat{L}_y + 2\hat{S}_y)|J, J_z\rangle &= \mp g'\sqrt{(J \pm J_z + 1)(J \pm J_z + 2)}, \end{aligned} \right\} \tag{3.42}$$

where

$$g' = \left\{ \frac{(J+L+S+2)(-J+L+S)(J-L+S+1)(J+L-S+1)}{4(J+1)^2(2J+1)(2J+3)} \right\}^{\frac{1}{2}}. \tag{3.43}$$

The values of g_0 and g' for individual ions are listed in Table 3.6.

The perturbation matrix of second rank has a trace equal to zero and can be represented in the form $\beta \vec{H}_0 g \vec{S}'$, where $\vec{S}'$ is the Pauli mat-

TABLE 3.6

1 Элемент [1]	α	β	γ	α'	β'	r'	ε₀	ε'	N	N'
Ce³⁺	$-\dfrac{2}{5\cdot7}$	$\dfrac{2}{3^2\cdot5\cdot7}$	0	$\dfrac{2^2}{3\cdot5\cdot7}$	$\dfrac{-2^2}{3^2\cdot7\cdot11}$	$\dfrac{2^2}{3^2\cdot11\cdot13}$	$\dfrac{6}{7}$	$\dfrac{1}{7}$	$\dfrac{2^2\cdot3}{5\cdot7}$	$\dfrac{1}{14}$
Pr³⁺	$-\dfrac{2^2\cdot13}{3^2\cdot5^2\cdot11}$	$-\dfrac{2^2}{3^2\cdot5\cdot11^2}$	$\dfrac{2^4\cdot17}{3^4\cdot5\cdot7\cdot11^2\cdot13}$	$\dfrac{13\sqrt{66}}{3^3\cdot5^2\cdot11}$	$\dfrac{2^3\sqrt{66}}{3^3\cdot7\cdot11^2}$	$\dfrac{-17\sqrt{66}}{3^4\cdot5\cdot11^2\cdot13}$	$\dfrac{4}{5}$	$\dfrac{\sqrt{66}}{5\cdot11}$	$\dfrac{2^4\cdot37}{3^3\cdot5^2}$	$\dfrac{-7\sqrt{66}}{2\cdot3^3\cdot5^2}$
Nd³⁺	$-\dfrac{7}{3^2\cdot11^2}$	$-\dfrac{2^3\cdot17}{3^3\cdot11^3\cdot13}$	$\dfrac{-5\cdot17\cdot19}{3^3\cdot7\cdot11^3\cdot13^2}$	$\dfrac{2^3\sqrt{14}}{11^2\cdot13}$	$\dfrac{2^3\cdot17\sqrt{14}}{3^3\cdot7\cdot11^3\cdot13}$	$\dfrac{2\cdot5\cdot19\sqrt{14}}{3^3\cdot7\cdot11^3\cdot13^2}$	$\dfrac{8}{11}$	$\dfrac{\sqrt{14}}{2\cdot11}$	$\dfrac{2^2\cdot7\cdot17}{3\cdot11^2}$	$\dfrac{-193\sqrt{14}}{2^2\cdot3^3\cdot11^3}$
Pm³⁺	$\dfrac{2\cdot7}{3\cdot5\cdot11^2}$	$\dfrac{2^3\cdot7\cdot17}{3^3\cdot5\cdot11^2\cdot13}$	$\dfrac{2\cdot17\cdot19}{3^3\cdot7\cdot11^2\cdot13^2}$	$\dfrac{-1}{3\cdot5\cdot11}\sqrt{\dfrac{14}{11}}$	$\dfrac{-2^5\cdot17}{3^3\cdot11^2\cdot13\cdot\sqrt{154}}$	$\dfrac{-2\cdot17\cdot19}{3^3\cdot7\cdot11^2\cdot13^2\cdot\sqrt{154}}$	$\dfrac{3}{5}$	$\dfrac{1}{5}\sqrt{\dfrac{14}{11}}$	$\dfrac{2^3\cdot7}{3\cdot5\cdot11}$	$\dfrac{-133}{5\cdot2^2\cdot3\cdot11}\sqrt{\dfrac{14}{11}}$
Sm³⁺	$\dfrac{13}{3^2\cdot5\cdot7}$	$\dfrac{2\cdot13}{3^3\cdot5\cdot7\cdot11}$	0	$\dfrac{-2^3\cdot13}{3^3\cdot7\cdot11^2\cdot\sqrt{30}}$	$\dfrac{-2^4\cdot5\cdot17}{3^4\cdot7\cdot11^2\cdot\sqrt{30}}$	$\dfrac{2^4\cdot5\cdot17}{3^4\cdot11^2\cdot13\sqrt{30}}$	$\dfrac{2}{7}$	$\dfrac{\sqrt{30}}{2\cdot7}$	$\dfrac{2^5\cdot61}{3^3\cdot5\cdot7}$	$\dfrac{-19\cdot23\cdot\sqrt{30}}{4\cdot3^3\cdot5^3\cdot7}$
Tb³⁺	$-\dfrac{1}{3^2\cdot11}$	$\dfrac{2}{3^3\cdot5\cdot7\cdot11^2}$	$\dfrac{-1}{3^4\cdot7\cdot11^3\cdot13}$	$\dfrac{1}{3\cdot5\cdot7}\sqrt{11}$	$\dfrac{-1}{3^3\cdot11\cdot\sqrt{11}}$	$\dfrac{1}{3^4\cdot11\cdot13\cdot\sqrt{11}}$	$\dfrac{3}{2}$	$\dfrac{1}{2\sqrt{11}}$	$\dfrac{7^2}{2\cdot3^3\cdot5}$	$\dfrac{-\sqrt{11}}{2\cdot3^3}$
Dy³⁺	$-\dfrac{2}{3^2\cdot5\cdot7}$	$-\dfrac{2^3}{3^3\cdot5\cdot11^2}$	$\dfrac{2^3}{3^4\cdot7\cdot11^2\cdot13}$	$\dfrac{2^3\sqrt{7}}{3\cdot5\cdot7\cdot13}$	$\dfrac{2^5\sqrt{7}}{3^3\cdot7\cdot11^2\cdot13}$	$\dfrac{-2^5\sqrt{7}}{3^4\cdot11^2\cdot13^2}$	$\dfrac{4}{3}$	$\dfrac{1}{3\sqrt{7}}$	$\dfrac{2^5}{3^3\cdot5}$	$\dfrac{-\sqrt{7}}{2\cdot3^3}$
Ho³⁺	$-\dfrac{1}{2\cdot3^2\cdot5^2}$	$\dfrac{-1}{2\cdot3\cdot5\cdot7\cdot11\cdot13}$	$\dfrac{-5}{3^3\cdot7\cdot11^2\cdot13^2}$	$\dfrac{-1}{2\cdot3\cdot5\cdot7\cdot\sqrt{5}}$	$\dfrac{\sqrt{5}}{2\cdot3^3\cdot7\cdot11^2\cdot13}$	$\dfrac{5\sqrt{5}}{3^2\cdot11^2\cdot13^2}$	$\dfrac{5}{4}$	$\dfrac{1}{4\sqrt{5}}$	$\dfrac{23}{2\cdot3\cdot5}$	$\dfrac{-4}{3\cdot5\cdot\sqrt{5}}$
Er³⁺	$\dfrac{2^2}{3^2\cdot5^2\cdot7}$	$\dfrac{2}{3^2\cdot5\cdot7\cdot11\cdot13}$	$\dfrac{2^3}{3^3\cdot7\cdot11^2\cdot13}$	$\dfrac{-1}{3\cdot5^2\cdot7\cdot13}\sqrt{14}$	$\dfrac{-2^4\sqrt{14}}{3^3\cdot7\cdot11^2\cdot13}$	$\dfrac{-2\sqrt{14}}{3^4\cdot11^2\cdot13^2}$	$\dfrac{6}{5}$	$\dfrac{2}{5\sqrt{14}}$	$\dfrac{2^4\cdot11}{3^3\cdot5^2}$	$\dfrac{-83}{3^3\cdot5^2\cdot\sqrt{14}}$
Tm³⁺	$\dfrac{1}{3^2\cdot11}$	$\dfrac{2^3}{3^4\cdot5\cdot7\cdot11^2}$	$\dfrac{-5}{3^4\cdot7\cdot11^2\cdot13}$	$\dfrac{-1}{3\cdot5\cdot7}\sqrt{55}$	$\dfrac{2^3}{3^2\cdot11\cdot\sqrt{55}}$	$\dfrac{\sqrt{55}}{3^4\cdot11^2\cdot13}$	$\dfrac{7}{6}$	$\dfrac{5}{6\sqrt{55}}$	$\dfrac{7}{3^2}$	$\dfrac{-11}{2\cdot3^3\cdot\sqrt{55}}$
Yb³⁺	$\dfrac{2}{3^2\cdot7}$	$-\dfrac{2}{3^2\cdot5\cdot7\cdot11}$	$\dfrac{2^2}{3^3\cdot7\cdot11\cdot13}$	$\dfrac{-2^2}{3\cdot5\cdot7}$	$\dfrac{2^2}{3^2\cdot7\cdot11}$	$\dfrac{-2^2}{3^2\cdot11\cdot13}$	$\dfrac{8}{7}$	$\dfrac{1}{7}$	$\dfrac{2^4}{3\cdot7}$	$\dfrac{-1}{14}$

1) Element.

rix vector and $\underline{g}$ is a certain tensor with principal values $g_\parallel$, $g_\perp$, $g_\perp$. If the wave functions of our doublet, which we symbolically denote by $|+\rangle$ and $|-\rangle$, are so chosen as to make the matrix $L_z + 2S_z$ diagonal, then

$$
\begin{aligned}
g_\parallel &= 2|\langle +|\hat{L}_z + 2\hat{S}_z|+\rangle|, \\
g_\perp &= 2|\langle +|\hat{L}_x + 2\hat{S}_x|-\rangle|.
\end{aligned}
\qquad (3.44)
$$

Thus, the paramagnetic resonance spectrum can be interpreted with the aid of a spin Hamiltonian with effective spin $S' = 1/2$:

$$
\mathscr{H}_{cn} = \beta g_\parallel H_{0z}\hat{S}_z' + \beta g_\perp (H_{0x}\hat{S}_x' + H_{0y}\hat{S}_y').
\qquad (3.45)
$$

Ions with an even number of electrons call for a special analysis. In this case it is easy to show that the nondiagonal matrix element is $\langle +|\hat{L}_x + 2\hat{S}_x|-\rangle = 0$. It follows therefore that there should be no paramagnetic resonance effect. Indeed, if the field H_0 is parallel to the trigonal axis of the crystal, then the magnetic dipole transitions between magnetic sublevels will be forbidden, but if H_0 is perpendicular to the trigonal axis then $g_\perp = 0$.

This effect was nevertheless observed in experiment, for example, in praseodymium salts. An explanation of this effect was found with the aid of the Jahn-Teller theorem [12]: in crystals containing ions having an even number of electrons the symmetry of the electric field is lowered to such an extent that the degeneracy is completely lifted and the doublets are split. These splittings, assumed by Van Vleck [13] are very small in the case of rare-earth ions and do not prevent the observation of paramagnetic resonances under usual magnetic field intensities. The paramagnetic resonance spectrum of ions with an even number of electrons can be calculated with the aid of the spin Hamiltonian

$$
\mathscr{H}_{cn} = \beta g_\parallel H_{0z}\hat{S}_z' + \Delta_x\hat{S}_x' + \Delta_y\hat{S}_y',
\qquad (3.46)
$$

where $\Delta = \sqrt{\Delta_x^2 + \Delta_y^2}$ is the doublet splitting due to the Jahn-Teller ef-

fect in the absence of the magnetic field H_0.

Many papers have been devoted to a detailed theoretical analysis of paramagnetic resonance spectra of individual rare earth elements: cerium ethyl sulfate [53, 50], the ethyl sulfates of Nd, Sm, Dy, Er, and Yb [54, 55], to the double nitrates of Ce, Pr, Nd, and Sm [56]. Attempts to interpret the observed paramagnetic resonance spectrum in dysprosium double nitrate have led to an interesting result. It turned out that the crystalline field can be divided into two parts [57]: a strong field of very high symmetry, namely icosahedral, and a weak trigonal field. For the field of icosahedral symmetry

$$A_6^5 = \left(\pm \frac{14}{\sqrt{5}} \right) A_6^0, \quad A_6^5 = 14 A_6^0 \qquad (3.47)$$

and all the remaining A_n^m vanish. To calculate the level splitting in fields of high symmetry it is convenient to use the method proposed in [58].

A large number of field constants A_n^m (up to six) makes difficult a unique interpretation of the observed paramagnetic resonance spectra. It is therefore customary to make use also of optical data, of results obtained by investigating the dependence of the static magnetic susceptibility on the temperature, or of information on the Faraday effect. To be sure, some difficulties arise from the fact that paramagnetic resonance is observed in strongly dilute solid solutions of paramagnetic salts, whereas other experiments are made with concentrated paramagnetic crystals. Dilution changes the electric crystalline field appreciably; in cerium ethyl sulfate these changes cause even the inversion of the two lower neighboring energy levels.

Reference [45] deals also with the general theory of the hyperfine structure of paramagnetic resonance spectra of rare earth ions. Calculation of the hyperfine splitting of the electron energy levels

can be made with the aid of the spin Hamiltonian (3.29) with effective spin $S' = 1/2$. If we denote here the operator of magnetic electron-nucleon interaction by $(\bar{a}/I)NI$, then the hyperfine structure constant will be equal to

$$A = 2\bar{a}\langle +|\hat{N}_z|+\rangle, \quad B = 2\bar{a}\langle +|\hat{N}_x|-\rangle. \tag{3.48}$$

The nonvanishing matrix elements of the operator $\hat{N}$ can be calculated with the aid of the following formulas

$$\left.\begin{array}{l} \langle J, \ldots |\hat{N}|J, \ldots \rangle \equiv N\langle J, \ldots |\hat{J}|J, \ldots \rangle, \\ \langle J+1, J_z |\hat{N}_z|J, J_z\rangle = N'\sqrt{(J+1)^2 - J_z^2}. \end{array}\right\} \tag{3.49}$$

The coefficients N and N' are listed in Table 3.6.

Rare earth ions can be artificially introduced into crystals which produce a field of cubic symmetry around these ions. The splitting of the energy levels in a field of cubic symmetry was considered theoretically in [59], where only part of the potential, proportional to $\overline{r^4}$, was considered. Bleaney [88] has shown that splitting in a cubic field can be calculated with the aid of a special type of spin Hamiltonian.

We wish to note in conclusion that many papers [4, 6], which in their day have played a major role in the explanation of the magnetic properties of rare earth salts, have lost their importance because of incorrect assumptions made concerning the symmetry of the crystalline field.

§3.8. Ions in the S State

Paramagnetic ions which have electron configurations $3d^5$ and $4f^7$ are in states

$$^6S_{5/2} (Mn^{2+}, Fe^{3+}) \text{ and } ^8S_{7/2}(Gd^{3+}, Eu^{2+}, Cm^{3+}).$$

The resultant orbital moment of the electrons is zero, and the electric crystalline field should therefore not split the ground levels of these ions. Actually, a small splitting has been ascertained both in experi-

ments on adiabatic demagnetization and from observations of paramagnetic resonance.

The complexity of the processes that bring about the splitting of the energy levels of ions in the S state makes it difficult to attempt direct calculations. It is therefore customary to use the spin Hamiltonian method. In the absence of an external magnetic field, the spin Hamiltonian will be an even polynomial of fourth degree (for Mn^{2+} and Fe^{3+}) or of sixth degree (for Gd^{3+}, Eu^{2+}, Cm^{3+}) in the projections of the spin momenta $\hat{S}_x$, $\hat{S}_y$, $\hat{S}_z$. The number of terms of this Hamiltonian is greatly reduced if we take into consideration the symmetry of the crystalline field. Thus, for example, for the Mn^{2+} or Fe^{3+} ion we can write the spin Hamiltonian in the form

$$\mathcal{H}_{cn} = D\left(\hat{S}_z^2 - \frac{35}{12}\right) + E(\hat{S}_x^2 - \hat{S}_y^2) + \frac{a}{6}(\hat{S}_1^4 + \hat{S}_2^4 + \hat{S}_3^4) + g\beta H_0\hat{S}. \qquad (3.50)$$

Here the first term takes into account the effect of the trigonal or tetragonal field with symmetry axes directed along the Z axis; the second term is connected with the small deviations toward the lower symmetries; the third term specifies the action of the cubic-symmetry field, and S_1, S_2, and S_3 are the spin components referred to the cubic axes; the last term takes into account the effect of the external magnetic field. The g factor of ions in the S state is isotropic. Detailed calculations of the positions and intensities of paramagnetic resonance absorption lines were made in [31, 60] for ions with S = 5/2 and S = 7/2 under the assumption that the crystalline field has a cubic symmetry. Both strong and weak magnetic fields were considered there.

Let us dwell briefly on different mechanisms capable of splitting the ground levels of ions in the S state under the influence of the crystalline field. The origin of the third term in spin Hamiltonian

(3.50) was explained by Van Vleck and Penney [61], who showed that if the effect of a cubic-symmetry electric field and of the spin-orbit interaction are taken into consideration simultaneously, then the ground level of an ion with configuration d^5 is split in the fifth-order approximation. The constant $\underline{a}$ can be estimated from the formula

$$a \approx \frac{K\lambda^4}{E_{PS}^4}. \tag{3.51}$$

Here K stands for the matrix element of the potential of the crystalline cubic field $\langle 3d | V_{kub} | 3d \rangle$, calculated with the aid of the single-electron functions; E_{PS} is the energy interval between the ^4P and ^6S terms of the free ion. Putting $K = 10^4$ cm^{-1}, $\lambda = 300$ cm^{-1}, and $E_{PS} = 2.5 \cdot 10^4$ cm^{-1}, we get $a \approx 10^{-4}$ cm^{-1}. It is known from experiment that the constant $\underline{a}$ is approximately one order of magnitude larger for Fe^{3+} than for Mn^{2+}. The reason for it is that the ratio λ / E_{PS} is somewhat larger for Fe^{3+} than for Mn^{2+}; furthermore, the quantity K is obviously larger for a trivalent ion than for a divalent one.

The origin of the first (and second) term of the spin Hamiltonian can be explained in two ways. Abragam and Pryce [17] called attention to the following splitting mechanism. The magnetic dipole interaction of the electron spins inside a paramagnetic atom depends not only on their relative orientation, but also on the electron coordinates. If the electron probability cloud has a cubic or spherical symmetry, then the averaged energy of the spin-spin interaction is independent of the orientations of the spins relative to one another; consequently the ground state of the paramagnetic ion is fully spin-degenerate. A field of tetragonal or trigonal symmetry slightly deforms the electron clouds and makes it ellipsoidal in shape. In this case the spin-spin interaction averaged over the electron cloud will depend on the relative orientations of the spins. The splitting of the energy ground level of a

paramagnetic ion occurs already in the second approximation and it will be proportional to $\hat{S}_z^2 - 35/12$. The constant D can be estimated from the formula

$$D \approx \frac{U\left(\frac{\beta^4}{r^4}\right)}{E_{DS}}. \tag{3.52}$$

Here $U = \langle 3d|U_2^0|4s\rangle$, and E_{DS} is the interval between the $3d^44s\,^6D$ and $3d^5\,^6S$ terms. According to Watanabe [62] a term of the type $D\hat{S}_z^2$ arises in fourth-order perturbation-method calculations, if simultaneous account is taken of the spin-orbit interaction and the effect of cubic and axial symmetry fields. An estimate of the splitting can be made with the aid of the formula

$$D \approx \frac{\lambda^3 KU'}{E_{DS}^3}, \tag{3.53}$$

where $U' = \langle 3d|U_2^0|3d\rangle$. Both formulas (3.52) and (3.53) yield $|D| \approx 0.1$ cm^{-1} if we assume $U = U' = 10^3$ cm^{-1}, $E_{DS} = 2.5 \cdot 10^4$ cm^{-1}, and $\overline{r^{-3}} = 5a_0^{-3}$; this is in good agreement with the experimental data.

Analogous splitting mechanisms were considered in other papers [62] devoted to calculations of the principal terms of ions in the S state.

If the paramagnetic resonance spectra of ions in the S state display a hyperfine structure, this structure can be calculated by adding to (3.50) the spin Hamiltonian (3.29). The presence of a hyperfine structure in electron energy levels of ions in the S state is apparently due exclusively to the configuration interaction.

§3.9. Covalent Bonds; 3d, 4d, and 5d Transition Groups

Ionic crystals, the paramagnetism of which is due to elements of the 3d, 4d, and 5d transition groups, frequently contain octahedral complexes MX_6: the center of such a complex is occupied by an atom M with unfilled $\underline{d}$ shell, and the vertices of the octahedron are either

water molecules, CN radicals, or atoms of chlorine, fluorine, etc. The bond inside the MX_6 complex is frequently covalent, something first pointed out by Pauling [63], who attempted to explain the singularities of magnetic properties of potassium ferrocyanide with the aid of the theory of localized pairs. Van Vleck [64] showed, however, that the experimental facts pertaining to static magnetic susceptibility can be equally well explained by assuming covalent forces within the complex $Fe(CN)_6$ or by advancing the hypothesis that the interaction is purely ionic, but that a strong crystalline field disturbs the normal type of bond between the electrons of the iron atom.

If the molecular orbital method is compared with the localized pair method, it turns out that the results obtained by the former method are more general and closer to the experimental facts. Detailed calculations of the energy splittings in a strong crystalline field were made for an atom with configuration d^5 [65]. Van Vleck's theory was later extended to include cyanides of other elements with electron configurations from d^1 to d^4 [66]. A further impetus in the development of the theory of the covalent bond inside the MX_6 complex was produced by the discovery of the unusual hyperfine structure of the paramagnetic resonance spectrum of iridium [67]. It turned out that the absorption line of the iridium contained in $[IrCl_6]$ has a structure due to the magnetic moment of the chlorine nucleus, and this fact points clearly to the covalent character of the bond within the complex. A detailed analysis shows that the hyperfine structure of the spectrum of Ir cannot be attributed to the σ bond, which was already investigated by Van Vleck, so that it becomes necessary to assume that the π bond between the iridium and the chlorine also plays a noticeable role. A general analysis of the theory of paramagnetic resonance in MX_6 complexes with covalent σ and π bonds was made by Stevens [68].

- 98 -

Data were soon compiled on the absorption of light by hydrated salts of the iron-group elements as well as experimental results on paramagnetic resonance in these substances [69].

Contradictions arose, and these could be eliminated by assuming that the bond in the octahedral complex is partially covalent. Double covalent bonds were established in the vanadium complex of vanadium sulfate [70] by comparing the paramagnetic resonance data with results of observation of optical absorption spectra and x-ray structural analysis. Further generalization of the theory became necessary to explain the spectra of paramagnetic resonance of chelates [71] and fluorites of the iron-group elements [72]; to set up the molecular orbitals for fluorides it was necessary to involve not only the 2s and 2p functions of the fluorine but also states with principal quantum number n = 3. We note also that to explain the hyperfine structure of Mn^{2+} ions introduced into the ZnF_2 crystal it becomes necessary to take the covalent bonds into account [89].

We shall present a general analysis of the effect of covalent bonds on paramagnetic resonance spectra of the elements of d transition groups by following Stevens [68] and Owen [69] and using the method of molecular orbitals.

a) Energy levels and molecular orbitals of a complex

If the bond were purely ionic in nature, the atom would be a positive ion with unfilled nd shell (n = 3, 4, 5), inside of which the electrons are distributed over the following orbitals*: $d_{3z^2-r^2}$, $d_{x^2-y^2}$, d_{xy}, d_{yz}, d_{zx}. The subscripts indicate the angular dependence of the real d wave functions. If we disregard the interaction between the electrons, then the ground level of the atom M splits in a crystal field of cubic symmetry in accordance with (3.11) into a lower triplet and an upper doublet. The first two of the listed orbitals belong to

- 99 -

the doublet and are called after Bethe [1], the dγ-orbitals. The functions d_{xy}, d_{yz}, and d_{zx} belonging to the triplet are called dε-orbitals.

In the ion approximation the particle X is diamagnetic and is a negative ion with a p shell that is filled as a rule; examples are X = $= Cl^{-1}$ or O^{-2}.* The orbital functions of the atoms M and X_6 must be used to set up the molecular orbitals of the entire octahedral complex.

We first consider the covalent σ bond, which is formed by the orbitals of the central atom ndγ, (n + 1)s, (n + 1)p and the p_σ orbitals of the surrounding atoms, which overlap the former appreciably. We include among the p_σ orbitals also the s functions of the X atoms. Altogether, we can construct 6[2(dγ) + 1(s) + 3(p)] binding six disintegrating orbitals, four of which contain magnetic dγ orbits [64]:

$$
\begin{aligned}
\sigma^{*}_{3z^2-r^2} &= \alpha d_{3z^2-r^2} - \sqrt{1-\alpha^2}\frac{1}{\sqrt{21}} \times \\
& \qquad \times [2p_6 - 2p_3 + p_1 + p_2 - p_4 - p_5]_\sigma, \\
\sigma^{*}_{x^2-y^2} &= \alpha d_{x^2-y^2} - \sqrt{1-\alpha^2}\frac{1}{2}[p_2 + p_4 - p_1 - p_5]_\sigma;
\end{aligned}
\qquad (3.54)
$$

$$
\begin{aligned}
\sigma_{3z^2-r^2} &= \sqrt{1-\alpha^2}d_{3z^2-r^2} + \alpha\frac{1}{\sqrt{21}} \times \\
& \qquad \times [2p_6 - 2p_3 + p_1 + p_2 - p_4 - p_5]_\sigma, \\
\sigma_{x^2-y^2} &= \sqrt{1-\alpha^2}d_{x^2-y^2} + \alpha\frac{1}{2}[p_2 + p_4 - p_1 - p_5]_\sigma.
\end{aligned}
\qquad (3.55)
$$

We denote here the binding orbits by σ, the disintegrating orbits by σ*, and use the subscripts 1, 2, 3, 4, 5, and 6 for the X atoms located on the axes X, Y, Z, —X, —Y, —Z, respectively. The coefficient α shows to what extent the ψ functions of the central atom and of the environment are mixed. If α = 1, the bond is purely ionic; on the other hand, if $\alpha^2 = 1 - \alpha^2 = 0.5$, the electrons are shared by M and X_6 with equal probability.

The covalent π bond can be formed by mixing the dε orbitals of the central atom with the p_π orbitals of X_6. This bond should generally speaking be weaker, since the directions of the combining orbitals are such that they overlap little. The molecular orbitals have the follow-

- 100 -

ing form [68, 69]:

$$\pi_{xy}^* = \beta d_{xy} - \sqrt{1 - \beta^2} \, \frac{1}{2} \, [p_1 + p_3 - p_4 - p_6]_\pi, \qquad (3.56)$$

$$\pi_{xy} = \sqrt{1 - \beta^2} \, d_{xy} + \beta \, \frac{1}{2} \, [p_1 + p_3 - p_4 - p_6]_\pi. \qquad (3.57)$$

The other four combinations π_{yz}, π^*_{yz}, π_{zx}, π^*_{zx} are obtained from (3.56) and (3.57) by cyclic permutation of the indices. The coefficient β shows how large the π bond is; when $\beta = 1$ there is no π bond. In expressions (3.54)-(3.57) we have neglected the influence of the overlap of the atomic orbitals of M and X_6 and the normalizations of the σ and π functions.

Figure 3.3 shows a possible level scheme for the free atoms M and X_6 and for the complex MX_6. We see that the σ bond increases the splitting Δ due to the cubic field of the crystal, while the π bond decreases it somewhat. This scheme applies to the cases $X = Cl^{-1}$ and H_2O; on the other hand if $X = CN^-$, then the formation of the π bond with M occurs with the aid of the orbitals of the excited level of the carbon atom, which lies above the dε level. Because of this, the sign of β should be reversed in (3.56) and (3.57), so that the binding orbitals become disintegrating orbitals and vice versa. Now the π bond also leads to an increase in Δ.

To develop the theory further, as already mentioned in §3.1, it is important to compare the action of the cubic field with the interaction between electrons, leading to the formation of the term. In hydrated salts of the iron group elements the value of Δ is much smaller than the interval between the different terms of the free paramagnetic ions; in cyanide and in a few other salts of the element of the same group, the inverse relation holds true in the compounds of the elements of the 4d and 5d transition groups. The apparent reason for the latter is that in heavy elements, first, the Russel-Saunders coupling

- 101 -
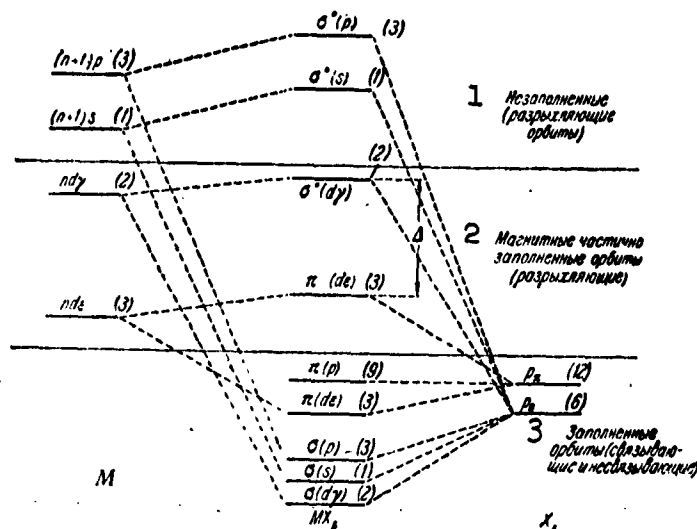
Fig. 3.3. Scheme showing the transition from the orbital energy levels of a paramagnetic atom M and of diamagnetic atoms X_6 to the energy levels of the complex MX_6. The figures in the parentheses indicate the degrees of orbital degeneracy of the levels. 1) Unfilled (disintegrating orbitals); 2) magnetic partially filled orbitals (disintegrating); 3) filled orbitals (binding and nonbinding).

is weak and, second, the $\underline{d}$ orbits lie farther away from the nucleus and therefore overlap more strongly the orbits of the X_6 atoms.

b) Hydrated salts of the iron group elements

The procedure for calculating the spectrum of the paramagnetic resonance is the same as in §3.3, but only the perturbation matrix elements (3.12) need now be calculated with allowance for the presence of the covalent bonds. For this purpose, it is necessary to expand the wave function of the entire unfilled electron shell in terms of $\underline{d}$ functions of the individual electrons, and the latter must then be replaced by the orbitals (3.54)-(3.57). Owen [69], who took only σ bonds into account, has shown that systematic discrepancies between the optical and magnetic data on the intervals Δ can be eliminated by choosing suitable values of the coefficient α. Thus, for example, for Ni^{2+}

we have in accord with the previously developed purely ionic theory $g = 2.0023 - 8\lambda/\Delta$; on the other hand, if we take the covalent σ bonds into account, we obtain

$$g = 2,0023 - \alpha^4\frac{8\lambda}{\Delta}. \qquad (3.58)$$

This result can be interpreted in the following fashion: each of the two unpaired electrons has a probability α^2 of being in the nickel atom and a probability $1/6(1 - \alpha^2)$ of being in each water molecule. As a result the spin-orbit coupling is reduced and in place of λ we have $\lambda' = \alpha^2\lambda$. For the complex $[Ni(H_2O)_6]^{2+}$ the experimental values of Δ and λ, taken from optical observations, as well as the values of g obtained by measuring paramagnetic resonance, lead in accord with (3.58) to a value $\alpha = 0.83$. The covalent bonds should also decrease the hyperfine splitting, something indeed observed in copper salts [25].
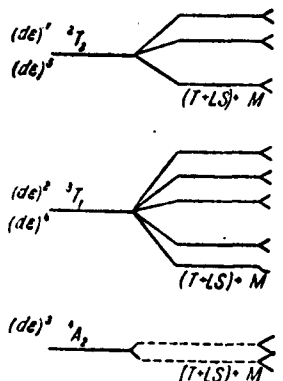
Fig. 3.4. Level splitting scheme of the ground state of the octahedral complex under the influence of the spin-orbit interaction (LS), the tetragonal field (T), and the magnetic field (M). It is assumed that the constant of the tetragonal field is $\delta > 0$; if $\delta < 0$, then the lower state for the configuration $(d\varepsilon)^2$ will be a doublet. The dashed lines indicate the splitting occurring only in the second perturbation theory approximation.

THIS
PAGE
IS
MISSING
IN
ORIGINAL
DOCUMENT

exception of $(d\varepsilon)^3$ have triple orbital degeneracy. Therefore, owing to the Jahn-Teller effect, the octahedral symmetry should be lowered.

We shall assume that a weak field of lower symmetry, such as tetragonal, is superimposed on the cubic field. We denote the total splitting due to this field by δ. If we furthermore take the spin-orbit interaction into account, we obtain the following series of values for the energy E_k*:

$$(d\varepsilon)^{1\,2}T_2: \quad E_1 = E_2 = -\frac{\delta}{3} - \frac{1}{2}\lambda,$$

$$E_{3,5} = E_{4,6} = \frac{1}{2}\left[\left(\frac{\lambda}{2} + \frac{\delta}{3}\right) \pm \sqrt{\frac{9}{4}\lambda^2 - \delta\lambda + \delta^2}\right]; \tag{3.59}$$

$$(d\varepsilon)^{2\,3}T_1: \quad E_{1,3} = E_{2,4} = \frac{1}{2}\left[-\frac{\delta}{3} \pm \sqrt{\delta^2 + \lambda^2}\right],$$

$$E_5 = E_6 = \frac{\delta}{3} - \frac{\lambda}{2},$$

$$E_{7,8} = \frac{1}{2}\left[-\frac{\delta}{3} + \frac{\lambda}{2} \pm \sqrt{\frac{9}{4}\lambda^2 + \delta\lambda + \delta^2}\right], \tag{3.60}$$

$$E_9 = \frac{\delta}{3} + \frac{\lambda}{2}.$$

The energy levels $(d\varepsilon)^{5\,2}T_2$ are obtained from $(d\varepsilon)^1$ and $(d\varepsilon)^{4\,3}T_1$ are obtained from $(d\varepsilon)^2$ by reversing the signs of δ and λ. The splitting of the level $(d\varepsilon)^3$ occurs only if the higher approximations of perturbation theory are included. In the case of an odd number of electrons we have Kramers' doublet, and therefore paramagnetic resonance can always be observed. If the number of electrons is odd, observation of paramagnetic resonance is possible (the ground states are singlets); an exception is the configuration $(d\varepsilon)^2$ if $\delta < 0$. Calculation of doublet splitting in a magnetic field shows that the g factor decreases, owing to the covalent bond. Thus, for $[IrCl_6]^{2-}$ we have, for example,

$$g = 2 - \frac{2}{3}(1 - \beta^2). \tag{3.61}$$

We have already indicated that covalent bonds produce a hyperfine structure in paramagnetic resonance lines, due not only to the momentum of the M nucleus, but also the momenta of the X_6 nuclei. Calcula-

tion of the hyperfine structure can be made with the aid of the spin Hamiltonian (3.20), containing an additional series of terms that take into account the spins of the X_6 nuclei. Thus, if a strong magnetic field is applied along the Z axis and only the octahedral symmetry of the crystalline field is taken into account, then the spin Hamiltonian has the form

$$\mathcal{H}_{cn} = g_{\parallel}\beta_0 H_0 \hat{S}_z + A(\hat{S}'_z \hat{I}_z)_0 + A'\{(\hat{S}'_z \hat{I}_z)_3 + (\hat{S}'_z \hat{I}_z)_6\}, \qquad (3.62)$$

where $A' = -(32/15)\beta^2(1 - \beta^2)g_0\beta_0\beta_N(\overline{r}^{-3})$. The subscript 0 pertains here to the central atom and the subscripts 3 and 6 to the X atoms located on the Z axis.

In conclusion we must note that the spin-orbit interaction can be described with the aid of a single constant λ only in the case of octahedral symmetry. Deviations of the field symmetry from octahedral cause anisotropy of the spin-orbit interaction.

§3.10. The Actinides

It is firmly established by now that the transition group of elements starting with thorium contains a partially filled 5f shell [44]. The actinides differ from the 4f transition rare-earth group in their tendency to form compounds that contain complexes which are rather stable chemically, similar to the uranyl ion $(UO_2)^{2+}$. A systematic investigation of the magnetic properties of the actinides, and particularly paramagnetic resonance, began only recently, and so far only compounds containing UO_2, NpO_2, and PuO_2 have been well investigated. The experimental data on these complexes have been theoretically interpreted in [74-76].

Let us start with an examination of the complex UO_2, although it does not have normal paramagnetism and therefore does not give rise to paramagnetic resonance.

The structure of this complex is linear: O–U–O. The free uranium

atom has a closed core and six valence electrons, forming a configuration $5f^3 6d 7s^2$. Two of these electrons are lost in $(UO_2)^{2+}$, and the four remaining ones produce a strong covalent bond with the oxygen atoms. In the simplest model used in [74, 75], only the σ bond is assumed. The linear combinations of the $5f_\sigma$, $6d_\sigma$, and $7s$ functions form orbitals which are highly elongated in the direction of the oxygen atoms, and strongly overlap the sp_σ orbitals of oxygen. Thus, no unpaired electrons remain in the ground state of $(UO_2)^{2+}$, and consequently compounds containing uranyl will either be diamagnetic or will have a weak temperature-independent paramagnetism.

The ions $(NpO_2)^{2+}$, $(PuO_2)^{2+}$ and $(AmO_2)^{2+}$ have a structure and chemical properties similar to those of $(UO_2)^{2+}$. It is natural to assume that the character of the bond of all these ions is the same, and that the additional electrons fill the $5f$ shell, similar to the $4f$ electrons of the trivalent ions Ce, Pr, and Nd. However, the trans-uranyl compounds differ greatly from the solid salts of the lanthanides in that the magnetic properties of the former are more sensitive to the crystalline field, whereas for the $5f$ electrons of the actinides the dominating effect is produced by the axially symmetrical field due to the binding electrons of the complex. In first approximation, the magnetic properties of a compound containing a transuranyl complex will be the same as those of a linear molecule; the crystalline field introduces small corrections.

The complex $(NpO_2)^{2+}$ contains one unpaired $\underline{f}$ electron, which moves in a strong field of axial symmetry. Therefore the conserving quantities will in first approximation be the components of its total (j_z), orbital $(\underline{1}_z)$ and spin (s_z) angular momenta about the symmetry axis, which we choose to be the Z axis. In an axial field, all possible values $|\underline{1}_z| = 3, 2, 1, 0$ will correspond to different energy

levels. The very lowest level, which is located about 10^4 cm^{-1} away from the neighboring one, corresponds to a state with $|l_z| = 3$, for in this case the charge of the unpaired electron is located in the equatorial plane, so that the repulsion between it and the electrons forming the σ bond will be minimal. This quadruply degenerate level ($l_z = \pm 3$, $s_z = \pm 1/2$) is split as a result of the spin-orbit interaction into two doublets: $j_z = \pm 5/2$, $\pm 7/2$. The first doublet lies 3000-4000 cm^{-1} below the second, and consequently it is the only one responsible for the paramagnetism of neptunyl.

The paramagnetic resonance spectrum can be calculated with the aid of the following simple spin Hamiltonian

$$\mathcal{H} = g_\parallel \beta H_z \, \hat{S}'_z + g_\perp \beta (H_x \, \hat{S}'_x + H_y \, \hat{S}'_y) + A \hat{I}_z \hat{S}'_z + $$
$$+ B(\hat{I}_x \hat{S}'_x + \hat{I}_y \hat{S}'_y) + P \left[\hat{I}_z^2 - \frac{1}{3} I(I+1) \right] - \gamma \beta_N H \hat{I}_z. \qquad (3.63)$$

Here $g_\parallel = 2\langle +| \hat{l}_z + 2\hat{s}_z |+\rangle$, $g_\perp = 2\langle +| \hat{l}_x + 2\hat{s}_x |-\rangle$, $|+\rangle$ and $|-\rangle$ denote the wave functions of the lower doublet, while S' is the effective spin with value 1/2. In the approximation that takes only the σ bond into account we have $g_\parallel = 4$, $g_\perp = 0$. If the possibility of the π bond is also taken into account then, as we have seen in the preceding section, the orbital momentum drops and l_z is replaced by kl_z; $k < 1$. Now $g_\perp \neq 0$, $g_\parallel = 6k - 2$. Comparison with the experimental data shows that $k = 0.9$.

Finally, it should be noted that the large electric field gradient produced by the electrons forming the covalent bond will give rise to a large hyperfine structure, due to the quadrupole moment of the Np nucleus.

The complex $(PuO_2)^{2+}$ contains two unpaired electrons, the motion of which is perturbed primarily by the axial field and by the electrostatic repulsion between them. For the same reason as in the case of neptunyl, it might appear that the unpaired electrons should occupy

the state $\underline{l}_z = \pm 3$. Actually, however, because of the electrostatic repulsion between the electrons, the ground state of the "configuration" $5f^2$ is determined by the modified Hund rule: the electron spin projection should be maximal, $S_z = 1$; the projection of the orbital momentum should have a maximum value compatible with $S_z = 1$, namely: $|\underline{l}_{1z}| = 3$, $|\underline{l}_{2z}| = 2$ and, consequently, $L_z = \pm 5$. The spin-orbit interaction causes further splitting of the energy levels, after which the lower level turns into a doublet with $J_z = \pm(5 - 1) = \pm 4$.

Elementary calculation shows that if we again introduce an effective spin $S' = 1/2$, then for this doublet $g_{\parallel} = 6$, $g_{\perp} = 0$. The probability of transition between magnetic sublevels is in this case equal to zero independently of the direction of the external magnetic field H. A detailed analysis shows that an account of different corrections does not change the fact that $g_{\perp} = 0$. As a result, the paramagnetic resonance has a maximum when the alternating magnetic field is parallel to the Z axis. The reason for it is that the previously unaccounted for crystalline field of lower symmetry causes an intermixing of the wave functions with $J_z = \pm 4$. It must be kept in mind that the doublet considered here is not a Kramers' doublet, for the number of unbound electrons is even in our case. Thus, the spin Hamiltonian will have the form

$$\mathcal{H} = g_{\parallel}\beta H_z \hat{S}'_z + A\hat{S}'_z\hat{I}_z + P\left[\hat{I}_z^2 - \tfrac{1}{3}I(I+1)\right] + \Delta_x\hat{S}'_x + \Delta_y\hat{S}'_y \quad (3.64)$$

The last two terms take into account the splitting due to a low-symmetry crystalline field.

§3.11. Influence of Exchange and Dipole Interactions on the Form of the Paramagnetic Resonance Spectrum

Interesting exchange effects were observed in certain salts of copper. The temperature dependence of the static magnetic susceptibility of copper acetate is unusual [77]. Sharp anomalies in the magnetic

behavior of this substance were also observed by the paramagnetic resonance method [78]. All these singularities can be explained as follows. The crystalline cell of copper acetate has two closely adjacent paramagnetic ions, which behave, as the result of the strong exchange bonds between them, in a manner similar to a single "molecule," capable of being either in a paramagnetic state with spin $S = 1$, or in a diamagnetic state with spin $S = 0$. It is well known [10] that the exchange bond is characterized in the absence of other forces acting on the spins by a cosinusoidal dependence on the spin direction; the exchange energy is equal to $-J\vec{S}_1\vec{S}_2$, where J stands for the exchange integral and S_1 and S_2 are the spins of the interacting atoms. It has been shown at the same time that if there are other than exchange forces, which also strongly influence the spin directions, then the cosinusoidal law may still be valid, but only for the "effective" spins [21, 22]. In copper acetate the exchange interactions are much stronger than the spin-orbit coupling (which appears only in the second approximation), and therefore the Hamiltonian for the system of two copper ions under consideration will have the form

$$\mathscr{H} = \hat{X}_1 + \hat{X}_2 - J\hat{S}_1\hat{S}_2 + \lambda(\hat{L}_1\hat{S}_1 + \hat{L}_2\hat{S}_2) +$$
$$+ \beta H_0(\hat{L}_1 + 2\hat{S}_1 + \hat{L}_2 + 2\hat{S}_2). \qquad (3.65)$$

The subscripts 1 and 2 are the numbers of the copper ions in the crystal cell, while the remaining terms of the Hamiltonian stand for the energy in the crystalline field, the exchange interaction, the spin-orbit coupling, and the energy in the external magnetic field. The exchange interactions split the lower orbital level of the "molecule" into a spin singlet and a triplet. It is possible to explain with the aid of (3.65) in natural fashion all the known facts concerning the static magnetic properties of copper acetate, the paramagnetic resonance spectrum, and its hyperfine structure.

- 110 -

The exchange interactions influence the form of the paramagnetic resonance spectrum also in copper sulfates [79], but here the anomalies have a different character, since the exchange energy is comparable in order of magnitude with the radio frequency quantum; its value is approximately 0.15 cm^{-1}, whereas in copper acetate $J = 300$ cm^{-1}.

The magnetic dipole interactions usually are causes of broadening of resonance lines. In some cases, however, when the substance is magnetically dilute and contains at the same time magnetic particles that lie closely to each other, these interactions can bring about the appearance of a fine structure of the paramagnetic absorption spectrum. Such a structure was observed in neodymium ethyl sulfate [80]. If the static magnetic field is parallel to the hexagonal axis of the crystal, then the spectrum comprises a symmetrical triplet with intervals of 360 oersteds between the extreme absorption peaks. The central peak has approximately double the intensity of the extreme ones. Simple calculation of the energy of dipole interaction between the ion and the neighboring particles yields values $\pm 2g_{\parallel}\beta/c^3, 0, 0$; here $c = 7A$ is the distance between two closest particles, located along the hexagonal axis. Thus, the satellites may be located $50g_{\parallel} = 180$ oersteds away from the central peak. A more complicated spectrum structure was established for gadolinium ethyl sulfate, this being due to the larger spin of the Gd^{3+} ion.

§3.12. Forbidden Spectral Lines. Multiple Quantum Transitions

So far, when speaking of a paramagnetic resonance spectrum, we had in mind resonance lines pertaining to such spin levels, the transition probabilities between which differ from zero in the first perturbation theory approximation. Let us consider now several causes of the appearance of additional "forbidden" resonance absorption lines.

a) Dipole interaction between magnetic centers

Let us assume that the crystalline field does not split the spin levels and that consequently each level corresponds to a definite value M of the spin momentum projection on the direction of the field H_0. Because of this, magnetic dipole transitions are possible in the first approximation only between neighboring levels ($\Delta M = \pm 1$) under the influence of the oscillating magnetic field perpendicular to the field H_0. We now take into account the magnetic dipole interactions between the paramagnetic centers of the crystals. Because of the interactions, the wave functions η_M(M = S, S − 1, ..., −S), pertaining to different spin levels become intermixed and assume the form (see

§5.2) $\eta_M + \sum_{l=M-2}^{M+2} \epsilon_l \eta_l$, where $\epsilon_1 \sim \beta^2/a^3 (g\beta H_0)^{-1}$; here $\underline{a}$ is the average distance between two neighboring magnetic centers. Now the nondiagonal matrix elements of the vector $\vec{S}$ will be different from zero not only in the case when $\Delta M = \pm 1$, but also for the transitions $\Delta M = \pm 2$ and ± 3. If we assume the intensity of the principal resonance line ($\Delta M = \pm 1$) to be equal to one, then the intensity of the lines $\Delta M = \pm 2$ and $\Delta M = \pm 3$ will be $\sim 4|\epsilon_1|^2$ and $9|\epsilon_1|^2$, respectively, if the oscillating field is perpendicular to the field H_0. If the fields are parallel, the transitions $\Delta M = \pm 1$ and $\Delta M = \pm 2$ give rise to two forbidden resonance lines, the intensity of which is $\sim |\epsilon_1|^2$ and $4|\epsilon_1|^2$. The existence of forbidden lines was first established experimentally by Zavoyskiy in manganese salts [81], and was later on observed by others [82].

b) Hyperfine interactions

With increasing concentration of the paramagnetic centers, the intensity of the additional absorption lines, due to the magnetic dipole interaction between centers, will become weaker. However, other forbidden absorption peaks can arise in this case, if the nuclei of the
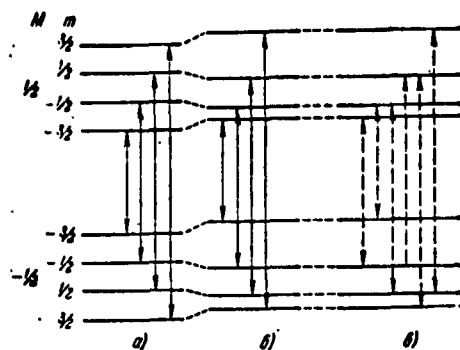
Fig. 3.5. Level scheme and transitions between levels in the case $S = 1/2$, $I = 1/2$. a) Quadrupole moment of the nucleus is equal to zero, the alternating magnetic field is perpendicular to H_0; b) quadrupole moment different from zero, the alternating field is perpendicular to H_0; c) quadrupole moment different from zero, alternating field parallel to H_0 (forbidden transitions).

paramagnetic atoms have a spin different from zero. Let us assume that the spectrum of the paramagnetic resonance can be described by the following spin Hamiltonian:

$$\mathcal{H}_{cn} = D\{\hat{S}_z^2 - \tfrac{1}{3}S(S+1)\} + \beta \{g_{\parallel}H_z\hat{S}_z + g_{\perp} (H_x\hat{S}_x + H_y\hat{S}_y)\} +$$
$$+ A\hat{S}_z\hat{I}_z + B(\hat{S}_x\hat{I}_x + \hat{S}_y\hat{I}_y) + P\{\hat{I}_z^2 - \tfrac{1}{3}I(I+1)\}. \qquad (3.66)$$

We assume first that the field H_0 is parallel to the Z symmetry axis of the crystalline field. Figure 3.5a shows the system of energy levels arising under the influence of the magnetic hyperfine interaction for the particular case $S = 1/2$, $I = 3/2$. Because of the quadrupole interaction, the energy levels cease to be equidistant (Fig. 3.5b). To each level there corresponds a wave function $\eta_{M,m}$ with a definite magnetic quantum number M of the electron spin and a magnetic quantum number $\underline{m}$ of the nuclear spin. The arrows in Fig. 3.5b denote the transitions that are allowed by the selection rule $\Delta M = \pm 1$, $\Delta m = 0$, provided

- 113 -

the oscillating field is perpendicular to the permanent field.

In the second approximation of perturbation theory, owing to the term $B(\hat{S}_x\hat{I}_x + \hat{S}_y\hat{I}_y)$, the wave functions assume the form $\eta_{M,m}$ + + $\alpha\eta_{M\pm1,m\mp1}$, where $\alpha \sim B/g_{\parallel}\beta H_0$. It is easy to verify that now, if the magnetic oscillating field is parallel to H_0, there should appear additional absorption peaks, corresponding to the transitions $\Delta M = \pm1$, $\Delta M = \pm2$. These transitions are shown in Fig. 3.5c by the dotted arrows. The intensity of the forbidden lines is related to the intensity of the principal lines of paramagnetic resonance approximately as $|\alpha^2|:1$. Forbidden absorption lines in parallel fields were observed experimentally in salts of cobalt, manganese, and vanadium [83].

If the field H_0 is inclined to the Z axis of the crystal, then the possibilities for forbidden transitions become greater. The additional lines appear not only in parallel but also in perpendicular fields. The spectrum becomes particularly enriched with forbidden lines if the quadrupole interactions between the nuclei and the crystalline field are large [84].

c) Multiple quantum transitions

The reason for the appearance of additional absorption lines may be quantum transitions connected with simultaneous absorption of several
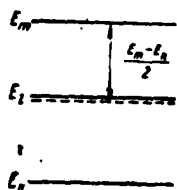
Fig. 3.6. Scheme of two quantum transitions between levels k and m.

eral photons by the paramagnetic atoms. Such transitions, which are forbidden in the first perturbation theory approximation, become possible in the higher approximations via one or several intermediate states of the atom. Multiple quantum transitions produced under the influence of a powerful radio frequency field, were first discovered in experiments with molecular beams [85], and then by the method of nuclear magnetic resonance [86]. Observation of electron paramagnetic

resonance has recently disclosed the existence of multiple quantum transitions in Mn^{2+} ions introduced into the MgO lattice [87].

Let us assume that among the energy spin levels there are three such levels E_k, $E_{\underline{l}}$, and E_m (Fig. 3.6) that $\omega_{\underline{l}k} \neq \omega_{m\underline{l}}$, but $|\omega_{m\underline{l}} - \omega_{\underline{l}k}| \ll \ll 1/2\omega_{mk}$ $(\omega_{\underline{i}\underline{j}} = (E_{\underline{i}} - E_{\underline{j}})/\hbar)$. We assume also that in first approximation the transitions between neighboring levels $k \longleftrightarrow \underline{l}$ and $\underline{l} \longleftrightarrow m$ are allowed, but the transition $k \longleftrightarrow m$ is forbidden. The state of the paramagnetic center can be described with the aid of the Hamiltonian

$$\mathscr{H} = \mathscr{H}_{cn} + \mathscr{H}', \quad \mathscr{H}' = g\beta H_1 \hat{S} = \tfrac{1}{2} g\beta H_1 \{\hat{S}_- e^{i\omega t} + \hat{S}_+ e^{-i\omega t}\}, \qquad (3.67)$$

where $\hat{H}_{sp}$ is the spin Hamiltonian which determines the system of spin energy levels of the paramagnetic center, and $\hat{H}'$ is the time-dependent part of the Hamiltonian representing the interaction with the radio frequency magnetic field, while $\hat{S}_\pm = \hat{S}_x \pm i\hat{S}_y$. In this case we consider, to simplify the calculations, a field rotating with angular velocity ω in place of an oscillating field.

We assume that at the initial instant of time the atom is in the state $\underline{k}$. Then in first approximation of the theory of time-dependent perturbations, the probability that the atom will be in the state $\underline{l}$ at the instant of time $\underline{t}$ is

$$|a_{k\underline{l}}^{(1)}(t)|^2 = \frac{g^2\beta^2 H_1^2}{4\hbar^2} |\langle k|\hat{S}_+|l\rangle|^2 \left|\frac{e^{i(\omega_{\underline{l}k} - \omega)t} - 1}{\omega_{\underline{l}k} - \omega}\right|^2; \qquad (3.68)$$

and in the second approximation of perturbation theory we have

$$|a_{km}^{(2)}(t)|^2 = \frac{g^4\beta^4 H_1^4 |\langle k|\hat{S}_+|l\rangle|^2 |\langle l|\hat{S}_+|m\rangle|^2}{16\hbar^4(\omega_{\underline{l}k} - \omega)^2} \times$$
$$\times \left|\frac{e^{i(\omega_{mk} - 2\omega)t} - 1}{\omega_{mk} - 2\omega}\right|^2. \qquad (3.69)$$

We see that the probability of the transition $k \longleftrightarrow m$ is appreciably different from zero if, first, the frequency of the alternating field is equal approximately to $\omega_{mk}/2$, and, second, if the matrix elements of the perturbation, which relate the levels $\underline{m}$ and $\underline{k}$ with the inter-

- 115 -

mediate level $\underline{1}$, are not equal to zero. Let us now take account of the fact that the absorption line is finite, for which purpose we introduce the form function $g(\omega)$ (see §1.3). Carrying out, as usual, the integration

$$W_{ij} = \int |a_{ij}(t)|^2 g_{ij}(\omega) \, d\omega, \tag{3.70}$$

we see that the probabilities of the transition are proportional to the time $\underline{t}$. If we take also account of the difference in the populations of the levels E_k, $E_{\underline{1}}$, and E_m and recognize that the quantity $g_{ij}(0)$ is inversely proportional to the absorption line width $\Delta\nu_{ij}$, then we obtain for the ratio of the intensity I_2 of the line due to the two-quantum transitions, to the intensity I_1 of the ordinary $\underline{1} \longleftrightarrow k$ resonant line the following expression:

$$\frac{I_2}{I_1} = \frac{1}{2} \left(\frac{\frac{g\beta H_1}{\hbar}}{\omega_{1k} - \frac{1}{2}\omega_{mk}} \right)^2 \frac{\Delta\nu_{kl}}{\Delta\nu_{km}} |\langle l|\hat{S}_+|k\rangle|^2. \tag{3.71}$$

We see that the intensity of the line, resulting to the two-quantum transitions, becomes larger if the frequency of the Larmor precession, corresponding to the magnetic field H_1, is comparable with the frequency interval between the ordinary absorption line, connected with the transitions $k \longleftrightarrow \underline{1}$ and $\underline{1} \longleftrightarrow m$. We note that when the power of the radio frequency field is so large that $g\beta H_1/\hbar \sim (\omega_{\underline{1}k} - 1/2\omega_{mk})$, then the use of perturbation theory is not justified, and formula (3.71) is no longer valid.

Along with the two-quantum transitions which we have considered, other transitions are also possible, due to the absorption of three or more photons. In the third perturbation-theory approximation we obtain for the probability of a three-quantum transition

$$|a_{kn}^{(3)}(t)|^2 = \frac{g^3\beta^3 H_1^3 |\langle k|S_+|l\rangle|^2 |\langle l|S_+|m\rangle|^2 |\langle m|S_+|n\rangle|^2}{64\hbar^6 (\omega_{lk}-\omega)^2 (\omega_{mk}-2\omega)^2} \times$$
$$\times \left|\frac{e^{i(\omega_{nk}-3\omega)t}-1}{\omega_{nk}-3\omega}\right|^2 . \qquad (3.72)$$

Here $\underline{l}$ and $\underline{m}$ are intermediate states through which the transition under consideration becomes possible.

REFERENCES (Chapter 3)

1. Bethe, H.A., Ann. Phys. 3, 133, 1929; Runchiman, W.A., Phil. Mag. 1, 1075, 1956.

2. Kramers, H.A., Proc. Acad. Sci. Ams. 33, 959, 1930.

3. Van Vleck, J.H., The theory of electric and magnetic susceptibilities, Oxford, 1932; Phys. Rev. 41, 208, 1932.

4. Penney, W.G., Schlapp, R., Phys. Rev. 41, 194, 1932.

5. Schlapp, R., Penney, W.G., Phys. Rev. 42, 666, 1932.

6. Kynch, G.F., Trans. Faraday Soc. 33, 1402, 1937; Penney, W.G., Kynch, G.F., Proc. Roy. Soc. A170, 112, 1939; Polder, D., Physica 9, 709, 1942.

7. Landau, L., Lifshits, Ye., Kvantovaya mekhanika [Quantum Mechanics], Gostekhizdat [State Publishing House for Technical and Theoretical Literature], 1948.

8. Stevens, K.W.H., Proc. Phys. Soc. A65, 209, 1952.

9. Bleaney, B., Stevens, K.W.H., Rep. Progr. Phys. 16, 108, 1953.

10. Vonsovskiy, S.V., Sovremennoye ucheniye o magnetizme [Modern Theory of Magnetism], Gostekhizdat, 1952.

11. Pryce, M.H.L., Phys. Rev. 80, 1107, 1950.

12. Jahn, H.A., Teller, E., Proc. Roy. Soc. A161, 220, 1937; Jahn, H.A., Proc. Roy. Soc. A164, 117, 1938.

13. Van Vleck, J.H., J. Chem. Phys. 7, 72, 1939.

14. Öpik, U., Pryce, M.H.L., Proc. Roy. Soc. A238, 425, 1957; Lonquet, H.C., Öpic, U., Pryce, M.H.L., Sack, R.A., Proc. Roy. Soc.

A244, 1, 1958.

15. Gorter, C.J., Phys. Rev. 42, 437, 1932.

16. Pryce, M.H.L., Proc. Phys. Soc. A63, 25, 1950.

17. Abragam, A., Pryce, M.H.L., Proc. Roy. Soc. A205, 135, 1951.

18. Pryce, M.H.L., Nature, London, 164, 117, 1949; Abragam, A., Pryce, M.H.L., Proc. Roy. Soc. A206, 173, 1951.

19. Kambe, K., Koide, S., Usui, T., Progr. theor. Phys. 7, 15, 1952.

20. Ollom, J.F., van Vleck, J.H., Physica 17, 205, 1951.

21. Stevens, K.W.H., Proc. Roy. Soc. A214, 237, 1952.

22. Ishiguro, E., Kambe, K., Usui, T., Physica 17, 310, 1951.

23. Pryce, M.H.L., Nature, London, 162, 539, 1948.

24. Abragam, A., Pryce, M.H.L., Proc. Roy. Soc. A205, 135, 1951; A206, 164, 1951.

25. Bleaney, B., Bowers, K.D., Pryce, M.H.L., Proc. Roy. Soc. A228, 166, 1955.

26. Van Vleck, J.H., J. Chem. Phys. 7, 61, 1939.

27. Becquerel, J., Opechowski, W., Physica 6, 1039, 1939.

28. Finkelstein, R., van Vleck, J.H., J. Chem. Phys. 8, 790, 1940.

29. Broer, L.J.F., Physica 9, 547, 1942.

30. Weiss, P.R., Phys. Rev. 73, 470, 1948; 74, 1478, 1948.

31. Kittel, C., Luttinger, J.M., Phys. Rev. 73, 162, 1948.

32. Brovetto, P., Ferroni, S., Nuovo Cimento 9, 628, 1952.

33. Mejer, P.H.E., Gerritsen, H.J., Phys. Rev. 100, 742, 1955.

34. Davis, C.F., Strandberg, M.W.P., Phys. Rev. 105, 446, 1957.

35. Abragam, A., Pryce, M.H.L., Nature, London, 163, 992, 1949.

36. Abragam, A., Pryce, M.H.L., Proc. Phys. Soc. A63, 409, 1950.

37. Abragam, A., Phys. Rev. 79, 534, 1950; Physica 17, 209, 1951.

38. Fermi, E., Zs. f. Phys. 60, 320, 1930.

39. Bleaney, B., Phil. Mag. 42, 441, 1951; Physica 17, 441, 175, 1951.

40. Abragam, A., Horowitz, J., Pryce, M.H.L., Proc. Roy. Soc. A230, 169, 1955.

41. Lipson, H., Beevers, C.A., Proc. Roy. Soc. A148, 664, 1935; Lipson, H., Proc. Roy. Soc. A151, 347, 1935.

42. Kleiner, W.H., J. Chem. Phys. 20, 1784, 1952.

43. Tanabe, Y., Sugano, S., J. Phys. Soc. Japan, 9, 753, 766, 1954; 11, 864, 1956.

44. Yel'yashevich, M.A., Spektry redkikh zemel' [Rare-Earth Spectra], Gostekhizdat, 1953.

45. Elliott, R.J., Stevens, K.W.H., Proc. Roy. Soc. A218, 553, 1953.

46. Lang, R., Canad. J. Res. 14, 127, 1936.

47. Hellwege, K.H., Kahle, H.C., Zs. f. Phys. 129, 62, 1950.

48. Gobrecht, H., Ann. Phys. 31, 300, 1938.

49. Bethe, H.A., Spedding, F.H., Phys. Rev. 52, 454, 1937.

50. Elliott, R.J., Stevens, K.W.H., Proc. Roy. Soc. A215, 437, 1952; Elliott, R.J., Rev. Mod. Phys. 25, 167, 1953.

51. Judd, B.R., Proc. Roy. Soc. A227, 552, 1955.

52. Elliott, R.J., Judd, B.R., Runchiman, W.A., Proc. Roy. Soc. A240, 509, 1957.

53. Elliott, R.J., Stevens, K.W.H., Proc. Phys. Soc. A64, 932, 1951.

54. Elliott, R.J., Stevens, K.W.H., Proc. Roy. Soc. A219, 387, 1953.

55. Elliott, R.J., Stevens, K.W.H., Proc. Phys. Soc. A64, 205, 1951; A65, 370, 1952.

56. Judd, B.R., Proc. Roy. Soc. A232, 458, 1955.

57. Judd, B.R., Proc. Roy. Soc. A241, 122, 1957.

58. Judd, B.R., Proc. Phys. Soc. B70, 880, 1957.

59. Afanas'yeva, N.V., Dissertation, Leningrad, GPI [State Polytechnic Institute], 1955.

60. Boer, J., Lieshout, R., Physica 15, 569, 1949; Debye, P., Ann.

Phys. 32, 85, 1937; Kronig, R. de L., Bouwkamp, C.J., Physica 6, 290, 1939; Lacroix, R., Helv. Phys. Acta 30, 374, 1957.

61. Van Vleck, J.H., Penney, W.G., Phil. Mag. 17, 961, 1934.

62. Watanabe, H., Progr. theor. Phys. 18, 405, 1957; Hutchison, C.A., Judd, B.R., Pope, D.F.D., Proc. Phys. Soc. B70, 514, 1957; La- croix, R., Helv. Phys. Acta 30, 478, 1957.

63. Pauling, L., J. Amer. Chem. Soc. 53, 1367, 1931.

64. Van Vleck, J.H., J. Chem. Phys. 3, 807, 1935.

65. Howard, J.B., J. Chem. Phys. 3, 207, 1935.

66. Kotani, M., J. Phys. Soc. Japan 4, 293, 1949; Kamimura, H., J. Phys. Soc. Japan 11, 1171, 1956.

67. Owen, J., Stevens, K.W.H., Nature, London, 171, 836, 1953.

68. Stevens, K.W.H., Proc. Roy. Soc. A219, 542, 1953.

69. Owen, J., Proc. Roy. Soc. A227, 183, 1955; Disc. Faraday Soc. 19, 127, 1955.

70. Palma-Vittorelli, M.B., Palma, M.U., Palumbo, D., Sgarlata, F., Nuovo Cimento 3, 718, 1956.

71. Maki, A.H., McGarvey, B.R., J. Chem. Phys. 29, 31, 35, 1958.

72. Tinkham, M., Proc. Roy. Soc. A236, 549, 1956.

73. Mulliken, K., Phys. Rev. 43, 279, 1933; J. Chem. Phys. 3, 375, 1935.

74. Elliott, R.J., Phys. Rev. 89, 659, 1953.

75. Eisenstein, J.C., Pryce, M.H.L., Proc. Roy. Soc. A229, 20, 1955.

76. Eisenstein, J.C., Pryce, M.H.L., Proc. Roy. Soc. A238, 31, 1956.

77. Guha, B.C., Proc. Roy. Soc. A206, 353, 1951.

78. Bleaney, B., Bowers, K.D., Phil. Mag. 43, 372, 1952.

79. Bagguley, D.M.S., Griffiths, J.H.E., Proc. Roy. Soc. A201, 366, 1950.

80. Bleaney, B., Elliott, R.J., Scovil, H.E.D., Proc. Phys. Soc. A64, 933, 1951.

81. Zavoyskiy, Ye.K., DAN [Proceedings Acad. Sci. USSR], 57, 887, 1947.

82. Buckmaster, H.A., Canad. J. Phys. 34, 150, 341, 1956; Gorter, K.D.,
    UFN [Progress in the Physical Sciences] 53, 545, 1954.

83. Jeffries, C.D., Phys. Rev. 106, 164, 1957; Abragam, M., Kedzie,
    R.W., Jeffries, C.D., Phys. Rev. 106, 165, 1957; Jeffries, C.D.,
    Low Temperat. Phys. and Chem., Madison. Univ. Wisconsin Press,
    634, 1958; Anderson, W.A., Piette, L.H., J. Chem. Phys. 30, 591,
    1959.

84. Bleaney, B., Phil. Mag. 42, 441, 1951.

85. Hughes, V., Grabner, L., Phys. Rev. 79, 314, 1950; Kusch, P.,
    Phys. Rev. 93, 1022, 1954; Besset, C., Horowitz, J., Messiah, A.,
    Winter, J., J. Phys. Radium 15, 251, 1954; Brossel, J., Cagnac, B.,
    Kastler, A., J. Phys. Radium 15, 6, 1954; Hughes, V., Geiger, J.S.,
    Phys. Rev. 99, 1842, 1955.

86. Anderson, W., Phys. Rev. 104, 850, 1956; Kaplan, J.I., Meibloom,
    S., Phys. Rev. 106, 499, 1957; Bloembergen, N., Sorokin, P., Phys.
    Rev. 110, 865, 1958; Salwen, H., Phys. Rev. 101, 623, 1956; Yat-
    siv, S., Bull. Am. Phys. Soc., ser. II, 3, 144, 1958.

87. Sorokin, P.P., Gelles, I.L., Smith, W.V., Phys. Rev. 112, 1513,
    1958.

88. Bleaney, B., Proc. Phys. Soc. 73, 937, 939, 1959.

89. Mukherji, A., Das, T.P., Phys. Rev. 111, 1479, 1958.

Manu-script Page No.	[Footnotes]
56	Certain exceptions will be discussed later (see §3.11).
88	In this section we do not concern ourselves with salts having ions in the S state.
90	Exceptions are encountered. For example, in cerium ethyl sulfate the two lower levels of the ion are noticeably populated even at liquid-helium temperature.
99	By orbitals we mean, as is customary in quantum chemistry, the "orbital" wave functions of individual electrons.
100	If the octahedral complex is formed by water molecules, then the oxygen atom faces the M atom.
105	We use Mulliken's notation for the terms of the octahedral complex [73].

Manu-script Page No.	[List of Transliterated Symbols]
59	кр = kr = kristallicheskiy = crystalline
61	тетр = tetr = tetragonal'nyy = tetragonal
61	триг = trig = trigonal'nyy = trigonal
61	гекс = geks = geksagonal'nyy = hexagonal
61	ромб = romb = rombicheskiy = rhombic
61	трикл = trikl = triklinicheskiy = triclinic
61	куб = kub = kubicheskiy = cubic
71	сп = sp = spin = spin
81	эфф = eff = effektivnyy = effective

Chapter 4

SPECTRA OF IONIC CRYSTALS. EXPERIMENT

§4.1. Introduction. Crystallographic Data

The experimental data on the paramagnetic resonance spectra in solids are listed below in the form of tables in §4.2. The data on spectra in liquid solutions of salts are contained in §4.3. Finally, §4.4 gives information on nuclear spins discovered with the aid of paramagnetic resonance. In the first column of the tables in §4.2 there are contained, in addition to the chemical formulas for the paramagnetic substance, also the degree of its dilution by the diamagnet (usually in atomic percent) and data on the crystal structure. If the latter is included among the ten most important types considered in the present section (see below, pages 126-129), the corresponding number is listed in the first column. For example, cr. st. 1 denotes that the compound is of the alum type. For other crystal structures, reference is made to the corresponding crystallographic literature; the number of such reference is accompanied by the letter "k." A list of these references is given for all the ions at the end of the chapter. The next columns give the temperature of the experiment and the basic spin-Hamiltonian constants in cm^{-1},* determined from the type of the spectrum.

The arrangement of the material follows that used in the preceding chapter. We first consider the ions of the iron group, the lower orbital level of which in octahedral magnetic complexes is a singlet (V^{2+}, Cr^{3+}, Ni^{2+}), and the neighboring ions Cr^{2+}, Mn^{3+} and Cu^{2+}, which

- 123 -

also have a lower orbital singlet in a crystal field with tetragonal component. Finally, it is necessary to include in the same group such compounds as $CsCoCl_5$, in which the magnetic ion Co^{2+} is surrounded by a distorted tetrahedron of Cl^-. In a tetrahedral magnetic complex, the sign of the cubic field is opposite that in an octahedral complex. Consequently, the orbital levels are inverted, and the Co^{2+} ion produces in this compound a spectrum which is similar to the spectra of the compounds of trivalent chromium or divalent vanadium.

The next group of tables contains data on the ions Ti^{3+}, V^{4+}, V^{3+}, Fe^{2+}, and Co^{2+} (Table 4.2). These are followed by the rare earths. We first give data for the rare-earth ions with odd number of electrons (Table 4.3), and then for those with even numbers (Table 4.4).

The ions of all the periodic-system groups in the S state (Mn^{2+}, Fe^{3+}, Gd^{3+}, Eu^{2+}, and Cm^{3+}) are listed separately (Table 4.5).

The next set of tables is devoted to compounds in which strong covalent bonds occur between the paramagnetic ion and its surroundings (individual compounds of the iron group, and also compounds of the palladium and platinum groups, and finally the actinides; see Table 4.6).

Table 4.7 lists some data on the compounds containing atoms of metals in anomalous valence states.

Within each group of tables, the ions appear in order of increasing atomic number of the element in the periodic system.

To facilitate the use of the bibliography, the references are given for each ion separately. The remarks contain certain special information concerning the structure of the given compound and other properties. The symbols used in the tables are explained on page 3.

For each ion, the data obtained with dilute single crystals are followed by a list of substances investigated only in the form of pow-

ders or magnetically concentrated single crystals, together with those constants which were determined by this investigation.

To explain the form of the paramagnetic resonance spectrum of an ionic crystal it is necessary to have certain crystallographic data, usually obtained by x-ray structural analysis. The paramagnetic properties of salts are determined essentially by the magnetic complexes contained in these salts. It is very important to know how many such complexes there are in each crystal cell, and what their arrangement is. We therefore relate with each magnetic complex a rectangular coordinate system X, Y, Z. If the crystal cell contains only one magnetic complex or if there are several complexes which are all equivalent and identically oriented, then the axes X, Y, Z coincide with the principal axes K_1, K_2, K_3 of the magnetic susceptibility tensor. In the general case, on the other hand, the axes K_1, K_2, and K_3 are the result of the averaging of the axes X, Y, Z of different magnetic complexes. It must be borne in mind that the axes K_1, K_2, K_3 do not coincide in the majority of cases with the crystallographic axes $\underline{a}$, $\underline{b}$, $\underline{c}$.

The magnetic complexes of the compounds of the 3d, 4d, and 5d transition groups frequently are octahedra with a paramagnetic ion M at the center and identical particles X on the vertices, at a distance R from the center. Such particles can be water molecules (the interval between M and the oxygen atom is approximately 2 A), halide ions (R ≈ ≈ 2.5 A), CN radicals (distance from M to C ≈ 1.8 A and to N ≈ 3 A). Owing to the Jahn-Teller effect and to the particles surrounding the magnetic complex, the octahedron is so deformed that the electric field acting on the ion M acquires either trigonal or tetragonal or even lower symmetry. The first of these factors explains why the crystal field can change appreciably when the particle M is replaced by another one, even if the surrounding remains completely the same. The second

reason explains why perfectly identical complexes MX_6 can have different symmetries in different salts.

We consider first the most widely investigated hydrated salts of the iron-group elements, the octahedral complexes of which contain six water molecules.

1) Alums [1-3]: $M'M'''(S^*O_4)_2 \cdot 6H_2O$, where $M' = K$, Na, Rb, Cs, NH_4, ..., $M''' = Al$, Gd, La, ... or the trivalent ion of the 3d group $S^* = S$, Se. The symmetry of the crystal is cubic. Each cell contains four complexes, the positions of which change in different allotropic modifications. The existence of α, β, and γ modifications is apparently connected with the difference in the dimensions of the monovalent ions M'. In the α modifications, the octahedral complexes are somewhat deformed along the trigonal axes of the crystal: [111], [1$\bar{1}$1], [1$\bar{1}\bar{1}$], [11$\bar{1}$]; the cubic axes of the octahedra, on the other hand, are turned about the [111] crystal axis. All four complexes of the unit cell of the β modification are perfectly equivalent; the cubic axes of the octahedra coincide with the cubic axes of the crystal. The paramagnetic resonance in the crystals of the γ modification was not investigated. At temperatures 80-160°K one observes phase transitions which change the symmetry of the magnetic complexes. The α structure of the alums usually occurs in salts with $M' = K$, Rb, Tl, and NH_4, β alums occur for $M' = Cs$, (NH_3CH_3), and γ alums occur for $M' = Na$.

2) Tutton's salts [1, 4, 5]: $M'_2M''(S^*O_4)_2 \cdot 6H_2O$, where $M' = K$, Rb, NH_4, ..., $M'' = Mg$, Zn, or a divalent ion of the 3d group. The crystal is monoclinic and contains in each cell two $M''(H_2O)_6$ complexes. Four water molecules are located at a distance 1.9 A from M'', forming almost a square, while the two other molecules are 2.15 A away from M''. Thus, the symmetry of the complex is close to tetragonal. One can choose the Z axis as the tetragonal symmetry axis.

A reflection from the ac plane transfers the X, Y, Z axes of one of the complexes into the axes of the other complex. The angle between the Z axis and the ac plane is designated α. ψ denotes the angle between c and the projection of Z on the ac plane.

3) Double nitrates [1]: $M''_3 M'''_2 (NO_3)_{12} \cdot 24 H_2 O$, where $M'' = Mg$, Zn, or a divalent ion of the 3d group, $M''' = Bi$, ..., or a trivalent ion of the 4f group. The crystal is trigonal and contains one trivalent and two divalent ions in each unit cell. The two 3d-magnetic complexes $M''(H_2 O)_6$ have trigonal deformations that are somewhat different in magnitude.

4) Fluorosilicates [1, 6, 7]: $M''SiF_6 \cdot 6H_2 O$, where $M'' = Zn$, Mg, or a divalent ion of the 3d group. The crystal is trigonal; it has been assumed that it contains one molecule per cell and that the magnetic complex is slightly deformed in the direction of the trigonal axis. Paramagnetic resonance investigations have shown that there are six magnetic complexes in each unit crystal cell, differing only in the orientation of the deformation axes.

5) Bromates [1, 8]: $M''(BrO_3)_2 \cdot 6H_2 O$, where $M'' = Zn$ or a divalent ion of the 3d group. The crystal has a cubic symmetry. The four $M''(H_2 O)_6$ complexes contained in the unit cell are octahedra distorted along the trigonal axes, similar to the analogous complexes of the α alums.

6) Sulfates [1, 9]: $M''SO_4 \cdot 7H_2 O$. A study was made of the structure of crystals in which $M'' = Ni$, Zn, Mg; the symmetry is orthorhombic. Each unit cell of the crystal contains four complexes, the axes of which go over into one another upon reflection from the symmetry planes (100), (010), and (001).

In addition to the hydrated salts of the 3d-group elements, the most thorough investigations were made of the cyan compounds, in which

the octahedral complexes contain six CN radicals. Two isomorphic series of cyanides were investigated:

7a) $K_3M'''(CN)_6$, $M''' = Cr$, Mn, Fe, Co. The crystal has a symmetry which is very close to orthorhombic [1, 10-12].

7b) $K_4M''(CN)_6 \cdot 3H_2O$, $M'' = V$, Mn, Fe. The symmetry of the crystal is monoclinic and very close to tetragonal [1, 13].

In both series, a unit cell of the crystal contained four magnetic complexes which were pairwise equivalent.

The X, Y, Z axes of one pair can be obtained by reflecting the axes of the second pair of complexes from three mutually perpendicular planes of the crystal. Among the compounds of the 4d and 5d group elements, the crystals investigated in greater detail are those containing octahedral complexes formed by halides, namely:

8a) $M'_2M^{IV}X_6$, $M' = K$, NH_4, ..., $M^{IV} = Pt$, Ir, Mo, ..., $X = Cl$, Br [1, 14]. The crystals have a cubic symmetry. In the case when $X = Cl$, all the magnetic complexes of the crystal cell turn out to be fully equivalent to one another. On the other hand, if $X = Br$, then the octahedra of the three complexes contained in the crystal cell are somewhat distorted along the three different cubic axes.

8b) $Na_2M^{IV}X_6 \cdot 6H_2O$, $M^{IV} = Ir$, Pt, $X = Cl$, Br [1]. The crystal is triclinic; the number of complexes per unit cell is unknown, but they are all perfectly equivalent magnetically. There is a large rhombic predominantly tetragonal distortion of the symmetry of the octahedral complex.

There are apparently no octahedral complexes in salts of the rare earth elements. The following compounds were investigated in detail:

9) Ethyl sulfates [1, 15]: $M'''(C_2H_5SO_4)_3 \cdot 9H_2O$, where M''' is a trivalent ion of the 4f group. The crystals are trigonal, and each unit cell contains two complexes which are perfectly equivalent. Nine

water molecules are located at the vertices of three identical equilateral triangles, which are parallel to one another and whose planes are perpendicular to the trigonal axes of the crystal. In the center of the middle triangle is located the rare-earth ion; the outermost triangles are turned by an angle $\pi/3$ relative to the middle triangle.

The double nitrates $(M'_3M'''_2(NO_3)_{12} \cdot 24H_2O)$ were considered above (see item 3). We note that the rare-earth ion is surrounded by (NO_3) groups which produce a field of trigonal symmetry.

10) Nitrates. From among the compounds of the 5f-group elements, the ones investigated in detail are rubidium nitrates, containing groups of the uranyl type [16] $(M^{IV}O_2Rb(NO_3)_3$, where M^{IV} = U, Np, Pu, ...). The symmetry of the crystal is rhombohedral; each unit cell has two equivalent complexes. Each complex contains the linear group $O-M^{IV}-O$, parallel to the hexagonal axis of the crystal, and surrounded by three nitrate groups situated in a plane perpendicular to the hexagonal axis.

REFERENCES (§4.1)

1. Bowers, K.D., Owen, J., Rep. Progr. Phys. 8, 304, 1955.

2. Lipson, H., Proc. Roy. Soc. A151, 347, 1935; Lipson, H., Beevers, C.A., Proc. Roy. Soc. A148, 664, 1935.

3. Wells, A.F., Stroyeniye neorganicheskikh veshchestv (Structure of Inorganic Substances), IL (Foreign Literature Press), Moscow, 1948.

4. Tutton, A.E.H., Phil. Trans. Roy. Soc. A216, 1, 1916.

5. Hofmann, W., Z. Kristall. (J. Crystallography) 78, 279, 1931.

6. Pauling, L., Z. Kristall. 72, 482, 1930.

7. Wyckoff, R.W., Crystal Structures, New York, Interscience Publishers Inc. 2, chap. 10, 1951.

8. Yu, S.H., Beevers, C.A., Z. Kristall. 95, 426, 1936.

9. Beevers, C.A., Schwartz, C.M., Z. Kristall. 91, 157, 1935.

10. Gottfried, C., Nagelschmidt, J.G., Z. Kristall. 73, 357, 1930.

11. Barkhatov, V., Acta Phys.-chim. URSS 16, 123, 1942.

12. Barkhatov, V., Zhdanov, G., Acta Phys.-chim. URSS 16, 43, 1942.

13. Pospelov, V.A., Zhdanov, G.S., ZhFKh (J. Phys. Chem.), 21, 405, 1947.

14. Bokiy, G.B., Usikov, P.I., DAN SSSR (Proc. Acad. Sci. USSR), 26, 782, 1940.

15. Ketelaar, J.A.A., Physica 4, 619, 1937.

16. Dieke, G.H., Duncan, A.B.F., Spectroscopic Properties of Uranium Compounds, National Nuclear Energy Series, III, 2 (New York, Mc-Graw-Hill), 1949.

Manu-
script
Page
No.

[Footnote]

123   The hyperfine structure constant is sometimes marked by an index indicating the mass number of the isotope to which it pertains.

§4.2. Spin-Hamiltonian Constants for Solid Paramagnets

1. Iron group ions (L ≠ 0) with lower orbital singlets (see Table 4.1, pages 138-151).

$3d^3$ (V^{2+} and Cr^{3+})

The lower orbital singlet arising under the influence of the octahedral field has a fourfold spin degeneracy, which is split by the lower-symmetry fields into two Kramers doublets. The spin Hamiltonian has the form

$$\mathcal{H} = g\beta(H_z\hat{S}_z + H_x\hat{S}_x + H_y\hat{S}_y) + D\left(\hat{S}_z^2 - \frac{5}{4}\right) + E(\hat{S}_x^2 - \hat{S}_y^2) +$$
$$+ A(\hat{S}_z\hat{I}_z + \hat{S}_x\hat{I}_x + \hat{S}_y\hat{I}_y),$$

with $S = 3/2$, $I = 0$ for the even isotopes Cr^{3+}, $3/2$ for ^{53}Cr, $7/2$ for ^{51}V, and 6 for ^{50}V. The value of I for ^{50}V has been determined from experiments on paramagnetic resonance.

If the hyperfine structure is disregarded, the levels in a field $H_0 || Z$ are described by the formula

$$\frac{1}{2}g\beta H_0 \pm \{(D + g\beta H_0)^2 + 3E^2\}^{\frac{1}{2}},$$
$$-\frac{1}{2}g\beta H_0 \pm \{(D - g\beta H_0)^2 + 3E^2\}^{\frac{1}{2}}.$$

The hyperfine structure in Cr^{3+} salts is frequently unresolved owing to the smallness of the constant A and the considerable width of the absorption lines.

In salts of ^{51}V, with a field $H_0 || Z$ and when $g\beta H_0 \gg E$ and A, account of the hyperfine structure yields for the levels

$$\pm\frac{3}{2}g\beta H_0 + D \pm \frac{3}{2}Am, \quad \pm\frac{1}{2}g\beta H_0 - D \pm \frac{1}{2}Am$$
$$\left(m = \frac{7}{2}, \frac{5}{2}, \dots, -\frac{7}{2}\right).$$

In analogy with the V^{2+} and Cr^{3+} in an octahedral environment, the Co^{2+} in a tetrahedral complex has a lower orbital singlet which is fourfold spin-degenerate. The only investigated compound Cs_3CoCl_5 yielded a spectrum described by means of a spin Hamiltonian

$$\mathcal{H} = g_1 \beta H_z \hat{S}_z + g_\perp \beta (H_x \hat{S}_x + H_y \hat{S}_y) + D \left(\hat{S}_z^2 - \frac{5}{4} \right)$$

with $S = 3/2$, without a resolved hyperfine structure, owing to the large width of the lines.

$3d^4$ (Cr^{2+}, Mn^{3+})

The cubic field of the octahedron and the trigonal field leave the lower orbital doublet degenerate. The orbital degeneracy is lifted by a tetragonal field; the lower orbital level remains quintuply spin-degenerate, with the degeneracy lifted by a rhombic field.

Only the sulfate of divalent chromium was investigated. The hyperfine structure due to ^{51}Cr was not resolved. The spin Hamiltonian has the form ($S = 2$):

$$\mathcal{H} = \beta g_1 H_z \hat{S}_z + \beta g_\perp (H_x \hat{S}_x + H_y \hat{S}_y) + D(\hat{S}_z^2 - 2) + E(\hat{S}_x^2 - \hat{S}_y^2).$$

The levels in a field $H_0 || Z$ are situated at

$$-2D; \quad -D \pm (g_1^2 \beta^2 H^2 + 9E^2)^{\frac{1}{2}}; \quad 2D \pm 2g_1 \beta H.$$

The Mn^{3+} compounds were not investigated.

$3d^8$ (Ni^{2+})

In an octahedral field the lower orbital level is a singlet that is triply spin degenerate; the trigonal and tetragonal fields split this level into a doublet and a singlet, while rhombic fields split it into three singlets. The experimental results are described by a spin Hamiltonian

$$\mathcal{H} = g\beta (H_z \hat{S}_z + H_x \hat{S}_x + H_y \hat{S}_y) + D \left(\hat{S}_z^2 - \frac{2}{3} \right) + E(\hat{S}_x^2 - \hat{S}_y^2)$$

with $S = 1$ and isotropic g; no hyperfine structure was observed. For a field $H_0 || Z$ the levels corresponded to

$$-\frac{2}{3}D, \; \frac{1}{3}D \pm (E^2 + g^2 \beta^2 H^2)^{\frac{1}{2}}.$$

$3d^9$ (Cu^{2+})

In an octahedral field, the lower orbital level is a "nonmagnetic"

doublet. A field of rhombic or tetragonal symmetry splits this level into two Kramers doublets. A trigonal field does not split the lower orbital doublet; in this case the orbital degeneracy is lifted by the Jahn-Teller effect or by the spin-orbit coupling. The experimental results are described by a spin Hamiltonian

$$\mathcal{H} = \beta(g_z H_z \hat{S}_z + g_x H_x \hat{S}_x + g_y H_y \hat{S}_y) + A_z \hat{S}_z \hat{I}_z + A_x \hat{S}_x \hat{I}_x +$$
$$+ P\left(\hat{I}_z^2 - \frac{5}{4}\right) + P'(\hat{I}_x^2 - \hat{I}_y^2) + g_n \beta_n H \hat{I}$$

with

$$S = 1/2 \text{ and } I = 3/2.$$

When $H_0 || Z$ and $g\beta H_0 \gg A \gg P'$ the levels are at $\pm 1/2 g_z \beta H_0 \pm$ $\pm 1/2 A_z m + P (m^2 - 5/4)$, where $m = 3/2, 1/2, -1/2, -3/2$. A special case is copper acetate, which was considered above in Chapter 3.

The behavior of the Ti^{3+} in a tetrahedral surrounding should be analogous to that of the copper ions.

2. Iron-group ions (L ≠ 0) with lower orbital triplet (see Table 4.2, pages 152-155)

$3d^1$ (Ti^{3+}, V^{4+}, Mn^{6+})

In an octahedral field, the lower level is an orbital triplet, which is split into three Kramers doublets by the lower-symmetry field. When the octahedral complex is weakly distorted, the spin-lattice relaxation time is quite short and the effect is observed only at very low temperatures. In the case of strong distortion (the VO^{2+} or MnO_3^- ion), the relaxation time is long enough to observe the effect at room temperatures. In Ti^{3+} salts, the results are described by the following Hamiltonian (S = 1/2):

$$\mathcal{H} = g_{||} \beta H_z \hat{S}_z + g_\perp \beta (H_x \hat{S}_x + H_y \hat{S}_y).$$

The hyperfine structure has not been resolved for Ti^{3+}. It is observed in dilute vanadyl salts (I = 7/2 for ^{51}V).

$3d^2$ (V^{3+}, Fe^{2+})

In an octahedral field, the lower level is an orbital triplet with quintuple spin degeneracy. A rhombic field lifts the degeneracy completely. In the case of (Fe, Zn)F_2 one observes a weakly split lower doublet. The spectrum is described by a Hamiltonian ($S = 1/2$, $g_\perp = 0$)

$$\mathscr{H} = g_{\|} \beta H_z \hat{S}_z + \Delta \hat{S}_x,$$

where Δ characterizes a weak splitting of the doublet by the low-symmetry components of the crystalline field.

$3d^7$ (Co^{2+})

In an octahedral field the lower orbital triplet is degenerate and is split into Kramers doublets by the lower-symmetry fields and by the spin-orbit coupling. The results of the experiments are described by a Hamiltonian ($S = 1/2$, $I = 7/2$)

$$\mathscr{H} = \beta (g_z H_z \hat{S}_z + g_x H_x \hat{S}_x + g_y H_y \hat{S}_y) + A_z \hat{S}_z \hat{I}_z + A_x \hat{S}_x \hat{I}_x + A_y \hat{S}_y \hat{I}_y.$$

Sometimes one obtains $g_x = g_y = g_\perp$; $A_x = A_y = A_\perp$ (axial symmetry).

3. Rare-earth ions ($L \neq 0$) with odd number of electrons (see Table 4.3, pages 156-158)

$4f^1$ (Ce^{3+}), $4f^3$ (Nd^{3+}), $4f^5$ (Sm^{3+}), $4f^9$ (Dy^{3+}), $4f^{11}$ (Er^{3+}), $4f^{13}$ (Yb^{3+})

In the investigated cases, the experimental data are described by a Hamiltonian ($S' = 1/2$)

$$\mathscr{H} = g_{\|} \beta H_z \hat{S}_z + g_\perp \beta (H_x \hat{S}_x + H_y \hat{S}_y),$$

to which one adds in the case of odd isotopes the terms of the hyperfine interaction $A\hat{S}_z \hat{I}_z + B(\hat{S}_x \hat{I}_x + \hat{S}_y \hat{I}_y)$. Sometimes (in ethyl sulfates of Ce^{3+}) a second doublet is observed, described by the same Hamiltonian and located several cm^{-1} away from the lower one.

4. Rare-earth ions with even number of electrons (see Table 4.4, pages 159-160)

$$4f^2(Pr^{3+}), \quad 4f^4(Pm^{3+}), \quad 4f^6(Eu^{3+}), \quad 4f^8(Tb^{3+}),$$
$$4f^{10}(Ho^{3+}), \quad 4f^{12}(Tm^{3+})$$

Since the number of electrons in these ions is even, the lower spin doublet can be nondegenerate. However, a trigonal field does not lift the degeneracy, and the components of the lower symmetry in ethyl sulfate and double nitrate crystals are small. Paramagnetic resonance is therefore observable; the available experimental data are described by a Hamiltonian

$$\mathscr{H} = g_{\parallel}\beta H_z \hat{S}_z + \Delta_x \hat{S}_x + \Delta_y \hat{S}_y + A\hat{S}_z \hat{I}_z.$$

In this case $g_{\perp}$ is assumed equal to zero; the terms Δ represent small splittings, due to distortion by a field which has a symmetry lower than trigonal.

5. Ions in the S state (see Table 4.5, pages 160-169)

$$3d^5(Mn^{2+}, Fe^{3+})$$

The lower orbital level is a singlet with sixfold spin degeneracy. The electric field of the water octahedron splits the singlet into three Kramers doublets which are usually spaced less than 1 cm^{-1} apart. The spin Hamiltonian (for the odd isotopes) has the form

$$\mathscr{H} = g\beta(H_z\hat{S}_z + H_x\hat{S}_x + H_y\hat{S}_y) + \frac{1}{6}a\left(\hat{S}_\xi^4 + \hat{S}_\eta^4 + \hat{S}_\zeta^4 - \frac{707}{16}\right) +$$
$$+ D\left(\hat{S}_z^2 - \frac{35}{12}\right) + \frac{7}{36}F\left(\hat{S}_z^4 - \frac{95}{14}\hat{S}_z^2 + \frac{81}{16}\right) + A(\hat{S}_z\hat{I}_z + \hat{S}_x\hat{I}_x + \hat{S}_y\hat{I}_y).$$

Here $\underline{a}$ is the splitting by the cubic field, ξ, η, ζ are mutually perpendicular axes, with respect to which the Z axis is in the [111] direction.

If the symmetry of the magnetic complex is not higher than orthorhombic (for example, in Tutton's salts of Mn^{2+}), then a term $E(\hat{S}_x^2 - \hat{S}_y^2)$ is added to the Hamiltonian.

$4f^7(Gd^{3+}, Eu^{2+})$

Because of the large value $S = 7/2$, the spin Hamiltonian is very complicated and will not be written out here. It can be written (without account of the hyperfine structure) in the form

$$\mathcal{H} = g\beta(H_z\hat{S}_z + H_x\hat{S}_x + H_y\hat{S}_y) + \\ + B_2^0\hat{U}_2^0 + B_2^2\hat{U}_2^2 + B_4^0\hat{U}_4^0 + B_4^4\hat{U}_4^4 + B_6^0\hat{U}_6^0.$$

Here each $\hat{U}_n^m$ is an operator; the coefficients B_n^m are determined from experiment. For the sake of convenience, one frequently uses the following notation

$$b_2^0 = 3B_2^0, \quad b_2^2 = 3B_2^2, \quad b_4^0 = 60B_4^0, \quad b_4^4 = 1260B_4^4, \quad b_6^0 = 1260B_6^0,$$

with $b_2^0 = D$, $b_2^2 = E$, $3b_4^6 = F$.

In the case of Eu^{2+}, which was investigated in a field of cubic symmetry, g and A are isotropic, but the complete spin Hamiltonian was not established.

6. Compounds with strong covalent bond (see Table 4.6, pages 169-173)

Included among such substances are the cyanides of trivalent iron and divalent manganese from the 3d group, and also all the investigated paramagnets from among the compounds of elements of the 4d and 5d groups.

For Fe^{III}, Mn^{II}, Mo^V, Ru^{III}, Ag^{II}, and Ir^{IV}, the effective spins have a value $S' = 1/2$ and the spectrum is described by a spin Hamiltonian

$$\mathcal{H} = \beta(g_z H_z\hat{S}_z + g_x H_x\hat{S}_x + g_y H_y\hat{S}_y),$$

to which the corresponding terms that take the hyperfine structure into account are added for the odd isotopes. In some cases one must also take into account the hyperfine structure due to the interaction between the uncompensated electron and the spins of the nuclei of the atoms which are covalently bound with the central atom (for example, in the case of $(NH_4)_2[IrCl_6]$, diluted with the corresponding platinum salt).

For Mo^{III} and Re^{IV}, the spin Hamiltonian has the form

$$\hat{\mathcal{H}} = \beta\,(g_z H_z \hat{S}_z + g_x H_x \hat{S}_x + g_y H_y \hat{S}_y) + \\ + D\left\{\hat{S}_z^2 - \tfrac{1}{3}S(S+1)\right\} + E\,(\hat{S}_x^2 - \hat{S}_y^2)$$

with effective spin S' = 3/2. For odd isotopes one should add to the Hamiltonian the terms characterizing the hyperfine structure of the spectrum.

The number of compounds of the elements of the 4d and 5d groups, in which paramagnetic resonance spectra were investigated, is very small; one of the difficulties entailed in the investigation is the choice of isomorphous diamagnetic salts necessary to weaken the magnetic dipole interactions, for the latter are quite appreciable when the indicated compounds are in the undilute state. The last group in the class of substances with strong covalent bonds is made up of the actinide compounds. Paramagnetic resonance is these compounds has also been investigated in a very small number of cases. In double neptunyl nitrate, the spectrum is described by a spin Hamiltonian

$$\hat{\mathcal{H}} = g_\| \beta H_z \hat{S}_z + g_\perp \beta\,(H_x \hat{S}_x + H_y \hat{S}_y) + A \hat{S}_z \hat{I}_z + \\ + B(\hat{S}_x \hat{I}_x + \hat{S}_y \hat{I}_y) + P\left(\hat{I}_z^2 - \tfrac{35}{12}\right)$$

with effective spin S' = 1/2 and I = 5/2 (for the odd isotope ^{237}Np).

For plutonyl we have $g_\perp = 0$ and the spin Hamiltonian has the form

$$\hat{\mathcal{H}} = g_\| \beta H_z \hat{S}_z + A \hat{S}_z \hat{I}_z + \Delta_x \hat{S}_x + \Delta_y \hat{S}_y.$$

The effective spin is S' = 1/2; the value of I is 1/2 for ^{239}Pu and 5/2 for ^{241}Pu. The last two terms of the Hamiltonian describe small splittings due to the distortions of the crystal and to thermal fluctuations.

TABLE 4.1

V^{2+}

1 Формула	T, °K	g	D	E	A	Литература	3 Замечания
(NH₄)₂ V (SO₄)₂ · 6H₂O (кр. ст. 2)							
V : Zn = 1 : 3	290		0,155 ±0,005			[1]	ψ = +4°, α = 23,5°
V : Zn = 10⁻³	20	1,951 ±0,002	0,158 ±0,010	0,049 ±0,005	⁵¹A 0,0088 ±0,0002	[2, 3]	ψ = +2°, α = 22° ⁵⁰A = 0,3792 ⁵¹A ±0,0008
K₄V (CN)₆ · 3H₂O (кр. ст. 7)		gx gy gz					
V : Fe = 0,1—5 · 10⁻³	90, 20	1,9919 1,9920 1,9920 ±0,0006 ±0,0006 ±0,0006	— 0,0264 ±0,0004	— 0,0072 ±0,0004	⁵⁰A — 0,00211 ±0,00003 ⁵¹A — 0,00555 ±0,00003	[4, 5]	a)
V²⁺ в Al₂O₃	290	~1,98	~0,31			[9]	
V²⁺ в MgO	290	1,9803 ±0,0005			A ≈ B = 0,0091 ⁵¹A = 0,00740 ±0,00002	[6]	
V : Mg ~ 2·10⁻⁷							
V²⁺ в ZnSiF₆ · 6H₂O	20	g∥ g⊥ 1,970 1,976	0,0804		— 0,00839	[10]	

Paramagnetic resonance is observed also in VSO₄ (T = 290°K) [7]; V(C₆H₄)₄(CN)₈ (T = from 270 to 20°K, g = 2.0) [8]; V²⁺ in phthalocyanine (T = 290, 20°K, g = 2.0) [11].

Remarks. a) The direction cosines are:

	a	b	c
X	0,707	0	—0,707
Y	0,523	± 0,676	—0,523
Z	0,470	∓ 0,737	—0,470

Cr^{3+}

1 Формула	T, °K	g	D	E	A	Литература	3 Замечания
CsCr (SO₄)₂ · 12H₂O (кр. ст. 1)	290	1,98	0,072₅ ± 0,003			[1—3]	
	193	1,98 ± 0,02	— 0,067				
	90, 20	1,98 ± 0,02	— 0,066₅ ± 0,001				
KCr (SO₄)₂ · 12H₂O (кр. ст. 1)	290	1,98	0,060 ± 0,003			[1—6]	a)
	193	1,98 ± 0,02	0,027 ± 0,003				
	160	1,98 ± 0,02	0,017₅				
	90	1,98 ± 0,02	I : 0,130 II : 0,075 ± 0,005				
	20	1,98 ± 0,02	I : 0.135 ± 0,002 II : 0,075 ± 0,005				
(NH₆CH₃) Cr(SO₄)₂·12H₂O (кр. ст. 1) Cr : Al = 2 : 17	290	1,98	0,045₅			[1, 2, 7, 8]	б) b
	290	1,98	0,082₅ ± 0,003				
	90	1,97₅ ± 0,01	0,087 ± 0,002	0,009 ± 0,001			
	20	1,976 ± 0,007	— 0,0871 ± 0,0007	— 0,0092 ± 0,0008			
Cr : Al = 10⁻²	90	1,97₅ ± 0,01	0,095₅ ± 0,002	0,009 ± 0,001		[7]	а) c
	20	1,977 ± 0,003	— 0,0958 ± 0,0004	— 0,0092 ± 0,0008		[8]	

TABLE 4.1 (Continuation)

1 Формула	T, °К	ε	D	B	A	2 Литература	3 замечания
4 (NH₄) Cr (SO₄)₂ · 12H₂O (кр. ст. 1)	290	1,98	0,067₅ ± 0,003			[1—5, 9, 10]	г) d
	193	1,98 ± 0,02	0,042₅				
	90	1,98 ± 0,02	0,017₅				
	80	1,98 ± 0,02	I: 0,157 ± 0,002 II: 0,121 ± 0,002				
	20	1,98 ± 0,02	I: 0,158 ± 0,002 II: 0,120 ± 0,002				
Cr : Al = 2 : 17	290	1,97	0,050			[4]	
Cr : Al = 1 : 0	295	1,988 ± 0,001	0,0675 ± 0,0010			[11]	д) e
Cr : Al = 1 : 17		1,9771 ± 0,0010	0,0492 ± 0,0005				
Cr : Al = 1 : 47		1,9772 + 0,0010	0,0490 ± 0,0005				
Cr : Al = 1 : 47	77	1,9765 ± 0,0010					
4 [(NH₂)₂ C] Cr (SO₄)₂·6H₂O (кр. ст. 1) Cr : Al = 1 : 20	373	I : 1,980 ± 0,005 II : 1,980 ± 0,002	I : 0,0610 ± 0,0004 II : 0,0488 ± 0,0004			[12]	е) f
	290	I : 1,980 ± 0,003	I : 0,0750 ± 0,0002				
Cr : Al = 1 : 50	295	II : 1,977 ± 0,001 1,975 ± 0,005	II : 0,0590 ± 0,0002 I : 0,0576 ± 0,0005 II : 0,0730 ± 0,0005			[13]	
	195	1,975 ± 0,005	I : 0,0696 ± 0,0006 II : 0,0882 ± 0,0010				
	77	1,975 ± 0,005	I : 0,0822 ± 0,0010 II : 0,105 ± 0,003				
	35	1,975 ± 0,005	I : 0,085 ± 0,003 II : 0,109 ± 0,005				
4 Rb Cr (SO₄)₂ · 12H₂O (кр. ст. 1)	290	1,98	0,082₅ ± 0,003			[1—3]	
	193	1,98 ± 0,02	0,063				
	90, 20	1,98 ± 0,02	0,054 ± 0,001				
4 KCr (SeO₄)₂ · 12H₂O (кр. ст. 1)	90		0,064 ± 0,002			[7]	
	20		0,070 ± 0,002				
Cr : Al = 1 : 10	90		0,089₅ ± 0,001				
	20		0,098 ± 0,001				

TABLE 4.1 (Continuation)

1 Формула	Т, °К	g	D	E	A	2 Литература	3 Замечания
Cr : Al = 10⁻³	90	1,976 ± 0,002	0,0900 + 0,0003			[14]	
	20	1,976 ± 0,002	0,0983 ± 0,0003				
KCr (ScO₄)₂ · 12D₂O (кр. ст. 1)	90, 20	1,976 ± 0,002	0,10₈		0,0018₈ ± 0,0001	[14]	
Al : Cr K₃ Cr (CN)₆ (кр. ст. 7)	90, 20 4,2	1,998 ± 0,008	~0,045	~0,013		[39, 15, 16]	ж)g
Cr : Co = 0,1—10⁻⁴	90, 20	g_x 1,993 ± 0,001 g_y 1,991₄ ± 0,001 g_z 1,991 ± 0,001	+0,0831 ± 0,0010	+0,0108 ± 0,0010	+0,00147 ± 0,00005	[15, 16]	з) h
	4,2	g 1,992 ± 0,0002				[39]	
Cr : Mn = 0,1—10⁻⁴	90, 20	g_x 1,992 ± 0,002 g_y 1,995 ± 0,002 g_z 1,993 ± 0,002	+0,0538 ± 0,0010	+0,0120 ± 0,0010	+0,00147 ± 0,00010		и) j
Cr [(CH₃CO)₂ CH]₃ [к. 1] Cr : Al = 1 : 50 Cr[CH₃CF₂(CO)₂CH]₃	290	1,983 ± 0,002	0,592 ± 0,002	0,052 ± 0,002		[17]	к) k $M_m = 2$
Cr : Al	290	~1,98	0,59			[18]	$M_m = 2$, орторомбич. A
Cr [(CF₃CO)₂ CH]₃	290	~1,98	0,70			[18]	$M_m = 1$,
Cr³⁺ в TiO₂ Cr : Ti = 10⁻⁴	290	1,97	0,55	0,27	0,0017	[35]	гексагон. B

1 Формула	Т, °К	g	D	E	A	2 Литература	3 Замечания
Cr³⁺ в Al₂O₃ Cr : Al = 10⁻²—10⁻⁴ (Обогащен нечетным изотопом) C Cr : Al = 10⁻⁴	290 4,2 290	1,982 ± 0,002	1,979 ± 0,009	— 0,1912 ± 0,0010	A 0,001680 ± 0,000004 B 0,001680 ± 0,000006	[19—21, 23] [22, 23]	M = 2, $M_m = 1$, гексагон. B
Cr³⁺ в Al₂Be₃ (SiO₃)₆	78 1,6	1,973 ± 0,002	1,97 ± 0,01	— 0,893 ± 0,002		[34]	
Cr³⁺ в CaF₂ Cr : Ca = 10⁻⁴	90, 20	g 1,9800 ± 0,0006			~0,0010 0,00160 ± 0,00003	[40] [24, 36]	п) з) p
Cr³⁺ в MgO Cr : Mg = 10⁻³—10⁻⁴	290, 77	1,980 ± 0,001	1,986 ± 0,001	0,0819	A = B 0,00162 ± 0,00004	[24]	$M_m = 3$, м)
	290, 77 90, 20	g 1,98		0,031 ± 0,002 D_{max}	0,22 ± 0,01	[36, 37]	$M_m = 6$, н) n
Cr³⁺ в ZnF₂ Cr : Zn = 10⁻⁴	290	I : 1,976 ± 0,007 II : 1,975 ± 0,007	I : 1,958 ± 0,004 II : 1,959 ± 0,006	I : 0,602 ± 0,008 II : 0,581 ± 0,008		[25]	м) m $M_m = 2$ o)

Paramagnetic resonance absorption was observed also at room temperature in

Парамагнитное резонансное поглощение наблюдено также при комнатной температуре в CrBr₃ (g = 1,99) [6]; Cr(C₃H₅O₃)₃·H₂O [26]; Cr(C₆H₅N)₃(OH)₃(H₂O)Cl (g = 1,99) [27]; Cr (C₇H₅O₃)₃ H₂O (g = 2,07) [27]; Cr [(CH₃)₃(CH)₃ CH₃ (CO)₃]₃ (g ≈ 2, D > ~0,5) [17]; Cr [(C₆H₅)(CO)₃ CHCH₃]₃ (g ≈ 2, D > ~0,5) [17]; CrCl₃ (g = 1,99 — 2,37) [28, 41, 42]; CrF₃ (g = 2,00) [6]; [Cr (H₂O)₄ Cl₂] Cl (g = 1,95) [27]; [Cr (H₂O)₄ Cl₃] Cl · 2H₂O [28]; [Cr (H₂O)₆ Cl] Cl₂ · H₂O [28]; [Cr (NH₃)₆ Cl] Cl₂ (g = 1,97) [27]; [Cr (NH₃)₆] Cl₃ ·H₂O (g = 1,97) [27]; [Cr (NH₃)₆] (NO₃)₃· H₂O (g = 1,95) [27]; [Cr(NH₃CH₃)₆]₃ · (SO₄)₃ (g ≈ 2, D ≈ 0,15) [17]; Cr (NO₃)₃ ·9H₂O (g = 2,26) [27, 29]; Cr (OH)₃ [28]; Cr(OH)₃ · 2H₂O (g = 2,00) [27]; [Cr (SCN)₃ (C₅H₄ (NH₃)₃)] (SCN) (g = 1,98) [27, 30]; Cr₂O₃ [28]; Cr₂ (SO₄)₃ (g = 2,00) [6]; Cr₂ (SO₄)₃ (g = 1,98) [6]; Cr₂(SO₄)₃·5H₂O [26]; Cr₂ (SO₄)₃·15H₂O [26]; Cr₂ (SO₄)₃·18H₂O (g = 2,00) [27]; K₃Cr (C₂O₄)₃·3H₂O (g ≈ 2, D ≈ 0,4) [17]; Cr₂(CH₃NH₃)₃(SO₄)₃ ·24H₂O (T = 0,06 — 1 °K) [31]; CrPO₄· 3H₂O [26]; CrCl₆ (g = 1,997 ± 0,003) [32]; K₂Cr₂ (SO₄)₃ · 24H₂O [33]; Cr в CaF₂ [38].

A) Orthorhombic; B) hexagonal; C) (enriched with odd isotope).

Remarks:

a) Below 160°K there are two different magnetic complexes.

b) The temperature of the crystalline transition is $157 \pm 2^{\circ}$K. Below this point, the spectrum corresponds to rhombic symmetry; the direction cosines of the rhombic axes relative to the tetragonal axes <u>a</u>, <u>b</u>, <u>c</u> are:

	a	b	c
X	−0,35 ± 0,05	−0,35 ± 0,05	+0,87 ± 0,03
Y	+0,71 ± 0,04	−0,71 ± 0,04	0 ± 0,05
Z	+0,61 ± 0,04	+0,61 ± 0,04	+0,50 ± 0,04

The directions for the other three ions are obtained by rotating the XYZ system about the <u>c</u> axis through angles $\pi/2$. D and E remain unchanged between 90 and 13°K.

c) The temperature of the crystalline transition $170 \pm 2^{\circ}$K. Below this point the spectrum corresponds to rhombic symmetry.

d) Crystalline transition near 80°K. Below this temperature there are two different magnetic complexes.

e) δ decreases at an approximate rate 0.0005 cm^{-1} deg^{-1} in the temperature interval from 295 to 77°K, i.e., the trigonal component of the crystalline field decreases with decreasing temperature.

f) The crystal has three aluminum atoms per unit cell, located on the C_3 axis, but only two of them are equivalent. This explains the observed intensities of spectra I and II: spectrum I is twice as intense.

g) Only one line.

h) The direction cosines of the angles at $T = 20^{\circ}$K are:

	a	b	c
X	0,104	±0,994	0
Y	0	0	1
Z	0,994	±0,104	0

j) The direction cosines of the angles at $T = 90^{\circ}$K are:

	a	b	c
X	0	±0,996	0,087
Y	0	±0,087	0,996
Z	1	0	0

k) The nearest surrounding of Cr^{3+} in acetyl acetonate and its fluorine derivatives is a distorted octahedron made up of six oxygen atoms; the local field is essentially axial. Between 290 and $90^{\circ}K$ one observes in acetyl acetonate a gradual transition wherein the complex splits at $90^{\circ}K$ into three types with slightly different orientations of the Z axes, or having a somewhat different splitting; $\psi = +22.5^{\circ}$, $\alpha = 59^{\circ}$.

l) The spectrum, which consists of one isotropic line, shows that Cr^{3+} is in a strictly cubic crystalline field.

m) the spectrum belongs to the Cr^{3+} ions in an axial crystalline field. The axes of the nonequivalent ions are directed along the cubic axes. The spectrum arises at large concentrations of Cr^{3+}.

n) The spectrum belongs to the Cr^{3+} ions in a rhombic crystalline field. The directions of the X, Y, and Z axes are: X = (110), Y = (1$\bar{1}$0), Z = (001). The number of Cr^{3+} ions in the rhombic field constitutes 1/2 to 1/4 of the number of Cr^{3+} in the cubic field. The spectrum arises at large concentrations of Cr^{3+}.

o) The presence of two spectra is attributed to different relative arrangements of the Cr^{3+} ions and the compensating F^- ions; the hyperfine interaction with the F nuclei causes only a broadening of the lines. The constant of this interaction is approximately 3-5 oersteds. The constant of the hyperfine interaction with the ^{19}F nuclei is approximately 20 oersteds. Absorption in zero field occurs at a frequency $\nu = (2847 \pm 2) \cdot 10^{-4}$ sec^{-1}.

TABLE 4.1 (Continuation)

Co^{2+}

1 Формула	T, °K	$\varepsilon_{\parallel}$	$\varepsilon_{\perp}$	D	E	Лите-ратура (2)	3 Замечания	
Cs_3CoCl_5 [к 2]	90, 20	2,32 ± 0,04	2,27 ± 0,04	~ —4,5	0	[1]	$M=4$. Каждый ион окружен искаженным тетраэдром из 4Cl. $M_n=1$, спектр соответствует аксиальной симметрии с осью, параллельной c	A

Cr^{2+}

1 Формула	T, °K	$\varepsilon_{\parallel}$	$\varepsilon_{\perp}$	D	E	Лите-ратура (2)	3 Замечания	
$CrSO_4 \cdot 5H_2O$	290	1,95	1,99	2,24	0,10	[1]	$M_m=2$, угол между осями $Z=86°$	B

Ni^{2+}

1 Формула	T,°K	ε	D	E	$\varphi°$	$\theta°$	$\alpha°$	Лите-ратура (2)	Заме-чания (3)
4 $K_2Ni(SO_4)_2 \cdot 6H_2O$ (кр. ст. 2)	290	2,25 ± 0,05	—3,30	—0,51₇	—12,5	11	45	[1]	
			—3,50 ± 0,01	—0,55 ± 0,01				[2]	
4 $(NH_4)_2Ni(SO_4)_2 \cdot 6H_2O$ (кр. ст. 2)	290	2,25 ± 0,05	—2,24 ± 0,01	—0,38₇ ± 0,01	—14	3,5	45	[1, 2]	a)
	90	2,25 ± 0,05	—1,99	—0,48₈	—14	3,5	45	[1]	
4 $Tl_2Ni(SO_4)_2 \cdot 6H_2O$ (кр. ст. 2)	290	2,25 ± 0,05	—2,65	—0,10	—11	11	45		
4 $K_2Ni(SeO_4)_2 \cdot 6H_2O$ (кр. ст. 2)	290	2,25 ± 0,05	—3	—1	—13	0	45		
4 $(NH_4)_2Ni(SeO_4)_2 \cdot 6H_2O$ (кр. ст. 2)	290	2,25 ± 0,05	—1,89	—0,79	—28	0	50	[1]	
	90	2,25 ± 0,05	—1,73	—0,82	—28	0	50	[1]	
4 $Ni_3La_2(NO_3)_{12} \cdot 24H_2O$ (кр. ст. 3) Ni:Mg = 1:800	90	2,24	0,177 ± 0,002	0				[3]	

A) $M = 4$. Each ion is surrounded by a distorted tetrahedron made up of 4 chlorine atoms. $M_m = 1$, the spectrum corresponds to axial symmetry with an axis parallel to c.
B) $M_m = 2$, the angle between the Z axes is 86°.

TABLE 4.1 (Continuation)

1 Формула	T, °K	g	D	E	q⁰	f⁰	e⁰	2 Лите-ратура	3 Заме-чания
4 NiSiF₆ · 6H₂O (кр. ст. 4)	290	2,3	— 0,50	0				[4, 5]	6) b
	195	2,29	— 0,32	0					
	90	2,26	— 0,17	0					
	60		— 0,14	0					
	20	2,29	— 0,12	0					
	14		— 0,12	0					
	290	2,34 ± 0,02	— 0,6					[6]	в) c
4 Ni(BrO₃)₂ · 6H₂O (кр. ст. 5)	290	2,29 ± 0,04	1,93 ± 0,04	0				[7]	
4 NiSO₄ · 7H₂O (кр. ст. 6)	290	2,2₆	— 3,5₆	— 1,5₆				[8]	г) d
A Ni²⁺ в MgO (порошок)	290	2,225 ± 0,005						[9, 10]	д) e
	77	2,227 ± 0,005							
	4	2,234 ± 0,004							
A Ni²⁺ в CdCl₂ NiCl₂ (порошок)	20	2,28	1,4100					[16] [17]	с) f ж)g
	290	2,25							
	90	2,24							
	50,2	2,27							
	40,6	2,46							
	20,4	2,30							

A) (Powder).

Paramagnetic resonance absorption was observed also at room temperature in: $NiBr_2$ (g = 2.27) [11]; $NiBr_2(NH_3)_6$ (g = 2.14 and 2.16) [12, 13]; $NiCl_2$ (g = 2.21) [11]; $NiCl_2 \cdot 6H_2O$ [14]; $NiI_2(NH_3)_6$ (g = 2.14) [13, 7]; $Ni(C_6H_4)_4(CN)_8$ (g = 2.20; T = 270 − 20°K) [15]; $Ni(NH_3)_6ClO_4$ (g = 2.17) [13].

Remarks:

a) When Zn:Ni = 50, the parameters and the axes remain practically unchanged.

b) When Zn:Ni = 4.16, D is approximately 20% larger than in the undiluted salts at all temperatures.

c) The dependence of D and g on the hydrostatic pressure p was investigated; g is independent of p, $\partial D/\partial p = 0.834 \cdot 10^{-4}$ cm^{-1}/kg-cm^{-2}; D = 0 when p = 6200 kg/cm^2.

d) For one complex, the direction cosines of the axes are: Z (0.95; 0.31; 0), Y (−0.31; 0.95; 0.09). The axes of the other complex are ob-

tained by mirror reflection.

e) One line, the width of which hardly changes with temperature.

f) The cubic field is subject to trigonal distortion.

g) The low-temperature measurements may not be accurate (see Orton, J.W., Rep. progr. Phys. 22, 204, 1959). The axes Z_1 and Z_2 of two ions lie in the K_1OK_3 plane, with the angles Z_1OK_1 and Z_2OK_1 equal to $\pm\theta$, where the angle $K_1Cc = \psi$. X_1 is approximately parallel to Y_2, and both axes lie in the K_2OK_3 plane with the angle X_1OK_2 equal to α and the angle Y_2OK_2 equal to $90° - \alpha$.

TABLE 4.1 (Continuation)

Cu^{2+}
Tutton's Salts (cr. st. 2)

1 Формула	T, °K	g			A		P	ψ	α°	Лите-ратура	Замечания
$Cs_2Cu(SO_4)_2 \cdot 6H_2O$	90	$g_{min}(K_1K_3)$ 2,08 ±0,02	g_1 2,06 ±0,02	g_z 2,43 ±0,02				+114	40	[1]	
$K_2Cu(SO_4)_2 \cdot 6H_2O$	290	g_1 2,31 ±0,03	g_2 2,07 ±0,03	g_3 2,25 ±0,03				+105		[2]	
	90	g_x 2,14 ±0,02	g_y 2,04 ±0,02	g_z 2,36 ±0,02				+105	42	[1]	
$Cu:Zn =$ $= 2 \cdot 10^{-3} - 5 \cdot 10^{-4}$	290	g_z 2,05 ±0,03	$g_{max}(K_2K_3)$ 2,25 ±0,03	g_1 2,26 ±0,03				+15	32	[2]	
	20	g_z 2,44 ±0,02	$g_{min}(K_1K_3)$ 2,13 ±0,02		A_z 0,0103 ±0,0005	$A_{min}(K_1K_3)$ 0,0034 ±0,0005	0,0011 ±0,0001	≈+105	42 ±2	[3]	

TABLE 4.1 (Continuation)

1 Формула	T, °K	g			A			P	ψ°	a°	Литература	Замечания
$Cu:Zn = 5:10^{-3}$	77	$g_{\parallel}$ 2,47 ± 0,05	$g_{\perp}$ 2,08 ± 0,04		A −0,0083	B 0,0045		0,001			[42]	a)
$K_2Cu(SO_4)_2 \cdot 6D_2O$ $Zn:Cu = 200-1000$	20	g_x 2,16 ± 0,02	g_y 2,04 ± 0,02	g_z 2,42 ± 0,02	A_x <0,0017	A_y +0,0061 ± 0,0003	A_z −0,0099 ± 0,0001	+0,00110 ± 0,00005 P' 0,00013 ± 0,00006	≈+105	43	[3]	$\frac{^{65}A}{^{63}A}=1{,}069$ ±0,003 $\frac{^{65}P}{^{63}P}=1{,}08$ ±0,02
$K_2Cu(SO_4)_2 \cdot 6H_2O$	90	g_z 2,38 ± 0,02	$g_{min}(K_1K_2)$ 2,07 ± 0,02	g_3 2,04₆ ± 0,02					+73	37	[1]	
$(NH_4)_2Cu(SO_4)_2 \cdot 6H_2O$	290	g_1 2,32 ± 0,03	g_2 2,09 ± 0,03	g_3 2,25 ± 0,03					+77		[2], [45, 49]	
	90	g_z 2,45 ± 0,02	$g_{min}(K_1K_2)$ 2,12 ± 0,02	g_3 2,06 ± 0,02					+65	39	[1]	
$Zn:Cu = 50-2000$	290	g_z 2,04 ± 0,03	g_{max} 2,26 ± 0,03	g_1 2,28 ± 0,03					+167	32	[2]	
	20	g_x 2,12 ± 0,02	g_y 2,05 ± 0,02	g_z 2,46 ± 0,02	A_x 0,0025 ± 0,0005	A_y 0,0035 ± 0,0005	A_z 0,0130 ± 0,0005	0,0011 ± 0,0001	+65	38	[3]	
$(NH_4)_2Cu(SeO_4)_2 \cdot 6H_2O$	90	g_z 2,39 ± 0,02	$g_{min}(K_1K_2)$ 2,075 ± 0,02	g_y 2,06₅ ± 0,02					+72	37,5	[1]	
$Rb_2Cu(SO_4)_2 \cdot 6H_2O$	290	g_1 2,28 ± 0,03	g_3 2,24 ± 0,03						+105		[2]	
	90	g_z 2,45 ± 0,02	$g_{min}(K_1K_2)$ 2,11 ± 0,02	g_3 2,07 ± 0,02					+105	40	[1]	
$Zn:Cu = 50-2000$	290	g_z 2,08 ± 0,03	$g_{max}(K_2K_3)$ 2,27 ± 0,03	g_1 2,25 ± 0,03					+15	33	[2]	
	20	g_z 2,44 ± 0,02	$g_{min}(K_1K_2)$ 2,12 ± 0,02		A_z 0,0116 ± 0,0005	$A_{min}(K_1K_2)$ 0,0030 ± 0,0005		0,0011 ± 0,0001	~+105 ±2	42	[3]	б) b
$Rb_2Cu(SO_4)_2 \cdot 6D_2O$ $Zn:Cu = 200-1000$	20	g_x 2,15 ± 0,02	g_y 2,04 ± 0,02	g_z 2,43 ± 0,02	A_x <0,0020	A_y +0,0059 ± 0,0004	A_z −0,0110 ± 0,0002	+0,0012 ± 0,0001	~+105 ±2	42	[3]	б) b
$Tl_2Cu(SO_4)_2 \cdot 6H_2O$	90	g_z 2,40 ± 0,02	$g_{min}(K_1K_2)$ 2,08 ± 0,02	g_3 2,06 ± 0,02					+112	39,5	[1]	

TABLE 4.1 (Continuation)

Формула	T, °K	g			A			Литература	Замечания
$Cu_3Bi_2(NO_3)_{12} \cdot 24H_2O$ (кр. ст. 3) $Cu:Mg=1:100$	90	$g_{\parallel}$ 2,219 ± 0,003	$g_{\perp}$ 2,217 ± 0,003		A 0,0027 ± 0,0001	B 0,0026 ± 0,0001		[4]	
	20	$g_x=g_y$ 2,096 ± 0,003	g_z 2,454 ± 0,003		$A_x=A_y$ 0,0017 ± 0,0002	A_z 0,0110 ± 0,0002			
$Cu_3La_2(NO_3)_{12} \cdot 24H_2O$ (кр. ст. 3)	290		2,22					[5]	в) c
	90, 20	$g_x=g_y$ 2,10	g_z 2,41						
$Cu_3La_2(NO_3)_{12} \cdot 24D_2O$ $Cu:Mg=1:500$ (кр. ст. 3)	90	$g_{\parallel}$ 2,219 ± 0,003	$g_{\perp}$ 2,218 ± 0,003		A 0,00290 ± 0,00005	B 0,00275 ± 0,00005		[4, 5]	г) d
	45		2,235 ± 0,005						
	20	$g_x=g_y$ 2,097 ± 0,002	g_z 2,470 ± 0,002		A_x + 0,00190 ± 0,00005	A_y + 0,00123 ± 0,00005	A_z — 0,0113 ± 0,00005	[4]	$P=0,00111$ ± 0,00005 $P'=0,00004$ ± 0,00001
$CuSiF_6 \cdot 6H_2O$ (кр. ст. 4)	290		2,20					[6]	
$Cu:Zn$	90	$g_{\parallel}$ 2,221 ± 0,005	$g_{\perp}$ 2,230 ± 0,005		A 0,0021 ± 0,0005	B 0,0028 ± 0,0005		[4]	д) e
	20, 12	$g_x=g_y$ 2,10 ± 0,01	g_z 2,46 ± 0,01		$A_x=A_y$ < 0,0030	A_z 0,0110 ± 0,0003			
$Cu_x^r(BrO_3)_2 \cdot 6H_2O$ (кр. ст. 5) $Cu:Zn=1:100$	90	2,21$_7$ ± 0,01						0,0028 ± 0,0005 [4]	е) f
$CuSO_4 \cdot 5H_2O$ [ж3]	290	$g_{\parallel}$ 2,08	$g_{\perp}$ 2,27					[10, 25, 28, 39, 40, 41, 45]	ж) g
		$g_x=g_y$ 2,08	g_z 2,46						
		g_1 2,267	g_2 2,236	g_3 2,086					
	77	g_1 2,264	g_2 2,233	g_3 2,083					
$Cu(NH_3)_4SO_4 \cdot H_2O$ [ж4]	290	g_1 2,054 ± 0,003	g_2 2,104 ± 0,006	g_3 2,181 ± 0,005				[7, 24, 35, 36]	A Орторомб.,з)h
		$g_{\parallel}$ 2,22 ± 0,02	$g_{\perp}$ 2,05 ± 0,02					[33]	
[Cu(C₅H₅N)$_m$]SO$_4 \cdot n$H$_2$O	290	g_1 2,072 ± 0,004	g_2 2,081 ± 0,006	g_3 2,314 ± 0,010				[24]	A
$Cu(NH_3)_6(NO_3)_2$ [ж4]	290	g_a 2,07 ± 0,02	g_b 2,14 ± 0,02	g_c 2,02 ± 0,02				[7, 35, 36]	A Орторомб.

A) Orthorhombic.

- 147 -

TABLE 4.1 (Continuation)

1 Формула	T, °K	g			A		2 Литература	3 Замечания
Cu (C₅H₅N)₆ (NO₃)₂ [к4]	290	$g_{\parallel}$ 2,25 ± 0,02	$g_\perp$ 2,05 ± 0,02		A 0,0199 ± 0,0007	B < 0,0014	[23]	B $M_m = 1$, ромбич., и) J
[Cu(C₅H₅N)ₘ](NO₃)₂·nH₂O	290	g_1 2,056 ± 0,004	g_2 2,124 ± 0,015	g_3 2,161 ± 0,008			[24]	
CuCl₂·2H₂O [к5]	290 до 15	g_a 2,187 ± 0,005	g_b 2,037 ± 0,005	g_c 2,252 ± 0,005			[9, 45, 49]	A $M_m = 2$, орторомб., к) k
K₂CuCl₄·2H₂O [к6]	290	g_x 2,06	g_z 2,38				[11, 25, 45]	C $M_m = 2$, тетрагон., л) l
(NH₄)₂CuCl₄·2H₂O [к6]	290	$g_{\parallel}$ 2,06	$g_\perp$ 2,22				[11]	л) l
Cu (C₆H₄)₄ (CN)₆ [к7]	290 до 20	g_x < 2,10₅ $g_{\parallel}$ 2,165 ± 0,004	g_y 2,06 $g_\perp$ 2,045 ± 0,003	g_z > 2,30	A 0,0208 ± 0,0010	B 0,0031 ± 0,0010	[15, 16]	D $M = 2$, моноклин., м) m
Cu [C₂H₂ (NH₂)₂]₂Cl₂·H₂O [к8]	290	g_1 2,050 ± 0,004	g_2 2,057 ± 0,010	g_3 2,244 ± 0,010		•	[24]	E x = 1 или 2, $M_m = 2$, моноклин., н) n D

1 Формула	T, °K	g			D	B	2 Литература	3 Замечания
Cu (HCOO)₂·4H₂O [к9]	290	$g_{\parallel}$ 2,35	$g_\perp$ 2,06				[26, 31]	D $M_m = 2$, моноклин., о) O
Cu (HCOO)₂·2H₂O [к9]	290	g_{max} 2,24	g_{min} 2,10				[26]	$M_m = 4$, о) O
Cu (CH₃COO)₂·H₂O [к10]	290, 90	g_x 2,05₅ ± 0,005	g_y 2,09₅ ± 0,005	g_z 2,34₄ ± 0,01			[12, 13]	S = 1 D
	90	2,08 ± 0,03	2,08 ± 0,03	2,42 ± 0,03	0,345 ± 0,005	0,007 ± 0,003	[27]	M=4, M_m=2, моноклин., п) p
Cu (CH₃CH₂COO)₂·H₂O	290	I: 2,36₅ ± 0,015 II: 2,36₉ ± 0,015 III: 2,36₅ ± 0,015	2,11₁ + 0,015 2,10₀ ± 0,015 2,10₂ ± 0,015	2,09₂ ± 0,015 2,08₂ ± 0,015 2,10₂ ± 0,015	0,344 ± 0,007 2,08₂ 0,341 ± 0,007 2,10₂ 0,345 ± 0,007	0,004 0,004 0,002	[50]	S=1, три различных магнитных комплекса, см. § 3.11 F
		2,09	— 2,10	2,35	0,38	≈ 0	[14]	S = 1
Cu [(CH₃CO)₂ CH]₂	290 90	$g_{\parallel}$ 2,254 ± 0,001	$g_\perp$ 2,075 ± 0,0008				[8], [32]	
Cu : Pd = 1 : 200	77	$g_{\parallel}$ 2,266₁	g_1 2,055₁	g_2 2,051₆			[37]	A = — 0,0160, Q' = = 0,0007, B = — 0,0195 т) t
5 Cu²⁺ в AgCl	290 77	$g_{\parallel}$ A : 2,00 ± 0,02 B : 2,26 ± 0,02 C : 2,30 ± 0,02	$g_\perp$ 2,28 ± 0,02 2,07 ± 0,02 2,07 ± 0,02	A 0,00093 ± 0,00093 0,0100 ± 0,0006 0,0112 ± 0,0001	B 0,0090 ± 0,0006 0,0043 ± 0,0005 0,0044 ± 0,0005	Q 0,0019 ± 0,0005 0,0021 ± 0,0005 0,0021 ± 0,0005	[51]	

A) Orthorhombic; B) rhombic; C) tetragonal; D) monoclinic; E) or;
F) S = 1, three different magnetic complexes, see §3.11.

TABLE 4.1 (Conclusion)

1 Формула	T, °К	g			A			2 Литература	3 Замечания
5 B Cu²⁺ в MgO (порошок)		2,190 ±0,002			0,0019 ±0,0001			[52]	Поле кубической симметрии A
5 Cu²⁺ в NaCl	290	b c a) 2,07 б) 2,06 в) 2,16						[53]	у) u
5 Cu²⁺ в KCl	290	2,180 ±0,009						[53]	
C Диметилглиоксим Cu²⁺		g_x 2,065	g_y 2,033	g_z 2,136				[54]	
5 Cu²⁺ в CdCl₂	290	$g_{\parallel}$ 2,205 ±0,010	$g_{\perp}$ 2,19 ±0,01					[55]	ф) V
	90 20	2,34 ±0,01	2,07 ±0,01		0,0120 ±0,0010				M_m - 3

Paramagnetic resonance is observed also in the following compounds at room temperature:

$g = 2,23$ [17]; Cu (C₂O₄) ($g = 2,12$) [31]; CuC₄H₄O₆ · 3H₂O ($g = 1,97$) [17]; Cu [C₅H₅ (NH₂)₂]₂ SO₄ · 2H₂O CuBr₂ ($g = 2,25$, $g_{min} = 2,05$) [36]; Cu [C₂H₄(NH₂)₂]₂ (NO₃)₂ · 2H₂O ($g_{max} = 2,25$, $g_{min} = 2,05$) [36]; Cu (C₅H₅O₃)₂ · 2H₂O ($g = 2,09$) [17]; Cu (C₅H₅N)₄ (NO₃)₂ · H₂O ($g = 2,04$) [17]; Cu [(CH₃)₃ C (CO)₂ CH₂C₆H₁₁]₂ ($g = 2,04$) [17]; Cu [C₆H₅ (CH₃) (CO)₂ CH₃]₂ ($g = 2,02$) [17]; Cu (C₇H₅O₃)₂ · 2H₂O ($g = 1,97$) [17]; CuF₂ ($g = 2,15$) [17]; CuF₂ basic ($g = 2,08$) [18]; Cu (NH₄)₂ (C₂O₄)₂ · 2H₂O ($g (010) = 2,1 ÷ 2,28$, $g (100) = 2,05 + 2,23$, $M_m = 2$) [29, 31]; CuK₂ (C₂O₄)₂ ($g = 2,13$) [31]; CuNa₂ (C₂O₄)₂ ($g = 2,07$) [31]; Cu (NH₃)₂ Cl₂ · H₂O [19, 35]; Cu (NH₃)₂ SO₄ · H₂O ($g = 2,09$; $T = 300, 90, 4°$ K) [34, 35] [33]; CuSO₄ [19]; CuSO₄ · 3H₂O ($g = 2,19$) [34]; CuSO₄ · 5H₂O [$T = 300°$ K; $g = 2,20$; $T = 90$ K; $g = 2,22$] [29, 34, 43, 46, 49] CuSO₄ 4NH₃·H₂O ($g = 2,04 ÷ 2,19$) [45, 49]; CuSiF₆ · 4H₂O ($g_{\parallel} = 2,40$; $g_{\perp} = 2,10$) [6]; CuWO₄ · 2H₂O ($g = 2,17$) [17]; 2CuC₂O₄ · H₂O ($g = 2,07$) [17]; Cu₃CO₃ (CN)₁₂ ($g = 2,17$; $T = 290 - 12°$ K) [21];

chlorophyllates of copper (T = 270, 90°K; g = 2.05 ± 0.01; Mg:Cu, g = 2.06) [15, 44]; in silicate glass ($g_{\parallel} = 2.32$ $g_{\perp} = 2.06$) [38]; persulfate of diorthophenantrolinate of copper (T = 290, 90, 20°K, $g_{\perp} = 2.05$) [22]; copper derivative of salicylaldimin (Cu:Ni = 1:200) [47]; CuS [20]; chlorinated and nonchlorinated tetraphenylporphin Cu²⁺ (g = 2.18, $A_{Cu} = 0.0250$, $A_{Cl} = 0.0120$) [30].

A) Field of cubic symmetry; B) (powder); c) dimethylglyoxime Cu³⁺.

Remarks:

a) Measurements were made at $\nu \approx 5 \cdot 10^8$ cps.

b) A second anomalous spectrum appears when T > 20°K; the g factors of both spectra differ by less than 1%.

c) Transition temperature from 173 to 273°K.

d) Transition temperature from 33 to 45°K.

e) Transition temperature from 12 to 50°K.

f) Transition temperature from <7 to 35°K.

g) Each Cu²⁺ is surrounded by a distorted octahedron of 4H₂O and 2O; it can be assumed that the Cu²⁺ is in a tetragonal field (the

- 149 -

rhombic field is very small); the angle between the tetragonal axes is $86 \pm 2^\circ$; g_{max} and g_{min} are determined in the plane of the tetragonal axes of the nonequivalent ions.

h) The ratio of the constant λ' of the spin-orbit coupling of the Cu^{2+} ion in the crystal to the constant λ for the free ion is $\lambda'/\lambda = 0.55$.

j) The sharply anisotropic exchange leads to lifting of the hyperfine structure in a direction perpendicular to the Z axes; the structure is resolved in the direction of the Z axes.

k) Each Cu^{2+} has a plane surrounding of two H_2O and two Cl; an elongated octahedron results from two additional more remote Cl, belonging to the other ions of Cu. Only one line is observed. The substance is antiferromagnetic below $4.3^\circ K$.

l) Each Cu^{2+} is surrounded by four Cl's, forming a rhombus in the aa plane, and two molecules of H_2O on a normal to this plane. The two rhombi of the nonequivalent ions are turned through 90° relative to each other around the c axis — the H_2O-H_2O line (the Y axis); thus, the Cu is in a field of rhombic symmetry. The spectrum was measured at wavelengths of 5.4 and 6.6 millimeters, with an exchange frequency $1.1 \cdot 10^{10}$ cps.

m) Each Cu^{2+} is surrounded by a square made up of four N.

n) The Cu^{2+} is surrounded with four N; perpendicular to the N plane, opposite the Cu, an O on one side (at a distance 2.68 A) and Cl on the other (at a distance 2.89 A).

o) Each Cu^{2+} surrounded by four O and two H_2O, forming a distorted octahedron.

p) Bimolecular cell; each Cu^{2+} surrounded by a distorted octahedron made up of four O, an H_2O, and a neighboring Cu^{2+}; distance between two neighboring Cu^{2+} is 2.6 A. $D = 0.345 \pm 0.005$, $E = 0.007 \pm 0.003$,

$A_z = 0.008$, A_x, $A_y < 0.0010$. See §3.11.

r) It is seen from the paramagnetic resonance spectrum that the cell contains six magnetic complexes, each with two Cu^{2+}; three complexes are derived from the remaining three by reflection in the $\underline{ac}$ plane. Each complex is approximately tetragonal.

s) Each Cu^{2+} is surrounded by four O in a single plane. The hyperfine structure is described by the relation

$$K^2 g^2 = A^2 g_{\parallel}^2 \cos^4 \theta + B^2 g_{\perp}^2 \sin^4 \theta + 2C^2 g_{\parallel} g_{\perp} \sin \theta \cos \theta,$$

$C = \pm 0.0062$ cm^{-1} at $T = 77^\circ$K and $C = \pm 0.0043$ cm^{-1} at $T = 290^\circ$K.

t) Type A; axial distortion of the crystalline field due to interaction between Cu^{2+} and vacancy of the positive lattice site in the (110) direction; type B: the same, but the vacancy is in the (100) direction; type C: axial distortion of the cubic-symmetry field is due to the Jahn-Teller effect and is directed along (100). The effect is observed only in halogenated crystals.

u) Spectra a) and b) obtained in crystals grown from a melt, while spectrum c) is obtained from the aqueous solution.

v) There are trigonal distortions of the cubic field.

1) Formula; 2) literature; 3) remarks; 4) cr. st.; 5) in; 6) to.

TABLE 4.2

1 Формула	T, °K	ε‖	ε⊥	2 Литература	3 Замечания
4 $CsTi(SO_4)_2 \cdot 12H_2O$ (кр. ст. 1)	4,2—2,5	1,25 ±0,02	1,14 ±0,02	[1]	
$KTi(C_2O_4)_2 \cdot 2H_2O$	90—20	1,86	1,96	[2]	$M_m = 2$
$Ti[(CH_2CO)_2CH]_3$ [x1]	290	2,00	1,93	[3]	$M_m = 2$. Ближайшее окружение Ti^{3+}— октаэдр из 6O; локальное поле аксиальной симметрии
A $Ti : Al = 10^{-2}$ (порошок)					B
A $CsTi(SO_4)_2 \cdot 12H_2O$ (порошок)	7,88 6,33	1,53 1,35		[4]	g-фактор зависит от температуры, ширина линии очень велика и определяется временем спин-решеточной релаксации

V^{4+}

1 Формула	T, °K	g			2 Литература	3 Замечания
		g_1	g_2	g_3		
$K_2V_2O_5(C_2O_4)_2 \cdot 4H_2O$	290, 90	1,95₄	1,96₅	1,96₇	[1]	C В порошке, разбавленном солью Ti^{3+}, наблюдена сверхтонкая структура, обязанная $^{51}V\left(I = \frac{7}{2}\right)$; $^{51}A = 0,010 + 0,001$
$VOCl_2$	290	2,00			[2]	
$VO_2(C_6H_5)_2N_2(CH)_2$	290	2,02			[2]	
A $VOSO_4 \cdot 2H_2O$ / $VOSO_4 \cdot 5H_2O$ (порошок)	290 / 300 / 70 / 4	1,96 / 1,990₁ ±0,002 / 1,998₇ ±0,002 / 1,994 ±0,004			[3] [4]	

Mn^{6+}

1 Формула	T, °K	g	2 Литература	3 Замечания
MnO_3	290	1,96	[1]	

V^{0+}

1 Формула	T, °K	g‖	D	A	2 Литература	3 Замечания
5 V^{0+} в Al_2O_3	4,2 / 2 / 90	1,92 ±0,01	~+10	0,0193 ±0,0002 / 350 эрст	[1] [2]	D Наблюден переход $\Delta M = 2$

A) (Powder); b) $M_m = 2$. Nearest surrounding of Ti^{3+} is an octahedron of 6O; local field of axial symmetry. The g factor depends on the temperature, the line width is very large and is determined by the spin-lattice relaxation time. C) A hyperfine structure, due to ^{51}V (I = 7/2) is observed in powder diluted with a Ti^{3+} salt; D) The transition $\Delta M = 2$ is observed.

TABLE 4.2 (Continuation)

1 Формула	T, °K	g			A			2 Литература	3 Замечания
4 K₂Co(SO₄)₂ · 6H₂O (кр. ст. 2) Co : Zn = 1 : 500 — 10⁻⁵	20	g_z 6,56 ± 0,13	g_{min} 2,50 ± 0,05	g_0 3,35 ± 0,07	A_z 0,0286 ± 0,0006	A_{min} 0,0065 ± 0,0003	A_0 0,0080 ± 0,0004	[1]	ψ = + 163°, α = 35°
4 (NH₄)₂Co(SO₄)₂ · 6H₂O (кр. ст. 2) Co : Zn = 1 : 500 — 10⁻⁵	20	g_z 6,45 ± 0,13	g_{min} 3,06 ± 0,06	g_0 3,06 ± 0,06	A_z 0,0245 ± 0,0005	A_{min} 0,0020 ± 0,0001	A_0 0,0020 ± 0,0001	[1]	ψ = + 130°, α = 34°
4 (NH₄)₂Co(SO₄)₂ · 6D₂O (кр. ст. 2) Co⁶⁰ : Co⁵⁹ : Zn = 1 : 50 : 10 000	20	g 6,41				⁶⁰A 0,0251	⁶⁰A 0,0144	[2]	$\frac{\mu(Co^{60})}{\mu(Co^{59})}$ = 0,8191 ± ± 0,0016
4 Rb₂Co(SO₄)₂ · 6H₂O (кр. ст. 2) Co : Zn	20	g_z 6,65	g_{min} 2,7	g_0 3,3	A_z 0,0293 ± 0,0003	A_{min} 0,0049 ± 0,0005		[3]	ψ = + 157°, α = 37°
4 Co₃Bi₂(NO₃)₁₂ · 24H₂O (кр. ст. 3) Co : Mg = 10⁻³	20	$g_\parallel$ I: 7,29 ± 0,01 $g_\parallel$ II: 4,108 ± 0,003	$g_\perp$ 2,338 ± 0,004 $g_\perp$ 4,385 ± 0,003		A 0,0283 ± 0,0001 A 0,0085 ± 0,0001	B ≤ 0,0001 B 0,0103 ± 0,0001		[4]	A Два различных магнитных комплекса
4 (Ce + Bi)₂Co₃(NO₃)₁₂ · 24H₂O (кр. ст. 3) Co : Mg = 1 : 200 Ce — 0%, Bi — 100% Ce — 10%	4	$g_\parallel$ I : 4,145 ± 0,002 4,12 ± 0,01	$g_\perp$ 4,415 ± 0,002 4,45 ± 0,01		A 0,0095 ± 0,0003 0,0082 ± 0,0009	B 0,0103 ± 0,0003 0,0114 ± 0,0009		[5]	A Два различных магнитных комплекса
Ce — 20%		$g_\parallel$ 4,22 ± 0,01	$g_\perp$ 4,22 ± 0,01		0,0090 ± 0,0009	0,0090 ± 0,0009			
Ce — 50%		4,30 ± 0,01	4,31 ± 0,01		0,00897 ± 0,0009	0,0107 ± 0,0009			
Ce — 80%		4,02 ± 0,01	4,45 ± 0,01						
Ce — 100%		4,14 ± 0,01							
Ce — 0%, Bi — 100%		II: 7,20 ± 0,01	2,39 ± 0,02		0,0302 ± 0,0006	<0,0001			
Ce — 10%			2,37 ± 0,01						
Ce — 20%		7,41	2,36 ± 0,01						
Ce — 50% Ce — 80%		10,55 7,33	2,36 ± 0,01						
Ce — 100% La₃Co₃(NO₃)₁₂ · 24H₂O	4	7,3 I: 4,050 ± 0,002 II : 7,23 ± 0,01	4,430 ± 0,002 2,810 ± 0,002		0,00807 ± 0,00030 0,02788 ± 0,00060	0.01033 ± 0,00030 <0,0001		[5]	A Два различных магнитных комплекса
4 CoSiF₆ · 6H₂O (кр. ст. 4) Co : Zn = 1 : 500 — 10⁻⁵	20	5,82 ± 0,12	3,44 ± 0,07		0,0184 ± 0,0004	0,0047 ± 0,0002		[1]	а) a
		6,6 ± 0,1	2,62 ± 0,05		0,023	0,0009			
		6,6 ± 0,2	2,82 ± 0,06		0,025	0,0013			б) b

A) Two different magnetic complexes.

TABLE 4.2 (Continuation)

1 Формула	T,°K	g			A			2 Литература	3 Замечания
		3,58 ± 0,05	4,09 ± 0,05		0,01	0,01			б) b
4 CoSO₄·7H₂O (кр. ст. 6)	20	g_x 2,90 ± 0,05	g_y 3,30 ± 0,07	g_z 6,90 ± 0,014	A_x 0,0028 ± 0,0001		A_z 0,0254 ± 0,0005	[1]	в) c
5 Co:Zn = 10⁻³ Co²⁺ в ZnF₂	20	g_x 2,6	g_y 6,05 ± 0,01	g_z 4,1 ± 0,1	A_x −0,0043	A_y 0,0217 ± 0,0002	A_z 0,0067	[6]	M_m = 2, г)d
5 Co²⁺ в NaF; 8·10¹⁵ A центров в 0,05 см³ кристалла; после облучения	20	g_x 4,3	g_y 8,3	g_z 5,7		A_y 0,0082	A_z 0,0250	[7]	л) e
5 Co²⁺ в MgO Co:Mg = 10⁻³ — 2·10⁻³	20 4	g ∼4,5 4,2785 ± 0,0001			A 0,00977₈ ± 0,00002			[8]	
5 Co²⁺ в Al₂O₃	1,6	$g_{||}$ 2,316 ± 0,005		$g_\perp$ 4,98 ± 0,01	A 0,00334 ± 0,00005		B 0,00974 ± 0,00013	[13]	
5 Co²⁺ в CaF₂ Co:Ca ∼ 10⁻³	4,2 20	2,27 ∼6,6		4,95 3,40 ± 0,05			0,0170 ± 0,0004	[15] [14]	е) f
5 Co²⁺ в CdCl₂	20	3,06 ± 0,02		4,98 ± 0,02	0,0035		0,0170	[17]	ж) g

Paramagnetic resonance observed also in: $Co(C_6H_4)_4(CN)_8$ (T = 270-20°K, two complexes I: g = 2.9, II: g = 2.4-1.98) [9]; (T = 290°K, g = 1.98; T = 20°K, g = 2.90) [10]; $K_2Co(SO_4)_2·6D_2O$ (T = 20°K, Co:Zn, sample contained 4 mC Co^{56}, μ^{56}/μ^{59} = 0.829 ± 0.002; sample contained 4 mC Co^{58}, μ^{58}/μ^{59} = 0.8734 ± 0.0024 [11, 12, 16].

A) Centers in 0.05 cm³ of the crystal; after irradiation.

Remarks:

a) Principal line, $g_{||}$ corresponds to the c axis of the crystal.

b) Much weaker lines (lattice imperfections).

c) For one complex, the Z axis lies in the plane (110) with ∠ZOc = = 13°, the X axis in (110) with ∠XOc = 103°, the Y axis is parallel to (110) plane. The axes of the second complex are obtained by mirror reflection. For an undilute salt, g is anisotropic in the ab plane and ranges from 1.4 to 5.8.

d) Hyperfine structure due to the F nuclei is observed: A_y^N = = (32 ± 1)·10⁻⁴ cm⁻¹, A_z^N = (21 ± 5)·10⁻⁴ cm⁻¹.

e) There are six types of magnetic ions with similar spectra. A well resolved structure due to the interaction not only with Co nuclei but also with F nuclei, is observed. After irradiation, this spectrum

vanishes and two isotropic lines appear, one of which is without a re-
solved structure and possibly belongs to Co^{2+} in a weakly distorted
cubic surrounding, while the other belongs to Co^+ (see page 193). All
the irradiated centers vanish after heating to $150°C$.

f) Hyperfine structure is observed, due to the interaction with
the F^- nuclei, $A_F \approx 0.0030$ cm^{-1}.

g) There are trigonal distortions of the cubic field.

TABLE 4.2 (Conclusion)

1 Формула		T. °K	ε_z	Δ	2 Литература	3 Замечания
FeF₃ [к13] Fe : Zn = 1 : 3000		90	8,97 ± 0,05	0,224 ± 0,010	[1]	$M=2$, $M_m=1$, каждый Fe окружен искаженным октаэдром из шести F A
		20	8,97 ± 0,02	0,203 ± 0,004	[1, 2]	Наблюдена сверхтонкая структура, обязанная ядрам F (константы определены при $T=12°$ K): $A_z^I = (9{,}98 \pm 0{,}52) \cdot 10^{-3}$ см⁻¹, 6 $A_z^{II} = (6{,}39 \pm 0{,}43) \cdot 10^{-3}$ см⁻¹ 6
5	Fe²⁺ в ZnS		2,26		[3]	
5	Fe²⁺ в MgO		3,428; 6,9		[3]	
5	Fe²⁺ в CdCl₂	20	g∥ 7,4		[6]	B Линия асимметрична

Paramagnetic resonance observed also for $T = 20°K$ in $K_2Fe(SO_4)_2 \cdot 6H_2O$,
$(NH_4)_2Fe(SO_4)_2 \cdot 6H_2O$, $FeSiF_6 \cdot 6H_2O$ [4]; $(C_3H_4N_2)_4Fe$ ($T = 290$, $20°K$, $g = 3.8$; 2.0) [5].

A) $M = 2$, $M_m = 1$, each Fe surrounded by a distorted octahedron of F.
A hyperfine structure is observed, due to the F nuclei (the con-
stants were determined at $T = 12°K$):

B) Asymmetrical line.

1) Formula; 2) literature; 3) remarks; 4) cr. st.; 5) in; 6) cm^{-1}.

TABLE 4.3

Ce^{3+}

1 Формула	T, °K	$\varepsilon_\parallel^a$	$\varepsilon_\perp^a$	$\varepsilon_\parallel^b$	$\varepsilon_\perp^b$	2 Литература	3 Замечания
4 $Mg_3Ce_2(NO_3)_{12} \cdot 24H_2O$ (кр. ст. 3) Ce : La = 1 : 20	4,2	0,25 ±0,05	1,84 ±0,02			[1]	
$^{141}Ce : La = 10^{-5}$	4,2		1,84			[2]	$A^{141} = 0,002$ $B^{141} = 0,0126 \pm 0,0001$
4 $Ce(C_2H_5SO_4)_3 \cdot 9H_2O$ (кр. ст. 9) Ce : La = 1 : 200	2,5	1,0 ±0,2	2,25 ±0,2	3,80 ±0,04	$\leqslant 0,4$	[3]	A Дублет b нижний
	4,2	0,955 ±0,005	2,185 ±0,01	3,72 ±0,01	0,20 ±0,005	[3, 4]	B Дублет b на (3±1) см⁻¹ выше дублета a
5 Ce^{3+} в CaF_2 Ce : Ca ~ 10⁻⁴	20	$g_\parallel$ 3,030 ±0,003	$g_\perp$ 1,396 ±0,002			[5]	C $M_{экв} = 3$, кристаллические оси неэквивалентных ионов направлены вдоль ребер куба
5 Ce^{3+} в $LaCl_3$ Ce : La = 2 : 100	4	4,0366 ±0,0015	0,17 ±0,08			[6]	

Nd^{3+}

1 Формула	T, °K	$\varepsilon_\parallel$	$\varepsilon_\perp$	Изотоп	A	B	2 Литература	3 Замечания
4 $Mg_3Nd_2(NO_3)_{12} \cdot 24H_2O$ (кр. ст. 3) Nd : La = 10⁻²	4,2	0,45 ±0,05	2,72 ±0,02	143	0,0052 ±0,0005	0,0312 ±0,0001	[1]	
				145	0,0032 ±0,0003	0,0194 ±0,0001		
Nd : La = 10⁻⁶	4,2		2,72	147	~0,004	0,0237 ±0,0001	[7]	
4 $Nd(C_2H_5SO_4)_3 \cdot 9H_2O$ (кр. ст. 9)	20	3,535 ±0,001	2,072 ±0,001	143	0,03803 ±0,00001	0,01989 ±0,00005	[2]	$\dfrac{^{145}A}{^{143}A} = 1,6083 \pm 0,0012$
Nd : La = 1 : 200				145	0,02364 ±0,00001	0,01237 ±0,00005		
$Nd(NO_3)_3 \cdot 6H_2O$ Nd : La = 1 : 200	20—18	g_x 3,88 ±0,01 g_y 1,72 ±0,01	g_z 0,74 ±0,01	143	A_x 0,0432 ±0,0002 A_y 0,0193 ±0,0002	A_z 0,0082 ±0,0010	[6]	D Для обоих изотопов $|P_x - P_z| < 0,005,$ $|P_y - P_z| < 0,005$
				145	A_x 0,0270 ±0,0002 A_y 0,0119 ±0,0002	A_z 0,0051 ±0,0010		
5 Nd^{3+} в CaF_2 Nd : Ca = 10⁻³	20	$g_\parallel$ 4,412 ±0,008	$g_\perp$ 1,301 ±0,002				[5]	a)
5 Nd^{3+} в SrF_2 Nd : Sr = 10⁻²	20	4,289 ±0,006	1,505 ±0,002				[5]	a)

A) Doublet b is the lower one; B) doublet b is (3±1) cm⁻¹ higher than doublet a; C) $M_m = 3$, crystalline axis of nonequivalent ions directed along the edges of a cube; D) for both isotopes.

TABLE 4.3 (Continuation)

1 Формула	T, °K	$\varepsilon_{\parallel}$	$\varepsilon_{\perp}$	Изотоп 1а	A	B	Литература 2	3 Замечания
5 Nd³⁺ в LaCl₃ Nd:La = 2:10⁴	4	8,996 ±0,001	1,763 ±0,001	143	0,0425 ±0,0002	0,0167 ±0,0001	[8]	¹⁴³P < 1·10⁻⁴
				145	0,0264 ±0,0002	0,0104 ±0,0001		¹⁴⁵P < 1·10⁻⁴

Paramagnetic resonance observed also in $Nd_2(SO_4)_3$ (T = 90°K) [3]; $Nd_2(SO_4)_3 \cdot 8H_2O$ (T = 90°K) [3]; Nd_2O_3 (T = 290°K, g = 3.2) [4].

Remarks. a) M_m = 3. There is an axial electric field near each ion; the crystalline axes of the nonequivalent ions are the axes of a cube.

$$Sm^{3+}$$

1 Формула	T, °K	$\varepsilon_{\parallel}$	$\varepsilon_{\perp}$	Изотоп 1а	A	B	Литература 2	3 Замечания
4 Mg₃Sm₂(NO₃)₁₂ · 24H₂O (кр. ст. 3)	4,2	0,76 ±0,01	0,40 ±0,05	147	0,0346 ±0,0005	<0,010	[1]	
				149	0,0287 ±0,0005	<0,010		
4 Sm (C₂H₅SO₄)₃ · 9H₂O (кр. ст. 9)	4,2	0,596 ±0,002	0,604 ±0,002	147	0,0060 ±0,0001	0,0251 ±0,0001	[2]	P < 0,0004
Sm:La = 10⁻³				149	0,0049 ±0,0001	0,0205 ±0,0001		$\frac{^{147}A}{^{149}A}$ = 1,222 ± 0,008
5 Sm³⁺ в LaCl₃ Sm:La = 1:50	4	0,5841 ±0,0003	0,6127 ±0,0006	147	0,00607 ±0,00002	0,0245 ±0,0001	[4]	
				149	0,00499 ±0,00002	0,0202 ±0,0001		

Paramagnetic resonance observed also in Sm in SrS (T = 77-20°K) and in Sm in SrS·SrSe [3].

$$Dy^{3+}$$

1 Формула	T, °K	g		Изотоп 1а	A_x		Литература 2	3 Замечания
Dy (CH₃COO)₃ · 4H₂O	4,2	g_x 13,60 ±0,06		161	0,0381 ±0,0005		[1]	
Dy:Y = 1:150				163	0,0540 ±0,0005			a)
		$g_{\parallel}$ 4,281	$g_{\perp}$ 8,923		A	B		
Dy₃Mg₃ (NO₃)₁₂ · 24H₂O		4,281	8,923	161	0,01161	0,02463	[2]	¹⁶¹P = 0,00142 ± 0,00010
Dy:La = 2·10⁻⁴		±0,006	±0,160		±0,00007	±0,00015		¹⁶³P = −0,00168 ± 0,00010
				163	0,01622 ±0,00007	0,03415 ±0,00015		$\frac{^{163}Q}{^{161}Q}$ = 1,18 ± 0,15

Remark. a) M_m = 1, triclinic crystal. All principal values of the g factor are different; the direction of the magnetic field corresponds to the maximum value of the g factor.

TABLE 4.3 (Continuation)

$$Er^{3+}$$

1 Формула	T, °K	$g_\parallel$	$g_\perp$	A	B	2 Литература	3 Замечания
Er $(C_2H_5SO_4)_3 \cdot 9H_2O$ Er : La = 1 : 200	4	1,47 ±0,03	8,85 ±0,2	0,0052 ±0,0001	0,0314 ±0,0001	[1]	P = 0,0030 ± 0,0003
5 Er³⁺ в CaF₂ Er : Ca = 10⁻⁶	20, 14	g 6,78 ±0,01				[2]	a)

1 Формула	T, °K	$g_\parallel$	$g_\perp$	A	B	2 Литература	3 Замечания
		7,76 ±0,02	6,253 ±0,006	0,0261 ±0,0003	0,0219 ±0,0003		б) b
Er₂Mg₃(NO₃)₁₂ · 24H₂O	4,2	6,76 ±0,02	9,11 ±0,01				в) с
5		4,21 ±0,01	7,990 ±0,010	0,0142 ±0,0001	0,0274 ±0,0001	[3]	P ≈ 0,0013
Er³⁺ в LaCl₃ Er : La = 5 · 10⁻³		1,989 ±0,001	8,757 ±0,002	0,00664 ±0,00003		[4]	P = 0,00086

Remarks:
a) Isotropic line.
b) Line from ground-state doublet.
c) Line from excited doublet.

$$Yb^{3+}$$

1 Формула	T, °K	g_x	1а Изотоп	A_x	2 Литература	3 Замечания
Yb (CH₃COO)₃ · 4H₂O Yb : Y = 10⁻³	4,2	4,57 ±0,02	171	0,122 ±0,001	[1]	a)
			173	0,0341 ±0,0003		

Remark. a) $M_m = 1$, triclinic crystal; all principal bodies of the **g** factor different; direction of magnetic field corresponds to maximum value of **g** factor.

1) Formula; 1a) isotope; 2) literature; 3) remarks; 4) cr. st.; 5) in.

TABLE 4.4

Pr³⁺

1 Формула	T, °K	$\varepsilon_{\parallel}$	$\varepsilon_{\perp}$	Δ	A	2 Литература	3 Замечания
4 Mg₃Pr₂(NO₃)₁₂ · 24H₂O (кр. ст. 3) Pr : La = 10⁻²	4,2	1,55 ±0,02			0,077 ±0,002	[1]	
4 Pr(C₂H₅SO₄)₃ · 9H₂O (кр. ст. 9) Pr : La = 1 : 200 Pr : Y	20	1,69 ±0,01 1,52₃ ±0,02	<0,03	~0,19 0,11 ±0,04	0,083 ±0,001 A_f 0,0755 ±0,0020	[2, 5] [5, 7, 3]	$V_2^0 = 50$ см⁻¹, $V_4^0 = -100$ см⁻¹, $V_4^3 = -48$ см⁻¹, $V_6^3 = 660$ см⁻¹
PrCl₃ · 7H₂O	4	3,02	2,23			[3]	A $M_m = 2$, триклинный кристалл
PrCl₃ Pr : La = 0,11	4,2	1,791	3,975			[4]	B Наблюдалась 1 линия
PrCl₃ Pr : La = 1 : 50	4	1,035 ±0,005	0,10 ±0,15		0,0502 ±0,0003	[8]	
5 Pr³⁺ в LaAlO₃ Pr : La = 10⁻²	4,2	2,67 ±0,02			0,119 ±0,003	[6]	C Кристалл типа перовскита

A) $M_m = 2$, triclinic crystal; B) one line observed; C) crystal of perovskite type.

Tb³⁺

1 Формула	T, °K	$\varepsilon_{\parallel}$	$\varepsilon_{\perp}$	Δ	A	2 Литература	3 Замечания
Tb(C₂H₅SO₄)₃ · 9H₂O (кр. ст. 9) Tb : Y = 10⁻²	20	17,72 ±0,02	<0,3	0,387 ±0,001	0,209 ±0,002	[1, 4]	$V_2^0 = (220 \pm 30)$ см⁻¹, $V_4^0 = 37$ см⁻¹
Tb(NO₃)₃ · 6H₂O Tb : La = 10⁻²	13	$g_x, g_y < 1$ 18,0 ±0,4		0,210 ±0,007	A_f 0,212 ±0,005	[2]	A Наблюдалась СТС от F⁺, число компонент четное, расстояния между ними порядка 5 эрст
Tb³⁺ в CaF₂ Tb : Ca = 10⁻⁴	20—10	17,8 ±0,1		0,173 ±0,001	0,209 ±0,001	[5]	
Tb³⁺ в LaCl₃ Tb : La = 5 · 10⁻³ — 2 · 10⁻³	4	17,78 ±0,01	<0,1	0,2010	0,2120 ±0,0030	[6]	

Paramagnetic resonance observed also in Tb³⁺ in SrS (T = 290°K) [3].

A) Hyperfine structure due to F⁺ observed, number of components even, distances between components on the order of 5 oersted.

TABLE 4.4 (Continued)

Ho^{3+}

Формула	T, °K	ε_z	Δ	A	B	P	Литература	Замечания
Ho (C₂H₅SO₄)₃ · 9H₂O Ho : Y = 10⁻²	13	15,410 ±0,010	0,065 ±0,015	0,3340 ±0,0010	0,0200 ±0,0040	0,0003 ±0,0003	[1]	
		$\varepsilon_{\parallel}$ 7,705 ±0,005			0,083		[2]	$D=(-5,8\pm0,2)$ см⁻¹ a)
		$\varepsilon_\perp$ 3,86						
Ho³⁺ в LaCl₃ Ho : La = 5 · 10⁻³		$\varepsilon_{\parallel}$ 16,010 ±0,018	$\varepsilon_\perp$ ~0	0,3510 ±0,0070			[3]	

Remark. a) A detailed investigation has shown that the best explanation of the experimental data can be obtained by ascribing S = 1 to the ground level.

1) Formula; 2) literature; 3) remarks; 4) cr. st.; 5) in; 6) cm⁻¹.

TABLE 4.5

Mn^{2+}

1 Формула	T, °K	g	D	E	a	A	Литература 2	3 Замечания
(NH₄)₂ Mn (SO₄)₂ · 6H₂O (кр. ст. 2)	290		0,0231 ±0,0002	0,006	0,0003	0,0090 ±0,0002	[1]	ψ=+60°, α=30°
Mn : Mg = 1 : 250	290		0,022₆	0,004₁		0,0095	[2]	ψ=+59°, α=30,5°
Mn : Zn	290	2,000 ±0,005	0,0238	0,007₅	0,0005	0,0091	[3]	
Mn : Zn = 10⁻²	230		+0,0243 ±0,0005	0,010 ±0,002	+0,0005 ±0,0001	−0,0091₁ ±0,0001	[4]	ψ=+58°, α=32°
	195		+0,0258 ±0,0005	0,008 ±0,001₀	+0,0007 ±0,0001	−0,0089₀ ±0,0001		
	90		+0,0275 ±0,0005	0,007 ±0,001	+0,0007 ±0,0001	−0,0089₀ ±0,0001		
	20		+0,0277 ±0,0005	0,005 ±0,001	+0,0008 ±0,0002	−0,0093		
Mn₃Bi₂ (NO₃)₁₂ · 24H₂O (кр. ст. 3) Mn : Mg = 1 : 200	90	I:1,99 ±0,02	−0,0211 ±0,0001	0	+0,0008 ±0,0001	−0,0090	[5]	Два различных магнитных комплекса
	20	1,997 ±0,003	−0,0215 ±0,0001	0	+0,0008 ±0,0001	−0,0090		
	90	II:1,99 ±0,02	−0,0064 ±0,0001	0	+0,0010 ±0,0001	−0,0089		
	20	1,997 ±0,003	−0,0080 ±0,0001	0	+0,0010 ±0,0001	−0,0090		
MnSiF₆ · 6H₂O (кр. ст. 4) Mn : Mg = 1 : 20 — 1 : 150	290		−0,0274	0,0080	+0,0007	−0,0092	[6]	$M_m=6$
Mn : Zn	290	2,000 ±0,005	0,0171	0	0,0007₅	0,0090	[3]	
Mn : Zn = 10⁻²	290		−0,0179 ±0,0008	0	+0,0007 ±0,0001	−0,0095	[4]	

TABLE 4.5 (Continuation)

1 Формула	T, °K	g	D	E	a	A	Литература [2]	3 Замечания
	195		−0,0161 ±0,0003	0	+0,0010 ±0,0002	−0,0092		
	90	2,000 ±0,001	−0,0141 ±0,0003	0	+0,0011 ±0,0002	−0,0092		
	20		−0,0134 ±0,0003	0	+0,0009 ±0,0002	−0,0091		
4 MnSO₄ · 7H₂O (кр. ст. 6) Mn : Mg	290	2,000 ±0,005	0,040₀	∼0		0,0088	[3]	з) a
MnCO₃ [к14] Mn : Ca = 1 : 2000	290	2,002	0,0075	≈ 0		0,00878	[7]	F = 0,0058, в) c
Mn²⁺ в ZnS 6	290	2,0016 ±0,0001	−0,0105			−0,0065	[33]	M_m = 2, F = −0,00076, гексагон. 9
Mn²⁺ в ZnS 6	290, 90, 4	2,0025 ±0,0002	0		−0,000781 ±0,000006	−0,00637 ±0,00001	[34, 35, 38, 53]	Кубич. 10
Mn²⁺ в ZnF₂ Mn : Zn = 5 · 10⁻⁶	290	2,002 ±0,005	−0,0186 ±0,0008	−0,0041 ±0,0008		−0,0096 ±0,0003	[21]	M_m = 2, 6) b
Mn (HCOO)₂ · 2H₂O Mn : Zn	290	1,999 ±0,001₅	0,0485 ±0,0005	0,011	0,0009₅	0,0091 ±0,0001	[10]	г) d
Mn (CH₃COO)₂ · 3H₂O Mn : Zn	290		0,0235	0,002₅		0,0084	[3, 11]	д) e
Mn (CH₃COO)₂ · 4H₂O Mn : Zn = 1 : 100	290	2,00 ±0,01	0,0412	0,006₀	0,0008	0,0087	[1]	е) f
6 Mn²⁺ в NaCl Mn²⁺ : Na⁺ = 10⁻³ — 4·10⁻⁶	290	2,0011 ±0,0005				0,00829 ±0,00005	[52]	
7 (при медленном охлаждении из расплава)	290	2,004					[40]	ж) g
8 (из расплава при быстром охлаждении)	290	2,015						
11 (из водного раствора)	290	2,020 ±0,005						з) h
11 (из водного раствора)	290	2,018						
11 (из водного раствора)	290	2,0012 ±0,0008	0,01285 ±0,00010	0,00479 ±0,00004		−0,00827 ±0,00008	[47]	п) o
12 Mn²⁺ 0,001—0,02% по весу	290	2,010 ±0,005					[28, 29]	з) h
6		2,0022 ±0,0008				0,00807 ±0,00002		и) 1
Mn²⁺ в KCl Mn²⁺ 10⁻³ — 10⁻⁶ (из расплава)	290 290, 80	2,0041 2,002				0,00886	[30] [28]	и) 1 з) h
13 Mn²⁺ в KCl, KBr, KI (из раствора)	290 80	2,0047				0,00887	[28] [52]	и) 1
14 Mn²⁺ в KBr 6 Mn²⁺ 0,001—0,02% по весу		2,0043 ±0,0005				0,00886 ±0,00002	[29]	
13 Mn²⁺ в NaF 6 4 · 10⁶ Mn²⁺ 15 в 0,05 см³ кристалла 6	90	I : 1,996 ±0,006 II : 2,00 ±0,01	I : 0,0089 ±0,0005 II : 0,0225 ±0,0008			I : 0,0091 ±0,0004 II : 0,0092 ±0,0004	[20]	к) j
Mn²⁺ в MgO 12 0,001—0,1% Mn²⁺ по весу	290 70, 4	2,0015 ±0,0001			+0,00186 ±0,00003	−0,00812 ±0,00005	[22, 23, 29]	
6 Mn²⁺ в CaF₂ 0,04%—0,5% Mn²⁺ 12 по весу	290 4	2,0013 ±0,001 2,0012 ±0,001				0,00954 ±0,00001 0,00945 ±0,00001	[23] [23]	
13 Mn : Ca = 10⁻⁴ 6 (из расплава)	90	1,998 ±0,003			+0,00006 ±0,00004	−0,00978 ±0,00010	[48]	и) m
Mn²⁺ в ZnO Mn : Zn = 10⁻⁶	77	2,0016 ±0,0006	−0,02169 ±0,0022		−0,00020 ±0,00006	−0,00760 ±0,00004	[49]	9 Гексагон.
6 Mn²⁺ в CdS Mn : Cd = 10⁻⁶	300	2,0029 ±0,0006	+0,00062 ±0,00022		−0,00014 ±0,00006	−0,00653 ±0,00004	[49]	9 Гексагон., о) n

- 161 -

TABLE 4.5 (Continuation)

1 Формула	Т, °К	g	D	B	ε	A	Литература	Замечания
6 Mn²⁺ в AgCl Mn : Ag = 10⁻⁴ — 10⁻³	290	I: 2,006 ±0,003				I: 0,0081 ±0,0004	[18]	з)к
13 (из расплава) Mn²⁺ в AgBr Mn : Ag = 10⁻⁴ — 10⁻³	290	II: 2,000 +0,003						
13 (из расплава) Mn²⁺ в Ge	290	2,006 −2,006 ±0,010				0,0077 ±0,0004	[18]	
16 MnCl₂ (порошок) Mn : Sr = 1 : 1000	77 1,5 20	2,0061 ±0,0002 2,00			+0,00088 ±0,00005	−0,00425 ±0,00003 ⁵⁵A = 0,00907 ⁵⁵A = 0,00871	[19] [32]	м)1
Mn²⁺ в фосфорах **17** 0,1—0,005% Mn²⁺ (порошки **16** KMgF₃	290	2,004 ±0,0025				0,00918	[37]	
CaF₂		2,004 ±0,0025				0,00922	[37, 50]	
CaCaF₂		2,004 ±0,0025				0,00908	[37]	
CaO		2,004 ±0,0025				0,00849	[37, 50]	
MgAl₂O₄, 4MgO·3Al₂O₃, 6MgO·Al₂O₃		1,999 2,004 ±0,0025				0,00877 0,00811	[37]	
CdS		2,006 ±0,0025				0,00607	[37, 50]	
CdTe		2,002 2,008 ±0,0025				0,00648 0,00551	[37, 50]	
ZnO·Al₂O₃		2,004 ±0,0025				0,00756	[37]	
ZnS		2,004 ±0,0025				0,00644 0,00638	[37] [9, 25, 50]	
16 MnS (порошок)	290	2,001 2,0024 ±0,0004	0,002			0,0063	[8, 37]	9 Гексагон
Mn : Zn = 10⁻³ — 10⁻⁴	290		0,001			0,0065 ±0,0001	[9]	
13 Mn²⁺ в NaBr (из расплава)	290	2,07 ±0,01						
Mn²⁺ в SrCl₂ (порошок) Mn : Sr = 10⁻³ **16**	20	2				⁵⁵A = 0,00974 ⁵⁵A = 0,00910	[52] [54]	**19** Два типа спектра, видимо, в зависимости
16 Mn²⁺ в SrS — SrSe (порошок)	290	2,00				A₁ = 0,0089 A₂ = 0,0086	[55]	от окружения S или Se Тригональное ис-
Mn²⁺ в CdCl₂	290, 90, 20	2,00	0,0015 ±0,0005			0,0082 ±0,0005	[56]	кажение кубического поля **20**
13 Mn²⁺ в LiCl (из расплава)		2,003 ±0,001				0,0076 ±0,0005	[57]	
18 Пары Mn — Au в Si	20	ε‖ 2,0	ε⊥ 4,0			A = 0,0060 B = 0,0096	[51]	P = 0,00009, р)

21 Парамагнитный резонанс наблюден также при комнатной температуре в: а) фосфорах, содержащих малые концентрации Mn²⁺: ZnAl₂O₄ (g ≈ 2,0, A = 0,00765) [9]; MgO (g = 2,001, A = 0,00812; 0,0072) [9, 50]; CdSiO₃ (g ≈ 2,0) [9]; Mg₂GeO₄ (g ≈ 2,0) [9]; ZnF₂ (g ≈ 2,0) [9]; ZnS Tb (g ≈ 2,0) [9]; Zn₂SiO₄ (g ≈ 2,0) [9]; 8ZnO·BeO·5SiO₂ (g ≈ 2,0) [9]; Zn₂GeO₄ (g ≈ 2,0) [9]; Zn₃(PO₄)₂ (g ≈ 2,0) [9]; MgF₂ (g = 2,001, A = 0,00906) [50]; CdF₂ (g = 2,001, A = 0,00906) [50]; SrF₂ (g = 2,002, A = 0,0093) [50]; BaF₂ (g = 2,004, A = 0,0091) [50]; CdO (g = 2,001, A = 0,00873) [50]; MgS (g = 2,001, A = 0,00719) [50]; CaS (g = 2,001, A = 0,00757) [50]; SrS (g = 2,000, A = 0,00750) [50]; MgSe (g = 2,004, A = 0,00712) [50]; CaSe (g = 2,004, A = 0,00729) [50]; CaTl (g = 2,003, A = 0,00672) [50]; ZnO (A = 0,0079) [50]; CdSe (g = 2,003, A = 0,00615) [50]; CdTl (g = 2,013, A = 0,00581) [50]; ZnSe (g = 2,01, A = 0,0060) [50]; ZnTl (A = 0,0056) [50]; б) нераз-

22 бавленных соединениях: Mn (BO₂)₂ (g = 2,01) [12]; MnB₄O₇ [42]; Mn (CH₃COO)₂·2H₂O (g = 2,00) [13]; Mn (C₂H₃O₂)₂·3H₂O [14]; Mn (C₅H₅)₄ (CN)₂ (g = 2,0, до 20° K) [15]; Mn (C₁₇H₃₁COO)₂ (g = 2,00) [16]; Mn (C₁₇H₃₃COO)₂ (g = 2,00) [16]; MnCO₃ (g = 2,00) [12, 36, 42, 47]; MnC₂O₄·2H₂O (g = 2,00) [16]; MnCl₂ [42, 45]; MnCl₂·2H₂O [45]; MnCl₂·4H₂O (g = 2,00 и 2,00) [12, 13, 26, 31, 42, 45]; MnF₂ [14, 42]; Mn (H₂PO₂)₂·H₂O [14, 42]; MnK₂(SO₄)₂·6H₂O [14]; Mn (NH₄)₂ (SO₄)₂·6H₂O [24]; Mn (NO₃)₂·6H₂O [24, 44]; MnS (g = 2,0) [42]; MnSO₄ (g = 2,00) [13, 17, 42, 45, 46]; MnSO₄·H₂O (g = 2,00) [13, 17, 42, 45, 46]; MnSO₄·4H₂O (g = 2,00—2,07) [17, 25, 42, 45, 46]; MnSO₄·5H₂O (g = 2,00) [17, 45, 46]; Mn₂Fe (CN)₆·7H₂O [14]; Mn₂(P₂O₇)·3H₂O [14, 42]; Mn₃(AsO₄)₂ [14]; Mn₃(C₆H₅O₇)₂ [14]; Mn₃(PO₄)₂·3H₂O [42]; Mn₃(PO₄)₂·7H₂O [14]; MnCl₂·4H₂O (T = 1,6—2,5° K) [31].

In addition, the absorption lines of Mn^{2+} were investigated in paramagnetic Tutton's salts $R(NH_4)_2(SO_4)_2 \cdot 6H_2O$ ($R = Ni^{2+}$, Co^{2+}, Fe^{2+}, Cu^{2+}), and also in $CuSO_4 \cdot 5H_2O$ [44]). The intermetallic compound $MnAu_2$ was investigated (polycrystal); when $T > 90°C$ we have $g \approx 2.0$; below $90°C$, $MnAu_2$ is an antiferromagnet [43]. Finally, the paramagnetic resonance was measured for Mn^{2+} in amorphous phthalocyanine ($g = 2.0$) [41].

Remarks:

a) The direction cosines of the Z axis are (0.282, ±0.952, 0.122).

b) The Zn is surrounded in ZnF_2 by a distorted octahedron made up of six F ions, four of which (type I) form a rectangle with sides 2.59 and 3.13 A, and the two other F ions (type II) lie on a perpendicular to the plane of the rectangle at a distance 2.04 A. The Z axis is chosen along the long side of the rectangle (c axis), the X axis passes through the type II F ions and is parallel to the short side of the rectangle. The following hyperfine structure due to the F nuclei was observed:

$$A_y^I = (16.5 \pm 0.7) \cdot 10^{-4} \text{ cm}^{-1}, \quad A_y^{II} = (14.6 \pm 1.2) \cdot 10^{-4} \text{ cm}^{-1},$$
$$A_z^I = (18.2 \pm 0.2) \cdot 10^{-4} \text{ cm}^{-1}, \quad A_z^{II} = (12.5 \pm 0.2) \cdot 10^{-4} \text{ cm}^{-1}.$$

c) $CaCO_3$ — calcite, M = 2. The nearest neighbors of the Ca are six O with trigonal symmetry. The magnetic complexes with Mn are equivalent. The structure of the crystal is hexagonal.

d) $M_m = 2$, $\psi = +97°$, $\alpha = 62°$, monoclinic structure.

e) $M_m = 1$, $Z \equiv c$, $X \equiv b$, monoclinic structure.

f) $M_m = 2$, $\psi = +47°$, $\alpha = 29°$.

g) If a sample obtained from the melt is heated and soaked for a certain time at a temperature T, and then cooled rapidly to room temperature, then: 1) if $T < 300°C$, the resonant curves do not change; 2) if $T > 500°C$, then curve I goes over into II. A superposition of curves

I and II is observed at intermediate temperatures. There are probably two different states of Mn^{2+} in NaCl, one of which is stable above $500°C$, and the other stable below. The former is contained in the rapidly cooled samples and the latter in the slowly cooled ones.

h) Lines without structure.

j) Line with hyperfine structure of Mn^{55}.

k) There are two types of centers, each containing three nonequivalent magnetic ions. Because of the complexity of the spectrum, the values of D, $\underline{g}$, and A are determined only along the axis of the crystalline field. The intensity of the second spectrum is one hundredth of that of the first. Each of the hyperfine structure lines of Mn has a resolved structure, due to the interaction with the F nuclei. The constants of this interaction are: $A_s = 0.00144 \pm 0.00003$, $A_p = 0.00028 \pm 0.00007$. The intensity of the Mn^{2+} spectrum is greatly weakened after irradiation.

l) Spectrum I of six peaks corresponds to isolated Mn^{2+} ions. Spectrum II having one peak is observed only in samples with higher concentration of Mn^{2+}, and is probably brought about by the aggregation of the Mn^{2+} ions.

m) $\mu^{53}/\mu^{55} = 1.455 \pm 0.002$.

n) $a = (+0.6 \pm 0.4) \cdot 10^{-4}$ cm^{-1}, $A_s = (9.5 \pm 0.3) \cdot 10^{-4}$ cm^{-1}, $A_p = (2.7 \pm 0.5) \cdot 10^{-4}$ cm^{-1}. A_s and A_p are the constants of the hyperfine structure due to the interaction between the spin of the F nucleus with the $\underline{s}$ and p_σ orbitals, respectively.

o) In addition to the ordinary hyperfine structure, a hyperfine structure was also observed due to the magnetic interaction between the Mn^{2+} electrons with the nearest Cd nuclei.

p) The spectrum is due to the complex made up by Mn^{2+} and the Na^+ vacancy; the Z axis is directed along the bond between Mn^{2+} and the

Na$^+$ vacancy, and the y axis is parallel to the cubic axis. The complexes are unstable.

r) At 20°K each Mn^{2+} line is split by the interaction with the Au nuclei; it is suggested that the quadrupole interaction with Au is stronger than the magnetic interaction.

TABLE 4.5 (Continuation)

Fe^{3+}

1 Формула	T, °K	g	D	a	F	Литература 2	3 Замечания
4 KFe(SeO$_4$)$_2$ · 12H$_2$O (кр. ст. 1) Al:Fe = 1:300	90	2,003 ±0,003	—0,0103 ±0,0001	—0,0127 ±0,0002	—0,0002 ±0,0002	[1]	$\varphi = (10,5\pm0,5)°$
	20	2,003 ±0,001	—0,0115 ±0,0001	—0,0127 ±0,0001	—0,0002 ±0,0001		
4 (NH$_3$CH$_3$)Fe(SO$_4$)$_2$ · 12H$_2$O (кр. ст. 1) Fe:Al = 1:200	90		(—)0,188 ±0,014	(—)0,010 ±0,004		[1]	
NH$_4$Fe(SO$_4$)$_2$ · 12H$_2$O Fe:Al = 1:80	4		0,016 ±0,001	(—)0,0128 ±0,0004		[23]	
4 RbFe(SO$_4$)$_2$ · 12H$_2$O (кр. ст. 1) Fe:Al = 1:300	90	2,003 ±0,003	+0,0022 ±0,0002	—0,0134 ±0,0002	—0,0003 ±0,0002	[1]	$\varphi = (7,5\pm0,5)°$
	20	2,003 ±0,001	+0,0031 ±0,0001	—0,0134 ±0,0001	—0,00033 ±0,0001		
Fe^3 в Al$_2$Be$_3$(SiO$_3$)$_6$	290	2,00	0,01658	0,01445	0,00045	[15]	$\delta_1 = 0,058$ см$^{-1}$, $\delta_2 = 0,050_5$ см$^{-1}$.
Fe^{3+} в MgO	290	2,0037 ±0,0007		+0,0205		[16]	
Fe^{3+} в SrTiO$_3$ Fe^{3+}:Ti^{4+} = 10^{-4}	290	2,004 ±0,001	0	0,0198 ±0,0010		[11, 17]	6) b
	77		0,00077 ±0,00003	0,02201 ±0,0011			
23 Fe^{3+} в Si (обогащ. и необогащ.)	10	2,0699		+0,00373		[19, 21]	$A^{67} = 7,0 \cdot 10^{-4}$см$^{-1}$, r) d
Fe[(CH$_3$CO)$_2$CH]$_3$ Fe:Co = 10^{-2}	290		0,07			[10]	в) c
Fe^{3+} в MgWO$_4$ [c18]	73	2,0	—0,687			[23]	$E = +0,174$ см$^{-1}$, д) e
Fe^{3+} в Al$_2$O$_3$ Fe:Al = 10^{-5}	290	2,003 ±0,001	+0,1679 ±0,0001	0,0241 ±0,0004	+0,0329 ±0,0002	[12, 22]	а)

TABLE 4.5 (Continuation)

1 Формула	T, °K	g	D	a	F	Литера-тура [2]	3 Замечания
6 Fe³⁺ в BaTiO₃ Fe:Ti = 10⁻⁴ — 4·10⁻⁴	77	2,003 ±0,001	+0,1716 ±0,0001	0,0236 ±0,0004	+0,0337 ±0,0002		
	4,2	2,003 ±0,001	+0,1719 ±0,0001	0,0224 ±0,0004	+0,0339 ±0,0002		
	290	2,00	~0,0830	0,0094		[20]	

24 Парамагнитный резонанс наблюден также при комнатной температуре в Fe[CH₂CF₂(CO)₂CH]₃ (Fe:Al) [10]; Fe(C₄H₇O₂)₃ (g≈1,95) [4]; Fe(C₇H₅O₂)₃ [5]; Fe(C₁₇H₃₅COO)₃ (g∼2,00) [6]; FeCl(C₆H₄)₄(CN)₃ (T=270 — 20° K, g=3,8; 2,0) [7]; FeCl₃ [5]; FeP₃ · 4,5 · H₂O [13]; FeK(SO₄)₂ · 12H₂O (Fe:Al=1:385, δ=0,03 см⁻¹) [14]; FeNH₄(SO₄)₂ · 12H₂O (g=2, δ=0,032 см⁻¹) [14]; Fe(NH₄)(SO₄)₂ · 12H₂O (g≈1,97) [13]; Fe(NH₄)₃(C₆H₅O₇)₂ · 24H₂O (g≈1,98) [4]; Fe₄[Fe(CN)₆]₃ [5]; FeOH(C₂H₅O₂)₂ (5); FePO₄ · 4H₂O [5]; (FeP₃)₂ · 9H₂O (g=2,02) [4]; Fe₂(SO₄)₃ · 3H₂O (g≈2,01) [8]; Fe₂(C₂O₄)₃ [5]; Fe₂(SO₄)₃ · 9H₂O (g≈2,01) [4]; Fe₃(CH₃COO)₆(OH)₂NO₃ · 6H₂O (T=15° K, g=2,0) [9]; Fe₃[C₆H₅(OH)₂OPO₃]₃ [5]; Fe³⁺ в 3Y₂O₃ · 5Ga₂O₃ [24].

Remarks:

a) $M_m = 2$, nonequivalence due to the difference in the directions of the cubic-field axes.

b) Below the phase-transition point (near 100°K) the single crystal consists of tetragonal domains.

c) $M_m = 2$, the crystal is orthorhombic. Upon dilution of the aluminum, a similar but not identical spectrum was obtained. Thus, the crystalline field acting on the Fe³⁺ may vary from diluent to diluent.

d) Isotropic line.

e) The Y axis is parallel to the b axis, the Z axis lies in the ac plane and forms a 41.5° angle with the a axis. The signs of D and E are determined from a comparison of the intensities at 2 and 4°K.

Gd³⁺

	T, °K	g	D	a		F		Литература [2]	Замечания
4 Mg₃Gd₂(NO₃)₁₂·24H₂O (кр. ст. 3) Gd:Bi = 1:5000	290, 77	1,991						[15]	¹⁵⁵A = (3,7±0,3) × × 10⁻⁴ см⁻¹, ¹⁵⁷A = (4,95±0,16)× × 10⁻⁴ см⁻¹
Gd:Bi = 10⁻³	90, 20	1,992 ±0,003	0,0124 ±0,0001	+0,00009 ±0,00001	+0,00006 ±0,00001	+0,0012 ±0,0001		[1]	
4 Gd(C₂H₅SO₄)₃ · 9H₂O (кр. ст. 9)	90	1,990 ±0,002	+0,0204₇ ±0,0002	−0,00039₄ ±0,00003	+0,00006₈ ±0,00001	+0,00035 ±0,00005		[2] [13]	
Gd:La = 1:200	20	1,990 ±0,002	+0,0199₈ ±0,0001	−0,000391 ±0,000015	+0,000053 ±0,000005	+0,00040 ±0,00005			
Gd₂(SO₄)₃ · 8H₂O [к16]									
Gd:Sm = 1:200	300		(+)0,0633 ±0,0005	(+)0,0038 ±0,005	(−)0,0013 ±0,0003			[12] [3]	а), б)
Gd Cl₃ [к16]	290	1,991 ±0,001	+0,000836 ±0,000010	+0,000168 ±0,000004	+0,000064 ±0,000015			[7]	в)
Gd:(La, Ce) = 10⁻⁴	90	1,991 ±0,001	+0,001600 ±0,000002	+0,000213 ±0,000005	+0,000025 ±0,000005	+0,000140 ±0,00003		[7]	г)
Gd:La = 5 · 10⁻³	4	1,991 ±0,001						[21]	¹⁵⁵A = (3,8±0,2) × × 10⁻⁴ см⁻¹, ¹⁵⁷A = (5,0±0,2) × × 10⁻⁴ см⁻¹
GdCl₃ · 7H₂O Gd:La	290	gₓ 1,996 ±0,003 gᵧ 2,000 ±0,003	+0,01313 ±0,00005	−0,00752 ±0,00020	+0,0002 ±0,0001			[19]	

TABLE 4.5 (Continuation)

1 Формула	T.°K	g	b₂⁰	b₂²	b₄⁰	b₄²	b₄⁴	Лите-ратура 2	3 Замечания
GdCl₃·7D₂O Gd:La = 2·10⁻⁴	99—77 290 77	$g_{\|}$ 1,989 ±0,003 1,99	+0,0099 ±0,0030	—0,0115 ±0,0007				[15]	$\frac{\mu^{155}}{\mu^{157}} = 0,75\pm0,07$ $^{157}A = (5,3\pm0,3) \times$ $\times 10^{-4}$ см⁻¹ e)
Gd³⁺ в LaF₃ Gd:La = 10⁻⁴	90	1,990 ±0,001	+0,0239 ±0,0001	—0,0005 ±0,0002	—0,00056 ±0,00002	+0,000014 ±0,000020		[22]	

Формула	T.°K	g	ΔE, д)	Литература	Замечания
Gd в ThO₂ Gd:Th = 10⁻⁴	290 90	1,9913 ±0,0005 1,991 ±0,001	0,1755 ±0,0003 0,1796 ±0,0008	[16] [16]	$c = (219,9\pm0,3)\cdot10^{-4}$ см⁻¹, $d = (1,0\pm0,3)\cdot10^{-4}$ см⁻¹, $c = (225,0\pm0,8)\cdot10^{-4}$ см⁻¹, $d = (1,7\pm0,8)\cdot10^{-4}$ см⁻¹, $M_m = 1$, $\frac{\mu^{155}}{\mu^{157}} = 0,744\pm0,007$
Gd³⁺ в CaF₂	290, 4 90	1,9918 ±0,0010	0,1491 ±0,0008 ~2,1	[8, 9, 10, 14] [20]	$M_m = 3$ 25 Главные оси тетрагонального поля параллельны ребрам куба, $a = +0,0175$

26 Парамагнитный резонанс наблюдался также на: Gd³⁺ в LaAlO₃ (T=4,2; 295; 195; 83°K, линия без структуры с g=1,992±0,002, шесть пиков тонкой структуры с g=1,55—2,7) [18]; Gd(NO₃)₃·6H₂O (Gd:La=10⁻⁴) [4]; GdCl₃·6H₂O [6]; Gd(BrO₃)₃·9H₂O [5]; Gd³⁺ в SrS (T=290°K, Gd:Sr=10⁻⁴, $\frac{\mu^{155}}{\mu^{157}}$=0,73±0,03) [11, 17].

Remarks:

a) The value of b_2^0 may not be exact (see Bowers, K.D., Owen, J., Rep. Progr. Phys. 18, 304, 1955).

b) Monoclinic. M = 8, M_m = 2. The axes are specified by the angles $\psi_z = 28°$, $\alpha_z = \pm35°$, $\psi_y = 0°$, $\alpha_y = \pm52°$, where ψ_1 is the angle between c and the plane containing the Z axes; α_1 is the angle between the i-th axis and the ac plane (i = z, y).

c) Hexagon. The crystalline field on Gd has a C_{3h} symmetry.

d) The sign of the coefficients b_n^m is determined from measurements of the relative intensities in parallel fields at 20°K.

e) $\Delta E = 8c - 2d$ is the total splitting in the cubic field.

f) $M_m = 3$, the ion is acted upon by a rhombic crystalline field; $b_4^2 = 60B_4^2 = +0.0027 \pm 0.0003$; $b_4^4 = 60B_4^4 = -0.0043 \pm 0.0003$; $b_6^2 + b_6^6 = 1260(B_6^2 + B_6^6) = +0.00085 \pm 0.00030$; $b_6^4 = 1260B_6^4 = -0.0001 \pm 0.0005$.

TABLE 4.5 (Continuation)

$$Eu^{2+}$$

1 Формула	T, °K	g	ΔE	Изотоп [27]	A	Литература [2]	3 Замечания [28]
Eu²⁺ в CaF₂	290	1,971 ±0,001		151	0,00346 ±0,00001	[4]	Магнитные моменты ¹⁵¹Eu и ¹⁵³Eu имеют одинаковый знак
				153	0,00154 ±0,00001		
	290	1,9927 ±0,0010	0,1784 ±0,0009	151	0,00303 ±0,00001	[2,3,5,6,9]	$R = 0,612 \pm 0,003$ $\frac{\mu^{151}}{\mu^{153}} = 2,26 \pm 0,02$
				153	0,00151 ±0,00001		
(естествен.) [13] (из расплава) Eu : Ca = 10⁻⁴	290 [29] 90	1,993 1,989 ±0,002	0,1810 ±0,0050	151	0,00345 ±0,00002	[12] [11, 14]	$a = 0,0186$ см⁻¹ $b_4^0 = (57,9 \pm 0,2) \cdot 10^{-4}$ см⁻¹ $b_4^4 = (0,5 \pm 0,2) \cdot 10^{-4}$ см⁻¹
				153	0,00153 ±0,00004		
Eu²⁺ в SrCl₂	290	1,996 ±0,006		151	0,00322 ±0,00003	[7]	
				153	0,00144 ±0,00003		
Eu²⁺ в SrS (порошок) Eu : Sr ~ 10⁻⁴	290 [16]	1,992 ±0,001		151	0,00300 ±0,00001	[1, 4, 13]	$\frac{\mu^{151}}{\mu^{153}} = 2,24 \pm 0,03$
				153	0,00134 ±0,00001		
				152	0,00139 ±0,00001		
Eu²⁺ в SrS — SrSe	90—20 90—20	2,0 2,0	0,18 0,18			[8, 9] [8]	

[30] Парамагнитный резонанс наблюден также на Eu²⁺ в KCl ($\frac{\mu^{154}}{\mu^{153}} = 1,308 \pm 0,004$, $\frac{\mu^{152}}{\mu^{151}} = 0,5574 \pm 0,006$, $\frac{\mu^{151}}{\mu^{153}} = 2,264 \pm 0,006$, $T = 77$ K, $g = 2$, $^{151}A = (32,56 \pm 0,06) \cdot 10^{-4}$ см⁻¹, $^{153}A = (15,12 \pm 0,15) \cdot 10^{-4}$ см⁻¹, $^{152}A = (14,38 \pm 0,03) \cdot 10^{-4}$ см⁻¹, $^{154}A = (15,67 \pm 0,06) \cdot 10^{-4}$ см⁻¹) [9].

$$Cm^{3+}$$

1 Формула	T, °K	g	b_2^0	Литература [2]	3 Замечания
Cm³⁺ в LaCl₃ Cm : La = 1 : 2000	290, 77	1,9914 ±0,0008	0,00076 ±0,00002	[1, 2]	$(b_2^0 - 5b_4^0) \geq 0,00034 \pm 0,00005$
Mg₃Cm₂(NO₃)₁₂ · 24H₂O Cm : Bi	290	2,003	0,00020 ±0,00002	[1]	$b_2^0 = 0,00020 \pm 0,00002$

31 Парамагнитный резонанс наблюдался также на Cm³⁺ в ThO₂ и CaCl₂ [1].

1) Formula; 2) reference; 3) remarks; 4) cr. st.; 5) two different magnetic complexes; 6) in; 7) (slow cooling from melt); 8) (fast cooling from melt); 9) hexagonal; 10) cubic; 11) (from aqueous solution); 12) by weight; 13) (from melt); 14) (from solution); 15) in 0.05 cm³ of the crystal; 16) (powder); 17) in phosphors; 18) Mn-Au pairs in Si; 19) two spectrum types, apparently depending on the S or Se surrounding; 20) trigonal distortion of cubic field; 21) paramagnetic resonance observed also at room temperature in: a) phosphorus containing small concentrations of .....; 22) b) undiluted compounds: .....; 23) (enriched and

not enriched); 24) paramagnetic resonance observed also at room temperature in .....; 25) the principal axes of the tetragonal field are parallel to the edges of the cube, $a = +0.0175$; 26) paramagnetic resonance is observed also in Gd^{3+} in $LaAlO_3$ (T = 4.2, 295, 195, $83°K$, lines without structure with $g = 1.992 \pm 0.002$, six fine-structure maxima with $g = 1.55.....$; 27) isotope; 28) the magnetic moments of ^{151}Eu and ^{153}Eu have the same sign; 29) (natural); 30) paramagnetic resonance was also observed in Eu^{2+} in $KCl.....$; 31) paramagnetic resonance observed also in Cm^{3+} in ThO_2 and $CaCl_2$ [1].

TABLE 4.6

$$Fe^{III}$$

1 Формула	T, °K	g			Литература	3 Замечания
$K_3[Fe(CN)_6]$ (кр. ст. 7)	20	g_a 2,30 ±0,03	g_b 2,18 ±0,03	g_c 0,94 ±0,03	[1]	5. Направляющие косинусы осей
Fe : Co = 10^{-2}	20	2,35 ±0,02	2,10 ±0,02	$0,91_5$ ±0,01	[2]	$\quad a \quad b \quad c$ $Z \quad 0 \quad 0 \quad 1$ $X \pm 0,866 \quad 0,500 \quad 0$ $Y \pm 0,500 \quad 0,866 \quad 0$
6 Fe^{III} в монокристаллах миоглобина, полученного из китовой мышцы	20	g_1 6	g_2 2,00 ±0,01	g_3 6,00 ±0,05	[3]	$\Delta > 2$ см$^{-1}$
7 Fe^{III} в монокристаллах гемоглобина	20	$g_{||}$ 2,00 ±0,01	$g_\perp$ 5,95 ±0,05		[4]	$\Delta > 2$ см$^{-1}$
$ClFe(C_6H_4)_4(CN)_3$	290—20	3,8			[5]	
8 Fe^{III} в азиде феррримиоглобина и ферригемоглобина	290, 20	g_x 1,72	g_y 2,22	g_z 2,80	[4—6]	15. Ось Z перпендикулярна к плоскости гема
9 в перле буры	77	4			[7]	Расстояние между пиками сверхтонкой структуры, обязанной ядру ^{57}Fe, равно ∼10 эрст 16
10 в поликристаллическом гемине		$g_{||}$ 6,0			[5]	
11 в кислом метаферригемоглобине						
12 в кислом метаферримиоглобине		$g_{||}$ 5,90 ±0,05				17. Линия асимметрична
13 в фториде ферригемоглобина					[5]	
14 в фториде феррримиоглобина						
4 $K_4[Mn(CN)_6]·3H_2O$ (кр. ст. 7) Mn : Fe = 10^{-2}	12	g_x 2,624 ±0,008	g_y 2,182 ±0,008	g_z 0,72 ±0,05	[1]	$\quad a \quad b \quad c$ $Z \, 0,205 \pm 0,899 \; -0,322$ $X \, 0,864 \pm 0,105 \; -0,495$ $Y \, 0,410 \pm 0,423 \; -0,807$
		A_x 0,00845 ±0,00006	A_y 0,00465 ±0,00006	A_z 0,0083 ±0,0013		

TABLE 4.6 (Continuation)

Mo^V, Mo^{III}, Tc^{IV}

1 Формула	T, °K	$\varepsilon_\parallel$	$\varepsilon_\perp$	A	B	Литература	3 Замечания
18 $\overline{Mo^V}$ в виде загрязнения в $K_3[InCl_6] \times$ $\times 2H_2O$ Mo : In = 10^{-3}	290, 20	I: 1,951 ±0,005 II: 1,959 ±0,004	1,939 ±0,006 1,939 ±0,006	0,0079 ±0,0002 0,0077 ±0,0002	0,00385 ±0,0002 0,00385 ±0,0002	[1]	В единичной ячейке два магнитно неэквивалентных комплекса; наблюдена сверхтонкая структура, обязанная ядрам Cl 20
19 $K_3[Mo(CN)_8]$ (порошок)	290, 20	g. 2,005 ±0,005				[2]	
$K_3[MoCl_6] \cdot 2H_2O$ Mo^{III} : In = 1 : 200	90, 20	I: 1,93 ±0,06 II: 1,93 ±0,06	$\frac{D>1}{E}$ $\frac{E}{D}=0,08$ $D>1$ $\frac{E}{D}=0,15$	A_g 0,0039 ±0,0005 0,0039 ±0,0005		[1]	21 В единичной ячейке несколько магнитно неэквивалентных комплексов; измерены только два
19 K_2MoCl_6 (порошок)	290	1,76				[2]	
19 $K_3MoCl_6 \cdot H_2O$ (порошок)	290—20	1,96				[3]	
19 $KMoF_4$ (порошок)	14	1,95				[3]	
Tc^{++} в K_2PtCl_6 (кр. ст. 8) Tc : Pt = 10^{-4}	4,2	1,9896 ±0,0005		A_{max} 0,01378 ±0,00004	A_{min} 0,01334 ±0,00004	[1]	

Ru^{III}

1 Формула	T, °K	ε_x	ε_y	ε_z	A_x	A_y	A_z	Литература	3 Замечания
$[Ru(NH_3)_6]Cl_3$ Ru : Co = 1 : 200	20	I: 2,06 ±0,01	2,02 ±0,01	1,72 ±0,01	0,0048 ±0,0002	0,0048 ±0,0002	0,0049 ±0,0002	[1—3]	a)
		II: 1,80 ±0,01	1,90 ±0,01	2,06 ±0,01	0,0048 ±0,0002	0,0048 ±0,0002	0,0050 ±0,0002		
		III: 1,15 ±0,01	1,84 ±0,01	2,66 ±0,01	0,0045 ±0,0002	0,0041 ±0,0002	0,0054 ±0,0002		$\frac{^{101}A}{^{99}A} = 1,09 \pm 0,03$
$K_3[RuCl_6] \cdot 2H_2O$ Ru : In = 10^{-3}	20	1,0 ±0,01	1,22 ±0,02	3,24 ±0,02				[4]	
$[Ru(NH_3)_6]Cl_3$ $3HgCl$	20	2,21	2,05	1,5 ±0,1				[1]	

22 Парамагнитный резонанс наблюден также в неразбавленных кристаллах $[Ru(NH_3)_6]$ Cl_6, $[Ru(NH_3)_6 Cl]Cl_2$ при $T = 20$ K [1].

Remark. a) The unit cell contains three pairs of magnetically non-equivalent complexes, types I, II, III. The plane ac is the mirror-symmetry plane for the ions of each pair.

TABLE 4.6 (Continuation)

Ag^{II}, Re^{IV}

Формула	T, °K	$g_{\parallel}$	$g_{\perp}$	Литература	Замечания
Ag (C$_5$H$_5$N)$_4$ S$_2$O$_8$ (порошок)	297, 20	2,18	2,04	[1]	
Ag : Cd = 1 : 20 (порошок)	4,2	$g = 2,06$		[1]	
Ди-о-фенантролин персульфат серебра	290, 90, 20	2,18	2,04	[2]	
K$_2$ [ReCl$_6$] (кр. ст. 6) Re : Pt = 1 : 200	90, 20	$g = 1,8$		[1]	Наблюдено 6 линий (возможно, сверхтонкая структура от ^{185}Re, ^{187}Re)

Ir^{IV}

1 Формула	T, °K	g	25 СТС Ir	26 СТС Cl или Br	2 Литература	3 Замечания
4 K$_2$ [IrBr$_6$] (кр. ст. 6) Ir : Pt = 1 : 200	20	$g_{\parallel}$ 1,60 ±0,10 $g_{\perp}$ 1,87 ±0,04			[1]	27 $M_m = 3$, оси неэквивалентных комплексов параллельны ребрам кубической единичной ячейки
4 K$_2$ [IrCl$_6$] (кр. ст. 6) Ir : Pt = 1 : 200	20	$g_x = g_y = g_z$ 1,78 ±0,02			[2]	28 Все комплексы эквивалентны
4 (NH$_4$)$_2$ [IrCl$_6$] (кр. ст. 6) Ir : Pt = 1 : 200	20	$g_x = g_y = g_z$ 1,775 ±0,001	$A_x = A_y = A_z$ 0,00265 ±0,00010	$A'_x = A'_y = A'_z$ 0,00088 ±0,00004	[1]	29 Все комплексы эквивалентны; оси X, Y, Z параллельны ребрам кубической единичной ячейки и осям октаэдра Cl$_6$. Значение A' для ^{35}Cl
4 Na$_2$ [IrBr$_6$] · 6H$_2$O (кр. ст. 6) Ir : Pt = 1 : 200	20	g_x 2,25 ±0,02 g_y 2,21 ±0,02 g_z 0,75 ±0,10	$A_x = A_y$ 0,00255 ±0,00010	$A'_x = A'_y$ 0,0057 ±0,0002	[1]	30 Все комплексы эквивалентны; оси X, Y, Z параллельны осям октаэдра Br$_6$. Значение A' для ^{79}Br, ^{81}Br
4 Na$_2$ [IrCl$_6$] · 6H$_2$O (кр. ст. 6) Ir : Pt = 1 : 200	20	g_x 2,20 ±0,02 g_y 2,07 ±0,02 g_z 1,05 ±0,02	A_x 0,00255 ±0,00010 A_y 0,00255 ±0,00010 A_z 0,0024 ±0,0001	A'_x 0,00116 ±0,00004 A'_y 0,00107 ±0,00004 $A'_z < 0,0005$	[1]	31 Все комплексы эквивалентны; оси X, Y, Z параллельны осям октаэдра Cl$_6$. Значение A' для ^{35}Cl

32 Парамагнитный резонанс наблюден также в (NH$_4$)$_2$ IrCl$_6$ при $T = 20 - 2$° К и разбавлении Ir : Pt = 1 : 10, 1 : 100 [3].

TABLE 4.6 (Continuation)

U^{III}

1 Формула	T, °K	$g_\parallel$	$g_\perp$	A	B	P	2 Литература	3 Замечания
34 U^{III} в CaF_2 U:Ca = 10^{-3}	20	3,501 ±0,008	1,866 ±0,002				[1]	33 a); $M_m = 3$; на ион действует аксиальное поле, кристаллические оси неэквивалентных ионов направлены по ребрам куба
U^{III} в SrF_2 U:Sr = 10^{-3}	20	3,433 ±0,008	1,971 ±0,002				[6]	
U^{III} в BaF_2 U:Ba = 10^{-4}	20—10	3,337 ±0,002	2,115 ±0,001				[6]	
UCl_3				A^{235}	B^{235}	P^{235}	[2, 3]	
35 U:La = 10^{-3} (обогащен U^{233})	20, 4	4,153 ±0,005	1,520 ±0,002	0,0176 ±0,001	0,00575 ±0,00005	0,00055 ±0,00005		
U:Nd	20, 4	3,991	1,769	A^{233}	B^{233}	P^{233}	[3]	
36 U^{233}:La = 10^{-3} (образец обогащен)	4, 2	4,149	1,520	0,03786 ±0,00012	0,01236 ±0,00010	0,00099 ±0,00010	[4]	
19 UF_3 (порошок)	290, 90	2,8—2,9	2,1—2,2				[5]	
19 UF_4 (порошок)	290	$g=2,1_5$					[5]	

Remark. a) A complex hyperfine structure due to the F⁻ nuclei was observed in CaF_2 and SrF_2. It is well resolved into an even number of components in some directions.

NpO_2^{II}, PuO_2^{II}

| 1 Формула	T, °K	$g_\parallel$	$g_\perp$	A	B	P	2 Литература	3 Замечания
4 $(NpO_2)Rb(NO_3)_3$ (кр. ст. 10)	20—12, 4,3	3,40 ±0,01	$0,20_5$ ±0,02	A^{237} (+)$0,1654_5$ ±0,0002	B^{237} $0,0178_5$ ±0,0002	P^{237} (—)$0,0301_5$ ±0,0003	[1—3]	37 Относительные знаки A и P определены непосредственно
NpO_2 : UO_2								
4 $(PuO_2)Rb(NO_3)_3$ (кр. ст. 10)	20—12	5,32 ±0,02	≤0,4	^{239}A 0,0862 ±0,0005	^{241}A 0,0609 ±0,0004		[1]	38 Δ мало $\frac{^{241}A}{^{239}A} = 0,706$ ±0,004
PuO_2 : UO_2 = 1:17—1:200								
$Na(PuO_2)(CH_3COO)_3$ [a17]	4	5,92	~0				[2]	a)
$(Pu, U)O_2Rb(NO_3)_3$	7—1,5	3,18 ±0,01	~0	0,0504 ±0,001	~0		[3]	б)b

Remarks:
a) Cubic; M = 4. Linear groups O-U-O lie along the body diagonals of the cube; each U is also surrounded with six O from the acetate

groups. Eight 0 form a distorted cube.

b) The spectrum is apparently due to unusual oxides of Pu, the composition of which has not yet been established.

1) Formula; 2) reference; 3) remarks; 4) cr. st.; 5) direction cosines of the axes are:; 6) Fe^{III} in single crystals of myoglobin obtained from whale muscle; 7) Fe^{III} in single crystals of hemoglobin

$$ClFe(C_6H_4)_4(CN)_8;$$
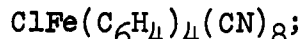
8) Fe^{III}: in ferrimyoglobin and ferrihemoglobin azide; 9) in borax beads; 10) in polycrystalline hemin; 11) in acid metaferrihemoglobin; 12) in acid metaferrimyoglobin; 13) in fluoride of ferrihemoglobin; 14) in fluoride of ferrimyoglobin; 15) Z axis perpendicular to hema plane; 16) the distance between maxima of the hyperfine structure, due to the ^{57}Fe nucleus is approximately 10 oersted; 17) asymmetrical line; 18) Mo^V in the form of contamination in $K_3[InCl_6]$ x $2H_2O$; 19) (powder); 20) the unit cell contains two magnetically nonequivalent complexes; a hyperfine structure due to the Cl nuclei is observed; 21) the unit cell has several magnetically nonequivalent complexes; only two were measured; 22) paramagnetic resonance was observed also in undilute crystals of $[Ru(NH_3)_6]Cl_3$, $[Ru(NH_3)_5Cl]Cl_2$ at T = $20°$K [1]; 23) di-o-phenanthroline persulfate of silver; 24) six lines observed (possibly the hyperfine structure of ^{185}Re, ^{187}Re); 25) HFS Ir; 26) HFS Cl or Br; 27) M_m = 3, axes of nonequivalent complexes parallel to the edges of a cubic unit cell; 28) all complexes equivalent; 29) all complexes equivalent; the X, Y, and Z axes are parallel to the edges of the cubic unit cell and to the axes of the Cl_6 octahedron. The value of A' is for ^{35}Cl; 30) all complexes equivalent; the X, Y, and Z axes parallel to the axes of the Br_6 octahedron. The value of A' is for ^{79}Br and ^{81}Br; 31) all complexes equivalent; the X, Y, and Z axes parallel to the axes of the Cl_6 octahedron. The value of A' is for ^{36}Cl; 32) paramagnetic resonance was also observed in $(NH_4)_2IrCl_6$ at T = $20-2°$K with a dilution ratio Ir:Pt = 1:10 and 1:100 [3]; 33) a); M_m = 3; the ion is acted upon by an axial field, the crystalline axes of the nonequivalent ions are directed along the edges of the cube; 34) in; 35) (enriched with U^{235}); 36) (specimen enriched); 37) relative signs of A and P determined directly; 38) Δ small.

7. Compounds with anomalous valence

TABLE 4.7

1 Вещество	T, °K	g	A	2 Ссылка	3 Замечания
Cr+ в NaF 6·10¹⁵ Cr+ в 0,05 см³ кристалла	90	$2,000 \pm 0,002$	$0,00140 \pm 0,00005$	[1]	**B** До облучения Cr++ в NaF вплоть до 20°K спектра не дает, после облучения появляется спектр, который, как предполагают, возникает от Cr+. Величина параметра кубического расщепления $a = 0,00036 \pm 0,00004$. Константы взаимодействия с ядрами фтора: $A_s = 0,00128 \pm 0,00002$, $A_\sigma = 0,00009 \pm 0,00007$. При нагревании до 150°C эффекты облучения пропадают.
Co+ в NaF	90	$2,31 \pm 0,02$		[1]	**C** Линия появляется при 90°K после облучения и имеет плоскую вершину, шириной около 200 эрст; что предполагают, Co+ она обязана. После нагревания до 150°C эффекты облучения пропадают.
A Ni+ в NaF 5·10¹⁵ Ni+ в 0,05 см³ кристалла	20	$g_\parallel\ 2,766 \pm 0,002$ $g_\perp\ 2,114 \pm 0,002$		[1]	**D** До облучения спектр не наблюдался до 20°K. После облучения появляется спектр, приписываемый Ni+. $M_{in} = 3$; спектры неэквивалентных ионов подобны и отвечают аксиальной симметрии; оси симметрии неэквивалентных ионов расположены по ребрам куба. Константы взаимодействия с ядрами F: $A_s^i = 0,0041 \pm 0,0002$, $A_\sigma^i = 0,0016 \pm 0,0003$,

1 Вещество	T, °K	g	A	2 Ссылка	3 Замечания
Fe+ в MgO Fe:Mg ≈ 10⁻³	20	$4,15 \pm 0,01$			**E** $A_s'' = 0,0010 \pm 0,0001$, A_σ'' очень мала. Индекс I относится к 4P, расположенным в плоскости, перпендикулярной к оси симметрии, индекс II — к 2P на оси симметрии. При нагревании до 150°C эффекты облучения пропадают.
Fe+ в NaF Fe:Na ≈ 10⁻⁴	20,4	$4,344 \pm 0,002$		[2]	
				[3]	**F** Константы сверх-тонкой структуры от взаимодействия с F: $A_s = 0,00283$, $A_\sigma = 0,0010 \pm 0,00010$ $\pm 0,001$, $a = 0,00088 \pm 0,00005$
G Mn²⁻ в Ge Растворы: (C₄H₉)₃CrI	290	$2,0061 \pm 0,0002$	$-0,00424 \pm 0,00003$	[4]	
(C₄H₅·C₅H₁₁)₂CrI	290	$1,988_3 \pm 0,002$	$3,6 *) \pm 0,5$	[6,7]	
(C₆H₅·C₆H₅)(C₅H₅)CrI	290	$1,986_5 \pm 0,002$	$3,7 *) \pm 0,5$	[6]	
(C₆H₅·C₆H₅)₂ CrI	290	$1,986_6 \pm 0,002$	$3,6 *) \pm 0,3$	[6]	
(C₅H₅·C₅H₅) OC₆H₅Cr	290	$1,986_6 \pm 0,002$ $1,993 \pm 0,007$	$3,6 *) \pm 0,3$	[6, 8] [8]	
H Дипиридил хрома (I)		$1,993$		[5]	
I Дипиридил ванадия (0)		$1,980$		[5]	
J Дипиридил титана (—I)		$2,007$		[5]	

K Замечание. A_s определяется контактным взаимодействием s-электронов, A_σ включает дипольные взаимодействия и связь через p-орбиты. Считается, что A_s и A_σ одинаковы для всех шести F.

1) Substance; 2) reference; 3) remarks.

A)   in 0.05 cm^3 of the crystal

B)   Prior to irradiation, Cr^{3+} in NaF yields no spectrum down to 20°K, but after irradiation a spectrum appears which is presumed to be due to the Cr^+. The value of the cubic splitting parameter is a = = 0.00036 $\pm$ 0.00004.
The constants of the interaction with the fluorine nuclei are:
$$A_s = 0.00128 \pm 0.00002, \quad A_\sigma = 0.00009 \pm 0.00007.$$
On heating to 150°C, the irradiation effects disappear.

C)   The line appears at 90°K after irradiation and has a flat top, with a width of about 200 oersted; it is presumed that it is due to Co^+. After heating to 150°C, the irradiation effects disappear.

D)   Prior to irradiation no spectrum is observed down to 20°K. After irradiation spectrum appears, ascribed to Ni^+. $M_m = 3$; the spectra of the nonequivalent ions are similar and correspond to axial symmetry; the symmetry axes of the nonequivalent ions are located along the edges of a cube. The interaction constants with the F nuclei are:
$$A_s^I = 0.0041 \pm 0.0002, \quad A_\sigma^I = 0.0016 \pm 0.0003,$$

E) A_σ^{II} very small.
The index I pertains to the four F located in a plane perpendicular to the symmetry axis, and the index II to the two F on the symmetry axis. After heating to 150°C, the irradiation effects drop out.

F)   The hyperfine structure constants due to the interaction with F^- are:

G) Solutions: H) dipyridyl of chromium; I) dipyridyl of vanadium; J) dipyridyl of titanium.

K)   Remark. A_s is determined by the contact interaction of the s electrons, A_σ includes the dipole interactions and the coupling via

the p_σ orbitals. It is assumed that A_s and A_σ are the same for all six F.

REFERENCES (§4.2)

To Table 4.1

$$V^{2+}$$

1. Hutchison, C.A., Singer, L.S., Phys. Rev. 89, 256, 1953.

2. Bleaney, B., Ingram, D.J.E. Scovil, H.E.D., Proc. Phys. Soc. A64, 601, 1951.

3. Kikuchi, C., Sirvetz, H.M., Cohen, V.W., Phys. Rev. 92, 109, 1953.

4. Baker, J.M., Bleaney, B., Proc. Phys. Soc. A65, 952, 1952.

5. Baker, J.M., Bleaney, B., Bowers, K.D., Proc. Phys. Soc. B69, 1205, 1956.

6. Low, W., Phys. Rev. 101, 1827, 1956.

7. Bagguley, D.M.S., Bleaney, B., Griffiths, J.H.E., Penrose, R.P., Plumpton, B.I., Proc. Phys. Soc. 61, 551, 1948.

8. Ingram, D.J.E., Bennett, J.E., J. Chem. Phys. 22, 1136, 1954.

9. Lambe, J., Ager, R., Kikuchi, C., Bull. Am. Phys. Soc., ser. II, 4, 261, 1959.

10. Baker, J.M. (see Orton, J.W., Rep. progr. Phys. 22, 204, 1959).

11. Ingram, D.J.E., Bennett, J.E., J. Chem. Phys. 22, 1136, 1954.

$$Cr^{3+}$$

1. Bagguley, D.M.S., Griffiths, J.H.E., Proc. Roy. Soc. A204, 188, 1950.

2. Bleaney, B., Proc. Roy. Soc. A204, 203, 1950.

3. Kip, A.F., Davis, S.F., Jennings, L., Reiner, D., Malvano, R., Nuovo Cimento 8, 683, 1951.

4. Whitmer, C.A., Weidner, R.T., Hsiang, J.S., Weiss, P.R., Phys. Rev. 74, 1478, 1948.

5. Halliday, D., Wheatley, J., Phys. Rev. 74, 1712, 1948.

6. Ting, Y., Williams, D., Phys. Rev. 82, 507, 1951.

7. Baker, J.M., Bleaney, B., International low temperature confer-
    ence, Paris [Paris: Institute International du Froid (Interna-
    tional Institute for Low Temperatures)], 1955.

8. Baker, J.M., Proc. Phys. Soc. B69, 633, 1956.

9. Bleaney, B., Penrose, R.P., Proc. Phys. Soc. 60, 395, 1948.

10. Yager, W.A., Merritt, F.R., Holden, A.N., Kittel, C., Phys. Rev.
    75, 1630, 1949.

11. Davis, C.F., Strandberg, M.W.P., Phys. Rev. 105, 447, 1957.

12. Bogle, G.C., Gabrill, J.R., Botomley, G.A., Trans. Faraday Soc.
    53, 1058, 1957.

13. Daniels, J.M., Wesemeyer, H., Canad. J. Phys. 36, 144, 1958.

14. Bleaney, B., Bowers, K.D., Proc. Phys. Soc. A64, 1135, 1951.

15. Bowers, K.D., Proc. Phys. Soc. A65, 860, 1952.

16. Baker, J.M., Bleaney, B., Bowers, K.D., Proc. Phys. Soc. B69,
    1205, 1956.

17. Singer, L.S., J. Chem. Phys. 23, 379, 1955.

18. Jarrett, H.S., J. Chem. Phys. 27, 1298, 1957.

19. Manenkov, A.A., Prokhorov, A.M., ZhETF (J. Exp. Theor. Phys.), 28,
    762, 1955.

20. Zaripov, M.M., Shamonin, Yu.Ya., ZhETF 30, 291, 1956.

21. Geusic, J.E., Phys. Rev. 102, 252, 1956.

22. Manenkov, A.A., Prokhorov, A.M., ZhETF 31, 346, 1956.

23. Zverev, G.M., Prokhorov, A.M., ZhETF 34, 513, 1958.

24. Low, W., Phys. Rev. 105, 801, 1957.

25. Tinkham, M., Proc. Roy. Soc. A236, 535, 1956.

26. Bagguley, D.M.S., Bleaney, B., Griffiths, J.H.E., Penrose, R.P.,
    Plumpton, B.J., Proc. Phys. Soc. 61, 551, 1948.

27. Lancaster, F.W., Gordy, W., J. Chem. Phys. 19, 1181, 1951.

28. Kozyrev, B.M., Salikhov, S.G., Shamonin, Yu.Ya., ZhETF 22, 56, 1952.

29. Tishkov, P.G., ZhETF 32, 620, 1957.

30. Lancaster, F.W., Gordy, W., J. Chem. Phys. 20, 740, 1952.

31. Ambler, E., Hudson, R.P., Physica 22, 866, 1956.

32. Ting, Y., Farringer, L.D., Williams, D., Phys. Rev. 97, 1037, 1955.

33. Sundaramma, K., Proc. Indian Acad. Sci. A44, 345, 1956.

34. Geusic, J.E., Peter, M., Schulz-Du Bois, E.O., Bull. Am. Phys. Soc., ser. II, 4, 21, 1959; Bell Syst. Techn. J. 38, 291, 1959.

35. Gerritsen, H.J., Harrison, S.E., Lewis, H.R., Wittke, J.R., Bull. Am. Phys. Soc., ser. II, 4, 165, 1959.

36. Wertz, J.E., Auzins, P., Phys. Rev. 106, 484, 1957.

37. Griffiths, J.H.E., Orton, J.W., Proc. Phys. Soc. 73, 948, 1959.

38. Baker, J.M., Hayes, W., Jones, D.A., Proc. Phys. Soc. 73, 942, 1959.

39. Swarup, P., Canad. J. Phys. 37, 848, 1959.

40. Baker, J.M. (see Orton, J.W., Rep. Progr. Phys. 22, 204, 1959).

41. Ting, Y., Farringer, L.D., Williams, D., Phys. Rev. 97, 1037, 1955.

42. Leech, J.W., Manuel, A.J., Proc. Phys. Soc. B69, 210, 1956.

43. Sierro, J., Lacroix, R., Muller, K.A., Helv. Phys. Acta 32, 286, 1959.

$$Co^{2+}$$

1. Owen, J. (see Bowers, K.D., Owen, J., Rep. Progr. Phys. 18, 304, 1955).

$$Cr^{2+}$$

1. Ono, K., Koide, S., Sekiyama, H., Abe, H., Phys. Rev. 96, 38, 1954; Ono, K., J. Phys. Soc. Japan 12, 1231, 1957.

$$Ni^{2+}$$

1. Griffiths, J.H.E., Owen, J., Proc. Roy. Soc. A213, 459, 1952.

2. Date, M., Sci. Repts. Res. Inst., Tohoku Univ. A6, 390, 1954.

3. Trenam, R.S. (see Bowers, K.D., Owen, J., Rep. Progr. Phys. 18, 304, 1955).

4. Holden, A.N., Kittel, C., Yager, W.A., Phys. Rev. 75, 1443, 1949.

5. Penrose, R.P., Stevens, K.W.H., Proc. Phys. Soc. A63, 29, 1950.

6. Walsh, W.M., Bloembergen, N., Phys. Rev. 107, 904, 1957.

7. Owen, J. (see Bowers, K.D., Owen, J., Rep. Progr. Phys. 18, 304, 1955).

8. Ono, K., J. Phys. Soc. Japan 8, 802, 1953.

9. Low, W., Phys. Rev. 109, 247, 1958.

10. Low, W., Phys. Rev. 101, 1827, 1956.

11. Ting, Y., Williams, D., Phys. Rev. 82, 507, 1951.

12. Lancaster, F.W., Gordy, W., J. Chem. Phys. 19, 1181, 1951.

13. Lütze, E., Z. phys. Chem. (J. Phys. Chem.) 8, 32, 1956.

14. Bagguley, D.M.S., Bleaney, B., Griffiths, J.H.E., Penrose, R.P., Plumpton, B.I., Proc. Phys. Soc. 61, 551, 1948.

15. Ingram, D.J.E., Bennett, J.E., J. Chem. Phys. 22, 1136, 1954.

16. Partridge, M.F. (see Orton, J.W., Rep. Progr. Phys. 22, 204, 1959).

17. Leech, J.W., Manuel, A.J., Proc. Phys. Soc. B69, 210, 1956.

Cu^{2+}

1. Bleaney, B., Penrose, R.P., Plumpton, B.I., Proc. Roy. Soc. A198, 406, 1949.

2. Bagguley, D.M.S., Griffiths, J.H.E., Proc. Phys. Soc. A65, 594, 1952.

3. Bleaney, B., Bowers, K.D., Ingram, D.J.E., Proc. Roy. Soc. A228, 147, 1955.

4. Bleaney, B., Bowers, K.D., Trenam, R.S., Proc. Roy. Soc. A228, 157, 1955.

5. Bijl, D., Rose-Innes, A.C., Proc. Phys. Soc. A66, 954, 1953.

6. Yokozawa, Y., Monogr. Res. Inst. Appl. Elect. Hokkaido Univ. 4, 95, 1954.

7. Okamura, T., Date, M., Phys. Rev. 94, 314, 1954.

8. Bagguley, D.M.S., Griffiths, J.H.E., Owen, J. (see Bowers, K.D., Owen, J., Rep. Progr. Phys. 18, 304, 1955).

9. Gerritsen, H.J., Bolger, B., Okkes, R.F. (see Bowers, K.D., Owen, J., Rep. Progr. Phys. 18, 304, 1955).

10. Bagguley, D.M.S., Griffiths, J.H.E., Proc. Roy. Soc. A201, 366, 1950.

11. Abe, H., Ono, K., Hayashi, I., Shimada, J., Iwanaga, K., J. Phys. Soc. Japan 9, 814, 1954.

12. Abe, H., Shimada, J., Phys. Rev. 90, 316, 1953.

13. Bleaney, B., Bowers, K.D., Proc. Roy. Soc. A214, 451, 1952.

14. Abe, H., Phys. Rev. 92, 1572, 1953.

15. Ingram, D.J.E., Bennett, J.E., J. Chem. Phys. 22, 1136, 1954.

16. Bennett, J.E., Ingram, D.J.E., Nature, London, 175, 130, 1955.

17. Lancaster, F.W., Gordy, W., J. Chem. Phys. 19, 1181, 1951.

18. Ramaseshan, S., Suryan, G., Proc. Ind. Acad. Sci. A36, 211, 1952.

19. Bagguley, D.M.S., Bleaney, B., Griffiths, J.H.E., Penrose, R.P., Plumpton, B.I., Proc. Phys. Soc. 61, 551, 1948.

20. Kozyrev, B.M., Salikhov, S.G., Shamonin, Yu.Ya., ZhETF 22, 56, 1952.

21. Perakis, N., Wucher, J., Gijsman, H.M., Compt. Rend. 239, 243, 1954.

22. Bowers, K.D., Proc. Phys. Soc. A66, 666, 1953.

23. Abe, H., Ohtsuka, M., J. Phys. Soc. Japan 11, 896, 1956.

24. Abe, H., Ono, K., J. Phys. Soc. Japan 11, 947, 1956.

25. Ono, K., Ohtsuka, M., J. Phys. Soc. Japan 13, 206, 1958.

26. Shimoda, J., Abe, H., Ono, K., J. Phys. Soc. Japan 11, 1956, 137,

1956.

27. Abe, H., Shimoda, J., J. Phys. Soc. Japan 12, 1255, 1957.

28. Sundaramma, K., Proc. Indian Acad. Sci. A46, 232, 1957.

29. Sundaramma, K., Proc. Indian Acad. Sci. A44, 345, 1956.

30. Bennett, J.E., Ingram, D.J.E., Phil. Mag. 1, 970, 1956.

31. Sundaramma, K., Proc. Indian Acad. Sci. A42, 292, 1955.

32. McGarvey, B.R., J. Phys. Chem. 60, 71, 1956.

33. Karlson, E.H., Spence, R.D., J. Chem. Phys. 24, 471, 1956.

34. Lütze, E., Z. phys. Chem. 8, 32, 1956.

35. Date, M., J. Phys. Soc. Japan 11, 1016, 1956.

36. Miduno, Z., Matumura, O., Hukuda, K., Horai, K., Mem. Fac. Sci. Kuysyu Univ. B2, 13, 1956.

37. Maki, A.H., McGarvey, B.R., J. Chem. Phys. 29, 31, 1958.

38. Sands, R.H., Phys. Rev. 99, 1222, 1955.

39. Sundaramma, K., Suryan, S., Current Sci. 26, 80, 1957.

40. Palma-Vittorelli, M.B., Palma, M.U., Palumbo, D., Santangelo, M., Ricerca Sci. 25, 2364, 1955.

41. Palma-Vittorelli, M.B., Palma, M.U., Palumbo, D., Santangelo, M., Nuovo Cimento 2, 811, 1955.

42. Garif'yanov, N.S., Zaripov, M.M., ZhETF 28, 629, 1955.

43. Lütze, E., Naturwiss. (Natural Sciences) 41, 279, 1954.

44. Ingram, D.J.E., Bennett, J.E., Disc. Faraday Soc. 19, 140, 173, 1955.

45. Kumagai, H., Ono, K., Hayashi, I., Abe, H., Shimoda, J., Shono, H., Ibamoto, H., Tachimori, S., J. Phys. Soc. Japan 9, 369, 1954.

46. Kumagai, H., Hayashi, I., Ono, K., Abe, H., Shimoda, J., Shono, H., J. Phys. Soc. Japan 9, 376, 1954.

47. Maki, A.H., McGarvey, B.R., J. Chem. Phys. 29, 35, 1958.

48. Vittorelli, M.B.P., Palma, M.U., Palumbo, D., Santangelo, M.,

Ricerca Sci. 23, 1423, 1953.

49. Ubbink, J., Poulis, J.A., Gerritsen, H.J., Gorter, C.J., Physica 18, 361, 1952.

50. Abe, H., J. Phys. Soc. Japan 13, 987, 1958.

51. Tucker, R.J., Jr., Phys. Rev. 112, 725, 1958.

52. Hayes, W. (see Orton, J.W., Rep. Progr. Phys. 22, 204, 1959).

53. Abe, H., Nagano, H., Nagusa, M., Oshima, K., J. Chem. Phys. 25, 378, 1956.

54. Jarrett, H.S., J. Chem. Phys. 28, 1260, 1958.

55. Partridge, M.F. (see Orton, J.W., Rep. Progr. Phys. 22, 204, 1959).

To Table 4.2

Ti^{3+}

1. Bleaney, B., Bogle, G.S., Cooke, A.H., Duffus, R.J., O'Brien, M.C.M., Stevens, K.W.H., Proc. Phys. Soc. A68, 57, 1955.

2. Bogle, G.S., Owen, J. (see Bowers, K.D., Owen, J., Rep. Progr. Phys. 18, 304, 1955).

3. Jarrett, H.S., J. Chem. Phys. 27, 1298, 1957.

4. Bijl, D., Proc. Phys. Soc. A63, 405, 1950.

V^{4+}

1. Griffiths, J.H.E., Ward, I.M. (see Bowers, K.D., Owen, J., Rep. Progr. Phys. 18, 304, 1955).

2. Lancaster, F.M., Gordy, W., J. Chem. Phys. 19, 1181, 1951.

3. Hutchinson, C.A., Singer, L.S., Phys. Rev. 89, 256, 1953.

4. Palma-Vittorelli, M.B., Palma, M.U., Palumbo, D., Sgarlata, F., Nuovo Cimento 3, 718, 1956.

5. Ingram, D.J.E., Bennett, J.E., Disc. Faraday Soc. 19, 140, 173, 1955.

Mn^{6+}

1. Lancaster, F.W., Gordy, W., J. Chem. Phys. 19, 1181, 1951.

$$V^{8+}$$

1. Zverev, G.M., Prokhorov, A.M., ZhETF, 34, 1023, 1958.

2. Lambe, J., Ager, R., Kikuchi, C., Bull. Am. Phys. Soc., ser. II, 4, 261, 1959.

$$Co^{2+}$$

1. Bleaney, B., Ingram, D.J.E., Proc. Roy. Soc. A208, 143, 1951.

2. Dobrowolski, W., Jones, R.V., Jeffries, C.D., Phys. Rev. 101, 1001, 1956.

3. Bowers, K.D. (see Bowers, K.D., Owen, J., Rep. Progr. Phys. 18, 304, 1955).

4. Trenam, R.S., Proc. Phys. Soc. A66, 118, 1953.

5. Gager, W.B., Jastram, P.S., Daunt, J.G., Phys. Rev. 111, 803, 1958.

6. Tinkham, M., Proc. Roy. Soc. A236, 535, 1956.

7. Hayes, W., Jones, D.A., Proc. Phys. Soc. 71, 459, 1958.

8. Low, W., Phys. Rev. 109, 256, 1958.

9. Ingram, D.J.E., Bennett, J.E., J. Chem. Phys. 22, 1136, 1954.

10. Ingram, D.J.E., Bennett, J.E., Disc. Faraday Soc. 19, 140, 173, 1955.

11. Jones, R.V., Dobrowolski, W., Jeffries, C.D., Phys. Rev. 102, 738, 1956.

12. Dobrow, W., Jeffries, C.D., Phys. Rev. 108, 60, 1957.

13. Geusic, J.E., Bull. Am. Phys. Soc., ser. II, 4, 261, 1959.

14. Baker, J.M., Hayes, W., Jones, D.A., Proc. Phys. Soc. 73, 942, 1959.

15. Zverev, G.M., Prokhorov, A.M., ZhETF 36, 647, 1959.

16. Baker, J.M., Bleaney, B., Llewellyn, P.M., Shaw, P.F.D., Proc. Phys. Soc. A69, 353, 1956.

17. J. Partridge, M.F. (see Orton, J.W., Rep. Progr. Phys. 22, 204, 1959).

$$Fe^{2+}$$

1. Tinkham, M., Proc. Phys. Soc. A68, 258, 1955.

2. Tinkham, M., Proc. Roy. Soc. A236, 535, 1956.

3. Low, W., Phys. Rev. 101, 1827, 1956.

4. Bleaney, B., Stevens, K.W.H., Rep. Progr. Phys. 16, 108, 1953.

5. Ingram, D.J.E., Bennett, J.E., J. Chem. Phys. 22, 1136, 1954.

6. Partridge, M.F. (see Orton, J.W., Rep. Progr. Phys. 22, 204, 1959).

To Table 4.3

$$Ce^{3+}$$

1. Cooke, A.H., Duffus, H.J., Wolf, W.P., Phil. Mag. 44, 623, 1953.

2. Kedzie, R.W., Abraham, M., Jeffries, C.D., Phys. Rev. 108, 54, 1957.

3. Bogle, G.S., Cooke, A.H., Whitley, S., Proc. Phys. Soc. A64, 931, 1951.

4. Bogle, G.S., Cooke, A.H. (see Bowers, K.D., Owen, J., Rep. Progr. Phys. 18, 304, 1955).

5. Baker, J.M., Hayes, W., Jones, D.A., Proc. Phys. Soc. 73, 942, 1959.

6. Hutchison, C.A., Wong, E., J. Chem. Phys. 29, 754, 1958.

$$Nd^{3+}$$

1. Cooke, A.H., Duffus, H.J., Proc. Roy. Soc. A229, 407, 1955.

2. Bleaney, B., Scovil, H.E.D., Trenam, R.S., Proc. Roy. Soc. A223, 15, 1954.

3. Kurenev, V.Ya., Salikhov, S.G., ZhETF 21, 864, 1951.

4. Garif'yanov, N.S., Dissertation, Kazan', 1952.

5. Bleaney, B., Llewellyn, P.M., Jones, D.A., Proc. Phys. Soc. B69, 858, 1956.

6. Sanadze, T.I., ZhETF 33, 1042, 1957; Tr. Gruz. politekhn. in-ta (Trans. Georgian Polytechnic Institute), No. 4, 177, 1957.

7. Kedzie, R.W., Abraham, M., Jeffries, C.D., Phys. Rev. 108, 54, 1957.

8. Hutchison, C.A., Wong, E., J. Chem. Phys. 29, 754, 1958.

$$Sm^{3+}$$

1. Cooke, A.H., Duffus, H.J., Proc. Roy. Soc. A229, 407, 1955.

2. Bogle, G.S., Scovil, H.E.D., Proc. Phys. Soc. A65, 368, 1952.

3. Low, W., Phys. Rev. 98, 426, 1955.

4. Hutchison, C.A., Wong, E., J. Chem. Phys. 29, 754, 1958.

$$Dy^{3+}$$

1. Cooke, A.H., Park, J.G., Proc. Phys. Soc. A69, 282, 1956.

2. Park, J.G., Proc. Roy. Soc. A245, 118, 1958.

$$Er^{3+}$$

1. Bogle, G.S., Duffus, H.J., Scovil, H.E.D., Proc. Phys. Soc. A65, 760, 1952.

2. Baker, J.M., Hayes, W., Jones, D.A., Proc. Phys. Soc. 73, 942, 1959.

3. Judd, B.R., Wong, E., J. Chem. Phys. 28, 1097, 1958.

4. Hutchison, C.A., Wong, E., J. Chem. Phys. 29, 754, 1958.

$$Yb^{3+}$$

1. Cooke, A.H., Park, J.G., Proc. Phys. Soc. A69, 282, 1956.

To Table 4.4

$$Pr^{3+}$$

1. Cooke, A.H., Duffus, H.J., Proc. Roy. Soc. A229, 407, 1955.

2. Bleaney, B., Scovil, H.E.D., Phil. Mag. 43, 999, 1952.

3. Davis, C.F., Kip, A.F., Malvano, R., R.C. Acad. Lincei 11, 77, 1951.

4. Anderson, J.H., Hutchison, C.A., Phys. Rev. 97, 76, 1955.

5. Baker, J.M., Bleaney, B., Proc. Phys. Soc. A68, 936, 1955.

6. Gränischer, H., Hubner, K., Müller, K.A., Helv. phys. Acta 30, 480, 1957.

7. Baker, J.M., Bleaney, B., Proc. Roy. Soc. A245, 156, 1958.

8. Hutchison, C.A., Wong, E., J. Chem. Phys. 29, 754, 1958.

$$Tb^{3+}$$

1. Baker, J.M., Bleaney, B., Proc. Phys. Soc. A68, 257, 1955.

2. Sanadze, T.I., Kalach, M., Tsintsadze, G.A., Tr. In-ta fiziki AN Gruz. SSSR (Trans. Inst. Physics Acad. Sci. Georgian SSR), 5, 271, 1957.

3. Manenkov, A.A., Prokhorov, A.M., Trapeznikova, Z.A., Fok, M.V., Izv. AN SSSR, ser fiz. (Bull. Acad. Sci. USSR, Physics Series), 21, 779, 1957; Optika i spektroskopiya (Optics and Spectroscopy) 2, 470, 1957.

4. Baker, J.M., Bleaney, B., Proc. Roy. Soc. A245, 156, 1958.

5. Berulava, B.G., Sanadze, T.I., Soveshchaniye po paramagnitnomu rezonansu (Conference on Paramagnetic Resonance), Kazan', 1959.

6. Hutchison, C.A., Wong, E., J. Chem. Phys. 29, 754, 1958.

$$Ho^{3+}$$

1. Baker, J.M., Bleaney, B., Proc. Phys. Soc. A68, 1090, 1955.

2. Baker, J.M., Bleaney, B., Proc. Roy. Soc. A245, 156, 1958.

3. Hutchison, C.A., Wong, E., J. Chem. Phys. 29, 754, 1958.

To Table 4.5

$$Mn^{2+}$$

1. Ingram, D.J.E., Proc. Phys. Soc. A66, 412, 1953.

2. Brovetto, P., Cini, G., Ferroni, S., Nuovo Cimento 10, 1325, 1953.

3. Hayashi, I., Ono, K., J. Phys. Soc. Japan 8, 270, 1953.

4. Bleaney, B., Ingram, D.J.E., Proc. Roy. Soc. A205, 336, 1951.

5. Trenam, R.S., Proc. Phys. Soc. A66, 118, 1953.

6. Arakawa, T., J. Phys. Soc. Japan 9, 790, 1954.

7. Hurd, F.K., Sachs, M., Herschberger, W.D., Phys. Rev. 93, 373, 1954.

8. Schneider, E.E., England, T.S., Physica 17, 221, 1951.

9. Herschberger, W.D., Leifer, H.N., Phys. Rev. 88, 714, 1952.

10. Ingram, D.J.E., Phys. Rev. 90, 711, 1953.

11. Kumagai, H., Ono, K., Hayashi, I., Kambe, K., Phys. Rev. 87, 374, 1952.

12. Lancaster, F.W., Gordy, W., J. Chem. Phys. 19, 1181, 1951.

13. Kozyrev, B.M., Salikhov, S.G., Shamonin, Yu.Ya., ZhETF 22, 56, 1952.

14. Bagguley, D.M.S., Bleaney, B., Griffiths, J.H.E., Penrose, R.P., Plumpton, B.I., Proc. Phys. Soc. 61, 551, 1948.

15. Ingram, D.J.E., Bennett, J.E., J. Chem. Phys. 22, 1136, 1954.

16. Abe, H., Shimoda, J., National Science Report, Ochanomizu University 4, 77, 1953.

17. Kumagai, H., Ono, K., Hayashi, I., Abe, H., Shimoda, J., Shono, H., Ibamoto, H., Phys. Rev. 83, 1077, 1951.

18. Abe, H., J. Phys. Soc. Japan 12, 435, 1957.

19. Watkins, G.D., Bull. Am. Phys. Soc., ser. II, 2, 345, 1957.

20. Hayes, W., Jones, D.A., Proc. Phys. Soc. 71, 459, 1958.

21. Tinkham, M., Proc. Roy. Soc. A236, 535, 1956.

22. Low, W., Phys. Rev. 105, 792, 1957.

23. Low, W., Phys. Rev. 105, 793, 1957.

24. Kurushin, A.I., ZhETF 32, 938, 1957.

25. Sundaramma, K., Proc. Indian Acad. Sci. A44, 345, 1956.

26. Kurushin, A.I., Izv. AN SSSR, ser. fiz., 20, 1232, 1956.

27. Lütze, E., Z. phys. Chem. 8, 32, 1956.

28. Forrester, P.A., Schneider, E.E., Proc. Phys. Soc. B69, 833, 1956.

29. Low, W., Proc. Phys. Soc. B69, 837, 1956.

30. Low, W., Phys. Rev. 101, 1827, 1956.

31. Ambler, E., Hudson, R.P., Physica 22, 866, 1956.

32. Dobrowolski, W., Jones, R.V., Jeffries, C.D., Phys. Rev. 104, 1378, 1956.

33. Keller, S.P., Gelles, I.L., Smith, W.V., Phys. Rev. 110, 850, 1958.

34. Matarese, L.M., Kikuchi, C., J. Phys. Chem. Solids 1, 117, 1956.

35. Watkins, G.D., Phys. Rev. 110, 986, 1958.

36. Hurd, F.K., Sachs, M., Herschberger, W.D., Phys. Rev. 93, 373, 1954.

37. Van Wieringen, I.S., Disc. Faraday Soc. 19, 118, 173, 1955.

38. Müller, K.A., Helv. phys. Acta 28, 450, 1955.

39. Lütze, E., Naturwiss 41, 279, 1954.

40. Oshima, K., Abe, H., Nagano, H., Nagusa, M., J. Chem. Phys. 23, 1721, 1955.

41. Ingram, D.J.E., Bennett, J.E., Disc. Faraday Soc. 19, 140, 173, 1955.

42. McLean, C., Kor, G.J.W., Appl. Sci. Res. B4, 425, 1955.

43. Asch, G., Meyer, A.J.P., Compt. Rend. 246, 1180, 1958.

44. Ono, K., Hayashi, I., J. Phys. Soc. Japan 8, 561, 1953.

45. Kumagai, H., Ono, K., Hayashi, I., Abe, H., Shimada, J., Shono, H., Ibamoto, H., Tachimori, S., J. Phys. Soc. Japan 9, 369, 1954.

46. Kumagai, H., Hayashi, I., Ono, K., Abe, H., Shimada, J., Shono, H., J. Phys. Soc. Japan 9, 376, 1954.

47. Morigaki, K., Fujimoto, M., Iton, J., J. Phys. Soc. Japan 13, 1174, 1958.

48. Baker, J.M., Bleaney, B., Hayes, W., Proc. Roy. Soc. A247, 141, 1958.

49. Dorain, P., Phys. Rev. 112, 1058, 1958.

50. Matumura, O., J. Phys. Soc. Japan 14, 108, 1959.

51. Ludwig, G.W., Carlson, R.O., Woodbury, H.H., Bull. Am. Phys. Soc., ser II, 4, 22, 1959.

52. Abe, H., Nagano, H., Nagusa, M., Oshima, K., J. Chem. Phys. 25, 378, 1956.

53. Matarese, L.M., Kikuchi, C., Phys. Rev. 100, 1243, 1955.

54. Dobrowolski, W., Jones, R.V. Jeffries, C.D., Phys. Rev. 104, 1378, 1956.

55. Low, W., Phys. Rev. 98, 426, 1955.

56. Partridge, M.F. (see Orton, J.W., Rep. Progr. Phys. 22, 204, 1959).

57. Fukuda, K., Uchida, J., Joshimura, H., J. Phys. Soc. Japan 13, 971, 1958.

Fe^{3+}

1. Bleaney, B., Trenam, R.S., Proc. Roy. Soc. A223, 1, 1954.

2. Ubbink, J., Poulis, J.A., Gorter, C.J., Physica 17, 213, 1951.

3. Meijer, P.H.E., Physica 17, 899, 1951.

4. Lancaster, F.W., Gordy, W., J. Chem. Phys. 19, 1181, 1951.

5. Bagguley, D.M.S., Bleaney, B., Griffiths, J.H.E., Penrose, R.P., Plumpton, B.I., Proc. Phys. Soc. 61, 551, 1948.

6. Abe, H., Shimoda, J., National Science Report, Ochanomizu University 4, 77, 1953.

7. Ingram, D.J.E., Bennett, J.E., J. Chem. Phys. 22, 1136, 1954.

8. Ting, Y., Williams, D., Phys. Rev. 82, 507, 1951.

9. Gerritsen, H.J., Bolger, B., Okkes, R.F. (see Bowers, K.D., Owen, J., Rep. Progr. Phys. 18, 304, 1955).

10. Jarrett, H.S., J. Chem. Phys. 27, 1298, 1957.

11. Müller, K.A., Arch. Sci. 10, fasc. spec., 130, 1957.

12. Korniyenko, L.S., Prokhorov, A.M., ZhETF 33, 805, 1957.

13. Lütze, E., Z. phys. Chem. 8, 32, 1956.

14. Date, M., Sci. Repts. Res. Insts., Tohoku Univ. A6, 497, 1954.

15. Zaripov, M.M., Shamonin, Yu.Ya., Izv. AN SSSR, ser. fiz., 20, 1224, 1956.

16. Low, W., Phys. Rev. 105, 792, 1957.

17. Müller, K.A., Helv. phys. Acta 31, 173, 1958.

18. Kumagai, H., Ono, K., Hayashi, I., Abe, H., Shimoda, J., Shono, H., Ibamoto, H., Tachimori, S., J. Phys. Soc. Japan 9, 369, 1954.

19. Ludwig, G.W., Woodbury, H.H., Carlson, R.O., Phys. Rev. Letters 1, 295, 1958.

20. Low, W., Shaltiel, D., Phys. Rev. Letters 1, 51, 286, 1958; Hornig, A.W., Rempel, R.C., Weaver, H.E., Phys. Rev. Letters 1, 284, 1958; Hornig, A.W., Jaynes, O.O., Weaver, H.E., Phys. Rev. 96, 1703, 1954.

21. Ludwig, G.W., Carlson, R.O., Woodbury, H.H., Bull. Am. Phys. Soc., ser. II, 4, 22, 1959.

22. Bogle, G.S., Symmons, H.F., Proc. Phys. Soc. 73, 531, 1959.

23. Peter, M., Phys. Rev. 113, 801, 1959.

24. Geschwind, S., Linn, D.F., Bull. Am. Phys. Soc., ser. II, 4, 261, 1959.

$$Gd^{3+}$$

1. Trenam, R.S., Proc. Phys. Soc. A66, 118, 1953.

2. Bleaney, B., Scovil, H.E.D., Trenam, R.S., Proc. Roy. Soc. A223, 15, 1954.

3. Bogle, G.S., Heine, V., Proc. Phys. Soc. A67, 734, 1954.

4. Garif'yanov, N.S., DAN SSSR 84, 923, 1952.

5. Bleaney, B., Elliott, R.J., Scovil, H.E.D., Trenam, R.S., Phil. Mag. 42, 1062, 1951.

6. Lancaster, F.W., Gordy, W., J. Chem. Phys. 19, 1181, 1951.

7. Hutchison, C.A., Judd, B.R., Pope, D.E.D., Proc. Phys. Soc. B70, 514, 1957.

8. Low, W., Phys. Rev. 109, 265, 1958.

9. Ruter, C., Helv. Phys. Acta 30, 353, 1957.

10. Low, W., Phys. Rev., 105, 792, 1957.

11. Manenkov, A.A., Prokhorov, A.M., ZhETF 33, 1116, 1957.

12. Kurushin, A.I., Izv. AN SSSR, ser. fiz., 20, 1232, 1956.

13. Buckmaster, H.A., Canad. J. Phys. 34, 341, 1956.

14. Ruter, C., Lacroix, R., Compt. Rend. 242, 2812, 1956.

15. Low, W., Phys. Rev. 103, 1309, 1956.

16. Low, W., Shaltiel, D., J. Phys. Chem. Solids 6, 315, 1958.

17. Manenkov, A.A., Prokhorov, A.M., Trapeznikova, Z.A., Fok, M.V., Izv. AN SSSR, ser. fiz., 21, 779, 1957.

18. Granisher, H., Müller, K.A., Nuovo Cimento 6, suppl. No. 3, 1217, 1957.

19. Weger, W., Low, W., Phys. Rev. 111, 1526, 1958.

20. Baker, J.M., Bleaney, B., Hayes, W., Proc. Roy. Soc. A247, 141, 1958.

21. Hutchison, C.A., Wong, E., J. Chem. Phys. 29, 754, 1958.

22. Jones, D.A., Baker, J.M., Pope, D.F.D., Proc. Phys. Soc. 74, 249, 1959.

$$Eu^{2+}$$

1. Bleaney, B., Low, W., Proc. Phys. Soc. A68, 55, 1955.

2. Ryter, C., Helv. phys. Acta 30, 353, 1957.

3. Lacroix, R., Ryter, C., Arch. Sci. 10, fasc. spec., 132, 1957.

4. Manenkov, A.A., Prokhorov, A.M., DAN SSSR 107, 402, 1956.

5. Ryter, C., Lacroix, R., Compt. Rend. 242, 2812, 1956.

6. Lacroix, R., Ryter, C., Colloq. AMPERE, Inst. Phys., Univ., Geneve, 55, 1956.

7. Low, W., Phys. Rev. 101, 1827, 1956.

8. Low, W., Phys. Rev. 98, 426, 1955.

9. Abraham, M., Kedzie, R., Jeffries, C.D., Phys. Rev. 108, 57, 1957.

10. Manenkov, A.A., Prokhorov, A.M., Trapeznikova, Z.A., Fok, M.V., Izv. AN SSSR, ser. fiz., 21, 779, 1957; Optika i spektroskopiya 2, 470, 1957.

11. Baker, J.M., Bleaney, B., Hayes, W., Proc. Roy. Soc. A247, 141, 1958.

12. Matumura, O., Horai, K., Miduno, J., J. Phys. Soc. Japan 13, 768, 1958.

13. Manenkov, A.A., Prokhorov, A.M., Trukhlyayev, N.S., Yakovlev, G.N., DAN SSSR 112, 623, 1955.

14. Ryter, C., Lacroix, R., Compt. Rend. (Proceedings) 242, 2812, 1956.

$$Cm^{3+}$$

1. Fields, P., Friedman, A., Smaller, B., Low, W., Phys. Rev. 105, 757, 1957.

2. Abraham, M., Cunningham, B.B., Jeffries, C.D., Kedzie, R.W., Bull. Am. Phys. Soc. 1, 396, 1956.

To Table 4.6

$$Fe^{III}$$

1. Bleaney, B., Ingram, D.J.E., Proc. Phys. Soc. A65, 953, 1952.

2. Baker, J.M., Bleaney, B., Bowers, K.D., Proc. Phys. Soc. B69, 1205, 1956.

3. George, P., Bennett, J.E., Ingram, D.J.E., J. Chem. Phys. 24, 627, 1956.

4. Bennett, J.E., Ingram, D.J.E., Nature, London 177, 275, 1956.

5. Ingram, D.J.E., Bennett, J.E., Disc. Faraday Soc. 19, 140, 173, 1955.

6. Gibson, J.F., Ingram D.J.E., Nature, London 180, 29, 1957.

7. Garif'yanov, N.S., Zaripov, M.M., Kozyrev, B.M., DAN SSSR 113, 1243, 1957.

$$Mn^{II}$$

1. Baker, J.M., Bleaney, B., Bowers, K.D., Proc. Phys. Soc. B69, 1205, 1956.

$$Mo^{V}$$

1. Owen, J., Ward, I.M., Phys. Rev. 102, 591, 1956.

2. Griffiths, J.H.E., Owen, J., Ward, I.M., Proc. Roy. Soc. A219, 526, 1953.

Mo[III]

1. Owen, J., Ward, I.M. (see Bowers, K.D., Owen, J., Rep. Progr. Phys. 18, 304, 1955).

2. Ramaseschan, S., Suryan, G., Phys. Rev. 84, 593, 1951.

3. Griffiths, J.H.E., Owen, J., Ward, I.M., Proc. Roy. Soc. A219, 526, 1953.

Tc[IV]

1. Low, W., Llewellyn, P.M., Phys. Rev. 110, 842, 1958.

Ru[III]

1. Griffiths, J.H.E., Owen, J., Ward, I.M., Proc. Roy. Soc. A219, 526, 1953.

2. Griffiths, J.H.E., O'Brien, M.C.M., Owen, J., Ward, I.M. (see Bowers, K.D., Owen, J., Rep. Progr. Phys. 18, 304, 1955).

3. Griffiths, J.H.E., Owen, J., Proc. Phys. Soc. A65, 951, 1952.

4. Owen, J., Ward, I.M. (see Bowers, K.D., Owen, J., Rep. Progr. Phys. 18, 304, 1955).

Ag[II]

1. Gijsman,H.M., Gerritsen, H.J., van den Handel, J., Physica 20, 15, 1954.

2. Bowers, K.D., Proc. Phys. Soc. A66, 666, 1953.

Re[IV]

1. Owen, J., Ward, I.M., Phys. Rev. 102, 591, 1956.

Ir[IV]

1. Griffiths, J.H.E., Owen, J., Proc. Roy. Soc. A226, 96, 1954.

2. Griffiths, J.H.E., Owen, J., Ward, I.M., Proc. Roy. Soc. A219, 526, 1953.

3. Griffiths, J.H.E., Owen, J., Park, J.G., Partridge, M.F., Phys. Rev. 108, 1345, 1957.

U^{III}

1. Bleaney, B., Llewellyn, P.M., Jones, D.A., Proc. Phys. Soc. B69, 858, 1956.

2. Bleaney, B., Hutchison, C.A., Llewellyn, P.M., Pope, D.F.D., Proc. Phys. Soc. B69, 1167, 1956.

3. Hutchison, C.A., Llewellyn, P.M., Wong, E., Dorain, P.B., Phys. Rev. 102, 292, 1956.

4. Dorain, P.B., Hutchison, C.A., Wong, E., Phys. Rev. 105, 1307, 1957.

5. Ghosh, S.N., Gordy, W., Hill, D.G., Phys. Rev. 96, 36, 1954.

6. Berulava, B.G., Sanadze, T.I., Soveshchaniye po paramagnitnomu rezonansu, Kazan', 1959.

Np^{II}

1. Bleaney, B., Llewellyn, P.M., Pryce, M.H.L., Hall, G.R., Phil. Mag. 45, 992, 1954.

2. Abraham, M., Jeffries, C.D., Kedzie, R.W., Wallmann, J.C., Phys. Rev. 106, 1357, 1957.

3. Abraham, M., Jeffries, C.D., Kedzie, R.W., Wallmann, J.C., Phys. Rev. 112, 553, 1958.

Pu^{II}

1. Bleaney, B., Llewellyn, P.M., Pryce, M.H.L., Hall, G.R., Phil. Mag. 45, 991, 1954.

2. Hutchison, C.A., Lewis, W.B., Phys. Rev. 95, 1096, 1954.

3. Abraham, M., Jeffries, C.D., Kedzie, R.W., Wallmann, J.C., Phys. Rev. 112, 553, 1958.

To Table 4.7

1. Hayes, W., Jones, D.A., Proc. Phys. Soc. 71, 503, 1958.

2. Orton, J.W. (see Orton, J.W., Rep. Progr. Phys. 22, 204, 1959).

3. Bleaney, B., Hayes, W., Proc. Phys. Soc. B70, 626, 1957.

4. Watkins, G.D., Bull. Amer. Phys. Soc. 2, 345, 1957.

5. Elschner, Herzog, VII Colloq. AMPERE, Paris, July 1958.

6. Voyevodskiy, V.V., Molin, Yu.N., Chibrikin, V.M., ZhOS (J. Optics and Spectroscopy) 5, 90, 1958.

7. Feltham, R.D., Sogo, P., Calvin, M., J. Chem. Phys. 26, 1354, 1957.

8. Tsvetkov, Yu.D., Voyevodskiy, V.V., Razuvayev, G.A., Sorokin, Yu.V., Domrachev, G.A., DAN SSSR 115, 118, 1957.

§4.3. Paramagnetic Resonance Spectra in Electrolyte Solutions

Paramagnetic absorption in liquid solutions of salts was first observed by Zavoyskiy [1] in 1944.

From among the inorganic compounds in solution, the salts studied predominantly to date have been those of the iron group ions. The solvent used for the most part was water; in addition, various monatomic and diatomic alcohols, glycerine, acetone, dioxane, and other organic liquids were used.

A measurable resonant effect was found in solutions containing the ions VO^{2+}, Cr^{3+}, Mn^{2+}, Fe^{3+}, and Cu^{2+}. The observation of paramagnetic resonance in solutions of Gd^{3+} and $[W(CN)_8]^{3-}$ salts is also reported.

The investigated absorption lines are either single or display a hyperfine structure. The maxima of the fine structure are not resolved, although it is known that in certain polycrystals (for example, in chrome alum powder) they can be observed. In solutions, on the other hand, the fine structure is manifest only in the width of the line.

The values of the effective g factors are close to 2, but for some ions, particularly for Cu^{2+}, their exact value depends appreciably on the nearest surrounding of the ion. In particular, a change in solvent or complex formation lead to a change in g.

A hyperfine structure of paramagnetic resonance lines was observed in aqueous solutions of the simple salts $^{55}Mn^{2+}$ [2-4], $^{51}VO^{2+}$ [4, 5], and also in solutions of the complex salts $^{63,65}Cu^{2+}$ [6] and $^{183}W^{5+}$ [7].

The spectrum is described by a spin Hamiltonian

$$\mathscr{H} = g\beta H_0 \hat{S} + A \hat{I} \hat{S}.$$

The resonant value of the field $H_0 = H^*_0$ for the transitions (M,m) → → (M − 1,m) are given by the expression

$$H^*_0 = H - Am - \frac{A^2}{2H}[I(I+1) - m^2],$$

where $H = h\nu/g\beta$, which is in good agreement with experiment in the case of solutions of Mn^{2+} and VO^{2+} in water.

When the frequency of the oscillating field is low ($\nu \approx 100$ Mcs), i.e., under conditions corresponding to the Zeeman effect, a single peak with g = 1.00 is observed in the hyperfine structure in weak fields in aqueous solutions of Mn^{2+}. The position of this peak is described by the formula

$$h\nu = g_F \beta H, \tag{a}$$

where F is the quantum number of the resultant momentum of the electron shell and of the nucleus and $g_F = \dfrac{F(F + 1) + J(J + 1) - I(I + 1)}{2F(F + 1)}$.

Indeed, when J = I = 5/2 we obtain $g_F = 1$ for Mn^{2+}. This effect, discovered by Al'tshuler, Kozyrev, and Salikhov [2],* was the first evidence of the influence of nuclear spin on the electron paramagnetic resonance line. The fact that formula (a) is applicable to the description of the effect in aqueous solutions of Mn^{2+} salts shows that in this case the fine splittings are quite small as compared with the hyperfine splittings. Measurements in solutions of other ions (for example, VO^{2+}) under weak field conditions have shown no agreement with this formula.

In solutions containing the ions $^{57}Fe^{3+}$, $^{53}Cr^{3+}$, and the hydrated ions $^{63,65}Cu^{2+}$, no hyperfine structure is observed because its constant is small compared with the line width. For $^{57}Fe^{3+}$ and $^{53}Cr^{3+}$, the hyperfine structure constants are quite small also in all the solid compounds of these ions. On the other hand, for the ions of $^{63,65}Cu^{2+}_{aq}$ the situation is to some extent close to that observed in solid copper salts, which have trigonal symmetry; in the latter, the hyperfine structure constant is small at sufficiently high temperatures and is close to isotropic; the g factor is likewise close to isotropic (see the foregoing tables for the solid salts of Cu^{2+}).

In aqueous solutions the copper ion is surrounded by a deformed octahedron of water molecules; one of its axes is elongated because of the Jahn-Teller effect. It is obvious that we have three possible deformations of this type, corresponding to the same energy. Transitions can occur between these deformations and impart to the Jahn-Teller effect a dynamic character in this case. Calculation [8] has shown that one can explain on this basis the single line observed in aqueous solutions of copper salts. On the other hand, the presence of a resolved hyperfine line structure in solutions of several complex copper salts is due to the fact that owing to the large mass of the ligands and to their stronger bond with the Cu^{2+} ion, the Jahn-Teller effect loses its dynamic character to some degree. Accordingly, the hyperfine structure constants increase and, like the g factor, they become less isotropic. The values of the g factors and of the hyperfine structure constants of the ions investigated in solution are listed in Table 4.8.

We note in conclusion that paramagnetic resonance was investigated also in certain supercooled solutions (glasses) [12-14]. In this case a hyperfine structure of absorption lines, which was anisotropic for VO^{2+} and Cu^{2+}, was observed for the ions $^{51}VO^{2+}$, $^{53}Cr^{3+}$, $^{55}Mn^{2+}$, and $^{63,65}Cu^{2+}$. In the case of Mn^{2+} the structure is isotropic, and at low frequencies a single peak with $g = 1$ is observed, as in aqueous solutions of this ion, but broader. One of the results of work done in this field was the establishment of the value of the spin $I = 1/2$ for the ^{57}Fe nucleus [15]. The experiments were set up in cooled melts of borax containing ^{57}Fe.

TABLE 4.8

g Factors and Hyperfine Structure Constants in Liquid Solutions of Paramagnetic Salts at Room Temperature

1 Соединение	Концентрация иона, моль/л 2	3 Растворитель	g	A, эрст 4	Лите-ратура 5
1) VO^{2+} $VOCl_2$; $VOSO_4$	0,5÷0,1	10 Вода	1,962±0,002	116	[4]
	0,3	11 Вода:ацетон = 1:19	1,962 ±0,002	110	[4]
2) Cr^{3+} Cr (NO₃)₃	3÷0,25	10 Вода	1,972 ±0,008		[9]
3) Mn^{2+} MnCl₂; MnSO₄; Mn (NO₃)₂	0,2÷0,01	10 Вода	2,000 ±0,002	95,6	[4]
4) Fe^{3+} [FeF₆]¹⁺ [FeF₃]	0,3	10 Вода	(~2)		[6]
	0,3	10 Вода	(~2)		[6]
5) Cu^{2+}	4÷0,01	10 Вода 12	2,184 ±0,004		[9]
Cu (NO₃)₂ · 3H₂O	2,5	Этиловый спирт	2,184 ±0,004		[9]
»	2	13 Ацетон	2,156 ±0,004		[9]
»	2÷1	14 Глицерин 15	2,088* ±0,004		[9]
6 Cu — ацетилацетонат	1	Диоксан + толуол	2,138*	~70*	[10]
»	0,08	»	2,130*	~73*	[10]
»	1	16 Хлороформ + толуол	2,127*	~79*	[10]
»	0,14	16 Хлороформ + толуол	2,124*	~79*	[10]
»	0,19	17 Хлороформ+четыреххлористый углерод	1,126*	~77*	[10]
7 Cu 3-этилацетонат	1	18 Диоксан-толуол	2,134*	~73*	[10]
»	0,27	»	2,129*	~75*	[10]
»	0,15	19 Диоксан	~2,2*	~36*	[11]
8 Cu этаноламин	0,15	10 Вода	2,11*	~75*	[11]
9 Cu диэтаноламин	0,15	10 Вода	2,12*	~75*	[11]

Remark on Table 4.8. the values of the g factors and hyperfine structure constants noted with an asterisk have been obtained without account of the second approximation.

1) Compound; 2) ion concentration, mole/liter; 3) solvent; 4) A, oersted; 5) literature; 6) Cu — acetyl acetonate; 7) Cu 3-ethylacetonate; 8) Cu ethanolamine; 9) Cu diethanolamine; 10) water; 11) water:acetone = 1:19; 12) ethyl alcohol; 13) acetone; 14) glycerine; 15) dioxane + toluol; 16) chloroform + toluol; 17) chloroform + carbon tetrachloride; 18) dioxane-toluol; 19) dioxane.

REFERENCES (§4.3)

1. Zavoyskiy, Ye.K., Doctor's Dissertation, Moscow, FIAN (Physics Institute Acad. Sci.), 1944.

2. Al'tshuler, S.A., Kozyrev, B.M., Salikhov, S.G., DAN SSSR (Proc. Acad. Sci. USSR), 71, 855, 1950.

3. Tinkham, M., Weinstein, R., Kip, A.F., Phys. Rev. 84, 848, 1951.

4. Garif'yanov, N.S., Kozyrev, B.M., DAN SSSR 98, 929, 1954.

5. Pake, G.E., Disc. Faraday Soc. 19, 184, 1955.

6. McGarvey, B.R., J. Phys. Chem. 61, 1232, 1957.

7. Weissman, S.I., Garner, Clifford S., J. Am. Chem. Soc. 78, 1072, 1956.

8. Avvakumov, V.I., ZhETF (in preparation).

9. Kozyrev, B.M., Doctor's Dissertation, Moscow, FIAN, 1957.

10. McGarvey, B.R., J. Phys. Chem. 60, 71, 1956.

11. Kozyrev, B.M., Rivkind, A.I., DAN SSSR 127, 1044, 1959.

12. Garif'yanov, N.S., DAN SSSR 103, 41, 1955.

13. Sands, K.H., Phys. Rev. 99, 1222, 1955.

14. Garif'yanov, N.S., Izv. AN SSSR, ser. fiz., 21, 824, 1957.

15. Garif'yanov, N.S., Zaripov, M.M., Kozyrev, B.M., DAN SSSR 113, 1243, 1957.

§4.4. Use of Electron Paramagnetic Resonance for the Determination of the Spins of Atomic Nuclei

One of the important results of investigations on the spectra of paramagnetic resonance was the determination of the spins of several atomic nuclei. Table 4.9 lists the corresponding data. It must be noted that this table does not indicate the many cases when the value of the nuclear spin, previously determined by other means (and sometimes unreliable), was confirmed by the electron paramagnetic resonance method. Nor do we present in the form of a separate table the values of the magnetic moments of the nuclei, obtained by this method, since they cannot compete in accuracy with the data obtained by the nuclear paramagnetic resonance method. Some information pertaining to magnetic moments is given in the remarks for Tables 4.1-4.6.

TABLE 4.9

Values of Nuclear Spins Determined by the Electron Paramagnetic Resonance Method

1 Изотоп	2 Ядерный спин	3 Литература	1 Изотоп	2 Ядерный спин	3 Литература	1 Изотоп	2 Ядерный спин	3 Литература
V^{50}	6	[1]	Mo^{97}	$\frac{5}{2}$	[9]	Sm^{149}	$\frac{7}{2}$	[13]
Cr^{53}	$\frac{3}{2}$	[2]	Ru^{99}	$\frac{5}{2}$	[10]	$*Eu^{151}$	3	[14]
Mn^{53}	$\frac{7}{2}$	[3]	Ru^{101}	$\frac{5}{2}$	[10]	$*Eu^{154}$	3	[15]
Fe^{57}	$\frac{1}{2}$	[4]	$*Ce^{141}$	$\frac{7}{2}$	[11]	Dy^{161}	$\frac{5}{2}$	[16]
$*Co^{56}$	4	[5]	Nd^{143}	$\frac{7}{2}$	[12]	Dy^{163}	$\frac{5}{2}$	[16]
$*Co^{57}$	$\frac{7}{2}$	[6]	Nd^{145}	$\frac{7}{2}$	[12]	Er^{167}	$\frac{7}{2}$	[17]
$*Co^{58}$	5	[7]	Nd^{147}	$\frac{5}{2}$	[11]	$*Pu^{239}$	$\frac{1}{2}$	[18]
Ni^{61}	$\frac{3}{2}$	[8]	Sm^{147}	$\frac{7}{2}$	[13]	$*Pu^{241}$	$\frac{5}{2}$	[19]
Mo^{95}	$\frac{5}{2}$	[9]						

1) Isotope; 2) nuclear spin; 3) literature.

REFERENCES (§4.4)

1. Baker, J.M., Bleaney, B., Proc. Phys. Soc. A65, 952, 1952.

2. Bleaney, B., Bowers, K.D., Proc. Phys. Soc. A64, 1135, 1951.

3. Dobrowolsky, W., Jones, R.V., Jeffries, C.D., Phys. Rev. 104, 1378, 1956.

4. Garifyanov, N.S., Zaripov, M.M., Kozyrev, B.M., DAN SSSR (Proc. Acad. Sci. USSR) 113, 1243, 1957.

5. Baker, J.M., Bleaney, B., Llewellyn, P.M., Shaw, P.F.D., Proc. Phys. Soc. A69, 353, 1956.

6. Baker, J.M., Bleaney, B., Bowers, K.D., Shaw, P.F.D., Trenam, R.S., Proc. Phys. Soc. A66, 305, 1953.

7. Dobrowolsky, W., Jones, R.V., Jeffries, C.D., Phys. Rev. 101, 1001, 1956.

8. Woodbury, H.H., Ludwig, S.W., Phys. Rev. Letters 1, 16, 1958.

9. Owen, J., Ward, I.M., Phys. Rev. 102, 591, 1956.

10. Griffiths, J.H.E., Owen, J., Proc. Phys. Soc. A65, 951, 1952.

11. Kedzie, R.W., Abragam, M., Jeffries, C.D., Phys. Rev. 108, 54, 1956.

12. Bleaney, B., Scovil, H.E.D., Proc. Phys. Soc. A63, 1369, 1950.

13. Bogle, G.S., Scovil, H.E.D., Proc. Phys. Soc. A65, 368, 1952.

14. Manenkov, A.A., Prokhorov, A.M., Trukhlyayev, P.S., Yakovlev, G.N., DAN SSSR 112, 623, 1955.

15. Abragam, M., Kedzie, R.W., Jeffries, C.D., Phys. Rev. 108, 58, 1956.

16. Cooke, A.H., Park, J.G., Proc. Phys. Soc. A69, 282, 1956.

17. Bleaney, B., Scovil, H.E.D., Proc. Phys. Soc. A64, 204, 1951.

18. Bleaney, B., Llewellyn, P.M., Pryce, M.H.L., Hall, G.R., Phil. Mag. 54, 773, 1954.

19. Bleaney, B., Llewellyn, P.M., Pryce, M.H.L., Hall, G.R., Phil. Mag. 45, 991, 1954.

1. Astbury, W.F., Proc. Roy. Soc. A112, 448, 1926; Morgan, G.F., Drew, H.D.H., J. Chem. Phys. 119, 1059, 1921; Roof, R.B., Acta Cryst. 9, 791, 1956.

2. Powell, H.M., Wells, A.F., J. Chem. Phys. 359, 1935.

3. Beevers, C.A., Lipson, H., Proc. Roy. Soc. A146, 570, 1934.

4. Groth, P., Chem. Kristall. (Chem. Crystals) 2, 438, 1908.

5. Harker, D., Z. Kristall. (J. Crystallography) 93, 136, 1936.

6. Chrobak, L., Z. Kristall. 88, 35, 1934; Wyckoff, R.W., Crystal structures (New York, Interscience Publishers, Inc.), v. 2, chap. 10, 1951.

7. Robertson, J.M., J. Chem. Soc. 615, 1935.

8. Mazzi, F., Rend. Soc. Mineral Italiana 9, 148, 1953.

9. Kiriyama, R., Ibamoto, H., Matsuo, K., Acta Cryst. 7, 482, 1954.

10. Van Niekerk, J.N., Schoening, F.R.L., Acta Cryst., Camb. 6, 227, 1953; Groth, P., Chem. Kristall. 3, 66, 1918.

11. Groth, P., Chem. Kristall. 3, 341, 1916.

12. Cox, E.G., Webster, K.C., J. Chem. Soc., 731, 1935.

13. Ferrari, A., R.C. Accad. Lincei 3, 224, 1926.

14. Wyckoff, R.W., Am. J. Sci. 50, 317, 1920.

15. Zachariasen, W.H., J. Chem. Phys. 3, 197, 1935.

16. Zachariasen, W.H., J. Chem. Phys. 16, 254, 1948.

17. Fankuchen, I., Z. Kristall. 91, 473, 1935.

18. Keeling, R.O., Acta cryst. 10, 209, 1957.

Manu-
script
Page
No.

[Footnote]

197   Reference [2] was delivered to the USSR Academy of Sciences on 7 March 1948.

FORM OF PARAMAGNETIC RESONANCE ABSORPTION LINES IN
IONIC CRYSTALS AND ACOUSTIC PARAMAGNETIC RESONANCE

§5.1. Introduction

The construction of a theory for the form of paramagnetic reso-
nance lines is a much more complicated task than a theoretical inter-
pretation of the paramagnetic spectra. Furthermore, the problem has
been very little investigated experimentally. Therefore, in spite of
the existence of several basic researches, many unsolved problems
still remain.

The deep analogy between the electron and nuclear resonances
frequently makes it possible to extend the results obtained in one
field to the other field. In investigations of the form of nuclear
resonance lines, an important role is played by Bloch's phenomenologi-
cal equation [1]

$$\left. \begin{array}{l} \frac{dM}{dt} = \gamma\,[M,\,H] - i\frac{M_x}{T_2} - j\frac{M_y}{T_2} - k\frac{M_z - M_0}{T_1}, \\ H = kH_0 + iH_r \cos 2\pi\nu t, \end{array} \right\} \tag{5.1}$$

where M is the magnetization at the instant of time $\underline{t}$, M_0 the equilib-
rium value of the magnetization corresponding to the static magnetic
field H_0, γ the gyromagnetic ratio, T_1 and T_2 the times of longitudinal
and transverse relaxation, respectively, and $\underline{i}$, $\underline{j}$, and $\underline{k}$ are the unit
vectors of the coordinate system. If the interactions between the mag-
netic moment of the particle and the surrounding is much stronger, un-
der conditions where the lattice is stationary (spin-spin interactions),
than the interactions with the lattice vibrations (spin-lattice inter-

actions), then the longitudinal relaxation time T_1 can be identified with the spin-lattice relaxation time τ, and the transverse relaxation time T_2 can be called the spin-spin relaxation time. If the spin-lattice interactions are stronger than the spin-spin interactions, then both the longitudinal and the transverse relaxation times are determined by the spin-lattice interactions, and therefore $T_1 = T_2 = \tau$.

Solution of (5.1) under stationary conditions leads to the following expressions for the real and imaginary parts of the paramagnetic susceptibility:

$$
\left.
\begin{aligned}
\chi' &= \frac{1}{2}\chi_0 \nu_0 T_2 \frac{\pi^2 T_2 (\nu_0 - \nu)}{1 + 4\pi^2 T_2^2 (\nu_0 - \nu)^2 + \frac{1}{4}\gamma^2 H_r^2 T_1 T_2}, \\
\chi'' &= \frac{1}{2}\chi_0 \nu_0 T_2 \frac{2\pi}{1 + 4\pi^2 T_2^2 (\nu_0 - \nu)^2 + \frac{1}{4}\gamma^2 H_r^2 T_1 T_2}.
\end{aligned}
\right\}
\qquad (5.2)
$$

In most cases the observation of the electron paramagnetic resonance is carried out under such conditions that the saturation factor is small ($1/4\gamma^2 H_r^2 T_1 T_2 \ll 1$) and can be neglected. It must be borne in mind that in formulas (5.2) we take into account only the component of the alternating magnetic field which is circularly polarized in the direction of the Larmor precession. The values of χ' and χ'' depend therefore on the sign of the static magnetic field and consequently on the sign of ν_0. It follows from (5.2) also that $\chi'' = 0$ if $\nu_0 = 0$. This is of course incorrect, since absorption exists also in the absence of a static magnetic field. This shortcoming was eliminated by Garsten [2], who obtained the following formulas for a linearly polarized wave:

$$
\left.
\begin{aligned}
\chi' &= \frac{1}{2}\chi_0 \left[\frac{1 + 4\pi^2 \nu_0 (\nu - \nu_0) T_2^2}{1 + 4\pi^2 (\nu - \nu_0)^2 T_2^2} + \frac{1 - 4\pi^2 \nu_0 (\nu + \nu_0) T_2^2}{1 + 4\pi^2 (\nu + \nu_0)^2 T_2^2} \right], \\
\chi'' &= \frac{1}{2}\chi_0 \nu T_2 \left[\frac{4\pi^2}{1 + 4\pi^2 (\nu - \nu_0)^2 T_2^2} + \frac{4\pi^2}{1 + 4\pi^2 (\nu + \nu_0)^2 T_2^2} \right].
\end{aligned}
\right\}
\qquad (5.3)
$$

We note that these expressions coincide with the known dispersion formulas of Van Vleck and Weisskopf [3].

Shaposhnikov [4] developed a thermodynamic method of investigating

relaxation phenomena. In considering paramagnetic resonance [5], he arrived at the formulas of Van Vleck and Weisskopf by solving the difference equations for the magnetization of a paramagnet, derived thermodynamically by assuming the existence of a spin system that interacts weakly with the vibrations of the lattice. Skrotskiy and Kurbatov [6], following the Shaposhnikov method, presented a general thermodynamic theory of relaxation and resonance phenomena in two spin systems. Systems of this type are frequently encountered among paramagnets, for many substances contain two sorts of magnetic particles.

Wangsness and Bloch [7] developed a statistical quantum theory for dynamic phenomena in paramagnets, starting out from the equation of motion of a corresponding statistical operator. It turned out that Bloch's phenomenological equation (5.1) is valid if there are no spin-spin interactions and if the paramagnetism is of pure spin nature (there are no splittings of the energy spin levels by electric fields). Thus, Bloch's phenomenological equation (as well as its various modifications) is applicable in a rather limited region. Nevertheless, it is used quite extensively because it gives a qualitative explanation of various aspects of the phenomenon of paramagnetic resonance: 1) it follows from the equation that the form of the resonance line is determined by the time $T_2 = \tau'$ and is independent of $T_1 = \tau$ if the spin-spin interactions are stronger than the spin-lattice interactions, and conversely the line shape is determined by the time $T_2 = T_1 = \tau$ and is independent of the spin-spin interactions if they are weaker than the spin-lattice interactions; 2) the equation makes it possible to account for the dependence of the line shape on the intensity of the alternating magnetic field which is capable of producing "saturation"; 3) the equation makes it possible to analyze quantitatively various transients in radio devices containing paramagnets.

The difficulties in constructing a microscopic quantum theory of the processes that determine the paramagnetic resonance line shape make it necessary to consider two extreme cases: either the spin-spin interactions are much stronger than the spin-lattice ones, or are much weaker. Because of this it is possible to assume that in the former case we deal with interactions in a system of magnetic particles that are in adiabatic conditions, and that there is no energy exchange with the lattice vibrations (or with the Brownian movement of the particles in a liquid). In the second case it is usually assumed that the magnetic particles are isolated from one another and each interacts individually with the lattice vibrations. In the sections that follow we shall discuss the theoretical and experimental investigations of spin-spin and spin-lattice interactions in ionic crystals and in their liquid solutions. In addition, we shall consider the theory of acoustic paramagnetic resonance, a phenomenon whose study can yield valuable information on spin-lattice interactions.

§5.2. Spin-Spin Interactions

1. If two neighboring magnetic atoms are at a distance $\underline{r}$ from each other, then each Zeeman energy level will be broadened by dipole interaction by an amount $\sim h/\beta^2 r$. This can be visualized in the following fashion. Each atom is acted upon not only by the external magnetic field H_0 but also by a local field H_{lok}, produced by the neighboring particles. The resonance condition therefore assumes the form $h\nu = = g\beta(H_0 + H_{lok})$. Since the average scatter of the possible values of H_{lok} is of the order of β/r^3, it is clear that we obtain for the width of the resonant line $\Delta\nu$ the value given above.

If all the magnetic particles are identical, then in addition to the "magnetostatic" broadening mechanism which we have already considered, there is also a second broadening mechanism, a "dynamic" one.

Let us consider two precessing dipoles with oppositely directed moments. Each of these produces at the location of the other an alternating field of resonant frequency, under the influence of which the moments can exchange orientations, for the total energy is conserved in this case. The limitation on the lifetime of each particle at a definite Zeeman energy level leads to a broadening, which again, in accordance with the uncertainty relation, has a value $\sim h/\beta^2 r^{-3}$.

The computation methods developed to date make it possible to calculate the moments of the resonance absorption curve. By k-th moment of an absorption line is meant the quantity

$$M_k = \int (\nu - \nu_0)^k g(\nu)\, d\nu. \tag{5.4}$$

If the paramagnetic resonance line has a Gaussian shape (1.20), then at $M_2 = \sigma^2$, $M_4 = 3\sigma^4$. If the line shape is Lorentzian (1.21), then in order for the integrals M_k to converge for positive k, the $g(\nu)$ curve must be cut off. If we assume that the function $g(\nu) = 0$ when $M_2 = \alpha\Delta\nu/\pi$, $M_4 = \alpha^3\Delta\nu/3\pi$, then $|\nu - \nu_0| \geq \alpha$.

This method was first used by Waller [8], and then by Broer [9] to estimate the magnitude of the spin-spin interaction. An analysis of the paramagnetic resonance absorption line shape by the method of moments was carried out by Van Vleck [10]. Van Vleck's theory is based on the following assumptions: a) the particle magnetism is of the pure spin type; b) there is no paramagnetism; c) the frequency of the oscillating field is so high that the Zeeman energy is much larger than the average energy of the spin-spin interaction of the neighboring particles; d) the exchange forces are isotropic; e) the temperature is so high that all the Zeeman levels are equally populated.

The Hamiltonian of the spin system contains the Zeeman energy as well as the dipole-dipole and exchange interactions:

$$\mathcal{H}' = \mathcal{H}'_{\text{зеем}} + \mathcal{H}_{\text{дип}} + \mathcal{H}_{\text{обм}},\tag{5.5}$$

where

$$\mathcal{H}_{\text{зеем}} = g\beta H_0 \sum_j \hat{S}_{zj},\tag{5.6}$$

$$\mathcal{H}_{\text{дип}} = g^2\beta^2 \sum_{\substack{j,k \\ j < k}} [r_{jk}^{-3}(\hat{S}_j\hat{S}_k) - 3r_{jk}^{-5}(r_{jk}\hat{S}_j)(r_{jk}\hat{S}_k)],\tag{5.7}$$

$$\mathcal{H}_{\text{обм}} = \sum_{j<k}' \tilde{A}_{jk}\hat{S}_j\hat{S}_k.\tag{5.8}$$

Here $\hat{S}_{zj}$ denotes the z-th component of the vector matrix of the spin momentum of the j-th atom, r_{jk} is the distance between the j-th and the k-th atoms, $\tilde{A}_{jk} = 2Z^2 I_{jk}$, where Z is the number of electrons in the unfilled atomic shell, and I_{jk} is the ordinary exchange integral. It is convenient to represent the dipole interaction matrix in the form

$$\left.\begin{aligned}
\mathcal{H}_{\text{дип}} &= \hat{A} + \hat{B} + \hat{C} + \hat{D} + \hat{E} + \hat{F} = g^2\beta^2 \sum r_{jk}^{-3} \times \\
&\times (\hat{a}_{jk} + \hat{b}_{jk} + \hat{c}_{jk} + \hat{d}_{jk} + \hat{e}_{jk} + \hat{f}_{jk}), \\
\hat{a}_{jk} &= (1 - 3\cos^2\vartheta_{jk})\hat{S}_{zj}\hat{S}_{zk}, \\
\hat{b}_{jk} &= -\frac{1}{4}(1 - 3\cos^2\vartheta_{jk})(\hat{S}_{k+}\hat{S}_{j-} + \hat{S}_{k-}\hat{S}_{j+}), \\
\hat{c}_{jk} &= \hat{d}_{jk}^* = -\frac{3}{2}\sin\vartheta_{jk}\cos\vartheta_{jk}e^{-i\varphi_{jk}}(\hat{S}_{j+}\hat{S}_{zk} + \hat{S}_{j-}\hat{S}_{zk}), \\
\hat{e}_{jk} &= \hat{f}_{jk}^* = -\frac{3}{4}\sin^2\vartheta_{jk}e^{-2i\varphi_{jk}}\hat{S}_{j+}\hat{S}_{k+},
\end{aligned}\right\}\tag{5.9}$$

where $\hat{S}_\pm = \hat{S}_x \pm i\hat{S}_y$ and ϑ_{jk} is the angle between $\vec{H}_0$ and $\vec{r}_{jk}$.

We choose a representation in which the matrices S_{zj} are diagonal; their eigenvalues are denoted by m_j. The magnetic quantum number of the entire spin system will be $M = \sum_j m_j$. If we neglect the interactions between the spins, then we obtain a system of equidistant energy levels $E_M = g\beta H_0 M$, which will be strongly degenerate, since there exists a tremendous number of combinations of values of m_j which lead to one and the same value of M. The eigenfunctions $\hat{H}_{\text{zeem}}$ will be denoted $\Psi_{M; m_1, m_2, \ldots}$. If $\hat{H}_{\text{dip}} + \hat{H}_{\text{obm}}$ are considered as a perturbation and the ordinary perturbation method is used for the degenerate case, then to solve the problem in the first approximation we must calculate the

perturbation matrix elements with the aid of ψ functions that pertain to only one considered energy level E_M. We can readily see that the application of individual parts of the perturbation operator to ψ_M; m_1, m_2, ... will give new ψ functions for which the values of M, m_j, and m_k will change in the following manner:

$$
\begin{aligned}
&\hat{a}_{jk}: && \Delta M = 0, \ \Delta m_j = \pm 0, \ \Delta m_k = 0; \\
&\hat{d}_{jk}: && \Delta M = -1, \ \Delta m_j = \left\{ \begin{matrix} 0 \\ -1 \end{matrix} \right., \ \Delta m_k = \left\{ \begin{matrix} -1 \\ 0 \end{matrix} \right.; \\
&\hat{b}_{jk}: && \Delta M = 0, \ \Delta m_j = \pm 1, \ \Delta m_k = \mp 1; \\
&\hat{e}_{jk}: && \Delta M = 2, \ \Delta m_j = 1, \ \Delta m_k = 1; \\
&\hat{c}_{jk}: && \Delta M = 1, \ \Delta m_j = \left\{ \begin{matrix} 0 \\ 1 \end{matrix} \right., \ \Delta m_k = \left\{ \begin{matrix} 1 \\ 0 \end{matrix} \right.; \\
&\hat{f}_{jk}: && \Delta M = -2, \ \Delta m_j = -1, \ \Delta m_k = -1.
\end{aligned}
\qquad (5.10)
$$

The operator $\hat{H}_{obm}$ acts like $\hat{b}_{jk}$. From (5.10) and (5.8) it is seen that the nonvanishing matrix elements pertaining to the level E_M contain only the matrices $\hat{A}$, $\hat{B}$, and $\hat{H}_{obm}$.

The probability of transition between two Zeeman levels E_M and $E_{M'}$ under the influence of a radio frequency field directed along the $\underline{x}$ axis will obviously be proportional to $|\langle M| \hat{S}_x |M'\rangle|^2$. Since the matrix element of the operator $\hat{S}_x = \Sigma \hat{S}_{xj}$ is in first approximation different from zero, provided only $M' = M \pm 1$, then only one bright absorption line can appear, with the Larmor frequency ν_0. In the next approximation we must also take into consideration the operators $\hat{C}$, $\hat{D}$, $\hat{E}$, and $\hat{F}$ in order to calculate the perturbation energy, and consequently the wave functions corresponding to the energy level E_M assume the form $\psi_M + \varepsilon_1 \psi_{M-1} + \varepsilon_2 \psi_{M+1} + \varepsilon_3 \psi_{M+2} + \varepsilon_4 \psi_{M-2}$, where the ε_i are of the order of $\beta^2 r^{-3}/g\beta H_0$. It is clear that in the second approximation transitions are also possible from the level M to the levels $M' = M$, $M \pm 2$, and $M \pm 3$. Thus, satellites at frequencies 0, $2\nu_0$, and $3\nu_0$ appear at the fundamental line of frequency ν_0. The intensity of the satellites will be related to the intensity of the fundamental line

approximately as ε_1^2:1. If still higher approximations are taken into account, then weak satellites at even higher frequencies can appear.

2. When considering the principal resonance line, we must cut off the Hamiltonian (5.5) by discarding from it the terms $\hat{C}$, $\hat{D}$, $\hat{E}$, and $\hat{F}$, which do not commute with the principal part of the Hamiltonian H_{zeem}. The eigenvalues of the cut-off Hamiltonian H^+ will be denoted by H_n, and the transition frequencies by $\nu_{nn'}$. Then, by definition, we have for the mean square of the absorption-line frequency

$$\langle \nu^2 \rangle = \frac{\sum_{n,n'} \{\nu_{nn'}^2 |\langle n'| \hat{S}_x |n\rangle|^2\}}{\sum_{n,n'} |\langle n'| \hat{S}_x |n\rangle|^2}. \qquad (5.11)$$

This expression can be represented in the form

$$\langle \nu^2 \rangle = -\frac{Sp(\mathscr{H}^+ \hat{S}_x - \hat{S}_x \mathscr{H}^+)^2}{h^2 Sp(\hat{S}_x)^2}. \qquad (5.12)$$

It would be quite hopeless to attempt to calculate the eigenvalues of H_n, for their number is comparable with the number of atoms in the crystal. The great advantage of formula (5.12) lies in the fact that it contains only the diagonal sums, the invariance of which makes it possible to carry out the calculations in an arbitrary representation. The simplest obviously will be a representation in which the spatial quantization is carried out for each spin separately. After calculating the traces of the matrices contained in (5.12), we find that the second moment of the absorption line is

$$M_2 = \left\langle \left(\nu - \frac{g\beta H_0}{h}\right)^2 \right\rangle = \frac{3}{4} g^4 \beta^4 h^{-2} S(S+1) \sum_k r_{1k}^6 \cdot (3\cos^2\theta_{1k} - 1)^2, \qquad (5.13)$$

where $\underline{k}$ numbers all the magnetic particles of the lattice, and the index 1 pertains to a certain atom which is chosen as the reference point for the calculations. For a crystalline powder we have

$$M_2 = \frac{3}{5} g^4 \beta^4 h^{-2} S(S+1) \sum_k r_{1k}^6. \qquad (5.14)$$

- 211 -

For a simple cubic lattice, with a constant equal to $\underline{d}$, we obtain

$$\sum_k r_{1k}^{-6} = 8.5\, d^{-6}. \qquad (5.15)$$

If the quantum mechanical calculations are replaced by the magnetostatic calculations and the influence of the broadening mechanism which we have called dynamic is thereby discarded, then we obtain for M_2 the same expression (5.13), reduced by a factor 9/4. This reduced value should be used only when we deal with the broadening due to the interaction between dipoles of different sorts, for example of paramagnetic atoms with nuclear spins of surrounding diamagnetic particles. Thus, if we have magnetic particles of two sorts with spins S and S' and spectroscopic-splitting factors $\underline{g}$ and g', then the second moment of the resonance line produced by the particles of the first sort will consist of (5.13) and the following expression:

$$M_2' = \frac{1}{3} g'^{4} \beta^{4} \hbar^{-2} S' (S' + 1) \sum_j r_{1j}^{-6} (3\cos^2 \theta_{1j} - 1)^2, \qquad (5.16)$$

where the index 1 pertains to some particle of the first sort, which is chosen to be the reference for the calculations, and $\underline{j}$ numbers the particles of the second sort. If g' = g, then these formulas are not suitable, for now the resonance lines produced by the particles of the different sorts coalesce into one. This case was considered in [11].

Van Vleck also calculated the second moment $\widetilde{M}_2$ of the absorption curve which includes not only the fundamental line, but also the supplementary lines at frequencies 0, $2g\beta H_0$, and $3g\beta H_0$. It turned out that $\widetilde{M}_2 = 10/3 M_2$, and that this relation, as was already pointed out by Broer [9], is independent of H_0, since the heights of the supplementary absorption curves are inversely proportional to H_0, whereas the frequencies are approximately linear in H_0.

Let us turn to an examination of the fundamental paramagnetic res-

onance line. It is seen from (5.13) that the isotropic exchange forces do not affect the value of the second moment of the absorption line at all. Therefore, in order to evaluate the influence of the exchange forces on the line shape it is necessary to make use of higher moments. The fourth moment was calculated in the same paper of Van Vleck, while the sixth moment was calculated later by Glebashev [12]. We note that the odd moments vanish and consequently the absorption line is symmetrical. Calculations have shown that in case of pure dipole interactions the ratios of the moments are close to the values obtained for the Gaussian function, namely: $M_6^{1/6}:M_4^{1/4}:M_2^{1/2} = 1.57:1.32:1$. If the exchange interactions predominate over the dipole ones, then $M_4^{1/4}$: $:M_2^{1/2} \gg 1$ and consequently the line assumes a Lorentzian form. Insofar as the area of the absorption curve and its second moment do not contain exchange integrals, we can conclude that the absorption line becomes narrower in the center and becomes accordingly less steep on the edges.

This narrowing down of the lines under the influence of the exchange forces, which was noted already in [13, 14] is the consequence of the assumptions on which the Van Vleck theory is based, and which cannot be accepted in many cases for real crystals.

The theory of dipole broadening as developed by Van Vleck was extended by Kittel and Abrahams [15] to the case of solid paramagnetic solutions. It was found that if the concentration of the paramagnetic atoms is $f > 0.1$, then the line retains a Gaussian form and its width is proportional to $\sqrt{f}$; on the other hand, if $f < 0.01$, then the line shape becomes Lorentzian, and the width is proportional to f. Glebashev [16] generalized these calculations, taking also account of the influence of exchange isotropic forces.

3. The assumption that the paramagnetism has a purely spin nature

- 213 -

greatly limits the applicability of Van Vleck's theory. In fact, if the effective spin is $S' > 1/2$ then there are always small splittings of the spin levels by the electric field of the crystal. On the other hand, if $S' = 1/2$, then the influence of the crystalline field is still felt and the g factor becomes anisotropic.

Pryce and Stevens [17] generalized Van Vleck's theory and pointed out methods of calculating the moments of curves for a great variety of cases. The general calculation method consists in the following. The Hamiltonian of the spin system is represented in the form

$$\mathscr{H} = \mathscr{H}_0 + \hat{W},$$

(5.17)

where the principal part of the Hamiltonian $\hat{H}_0$ determines the energy levels the transitions between which produce individual lines of the paramagnetic resonance spectrum, while the perturbation W serves as the cause of broadening of these lines. Expressions of the type (5.12) are then set up for the calculation of the moments of the line. In order to separate only the absorption line of interest to us, the operators $\hat{W}$ and $\hat{S}_x$ are so cut off as to make the cut-off operator $\tilde{W}$ commute with $\hat{H}_0$, and the cut-off operator $\tilde{S}_x$ contains only nondiagonal matrix elements, which ensure the necessary quantum transitions. The matrices $\tilde{W}$ and $\tilde{S}_x$ are cut off either with the aid of the corresponding projection matrices, as was proposed by Pryce and Stevens [17], or by directly crossing out the unneeded matrix elements.

The following cases are considered in [17]: 1) there is one sort of particles, all the energy intervals of which are different in the unperturbed state; 2) the particles in the unperturbed state have coinciding or nearly degenerate levels; 3) there are two sorts of particles; 4) there exists a hyperfine structure of the energy levels of the particles. In addition, Pryce and Stevens considered the question of the dependence of the absorption line width on the temperature and

- 214 -

on the form of the crystal. The perturbation usually has a two-particle character and can be represented in the form $\hat{W} = \sum\limits_{i,j} \hat{W}_{ij}$. The resulting second moment, expanded in powers of $1/kT$, is

$$M_2 = a_0 \sum_{i,j} |\langle W_{ij} \rangle|^2 + \frac{a_1}{kT} \sum_{i,j} |\langle W_{ij} \rangle| + \ldots , \qquad (5.18)$$

where a_0 and a_1 are certain quantities independent of W and T. By virtue of the fact that W^2_{jk} decreases at least as fast as $1/r^6_{jk}$, we can carry out for the temperature-independent part of the moment M_2 the following transformation:

$$\sideset{}{'}\sum_{i,j} |\langle W_{ij} \rangle|^2 = N \sum_j |\langle W_{ij} \rangle|^2. \qquad (5.19)$$

It is immaterial whether the particle $\underline{i}$, chosen as the reference for the calculations, is located at the center of the crystal or near its boundary. The transformation (5.19) cannot be applied to that part of the moment which is proportional to $1/kT$, since W_{ij} decreases slowly with increasing r_{ij}. As a result the paramagnetic resonance line should shift near the Curie point, and the line width will depend on the temperature and on the form of the crystal. From the microscopic point of view it can be stated that the factor of demagnetization of the investigated specimen becomes essential near the Curie point. Glebashev [18] made detailed calculations of the dependence of the moments of the resonance line on the temperature. At sufficiently low temperatures the paramagnetic resonance lines will become asymmetrical and their width will change.

4. Ishiguro, Kambe, and Usui [19] calculated M_2 for nickel fluorosilicate, which has only one magnetic ion per crystal cell. The principal Hamiltonian has the form

$$\mathcal{H}_0 = \sum_i (g\beta H_v \hat{S}_i + D\hat{S}^2_{zi}). \qquad (5.20)$$

The spin level scheme for the individual particle was shown in Fig. 3.2. If the field H_0 is parallel to the hexagonal axis of the crystal (the Z axis) we have for both lines $-1 \rightarrow 0$ and $0 \rightarrow 1$

$$h^2 M_2 = \sum{}' \left[\tilde{A}_{jk}^2 + \frac{5}{4} \frac{g^4 \beta^4}{r_{jk}^6} (3 \cos^2 \theta_{jk} - 1)^2 \right]. \tag{5.21}$$

For the case $H_0 \perp Z$, this same formula will hold true if we assume $g \beta H_0 \gg D$. Calculation of the lattice sums yields

$$h^2 M_2 = 6 \tilde{A}^2 + \frac{3{,}13 g^4 \beta^4}{d^6}, \ H_0 \parallel Z; \ h^2 M_2 = 6 \tilde{A}^2 + \frac{6{,}50 g^4 \beta^4}{d^6}, \ H_0 \perp Z. \tag{5.22}$$

From a comparison with experiment [20] we can estimate the value of the exchange coefficient $|\tilde{A}| = 0.027 \text{ cm}^{-1}$.

Griffiths and Owen [21] observed a discrepancy between their measurements of the line shape of Tutton's salts of nickel and the theory of Ishiguro, Kambe, and Usui. Stevens [22] made detailed calculations and showed that the discrepancies are due, first, to the presence of two nonequivalent paramagnetic ions per crystal cell in Tutton's salts, and second to the more complicated form of the spin Hamiltonian, which contains the additional term $E(\hat{S}_x^2 - \hat{S}_y^2)$. From a comparison with the experimental data, Stevens estimated the exchange coefficient at $\tilde{A} = -0.026 \text{ cm}^{-1}$.

Kambe and Ollom [23] calculated the second moment of the central paramagnetic resonance line (transition $-1/2 \rightarrow 1/2$) for half-integer particle spin S. Because of the action of the crystalline field, other transitions give lines at different frequencies and are not considered in this work.

a) If all the particles are equivalent, then

$$h^2 M_2 = \left[\frac{S(S+1)}{3} + \frac{2S^2(S+1)^2 - 3S(S+1) + \frac{1}{8}}{2(2S+1)} \right] \sum{}'_k \tilde{A}_{jk}^2 +$$

$$+ \left[-\frac{2}{3} S(S+1) + \frac{2S^2(S+1)^2 + \frac{7}{8}}{2(2S+1)} \right] \sum{}'_k \tilde{A}_{jk} \frac{g^2 \beta^2}{r_{jk}^3} \times$$

$$\times (3\cos^2\theta_{jk}-1) + \left[\frac{S(S+1)}{3} + \frac{\frac{1}{2}S^2(S+1)^2 + \frac{3}{4}S(S+1) + \frac{13}{32}}{2(2S+1)}\right] \times$$

$$\times \sum_{k} \frac{g^2\beta^4}{r_{jk}^6}(3\cos^2\theta_{jk}-1)^2. \tag{5.23}$$

b) If there are particles of a different sort with g-factor g' and spin S', they make an additional contribution:

$$h^2 M_2' = \frac{1}{3}S'(S'+1)\sum_{k'}{}' \left[\tilde{A}_{jk'} + \frac{gg'\beta^2}{r_{jk'}^3}(1-3\cos^2\theta_{jk'})\right]^2. \tag{5.24}$$

c) If there are several nonequivalent particles of one and the same sort in the crystal cell, then the interaction between the considered type of particles with the other nonequivalent particles gives an additional contribution to the second moment:

$$h^2 M_2'' = \left[\frac{1}{3}S(S+1) - \frac{1}{4}(2S+1) + \frac{(2S+1)^2}{32}\right]\sum_{k'}\tilde{A}_{jk'} +$$

$$+ \left[-\frac{2}{3}S(S+1) + \frac{1}{8}(2S+1) + \frac{(2S+1)^2}{32}\right]\sum_{k'}\tilde{A}_{jk'}\frac{g'^2\beta^2}{r_{jk'}^3} \times$$

$$\times (3\cos^2\theta_{jk'}-1) + \left[\frac{1}{3}S(S+1) + \frac{1}{8}(2S+1) + \frac{(2S+1)^2}{128}\right] \times$$

$$\times \sum_{k'}\frac{g'^2\beta^4}{r_{jk'}^6}(3\cos^2\theta_{jk'}-1)^2. \tag{5.25}$$

If we denote the second moment, calculated by formula (5.13), which is valid in the absence of crystalline splittings, by M^*_2, then we obtain for purely dipole interactions:

Spin	$\frac{M_2}{M_2^*}$	$\frac{M_2''}{M_2^*}$
$\frac{1}{2}$	1	1
$\frac{3}{2}$	$\frac{9}{10}$	$\frac{4}{5}$
$\frac{5}{2}$	$\frac{107}{105}$	$\frac{257}{315}$
$\frac{7}{2}$	$\frac{881}{756}$	$\frac{16}{189}$

Abragam and Kambe [24] calculated the dipole broadening of the resonance line due to transitions between energy sublevels arising in

the electric field of the crystal, if the external magnetic field is equal to zero. The following assumptions were made there: a) the spin is $S = 1$ or $3/2$; b) the crystalline field has axial symmetry; c) the symmetry axis is the same for all particles. The following expressions were obtained for the second moment of the resonance lines:

$$S = 1: \quad M_2 = \frac{g^{\prime 3 \prime}}{4 h^3} \sum_{k}' r_{jk}^{-6} \times$$
$$\times [5(1 - 3\gamma_{jk}^2) + (1 - \gamma_{jk}^2)^2 - 2(1 - 3\gamma_{jk}^2)(\alpha_{jk}^2 - \beta_{jk}^2)],$$
$$S = \frac{3}{2}: \quad M_2 = \frac{g^{\prime 3 \prime}}{96 h^3} \sum_{k}' r_{jk}^{-6} \times$$
$$\times [207(1 - 3\gamma_{jk}^2)^2 + 1512\,\gamma_{jk}^2(1 - 3\gamma_{jk}^2) + 459(1 - \gamma_{jk}^2)^2 -$$
$$- 108(1 - 3\gamma_{jk}^2)(\alpha_{jk}^2 - \beta_{jk}^2)], \qquad (5.26)$$

where α_{jk}, β_{jk}, and γ_{jk} are the direction cosines of the radius vector $\vec{r}_{jk}$, if the Z axis is taken to be the symmetry axis of the crystalline field. For a cubic lattice with an electric field parallel to one of the axes

$$S = 1: \quad M_2 = 28.4 \frac{g^{\prime 3 \prime}}{h^3 d^6}; \quad S = \frac{3}{2}: \quad M_2 = 60.0 \frac{g^{\prime 3 \prime}}{h^3 d^6}. \qquad (5.27)$$

Calculations were also made for the broadening due to the presence of "nonresonant" particles (particles of the second sort, not participating in the production of the resonance line).

5. In all the investigations which we have just considered, where the existence of energy splittings due to the electric field of the crystals was taken into account, it was assumed that the action of the crystalline field is much stronger than the dipole and exchange interactions. If this is not so, then the appearance of the resonance lines becomes possible if the external magnetic field causes splittings that are much larger than the crystalline ones. In this case the Hamiltonian term that takes into account the influence of the crystalline field should be transferred from the main part $\hat{H}_0$ into the "perturbed" part $\hat{W}$. The crystalline field will participate in the broadening of the resonance line along with the dipole and the exchange interactions. This

case was considered by Berson [25], who proposed that the action of the crystalline field can be represented by an axially-symmetrical Hamiltonian $ES_z^2 + FS_z^4$. Calculations have shown that the second moment is equal to

$$
\begin{aligned}
h^2 M_2 = {} & \tfrac{3}{4} g^4 \beta^4 S(S+1) \sum_k r_{ik}^{-6} (3 \cos^2 \vartheta_{ik} - 1) + \\
& + \tfrac{1}{5} [4S(S+1) - 3] E^2 + \tfrac{1}{35} [48 S^2(S+1)^2 - 76S(S+1) + 30] EF + \\
& + \tfrac{1}{105} [80 S^3(S+1)^3 - 268 S^2(S+1)^2 + 336 S(S+1) - 135] F^2. \quad (5.28)
\end{aligned}
$$

Here, as in the case considered by Van Vleck, the second moment is independent of the isotropic exchange interactions.

6. In many crystals the paramagnetic ions of which contain an odd number of electrons, the ground level of these ions is a Kramers doublet. Among substances of this type are the investigated salts of rare-earth elements, many salts of the iron-group elements, etc. In spite of the fact that in all these cases the ground level can be characterized by an effective spin $S' = 1/2$, nonetheless the Van Vleck theory is unsuitable here, too. The electric field of the crystal cannot split a level with $S' = 1/2$, but it can give rise to a strong anisotropy of the g factor.

Kopvillem [26] calculated the second moment of the resonance line for this case under the following assumptions: a) the crystal temperature is so low that only the lowest Kramers doublet is populated; b) all the paramagnetic ions are equivalent and consequently have the same g-tensor. Since the spin-lattice interactions are for the most part very strong in paramagnets of this type and the observations of paramagnetic resonance must be made at low temperatures, the dependence of the line shape on the temperature can therefore be of importance and was consequently taken into account in the calculations of the moment M_2.

The calculations have shown the following: a) the line width de-

- 219 -

pends on the direction of the static magnetic field; b) the isotropic exchange forces influence the value of M_2, and consequently the exchange interactions generally speaking increase the width of the resonance line; this broadening is different for different magnetic field directions; c) the line width due to the dipole interactions decreases with decreasing temperature. The magnitude of the second moment due to the dipole interactions was found to be

$$
\left.
\begin{aligned}
M_2 &= \frac{\beta^4}{8(1+e^m)\hbar^2} \sum_{j}' \Big\{ (B_{ij}^{(x)} + B_{ij}^{(y)})^2 e^m + B_{ij}^{(z)2} \times \\
&\times \left(\frac{3}{2} + 2e^m + \frac{1}{2}e^{2m} \right) - B_{ij}^{(z)}(B_{ij}^{(x)} + B_{ij}^{(y)})(1 + 3e^m) \Big\}, \\
m &= -\frac{g_{zz}\beta H_0}{kT}, \quad B_{ij}^{(\alpha)} = g_{\alpha\alpha}^2 r_{ij}^{-3}(1 - 3\cos^2\vartheta_{ij}^{(\alpha)}), \quad \alpha = x, y, z,
\end{aligned}
\right\}
\tag{5.29}
$$

where $\underline{x}$, $\underline{y}$, and $\underline{z}$ are the principal axes of the $\underline{g}$ tensor, $\vartheta_{ij}^{(\alpha)}$ is the angle between r_{ij} and the α axis. Calculation of the lattice sums gives, for example for ethyl sulfates of rare earths and for a field H_0 parallel to the crystal symmetry axis,

$$
\left.
\begin{aligned}
M_2 &= 66.73\, g_\parallel^4 \beta^2 [(1 + e^m) a^6]^{-1} [e^m(x^4 + 3x^2 + 2) + \\
&\quad + 0.5\, e^{2m} + 1.5 + x^2], \\
x &= \frac{g_\perp}{g_\parallel},
\end{aligned}
\right\}
\tag{5.30}
$$

where $\underline{a}$ is the larger side of the ethyl sulfate elementary cell. Kopvillem's calculations were further developed in [114].

7. If the exchange interactions are sufficiently strong, they influence not only the paramagnetic resonance line widths, but can also change the line positions. One such case was experimentally investigated by Bagley and Griffiths [27] in the salt $CuSO_4 \cdot 5H_2O$. The crystal cell of this substance of this substance contains two ions with different magnetic axes. Two resonance lines of approximate width 115 oersted were therefore observed with the aid of a radio frequency field at a wavelength $\lambda = 0.85$ cm. Were we to have $\lambda = 3$ cm, then these lines would be approximately 500 oersted apart, but experience has

shown that they coalesce into a single line. A theoretical explanation of this fact was presented by Pryce [28]. The Hamiltonian of the spin system has the form

$$\mathscr{H} = \beta \hat{S}' g' H_0 + \beta \hat{S}'' g'' H_0 + \mathscr{H}_{\text{обм}},\qquad(5.31)$$

where S' and S" are the total spins of all particles of the first and second kind, and g' and g" are the corresponding g tensors. For simplicity no account was taken here of the dipole interaction. Formula (5.31) can be represented in the form

$$\left.\begin{array}{l}\mathscr{H} = \mathscr{H}_0 + \hat{W}, \\[4pt] \mathscr{H}_0 = \dfrac{\beta}{2}(\hat{S}' + \hat{S}'')(g' + g'')H_0 + \mathscr{H}_{\text{обм}}, \\[4pt] \hat{W} = \dfrac{\beta}{2}(S' - S'')(g' - g'')H_0. \end{array}\right\}\qquad(5.31a)$$

Were there no "perturbation" $\hat{W}$, then, in view of the fact that both terms of $\hat{H}_0$ commute with each other, a transverse radio frequency field should give rise to transitions between states, for which the components of the total spin S' + S" in the direction (g' + g")H_0 differ by unity, and the exchange energy is conserved. The result should be one sharp absorption line. The perturbation W changes the intervals between the unity levels, the transitions between which are allowed by the selection rules. The line broadens. In addition, the perturbation causes overlapping of the wave functions pertaining to different exchange-energy levels, and consequently the selection rules change together with the line shape. At higher frequencies, at large fields H_0, the value of $\hat{W}$ can no longer be regarded as a perturbation, for it becomes comparable with the exchange energy. It is easy to imagine that two absorption peaks can appear under such conditions.

A second example of the influence of exchange interactions on the form of the spectrum is the reduction in the hyperfine splittings of the resonance lines, occurring under the influence of the exchange forces. Assume that the interaction of the magnetic moments of the nu-

cleus and of the electron shell is characterized by an isotropic hyperfine structure constant A. If we disregard the nuclear spin, we can assume for simplicity that all the paramagnetic atoms precess about the external magnetic field with one and the same Larmor frequency. Because of the interaction between the electron and nuclear moments, different atoms will have one of the 2I + 1 precession frequencies, which differ by small amounts on the order of A/h, with equal probability. Let the period of the exchange be $\tau = h/J$ (J is the exchange integral). If $\tau \gg h/A$, then the precession will change during the course of the exchange by an amount ~A/h; if on the other hand $\tau \leq h/A$, then all these changes will average out and the individual peaks of the hyperfine structure will coalesce into a single line. Consequently, the reduction in the hyperfine splitting can be expected only when $J \geq A$. These arguments can be qualitatively confirmed by the method of moments. The Hamiltonian of the spin system can be written in the form

$$\mathcal{H} = g\beta H_0 \sum_j \hat{S}_{zj} + \sum_{j,k} \tilde{A}_{jk} \hat{S}_j \hat{S}_k + A \sum_j \hat{S}_j \hat{I}_j.$$

The first term denotes here the Zeeman energy, the second the exchange interactions, and the third the magnetic interactions of the nuclei and the electrons. Calculations made by Van Viringen [29] have led to the following expressions for the second and fourth moments of the resonance line:

$$\left.\begin{aligned}
M_2 &= \frac{1}{3} h^{-2} A^2 I(I+1), \\
M_4 &= h^{-4} I(I+1) \left\{ \frac{1}{5} \left[I(I+1) - \frac{1}{3} \right] A^4 + \right. \\
&\quad \left. + \frac{2}{9} S(S+1) A^2 \sum \tilde{A}_{jk}^2 \right\}.
\end{aligned}\right\} \qquad (5.32)$$

The exchange forces do not enter into M_2, but they do increase M_4. We can conclude from this that the exchange interactions shift the absorption from the center of the spectrum to its edges. This redistribution

of the intensities of the different parts of the spectrum can occur in two ways: 1) the intervals between the hyperfine components are decreased and the absorption is increased on the curves of the entire spectrum; 2) the intervals between the hyperfine components remain unchanged, but each line becomes narrower at the center and broader at the skirts. It was shown by the method of random functions that the first possibility is realized.

8. In most cases it is possible to calculate only the second moment of the absorption line, while calculations of the higher moments are exceedingly difficult. The information obtained on the paramagnetic resonance line shape by the moment method is therefore inadequate. Anderson and Weiss [30] proposed to use the method of random functions so as to obtain more detailed information on the absorption line shapes, particularly the exchange narrowing of these lines. This idea was developed in the papers by Anderson [31], Kubo and Tomita [32], and others. Since we are unable to describe in detail the results of all these investigations, we shall stop to discuss only the principal idea and the most important applications.

The narrowing down of the resonance line under the influence of the exchange forces can be visualized as being the consequence of frequency modulation of the precessional motion of the individual magnetic dipoles. How frequency modulation acts on the width of a resonance line is best understood from the following example, which was analyzed in [33, 31]. Let us consider an oscillator which is subjected to random collisions. Let the average time interval between two collisions be τ. We assume that the oscillator has two different natural frequencies, ν_1 and ν_2. Assume that after each collision the oscillator changes its frequency, going over from ν_1 to ν_2 and back. If the oscillator "suffers from complete lack of memory" and its state prior

to collision does not influence at all the subsequent motion, then the form function is

$$g(\nu) = \frac{1}{2\pi} \left\{ \frac{\frac{1}{2\pi\tau}}{(\nu - \nu_1)^2 + \frac{1}{(2\pi\tau)^2}} + \frac{\frac{1}{2\pi\tau}}{(\nu - \nu_2)^2 + \frac{1}{(2\pi\tau)^2}} \right\}. \qquad (5.33a)$$

A more complicated form function is obtained in the case of "good memory." If only the oscillator frequency changes after the collision, while its position and velocity are conserved, then

$$g(\nu) = \frac{2}{\pi} \frac{\frac{\nu_m^2}{2\pi\tau}}{(\nu - \nu_c)^4 + \nu_m^4 + (\nu - \nu_c)^2 \left(\frac{1}{\pi^2\tau^2} - 2\nu_m^2\right)},$$

where

$$\nu_c = \frac{1}{2}(\nu_1 + \nu_2), \quad \nu_m = \frac{1}{2}(\nu_1 - \nu_2). \qquad (5.33b)$$

In the case of (5.33a), the intensity under resonant conditions is proportional to τ, and consequently both resonant lines spread out with decreasing τ, and finally, when $\tau \ll 1/2\pi\nu_m$ they merge into one broad line with resonant frequency ν_c. In the case (5.33b), if $\nu = \nu_c$, the intensity is proportional to $1/\tau$, and therefore both resonant peaks merge at sufficiently small values of τ into one line, which becomes narrower with decreasing τ. An illustration of the foregoing is seen in Fig. 5.1.

In a paramagnetic crystal the precession frequency of the magnetic moment is $\nu_0 + \nu'$, where ν_0 is determined by the externally applied static magnetic field, and ν' is determined by the internal local fields. It can be assumed that the frequencies ν' have a Gaussian distribution. We denote the mean value of $(\nu')^2$ by ν_p^2. Owing to exchange interactions, the neighboring particles will exchange frequencies, in the mean, after time intervals $1/\nu_1 \approx h/J_{1k}$. If we concentrate our attention on one particle only, we see that its precession frequency will be constantly subject to random variations. If $\nu_1 \gg \nu_p$,

- 224 -
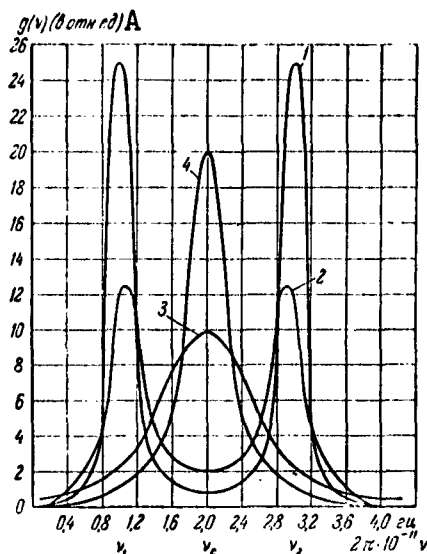
Fig. 5.1. Reduction in the width of the oscillator form function with decreasing collision time τ. It is assumed that the oscillator has alternately the frequencies ν_1 and ν_2, and retains its previous velocity and position after each collision. The curves have been drawn for different values of τ. 1) $\tau = 10^{-10}$ sec; 2) $\tau = 0.5 \cdot 10^{-10}$ sec; 3) $\tau = 10^{-11}$ sec; 4) $\tau = 0.5 \cdot 10^{-11}$ sec. A) (in relative units).

this frequency modulation can appreciably narrow down the resonant absorption line. Calculation shows that the form function of the line can be written as

$$g(\nu) = \frac{1}{2\pi} \operatorname{Re} \int_0^\infty \exp\left[-2\pi i (\nu - \nu_0) t - \nu_p^2 u\right] dt, \qquad (5.34)$$

where

$$u = \int_0^t (t - t') \exp\left(-\pi^3 \nu_i^2 t'^2\right) dt'. \qquad (5.34a)$$

The frequencies ν_p and $\underline{\nu_1}$ can be determined from the following equations:

$$\nu_p^2 = M_2, \quad 3\nu_p^4 + \frac{1}{2}\pi\nu_p^2\nu_l^2 = M_4. \qquad (5.35)$$

For a simple cubic lattice we have

$$\nu_l^2 = \frac{8.48}{3}\left(\frac{J_{lk}}{h}\right)^2 S(S+1). \qquad (5.36)$$

Inasmuch as $\nu_{\underline{1}} \gg \nu_p$, it follows from (5.34a) that

$$u = 1/2t^2, \quad \text{if } \nu - \nu_0 \gg \nu_{\underline{1}},$$
$$u = t/\nu_{\underline{1}}, \quad \text{if } \nu - \nu_0 \ll \nu_{\underline{1}}.$$

Substituting in (5.34), we obtain in the former case

$$g(\nu) = \frac{1}{\sqrt{2\pi}\nu_p}\, e^{-\frac{(\nu-\nu_0)^2}{2\nu_p^2}}, \qquad (5.37a)$$

and in the latter case

$$g(\nu) = \frac{1}{\pi}\, \frac{\frac{\nu_p^2}{\nu_l}}{(\nu-\nu_0)^2 + (\nu_p^2/\nu_l)^2}. \qquad (5.37b)$$

Thus, in the case of strong exchange interactions, the absorption line, being Lorentzian at the center, assumes on its skirts a Gaussian form, thus ensuring that its second and higher moments are finite. In place of the formula $\Delta\nu = 2.35\nu_p$ (see (1.21)), which is valid in the case of pure dipole interactions, we now have

$$\Delta\nu = 2\frac{\nu_p^2}{\nu_l}. \qquad (5.37c)$$

It must be noted that if the exchange energy is very large, so that $\nu_{\underline{1}} \gg \nu_0$, then the value of $\Delta\nu$ given by this formula should be multiplied by 10/3. The reason for it is that the cutoff of the Hamiltonian carried out in the calculation of (5.13) is no longer justified here, for the energy difference between two neighboring Zeeman levels $h\nu_0$ can be strongly modified by the exchange energy. Consequently, the alternating magnetic field of frequency $\nu = \nu_0$ can give rise not only to transitions $\Delta M = \pm 1$, but also transitions such as $\Delta M = 0, \pm 2, \pm 3$. Thus, in equating ν_p^2 to the second moment of the ab-

sorption curve, one must recognize that the principal resonance line coalesces with its satellites. Consequently,

$$\nu_p^2 = \tilde{M}_2 = \frac{10}{3} M_2.$$

If the resonant frequency ν_0 is increased enough to make $\nu_0 \gg \nu_1$, observation of the satellites becomes possible and the factor 10/3 in the formula for the width of the principal line must be discarded.

§5.3. Spin-Lattice Interactions

Before we start to consider the results of the spin-lattice interaction theory in different types of ionic paramagnetic crystals, let us dwell on some general problems.

1. Let us consider some pair of spin-system energy levels E_k and E_1 ($E_k > E_1$), the population of which is assumed to be N_k and N_1. We denote by A_{kl} the per-second probability of transition of the spin system from the level E_k to the level E_1 under the influence of the lattice vibrations. The condition for statistical equilibrium is the equation

$$N_k A_{kl} = N_l A_{lk}.$$

If a Boltzmann distribution can be assumed, it follows that

$$A_{lk} = A_{kl} e^{\frac{-(E_k - E_l)}{kT}}. \qquad (5.38)$$

We see that $A_{kl} > A_{lk}$. This circumstance plays an important role in paramagnetic resonance. Let the oscillating magnetic field of resonant frequency give rise to transitions between the levels E_k and E_1; the probability of such transitions per second will be denoted by p_{kl} (see formulas (1.3) and (1.4)). Under stationary conditions we have

$$N_k \left(\sum_j {}' A_{kj} + p_{kl} \right) = \sum_j {}' N_j A_{jk} + N_l p_{lk}. * \qquad (5.39)$$

We can assume with great degree of accuracy that $p_{kl} = p_{lk}$. If in addition $A_{kl} = A_{lk}$, then $N_k = N_1$ and no paramagnetic resonance is pos-

sible. The difference $A_{kl} - A_{lk}$ decreases with increasing temperature of the paramagnet, and consequently the resonant paramagnetic absorption decreases.

We have seen in §5.1 that under certain conditions the paramagnetic resonance line width is determined by the spin-lattice paramagnetic relaxation time τ. If the energy levels E_k and the transition probabilities A_{kl} are known, then this time can be calculated by means of the following formula [34]:

$$\tau = \frac{\sum\limits_{k>l} (E_k - E_l)^2}{\eta \sum\limits_{k>l} A_{kl} (E_k - E_l)^2},$$

(5.40)

where η is the number of all possible states of the spin system. Formula (5.40) has been derived under the assumption that $|E_l - E_k| \ll kT$ is valid for all $\underline{l}$ and $\underline{k}$. It follows from (5.40) that if we choose as the "spin system" a single particle with spin $S = 1/2$, then $\tau = A_{kl}/2$.

Paramagnetic resonance makes it possible to determine the transition probabilities A_{lk} by the saturation method. Experiments of this type are made to determine the saturation factors $q_{lk} = n_{lk}/n^0_{lk}$ (compare with §1.3), where n^0_{lk} is the difference in the populations of the energy levels E_l and E_k, if the paramagnet is in thermodynamic equilibrium state, and n_{lk} is the same quantity under saturation conditions. The saturation factors q_{lk} can be readily expressed in terms of the transition probabilities A_{lk} and p_{lk}, by setting up equations of the type (5.39) for each spin level of the paramagnetic particle. If all the intervals between these levels are different, and the resonance is observed as a result of transitions between the levels E_1 and E_2 under the influence of a radio frequency field, then it is easy to show [35] that

$$q_{12} = \left(1 + \frac{p_{12}}{A_R}\right)^{-1},$$

(5.41)

- 228 -

where the quantity W_R, which Lloyd and Pake call the relaxation probability, is equal to

$$W_R = A_{11} + \frac{1}{C_{11}} \sum_{k=3}^{\eta} A_{1k} C_{2k} \qquad (5.41a)$$

Here C_{2k} is the cofactor of the elements of the second row and the second column of the following matrix:

$$
\begin{vmatrix}
A_{11} - \sum\limits_{k=3}^{\eta} A_{1k}, & A_{21}, & A_{31},\dots, & A_{\eta 1} \\
A_{12} - \sum\limits_{k=3}^{\eta} A_{2k}, & -\sum\limits_{k=3}^{\eta} A_{2k}, & A_{32},\dots, & A_{\eta 2} \\
\cdot\ \cdot\ \cdot\ \cdot\ \cdot\ \cdot\ \cdot\ \cdot\ \cdot\ \cdot\ \cdot\ \cdot\ \cdot\ \cdot \\
A_{1m} + A_{2m}, & A_{2m}, & A_{3m},\dots, & A_{\eta m} \\
\cdot\ \cdot\ \cdot\ \cdot\ \cdot\ \cdot\ \cdot\ \cdot\ \cdot\ \cdot\ \cdot\ \cdot\ \cdot\ \cdot \\
A_{1\eta} + A_{2\eta}, & A_{2\eta}, & A_{3\eta},\dots, & -\sum\limits_{k=3}^{\eta} A_{\eta k}
\end{vmatrix}
\qquad (5.41b)
$$

The experimental conditions are frequency adjusted in such a way as to make $q_{12} = 1/2$. It is directly evident from (5.41) that in this case $W_R = p_{12}$.

2. For reasons stated in §5.1, the theory of spin-lattice relaxation usually deals not with the entire spin system but with an individual particle interacting with the lattice vibrations. The calculation of the transition probabilities A_{1k} between the energy levels of an individual magnetic particle as a result of energy exchange with the lattice is made by the perturbation method. In the unperturbed state, the system considered by us consists of two noninteracting parts: a paramagnetic ion and an aggregate of oscillators, which represent the elastic vibrations of the crystal. From among all the interactions between the paramagnetic ion and the surrounding particles, we are interested in those that depend on the magnitude of its magnetic moment. Under the influence of the lattice vibrations, the magnitude of these interactions will vary. This variable part of the energy of

the bond between the paramagnetic ion and its surrounding does indeed yield the spin-lattice interaction operator H'. We can then use the perturbation theory developed in the theory of radiation [36].

Energy exchange between the paramagnetic ion and the lattice vibrations under the influence of the perturbation H' can occur in different ways, of which the most important are the direct (single-phonon) processes and processes of combination scattering of phonons (two-phonon). We denote the difference in the energies of any two states of the paramagnetic ion by E_{1k}. A direct process consists in an increase (or decrease) of the ion energy by an amount E_{1k} due to the vanishing (or occurrence) of one quantum of elastic lattice vibrations (one phonon). Of all the lattice oscillators, the only ones that can participate in such processes are those whose frequency ν satisfies the condition

$$E_{1k} = h\nu. \qquad (5.42)$$

The probability that the paramagnetic ion will go over as a result of the direct processes from level E_1 to level E_k is

$$A_{1k}^{(1)} = \frac{4\pi^2}{h^2} \rho_\nu |\mathscr{H}_{1k}'|^2. \qquad (5.43)$$

Here ρ_ν is the spectral density of the oscillators with frequency ν, and H'_{1k} is the matrix element of the spin lattice interaction, averaged over the different states of the oscillators that satisfy condition (5.42). Frequently the matrix element H'_{1k} relating the energy levels E_1 and E_k turns out to be zero in first approximation. Higher approximations are then used and H'_{1k} is calculated through the intermediate state of the paramagnetic particles.

Combination scattering of phonons is a process consisting of an increase (or a decrease) in the ion energy by an amount E_{1k}, owing to the vanishing of an elastic-oscillation quantum of frequency ν and the

occurrence of a quantum of frequency ν'; in this case, obviously, the following condition should be satisfied:

$$E_{lk} = h\nu - h\nu'. \qquad (5.44)$$

For the probability of transition under the influence of combination phonon scattering processes we have

$$A_{lk}^{(2)} = \frac{4\pi^2}{h^2} \int |\mathcal{H}_{lk}|^2 \rho_\nu \rho_{\nu'} d\nu'. \qquad (5.45)$$

It is seen from (5.44) and (5.45) that elastic lattice vibrations of all frequencies participate in combination phonon scattering processes. Therefore, in spite of the fact that the combination scattering of phonons is a second-order process, it does play a principal role in the relaxation mechanism if the temperature of the paramagnet is relatively high. At low temperatures, the principal role is assumed by the direct processes.

We denote the quantity $A_{lk}^{(1)}$, averaged over different values of $\underline{l}$ and $\underline{k}$, by A_1, while the averaged value of $A_{lk}^{(2)}$ is denoted A_2. From (5.43) and (5.45) we obtain, if we assume that $E_{lk} \ll kT$,

$$A_1 = K_1 \frac{kT}{\rho v^5}, \qquad A_2 = K_2 \frac{J_8}{\rho^2 v^{10}}. \qquad (5.46)$$

Here ρ is the crystal density, T is the temperature, $\underline{v}$ the average velocity of sound, while K_1 and K_2 are quantities that depend on the nature of the relaxation mechanism and on the energy level structure of the magnetic particles, and consequently also on the applied magnetic field H_0. By J_n we denote

$$J_n = \int_0^{\frac{\theta}{T}} \frac{\nu^n \exp \frac{h\nu}{kT}}{\left[\exp \frac{h\nu}{kT} - 1 \right]^2} d\nu, \qquad (5.47)$$

where θ is the Debye temperature. This integral can be calculated from the following approximate formulas [37]:

$$J_n = n! \left(\frac{kT}{h} \right)^{n+1} \quad (T < \theta), \qquad (5.48)$$

- 231 -

$$J_n = \left(\frac{k\theta}{\hbar}\right)^{n+1}\left[\frac{e^{\frac{\theta}{T}}}{(n+1)(e^{\theta/T}-1)^2} + \right.$$
$$\left. + \frac{\theta}{(n+1)(n+2)T}\frac{(e^{\frac{\theta}{T}}+1)e^{\frac{\theta}{T}}}{(e^{\theta/T}-1)^3} - \dots\right](T\sim\theta), \qquad (5.49)$$

$$J_n = \frac{1}{n-1}\left(\frac{k}{\hbar}\right)^{n+1}\theta^{n-1}T^2 \quad (T>\theta). \qquad (5.50)$$

The value of $\underline{n}$ is usually 6 or 8. Therefore the relatively weak temperature dependence of the relaxation time when $T \gg \theta$ becomes very strong when $T \ll \theta$.

3. In the first theory of paramagnetic spin-lattice relaxation, presented by Waller [8], it was assumed that the reorientation of the atomic spin relative to the external magnetic field H_0 under the influence of the lattice vibrations is the result of a change in the magnetic interaction of the spins, brought about by these oscillations. Waller's calculations lead, however, to values of the relaxation time which are several orders of magnitude larger than the experimental data. A particularly sharp discrepancy between theory and experiment was observed in titanium-cesium alums. Kronig [38] and Van Vleck [37] therefore proposed a different relaxation mechanism. In many cases, however, as was shown by Al'tshuler [39], Waller's mechanism can play a principal role.

Waller's calculations were made for a paramagnet whose magnetic particles have a spin $S = 1/2$. Yet the probability of the particle spin reorientation under the influence of oscillations of the magnetic forces acting on it is proportional to the fourth power of the magnetic moment of the particle. In addition, this probability is inversely proportional to R^6, if R stands for the equilibrium distance between two neighboring crystal atoms having magnetic moments. Frequently several such atoms are contained in a single crystalline cell.

It is easy to see that in this case a more exact result will be obtained if R is defined not as the average distance between neighboring particles with magnetic moments, but the shortest one. It is clear therefore that the magnetic forces can determine the spin-lattice interaction in substances with large atomic magnetic moments and with large magnetic particle density. Calculations have shown that

$$K_1 = \frac{4\pi^2 Z}{3h^2}\left(\frac{g^2\beta^2}{R^3}\right)^2 (g\beta H_0)^2 S(2S+1)(S+1)^2,$$ (5.51)

$$K_2 = \frac{2\pi^2 Z}{3}\left(\frac{g^2\beta^2}{R^3}\right)^2 S(2S+1)(S+1)^2, \quad n=6.$$ (5.52)

Here Z is the number of nearest neighbors of the particle. It should be noted that Waller considered the relaxation due to the spin reorientation of one particle under the influence of the lattice vibrations under the condition that the other spins conserve their directions. Yet, as can be seen from (5.10), the matrix elements of the spin-lattice perturbation differ from zero even in the case of simultaneous reorientation of the spins of two neighboring particles. For this case it follows from the calculations that

$$K_1' = \frac{16\pi^2 Z}{3h^4}\left(\frac{g^2\beta^2}{R^3}\right)^2 (g\beta H_0)^2 (2S+1)^2(S+1)^2,$$ (5.53)

$$K_2' = 3,16\pi^2 Z\left(\frac{g^2\beta^2}{R^3}\right)^2 (2S+1)^2(S+1)^2, \quad n=6.$$ (5.54)

We see that simultaneous reorientations of the spins of two interacting particles is much more probable than the change in spin orientation of one particle alone.

In substances with large magnetic ion density, exchange forces assume appreciable values. The energy of the exchange interactions has for the most part the isotropic form $A_{12}(r)\vec{S}_1\vec{S}_2$; it is an integral of the motion, and consequently the exchange forces cannot cause, in first approximation, a transfer of energy from the spins to the lattice vibrations. On the other hand, if the exchange forces are anisotropic, the magnitude of the spin-lattice interactions which they pro-

duce has the same order as in the case of magnetic dipole forces.

4. In order to explain why the spin-lattice interaction is very large in titanium-cesium alums, Kronig [38] proposed the following relaxation mechanism. The elastic vibrations of the lattice modulate the electric field of the crystal, and this causes a change in the orbital motion of the magnetic-ion electrons. The action influences the electron spin through the orbital magnetic moment. This mechanism of spin-lattice interaction is the principal one for the majority of salts in the iron-group elements, in spite of the fact that the orbital motion is "frozen" in these salts. Calculations have shown that

$$K_1 = \left(\frac{\lambda}{\Delta}\right)^2 \left(\frac{r_0}{a}\right)^4 \left(\frac{ee'}{a\Delta}\right)^2 \left(\frac{g\beta H_0}{h}\right)^4,$$
$$K_2 = h^2 \left(\frac{\lambda}{\Delta}\right)^2 \left(\frac{r_0}{a}\right)^6 \left(\frac{ee'}{a\Delta}\right)^4, \quad n = 8.$$
(5.55)

Here Δ is the interval between two lower orbital sublevels, arising in the electric field of the crystal, r_0 is the average distance from the 3d electron to the nucleus, $\underline{a}$ is the equilibrium distance from the center of the magnetic particle to the nearest diamagnetic ion, and e' is the effective charge of this ion. The factor $(\lambda/\Delta)^2$ appears in (5.55) because changes in the crystalline electric field cannot produce directly a reorientation of the electron spin, and acts through the orbital momentum. Since the orbital motion is "frozen," the matrix element of the spin-lattice interaction differs from zero in the higher approximations of perturbation theory.

It is therefore clear that in ionic crystals containing the iron group elements the probabilities of relaxation transitions will always be inversely proportional to a high power of the interval Δ. It is known from experiment that the spin-lattice relaxation times at the same temperature can differ by several orders of magnitude for different elements. This is explained principally by the fact that the in-

terval Δ can change on going from one ion to another from about 10^2 to about 10^4 cm^{-1}. In particular, for the titanium ion (see §4.2) we have $\Delta \approx 500$ cm^{-1}.

An analogous but more complete theory of spin-lattice relaxation was developed by Van Vleck [37] independently of Kronig. He considered in addition to titanium salts also salts containing Cr^{3+}. Unlike the titanium ion, the simple orbital levels of which are Kramers doublets, in the chromium ion we have $S = 3/2$, and consequently the simple orbital level breaks up into two closely located Kramers doublets, the interval between which will be denoted by δ. The expressions for τ obtained by Van Vleck are very cumbersome. The principal difference between them and (5.55) lies in the following. In the case of the direct processes $(g\beta H_0)^4$ is replaced by $\lambda^2 \sqrt{g^4\beta^4 H_0^4 + c_1 \delta g^2 \beta^2 H_0^2 + c_2 \delta^2}$, where c_1 and c_2 are certain numbers on the order of unity. In the expression for K_2 we have $\lambda^2 J_6$ in place of $h^2 J_8$.

Bashkirov [40] calculated the spin-lattice relaxation time for copper salts, the electric fields of which have tetragonal symmetry. The copper ion Cu^{2+}, like the ion Ti^{3+}, has $S = 1/2$. However, unlike the titanium salts, the matrix element of the spin-orbit interaction, which relates the lowest orbital states, is in this case equal to zero. Therefore in place of one interval Δ, the formula for the relaxation time contains two intervals, Δ_0 and Δ, where Δ_0 is the splitting in the field produced by the octahedron of the water molecules surrounding the Cu^{2+} ion, and Δ is the interval between the lowest orbital sublevels, arising in the field of tetragonal symmetry. In formulas (5.55) it is necessary to replace Δ^{-6} by $\Delta_0^{-2}\Delta^{-4}$.

The following singularities were observed experimentally in many copper salts: 1) the spin-lattice relaxation time at room temperature depends strongly on the angle ϑ between the field H_0 and the tetragonal

axis of the crystal [41]; 2) the paramagnetic resonance spectrum in $CuSO_4 \cdot 5H_2O$ can be explained by assuming the constant λ to have appreciable anisotropy [42]. If the constant λ is replaced by a tensor with principal values $\lambda_{\parallel}$, $\lambda_{\perp}$, $\lambda_{\perp}$, then in formula (5.55) λ^2 must be replaced by $1/2[\lambda_{\parallel}^2 \sin^2 \vartheta + \lambda_{\perp}^2 (1 + \cos^2 \vartheta)]$. If we take for $\lambda_{\parallel}$ and $\lambda_{\perp}$ the values assumed in [42], we obtain good agreement with the measurements of [41].

It follows from Kramers'theorem that the spectra of ions with an even number of electrons should have many singularities. Avvakumov [43] undertook detailed theoretical calculations of the spin-lattice interaction for crystals with such ions (V^{3+}, Cr^{2+}, Mn^{3+}, Fe^{2+}, Ni^{2+}). In the case of Ni^{2+}, as in the case of the Cr^{3+} investigated by Van Vleck, the lower orbital level is simple under the action of a field of cubic symmetry. Therefore the interval is $\Delta \approx 10^4$ cm^{-1} and the relaxation time is relatively large. In the other ions considered by Avvakumov, the lower orbital level is degenerate under the action of a cubic field, and therefore Δ denotes the interval between sublevels produced in a weak field of low symmetry. Because of this, the relaxation time of salts containing these ions turned out to be relatively short and observation of paramagnetic resonance is impossible at room temperatures.

If the relaxation is due to the combination phonon scattering processes, then the temperature dependence of τ is determined by the integral J_n, in which n = 6 for the Cr^{2+}, Mn^{3+}, and Ni^{2+} ions and n = 8 for the Fe^{2+} and V^{3+} ions. Calculations have disclosed a strong dependence of the relaxation time on the value of the spin S; at low temperatures $\tau \sim S^{-12}$ and at high temperatures $\tau \sim S^{-8}$. A noticeable dependence of the relaxation time on the angle between the field H_0 and the axes of the crystal was established also for all ions, except Ni^{2+}.

As to the dependence of τ on the magnitude of the field H_0, this dependence becomes noticeable if $g\beta H_0 > \delta$.

5. A special analysis is necessary for ions in the S state. Al'tshuler [39], using the salts of trivalent iron as an example, considered relaxation due to the direct processes. Bashkirov [44] made detailed calculations of the relaxation which is due also to second-order processes for the ions Mn^{2+}, Fe^{3+}, Eu^{2+}, and Gd^{3+}. If we denote by δ the magnitude of the total splitting of the spin levels by the crystalline field, then the results of the calculations will essentially reduce to the following:

$$K_1 = \frac{\mathfrak{b}^2}{\hbar^4}(g\beta H_0)^2, \quad K_2 = \mathfrak{b}^2, \quad n = 6. \tag{5.56}$$

Comparison of these formulas with (5.52) and (5.53) shows that Waller's mechanism can play the principal role when

$$\delta < \frac{g^2\beta^2}{R^3}(2S+1)(S+1). \tag{5.57}$$

This is apparently the case with manganese salts, for which the splitting δ is relatively small.

6. The theory of spin-lattice relaxation for salts of the rare earth elements was given by Al'tshuler [45] with the cerium ion as an example; it was assumed there that the crystalline field consists of two parts, a strong field of cubic symmetry and a weak field of lower symmetry. Shekun [46] made a theoretical analysis of relaxation in ethyl sulfates of different rare earth elements. We recall that the crystalline field in ethyl sulfates has trigonal symmetry.

In rare earth compounds, the lattice vibrations, by changing the crystalline field, can directly change the direction of the moment of the paramagnetic ion, for in this case the coupling between the spin and orbital momenta is stronger than the action of the electric field of the crystal. One therefore obtains for K_1 and K_2 expressions of the

type (5.55), but without the factor $(\lambda/\Delta)^2$. Since the interval Δ is relatively small for rare earth ions, on the order of 10-100 cm^{-1}, the spin-lattice interaction turns out to be very strong, in spite of the fact that r_0 for 4f electrons is somewhat smaller than for the valence electrons of the iron group. In ions with an odd number of $\underline{f}$ electrons, the spin-lattice interaction due to the direct processes turns out to be particularly large if a nonKramers degeneracy of the ground level exists. In this case we have

$$K_1 = \frac{1}{h^4}\left(\frac{ee'}{a}\right)^2\left(\frac{r_0}{a}\right)^4 (g\beta H_0)^2. \tag{5.58}$$

Here the matrix element of the spin-lattice interaction differs from zero even in the first approximation of perturbation theory.

7. Great interest is attached to an explanation of how the spin-lattice interaction is changed if the concentration of the paramagnetic particles is decreased by isomorphically replacing them with diamagnetic ions. This question was considered theoretically by Kochelayev [112].

It would seem at first glance that relaxation due to the Kronig-Van Vleck mechanism should not depend on the concentration of the paramagnetic particles, since the forces bringing about the spin-lattice coupling are determined by the relative displacement of the paramagnetic ion and the diamagnetic atoms surrounding it. Actually, however, an appreciable role can be played by the following circumstance: practically any specimen contains crystal-lattice imperfections, on which the plane Debye waves are scattered.

Under the influence of the standing plane Debye wave, two neighboring atoms oscillate with amplitudes whose difference is proportional to the frequency ν of the elastic oscillations. Since the probability of the relaxation transition is proportional to the square of the rela-

tive displacement of the paramagnetic ion and of the neighboring dia-magnetic particle, we find in the case of direct processes, in accord with (5.45), that $A_1 \sim E_{kl}^2$. After the Debye wave is scattered by the randomly located paramagnetic center, a spherical wave is produced around this center, with an intensity that increases rapidly, of course, as it propagates. Consequently, two neighboring atoms located at distances r_1 and r_2 from the scattering center will oscillate with amplitudes whose difference is proportional to $(1/r_1 - 1/r_2)$. In spite of the fact that the intensity of the scattered waves is much smaller than the intensity of the plane Debye waves, simple calculation shows that over a wide range of paramagnetic particle concentrations and at reasonable values of the defect concentrations, the relaxation due to the scattered spherical waves plays the principal role if the ampli-tude of the scattered wave is independent of the frequency. Besides, whereas in accordance with the ordinary spin-lattice relaxation theory we have $A_1 \sim E_{kl}^n$, now, by virtue of the fact that the relative dis-placement of the neighboring particles is independent of the frequency ν, the relaxation probability will be $A_1 \sim E_{kl}^{n-2}$. As we have seen above, in many cases $n = 2$, and consequently the dependence of the probabil-ity of relaxation transitions between spin levels E_k and E_l on the magnitude of the interval E_{kl} should dispppear. When the number of de-fects in the crystal is small and when the crystal is strongly diluted by diamagnetic ions, the Kronig-Van Vleck relaxation mechanism will again predominate.

According to the views developed here, the spin-lattice interac-tion should also be appreciably influenced by such crystal lattice im-perfections, whose dimensions are comparable with the length of the incident wave.

The theory developed here is applicable in the case of low tem-
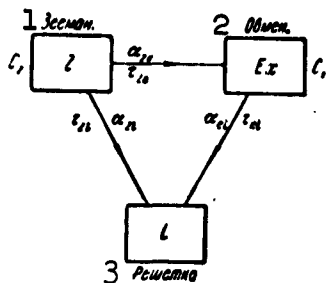
Fig. 5.2. Scheme showing the transfer of energy to the lattice vibrations in the case of strong exchange interactions. 1) Zeeman; 2) exchange; 3) lattice.

peratures, when the relaxation is due to single-phonon processes. At high temperatures, when the relaxation is determined by two-phonon processes, the principal role is assumed by the phonons with high frequencies v, and consequently the spin-lattice interaction due to the waves scattered by the imperfections ceases to predominate.

8. Akhiezer and Pomeranchuk [47] have considered the question of paramagnetic relaxation at super low frequencies by the method of elementary excitations. They have proposed that the paramagnet is a nonconducting crystal containing ions with an odd number of electrons. The spin system of the paramagnetic crystal has a spectrum whose form is determined by the crystalline electric field and by the magnetic and exchange interactions between the individual lattice ions. Deviations from the ground state of the spin system, a state which occurs when $T = 0$, are regarded as an assembly of elementary excitations, which, as in the case of the Bloch model of the ferromagnet, propagate over the entire crystal. Each elementary excitation represents a quasiparticle which can be assigned a definite energy and a certain quasimomentum. The calculations were made under the assumption that the quasiparticles obey the Fermi-Dirac statistics. Because of the interaction between the elementary excitations and the lattice vibrations, energy is exchanged between the spin system and the lattice. By calculating the probabilities of the collisions of the quasiparticles among themselves and with the phonons, one determines the amount of heat Q which is transferred per unit time from the lattice to the spin system. It was found that $Q = const\ T_s^6 q\ (T_s/T_l)$, where the function $q(T_s/T_l)$ is inversely pro-

- 240 -

portional to $(T_s/T_{\underline{1}})^6$ when $T_s \ll T_{\underline{1}}$ and proportional to $1 - T_s/T_{\underline{1}}$ when $T_s \approx T_{\underline{1}}$. If initially $T_{\underline{1}} \gg T_s$ and $T_s \sim 10^{-4}{}^{\circ}K$, then, as shown by calculation, the time after which $T_{\underline{1}}$ and T_s differ by 1% does not exceed 1 second.

9. If the exchange interactions are very large (anhydrous paramagnetic salts, free radicals, ferrites), then it is necessary, as shown by Blombergen and Wein [48], to divide the spin system into two parts, a Zeeman part and an exchange part.

The scheme whereby energy is transferred from the Z system to the lattice is shown in Fig. 5.2. Each of the three subsystems can be assigned a certain temperature. Let us denote the temperature of the Z system by T_Z, the temperature of the Ex system by T_e, and the lattice temperature as before by $T_{\underline{1}}$. The possibility of introducing separate concepts of Zeeman and exchange temperatures is connected with the fact that the operators of Zeeman energy (5.6) and exchange energy (5.8) commute. Therefore changes in the Zeeman energy can occur without affecting the exchange energy. The transfer of energy from the Z system to the Ex system is possible because of the existence of relatively weak magnetic dipole interactions which do not commute with $H._{zeem}$ and $H._{obm}$.

It can be assumed that direct transfer of energy from the Z system to the lattice has low probability and consequently the relaxation time $\tau_{z\underline{1}}$ is large compared with the times τ_{ze} and $\tau_{e\underline{1}}$. Let us denote by α_{ze} and $\alpha_{e\underline{1}}$ the corresponding heat conduction coefficients, and by C_z and C_e the specific heats of the Z and Ex systems. To explain the experimental data it becomes necessary to assume that $\alpha_{ze} < \alpha_{e\underline{1}}$ and $C_z \ll C_e$.

Inasmuch as the relaxation time is determined by the ratio of the specific heat to the corresponding heat conduction coefficient, it

turns out that $\tau_{ze} < \tau_{e\underline{l}}$. Therefore τ_{ze} plays the role of the spin-lattice relaxation time for ordinary paramagnetics. It is remarkable that the independence of τ_{ze} of the lattice temperature is confirmed in experiments on saturation. Under stationary conditions the amount of heat transferred from the Z system to the Ex system is equal to the heat flowing from the Ex system to the lattice, i.e., $\alpha_{ze}(T_z - T_e) =$ $= \alpha_{e\underline{l}}(T_e - T_{\underline{l}})$. It follows therefore that T_e is much closer to $T_{\underline{l}}$ than to T_z.

§5.4. Longitudinal Relaxation at Low Temperatures

1. It follows from the theory of spin-lattice relaxation due to single-phonon processes (§5.3) that the relaxation time τ, which is inversely proportional to the temperature T, decreases with increasing applied field H_0 and is generally speaking independent of the concentration of the paramagnetic centers and of the crystal dimensions. Yet many experiments [49-53] have established facts that are in direct contradiction with all these theoretical conclusions. Moreover, it was observed that in place of one time it becomes necessary sometimes to introduce a whole set of relaxation times. In spite of all these contradictions, there are no grounds for doubting the correctness of the theoretical choice of the mechanism of spin-lattice interaction. At least in some cases, these singularities of the relaxation occurring at helium temperatures can be explained as follows.

In the analysis of relaxation processes it is always assumed that the lattice vibrations can be regarded as a thermostat in which the spin system is embedded. The specific heat of the spin system was always considered to be small compared with the specific heat of the lattice. Yet if the temperature of the spin system is higher than that of the lattice, then establishment of equilibrium with the aid of single-phonon processes will occur by exciting oscillations in a narrow fre-

quency band, satisfying approximately the condition (5.44). The specific heat of these low-frequency lattice oscillators, which are in direct contact with the spin system, is low. The speed with which the energy acquired by these "effective" oscillators is transferred either to the oscillators of other frequencies or to the helium thermostat surrounding the crystal is therefore important. Let us denote the temperature of the spin system by T_s, the temperature of the "effective" oscillators by T_Z, and the thermostat temperature by T_0. If the energy transferred to the "effective" oscillators is drawn away sufficiently rapidly so that the relation $T_s - T_Z \gg T_Z - T_0$ holds true for the temperature differences, then the bottleneck in the chain linking the spin system with the thermostat will be the contact between the spin system and the lattice, and consequently the longitudinal relaxation time T_1 will be equal to the time τ. If on the other hand the stationary processes of striking the balance between the spin system and the thermostat is such that $T_s - T_Z \ll T_Z - T_0$, then along with the spin-lattice relaxation time τ it is necessary to introduce a time characterizing the exchange of energy between the "effective" oscillators and the helium thermostat (or with the oscillators of other frequencies). We shall denote this time T_1, since it will now determine the longitudinal relaxation, inasmuch as $T_1 \gg \tau$.

2. For what is to follow, it is necessary to calculate the number N_f of "effective" oscillators per unit volume. Were the energy spectrum of the spins and lattice oscillators a discrete one, then the number of oscillators participating in the energy exchange between the spins and the lattice would be infinitesimally small. Actually, however, owing to the spin-spin interactions on the one hand, and the finite lifetime of the oscillators in the excited state on the other, the energy levels become broadened. We shall see that the most appre-

- 243 -

ciable broadening occurs in the vibrational levels. We denote by $2\Delta\nu_L$ the frequency interval of the oscillators that interact strongly with distance. In accordance with the usual law governing the distribution of the frequencies of elastic lattice vibrations, we can assume that

$$N_f = \frac{12\pi\nu^2}{v^3}(2\Delta\nu_L).$$

(5.59)

The value of $\Delta\nu_L$ can be estimated in the following fashion. We assume for simplicity that the effective spin of the paramagnetic particles is 1/2. Then, according to (5.40), the probability per unit time A_1 of transition between the spin energy levels under the influence of the lattice vibrations is connected with the time τ by the relation $A_1 = 1/2 \ \tau^{-1}$. Each of the N_0 spins contained per unit volume can exchange one phonon with each of the N_f oscillators within a time 2τ. Therefore the oscillator vibrations will be interrupted in the mean after time intervals

$$\Delta t = 2\frac{N_f}{N_0}\tau.$$

Since $\Delta\nu_L = 1/2\pi\Delta t$, it follows from (5.59) that

$$\Delta\nu_L = \left(\frac{N_0 v^3}{96\pi^2\nu^2\tau}\right)^{\frac{1}{2}}.$$

(5.60)

By way of an example let us assume that $N_0 = 10^{19}$ cm^{-3}, $v = 2\cdot10^5$ cm/sec, and $\nu = 10^{10}$ cps, and $2\tau = 10^{-5}$ sec; then $\Delta\nu_L = 4\cdot10^8$ cps, which is much larger than the frequency interval $4N_0\beta^2/h$, connected with the spin-spin interactions. The number of "effective" oscillators in our example is, in accord with (5.59), $N_f \approx 5\cdot10^{14}$ cm^{-3}. We see that there are approximately 10^4 spins for each effective oscillator. It is clear that the specific heat of the "effective" oscillators is negligible compared with that of the spin system. Therefore, if $T_1 \gg \tau$, then the establishment of the thermal equilibrium between the spin system and the aggregate of the effective oscillators will consist of hav-

ing the "effective" oscillators assume the spin temperature, $T_Z \rightarrow T_s$. It can be shown that in this case the "effective" oscillators are directly coupled to the spin system.

We note that the formulas obtained are valid if $kT_s \ll h\nu$. On the other hand, if $kT_s \gg h\nu$, then it is necessary to introduce in place of N_0 the difference in the populations of two neighboring spin levels, i.e.,

$$\frac{N_0 h\nu}{2kT_s}.$$

3. What is the mechanism determining the longitudinal relaxation if $T_1 > \tau$? Equilibrium between the spin system and a helium thermostat can be established in various ways. Frelikh and Heitler [54] have shown that the heat conductivity of the spin system is very small. Therefore direct transfer of energy from the spin system to the thermostat is of low effectiveness. This can be readily understood by recognizing that the rate of propagation of the spin-system excitations (magnons) in substances that do not have too high a concentration of paramagnetic centers is much smaller than the velocity of sound: $v \gg \beta^2/hr^2$ (see §5.1).

Two possible mechanisms remain: a) the transfer of the energy of the "effective" oscillators to all other lattice vibrations; b) direct transfer of energy from the "effective" oscillations to the helium thermostat. Van Vleck [55] considered mechanism a), and took the anharmonicity of the lattice vibrations into account. Let dQ/dt be the quantity of heat transferred per second from the "effective" oscillators to the remaining lattice vibrations. Then

$$\frac{dQ}{dt} = b(T_Z - T_0), \tag{5.61}$$

where b is the heat conduction coefficient, equal to

$$b = \left(\frac{36}{35}\right)^2 \pi^2 \frac{k^2 T_1 V N \rho}{h^3 \rho_s v^6}\left[\left(\frac{18}{A} - \frac{15B}{A^3}\right)^2 + 2\left(\frac{5}{A} - \frac{3B}{A^3}\right)^2\right]. \tag{5.62}$$

If we denote by ΔV the change in the volume V of the crystal under the influence of the pressure $\underline{p}$, then the mean of the coefficients A and B becomes clear from the following formula:

$$\frac{\Delta V}{V} = Ap - Bp^2. \tag{5.62a}$$

For potassium chrome alums [56] $A = 6.3 \cdot 10^{-12}$ cm^2/dyn and $B = 1.08$ x x 10^{-22} cm^4/dyn^2. If we return to the numerical example considered in this section and assume furthermore that the specimen is in the form of a sphere of radius R, we obtain with the aid of (5.62) $b \approx 2 \cdot 10^{-4}$ x x R^3 w/deg.

In order to estimate the effectiveness of mechanism b), let us assume first that the elastic waves are not perturbed at all, with the exception of interaction with the spin system and the walls of the crystal [57]. The case which we are considering is most favorable for the penetration of heat from the thermostat inside the specimen. Let us imagine a spherical cavity in which the elastic waves striking the wall have a temperature T_Z and the waves radiated by the wall have a temperature T_0. If u(T) denotes the energy density of the "effective" oscillations at temperature T, then each unit surface of the wall will absorb per second an energy $vu(T_Z)/4$ and radiate an energy $vu(T_0)/4$. If the difference $T_Z - T_0$ is small, then

$$u(T_Z) - u(T_0) = N_f k (T_Z - T_0),$$

and consequently the heat transferred per second by the "effective" oscillations to the helium thermostat is $a(T_Z - T_0)$, where the heat conduction coefficient is

$$a = \pi R^2 N_f k v. \tag{5.63}$$

Substituting the previous values of N_f and $\underline{v}$ we obtain $a \approx 4 \cdot 10^{-3} \cdot R^2$ w/deg.

The longitudinal relaxation time T_1 can be defined as the ratio

of the specific heat of the spin system C_s to the heat conduction coefficient of the channel coupling the spin system with the thermostat. If we take both mechanisms a) and b) into account, we obtain

$$T_1 = C_s \left(\frac{1}{a} + \frac{1}{b} \right).$$

(5.64)

If S' = 1/2, then [34]

$$C_s = \frac{N_0 V h^2 v^2}{k T_s^2}.$$

(5.65)

In the example which we have considered a/b >> 1 and consequently mechanism a) is much more effective than b). In this case we obtain with the aid of (5.63)-(5.65)

$$T_1 = \left(\frac{1}{6} N_0 v \tau \right)^{\frac{1}{3}} \left(\frac{h}{k T_s} \right)^2 v R.$$

(5.66)

If $kT_s \ll h\nu$, then obviously

$$T_1 = \left(\frac{1}{12} N_0 v \tau \right)^{\frac{1}{3}} \left(\frac{h}{k T_s} \right)^{\frac{1}{3}} v^{\frac{1}{3}} R.$$

(5.66a)

Substituting again the previous values of the quantities used in our example, we obtain $T_1 \approx 10^{-2}$ sec.

If the mean free path of the "effective" phonons is small compared with the linear dimensions of the crystal, then the mechanism which we have described for the transfer of energy from the effective oscillations to the thermostat will be disturbed by diffusion processes. The mean free path of the phonon, the path of which is interrupted by collision with a magnon, is of the order of ~$v\tau$. Therefore, if R >> $v\tau$, the phonon diffusion processes begin to play a predominant role in the transfer of energy from the spin system to the thermostat. An estimate of the longitudinal relaxation time made for this case [58] has shown that for $h\nu \ll kT_s$ its approximate value is

$$T_1 = \frac{R^2 h^2 N_0 v}{18 \pi^2 (k T_s)^3}.$$

(5.67)

We note that in this case one cannot, strictly speaking, define a sin-

gle relaxation time. The temperature of the spin system and of the aggregate of "effective" oscillators will vary from the center of the crystal toward its boundary. As a result, a certain distribution of the relaxation times is produced.

The formulas which we have obtained for the longitudinal relaxation time apparently permit an explanation of the experimental facts concerning the character of the dependence of T_1 on the concentration N_0 of the paramagnetic centers, on the temperature T_s, on the dimensions R of the crystal, and on the intensity of the applied field H_0 (of frequency v).

Longitudinal relaxation at low temperatures has not been sufficiently well investigated experimentally. The discussion that arose in an examination of this question [59, 60] in connection with the development of paramagnetic amplifiers (see Chapter 8) has thus far not led to any definite results (see §5.9).

§5.5. Experimental Data on Ionic Crystals

1. Line width in solid paramagnets

Various types of interactions in paramagnets are experimentally investigated either by determining the width and the shapes of the paramagnetic resonance lines, or with the aid of a method that makes use of the saturation of these lines. In addition, information on the spin-spin and spin-lattice relaxation times is obtained by measuring parametric absorption and the dispersion of susceptibility on superposition of a static field and a high frequency magnetic field parallel to it.

By line width ΔH we mean the distance in oersteds between the points on the $\chi''(H_0)$ curve at which χ'' has a value equal to half the maximum. In some papers the width is defined differently, as the distance in oersteds between the points of inflection of the $\chi''(H_0)$ curve.

Such a definition is convenient when the result of the measurements is the differential curve $d\chi''/dH(H_0)$. We shall designate this width δH. For curves of Lorentzian shape $\Delta H = 1.73\delta H$ and for Gaussian curves $\Delta H = 1.26\delta H$. We note that at measurements at low frequencies it becomes necessary to use the definition of a "right half-width," i.e., the distance in oersteds between the point corresponding to the position of the absorption maximum and the point where $\chi'' = \chi''_{max}/2$, which lies in the region of H_0 above the maximum. The "right half-width" will be designated ΔH_{pr}.

In addition to measuring $\chi''(H_0)$, the width of resonance lines is also estimated by measuring the dependences of χ' and $d\chi'/dH$ on the field intensity H_0. In the latter case the difference between the Lorentzian and Gaussian line shapes can be readily established by determining the ratio of the values of $d\chi'/dH$ at the maximum and at the minima of the $d\chi'/dH(H_0)$ curve. The values of this ratio are 8:1 and 3.5:1 for Lorentzian and Gaussian shapes, respectively [61].

Measurement of the values of ΔH (or δH) gives much less accurate results than a determination of the positions of the lines in the spectrum. The inaccuracy of the resultant line shape and width, which is inherent to some degree or another in all the methods used to determine paramagnetic resonance, is due principally to the impossibility of separating completely the various effects due to the real and imaginary parts of the high-frequency susceptibility.

We shall discuss first data pertaining to pure paramagnetic salts, not diluted by the corresponding diamagnetic ions. The line widths in these salts range from several tens to thousands of oersteds. The lines become sometimes utterly unobservable. If we exclude the case of ions with even number of electrons (in which paramagnetic resonance cannot occur because of the smallness of the quantum of the radio fre-

quency field as compared with the initial splitting of the spin sub-levels), then the absence of the effect can be due only to excessively strong spin-lattice interactions. A sufficient reduction in temperature decreases these interactions and makes the effect observable. In general the narrowing down of the lines upon cooling is the most convincing proof that the spin-lattice interactions determine the line width.

Another way of elucidating the nature of the observed width is to study the dependence of ΔH on the frequency of the absorbed radiation. In the case when the width increases appreciably with increasing frequency, it is natural to attribute this increase to the influence of the anisotropy of the g factor; in this case the measurements aimed at determining the true relaxation line width should be carried out at the lowest frequencies. Of course, the influence of the anisotropy manifests itself most strongly in investigations of polycrystalline specimens; it is not excluded, however, from single crystals, since in most cases a unit cell contains several nonequivalent magnetic ions.

One of the most important methods of investigating the internal interactions in paramagnets is to analyze the absorption line shape. So far, however, this study has been carried out principally by calculating the second and fourth moments of the experimental $\chi''(H)$ curves and comparing the results obtained with the Van Vleck line-width theory [10]. That this theory has limited applicability to the greater part of real crystals was already noted earlier.

Some typical results of measurements of absorption line width and shape in undiluted paramagnetic salts of Mn^{2+} are listed in Table 5.1 [62].

From an examination of the data in this table we can conclude the following:

1) In magnetically concentrated salts, the line widths are considerably smaller than would be expected if only magnetic dipole interactions were taken into account; the line shape is Lorentzian or close to it. It follows therefore that in such salts considerable exchange interactions take place.

2) In salts with smaller magnetic ion concentration (for example, in Tutton's salts of Mn^{2+} and Cu^{2+} or in chrome alums), the line shape is close to Gaussian, and the width deviates little from dipole width; thus, the role of exchange is no longer large.

TABLE 5.1

1 Вещество	$(\Delta H_{\frac{1}{2}})_{эксп},$ эрст [4] [2]	$(\Delta H_{\frac{1}{2}})_{теор},$ эрст [4] [3]	$\dfrac{\langle \Delta H^4 \rangle^{\frac{1}{4}}}{\langle \Delta H^2 \rangle^{\frac{1}{2}}}$
$MnCl_2 \cdot 4H_2O$	1410	1530	1,23
$MnCl_2$	750	2950	1,40
$MnSO_4 \cdot 4H_2O$	1150	1560	1,28
$MnSO_4 \cdot H_2O$	320	2870	1,46
$MnSO_4$ [5]	665	3520	1,35
$MnCO_3$ (крист.)	460	4460	1,43
$Mn_3(PO_4)_2 \cdot 3H_2O$	465	1246	1,38
$Mn_2P_2O_7 \cdot 3H_2O$	1070	1250	1,32
$Mn(NO_3)_2 \cdot 6H_2O$	1210	1033	1,31
MnF_2	470	7020	1,39
MnS	780	7520	1,40

1) Substance; 2) eksp; 3) teor;
4) oersted; 5) crystalline.

It must be noted, however, that a study of the dependence of the exchange interaction on the average distances between magnetic particles in highly concentrated paramagnets is possible only by comparison of substances that have crystal lattices of the same type; otherwise it is easy to arrive at erroneous conclusions, for at high magnetic concentrations it is meaningless to operate with average interionic distances without taking into account the specific nature of concrete lattices. In particular, it was shown by Kashayev [63], for example, that the absorption line in $CuF_2 \cdot 2H_2O$ is considerably narrower

than in CuF_2, in spite of the fact that the average distances between the Cu^{2+} are smaller than in the former salts, and consequently the exchange narrowing of the lines in the latter salts should have been more manifest in the CuF_2. The point is that according to crystallographic data the distance between the nearest Cu^{2+} ions in CuF_2 is larger than in $CuF_2 \cdot 2H_2O$.

From among the substances with strong exchange interactions, let us stop to discuss $CrCl_3$, polycrystalline specimens of which were investigated many times under various conditions. The form of the absorption line is shown in Fig. 1.2. The value of ΔH was determined in the frequency interval between 10^{10} and 10^7 cps and was found to be constant and equal to 140 ± 5 oersteds [64] within the limits of measurement accuracy (if it is determined at low frequencies by multiplying the "right-hand half-width" by two). Temperature changes in the interval from 290 to 77°K do not affect ΔH. The value of ΔH, calculated following Van Vleck from only the magnetic dipole interactions, is much larger than the observed value and amounts to 1000 oersted. The ratio $\Delta H/\delta H$ corresponds to a Lorentzian form.

A good example of a Gaussian form is the line observed by Bleaney [65], corresponding to the transition $\frac{1}{2} \underset{\leftarrow}{\rightarrow} \frac{3}{2}$ in the spectrum of cesium chrome alum $CrCs(SO_4)_2 \cdot 12H_2O$ with the crystal optical axis oriented along the field. The width of this line is $\Delta H = 280$ oersted, and is shown in Fig. 5.3. The experimental data are marked on the figure by the points, and the curve is drawn to obey a Gaussian law, with a mean square width $\sigma_H = 118$ oersted. This last quantity was calculated by Bleaney after Van Vleck with account of the presence of nonequivalent Cr^{3+} ions in the crystal cell. The good agreement with experiment leads to the conclusion that the role of exchange interactions is small in cesium chrome alum.
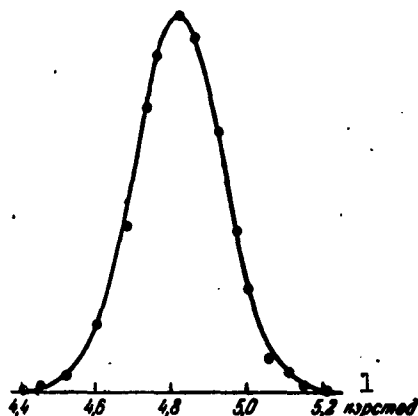
Fig. 5.3. Shape of the (1/2 ←→ 3/2) paramagnetic resonance line of cesium chrome alum [65]. 1) kilo-oersted.

Sometimes the line corresponds to neither Lorentzian nor Gaussian shape. In particular, an intermediate form was obtained by Japanese investigators [66] for $MnSO_4 \cdot 4H_2O$ and $MnSO_4 \cdot 5H_2O$. Deviations from the form expected by the Van Vleck theory have been observed by MacLean and Kor [67] in organic salts of Mn^{2+}.

We shall now stop to discuss the measurements of ΔH in dilute salts, in which some of the magnetic ions are replaced by diamagnetic ones. From the point of view of spectroscopy, such salts are of great interest. It is necessary to note here first of all that the narrowing down of the lines resulting from the reduction in the magnetic dipole interactions between the ions is observed down to sufficiently small relative concentrations of the magnetic ions ($f \leq 0.01$). If the residual line, which is independent of the further dilution, is not connected with the spin-lattice relaxation, it is usually due to magnetic dipole interactions with the moment of the near-lying atomic nuclei, particularly with the moment of the protons of the water in hydrated salts. Therefore in spectroscopic investigations the H_2O is frequently replaced by heavy water D_2O, which leads to a certain narrowing down of the line as the result of the smaller magnetic moment of D. During the initial stages of dilution (for $f > 0.1$) the absorption lines are weakly narrowed down, and sometimes they may even broaden a little, as was noted in [63]. The reason for this is that the exchange interactions decrease with increasing distance more rapidly than the magnetic dipole interactions. Examples of experimentally determined width in dilute paramagnetic salts are

TABLE 5.2

1 Вещество	2 Разве-дение	3 Полу-ширина	4 Условия опыта			6 Лите-ратура
			λ, см	T, °K	Состояние вещества	
$(Mn^{2+}, Zn^{2+})\,S$	10^{-3}	$7,5\pm0,5$	3,2	300—4,2	Монокр.	[68]
$(Pr^{3+}, La^{3+})\,Cl_3$	10^{-4}	$5,5\pm0,5$	3,2	»	»	[68]
8 H_0 параллельно оптической оси кристалла	0,11	25	3,2	4,2	»	[69]
9 H_0 перпендикулярно к оптической оси кристалла		180	3,2	4,2	»	[69]

1) Substance; 2) dilution; 3) half width; 4) conditions of experiment; 5) state of substance; 6) literature; 7) monocrystalline; 8) H_0 parallel to the optical axis of the crystal; 9) H_0 perpendicular to the optical axis of the crystal.

TABLE 5.3

1 Вещество	$2\pi\tau' \cdot 10^9$, сек 2
$VOCl_3$	10,5
$VOSO_4$	1,85
$CuCl_2 \cdot 2H_2O$	8,65
$CuSO_4 \cdot 5H_2O$	4,05
$Cu(NH_3)_4SO_4 \cdot H_2O$	15,3
$Cu(NO_3)_2 \cdot 6H_2O$	2,70
$CrCl_3$	3,50
CrF_3	0,77
$Cr_2(SO_4)_3$	0,60
$Cr_2(OH)_6 \cdot H_2O$	1,88

1) Substance; 2) sec.

listed in Table 5.2.

Information on the spin-spin interactions in paramagnets in the absence of constant fields H_0 can be obtained from absolute measurements of the absorption coefficient at $H_0 = 0$. Measurements of this type were made for several salts by Gorter [34] and later by Rivkind [70]. The values of $\tau'(0)$ obtained by the latter at 10 megacycles are listed in Table 5.3.

2. Spin-lattice relaxation in solid paramagnets

Investigations of spin-lattice relaxation were started by Gorter [34] even before the discovery of paramagnetic resonance, in the 1930's. His method consisted of measuring the dependence of the coefficients χ' and χ'' on the intensity of a static magnetic field $H_{||}$, situated parallel to an oscillating magnetic field of constant frequency ν. The frequency that Gorter used in his experiments was on the order of 10^6-10^7 cps. A phenomenological theory of spin-lattice relaxation in parallel fields was proposed by Casimir and du Pre [71] for the case $\tau \gg \tau'$.

The phenomenological theory of relaxation phenomena in parallel fields was further developed by Shaposhnikov [4], who took into account the role of the spin-spin interactions in the general relaxation effect. A summary of the experimental values of τ obtained up to 1947 by Gorter and his co-workers is contained in his book [34]. Later measurements of τ by the method of parallel fields can be found in [72-74, 41] and elsewhere. We shall note here only the principal results, without stopping to describe the experiments.

Measurements at temperatures from 300 to $64^\circ K$ were made in hydrated salts of the iron-group ions and in salts of Gd^{3+}. The longest spin-lattice relaxation times were found in salts of Mn^{2+}, Gd^{3+} and Cr^{3+}; they have an order of $10^{-7}-10^{-8}$ sec at room temperatures. Very short values of τ, which are observed for example in salts of Co^{2+} or particularly in salts of Ti^{3+} could not be measured by the parallel-field method in the indicated temperature interval, since the condition $\tau > \tau'$ is not satisfied there.

A small number of salts of Mn^{2+}, Fe^{3+}, Gd^{3+}, Cr^{3+}, and Co^{2+} and of a few other ions were investigated in the region of helium temperatures. Their relaxation times are on the order of $10^{-2}-10^{-4}$ sec.

We shall consider first the region of high temperatures, where combination processes predominate.

In this region, the dependence of τ on $H_\parallel$ is well described by a formula proposed by Brons [75], which was theoretically confirmed in a paper by Van Vleck [37]:

$$\tau = \tau_0 \frac{\frac{b}{C} + H_\parallel^2}{\frac{b}{C} + pH_\parallel^2},$$

(5.68)

Here $b = C_H T^2$ is the constant of magnetic specific heat, C is the Curie constant, τ_0 is the spin-lattice relaxation time at $H_0 \to 0$; $p =$

$= \tau_0/\tau_\infty$, where τ_∞ is the same time when $H_0 \to \infty$. According to Van Vleck $p < 1$, and therefore the value of τ should increase with increasing field intensity $H_{\parallel}$ and tend in the limit to τ_∞. The temperature dependence is contained essentially in the factor $\tau_0 \sim T^{-2}$ with $T \gg \theta$. Experiment shows, however, that the value of $\underline{p}$ sometimes varies with the temperature. The experimental data obtained for the temperature range from 300 to $64°K$ agree qualitatively in most cases with the theoretical predictions; the value of τ calculated by Van Vleck for chrome alums agrees with the experimental values also in order of magnitude. Nonetheless one cannot speak of strict agreement between theory and the experimental data. The main reason for the discrepancies is apparently the fact that the measurements of the spin-lattice relaxation time in parallel fields is possible only if $\tau \gg \tau'$ whereas in Van Vleck's theory the spin-spin interactions are taken into account only very approximately.

Another reason that leads in individual cases to major qualitative disagreements with the theory may be the phase transitions in the paramagnet occurring as the temperature of the experiment is varied. In particular, this may explain the reduction in τ on cooling, observed by Garif'yanov [76] in iron-ammonia alum, in which the phase transition point lies according to his measurements near $200°K$.

A similar behavior is exhibited by potassium chrome alum (phase transition point near $90°K$) and also by gadolinium sulfate [34].

Tables 5.4 and 5.4a contain certain data pertaining to the values of τ in the high temperature region ($77-300°K$), obtained by the parallel-field method.

In the region of helium temperatures, where the direct processes should predominate, Van Vleck's theory agrees much worse with experiment. In particular, for the direct processes the theory requires that

TABLE 5.4

Spin-Lattice Relaxation Time

1 Вещество	H_{ll}, эрст	$\frac{b}{c} \cdot 10^{-8}$, эрст²	$2\pi\tau \cdot 10^6$, сек 77° K	90° K	290° K	4 Другие температуры, °K (в скобках)	5 Литература
Cr(NO₃)₃·9H₂O	0	1,1	2,2	0,7			[72]
	800		3,2	1,1			
	1600		3,9	1,52			
	2400		5	2,13			
	3200		5,3	2,38			
	>4000		6,3	3,2			
CrK(SO₄)₂·12H₂O	0	0,65	0,9—0,7;	0,33—0,25;			[72]
	>4000		4,1—2,8;	2,1—2,0			[72]
	0				~0,01;	~0,001 (200)	[76]
Cr(NH₄)(SO₄)₂×12H₂O		2,68					
[Cr(H₂O)₆]Cl₃	0	0,96		2,5			[72]
	>4000			5			
[Cr(NH₃)₆]Cl₃	≤3200	13	0,2	0,18			
[Cr(H₂O)₄Cl₂]Cl×2H₂O	0	4,5	1,2	1,05			
	>4000		1,9	1,5			
	1000				0,04		[64]
	2000	4,1			0,085		
	3000				0,13		
[CrF₆]K₃	0	8	0,19	0,15			
	1600		0,22	0,18			
	2400		0,25	0,22			
	3200		0,28	0,24			
[Cr(—OOC—COO)₃]K₃	0	27	0,3	0,22			
	1600		0,32	0,24			
	2100		0,36	0,27			
	3200		0,41	0,33			
Fe(NO₃)₃·9H₂O	800	19,5	0,71	0,38		0,8 (64,4)	
	1600		0,78	0,49		1,1 (64,4)	
	2400		0,84	0,56		1,2 (64,4)	
	3200		0,98	0,69		1,35 (64,4)	[72]
Fe(NH₄)(SO₄)₂×12H₂O	0	0,27	0,25	0,04		0,75 (64); <0,02 (195)	[72]
	100		0,26	0,042			
	200		0,27	0,046			
	300		0,28	0,05			
	400		0,33	0,055			
	800		0,62	0,1			
	1600		1,1	0,23			
	3200		1,79	0,53			
	4800		2,06	0,8			
	>4000		2,1	0,9		3 (64)	
Fe(ND₄)(SO₄)₂× ×12D₂O (93%D)	0				~0,01	~0,001(200)	[74]
	0	0,27	0,32	0,08		0,75 (64)	
	>4000		2,2	1		3 (64)	[72]
(Fe, Al)(ND₄)(SO₄)₂·12D₂O	~0	0,27	<0,32	<0,08			
Gd₂(SO₄)₃·8H₂O	0	3,9	1,6	1,95	0,42		
	800		1,75	2,1	0,5		
	1600		2,1	2,5	0,55		
	2400		2,5	2,85	0,69		
	3200		2,8	3,15	0,79		
	>4000		4	4,2	1,25		
Gd(CH₃—COO—)₃·4H₂O	1600		0,67	0,41	0,11	0,27 (195)	[72]
	2400		0,71	0,46	0,125	0,28 (195)	
	3200		0,77	0,51	0,14	0,29 (195)	
Gd₂(—OOC—COO—)₃·10H₂O	0	1,8	1,5	1,5		0,24 (195)	
	800		1,75	1,8		0,31 (195)	
	1600		2	2		0,45 (195)	
	2400		2,7	2,7		0,69 (195)	
	3200		2,9	2,95		0,85 (195)	
	>4000		3,6	3,6		1,5 (195)	
Gd(NO₃)₃·6H₂O	800	2,06			0,55		
	1600				0,72		
	2400				0,86		
	3200				0,96		
	4000				1		
	5000				1,1		

TABLE 5.4 (Conclusion)

1) Substance	2) oersted						5)
$GdCl_3 \cdot 4H_2O$	800	5,1			0,53		[74]
	1600				0,59		
	2400				0,64		
	3200				0,69		
	4000				0,72		
	5000				0,75		
$MnCl_2 \cdot 4H_2O$	800	19,8			1,41		[98]
	1200				1,56		
	1600				1,6		
	2000				1,79		
$MnCl_2 \cdot 4H_2O$	2400				1,94		[98]
	2800				2,12		
	3200				2,2		
	3600				2,4		
$Mn(NO_3)_2 \cdot 6H_2O$	800	1,2					[73]
	1200				0,3		
	1600				0,35		
	2000				0,37		
	2400				0,38		
	3200				0,39		
$MnSO_4 \cdot 4H_2O$	0	6,2	4	3,2	0,32		$T=290°K$ [73], при низких температурах [72]
	800	5±2			0,28		
	1600				0,37		
	2400				0,47		
	3200				0,53		
$Mn(NH_4)_2(SO_4)_2 \times 6H_2O$	0	0,64		5,5	0,40	0,93 (195)	$T=290°K$ [98], при низких температурах [72]
	>4000			11	0,80	1,85 (195)	
	1200				0,66		
	1600				0,74		
	2000				0,77		
	2400				0,8		
	2800				0,82		
	3200				0,83		
	3600				0,835		
$NiSO_4 \cdot 7H_2O$		90?	0,1?	0,08?			[72]
$Ni(NH_4)_2(SO_4)_2 \times 6H_2O$		90?	0,14?	0,11?			
$V(NH_4)_2(SO_4)_2 \times 6H_2O$		4,8					

1) Substance; 2) oersted; 3) sec; 4) other temperatures, °K (in parentheses); 5) literature; 6) at low temperatures.

TABLE 5.4a

1 Вещество	$H_{\parallel}$ эрст (2)	$\frac{b}{C} \cdot 10^{-8}$ эрст²	$2\pi\tau \cdot 10^9$, сек (3)		290 K				Литература (4)
			77° K	90° K	поро-шок (5)	ось K_1	ось K_2	ось K_3	
$CuSO_4 \cdot 5H_2O$	800	0,47 (порошок)			0,01	0,01	0,01	0,008	При низких темпе-ратурах [72]
	1600	0,4 (ось K_1)			0,015	0,015	0,014	0,012	

- 258 -

TABLE 5.4a (Conclusion)

Вещество	$H_{||}$, эрст	$\frac{b}{C} \cdot 10^{-6}$, эрст³	$2\varkappa\tau \cdot 10^{-8}$, сек 77°K	90°K	290°K порошок	290°K ось K_1	290°K ось K_2	290°K ось K_3	Литература
CuK$_2$(SO$_4$)$_2$·6H$_2$O	2400	0,6 (ось K_2)			0,02	0,025	0,023	0,017	При $T=$290°K [41] (7)
	3200				0,025	0,03	0,027	0,02	
	4000				0,028	0,033	0,03	0,022	
	4800				0,03	0,035	0,032	0,023	
	5600				0,031	0,036	0,033	0,024	
	400	0,12 (порошок)	0,66	0,43					При низких температурах [72] (6)
	800		0,8	0,48	0,008	0,008		0,008	
	1600	0,11 (ось K_1)			0,009	0,009		0,009	при $T=$290°K [41] (7)
	2400	0,15 (ось K_2)	0,9	0,54	0,01	0,01		0,009	
	3200				0,01	0,01		0,009	
	4000				0,01	0,01		0,009	
	4800				0,01	0,01		0,009	
	5600				0,01	0,01		0,009	
Cu(NH$_4$)$_2$(SO$_4$)$_2$ × × 6H$_2$O	400	0,18	0,47	0,28					При низких температурах [72] (6)
	800	0,16 (порошок)	0,59	0,33	0,008	0,008		0,008	
	1600	0,16 (ось K_1)			0,01	0,012		0,01	при $T=$290°K [41] (7)
	2400	0,16 (ось K_2)	0,67	0,44	0,012	0,013		0,011	
	3200				0,013	0,014		0,012	
	4000				0,014	0,015		0,013	
	4800				0,014	0,015		0,013	
	5600				0,014	0,015		0,013	

Remark. K_1, K_2, and K_3 are the principal magnetic axes of the crystal, see §4.1.

1) Substance; 2) oersted; 3) sec; 4) literature; 5) powder; 6) at low temperatures; 7) at T = 290°K.

τ be proportional to H_0^{-2} and T^{-1}; in addition, naturally, there should be no observed dependence of τ on the magnetic concentration N_0. Yet, according to [77], experience shows in concentrated salts a stronger dependence on the temperature than T^{-1}, and the dependence on H_0 can be expressed up to rather strong fields by means of $\tau \sim (b + CH_0^2)$. Finally, an increase in τ is observed in most cases upon dilution* $\tau(\tau \sim N_0^{-1})$. Moreover, for concentrated salts the Casimir and du Pre formula itself is not in good agreement with the experimental results. They can be described satisfactorily only with the aid of an entire set of values of τ. However, when the magnetic dilution of the specimens increases, the deviations from the Casimir and du Pre formula de-

crease. The dependence of τ on the concentration also becomes weaker, and at sufficient degrees of dilution the relaxation time becomes constant.

The dependence $\tau(H_0)$ has a complicated form in dilute specimens. At small values of H_0 the relaxation time increases with the field but reaches rapidly a maximum (corresponding to several hundred oersted), after which τ becomes approximately proportional to H_0^{-1}. Thus, in dilute paramagnets the deviation from the theory turns out to be somewhat smaller, but is nevertheless not completely eliminated.

TABLE 5.5

Spin-Lattice Relaxation at Low Temperatures [72]

1 Вещество	T, °K	$H_{||}$, эрст (2)	$2\pi\tau\cdot10^4$, сек (3)	4 Метод
KCr (SO₄)₃ · 12H₂O	20,4	4000	0,21	5 Поглощение в параллельных полях
	14,3	4000	0,31	
Gd₂ (SO₄)₃ · 8H₂O	20,4	800	0,0054	Дисперсия восприимчивости в параллельных полях
		1600	0,006	
		2400	0,0074	
		3200	0,009	
		4000	0,012	6
MnSO₄ · 4H₂O	20,5	670	1,37	Поглощение и дисперсия в параллельных полях
		1120	1,52	
		1685	1,82	
		2250	2,13	
		3370	2,64	
		4030	2,78	
	18,4	670	2,56	7 То же
		1120	2,82	
		1685	3,30	
		2250	3,90	
		3370	4,90	
		4030	5,12	6
	14,4	670	9,3	Поглощение и дисперсия в параллельных полях
		1120	10,5	
		1685	12,5	
		2250	14,5	
		3370	18,2	
		4030	19,0	6
Mn (NH₄)₂ (SO₄)₂ × ×6H₂O	20,3	0	1,06	Поглощение и дисперсия в параллельных полях
		→∞	2,47	
	14,3	0	5,86	
		→∞	13,6	
	4,21	0	50,3	
		→∞	117	

1) Substance; 2) oersted; 3) sec; 4) method; 5) absorption in parallel fields. Dispersion of susceptibility in parallel fields; 6) absorption and dispersion in parallel fields; 7) the same.

TABLE 5.5a

Average Spin-Lattice Relaxation Times at Low Temperatures [72]

1 Вещество	$H_{\parallel}$, эрст	$2\pi\bar{\tau}\cdot 10^3$, сек	$\tau_{1/2}/\bar{\tau}$	T, °К
KCr(SO₄)₂·12H₂O Образец A	790	2,48	—	4,04
	2250	5,1	—	4,04
	3370	6,7	—	4,04
	790	9,8	—	2,58
	2250	19,5	—	2,58
	3370	23,5	—	2,58
	790	20,0	—	1,95
	2250	36,3	—	1,95
	3370	44,1	—	1,95
Образец B	710	1,6	1,3	2,68
	2480	3,6	1,29	2,68
	3100	4,2	1,34	2,68
	710	12,5	1,0	1,34
	2480	29	1,28	1,34
	3100	34	1,27	1,34
K₂Cu(SO₄)₂·6H₂O	225	30	1,6	4,015
	340	40	1,5	
	450	45	1,4	
	657	50	1,3	
	226—339			2,16
	226—339			1,0
Cu(NH₄)₂(SO₄)₂·6H₂O	286—428	210		2,18
	286—428	240—250		0,97
Fe(NH₄)(SO₄)₂·12H₂O Образец A	2250	2,40	1,24	3,61
	3370	4,78	1,27	3,61
	4500	7,58	1,33	3,61
	450	0,98	1,00	3,00
	675	1,50	1,11	3,00
	1120	3,01	1,14	3,00
	1685	5,74	1,21	3,00
	2250	9,90	1,30	3,00
	3370	18,0	1,31	3,00
	4500	26,9	1,40	3,00
	450	2,10	1,21	2,51
	675	3,38	1,11	
	1120	5,78	—	
	1685	11,3	1,27	
	2250	19,1	—	
	3370	42,0	—	
	113	4,26	—	1,89
	225	4,46	—	
	450	6,53	1,16	
	675	8,70	1,15	
	1120	18,7	1,17	
	225	9,09	.	1,61

1 Вещество	$H_{\parallel}$, эрст	$2\pi\bar{\tau}\cdot 10^3$, сек	$\tau_{1/2}/\bar{\tau}$	T, °К
	450	12,2	—	
	675	15,9	—	
	1120	36	—	
Образец B	450	1,82	4,02	4,08
	675	2,29	3,53	
	1120	5,72	3,49	
	1685	11,8	2,83	
	2250	15,9	2,50	
	3370	27	2,32	
	4500	36	1,68	
	450	8,5	2,12	2,98
	675	14,9	1,41	
	1120	29	2,24	
	2250	83	1,62	
	3370	133	1,47	
	4500	180	1,33	
Образец C	225	2,9		2,96
	450	4,6	2,01	
	675	7,5	1,98	
	1120	15,5	1,74	
	1685	31,7	1,81	
	113	11	1,2	2,32
	225	13,1	1,48	
	450	19,2	1,63	
	675	26,7	1,63	
	1120	58	1,53	
	1685	100	1,27	
Gd(SO₄)₃·8H₂O	1120	25		4,15
	1685	29		
	2250	37		
	3370	45		
	4030	55		
	570—851	44—50		2,16
	570—851	314		0,99

Remark. In order to calculate these data, which were obtained by measuring $\chi'(H_0)$ and $\chi''(H_0)$ in parallel fields H , the factors $(1 + \tau^2\omega^2)^{-1}$ and $\tau(1 + \tau^2\omega^2)^{-1}$ in the Casimir and du Pre formulas have been replaced by $\int \frac{g(\tau)}{1+\tau^2\omega^2}\,d\tau$ and $\int \frac{\tau g(\tau)}{1+\tau^2\omega^2}\,d\tau$, with $g(\tau)d\tau = 1$. $\bar{\tau}$ denotes the mean value of τ in the continuous distribution $g(\tau)$; $\tau_{1/2}$ denotes the value of τ given by the relation $g(\tau_{1/2}) = g(\tau)/2$; the ratio $\tau_{1/2}/\bar{\tau}$ characterizes the width of the distribution of the relaxation times.

1) Substance; 2) oersted; 3) sec; 4) sample.

Tables 5.5 and 5.5a list some data obtained by Gorter and his co-workers [72] in measurements of paramagnetic relaxation in the region of helium temperatures.

Along with the method of parallel fields, the relaxation time has been measured in recent years by the method of saturation of the paramagnetic resonance line. In this case it is possible to use in principle much greater magnetic dilutions. In addition, the saturation method makes it possible to determine the relaxation constants for individual resonance transitions, whereas the method of parallel fields gives only summary quantities. On the other hand, the saturation method is not free of shortcomings; it is very difficult to use it for the determination of the dependence $\tau(H_0)$ since this calls for measurements over a wide range of frequencies; to study short relaxation times it is necessary to use an oscillating field of very large power; finally, the experiments themselves are much more difficult to set up than in the method of parallel fields.

The first relaxation measurements by the saturation method were made in 1949 by Schlichter and Purcell [78] in undiluted salts of Mn^{2+} and Cu^{2+} at room temperature and at the temperature of dry ice. The sample was placed in a resonant cavity used to terminate one of the arms of a T-bridge. To generate the strong microwave magnetic field (with an approximate amplitude of 30 oersteds) needed to saturate the broad absorption lines, a pulse magnetron was used. In view of the transient effects connected with short pulses, the ordinary bridge technique was somewhat modified. The relaxation times T_1 for $Mn(NH_4)_2(SO_4)_2 \cdot 6H_2O$, the sulfate of Mn^{2+}, and the sulfate of Cu^{2+} were found to be on the order of 10^{-8} sec.

Schneider and England [79] measured T_2 in a specimen of ZnS with a small content of Mn^{2+} at 90°K. Since the absorption lines were nar-

- 262 -

row, experiments on the saturation were carried out with an ordinary
klystron as a source of microwave field. The measurements were made at
the temperature of liquid air and have led to values of the spin-lat-
tice relaxation time close to those observed by Gorter in undiluted
salts of Mn^{2+}.

Eschenfelder and Weidner [80] carried out saturation experiments
in single crystals of dilute potassium chrome alum and iron ammonia
alum at 2-4°K. The measurements were made by the reflection method us-
ing a T bridge. The source of the microwave field was a klystron with
1 watt output power. A toroidal sample of the substance was placed in
a cylindrical cavity coupled to a waveguide. To ensure thermal insula-
tion, part of the waveguide was made of glass coated with a thin layer
of silver.

The spin-lattice relaxation time was determined with the aid of
the formula

$$\frac{Q_M}{Q_L} = B \frac{T}{g(\nu)} + A \Gamma T_1 p_1 (1 - \Gamma)^2.$$

Here Q_M and Q_L are the Q factors of the cavity with and without mag-
netic losses, B is a certain constant,

$$A = \frac{4(2S+1)k}{N(h\nu)^2(1-\Gamma_0)},$$

Γ is the reflection coefficient at the resonant value of the field H =
= H_{rez}, Γ_0 the same quantity at H >> H_{rez}, p_1 is the incident power,
and

$$\frac{Q_M}{Q_L} = \frac{(1-\Gamma)}{(\Gamma-\Gamma_0)}.$$

From the experimental dependence $\Gamma(p_1)$ it is possible to deter-
mine the spin-lattice relaxation time $T_1 = 1/2W$, where W is the proba-
bility of the relaxation transitions. It is most convenient to do this
by plotting the quantity Q_M/Q_L as a function of $p_1(1 - \Gamma)^2$; the slope
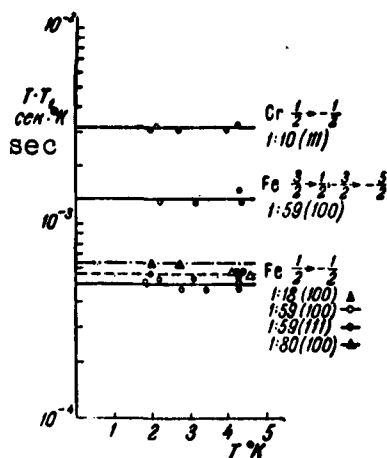
- 263 -

of the resultant line makes it possible to determine TT_1 independently of $g(v)$.

The basic results obtained for $KCr(SO_4)_2 \cdot 12H_2O$ and $Fe(NH_4)(SO_4)_2 \cdot 12H_2O$ are shown in Fig. 5.4. On the right side of this figure are indicated, for both salts, the corresponding resonant transitions, the magnetic dilutions, and the crystal orientations. It is seen from the figure that, in accordance with the theory, the time T_1 is inversely proportional to the absolute temperature. The magnetic dilution investigated in iron-ammonia alums lengthens the time T_1 by only a very small amount.

Fig. 5.4. Results of measurement of the temperature dependence of the relaxation time T_1 by the saturation method for $KCr(SO_4)_2 \cdot 12H_2O$ and $Fe(NH_4)(SO_4)_2 \cdot 12H_2O$ [80].

Bloembergen and Wang [48] continued the experiments of Slichter and Purcell on the study of the spin-lattice relaxation time in substances with broad absorption lines, using pulse techniques. Their setup made it possible to obtain in the resonant cavity a microwave magnetic field with a pulsed amplitude up to 50 oersted. The following relation, which is derivable from Bloch's formula (5.1), holds true under paramagnetic resonance conditions:

$$\frac{M_z}{M_0} = \frac{\chi''}{\chi_0} = \frac{1}{1 + \frac{1}{4}\gamma^2 H_1^2 T_1 T_2}.$$

Here χ'' and χ_0 are the absorption coefficients for the given amplitude H_1 and when $H_1 \rightarrow 0$, i.e., in the absence of saturation. If the value of γ and the width of the resonance line are known, then the time T_1 can be determined either by measuring χ''/χ_0 or by measuring M_z/M_0 at different amplitudes H_1. Measurements carried out by both methods in $MnSO_4 \cdot 4H_2O$ have shown good agreement with Gorter's data, as can be seen from Table 5.6.

TABLE 5.6

Relaxation Time in $MnSO_4 \cdot 4H_2O$

1 Метод	300° K	77° K
2 Нерезонансная дисперсия........	$1,0 \cdot 10^{-7}$ сек	$1,3 \cdot 10^{-8}$ сек
3 Насыщение	$0,78 \cdot 10^{-7}$ »	$1,2 \cdot 10^{-8}$ »

1) Method; 2) nonresonant dispersion; 3) saturation; 4) sec.

There is no doubt that extensive use of the saturation method will add in the very near future to the far from sufficient experimental data on the spin-lattice relaxation times in crystalline paramagnets.

An appreciable step forward toward the study of relaxation at low temperatures was made in a recent work by Giordmaine, Alsop, Nash, and Townes [58]. These authors measured the relaxation times in $Gd_2Mg_3(NO_3)_{12} \cdot 24H_2O$; $K_3Cr(CN)_6$ and $Cu(NH_4)_2(SO_4)_2 \cdot 6H_2O$ at temperatures $1-4°K$. Two methods were used: 1) the ordinary method of paramagnetic resonance line saturation, and 2) saturation of the lines by strong microwave pulses with subsequent measurement of the rate of reestablishment of equilibrium by observing the absorption of a weak microwave signal as a function of the time elapsed after the cessation of the strong pulse causing the saturation. This observation was made with the aid of a synchronized frequency sweep of the vicinity of paramagnetic resonance by means of two different klystrons. The pulses were usually repeated at a rate considerably smaller than the relaxation rate. The time between the saturation and the instant of measurement of the absorption can be readily varied by changing the difference in the frequencies radiated by the strong and weak generator or by changing the sweep rate. The relaxation times determined with the aid of both methods turned out to be close to one another, with the excep-

tion of the copper salt. The obtained values of T_1 together with the data on the line width are presented in Table 5.7.

For the Gd^{3+} salts, the observed width is connected with hyperfine interactions, and the times T_1 vary as functions of the studied transition by approximately two times. They depend also somewhat on the specimen chosen, on the concentration of the Gd^{3+} ion, and on the temperature.

TABLE 5.7

1 Вещество (концентрация ≤ 1 : 100 ат. %) и переход	2 Диамагнит- ный разба- витель	3 ΔH, эрст (ширина на по- ловине макси- мальной интен- сивности)	4 T_1 из времени экспоненциаль- ного спада, сек	5 T_1 из на- сыщения, сек
$Gd_2Mg_3(NO_3)_{12}\cdot24H_2O$ $M\left(-\dfrac{1}{2}\right)\to M\left(\dfrac{1}{2}\right)$	La	2,0	$7\cdot10^{-3}$	$15\cdot10^{-3}$
$K_3Cr(CN)_6$ $M\left(-\dfrac{1}{2}\right)\to M\left(\dfrac{1}{2}\right)$	Co	12	$3\cdot10^{-3}$	$4\cdot10^{-3}$
$Cu(NH_4)_2(SO_4)_2\cdot6H_2O$ $M\left(-\dfrac{1}{2}\right)\to M\left(\dfrac{1}{2}\right)$ $m\left(\dfrac{3}{2}\right)\to m\left(\dfrac{3}{2}\right)$	Zn	20	20	2

1) Substance (concentration <1:100 atomic %); and transition; 2) diamagnetic diluent; 3) ΔH, oersted (width at half the maximum intensity); 4) T_1 determined from the time of exponential decrease, sec; 5) T_1 determined from saturation, sec.

§5.6. Solutions of Paramagnetic Salts. Theory

1. Until now, calculations of the line shape of paramagnetic resonance in liquids have been made with the aid of the correlation theory. The use of the correlation method is quite natural, since it permits the simplest evaluation of the effect of Brownian motion of the particles on the width of the absorption lines. We shall describe briefly this method and its application to calculations of the broadening of resonance lines.

Let $F(t)$ be a certain random function of the time, the mean value of which is denoted $\langle F(t) \rangle$. Let us assume that $\langle F(t) \rangle = 0$. The correlation function, as is well known [81], is defined as

$$K(\tau) = \langle F(t) F(t+\tau) \rangle. \qquad (5.69)$$

Let us introduce the Fourier transform $I(\nu)$ of the correlation function defined in the following fashion:

$$K(\tau) = \int_{-\infty}^{\infty} I(\nu)\, e^{-2\pi i \nu \tau}\, d\nu, \quad I(\nu) = \frac{1}{2\pi} \int_{-\infty}^{\infty} K(\tau)\, e^{-2\pi i \nu \tau}\, d\tau. \qquad (5.70)$$

The correlation function obviously decreases with increasing τ. For most cases considered below, it can be proved that the decrease in the correlation function with time obeys the Markov law:

$$K(\tau) = \langle |F(t)|^2 \rangle\, e^{-\frac{|\tau|}{\tau_c}}, \qquad (5.71)$$

where τ_c is a certain parameter called the correlation time. Substituting (5.71) in (5.70) we obtain

$$I(\nu) = \frac{1}{2\pi} \langle |F(t)|^2 \rangle\, \frac{2\tau_c}{1 + 4\pi^2 \tau_c^2 \nu_{lk}^2}. \qquad (5.72)$$

Assume that we have a quantum system with energy levels E_l, subject to the action of time-varying random perturbations $\hat{H}'(t)$. The matrix element of the perturbation $H_{lk}(t)$ will be a random function of the time. Using the ordinary theory of time-dependent perturbations we can readily show that the probability of the transition of a quantum system from the state E_l to the state E_k under the influence of the perturbation $\hat{H}'(t)$ per second is

$$A_{lk} = \frac{4\pi^2}{h^2} I(\nu_{kl}). \qquad (5.73)$$

With the aid of (5.72) we obtain alternately

$$A_{lk} = \frac{2\pi}{h^2} \langle |\mathscr{H}'_{lk}(t)|^2 \rangle\, \frac{2\tau_c}{1 + 4\pi^2 \tau_c^2 \nu_{lk}^2}. \qquad (5.74)$$

- 267 -

For further calculations it is necessary to clarify the nature of the relaxation mechanism, or in other words, the origin of the perturbation $\hat{H}{}'(t)$.

2. The first theory of paramagnetic resonance line shape in liquids was proposed by Bloembergen, Pound, and Purcell [82]. To be sure, this paper dealt specifically with nuclear resonance, but its results can be directly applied to liquid electronic paramagnets. In the theory of Bloembergen et al, as was done by Waller in the case of crystals, it is assumed that the relaxation is due to magnetic interactions of the particles. Consequently, the perturbation $\hat{H}{}'(t)$ can be expressed with the aid of (5.9), assuming that $\underline{r}$, ϑ, and φ are time-varying as a result of Brownian motion. Let us assume that all the Zeeman levels of the magnetic particles are equidistant, so that there is only one Larmor precession frequency ν_0. If we calculate the nondiagonal matrix elements $\hat{H}{}'(t)$, carry out the necessary averaging, and then substitute the resultant expressions for A_{1k} in (5.40), we obtain for the time of longitudinal relaxation

$$\frac{1}{T_1} = \frac{8\pi^2}{5h^2}\, g^6\beta^2 S(S+1)\left[\frac{\tau_c}{1+4\pi^2\tau_c^2\nu_0^2} + \frac{4\tau_c}{1+16\pi^2\tau_c^2\nu_0^2}\right]\sum_k \left\langle\frac{1}{r_k^6}\right\rangle. \qquad (5.75)$$

If $\underline{r}$ is the distance between two interacting particles, then we must assume the correlation time to be the average time necessary for this distance to double as a result of Brownian motion. Thus, the quantity τ_c will naturally be a function of $\underline{r}$, namely $\tau_c = r^2/12D$, where D is the diffusion coefficient, the value of which is, by Stokes' formula:

$$D = \frac{kT}{6\pi a_0\eta}. \qquad (5.76)$$

Here a_0 is the radius of the particle and η the viscosity coefficient. Recognizing that the inequality $2\pi\nu\tau_c \ll 1$ holds true for all particles that are sufficiently close to one another to make their interaction significant in the relaxation process we obtain from formula

- 268 -

(5.75), after replacing the summation by integration with respect to $\underline{r}$,

$$\frac{1}{T_1} = \frac{8\pi^4 g^4 \beta^4 N_0 \eta S (S+1)}{h^6 kT}.$$ (5.77)

Bloembergen, Purcell, and Pound took account also of the influence of the Brownian motion on the magnitude of the transverse relaxation time. This question was subsequently investigated in detail in [30-32]. An estimate of the transverse relaxation time due to magnetic interaction of the particles can be carried out in accordance with the following formula:

$$\frac{1}{T_2} = \sqrt{\frac{3}{\pi} K_1 \arctan \frac{2\tau_c}{T_2}}, \quad K_1 = \frac{2}{5} \frac{g^2 \beta^2}{h^2} S(S+1) \sum_k \langle \frac{1}{r_k^6} \rangle.$$ (5.78)

If $\tau_c \ll T_2$, we obtain from (5.78), after carrying out the transformations involved in going over from (5.75) to (5.77),

$$\frac{1}{T_2} = \frac{48\pi^2}{5} \frac{g^4 \beta^4 N_0 \eta}{h^2 kT} S(S+1).$$ (5.79)

By way of an example let us point out that for an aqueous solution of a salt of divalent manganese we obtain for $N_0 \approx 6 \cdot 10^{20}$ cm^{-3} from (5.77) a value $1/T_1 \approx 4 \cdot 10^9$ sec^{-1}.

It must be borne in mind that at large paramagnetic-ion concentrations the line shape can be appreciably influenced also by exchange interactions. However, experiments on paramagnetic resonance in ionic solutions are set up for the most part at such low magnetic-particle concentrations that the relaxation mechanism is determined no longer by magnetic or exchange interactions.

3. From an analysis of the experimental data on paramagnetic absorption in solutions, Kozyrev [83] arrived at the conclusion that the solvate complex formed of the paramagnetic ion and the dipole molecules of the solvent surrounding it has so high a stability, that it can be regarded in experiments on paramagnetic resonance as a unique type of "microcrystal." Therefore the "spin-lattice" interactions in

solutions turned out to be in many respects analogous to those occurring in solids. The "spin-spin" share of the absorption line width is connected with the fact that the "microcrystals" are randomly oriented in the solution; this should lead to a broadening of the line due to the possible anisotropy of the g factor, and also because the splittings of the spin levels by the "crystalline" electric field depend on the orientation of the "microcrystal" in the external field H_0.

McConnell [84] considered the following relaxation mechanism, connected with the presence of stable solvate shells. When the "microcrystal" rotates under the influence of the Brownian forces, the intervals between the spin levels of the paramagnetic ion change. Therefore energy will be exchanged between the paramagnetic ions and the Brownian motion when the "microcrystal" rotates.

McConnell carried out calculations for the Cu^{2+} ion, for which he assumed the following spin Hamiltonian:

$$\mathscr{H}_{cn} = \beta[g_{\|}H_r S_r + g_\perp(H_p S_p + H_q S_q)] + A I_r S_r + B(I_p S_p + I_q S_q). \qquad (5.80)$$

Here $\underline{r}$, $\underline{q}$, and $\underline{p}$ are unit vectors of the rectangular coordinate system rigidly connected to the octahedron of water molecules. XYZ denotes a stationary system of coordinates; the direction of the external magnetic field H_0 is assumed to coincide with the Z axis. The spin Hamiltonian can be represented in the form

$$\mathscr{H}_{cn} = \mathscr{H}_\bullet + \mathscr{H}_t', \quad \mathscr{H}_\bullet = \tfrac{1}{3}(g_{\|} + 2g_\perp)\beta H S_z + \tfrac{1}{3}(A + 2B)SI. \qquad (5.81)$$

The principal part of the Hamiltonian $\hat{H}_0$ remains constant in time. Calculating the matrix elements of the time-varying perturbation $\hat{H}'_z(t)$ and substituting in (5.74) and (5.40), we obtain

$$\frac{1}{T_1} = \frac{8\pi^2}{15} \frac{(\Delta g \beta H_\bullet + b I_z)^2 h^{-2} \tau_c}{1 + 4\pi^2 \nu_0^2 \tau_c^2}, \qquad (5.82)$$

$$\Delta g = g_{\|} - g_\perp, \quad b = A - B.$$

For the correlation time we can assume an expression that follows from

the well-known Debye theory [82]:

$$\tau_c = \frac{4\pi\eta a_i^3}{3kT}.$$ (5.83)

McConnell considered also the contribution made to the transverse relaxation time T_2 by the Brownian rotation of the microcrystals, at which the resonant conditions vary. The broadening of the paramagnetic resonance lines of a particle whose state is described by the spin Hamiltonian (5.80) can be described with the aid of the following formula for the time T_2:

$$\frac{1}{T_2} = \frac{32\pi}{45}(\Delta g\beta H_0 + bI_z)^2 \hbar^{-2} \operatorname{arctg} \frac{2\tau_c}{T_2}.$$ (5.84)

From formulas (5.82) and (5.84) follow two interesting facts: 1) the absorption line width should depend strongly on the field intensity H_0; 2) different hyperfine components of the paramagnetic resonance line should have different widths.

McGarvey [85] extended McConnell's theory to include ions with $S > 1/2$. For Cr^{3+} he assumed a spin Hamiltonian

$$\mathcal{H}_{cn} = \beta g H_0 S + D\left[S_z^2 - \frac{1}{3}S(S+1)\right]$$ (5.85)

and obtained

$$\frac{1}{T_1} = \frac{32\pi^2}{5}\frac{D^2}{\hbar^2}\left[\frac{\tau_c}{1 + 4\pi^2\tau_c^2\nu_0^2} + \frac{\tau_c}{1 + 16\pi^2\tau_c^2\nu_0^2}\right],$$ (5.86)

$$\frac{1}{T_2} = \frac{64\pi}{15}\frac{D^2}{\hbar^2}\operatorname{arctg}\frac{2\tau_c}{T_2}.$$ (5.87)

For the ions Mn^{2+} and Fe^{3+}, the following term was added to the spin Hamiltonian (5.75):

$$\frac{1}{6}a\left[(S_x^4 + S_y^4 + S_z^4) - \frac{1}{5}S(S+1)(3S^2 + 3S - 1)\right].$$ (5.88)

Calculations have shown that

$$\frac{1}{T_1} = \frac{16\pi^2}{25}\frac{D^2}{\hbar^2}\left[\frac{67\tau_c}{1 + 4\pi^2\tau_c^2\nu_0^2} + \frac{52\tau_c}{1 + 16\pi^2\tau_c^2\nu_0^2}\right],$$ (5.89)

$$\frac{1}{T_2} = \frac{64\pi}{5}\frac{D^2}{\hbar^2}\operatorname{arctg}\frac{2\tau_c}{T_2} + \frac{656\pi}{105}\frac{a^2}{\hbar^2}\operatorname{arctg}\frac{0.6\tau_c}{T_2}.$$ (5.90)

In the calculation of T_1 it was assumed that a = 0. All the calcu-

lations were made under the assumption that the fine components of the Cr^{3+} and of the Mn^{2+} and Fe^{3+} lines merge into one line.

4. We shall show below that in many cases the experimental data on the dependence of the resonant line widths on the temperature and on the intensity of the static magnetic field cannot be explained by means of McConnell's theory. Al'tshuler and Valiyev [86] proposed that the principal mechanism that guarantees longitudinal (spin-lattice) relaxation consists of the following.

In solid paramagnetic ionic crystals, the paramagnetic particle M together with the nearest diamagnetic particles X usually forms a paramagnetic complex, for example MX_6 (M is the metal ion and X a water molecule or some other diamagnetic particle), the interactions within which must be taken into account first of all in explaining the magnetic properties of the substances. In liquids, the presence of the solvate shell enables us to make a similar assumption. It can be assumed that, at least for a time longer than the correlation time of the "spin-lattice interaction," the paramagnetic ion together with the nearest solvent molecules forms a stable complex, the oscillations of which can be characterized by a set of normal coordinates Q_i: the Brownian motion of the liquid molecules perturbs the oscillations of the paramagnetic complex and thereby changes the electric field in which the paramagnetic particle is situated. These changes influence the spin-orbit interaction of the electrons of the paramagnetic ion and consequently can lead to a reorientation of its magnetic moment.

If we expand the matrix element of the "spin-lattice perturbation" in normal coordinates

$$\mathcal{H}'_{ik}(t) = \sum_i V_{ik}^{(i)} Q_i(t) \qquad (5.91)$$

and denote the mean oscillation frequency of the paramagnetic complex

by ν_0, we obtain with the aid of (5.74)

$$A_{ik} = \frac{4\pi^2 \bar{Q}_l^2}{h^2} \sum_l |V_{ik}^{(l)}|^2 \frac{2\tau_c}{1 + 4\pi^2 \nu_{ik}^2 \tau_c^2}. \qquad (5.92)$$

Here $\bar{Q}^2$ is the average value of the square of the oscillator amplitude, which can be calculated from the formula [81]:

$$\bar{Q}^2 = \frac{h}{8\pi m\nu_0} \operatorname{cth}\left(\frac{h\nu_0}{2kT}\right), \qquad (5.93)$$

where $\underline{m}$ stands for the mass of the complex. The oscillations of the paramagnetic complex will be perturbed by the action of the surrounding particles, which execute Brownian motion. Therefore the correlation time is naturally defined as the reciprocal of the damping coefficient γ, which can be estimated from the line width of the satellites in the combination spectra of the paramagnetic ions: $\gamma \approx 10$ cm^{-1} and $\tau_c \sim 1/\gamma \approx$ $\approx 10^{-12}$ sec. From the experimental data [87] on the temperature dependence of the line width of the vibrational structure of the optical spectra of ions in crystals it follows that the width increases with the temperature approximately as $\sqrt{T}$.* In this case the temperature dependence of the probability of the relaxation transition will be determined by the formula

$$A_{ik} \sim \frac{1}{\sqrt{T}} \operatorname{cth}\left(\frac{h\nu_0}{2kT}\right) \qquad (5.94)$$

when $4\pi^2 \nu_{1k}^2 \tau_c^2 \ll 1$ and

$$A_{ik} \sim \sqrt{T} \operatorname{cth}\left(\frac{h\nu_0}{2kT}\right) \qquad (5.95)$$

when $4\pi^2 \nu_{1k}^2 \tau_c^2 \gg 1$.

Let us consider some typical paramagnetic ions.

Cu^{2+}. The system of energy levels arising in a strong cubic field, a weak field of lower symmetry, and an external magnetic field H_0 is shown in Fig. 5.5. This case is characterized by the presence of two relatively close orbital levels, the interval between which is on the order of 1000 cm^{-1} in solid salts. The width of the resonance lines in
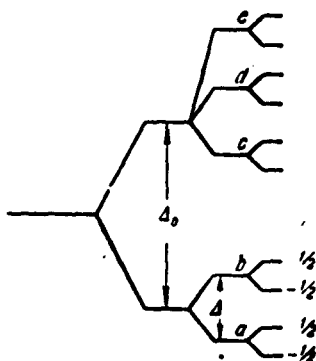
Fig. 5.5. Successive splitting of the energy level of Cu^{2+} under the influence of a strong cubic, weak tetragonal, and external magnetic field.

liquids turns out to be determined by the relaxation transitions between these energy levels without a change in spin direction. For the width of the resonance line we obtain the following expression

$$\Delta v = 2 A_{ab} =$$

$$= 12 \left(\frac{16}{7} \frac{e\mu}{R^3 \Delta_0} \frac{\overline{r^3}}{R^3} \right)^2 \frac{\overline{Q^2}}{R^2} \frac{e^{-\frac{\Delta}{2hT}}}{\tau_c}. \qquad (5.96)$$

Here R is the equilibrium distance from the Cu^{2+} ion to the water molecule, the dipole moment of which is equal to μ. In contradistinction to the McConnell theory, it follows from this formula that the width should be independent of the field H_0. If we assume $v_0 \approx 500$ cm^{-1} [88], then the temperature dependence will be given by the formula

$$\Delta v = \sqrt{\overline{T}} \exp \left(-\frac{\Delta}{2hT} \right). \qquad (5.97)$$

The connection between the relaxation time and the half-width is in this case somewhat unusual and has the form

$$\frac{1}{T_1} \approx \frac{\Delta v}{2} \frac{\exp \frac{\Delta}{hT}}{1 - \exp \left(-\frac{\Delta}{hT} \right)}. \qquad (5.98)$$

It is interesting to note that unlike Δv, quantity $1/T_1$ decreases with increasing temperature. This seemingly strange dependence of the relaxation time on the temperature is explained by the fact that in our case the specific heat of the spin system increases more rapidly upon heating than the probabilities of the relaxation transitions. It must be borne in mind that the nonequilibrium distribution of the particles among the levels a, -1/2 and a, 1/2 (or the levels b, -1/2 and b, 1/2) cannot be annihilated with the aid of the relaxation transitions a, -1/2 → b, -1/2 and a, 1/2 → b, 1/2. Therefore, in addition to

time T_1, there will exist still another relaxation time T'_1, the value of which can be estimated from the formula

$$\frac{1}{T_1} = 6 \frac{\overline{Q^2}}{\hbar^2 R^2} \left(\frac{\lambda g \beta H_0}{\Delta_0^2}\right)^2 \left(\frac{16}{7} \frac{e\mu}{R^2} \frac{\overline{r^2}}{R^2}\right)^2 2\tau_c. \tag{5.99}$$

Cr^{3+}. Calculations have been made for two extreme cases, a strong magnetic field and a weak one. If the field H_0 is strong and the spin levels are equidistant, then

where

$$\frac{1}{T_1} = \frac{96}{20} \frac{\overline{Q^2}}{\hbar^2} (13\varepsilon_1^2 + 4\varepsilon_2^2) \tau_{c_0}$$

$$\varepsilon_1 = 54 \sqrt{3} \frac{\lambda^2}{\Delta_0^2} \frac{e\mu}{R^2} \frac{\overline{r^2}}{R^2};$$

$$\varepsilon_2 = \frac{12 \cdot 324}{175} \frac{\lambda^2}{\Delta_0^2} \frac{e\mu}{R^2} \left(\frac{\overline{r^2}}{R^2} - \frac{55}{36} \frac{\overline{r^4}}{R^4}\right). \tag{5.100}$$

On the other hand if $H_0 = 0$, then

$$\frac{1}{T_1} = 36 \frac{\overline{Q^2}}{\hbar^2} (\varepsilon_1^2 + \varepsilon_2^2) \tau_c. \tag{5.101}$$

Taking into account the fact that for the chrome complexes $\nu_0 \approx$ $\approx 800 \text{ cm}^{-1}$ [88], we obtain $T_1 \approx T_2$.

Mn^{2+}. If we denote by D the spin Hamiltonian constant that determines the splitting of the spin levels in the zero magnetic field, we find that

$$\frac{1}{T_1} = C \frac{D^2}{\hbar^2} \frac{\overline{Q^2}}{R^2} \tau_c. \tag{5.102}$$

where in the case of a strong magnetic field $C = (274 \cdot 64 \cdot 12)/35$; on the other hand, if $H_0 = 0$, then $C = (36 \cdot 16 \cdot 157)/7$. At temperatures 300-400°K we have $h\nu_0 \approx kT$ for Mn^{2+} [56], and therefore the quantity $1/T_1$ first decreases on heating, and then begins to increase.

§5.7. Solutions of Paramagnetic Salts. Experimental Results

As was indicated in Chapter 4, paramagnetic absorption in liquid solutions of Mn^{2+} salts was first observed by Zavoyskiy. He investigated this absorption at frequencies 1-10 Mcs in the presence of static

magnetic fields, situated both perpendicular and parallel [89] to the oscillating magnetic field. Later on a series of measurements of the paramagnetic resonance line widths was undertaken not only in solutions of Mn^{2+} [90-94], but also for other ions of the iron group and the ion Gd^{3+} [64, 94, 84, 85]. Some complex ions were investigated along with the simple ones [95, 85]. The measurements have shown that ΔH in solutions depends strongly on the character of the ion, on the solvent, and on the temperature. The limiting width reached at sufficiently low concentrations, which is independent of further dilution, has different values for different ions. In particular, in solutions of the salts of hydrated ions Ti^{3+}, Fe^{3+}, and Co^{2+} the lines turned out to be so broad, regardless of the dilution, that no resonance effect was observed. The reason for failure to observe the effect is apparently the rather short spin-lattice relaxation time.*

TABLE 5.8

Absorption Line Width in Aqueous Solutions of Iron-Group Salts at Room Temperature

1 Вещество	2 Концентрация моль/л	ΔH, эрст 3	ν, Mгц 4
MnCl₂	4,0	300	10
»	3,0	255	10
»	2,0	200	10
»	1,0	131	10
»	0,5	90	10
»	0,1	48	10
»	0,05	41	10
»	0,03	38	10
»	0,01	35	10
Cr(NO₃)₃	3,0	440±20	9452
»	2,0	310±20	9452
»	1,5	270±20	9452
»	1,0	240±20	9452
»	0,6	220±20	9452
»	0,4	200±20	9452
»	0,2	190±20	9452
Cu(NO₃)₂	4	140	207
»	2	140	207
»	1	140	207
»	0,5	140	207
CuCl₂	4	225	207
»	3	185	207
»	2	160	207
»	1	140	207

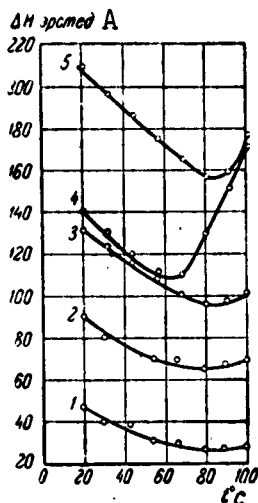1) Substance; 2) concentration, mole/liter; 3) oersted; 4) Mcs.

- 276 -

Fig. 5.6. Dependence of the line width ΔH on the temperature in aqueous solutions of $MnCl_2$ of varying concentrations. 1) 0.005 mole/liter; 2) 0.5 mole/liter; 3) 1 mole/liter; 4) 1 mole/liter $MnCl_2$ + 3 mole/liter LiCl; 5) 2 mole/liter $MnCl_2$. $v = 12.6$ Mcs. A) ΔH, oersted.

In investigations made in the frequency range $10\text{-}10^4$ Mcs [64], the effect is absent in salts of ions having an even number of electrons (Cr^{2+}, Ni^{2+}, V^{3+}); this can be attributed, as in the case of solid salts, to the smallness of the quantum of radio frequency fields as compared with the initial splitting of the spin sublevels.

Certain data on the values of ΔH in iron-group ions at room temperatures are listed in Table 5.8.

For certain ions (Mn^{2+}, Cr^{3+}, Cu^{2+}), an investigation was made of the temperature dependence of ΔH [94]. This dependence is shown in Figs. 5.6-5.8.

The following conclusions can be drawn concerning the line width in solutions.

1) In highly concentrated solutions one observes sometimes relatively narrow lines without a hyperfine structure. The lines broaden upon dilution and a hyperfine structure arises. An example of this are solutions of $VOCl_2$, investigated by Garif'yanov and Kozyrev [96]. It must be assumed that considerable exchange interactions take place in very concentrated solutions of this ion. An analogous fact was noted also in liquid melts of hydrated salts of Mn^{2+} [93].

2) In solutions of Cr^{3+} salts one observes at not too high concentrations a narrowing down of the lines on dilution [64, 85]. This narrowing down should be attributed to the reduction in the magnetic dipole interactions, and perhaps partially also to the increase in the symmetry of the local electric fields acting on the ions, and conse-
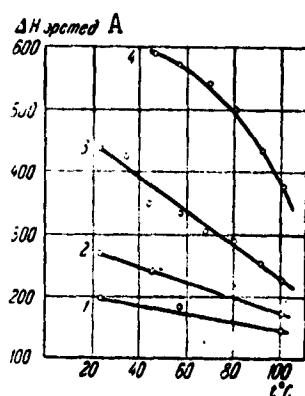
- 277 -

Fig. 5.7. Dependence of the line width on the temperature in aqueous solutions of trivalent chromium of varying concentration. 1) 0.4 mole/liter; 2) 1.5 mole/liter; 3) 3 mole/liter $Cr(H_2O)_6$-$(NO_3)_3$; 4) 1 mole//liter $[Cr(H_2O)_4$-$Cl_2]Cl$. A) ΔH, oersted.
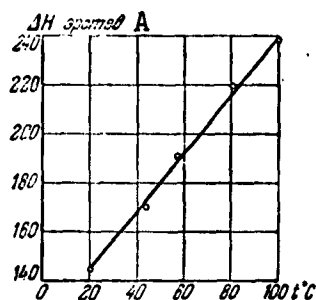

Fig. 5.8. Dependence of ΔH on the temperature in an aqueous solution of 1 mole/liter $Cu(NO_3)_2$. The curve is a plot of the equation $\Delta H = aT^2$. A) ΔH, oersted.

quently to the reduction in the "scatter" of the unresolved fine-structure peaks. As to the limiting line-width, which is no longer dependent on further dilution, it may be due either to spin-lattice interaction or to the scatter of the fine-structure peaks.

3) In aqueous solutions of Cu^{2+} salts [64], the line width is independent of the concentration and of the viscosity (inasmuch as the latter decreases to approximately one fifth as the concentration is varied from 4 to 0.5 moles/liter). Therefore the width cannot be related in this case to the spin-spin interactions, and should be ascribed to spin-lattice interactions.

A comparison of the experimental results with the proposed theories is best made for each ion individually.

Cr^{3+}. The independence of ΔH of the field intensity H_0 is equally well explained either by the calculations of Al'tshuler and Valiyev or by those of McGarvey. The same pertains also to the qualitative explanation of the $\Delta H(T)$ dependence. There are, however, experimental indications that at approximately 250°C the lines begin to broaden with increasing temperature; this broadening can be understood only with the aid of the theory of Al'tshuler and Valiyev.

Mn^{2+}, Fe^{3+}. The McGarvey calculations cannot explain the sharp

difference in the line width measured in the solutions of Mn^{2+} and Fe^{3+} ions, and also the broadening of the Mn^{2+} line resulting from heating above $70^\circ C$. The theory of Al'tshuler and Valiyev makes it possible to understand the observed $\Delta H(T)$ dependence, while the difference in the width of the Mn^{2+} and Fe^{3+} lines is at any rate not in contradiction with this theory.

Cu_{aq}^{2+}. For the Cu_{aq}^{2+} ion, the Al'tshuler and Valiyev theory explains both the independence of ΔH of H_0 and of the concentration, and the line broadening upon heating. However, in solutions of complex copper salts, which give resolved hyperfine structure peaks [97], one observes that I_z influences the width of the individual peaks. This dependence of ΔH on I_z in the case of complex copper ions is explained qualitatively by McConnell's theory. The same pertains, apparently, to solutions of vanadium salts, where the width of the hyperfine structure peaks also depend on I_z.

Recently, Tishkov [98] measured paramagnetic relaxation in parallel fields in solutions of Mn^{2+} salts in water, glycerine, and water-glycerine mixtures. The principal results obtained by him reduce to the following.

1) The experimental $\chi''(H_\parallel)$ are well described by the theory of Casimir and du Pre with account of the spin-spin relaxation as made by Shaposhnikov.

2) The value of τ increases with increasing field $H_\parallel$. The dependence of $\tau(H_\parallel)$ is in good agreement with the Brons-Van Vleck formula.

3) When the concentration of Mn^{2+} is decreased from 3 to 1 mole/liter in an aqueous solution of $Mn(NO_3)_2$, the value of τ increases somewhat; further dilution does not affect τ.

4) A change in the microscopic viscosity of the solution does not affect τ.

5) A change in the nearest surrounding of the Mn^{2+} ion brings about a change in τ.

6) The value of τ as a function of the temperature goes through a maximum corresponding to approximately $20^\circ C$ for 1 mole of solution of $Mn(NO_3)_2$ in water.

None of these results contradict the Al'tshuler and Valiyev theory, while the temperature dependence of τ confirms this theory directly.

Summarizing, we can state that in the case of ions with a small anisotropy of the g factor, the spin-lattice relaxation mechanism is the perturbation of the solvate complex by the Brownian motion. Such ions are, for example, Mn^{2+}, Cr^{3+}, and the hydrated Cu^{2+} ions. On the other hand, in the case of ions having a strong g-factor anisotropy (complex ions of Cu^{2+} and possibly of VO^{2+}), the stronger relaxation mechanism is the one connected with the rotation of the solvate complex.

§5.8. Line Shape under Saturation Conditions

One speaks of saturation of paramagnetic resonance when a noticeable dependence of the magnitude of the effect and of the resonance line shape on the power of the alternating field is observed. The character of the saturation can be twofold, corresponding to two possible types of absorption line broadening [99]. We shall call a broadening uniform, if the absorbed energy of the radio frequency field is distributed among all the spins in such a way that thermodynamic equilibrium is not disturbed during the paramagnetic resonance processes. One can name the following sources of uniform broadening:

1) dipole-dipole interaction between identical magnetic particles;

2) spin-lattice interaction;

3) interaction between the spins and the radiation field;

4) exchange interactions;

5) motion of paramagnetic centers in a radio frequency field;

6) diffusion of the excited spin system within the paramagnet.

We are already acquainted with some of these broadening mechanisms, while others are encountered in the study of the effect in metals, semiconductors, and other paramagnets.

If the broadening is due to inhomogeneity of the local magnetic field, then the radio frequency energy is transferred only to those spins for which the intensities of the magnetic field satisfy the resonance condition. If at the same time the processes within the spin system occur at a slower rate than the energy exchange between the spins and the lattice vibrations, then the spin system does not have time to reach thermodynamic equilibrium. A broadening of this type will be called nonuniform. In this case it is convenient to visualize the paramagnet as an aggregate of spin packets, which do not interact with one another at all. To each packet belongs a certain absorption line, the width of which is determined by the dipole-dipole interactions. The reaction of the entire paramagnet to the external interactions consists of the independent reactions of the individual packets. It is therefore clear that such a system will behave entirely differently from a paramagnet with uniform broadening mechanism.

By way of an example we can list the following sources of nonuniform broadening:

1) hyperfine interaction of the spins of the paramagnetic centers with the nuclear moments of the surrounding diamagnetic particles;

2) anisotropy of the spin-level splittings;

3) dipole interaction between spins with different Larmor precession frequencies;

4) inhomogeneity of the applied static magnetic field.

If the broadening is uniform, then it is easy to show that paramagnetic absorption is determined by the following formula:

$$\chi''(\nu) = \frac{\pi}{2}\chi_0\nu_0 \frac{g(\nu - \nu_0)}{1 + \frac{1}{8}\gamma^2 H_1^2 T_1 g(\nu - \nu_0)}. \qquad (5.103)$$

In the present case we write for the form function $g(\nu)$ (see §1.3) $g(\nu - \nu_0)$, for we are also interested in its dependence on the resonant frequency ν_0.

In order to obtain the Bloch formula under resonance conditions, we put

$$g(0) = 2T_2; \qquad (5.104)$$

then

$$\chi''(\nu_0) = \frac{\pi\chi_0\nu_0 T_2}{1 + \frac{1}{4}\gamma^2 H_1^2 T_1 T_2}, \qquad (5.105)$$

which coincides with formula (5.2) when $\nu = \nu_0$. The dispersion is characterized by the following expression:

$$\chi'(\nu) = \frac{\pi}{2}\chi_0\nu_0 \frac{1}{1 + \frac{1}{8}\gamma^2 H_1^2 T_1 g(\nu - \nu_0)} \int_0^\infty \frac{2}{\pi}\frac{\nu' g(\nu' - \nu_0)}{\nu'^2 - \nu^2} d\nu'. \qquad (5.106)$$

Let us assume now that the broadening is not uniform. Let the distribution of the local fields be specified by the function $h(\nu - \nu_0)$, so normalized that

$$\int_0^\infty h(\nu - \nu_0)\,d\nu = 1.$$

In analogy with (5.104) it is convenient to introduce the time

$$T_2^* = \frac{1}{2}h(0). \qquad (5.107)$$

For absorption in the nonuniform case we have

$$\chi''(\nu) = \frac{\pi}{2}\chi_0 \int_0^\infty \frac{\nu g(\nu - \nu')}{1 + \frac{1}{8}\gamma^2 H_1^2 T_1 g(\nu - \nu')} h(\nu - \nu')\,d\nu'. \qquad (5.108)$$

Since the total width is large compared with the width of the line of an individual spin packet, this expression can be simplified to the form

$$\chi''(\nu) = \frac{\pi}{2} \chi_0 \nu h (\nu - \nu_0) \int\limits_0^\infty \frac{g(\nu' - \nu_0)}{1 + \frac{1}{8} \gamma^2 H_1^2 T_{1} g (\nu' - \nu_0)} d\nu'. \qquad (5.109)$$

The corresponding formula for the dispersion has the form

$$\chi'(\nu) = \chi_0 \int\limits_0^\infty \frac{\nu'^2 h (\nu' - \nu_0)}{\nu'^2 - \nu^2} d\nu'. \qquad (5.110)$$

We see that in the case of nonuniform broadening the absorption line shape does not change upon saturation, since the integral in (5.109) is independent of ν. The character of the dependence of the maximum absorption on the power of the alternating magnetic field is determined by the form function $g(\nu - \nu_0)$. Consequently an experimental study of the saturation of lines with uniform broadening makes it possible to determine the form function $g(\nu - \nu_0)$, though it is masked in the present case by the total broadening.

In conclusion it must be noted that under saturation conditions the Kramers-Kronig relations (1.18) no longer are valid. Relations (1.18) are a direct consequence of the fact that the complex suscep- tibility becomes an analytic function of the frequency in the lower half of the complex plane. Van Vleck has shown that this condition follows from the linearity of the system. Since the linearity of the system is disturbed under saturation conditions, it is understandable why the Kramers-Kronig relations must be reviewed.

Recently Tomita [100] proposed a general theory of paramagnetic resonance under saturation conditions; he explained at the same time many interesting phenomena that are encountered in the observation of both electron and nuclear paramagnetic resonance.

In many cases of nonuniform broadening, the saturation is nevertheless uniform owing to cross correlation.

§5.9. Cross Correlation

The two characteristic time parameters T_1 and T_2 (or τ and τ') are not always sufficient for a description of the paramagnetic relaxation processes. Thus, at very low temperatures it becomes necessary to take into account the time required to establish thermal equilibrium between the lattice and the helium thermostat. In the case of strong exchange interactions it is necessary to separate the "exchange system" and introduce new time parameters characterizing the rate of establishment of equilibrium between this system and the lattice, the Zeeman system, etc. Developing further the researches of Kronig and Bouwkamp [101], of Gorter [102], and of Abragam and Proctor [103], Bloembergen [104] showed that a large group of phenomena can be explained from a unified point of view by introducing the concept of cross correlation.

We shall henceforth assume always that $T_2 \ll T_1$. The spin-spin relaxation time T_2 has a twofold significance: first, the quantity $1/T_2$ is of the order of the resonant paramagnetic absorption line width; second, the quantity T_2 is the time necessary to establish thermal equilibrium within the spin system.

If the Zeeman and the intracrystalline Stark splittings of the spin levels are much larger than the average interaction energy between the spins of two neighboring magnetic particles, the second interpretation of the time T_2 becomes meaningless. In this case, the conversion of the Zeeman and Stark energies into the energy of dipole-dipole interaction is difficult, and consequently one cannot speak of a single spin system. The rate of establishment of thermal equilibrium between the system of individual spin levels of the paramagnetic par-

ticles, on the one hand, and the system of dipole-dipole interactions on the other, will be characterized with the aid of the "cross relaxation time" T_{21}. Greatest interest is attached to the case $T_{21} < T_1$, which we shall now consider.

We assume first that the paramagnet contains magnetic particles of one sort with effective spin $S' = 1/2$. Let the Zeeman splitting of the individual ion $h\nu_{12} = g\beta H_0$ be so large that the energy of interaction between spins of different particles can be regarded as a perturbation. It is necessary to calculate the probability that an energy quantum $h\nu_{12}$ will be converted as a result of the realignment of the magnetic-dipole system into the energy of dipole-dipole interaction. Direct application of perturbation theory is impossible, owing to the tremendous number of degrees of freedom of the spin system. It is simplest to attain our purpose by means of a mixed method, which combines perturbation theory and the method of moments.

Successive application of perturbation theory calls for the knowledge of the eigenvalues of that part of the dipole-dipole interaction operator which commutes with the Zeeman-energy operator. In order not to consider the tremendous number of energy levels which are eigenvalues of the matrices A and B (5.9), which commute with the Zeeman-energy matrix, we introduce a form function $g(\nu)$, which has a symmetrical maximum at the point ν_{12}. The transitions between energy levels of these dipole systems are brought about by that part of the dipole-dipole interactions which is represented by matrices C and D, which do not commute with the Zeeman energy matrix. We shall see below that in our case we can disregard the terms E and F. In the first approximation of the theory of time-dependent perturbations, the probability of transition of the Zeeman energy $h\nu_{12}$ into dipole energy is

$$w \equiv (2T_{11})^{-1} \Rightarrow \hbar^{-1}|c_{11}|^2 N_{\bullet}^{-1} g(0). \tag{5.111}$$

We denote here by c_{12} the nondiagonal element of the matrix C, which relates the states 1 and 2. The form function $g(\nu)$ can be determined with the aid of its moments. The second moment of this function relative to the frequency ν_{21} can be calculated from the following formula

$$M_2 = -\frac{Sp\left\{\left[(A+B)\sum_{j>i}\hat{S}_{zi}\hat{S}_{+j}-\sum_{j>i}\hat{S}_{zi}\hat{S}_{+j}(A+B)\right]^2\right\}}{Sp\left\{\left[\sum_{j>i}\hat{S}_{zi}\hat{S}_{+j}\right]^2\right\}}. \qquad (5.112)$$

The difference from formula (5.12) consists in the fact that in place of the operator $\Sigma\hat{S}_x$, which is connected with the action of the external oscillating magnetic field applied along the $\underline{x}$ axis, we have here the matrix of the operator $\hat{C} \sim \Sigma\hat{S}_{z1}\hat{S}_{+j}$, the elements of which determine the intensity of the transitions that we are now considering. The moment (5.112) has obviously the same order as the moment (5.12), which pertains to the absorption line of the radio frequency field, but the two are not equal.

If we assume that $g(\nu)$ has a Gaussian form, then we obtain for the cross relaxation probability

$$w = \frac{\frac{3}{4}g^4\beta^4 S(S+1)}{\hbar^2\sqrt{2\pi M_2}}\sum_{j}' r_{ij}^{-6}\sin^2\theta_{ij}\cos^2\theta_{ij}e^{-\frac{g^2\beta^2 H_0^2}{2\hbar^2 M_2}}. \qquad (5.113)$$

At large fields H_0, the time T_2 increases very rapidly with increasing interval between the Zeeman levels of the ion. Therefore the processes $\Delta M = \pm 2$, caused by the terms E and F, can be neglected.

If $H_0 \to 0$, then $T_{21} \to T_2$ and we have in accordance with Kronig and Bouwkamp [101]

$$w = 2\pi\sqrt{M_2'}e^{-\frac{g^2\beta^2 H_0^2}{2M_2'}}. \qquad (5.114)$$

Here M'_2 is the second moment calculated with additional account of the terms E and F.

It must be kept in mind that the assumed Gaussian character of

the curve $g(v)$ can lead to serious errors, particularly in the case of strong exchange coupling and random paramagnetic dilution.

We now proceed to consider substances which contain either two sorts of paramagnetic centers, or magnetic particles of one sort but with spin $S > 1/2$. The establishment of equilibrium between the Zeeman and the dipole systems can become appreciably accelerated if there are two pairs of levels with almost equal intervals: $hv_\alpha \approx hv_\beta$. Then the following processes will take place under the influence of the dipole interactions: the ion $\underline{i}$ will absorb an energy hv_α, the ion $\underline{j}$ will lose an energy hv_β, and the energy $h(v_\alpha - v_\beta)$ is transferred to the dipole system. The probability of a process of this kind is

$$w_{ij} = \hbar^{-1} |\langle E_i, E_j | \mathscr{H}_{ij} | E_i + hv_a, E_j - hv_\beta \rangle|^2 g_{\alpha\beta}(0), \qquad (5.115)$$

where $\hat{H}_{ij}$ is the operator of interaction between the ions $\underline{i}$ and $\underline{j}$, and $g_{\alpha\beta}(v_\alpha - v_\beta)$ is a form function which has a maximum at the point $v_\alpha - v_\beta = 0$. The second moment of this function can be determined from a formula analogous to (5.112).

Let us point out a few important cases, where two pairs of energy levels with practically identical intervals are encountered: 1) the ion Ni^{2+} ($S = 1$) in an axial crystalline field and a weak magnetic field (Fig. 5.9a); 2) the ion Ni^{2+} in an intermediate crystalline field and an intermediate magnetic field (Fig. 5.9b); 3) the ion Cr^{3+} ($S = 3/2$) in a weak magnetic field parallel to the crystal axis (Fig. 5.9c); 4) two nonequivalent ions of Cu^{2+} ($S = 1/2$) (Fig. 5.9d).

We can calculate $g_{\alpha\beta}$ approximately if we know the form function g_α and g_β for the paramagnetic resonance absorption lines v_α and v_β, using the following formula:

$$g_{\alpha\beta} = \iint g_\alpha(v') g_\beta(v'') \delta(v' - v'') dv' dv''; \qquad (5.116)$$

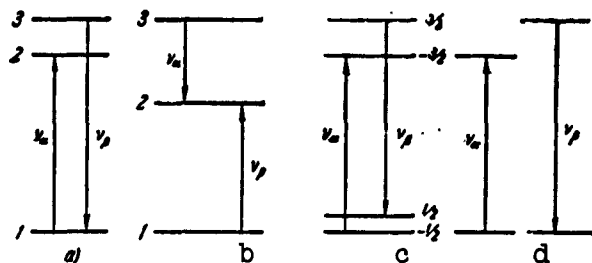if g_α and g_β have a Gaussian form, then

Fig. 5.9. Typical example of cross relaxation transitions.

$$w_{ij} = \frac{|\mathscr{H}_{ij}|^2}{\sqrt{2\pi}\,\hbar^2\,\sqrt{(\Delta\nu_a)^2+(\Delta\nu_\beta)^2}}\, e^{-\frac{(\nu_a-\nu_\beta)^2}{2[(\Delta\nu_a)^2+(\Delta\nu_\beta)^2]}}. \qquad (5.117)$$

Kopvillem [115] made detailed calculations of the form function $g_{\alpha\beta}(\nu)$ by the method of moments. He obtained a somewhat unexpected result, which contradicted Bloembergen's statements. It turned out that the form function $g_{\alpha\beta}(\nu)$ remains practically unchanged upon magnetic dilution, if the energy $h(\nu_\alpha - \nu_\beta)$ is smaller than the average energy E_{dip} of the magnetic dipole-dipole interactions, calculated per paramagnetic ion in a magnetically concentrated crystal. If on the other hand $h(\nu_\alpha - \nu_\beta) > E_{dip}$, then the increase in energy $h(\nu_\alpha - \nu_\beta)$ will lead to a rapid decrease in $g_{\alpha\beta}(0)$.

We have assumed in the preceding sections that a change in the spin-level populations can occur under the influence of an external applied oscillating magnetic field and as a result of spin-lattice interactions. The probabilities of the corresponding transitions were denoted by us by p_{ij} and A_{ij}. We see now that the populations of the spin levels can also be changed by cross relaxation. Thus, for example, for the case shown in Fig. 5.9a we have

$$\left(\frac{\partial N_2}{\partial t}\right)_{\text{кросс рел}} = -\left(\frac{\partial N_3}{\partial t}\right)_{\text{кросс рел}} = w\,[N_3 - N_2 - (N_3 - N_2)_{a.a}] +$$
$$+ N_\bullet^{-1} \sum w_{ij}\,[(N_3 N_1 - N_2 N_1) - (N_3 N_1 - N_2 N_1)_{a.a}]. \qquad (5.118)$$

Here $(N_k)_{ad}$ is the population of level $\underline{k}$ under conditions where the spin system is equilibrium, it being assumed that the spin system is

isolated from the lattice. If T is the lattice temperature and T_{ad} is the temperature of the spin system under adiabatic conditions, then we have the following system of differential equations for the level population of particles with spin S = 1:

$$
\begin{aligned}
\frac{dN_1}{dt} &= p_{31}(N_3 - N_1) + A_{13}\left(N_1 - N_3 - \frac{1}{3}N_0\frac{h\nu_{31}}{kT}\right) + \\
&\quad + A_{23}\left(N_2 - N_3 - \frac{1}{3}N_0\frac{h\nu_{32}}{kT}\right) + \\
&\quad + \left(w + \frac{1}{3}\sum_j w_{ij}\left[N_3 - N_2 - \frac{1}{3}N_0\frac{h\nu_{32}}{kT_{ad}}\right]\right), \\
N_1 + N_2 + N_3 &= N_0, \\
\frac{dN_3}{dt} &= p_{31}(N_1 - N_3) + A_{23}\left(N_3 - N_2 + \frac{1}{3}N_0\frac{h\nu_{32}}{kT}\right) + \\
&\quad + A_{13}\left(N_1 - N_3 - \frac{1}{3}N_0\frac{h\nu_{31}}{kT}\right) - \\
&\quad - \left(w + \frac{1}{3}\sum_j w_{ij}\left[N_3 - N_2 - \frac{1}{3}N_0\frac{h\nu_{32}}{kT_{ad}}\right]\right).
\end{aligned}
\qquad (5.119)
$$

We have assumed here that the frequency of the applied radio signal is ν_{32}.

A solution of equations such as (5.119) enables us to estimate the behavior of the paramagnet under specified external conditions and the role of cross relaxation. Since we are unable to examine in detail the phenomena that can be explained by cross relaxation, we shall stop to discuss some of them.

a) Intermediate relaxation in measurements made in parallel fields

Measurement of paramagnetic absorption in parallel fields made in dilute paramagnetic salts have shown [105] that in addition to ordinary relaxation maxima, the positions of which are determined by the values of τ and τ', intermediate temperature-independent absorption peaks are observed in many cases. A quantitative comparison shows that the experimentally established region of dispersion and absorption corresponds to a frequency $\nu \approx (1/2\pi)T_{21}$.

b) Thermal contact between two different spin systems

If a paramagnetic salt contains two sorts of paramagnetic particles, then the cross relaxation theory makes it possible to estimate

- 289 -

the energy that goes over from one spin system to the other if the thermal equilibrium between these systems has been disturbed.

c) "Crossing" saturation

In the previously mentioned experiments of Giordmaine et al [58], which were carried out at helium temperatures, it was shown that saturation of one of the hyperfine components of copper ions leads to a rapid saturation of all other components which have not been subjected to the action of the radio frequency field. The authors of this experiment have attempted to attribute this to the broadening of the energy levels of the "effective" oscillators of the lattice resulting from the weak coupling between these oscillators and the oscillators of other frequencies and with the helium thermostat (see §5.4). The real reason for the crossing saturation, however, is apparently cross relaxation. A principal role is played here by processes in which four ions participate simultaneously. Let the frequency of three resonant lines ν_α, ν_β, and ν_γ be such that $(\nu_\beta - \nu_\alpha) \approx (\nu_\gamma - \nu_\beta)$; besides, $h\nu_{\alpha,\beta,\gamma} = E_{\alpha,\beta,\gamma}^{(2)} - E_{\alpha,\beta,\gamma}^{(1)}$. Let us take four ions, of which two are at an energy level $E_\beta^{(2)}$ and one each are on the levels $E_\alpha^{(1)}$ and $E_\gamma^{(1)}$. As a result of dipole-dipole interaction between these ions, their spins can become simultaneously reoriented. In this way the energy of the radio frequency field applied at a frequency ν_β can be transferred and saturate paramagnetic resonance at the frequencies ν_α and ν_γ. The numerical estimate of T_{21} is in good agreement with the experimental data. Bloembergen et al [101] have set up special experiments which led to the following important conclusion: at temperatures above $1^\circ K$ processes connected with the heating of the system of "effective oscillators" do not play any role whatever in dilute paramagnetic salts.

d) Nonuniform broadening and uniform saturation

In sufficiently diluted paramagnetic salts, the greater part of

the resonance-line width is due to the initial magnetic field of the nuclear spins of the diamagnetic atoms and to the scatter of the parameters of the crystalline field. A nonuniform broadening of this type will be called microscopic to distinguish it from the macroscopic broadening, produced by the inhomogeneity of the external magnetic field and by the polycrystalline nature of the specimens.

Let the total width of the lines be determined by the quantity $1/T_2^*$, and the uniform part of the broadening by $1/T_2$. As a result of cross relaxation, the energy of the radio frequency field absorbed by the fields whose resonant frequencies are distributed within the region $\nu_0 \pm 1/T_2$ will be transferred to fields with resonant frequencies outside this region. If at the same time the corresponding cross relaxation time is $T_{21} > T_1$, then the saturation of the entire resonant line will occur as if the broadening were uniform; the expression for the saturation factor will contain T_2^* in lieu of T_2. The cross relaxation within the resonant line can be due either to processes of the Kronig-Bouwkamp type, or to multiple processes similar to those considered in item c). In the case of Kronig-Bouwkamp processes we readily obtain

$$T_{21} = \frac{T_2^*}{(T_2^*)^2}.$$ (5.120)

Thus, the saturation is uniform in the majority of practically realized conditions, even in the case of nonuniform broadening. Among the experiments directly confirming the considerations advanced here are those on saturation of paramagnetic resonance in nickel fluorosilicate by means of radio frequency pulses [106].

§5.10. Acoustic Paramagnetic Resonance

In analogy with ordinary paramagnetic resonance, in which a paramagnet selectively absorbs energy from an alternating magnetic field,

it is possible to have also paramagnetic resonant absorption of ultrasonic energy. The theory of this phenomenon was proposed by Al'tshuler [107], while the experimental observations were first made on nuclear paramagnets [108, 109] and recently also on Mn^{2+} ions introduced into quartz crystals [111].

Acoustic paramagnetic resonance consists of a transfer of ultrasonic energy to a system of magnetic particles; this transfer occurs when a quantum of elastic-vibration energy is equal to the difference between the energies of the magnetic levels. Thus, just as in the case of ordinary paramagnetic resonance, the acoustic effect will take place if condition (1.2) is satisfied, except that now v stands for the frequency of the ultrasound.

The mechanism that effects the transfer of the energy from the sound oscillations to the paramagnetic particles has the same nature as paramagnetic lattice relaxation, realized with the aid of single-phonon processes. Resonant absorption of ultrasound can therefore be regarded as a phenomenon inverse to paramagnetic relaxation. Under the influence of the sound oscillations, the forces acting on the magnetic particles will vary periodically and transitions will occur from one magnetic energy sublevel to another. The complete population of the lower sublevels will cause the number of transitions connected with absorption of energy to exceed the number of the inverse transitions. Equilibrium will be established by transferring the excess energy of the paramagnetic particles to the thermal vibrations of the lattice.

The calculation of the absorption of ultrasound by paramagnets is analogous to the calculation of the time of paramagnetic lattice relaxation produced by first-order processes. This makes it possible to obtain the following formula for estimating the effect in solids:

$$\sigma = \frac{h^3}{8\pi\tau} \frac{N_0 v^3}{kT \cdot kT_0 \Delta v}. \tag{5.121}$$

- 292 -

Here σ is the coefficient of sound absorption, that is, the ratio of the energy absorbed per cubic centimeter to the energy incident on a square centimeter per second; T is the temperature of the body; T_0 is the temperature at which the relaxation time τ was determined. The experimental data lead to values on the order of 0.1 cm^{-1} for the coefficient. Thus, the effect investigated is sufficient to become observable. Calculations of σ were therefore undertaken subsequently for many types of paramagnets assuming various mechanisms for the spin-lattice coupling.

The first to be investigated was resonant absorption of ultrasound by paramagnetic salts in which the spin-lattice coupling is by modulation of the internal electrical field of the crystal by elastic lattice oscillations. The coefficient σ was calculated for several typical salts of the iron-group elements (titanium and chrome alums), salts of rare-earth elements (cerium nitrate, praseodymium ethyl sulfate), and finally for salts whose magnetic ions are in the S state (iron alums). The absorption coefficient for titanium alum was found to be

$$\sigma \approx h^a P \left(\frac{\lambda}{4\xi}\right)^a \left(\frac{e\mu}{R^a}\right)^a \nu^a,$$
(5.122)

where $P = \pi^2 N_0 / \rho k T v^3 \Delta\nu$. At $T = 20^{\circ}K$, a numerical estimate yields $\sigma \approx$ $\approx 2\cdot10^{-88}$ cm^{-1}. For chrome alum we have

$$\sigma \approx \left(\frac{e\mu}{R^a}\right)^a \left(\frac{\lambda}{\Delta_a}\right)^a P \nu^a.$$
(5.123)

A numerical estimate yields at room temperature $\sigma \approx 10^{-21} \nu^2$ cm^{-1}.

Formula (5.123) pertains to transitions between spin levels belonging to different Kramers doublets. Consequently, unlike the titanium salts, we have here $\sigma \sim \nu^2$. In the perturbation-theory approximation that yields formula (5.123), we have $\sigma = 0$ for transitions within the Kramers doublets. In the higher-order approximation we obtain, as

for the ion Ti^{3+}, $\sigma \sim v^4$. Physically this result is understandable and has general significance. The lowering of the symmetry of the crystalline field, brought about by the elastic lattice vibrations, can change the splitting of the spin levels pertaining to different Kramers doublets, but can hardly influence the distribution of the Kramers doublets themselves.

Calculation for the salts of rare-earth elements has shown that the effect of resonant absorption of ultrasound is small in those cases when the crystalline field leaves in the magnetic ions only a Kramers energy-level degeneracy, which cannot be lifted by the changes induced in the electric field by the lattice vibrations.

In ethyl sulfates of rare earths, the crystalline field has hexagonal symmetry. If the rare-earth ion contains an even number of electrons, the energy levels retain the Kramers degeneracy and the effect of sound absorption should therefore be large. Thus, for praseodymium ethyl sulfate we obtain

$$\sigma \approx P \left(\frac{e\mu_e}{R^2}\right)^2 \left(\frac{\overline{r^2}}{R^3}\right)^2 v^2.$$
(5.124)

From this we have $\sigma \approx -10^{-15}$ cm^{-1} when $T = 20°K$. The effect is so large that this salt is apparently the most suitable for experimental observation of the effect. The acoustic effect in rare-earth salts is analyzed in detail in [110].

For iron alums in which the Fe^{3+} ion is in the S state, the absorption coefficient is relatively small, on the order of $10^{-24} v^2$ cm^{-1} at room temperature.

In gadolinium salts, in which, as is well known, the splitting of the ground energy level of the paramagnetic ion by the electric field of the crystal is much larger than in the iron ion, we can expect the acoustic effect to be approximately 10^4 times stronger.

Resonant absorption of ultrasound was considered also under the assumption that the spin-lattice coupling is produced by a change in the magnetic interaction of the particles by the elastic oscillations of the lattice (the Waller mechanism). In this case the absorption coefficient turns out to be

$$\sigma = \frac{253}{21} P_z \left(\frac{g^2 \beta^2}{a^3} \right)^2 S(S+1)^2 (2S+1) \nu^4. \qquad (5.125)$$

In substances with large density of magnetic atoms, of the MnF_2 type, this mechanism may make the coefficient σ at room temperature equal to approximately $10^{-19} \nu^2 cm^{-1}$.

Resonant absorption of ultrasounds will obviously take place not only in electronic paramagnets, but also in substances having nuclear paramagnetism. Favorable circumstances for the nuclear effect are the small line width of the paramagnetic absorption and the large density of the magnetic particles. Small values of nuclear magnetic and quadrupole moments are the cause of a relatively weak spin-lattice coupling, which naturally decreases the effect.

In solid dielectrics, in which the spin-lattice coupling is due to magnetic interaction between the nuclei, the coefficient of resonant absorption of ultrasound can be calculated by means of formula (5.125), where β now stands for the nuclear magneton. For example, for a NaBr crystal at $T = 300^\circ K$ we have $\sigma \approx 10^{-25} \nu^2 cm^{-1}$. For substances in which the spin-lattice coupling is due to quadrupole nuclear interactions, the coefficient σ can become appreciably larger, on the order of $10^{-20} \nu^2 cm^{-1}$. An even larger effect can be expected in metals in which the coupling between the nuclear spins and the lattice vibrations becomes intensified by the interaction between the nuclei and the conduction electrons. An appreciable effect can also be obtained in singlet electronic levels of paramagnetic particles, the nuclei of which

have nonzero magnetic moments [110].

It is interesting to compare the resonant absorption of ultra-sound with paramagnetic resonance under the influence of variable magnetic fields.

a) A comparison of the magnitudes of both effects can be readily carried out by recognizing that the coefficient of absorption of the electromagnetic-field energy is

$$\sigma_e = \frac{8\pi}{c} \nu \chi'' \approx \frac{8\pi^2}{c\Delta\nu} \chi_0 \nu^2. \qquad (5.126)$$

In many "electronic" paramagnets $\Delta\nu \approx 10^9$ cps, $\chi_0 \approx 10^{-6}$, and therefore $\sigma \approx 10^{-22} \nu^2$ cm^{-1}. In many cases we have also obtained for the coefficient of ultrasound absorption an expression proportional to ν^2, with the proportionality factor strongly dependent on the matrix element of the spin-lattice interaction operator. If this matrix element differs from zero in first approximation, then the values obtained for σ are much larger than σ_e. On the other hand, if higher approximations are needed, usually σ and σ_e are of the same order of magnitude.

It must be noted that the absorption coefficient for the longitudinal and transverse waves will generally speaking be different. We have cited in all cases the average values of the coefficient σ for solid bodies.

b) Ordinary paramagnetic resonance is strongly dependent on the angle between the static and alternating magnetic fields. The acoustic effect is little sensitive to changes in the direction of sound-wave propagation relative to the field H_0.

c) Absorption of ultrasound is frequently made possible by transitions between such sublevels, for which the magnetic dipole transitions are forbidden.

d) The absorption line shapes in the case of acoustic and ordinary

- 296 -

effects can be quite different. The reason for it is that in both phenomena we deal with the same energy-level bands, produced by the magnetic and other interactions, but the laws governing the transition probabilities between these levels under the influence of ultrasound and under the influence of an alternating magnetic field are quite different in nature.

In spite of the fact that in many cases the coefficient of ultrasound absorption greatly exceeds the coefficient of absorption of the energy from the radio frequency field, the low sensitivity of ultrasonic research methods makes it desirable to use indirect methods of detecting acoustic paramagnetic resonance. Such resonance can be observed by "saturation" of the magnetic sublevels of the nuclei, a saturation occurring at high sound intensities [108]. Another method can be based on the changes produced in the magnetization of the body under the influence of the ultrasound.

The generation, and particularly the transmission of sound oscillations at microwave frequencies from the generator to the investigated substance constitutes a very complicated experimental problem. Therefore great interest is attached to a determination of the conditions under which one can expect a noticeable effect in electronic paramagnets at relatively low frequencies, on the order of 100 Mcs. This question was considered in [113]. Since the greatest effect is connected with transitions between different Kramers doublets, it is apparently very convenient to observe transitions between spin levels near the points where the levels cross, as occurs, for example, in the case shown in Fig. 1.3.

We note finally that if magnetically diluted crystals are used, the scattering of the sound waves on the imperfections of the crystal lattice can become most appreciable. For reasons indicated in §5.3,

- 297 -

item 7, resonant absorption of these waves will be very strong. Therefore indirect measurement methods, which make it possible to evaluate directly the difference in the spin-level populations, should be very convenient.

An experimental study of resonant paramagnetic absorption of ultrasound can greatly supplement the data obtained by investigating ordinary resonance and paramagnetic relaxation; it makes possible a deeper explanation of the nature of the spin-lattice interaction, and a determination of the constants characterizing this interaction; it discloses new absorption lines, the appearance of which under the influence of a radio frequency field is impossible because of the absence of magnetic dipole transitions.

REFERENCES TO CHAPTER 5

1. Bloch F., Phys. Rev. 70, 460, 1946.

2. Garstens M.A., Phys. Rev. 93, 1228, 1954.

3. Van Vleck J.H., Weisskopf V.F., Rev. Mod. Phys. 17, 227, 1945.

4. Shaposhnikov I.G., ZhETF (Journal of Experimental and Theoretical Physics) 18, 533, 1948.

5. Shaposhnikov I.G., ZhETF 19, 225, 1949.

6. Skrotskiy G.V., Kurbatov L.V., Izv. AN SSSR, ser. fiz. (Bull. Acad. Sci. USSR, physics series), 21, 833, 1957.

7. Wangsness R.K., Bloch F., Phys. Rev. 89, 728, 1953.

8. Waller J., Z. Physik (Journal of Physics) 79, 370, 1932.

9. Broer L.J.F., Physica 10, 801, 1943.

10. Van Vleck J.H., Phys. Rev. 73, 1249, 1948.

11. Al'tshuler S.A., Odintsov M.G., Izv. KFAN SSSR, ser. fiz.-tekh. (Bull. Kazakh Branch Acad. Sci. USSR, Technical Physics Series), 3, 39, 1953.

12. Glebashev G.Ya., ZhETF 32, 82, 1957.

13. Al'tshuler S.A., Zavoyskiy Ye.K., Kozyrev B.M., ZhETF 17, 1122, 1947.

14. Gorter C.J., van Vleck J.H., Phys. Rev. 72, 1128, 1947.

15. Kittel C., Abrahams E., Phys. Rev. 90, 238, 1953.

16. Glebashev G.Ya., ZhETF 30, 612, 1956.

17. Pryce M.H.L., Stevens K.W.H., Proc. Phys. Soc. A63, 36, 1950.

18. Glebashev G.Ya., Uch. zap. KGU (Scientific Notes of the Kiev State University) 116, 121, 1956.

19. Ishiguro E., Kambe K., Usui T., Physica 17, 310, 1951.

20. Holden A.N., Kittel C., Yager W.A., Phys. Rev. 75, 1443, 1949.

21. Griffiths J.H.E., Owen J., Proc. Roy. Soc. A213, 459, 1952.

22. Stevens K.W.H., Proc. Roy. Soc. A214, 237, 1952.

23. Kambe K., Ollom F., J. Phys. Soc. Japan 11, 50, 1956.

24. Abragam A., Kambe K., Phys. Rev. 91, 894, 1953.

25. Bersohn R., J. Chem. Phys. 20, 1505, 1952.

26. Kopvillem U.Kh., ZhETF 34, 1040, 1958.

27. Bagguley D.M.S., Griffiths J.H.E., Nature 162, 538, 1948.

28. Pryce M.H.L., Nature 162, 539, 1948.

29. Van Wieringen J.S., Disc. Faraday Soc. 19, 118, 1955.

30. Anderson P.W., Weiss P.R., Rev. Mod. Phys. 25, 269, 1953.

31. Anderson P.W., J. Phys. Soc. Japan 9, 316, 1954.

32. Kubo R., Tomita K.J., J. Phys. Soc. Japan 9, 888, 1954; Kubo R., J. Phys. Soc. Japan 9, 935, 1954; Yokota M., Koide S., J. Phys. Soc. Japan 9, 953, 1954.

33. Archer D.H., Thesis, Harvard 1953; Gutowski H.S., McCall D.M., Slichter C.P., J. Chem. Phys. 21, 279, 1953.

34. Gorter K.D., Paramagnitnaya relaksatsiya (Paramagnetic relaxation), IL (Foreign Literature Press), Moscow, 1949.

35. Lloyd J.P., Pake G.E., Phys. Rev. 94, 579, 1954.

36. Gaytler V., Kvantovaya teoriya izlucheniya (Quantum Theory of Radiation), IL, Moscow, 1956.

37. Van Vleck J.H., Phys. Rev. 57, 426, 1052, 1940.

38. Kronig R.L., Physica 6, 33, 1939.

39. Al'tshuler S.A., Izv. AN SSSR, ser fiz., 20, 1207, 1956.

40. Bashkirov Sh.Sh., ZhETF 34, 1465, 1958.

41. Volokhova T.I., ZhETF 33, 856, 1957.

42. Abe H., Ono K., J. Phys. Soc. Japan 11, 947, 1956.

43. Avvakumov V.I., FMM (Physics of Metals and Metallography) 4, 199, 1957.

44. Bashkirov Sh.Sh., FMM 6, 577, 1958.

45. Al'tshuler S.A., ZhETF 24, 681, 1953.

46. Shekun L.Ya., Dissertation, Kiev State University, 1956.

47. Akhiyezer, A.I., Pomeranchuk I.Ya., ZhETF 14, 342, 1944; DAN SSSR (Proc. Acad. Sci. USSR) 87, 917, 1952.

48. Bloembergen N., Wang S., Phys. Rev. 93, 72, 1954.

49. Kramers H.A., Bijl D., Gorter C.J., Physica 16, 65, 1950.

50. Vrijer F.W., Gorter C.J., Physica 18, 549, 1952.

51. Benzie R.J., Cooke A.H., Proc. Phys. Soc. A63, 201, 1950.

52. Gorter C.J., Van der Marel L.C., Bolger B., Physica 21, 103, 1955.

53. Van der Marel L.C., Van den Broek J., Gorter C.J., Physica 23, 361, 1957.

54. Frölich H., Heitler W., Proc. Roy. Soc. A155, 640, 1936.

55. Van Vleck J.H., Phys. Rev. 59, 730, 1941.

56. Bridgman P.W., Proc. Ams. Acad. 64, 63, 1929.

57. Van Vleck J.H., Phys. Rev. 59, 724, 1941.

58. Giordmaine J.A., Alsop L.E., Nash F.R., Townes C.H., Phys. Rev. 109, 302, 1958.

59. Strandberg M.W.P., Phys. Rev. 110, 65, 1958.

60. Bloembergen N., Phys. Rev. 109, 2209, 1958.

61. Endryu E., Yadernyy magnitnyy rezonans (Nuclear Magnetic Resonance), IL, Moscow, 1957.

62. Van Vleck J.H., Nuovo cimento 6, suppl., No. 3, 1081, 1957.

63. Kashayev S.Kh.G., DAN SSSR 110, 362, 1956.

64. Kozyrev B.M., Doctorate Dissertation, FIAN (Institute of Physics Acad. Sci. USSR), Moscow, 1957.

65. Bleaney B., Proc. Roy. Soc. A204, 203, 1950.

66. Kumagai H., Ono K., Hayashi I., Abe H., Shono H., Ibamoto H., Shimoda J., Phys. Rev. 83, 1077, 1951.

67. MacLean C., Kor G.J., Appl. Sci. Rev. B4, 425, 1955.

68. Müller K.A., Helv. Phys. Acta 28, 450, 1955.

69. Anderson J.H., Hutchison C.A., Phys. Rev. 97, 76, 1955.

70. Rivkind A.I., Izv. AN SSSR, ser. fiz., 16, 541, 1952.

71. Casimir H.B.G., du Pre F.K., Physica 5, 507, 1938.

72. Gorter C.J., Smits L.J., Tables de constantes et donnees numeriques (Tables of Constants and Numerical Data). 7. Relaxation paramagnetique (Paramagnetic Relaxation). Masson et c^{ie}, 1957.

73. Kozyrev B.M., Izv. Kaz. ped. in-ta (Bull. Kazakh Pedagogical Institute) 1, 83, 1947.

74. Garif'yanov N.S., Dissertation, KGU, 1953.

75. Brons F., Thesis, Groningen, 1938.

76. Garif'yanov N.S., ZhETF 35, 612, 1958.

77. Kramers H.A., Bijl D., Gorter C.J., Physica 16, 65, 1950; de Vrijer F.W., Gorter C.J., Physica 18, 549, 1952; Benzie R.J., Cooke A.H., Proc. Phys. Soc. A63, 201, 1950.

78. Purcell E.M., Slichter C.P., Phys. Rev. 76, 466, 1949; Damon R.W., Rev. Mod. Phys. 25, 239, 1953.

79. Schneider E.E., England T.S., Physica 17, 221, 1951.

80. Eschenfelder A.H., Weidner R.T., Phys. Rev. 92, 869, 1953.

81. Landau L.D., Lifshits E.M., Statisticheskaya fizika (Statistical Physics), Gostekhizdat (State Publishing House for Theoretical and Technical Literature), Moscow, 1951.

82. Bloembergen N., Purcell E.M., Pound R.V., Phys. Rev. 73, 678, 1948.

83. Kozyrev B.M., Disc. Faraday Soc. 19, 135, 1955.

84. McConnell H.M., J. Chem. Phys. 25, 709, 1956.

85. McGarvey B.R., J. Phys. Chem. 61, 1232, 1957.

86. Al'tshuler S.A., Valiyev K.A., ZhETF 35, 947, 1958.

87. Yel'yashevich M.A., Spektry redkikh zemel' (Rare-Earth Spectra), Gostekhizdat, 1953.

88. Schultz M.L., J. Chem. Phys. 10, 194, 1942; Freed S., Weissman S.I., J. Chem. Phys. 8, 840, 1940; Kobajshi M., Fujita I., J. Chem. Phys. 23, 1354, 1955.

89. Zavoyskiy Ye.K., Doctorate Dissertation, FIAN, Moscow, 1944.

90. Kozyrev B.M., Izv. AN SSSR, ser. fiz., 16, 533, 1952.

91. Rivkind A.I., Dissertation, Ural'skiy gos. un-t (Urals State University), Sverdlovsk, 1951.

92. Tinkham M., Weinstein R., Kip F., Phys. Rev. 84, 848, 1951.

93. Garstens M., Liebson S., J. Chem. Phys. 20, 1677, 1952.

94. Kozyrev B.M., Izv. AN SSSR, ser. fiz., 21, 828, 1957.

95. Cohn M., Townsend J., Nature 173, 1090, 1954.

96. Garif'yanov N.S., Kozyrev B.M., DAN SSSR 98, 929, 1954.

97. McGarvey B.R., J. Phys. Chem. 60, 71, 1956.

98. Tishkov P.G., ZhETF 36, 1337, 1959.

99. Portis A.M., Phys. Rev. 91, 1071, 1953.

100. Tomita K., Progr. Theor. Phys. 19, 541, 1958.

101. Kronig R., Bouwkamp C.J., Physica 5, 521, 1938; 6, 290, 1939.

102. Verstelle J.C., Drewes G.W.J., Gorter C.J., Physica 24, 632, 1958.

103. Abragam A., Proctor W.G., Phys. Rev. 109, 1441, 1958.

104. Bloembergen N., Shapiro S., Pershan P.S., Artman J.O., Phys. Rev. 114, 445, 1959.

105. Smits L.J., Derksen H.E., Verstelle J.C., Gorter C.J., Physica 22, 773, 1956.

106. Bowers K.D., Mims W.B., Bull. Amer. Phys. Soc. ser. II, 3, 325, 1958.

107. Al'tshuler S.A., DAN SSSR 85, 1235, 1952; ZhETF 28, 38, 49, 1955.

108. Proctor W.G., Tantila W.H., Phys. Rev. 98, 1854, 1955; 101, 1757, 1956; Proctor W.G., Robinson W.A., Phys. Rev. 102, 1183, 1956; Kraus O., Tantilla W.H., Phys. Rev. 109, 1052, 1958; Jennings D.A., Tantilla W.H., Phys. Rev. 109, 1059, 1958.

109. Menes M., Bolef D.I., Phys. Rev. 109, 218, 1958.

110. Al'tshuler S.A., Zaripov M.M., Shekun L.Ya., Izv. AN SSSR, ser. fiz., 21, 844, 1957.

111. Jacobsen E.H., Shiren N.S., Tucker E.B., Phys. Rev. Letters 3, 81, 1959.

112. Kochelayev B.I., DAN SSSR 131, 1053, 1960.

113. Al'tshuler S.A., Bashkirov Sh.Sh., Soveshchaniye po paramagnitnomu rezonansu (Conference on Paramagnetic Resonance), Kazan', 1960, page 78.

114. Kopvillem U.Kh., Fizika metall. i metalloved. (Physics of Metals and Metallography), Vol. 8, 8, 1959; Izv. MVO (Bull. Ministry of Higher Education), Fizika (Physics), Vol. 3, 13, 1958; ZhETF 35, 506, 1958; Koloskova N.G., Kopvillem U.Kh., Fizika tverdogo tela (Physics of Solids) 2, 1368, 1960; Izv. MVO, Fizika 3, 223, 1960; Morozova I.D., Mineyeva R., Kopvillem U.Kh., Soveshchaniye po paramagnitnomu rezonansu, Kazan', 1960, page 92.

115. Kopvillem U.Kh., ZhETF 38, 151, 1960.

Manu- script Page No.	[Footnotes]
215	A primed summation sign denotes that $j \neq k$.
227	See footnote for page 215.
259	The only exception is the Tutton's salt of Cu^{2+}.
273	A detailed analysis of the interaction between the oscilla-tors Q_i and the Brownian motion, carried out by K.A. Valiyev (unpublished work), has shown that the constant τ_c can be given a different interpretation; the character of the tem-perature dependences of A_{ik} remains the same in this case.
276	Confirming this fact is the possibility of observing reso-nance in VO^{2+} [96], and also the reported [84] observation of the effect in a complex salt of Ti^{3+}. In these cases a strong low-symmetry component of the crystalline field can explain the sufficiently long time τ.

Manu- script Page No.	[List of Transliterated Symbols]
207	лок = lok = lokal'nyy = local
209	зеем = zeem = zeemanovskiy = Zeeman (adj.)
209	дип = dip = dipol'nyy = dipole
209	обм = obm = obmen = exchange
251	эксп = eksp = eksperimental'nyy = experimental
251	теор = teor = teoreticheskiy = theoretical
263	рез = rez = rezonansnyy = resonance
270	сп = sp = spin = spin
273	cth = coth
288	кроссрел = krossrel = krossrelaksatsiya = cross-relaxation
288	ад = ad = adiabaticheskiy = adiabatic

Chapter 6

METALS AND SEMICONDUCTORS. IMPERFECTIONS IN CRYSTALS

§6.1. Effect on Conduction Electrons

The carriers of paramagnetism in metals are the conduction electrons. In transition metals, paramagnetism may also be associated with the ions that form the core of the crystal lattice. One could expect in metals the appearance of paramagnetic resonant absorption lines, the positions of which would be determined by the g factors of both the conduction electrons and of the d and f shells of the atoms. However, the observation of paramagnetic resonance in metals entails several difficulties: 1) the skin effect reduces the absorption of energy from the radio frequency field and makes the form of the resonance line more complicated; 2) small paramagnetic inclusions may cause results that are quite erroneous; 3) in many metals, the spin-lattice interactions smear out the paramagnetic resonance curve.

To reduce the skin effect one usually employs minute metal particles, pulverized by ultrasound and embedded in paraffin. The metal specimens must be subjected to multiple purification to rid them of paramagnetic impurities. A confirmed effect on the conduction electrons was obtained in the following metals: Li, Na, K, Be, Cs [1-11]. Investigations of many other substances, such as Al, Mg, Pd, W, produced no positive results, apparently owing to the excessive width of the resonance line.

The first calculation of the g factor for conduction electrons was made by Jafet [12] with sodium as an example. Only the spin-orbit

- 305 -

interaction was taken into account there, since the correlation and exchange effects were insignificant, and the influence of interaction between the electronic and nuclear spins became noticeable only at temperature $T < 1°K$. The closeness of the experimental values of the g factors to the pure spin value $g_{spin} = 2.0023$ shows that the spin-orbit interaction can be regarded as a perturbation. The Bardeen method [13], in which it is possible to avoid calculation of the matrix elements, was used in the computations. This yielded $\Delta g = g -$ $- g_{spin} = -3.7 \cdot 10^{-4}$, whereas experiments [8, 9] implied that $\Delta g = -(8 \pm 12) \cdot 10^{-4}$. Brooks [14] made calculations based on the atomic value of the spin orbit coupling constants. The value $\Delta g = -6.6 \cdot 10^{-4}$ which we obtained agrees within the limits of error with the experimental data. The value $\Delta g = -6 \cdot 10^{-5}$ obtained theoretically for lithium [15] is very small, in agreement with the measurement results [8, 9]: $|\Delta g| \leq 10^{-4}$. For beryllium, experiment [8] yields $\Delta g = +(9 \pm 1) \cdot 10^{-4}$, and there are no theoretical calculations. For potassium, the g factor could at first not be determined, since the effect was small and became observable only at temperatures below $4°K$.

An original method of obtaining pure and finely ground specimens of metals was proposed by Levy [9]; he froze solutions of alkali metals in ammonia at liquid nitrogen temperature. He was thus able to measure paramagnetic resonance absorption in potassium at $180°K$ and in cesium at $25°K$. The measured values of the g factor were 1.99 and 1.93, respectively, in good agreement with the theoretical [14] values 1.99 and 1.94.

In metals in which the paramagnetism is due to the conduction electrons, the form of the resonance line is determined by the spin-lattice interactions. The spin-spin relaxation is insignificant, owing to the high velocity of the electrons and the relatively small value

of the spin-spin interactions. A theoretical analysis of paramagnetic relaxation in metals was first made by Overhauser [16], who used the single-electron model of degenerate gas for the calculation of the interactions between the conduction electron spins and the other parts of the metal. The interactions themselves were regarded in this case as small perturbations.

One might think that, just as in the case of ionic paramagnetic crystals at high temperatures, the principal role in the energy exchange between the electron spins and the lattice vibration would be assumed by second order processes (combination scattering of phonons). This assumption, however, must be rejected for the same reasons for which two-phonon processes are disregarded in the calculations of the electric resistivity of metals.

Overhauser considered the following relaxation mechanisms.

1) Interaction with transverse phonons. Let us assume that the relaxation is brought about by interaction between the magnetic moments of the electrons and the magnetic field produced by the charged particles (ions) participating in the lattice vibrations. It is obvious here that only transverse vibrations are significant. We denote the Fermi energy in the absence of an external magnetic field by $\varepsilon_0 = \hbar^2 k_0^2/2m_0$, the metal particle diameter by $\underline{d}$, the length of the side of the atomic dimension cube by $\underline{a}$, the number of electrons per cubic centimeter by N_e, and finally the density of the metal by ρ. If we neglect the correlation between the translational motion of the conduction electrons and the vibrational motion of the lattice, the calculations yield for the relaxation time the following expression:

$$\tau = \frac{3\rho m_0 \hbar k_0 c^4}{16\pi e^4 N_e^2 kT \ln \frac{d}{a}}. \tag{6.1}$$

From this we get, for example in the case of lithium, $\tau \approx 6 \cdot 10^{-2}$ sec

at room temperature.

2) Interaction with longitudinal phonons. Relaxation can be due to interaction between the electron spins and the electric field produced by the vibration of the positive lattice ions. Interactions of this type in atoms give rise to spin-orbit coupling. Transverse vibrations produce a relatively weak electric field; we can therefore confine ourselves to an analysis of longitudinal oscillations. Calculation shows that the relaxation time is

$$\tau = \frac{96 \rho k_0 m_0^3 c^4 v^2}{\pi^3 N_e^2 \hbar^4 \left(\frac{k\theta}{\hbar v}\right)^4 kT}.$$ (6.2)

Here $\underline{v}$ is the average velocity of sound and θ is the Debye temperature.

It follows from (6.2) that for lithium at room temperature $\tau \approx$ $\approx 3 \cdot 10^{-4}$ sec.

3) Magnetic dipole interaction of the electron spins. In this case the relaxation process may be the result of both simultaneous reorientation of the spins of both interacting electrons and of the spin of one electron only (see §§5.2 and 5.3). If only the former processes which play the principal role, are taken into account, we obtain for the relaxation time

$$\tau = \frac{15 m_0 \hbar^3 c^4}{8 \pi e^4 k^2 T^2}.$$ (6.3)

At room temperature we have hence $\tau \approx 6 \cdot 10^{-3}$ sec.

4) Interaction with nuclear spins. The relaxation may also be caused by interaction between the electrons and the nuclear spins. In this case, as in atoms, the principal role is assumed by the hyperfine interaction with the electrons in the S state [17]. Calculation shows that

$$\frac{\tau_N}{\tau} = \frac{8I(I+1)\varepsilon_0}{9kT},$$ (6.4)

where τ_N denotes the relaxation time of the nuclear spins; according

to calculations by Korringa [17], this time is equal to

$$N = \frac{9\pi \hbar^3 I^2}{6 \{m_0^* k_0^3\}^2 kT |\psi(0)|^4}.$$ (6.5)

Here $\psi(0)$ is the wave function of the electron situated on the Fermi surface; the vanishing of the argument denotes that it is necessary to take the value of the given function at the location of the nucleus. It is interesting that the relaxation time τ is independent of the temperature. One can therefore expect this relaxation mechanism to have the decisive significance at sufficiently low temperature.

5) Interaction of the electron spins with the magnetic field of the currents arising during the translational motion of the conduction electrons. This relaxation mechanism leads to the following expression:

$$\tau = \frac{9 m_0^3 c^4 \hbar}{20 e^4 k_0^3 kT \ln \frac{kT}{\beta H_0}}.$$ (6.6)

The weak dependence on the applied magnetic field H_0, which is implied in this formula, can be used to ascertain whether this mechanism plays an appreciable role in paramagnetic relaxation processes. Numerical calculation shows that when $H_0 = 5$ oersted and $T = 293^c K$ we obtain $\tau \approx$ $\approx 8 \cdot 10^{-7}$ sec.

Experimental determinations of the relaxation time [8, 9] have shown that even the shortest values of τ given by the latter of the mechanisms proposed by Overhauser are approximately two orders of magnitude higher than the measurement results. In addition, in contradiction to Formula (6.6), it was observed that the relaxation time is constant as the field H_0 is varied from 300 to 3000 oersted.

The inadequacy of the Overhauser theory lies evidently not in the fact that some important relaxation mechanism has been left out. The use of plane waves for the description of the conduction electron motion probably leads to excessively crude results. Elliott [18] obtained

- 309 -

good agreement with experiment by calculating the relaxation time using the ordinary band theory of metals, under the assumption that the energy exchange between the electron spins and the lattice vibrations is due to the spin-orbit interaction. The connection between the lattice vibrations and the motions of the electrons is so much stronger than the direct interaction between the electron spins and the lattice that even a weak orbit coupling is sufficient to create the most effective relaxation mechanism. Elliott obtained the following formula for the relaxation time

$$\tau = \frac{\alpha \tau_R}{(\Delta g)^2}.$$
(6.7)

Here τ_R is the impact time of the conduction electrons which, as is well known, can be readily determined if the electric resistivity of the metal is known. For lithium, sodium, and potassium the impact time is $\tau_R = 1 \cdot 10^{-14}$, $3 \cdot 10^{-14}$, $2 \cdot 10^{-14}$ sec, respectively. The impact time can be assumed, with sufficiently good approximation, to be proportional to the electric conductivity of the metal, and therefore it will be approximately proportional to $1/T$ at temperatures $T > \theta$, whereas at low temperatures $\tau_R \sim 1/T^5$. For temperature $T > \theta$, the numerical factor is $\alpha = 1/2^{5/3} \ln (d/a)$ (see (6.1)); when $T < \theta$, the factor α depends on the temperature and besides, as in the case of high temperatures, $\tau \sim 1/T$.

The attractive feature of Elliott's theory is the simple connection between the relaxation time τ and the deviation of the g factor from the pure spin value, which, as we have seen, is due to the spin-orbit interaction. Formula (6.7) readily explains why it was impossible to observe paramagnetic resonance in heavy metals. After all, with increasing atomic number of the element, the spin-orbit coupling increases rapidly, and with it also the deviation Δg.

Andreyev and Gerasimenko [19] have analyzed the problem of paramagnetic relaxation in metals by solving the kinetic equation for the conduction electrons. They have shown that at temperatures $T \gg \beta H_0/k$, under paramagnetic resonance conditions, the magnetization vector obeys Bloch's equation (5.1), in which the longitudinal and transverse relaxation times are equal to each other. At the same time they have made more precise and corrected Elliott's formula for the paramagnetic relaxation time, for which they obtained the following expression:

$$\tau = \frac{u}{T}\left(\ln\frac{\operatorname{th}\frac{\theta}{T}}{\operatorname{th}\frac{T_k}{T}}\right)^{-1}, \quad u = \frac{3\beta^2\hbar\rho v^2}{16\pi\chi_0 k\bar{\imath}^3(\Delta g)^2}, \tag{6.8}$$

where $\bar{\varepsilon}$ is the average electron energy in the lattice, and $T_k = (v/kv_F)2\beta H_0$, if the dimensions of the metal specimen are such that $d > \hbar v_F/2\beta H_0$; if on the other hand the specimen dimensions do not satisfy this inequality, then $T_k = \hbar vkd$; by v_F we denote here the velocity of the electron on the Fermi boundary. At a temperature $T \gg \theta$, Formula (6.8) assumes the form

$$\tau = \frac{u}{T}\ln\frac{\theta}{T_k}. \tag{6.9}$$

On the other hand, if $T \ll \theta$, then

$$\tau = \frac{u}{T}\ln\frac{T}{T_k}. \tag{6.10}$$

Experimental investigations of the relaxation time have shown that in the case of sodium, $\tau \sim 1/T$ as the temperature varies from 4 to 293°K, as called for by the theory.

The value $\tau = 9 \cdot 10^{-8}$ sec obtained by measurements at room temperature is in good agreement with the theoretical value $\tau \approx 10^{-6}\, T^{-1}$ sec.

In lithium and beryllium, experiment has disclosed that the relaxation time is constant as the temperature is varied over a wide range.* At the same time, it was established that if the specimen is purified

and the amount of lithium in it is raised from 99.0 to 99.9%, the relaxation time increases from $3 \cdot 10^{-9}$ to $2.5 \cdot 10^{-8}$ sec. All these facts can be simply explained. Because the value of Δg of light metals is small, the paramagnetic relaxation is determined by the spin-orbit coupling of the conduction electrons with the impurities. Success in the measurement of the "true" relaxation time will probably be attained in the case of specimens subjected to an exceedingly careful purification.

In potassium the width of the resonance line is approximately 50 times larger than in sodium [9]. In cesium at helium temperatures, the line width is approximately $2 \cdot 10^8$ cps.

Garif'yanov and Starikov [11] have established that negligible impurities of heavy metals (mercury or lead) in specimens of sodium and lithium are capable of broadening the resonance curve by a factor of 10^4. This broadening is apparently the result of the shortening of the relaxation time due to the strong spin-orbit coupling in the heavy-metal atoms.

In conclusion we note that the area under the paramagnetic resonance absorption curve is proportional to the purely paramagnetic part of the static susceptibility. Therefore, measurements of the paramagnetic resonance make it possible to separate the diamagnetic part of the susceptibility from the paramagnetic one [20]. The main difficulty arising in realization of this idea lies in the fact that it is exceedingly difficult to make absolute measurements of paramagnetic absorption. This difficulty was cleverly circumvented by Schumacher, Carver, and Slichter [5] who observed simultaneously both electronic and nuclear resonance in metallic lithium, at one and the same frequency, $1.7 \cdot 10^7$ cps. The absolute value of the intensity of the nuclear line could be readily calculated. By comparing both resonance curves

it was found that the static susceptibility is $(2.0 \pm 0.3) \cdot 10^{-6}$ cgs; theoretical calculation [21] yields $1.87 \cdot 10^{-6}$.

§6.2. Effect of Skin Effect and Diffusion of Electrons on the Form of the Resonance Line

It has been demonstrated theoretically and experimentally that the skin effect and the diffusion of electrons within the skin layer change appreciably the form of the paramagnetic resonance line. The distortion of the resonance line form should result even from the fact that, unlike paramagnetic dielectrics, in which the variable part of the magnetization is determined by the magnitude of the applied oscillating field, in a metal there exists also an inverse dependence of the local values of this field on the magnetization, owing to the skin effect. By virtue of this, whereas in dielectrics the absorbed energy is proportional to the coefficient χ'', in a metal it will also be proportional to the real part of the dynamic susceptibility, χ'. In addition, the line shape will be distorted also because diffusion causes the same electron, which moves inside the skin layer, to be subjected to the action of the oscillating magnetic field, the amplitude and phase of which are continuously varying. Thus, the interesting information concerning the nature of the metallic state, obtained by the paramagnetic resonance method, can be rid of distortion only if account is taken of the skin effect and of electron diffusion. A theoretical analysis of this question was made by Dyson [22] who used a very simple model of the metal in order to obtain formulas that are convenient in practical use. He suggested that the conduction electrons diffuse like free particles, and that the spin of each electron can be regarded as an independent quantum variable. The spin is very weakly coupled to the orbital motion and is therefore very weakly affected by the collisions experienced by the electrons. Judging from the value of the

- 313 -

spin-lattice relaxation time in the case of sodium, for example, only one out of 10^5 collisions causes reorientation of the spin. One can therefore assume that the spin responds primarily to changes in the local magnetic field.

We denote the thickness of the skin layer by δ and the mean free path of the electron by λ. In order for the electron to traverse the skin layer the time required on the average is

$$t_D = \frac{3}{2} \frac{\delta^2}{\lambda^2} \tau_R. \qquad (6.11)$$

During the time t_D, the amplitude and phase of the oscillating magnetic field change by approximately $\underline{e}$ times. Consequently, in place of a definite frequency of magnetic field acting on the electrons within the layer, we have a frequency band of width $1/t_D$. Since usually $t_D \ll \tau_R$, it appears at first glance that the width of the resonance line should increase from $1/\tau$ to $1/t_D$. Actually, however, the width remains practically constant, but the form of the line changes.

This unexpected result is explained as follows. The alternating magnetic field can be represented in the form

$$F(t) = f(t) e^{-2\pi i \nu t} + f^*(t) e^{2\pi i \nu t}, \qquad (6.12)$$

where $f(t)$ is a modulation factor which, however, cannot be regarded as a perfectly random function of the time. After a time τ, each electron experienced a large number of individual pulses, separated by unequal intervals. The pulses arise near the surface of the metal, where the amplitude $f(t)$ is large. During the intervals between the pulses, the electron is for the most part away from the surface, where $f(t)$ is close to zero. The decisive facts are as follows: 1) there is a large probability that the electron will encounter the surface of the metal many times during the time τ; 2) every time that the electron approaches the surface, the phase of $f(t)$ assumes the same value, and consequently

- 314 -

the integral of f(t) taken over the time interval between two pulses differs from zero.

Let us examine the spectral composition of F(t). Each pulse produces a spectrum distributed with approximately equal intensity over a band of width $1/t_D$. Owing to factors 1) and 2), the interference between the spectra produced by a large number of pulses causes a central maximum, corresponding to the frequency ν, to become separated within a band of width $1/\tau_D$. The interval between two successive pulses is a random quantity, which can assume values from zero to τ. Therefore, if we average the spectrum of each electron over all the electrons, we obtain a curve with a flat maximum of width $1/\tau_D$, on which is superimposed a sharp peak of approximate width $1/\tau$.

We present the results of Dyson's calculations. In addition to the time parameters τ and t_D which we have already encountered, we find it useful to introduce a third one, namely the time t_T needed by the electron to traverse the entire metal specimen. If the metallic particles are so fine that $t_T \ll t_D$, then the skin effect is negligible and the power absorbed by the paramagnetic material in the volume V can be represented, in accordance with (1.9), (1.19), and (5.2), in the following form:

$$P_{\bar{\nu}} = \pi^2 \nu H_r^2 V \nu_0 \chi_0 \tau \frac{1}{1 + 4\pi^2 (\nu - \nu_0)^2 \tau^2}. \qquad (6.13)$$

We assume here and throughout that there is no saturation; thereupon we assume that in the metal $T_2 = \tau$. In addition, we neglect here and in what follows the nonresonant absorption proportional to g_2 (see §§1.4 and 5.1).

In the opposite case, when $t_T \gg t_D$, it is necessary to distinguish in the solution of the problem concerning the form of the resonance line in metals between regions of normal and anomalous skin ef-

- 315 -

fect. In the former case the depth of penetration of the alternating field into the metal is determined by the classical value $\delta = c/2\pi\sqrt{\sigma}$, where σ is the electric conductivity of the metal, while in the latter case the depth of penetration is characterized by the mean free path λ. We first consider the case of normal skin effect. The general formula for the absorbed power is

$$P_v = -\pi^2 \nu H_r^2 (\delta A_0)\, \nu_0 \chi_0 \tau\, \frac{t_D}{2\tau} \left\{ \frac{R^4(x^2-1)+1-2R^2x}{[(R^2x-1)^2+R^4]^4} \times \right.$$
$$\times \left[\frac{2\xi}{R(1+x^2)^{\frac{1}{2}}} + R^2(x+1)-3 \right] + \frac{2R^2-2xR^4}{[(R^2x-1)^2+R^4]^3} \times$$
$$\left. \times \left[\frac{2\eta}{R(1+x^2)^{\frac{1}{2}}} + R^2(x-1)-3 \right] \right\}, \qquad (6.14)$$

where

$$x = 2\pi(\nu-\nu_0)\tau, \quad \xi = \frac{x}{|x|}[(1+x^2)^{\frac{1}{2}}-1]^{\frac{1}{2}},$$

$$\eta = [(1+x^2)^{\frac{1}{2}}+1]^{\frac{1}{2}}, \quad R = \left(\frac{t_D}{\tau}\right)^{\frac{1}{2}}$$

and A_0 is the area of the metal surface. This formula can be simplified for certain cases of practical importance.

Let us assume that $t_D/\tau \ll 1$. If this condition, which applies to metals with high conductivity (low temperatures and narrow lines), is fulfilled then, accurate to quantities proportional to R, we have

$$P_v = -[\pi^2 \nu H_r^2 (\delta A_0)\, \nu_0 \chi_0 \tau] \left(\frac{t_D}{\tau}\right)^{\frac{1}{2}} \frac{x}{|x|} \frac{[(1+x^2)^{\frac{1}{2}}-1]^{\frac{1}{2}}}{(1+x^2)^{\frac{1}{2}}}. \qquad (6.15)$$

If $t_D/\tau \gg 1$, which holds true when the diffusion of the magnetic dipoles is very slow, then (6.14) assumes the form

$$P_v = [\pi^2 \nu H_r^2 (\delta A_0)\, \nu_0 \chi_0 \tau] \cdot \frac{1}{2} \frac{1-2\pi\tau(\nu-\nu_0)}{1+4\pi^2\tau^2(\nu-\nu_0)^2}. \qquad (6.16)$$

This formula was derived already by Bloembergen [23], who investigated the influence of skin effect on the form of the resonance line in the case when diffusion does not play any role. The present case is encountered when one deals with paramagnetic resonance in metals, brought

about by paramagnetic impurities, nuclear spins, or the core of the crystal lattice (transition metals).

At low temperatures the skin effect becomes anomalous. If we assume furthermore that $t_D/\tau \ll 1$, then the formula for the absorbed power assumes the form

$$P_v = [\pi^2 \nu H_r^2 (\delta A)_\bullet \nu_0 \chi_0 \tau] \cdot 6 \frac{\tau_R}{\tau} \left\{ \frac{(Z_2 - Z_1)[(1 + x^2)^{\frac{1}{2}} + 1]^{\frac{1}{2}}}{(1 + x^2)^{\frac{1}{2}}} + \right.$$
$$\left. + 2Z_1 Z_2 \frac{[(1 + x^2)^{\frac{1}{2}} - 1]^{\frac{1}{2}} x}{(1 + x^2)^{\frac{1}{2}} |x|} \right\}, \qquad (6.17)$$

where Z_1 and Z_2 define the complex impedance $Z = Z_1 + iZ_2$.
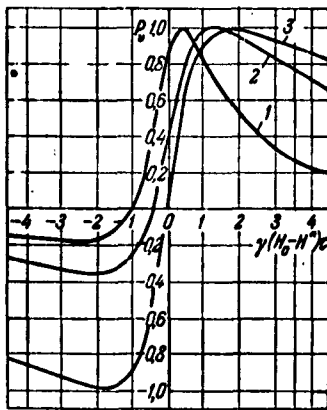
Fig. 6.1. Paramagnetic resonance absorption in a thick layer of metal. The curves show the dependence of the absorbed power P_v on the quantity $\gamma(H_0 - H^*)\tau$ for various values of R. 1) R = $= \infty$; 2) R = $\sqrt{0.1}$; 3) R = 0.

Many authors have rigorously established and developed the theory of paramagnetic resonance under conditions of both normal and anomalous skin effect. By means of a brilliant method using the kinetic equation for the statistical conduction electron density operator, Silin [24] derived for the magnetization vector the differential equation which served as the basis for Dyson's work. Lifshits, Azbel', and Gerasimenko [25], who derived independently of Silin an analogous kinetic equation, carried out a general analysis of the behavior of the conduction electrons in a constant magnetic and in an arbitrary alternating electron magnetic field.

From among the many results which they obtained, we note that they calculated the paramagnetic resonance line form under saturation conditions. It is interesting that resonance saturation in bulky spec-
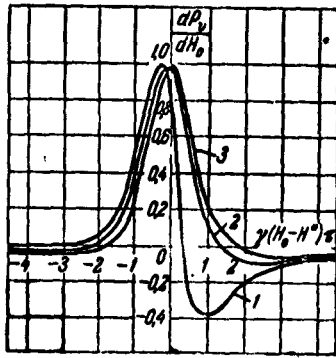
Fig. 6.2. Paramagnetic resonance absorption in a thick layer of metal. Curves showing the dependence of the derivative dP_v/dH_0 of the absorbed power with respect to the field on the quantity $\gamma(H_0 - H^*)\tau$ for various values of R. 1) R = ∞; 2) R = $\sqrt{0.1}$; 3) R = 0.

imens calls for much larger amounts of power than in the case when the skin effect is insignificant. The question of paramagnetic resonance in superconductors is considered in [26] where, in particular, it is shown that this effect is impossible in bulky conductors.

Let us proceed to compare the theoretical results with the experimental data, which are cited principally in [8]. Figure 6.1 shows the characteristic curve of paramagnetic resonance absorption in a thick layer of metal. We see that the curve is the result of a certain superposition of the usual curves for χ' and χ''. Figure 6.2 shows an analogous curve for the derivative of the absorption with re-
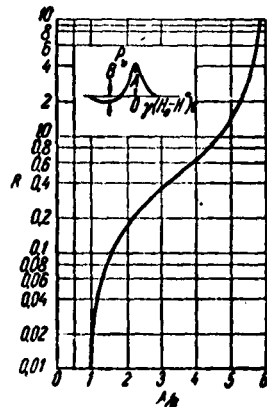

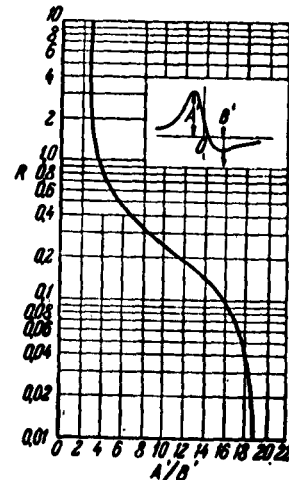Fig. 6.3a. Dependence of the ratio A/B on R = $(t_D/\tau)^{1/2}$.

Fig. 6.3b. Dependence of the ratio A'/B' on R = $(t_D/\tau)^{1/2}$.

spect to the field, dP_v/dH, which is frequently measured in the experiments. For comparison with experiment, it is convenient to trace the values assumed by the ratio A/B or A'/B'. Figure 6.3a shows the varia-

tion of these ratios as functions of $R = (t_D/\tau)^{1/2}$. It is easy to vary R over a wide range by changing over from room temperature to helium temperature. For sodium and beryllium, the specimen surfaces of which were very smooth, the experimental curves are quite close to the theoretical ones. For other metals, discrepancies were observed apparently connected with the appreciable variation of the diffusion time t_D resulting from unevenness in the metal surface.

The experimental values of A/B can obviously be used to determine the diffusion times t_D. The diffusion time measured in this fashion for beryllium turned out to be in good agreement with the value obtained with the aid of (6.11).

Knowledge of the ratio A/B or A'/B' is very important also because it makes possible separation of the effect exerted on the conduction electrons from the effect due to the paramagnetic impurities. It is seen from Fig. 6.3b that for the conduction electrons the ratio A'/B' always exceeds 2.7. It can be shown that for impurities A'/B' < 2.7.

For alkali metals the depth of penetration of a field of frequency $3 \cdot 10^8$ cps at a temperature 40°K becomes equal to the mean free path. It is therefore understandable why the experimental absorption curve obtained for sodium at 4°K corresponds to Formula (6.17), which holds true under the conditions of anomalous skin effect.

§6.3. Transition Metals

We can expect the paramagnetic resonance due to the atoms that form the core of the crystal lattice to be observable in transition metals. The first positive result in the case of the iron-group elements was obtained in copper-manganese alloys containing from 11 to 0.07% manganese [27, 28]. The choice of the substance was dictated by the following considerations: a) the conduction band of copper has a simple structure, since it contains 4s electrons with isotropic effec-

tive mass close to the mass of the free electrons; b) from data on the
static susceptibility one can conclude that two $4s$ electrons of the
manganese atoms are included among the particles that fill the conduc-
tion band, and therefore the manganese ions are in the $^6S_{5/2}$ state; c)
by virtue of the fact that the manganese ions are in the S state, we
can expect those mechanisms of spin-lattice relaxation, the effect of
which depends on the magnitude of the spin-orbit coupling, to be of
little effectiveness; d) we can expect the paramagnetic coupling be-
tween the manganese atoms to be due to indirect sd exchange forces.

The operator of sd exchange interaction has the simple form

$$\mathscr{H}'' = I\hat{S}\hat{s},\qquad\qquad (6.18)$$

where $\hat{S}$ pertains to the spin of the manganese ion, and $\hat{s}$ pertains to
the spin of the conduction electron. On the basis of optical data con-
cerning the magnitude of the exchange interactions in the free man-
ganese atom, we can estimate the sd coupling constant at $I = -7 \cdot 10^{-13}$
erg. The operator (6.18) has the same form as the operator $A\hat{I}\hat{s}$ of the
hyperfine interaction between the conduction electrons and the nuclear
spins of the metal. This interaction, as is well known, determines the
form of the paramagnetic nuclear resonance line in metals [17]. It
brings about, first of all, the so-called Knight shift [29] of the po-
sition of the resonant peak; owing to the magnetization of the conduc-
tion electrons under the influence of the external magnetic field H_0,
the nuclear spins will be acted upon not only by this field but also
by the internal field $H_A = \lambda M_e$, where

$$\lambda = -\frac{A}{4\beta^2 N_e},\qquad\qquad (6.19)$$

and M_e is the length of the magnetization vector of the conduction
electrons. Second, the $A\hat{I}\hat{s}$ interaction gives rise to the main mechanism
of spin-lattice relaxation.

- 320 -

Applying the deduction of nuclear theory to our case, we obtain for an alloy containing say 5% manganese the following formula, which determines the relative change in the g factor:

$$\frac{\Delta g}{g} = \frac{12}{T}.$$

(6.20)

The formula for the spin-lattice relaxation time (6.5) can be rewritten in the form

$$\tau = \frac{8h\omega_0^2}{9\pi^2 kTI^2}.$$

(6.21)

The experimental investigations were carried out at wavelengths 3.3 and 1.2 cm in the temperature interval from 2 to 300°K. The values of the g factor corrected for the line form distortion by the skin effect, using the method indicated in the preceding section, turned out to be very close to 2. On the other hand, the measured width of the resonance line turned out to be approximately 5 times smaller than the value given by Formula (6.21). Thus, if the exchange sd interactions do indeed determine the magnetic properties of the alloys which we are considering, then their magnitude should be approximately one order of magnitude smaller than in the case of free atoms.

The splitting of the spin levels by the electric field of the crystal could not be discerned at all experimentally; the reason for it is that the screening action of the conduction electrons makes these splittings very small. Nor was it possible to observe the hyperfine structure of the absorption lines, a fact which apparently indicates a very weak s-configuration interaction.

Along with copper-manganese alloys, silver-manganese and magnesium-manganese alloys were also investigated. All these alloys acquired antiferromagnetic properties at low temperatures.

Let us proceed to consider the rare earth metals. Experimental data on the paramagnetic resonance of this group of transition metals

are exceedingly scanty [30, 31] and do not allow us to make reliable theoretical generalizations. Some theoretical conclusions are given in [32].

With respect to their magnetic properties, the rare earth element metals occupy a special place, for the paramagnetism of these metals is almost completely due to the $4f$ electrons which lie deep inside the atoms; the conduction electrons exert a negligible influence on the magnetic susceptibility. Because of this we can assume that the general methods for calculating the paramagnetic properties, developed and applied successfully to the salts of the rare earth elements, are applicable in first approximation also to metals. The interpretation of the paramagnetic resonance spectra for rare earth metals becomes simpler by the fact that, unlike the salts, the symmetry of the internal electric field of a metal always coincides with the symmetry of the crystal lattice.

Of particular interest are the paramagnetic absorption lines, the positions of which are independent of the direction of the static magnetic field relative to the crystal axes, since the available experimental data pertain only to polycrystalline specimens. Such lines can appear in crystals that have a cubic lattice, for it is easy to show that if doubly or triply degenerate energy levels are produced under the influence of the cubic-symmetry electric field, then further splitting of these levels by a weak magnetic field will be independent of the direction of this field relative to the cube axes. Among the rare earth metals possessing a cubic lattice are β-cerium, β-praseodymium, europium, and ytterbium. The theoretical conclusions concerning the spectrum of β-cerium turn out to be in good agreement with the experimental results. It was assumed in the calculations that the metal atom lacks three electrons. This assumption follows from data on the static

susceptibility and is confirmed here directly.

From among the metals possessing hexagonal lattices, we shall dwell primarily on α-cerium, neodymium, and dysprosium, the ions of which have odd numbers of electrons.* The energy levels produced in these ions by the electric field of the crystals are doubly degenerate. If we make certain natural assumptions we find that there should exist only one absorption line, the position of which is determined by the spectroscopic splitting factor

$$g = g_0 \sqrt{1 + q \sin^2 \vartheta}, \quad q = J^2 + J - \tfrac{3}{4}, \qquad (6.22)$$

where g_0 is the Lande factor for the free ion and ϑ is the angle between the direction of the static magnetic field and the crystal hexagonal axis. Calculation shows that for a polycrystalline specimen the absorption line intensity is proportional to

$$P \sim \left(J + \tfrac{1}{2}\right)^2 g_0^2 \sin \vartheta \, \frac{2q \sin^2 \frac{\vartheta}{2}}{1 + q \sin^2 \vartheta}. \qquad (6.23)$$

Elimination of ϑ from Formulas (6.22) and (6.23) enables us to establish with the aid of (1.2) the dependence of the magnitude of the paramagnetic absorption on the intensity of the static field. The theoretical curves obtained in this fashion are in satisfactory agreement with the experimental absorption curves for cerium and neodymium.

The only rare earth metal with a tetragonal lattice, samarium, should have the same spectrum as α-cerium, provided very simple assumptions are made concerning the coefficients that determine the potential of the crystalline field. Metals whose ions contain an odd number of electrons (α-Pr, Tb, Ho, and Tm) have a hexagonal lattice. It is easy to show that in this case the probabilities of the magnetic dipole transitions between nearby Zeeman sublevels are equal to zero in first approximation.

If it is assumed that the theory of spin-lattice relaxation de-

- 323 -

veloped above for the rare earth element salts (see §5.3) is also applicable to metals, then we obtain for the time τ values that are several times larger because the density and velocity of sound in metals are appreciably larger; in addition, it is necessary to bear in mind that the electric field inside metal crystals is much weaker, owing to the screening effect of the conduction electrons. This probably makes it possible to observe paramagnetic resonance in rare earth metals at room temperature.

Gadolinium, the triply charged ion of which is in the S state, occupies a special position. Gadolinium is paramagnetic at temperatures above 16°C. The measurements of resonant absorption [30], made at a frequency $2.43 \cdot 10^{10}$ cps and at a temperature 105.5°C, have shown that $g = 1.95$, and the line width is independent of the temperature and has a value of approximately 4000 oersted.

The question of resonant absorption of ultrasound by rare earth metals was also considered theoretically [33]. In some cases this effect should be quite appreciable.

§6.4. Impurity Semiconductors

In the first work [34] devoted to paramagnetic resonance in impurity semiconductors, the effect was established at a frequency $\nu =$ $= 9 \cdot 10^9$ cps in powdered specimens of n-type silicon, containing between $1 \cdot 10^{18}$ and $2 \cdot 10^{18}$ phosphorus atoms per cubic centimeter. To eliminate the skin effect, minute silicon grains, with radius one order of magnitude smaller than the depth of the skin layer, were embedded in paraffin. The measurements were made at temperatures between 4 and 300°K. One absorption line was observed with Lorentzian shape. The position of the absorption peak was independent of the temperature and was determined by a factor $g = 2.001 \pm 0.001$. The width of the resonance line increased rapidly with temperature from about 2 oersted at

4°K to 30 oersted at 300°K. When working with a klystron generator, no paramagnetic resonance saturation could be observed even at helium temperatures. We can therefore conclude that the longitudinal relaxation time is $T_1 < 10^{-3}$ sec at a temperature 4°K. Willenbroek and Bloembergen [35] have observed at this same alternating field frequency paramagnetic resonance in both n-type and p-type silicon. The measurements were made at 78°K, and the impurity concentration was varied from 5 x x 10^{17} to $5 \cdot 10^{18}$ atoms per cubic centimeter. The position of the absorption peak was the same for electrons and for holes, and corresponded to g = 2.00. The intensity of the absorption line was proportional to the impurity concentration.

Fletcher et al. investigated paramagnetic resonance at helium temperatures in single crystals of silicon doped with phosphorus, arsenic [36], and antimony [37]. At concentrations of about 10^{18} atoms per cubic centimeter, one absorption peak is observed, the position of which varies somewhat depending on the slope of the static magnetic field relative to the crystal axes. When the field is parallel to the [100] axis, we have for the case of arsenic g = 2.0004 $\pm$ 0.0005. The line width was always less than 3 oersted.

From all the foregoing we can conclude that paramagnetic resonance absorption is due to the conduction band electron spins. This conclusion follows first of all from the possibility of observing the effect at temperatures corresponding to an average energy of thermal motion much larger than the ionization energy of the impurity atom (approximately 0.05 ev). Other evidence in favor of this conclusion is the relatively high impurity concentration in the tested specimens and the absence of hyperfine splitting of the resonance line.

The broadening of the paramagnetic absorption line has apparently a spin-lattice character. Indeed, it is easy to calculate that the

width due to magnetic dipole interactions of the electron spins should be of the order of 0.1 oersted. Hyperfine interactions of electron spins with phosphorus nuclei and with nuclei of the odd isotope of silicon* cannot make a noticeable contribution to the line width, owing to the rapid motion of the electrons. Nor can surface recombination of the electrons and holes play any appreciable role, since this process is quite slow.

Elliott [18] considered the influence of spin-orbit interaction of conduction electrons on the magnitude of the g factor and the spin-lattice relaxation time of semiconductors. He found that the change in the g factor is

$$\Delta g \approx \frac{\lambda}{\Delta E},$$ (6.24)

where ΔE is the interval between the lowest conduction band and the nearest band having the same transformation properties. If it is recommended that the spin-orbit coupling constant for a silicon atom is $\lambda \approx 100$ cm^{-1} and that experiment yields $\Delta g \approx 3 \cdot 10^{-3}$, we obtain with the aid of (6.24) a sensible value of approximately 4 ev for ΔE.

The spin-lattice relaxation time can be calculated from the following formula (see (6.7))

$$\tau \sim \frac{\tau_R}{(\Delta g)^2},$$ (6.25)

if Δg is small. For n-type silicon, the impact time at high temperatures is independent of the impurity concentration and its value is [38]

$$\tau_R \approx 10^{-9} T^{-\frac{3}{2}} \text{ sec.}$$ (6.26)

Hence $\tau \approx 10^{-9}$ sec at $T = 300°K$, i.e., the line width is equal to approximately 50 oersted, which is in good agreement with the measured value of approximately 30 oersted. For germanium, the constants τ_R and λ are larger than for silicon by 5 and 20 times, respectively. Conse-

quently, the line width of germanium should be approximately 10^2 times larger than for silicon, which apparently explains the negative results of the first experiments with germanium.*

At low temperatures and low impurity concentrations, the paramagnetic resonance absorption is due to the spins of the electrons bound to the donors. This fact manifests itself most clearly in the presence of a hyperfine structure of the resonance lines, which indicates that there is a definite coupling between the electron spin and the moment of the impurity atom nucleus. Measurements [36] carried out at a frequency $\nu = 2.4 \cdot 10^{10}$ cps at a temperature of 4.2°K, on specimens containing from $5 \cdot 10^{16}$ to 10^{18} atoms of arsenic per cubic centimeter, have disclosed four equidistant lines in accordance with a nuclear spin of $3/2$ for As^{75}. The interval between neighboring hyperfine components is approximately 73 oersted, and the width of each component is about 10 oersted. If silicon is doped with acceptors (boron), the magnitude of the effect is decreased. In addition, it was established that prior elastic deformation of the semiconductors at a temperature of 1000°C leads to a considerable increase in the intensity of the absorption lines; the nature of this phenomenon is not quite clear.

In the case of phosphorus-doped specimens, two components spaced 42 oersted apart were observed, in conformance with a value of $1/2$ for the nuclear spin of P^{31}.

In specimens containing $4 \cdot 10^{17}$ atoms of antimony per cubic centimeter, owing to the presence of two odd isotopes Sb^{121} and Sb^{123} with nuclear spins $5/2$ and $7/2$, respectively, the paramagnetic spectrum consists of $6 + 8$ hyperfine components [37]. The ratio of the intensities of these two groups of lines corresponds rigorously to the percentage content of the given isotopes, while the total splittings of these line groups (69 and 38 oersted) correspond exactly to the magnetic mo-

ments of the nuclei Sb^{121} ($\mu = 3.360\beta_N$) and Sb^{123} ($\eta = 2.547\beta_N$).

An attempt to observe paramagnetic resonance in semiconductors containing 10^{17} atoms of boron and $3 \cdot 10^{17}$ atoms of aluminum per cubic centimeter yielded negative results.

Honig and Kip [39] observed paramagnetic resonance at a frequency $\nu = 8.8 \cdot 10^9$ cps in the temperature range 4-20°K, in a silicon specimen containing $7 \cdot 10^{16}$ atoms of lithium per cubic centimeter. No hyperfine structure was established. The position of the single absorption peak corresponded to g = 1.999, the line width was 1.5 oersted, and the line shape was Gaussian.

Kohn and Lüttinger [40] undertook to ascertain to what degree the experimentally obtained values of the hyperfine splittings of paramagnetic resonance lines are compatible with the assumption that the hyperfine structure is due to the interaction between the donor nuclei and the electrons localized near the donors and situated in well-known donor states with ionization energy 0.04-0.05 ev. The total hyperfine splitting $(\Delta H)_{HFS}$ of the energy level, expressed in oersted, can be represented in the form

$$(\Delta H)_{HFS} = \frac{16\pi}{3} |\psi(0)|^2 \mu_D, \qquad (6.27)$$

where μ_D is the nuclear magnetic moment, $\psi(r)$ is the wave function of the electron bound to the donor, and $\underline{r}$ is the radius vector drawn from the nucleus to the electron. Table 6.1 lists the experimental values of $|\psi(0)|^2$.

The function $\psi(r)$ obeys the Schroedinger equation

$$\left[-\frac{\hbar^2}{2m} \nabla^2 + V(r) + U(r) - E \right] \psi(r) = 0, \qquad (6.28)$$

where $V(r)$ is the potential energy of the electron in the periodic field of the crystal lattice of silicon, and $U(r)$ is the initial energy that arises when one of the silicon atoms is replaced by an impurity

- 328 -

atom. At distances large compared with interatomic distances we have $U(r) = -e^2/\varepsilon r$, where ε is the dielectric constant of the medium; for silicon, $\varepsilon = 13$. The solution of (6.28) entails great difficulties since, first, the band wave function is unknown for silicon, and, second, the introduction of the concept of the electron effective mass is not allowed near the donor. As a result of detailed calculations undertaken for phosphorus, it was found that $|\psi(0)|^2 = 0.4 \cdot 10^{24}$ cm^{-3}, which is in much better agreement with the experimental data than would be expected from the assumptions made. A rough estimate gives a ratio $|\psi(0)|^2_{Li}/|\psi(0)|^2_P = 0.004$. So small a value of $|\psi(0)|^2_{Li}$ fully explains the negative results of attempts made to observe the hyperfine structure of the absorption line in silicon doped with lithium.

TABLE 6.1

Experimental Values of $|\psi(0)|^2$

I	ε_N	$\begin{array}{c}\|\psi(0)\|^2\times\\10^{-24},\\ cm^{-3}\end{array}$ 1	$\begin{array}{c}A\cdot10^{19},\\ erg\end{array}$ 2	T_x, мин. 3	T_{Si}/T_x
Li⁷	$\frac{3}{2}$	2,17	0,055	0,056	3,64·10⁶	0,1
P³¹	$\frac{1}{2}$	2,26	0,44	7,8	560	150
As⁷⁵	$\frac{3}{2}$	0,957	1,80	14,0	56	1000
Sb¹²¹	$\frac{5}{2}$	1,37	1,20	13,0	41	2000
Sb¹²³	$\frac{7}{2}$	0,724	1,20	7,0	97	820

1) cm^{-3}; 2) erg; 3) min.

During the observation of the hyperfine structure of paramagnetic resonance spectrum in silicon containing impurities of group V elements, weak satellites, located halfway between each pair of hyperfine components, were observed in addition to the $2I + 1$ lines [36, 37]. Slichter [41] has shown that such satellites should appear if one admits of exchange interactions of the type $I\vec{S}_1\vec{S}_2$ between an electron

pair belonging to two donors that are accidentally in the vicinity of each other. From this interpretation of the nature of the satellite it follows that: a) the intensity of the central satellite is twice that of the outer ones; b) the intensity of the satellites should depend on the concentration of the impurities: at low concentrations the intensities should be proportional to the concentration, and at large concentrations additional satellites should appear, connected with families of three or four electrons; c) if $I \sim kT$, then the intensity of the satellites should depend strongly on the temperature of the semiconductor, approximately as $\exp(-I/kT)$; d) a dependence on the mechanical working is also possible, if this working influences the character of the donor distribution.

In the experiments undertaken to check on Slichter's theory [42], the measurements were carried out at $1.2^{\circ}K$ and with an alternating field of frequency $\nu = 9 \cdot 10^9$ cps using two samples of silicon, containing 10^{17} and $4 \cdot 10^{17}$ phosphorus atoms per cubic centimeter. Additional absorption maxima, corresponding to the exchange between a pair, a triplet, and a quartet of electrons, were observed in the positions predicted by the theory.

Let us proceed to an analysis of the spin-lattice relaxation of the electrons localized near the donors. As a result of experiments made on silicon samples containing up to 10^{17} impurity atoms per cubic centimeter, it was established that the spin-lattice relaxation time at helium temperatures amounts to minutes [43, 44]. Such large relaxation-time values are usually characteristic of nuclear spins. With increasing impurity concentration, the time τ begins to decrease rapidly, apparently owing to the stronger interaction between the bound electrons and the conduction band electrons. The correctness of this explanation is confirmed directly by the fact that the time τ decreases

to several milliseconds if the semiconductor is exposed to light [45].

The theory of this phenomenon was presented by Pines, Bardeen, and Slichter [46] and was later developed by Abrahams [47]. The calculations were made in order to estimate the order of magnitude, and consequently several simplifications were made: a) the complex wave function of the bound electron was replaced by the function of an electron with effective mass $m^* = 0.3m_e$ in a minimal-energy state; b) all the angular dependences were left out; c) the action of only longitudinal phonons was taken into account. The following were considered from among the various relaxation mechanisms.

1. Modulation of electron-nuclear hyperfine interaction. Changes brought about by lattice vibration in the potential energy $V(r)$, which is contained in Eq. (6.28), manifest themselves on the wave function and consequently on the magnitude of the interaction between the electronic and nuclear spins. The relaxation time is

$$T_x = \frac{\hbar^3 v^6 \rho}{8\pi^3 v_1^5 kT \alpha^2 I A^4} ,$$ (6.29)

where v_0 is the resonant frequency, A is the hyperfine structure constant, and α is a numerical factor of order 10-100.

Table 6.1 lists the values of T_x for different impurities in silicon, calculated under the assumption that $\alpha = 50$, $v_0 = 9 \cdot 10^9$ cps, and $T = 1.2^\circ K$.

2. Modulation of the hyperfine interaction of the bound electrons with the Si^{29} nuclei. We designate the relaxation time due to the given mechanism by T_{Si}. Calculation shows (see Table 6.1) that $T_{Si}/T_x \gg 1$ in all cases, except lithium. Consequently, this mechanism can be significant only for silicon with lithium impurity.

3. Modulation of spin-orbit interaction of the electrons. This mechanism, which is the most important for the conduction electrons,

- 331 -

is of little effectiveness in our case, if single-phonon processes are taken into account. Combination scattering of phonons yields for the relaxation time

$$T_{LS} \sim 10^{18} T^{-12}.$$

(6.30)

It follows therefore that at temperatures above that of hydrogen, this mechanism should play the principal role.

4. Modulation of exchange interactions between neighboring impurity atoms. At the donor concentrations employed, the mechanism is quite ineffective.

To explain the dependence of the relaxation processes on the impurity concentration, mechanisms were considered, based on the following interactions between the bound electrons and the conduction band electrons:

1) Coulomb interactions; spin reorientation is possible if the spin-orbit coupling of the electron in the donor state is taken into consideration;

2) interaction between the bound electron spins and the magnetic field of the currents produced by the conduction electrons;

3) magnetic dipole-dipole interactions;

4) exchange interactions.

The most effective, in accordance with the calculations, is the last mechanism, since the spins of the bound electrons are subject after the exchange, when they enter the conduction band, to the strong influence of the lattice vibrations. However, even with this mechanism it is impossible to explain the experimental data. It is possible that a stronger spin-lattice interaction mechanism, which is not considered here, exists.

§6.5. Color Centers in Ionic Crystals

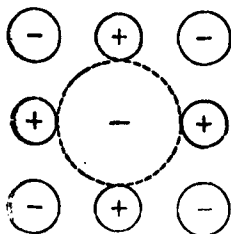It is known that crystals of halides of alkali metals become

- 332 -

Fig. 6.4. In an al-kali-halide crystal, the F center is an electron localized near the vacancy produced after a negative ion is removed from the crys-tal lattice site.

strongly colored if their stoichiometric com-position is disturbed in some manner and if they contain an excess of metal atoms. It was established that the reason for the coloring is the occurrence of color centers. There ex-ist various methods for obtaining colored crystals: passage of x-rays and γ rays, bom-bardment with α and β particles, neutrons, or protons; passage of current through a crystal placed between metallic electrodes; heating the crystal in vapors of alkali metals, etc. We note that the color centers are produced not only in alkali halide salts, but in other di-electric and semiconductor crystals. The experimental and theoretical study of various types of color centers has been the object of a large number of investigations (see, for example, the reviews [48]).

In most cases the color centers are also paramagnetic centers, so that their properties can be investigated by magnetic means, particu-larly with the aid of paramagnetic resonance.

From among the various types of color centers, the best investi-gated were the F centers, which have a characteristic light absorption band. It can be regarded as proved that the F center in an alkali halide crystal is an electron localized near a vacancy produced after a negative ion has been removed from the crystal lattice site (Fig. 6.4). Thus, a qualitative analogy exists between the hydrogen atom and the F center, since the vacancy of the anion can be identified with the positive charge.

The first to observe paramagnetic resonance on F centers was Hutchison [49], who used for this purpose crystals of LiF bombarded for 24 hours by a neutron flux of 10^{12} particles/sec·cm^2. The measure-

- 333 -

ments were made at a frequency of 9350 megacycles; one absorption peak was observed, the position of which corresponded to g = 2.00, while its width was approximately 160 oersteds. The effect was lost when the crystal was bleached by heating it to 500°C. Later, the circle of investigated substances was greatly broadened. A summary of the principal experimental results is given in Table 6.2.

As can be seen from the table, the values of the spectroscopic splitting factors are very close to the g factor of the free electron, thus evidencing the insignificant role of the orbital magnetism. Experiments show that the resonance line has a Gaussian form and that its width in alkali halide crystals is independent of the F center concentration. From this we can conclude that the dipole-dipole interactions of the electron spins of the F centers do not play a major role in the absorption line broadening. This conclusion is reached by simple calculation which shows that at the experimentally investigated F center concentrations the width should not exceed 0.1 oersted. It is seen from Table 6.2 that the experimental values for the line widths of the alkali halide crystals are 2 or 3 orders of magnitude higher.

Kip, Kittel, and others [53] have suggested that the resonance line broadening of the F centers is due to hyperfine interactions between the electron localized near the vacant lattice site and the nuclei of the surrounding atoms. This hypothesis was irrevocably proved. Measurement of paramagnetic resonance in KCl crystals [53], both with natural mixture of potassium isotopes and strongly enriched with the isotope K^{41}, have shown that the widths of the resonance lines are quite different in the two cases, and the ratio of these widths corresponds precisely to the values of the magnetic moments of the K^{39} and K^{41} nuclei.

Portis [58] measured by the saturation method the longitudinal

TABLE 6.2

1 Вещество	2 Количество F-центров в 1 см³	3 Способ окрашивания	4 g-фактор	5 Ширина линии в эрст	6 Литература
LiF	$10^{16}—10^{17}$	7 Поток нейтронов, протонов; рентгеновские лучи	2,008±0,001	77—160	[49, 54, 55, 60, 79, 108]
NaCl	$5·10^{16} — 10^{18}$		1,987	162	[53]
NaF			2,0021±0,0001		[55]
KBr	$10^{18}—10^{20}$	8 γ-лучи; электролитический	1,980	146	[50, 51, 52, 53]
KCl	$5·10^{16}—5·10^{18}$	9 Рентгеновские лучи	1,995±1	54	[51, 52, 53, 59]
K⁴¹Cl	$5·10^{16}$	» »	1,995±1	36	[53]
KI	—	—	1,971±0,001	200	[109]
MgO	$10^{16}—10^{18}$	10 Поток нейтронов, прогревание в парах	2,0028±0,0001	0,7—0,9	[56]
NaNO₃			2,000±0,003		[57]

1) Substance; 2) number of F centers per cubic centimeter; 3) method of coloring; 4) g factor; 5) line width in oersted; 6) literature; 7) neutron or proton flux; x-rays; 8) γ rays; electrolytic; 9) x-rays; 10) neutron flux, heating in vapor.

relaxation time for F centers of a KCl crystal at room temperature, and obtained $T_1 = 2.5·10^{-5}$ sec. These experiments have shown that the broadening is uneven in character, as should be the case if it is due to hyperfine interactions (see §5.8). We note that questions concerning the nature of spin-lattice relaxation of colored crystals or concerning the dependence of T_1 on the temperature, on the static magnetic field intensity, etc., have as yet not been investigated either theoretically or experimentally.

Lord [55] succeeded in resolving the hyperfine structure of the F center resonance lines in LiF and NaF crystals. A large number of components was observed, due to the interaction between the spin of the F electron and the nuclei of the six surrounding alkali metal atoms;

interactions with the following layer of fluorine atomic nuclei yield
an unresolved structure and determine the width of the resonance line.
The experiments make it possible to determine the hyperfine interac-
tion constants A and the values of $|\psi|^2$ on the nuclei of the alkali
metal and fluorine atoms (see Formula (6.27)). The corresponding data
are listed in Table 6.3, where the constants A_1 and A_2 are in oersteds.

TABLE 6.3

Веще- ство (1)	A_1 (щелоч- ной металл) (2)	$\left|\psi\left(\begin{smallmatrix}\text{щелочной}\\ \text{металла}\end{smallmatrix}\right)\right|^2$ см$^{-3}$ (3)	A_2 (F)	$|\psi(F)|^2$, см$^{-3}$ (4)
LiF	14,1±0,1	1,53·10^{24}	4,6±0,5	0,21·10^{24}
NaF	37,8±0,3	6,05·10^{24}	8,6±0,1	0,39·10^{24}

1) Substance; 2) (alkali metal);
3) (alkali metal) cm^{-3}; 4) cm^{-3}.

Feher [59] used a double resonance technique (see §8.2) to dis-
close the hyperfine structure of the paramagnetic resonance line in a
colored KCl crystal. The measurements were carried out with samples
containing $2\cdot10^{17}$ centers per cubic centimeter at a temperature 1.2°K;
the electron resonance absorption line was observed at a frequency
$\nu \approx 9000$ megacycles and had a width of approximately 150 megacycles,
while the frequency of the nuclear resonance was varied from 10 to 100
megacycles and the width of the nuclear resonance was approximately
20,000 cps. Since the nuclear resonance line is approximately 7500
times narrower than the electron line, it is natural for the nuclear
resonance to influence noticeably the form of the electron resonance
line, in spite of the relatively low intensity of its absorption lines.
The results obtained in this fashion can be explained with the aid of
the spin Hamiltonian

$$\mathcal{H} = a(\hat{I}\,\hat{S}) + b(3\,\hat{I}_z\hat{S}_z - \hat{I}\,\hat{S}) + Q'[\hat{I}_z^2 - \tfrac{1}{3}I(I+1)], \qquad (6.31)$$

from which it follows that the resonant frequencies due to the nuclear transitions are

$$h\nu = \pm q_N \beta_N H_0 + \frac{1}{2}[a + b(3\cos^2\vartheta - 1)] +$$
$$+ Q'\left(3\cos^2\vartheta - 1\right)\left(m - \frac{1}{2}\right), \qquad (6.32)$$

where ϑ is the angle between the field H_0 and the axial symmetry axis. If this formula is used, then it follows from the experimental data on the nuclear resonance frequencies that $(a/h) = 2.16$ megacycles, $(b/h) = 0.95$ megacycles, and $(Q'/h) = 0.20$ megacycles for K^{39} and $(a/h) = 700$ megacycles, $(b/c) = 0.5$ megacycles for Cl^{35}. The value of $\underline{a}$ in the case of K^{39} is in good agreement with the value obtained earlier from the width of the resonance line with unresolved hyperfine structure. Lord [60] applied Feher's double resonance technique to F centers in LiF crystals. He succeeded in making the previous results concerning the hyperfine interaction between the F electron and the nuclei of the second coordinate sphere more precise.

It is clear from all the foregoing that it would be of undoubted interest to measure paramagnetic resonance in crystals containing only atoms whose nuclear spins are equal to zero. Wertz and his coworkers [56] came close to solving this problem by setting up paramagnetic resonance experiments on F centers in MgO crystals. These crystals, to be sure, cannot be classified as ionic, but we shall consider them in the present section, since the properties of interest to us are independent of the character of the chemical bond.

Two methods were used for coloring single crystals of MgO: bombardment with a flux of neutrons of intensity $(1-3) \cdot 10^{19}$ particles per square centimeter (between 5 and 7 neutrons are necessary to form one center) and heating in magnesium vapor to a temperature of $1500°C$, followed by rapid cooling and x-raying.

Only the odd isotope Mg^{25}, the abundance of which in natural mag-

- 337 -

nesium is 10 or 11%, has in magnesium oxide a nonzero nuclear spin. Consequently, 53% of the magnesium isotope octahedra surrounding the vacancy contain only the isotopes Mg^{24} and Mg^{26}, 36% of the octahedra contain only a single Mg^{25} atom, and 10% contain each two Mg^{25} atoms. One can expect the paramagnetic resonance spectrum to consist of a narrow bright central line, a broad weak line containing six hyperfine components (I (Mg^{25}) = 5/2), and a family of 11 even weaker lines. The central line actually turns out to be very narrow, approximately 0.7 oersted wide; its position corresponds to the <u>g</u> factor, which coincides accurate to 0.0001 with the value for the free electron. The hyperfine structure has a rather complicated character, owing to the anisotropy of the electron-nuclear coupling constant.

From the value of the isotropic part of the hyperfine structure we can conclude with the aid of (6.2) that $|\psi(Mg)|^2 = 0.276 \cdot 10^{24}$ cm^{-3}, whereas in the free doubly charged magnesium ion $|\psi(Mg^{2+})|^2 = 17.1$ x x 10^{24} cm^{-3}. It is interesting to compare these values with the corresponding values for potassium in the KCl crystal: for the F center we have $|\psi(K)|^2 = 0.70 \cdot 10^{24}$, and for the free potassium ion $|\psi(K^+)|^2 = 7.5 \cdot 10^{24}$ cm^{-3}. From these data we see that the electron is localized in the MgO crystal inside the vacancy to a considerable greater degree than in KCl, and this apparently is explained by the relatively larger Madelung energy in divalent crystals.

Paramagnetic resonance on F centers can be used for certain practical purposes. By measuring the relative intensity of the paramagnetic absorption lines it becomes possible to determine the number of F centers with an accuracy which is 1 or 2 orders of magnitude higher than the accuracy of all other methods. Gordy [61] points out that paramagnetic resonance absorption on F centers can be used to construct a meter to measure the intensity of neutron and x-ray fluxes.

Let us proceed to consider the theory of paramagnetic resonance on F centers. As is well known, in the general theory of F centers, two models are used, the continual [62] and the orbital [63]. It is shown in [59, 64] that even elementary calculations based on the orbital model yield the correct order of magnitude of the displacement of the g factor and the width of the resonance line. According to the orbital model, the F center electron is a valence electron, bound in succession to each of the six atoms in the nearest surrounding of the vacancy. In other words, the wave function of the F electron is in first approximation a linear combination of the $\underline{s}$ functions pertaining to the metal atoms situated around the vacancy:

$$\Psi = \frac{1}{\sqrt{6}} \sum_{i=1}^{6} \psi_i.$$

(6.33)

It is assumed here that the ψ functions of the different atoms do not overlap one another. Since a negative vacancy is equivalent to a positive charge, it is necessary to take into consideration the polarization of the metal atoms under the influence of the given charge. Calculation by a perturbation method shows that a $\underline{p}$ function is added to the $\underline{s}$ function of the valence electron, so that for one of the atoms we have

$$\psi_1 = C \left[\psi_s - \frac{\varepsilon}{\sqrt{2}} (\psi_p^1 - \psi_p^{-1}) \right],$$

(6.34)

where ε is a numerical factor smaller than unity and C is a normalization factor. The wave functions of the other atoms are constructed in analogous fashion. Calculations with the aid of hydrogen functions yield ε = 0.9. In the next approximation it is necessary to take into account the spin-orbit coupling λLS, as a result of which the ψ function assumes the form

- 339 -

$$\psi_1 = c\left[\psi_s - \frac{i}{\sqrt{2}}\left(1 + \frac{\lambda}{2\Delta}\right)\psi_p^1 + \frac{i}{\sqrt{2}}\left(1 - \frac{\lambda}{2\Delta}\right)\psi_p^{-1}\right]. \qquad (6.35)$$

Here Δ is the interval between the s and p levels. Calculation with the aid of this function yields the following expression for the displacement of the g factor [64]:

$$\Delta g = -\frac{4}{3}\cdot\frac{\lambda}{\Delta}\cdot\frac{c^2}{1+c^2}. \qquad (6.36)$$

If we use the known value for potassium $\Delta = 13,200$ cm^{-1} and $\lambda = 38$ cm^{-1}, we obtain $\Delta g = -1.7\cdot10^{-3}$, which coincides in order of magnitude with the experimental value $\Delta g = -0.007 \pm 0.001$.

To calculate the resonance line broadening due to the hyperfine interactions of the F electron with the nuclei of the atoms surrounding the vacancy [53], we employ the Hamiltonian

$$\mathcal{H}' = \sum_i A_i \hat{S}\hat{I}_i, \qquad (6.37)$$

where

$$A_i = -\frac{16\pi}{3}\frac{\beta\mu_i}{I_i}|\psi(i)|^2. \qquad (6.38)$$

Here μ_i is the magnetic moment of the nucleus of the i-th atom, I_i is the spin of the given nucleus, and $\psi(i)$ is the value of the normalized wave function of the electron at the location of the i-th nucleus. With the aid of the Hamiltonian (6.37) we can readily calculate the second moment of the paramagnetic resonance absorption line; its value is

$$M_2 = \frac{1}{3}\sum_i A_i^2 I_i(I_i + 1). \qquad (6.39)$$

It can be shown that the absorption line has a nearly Gaussian shape, and consequently, the line width is $\Delta\nu = 2.36\sqrt{M_2}$. The hyperfine structure will be anisotropic, owing to the presence of the ψ_p functions in Expression (6.35). If we take into account only the principal isotropic part of the hyperfine structure, then we readily ob-

- 340 -

tain from (6.35), (6.38), and (6.39)

$$\Delta \nu = \frac{2{,}36}{\sqrt{18}} \cdot \frac{\sqrt{I(I+1)}}{1+\epsilon^s} A. \qquad (6.40)$$

Here A is the constant of the hyperfine interaction between the elec-
tron and the metal nucleus closest to the vacancy, and I is the spin
of this nucleus. For potassium $I = 3/2$, $A = 0.0077$ cm^{-1}, and the line
width is therefore 50 oersted, which is in splendid agreement with the
experimental value (54 ± 2) oersted.

The authors of [53] have also estimated the width by using the
continual model. According to this model, the F center is made up of
an electron moving in a spherically symmetrical potential field, the
center of which coincides with the vacancy, and the wave function of
the electron covers a large number of atoms. The calculated resonance
line width turned out to be several orders of magnitude lower than the
experimental value. It was therefore concluded that the continual
model is incompatible. The correctness of this conclusion was disputed
by several workers [65, 66, 67]. Deygen [67] called attention to the
following important circumstance. Kip, Kittel, et al. use in their
calculations Formula (6.38), in which the value of the wave function
taken for $\psi(1)$ is the one given by the continual model at the point
where the nucleus $\underline{1}$ is situated. Yet the formula (6.38), which is due
to Fermi [68], holds true only when the symmetry center of the wave
function coincides with the nucleus, something that precisely does not
occur in the F center, since the nuclei of the ions are shifted rela-
tive to the symmetry center of the wave function by an amount equal to
the lattice constant. The question of the hyperfine interaction between
the electron and a nucleus shifted relative to the symmetry center of
the wave function calls for a special analysis. Deygen offers a solu-
tion of this problem, using for the wave function of the F center the

following expression [69]:

$$\varphi(r) = a^{\frac{3}{2}} (1 + ar) e^{-\frac{ar}{\sqrt{12}}}. \qquad (6.41)$$

Assuming that the length $(1/a)$ does not far exceed the lattice constant, and therefore confining himself to a consideration of the hyperfine interaction with the nuclei of the first coordination sphere, he obtained for the resonance line width in KCl a value on the order of 1-2 oersted. With an aim toward improving this result, Deygen replaced the "smoothed" function (6.41) by a so-called detailed wave function in the form

$$\psi(r) = \Omega^{\frac{1}{2}} \varphi u. \qquad (6.42)$$

Here Ω is the volume of the principal region in the crystal and $\underline{u}$ is the normalized Bloch wave function of the electron at the bottom of the conduction band, which, as is well known, represents in the strong-coupling approximation a linear combination of the atomic wave functions. The line width calculated with the aid of the detailed function turned out to be equal to 15 oersted, which is already quite close to the experimental value.

In order to ascertain whether the line width is affected by an account of relativistic corrections, the usual Pauli equation for the motion of the electron was replaced in the calculation of the hyperfine structure by the Darwin relativistic approximation [70]; the corrections turned out to be negligible. Zevin [71] developed the theory proposed by Deygen and obtained a general expression for the spin Hamiltonian, describing the interaction between the F center electron and the nuclei of the atoms surrounding the vacancy. Shul'man [72], using the given spin Hamiltonian, calculated the broadening brought about by the second coordination sphere, consisting of the halide atoms. For the KCl crystal, the contribution made by the chlorine atoms to the

width amounts to 19%.

Gourary and Adrian [73] used a wave function obtained by a simplified Hartree method to calculate the hyperfine structure of paramagnetic resonance on F centers. The lattice ions were regarded here as being point charges. The distortions of the lattice near the vacancy were also taken into account. The theoretically obtained hyperfine splittings are in good agreement with the experimental results for LiF.

The method of Gourary and Adrian was applied to calculations of the isotropic and anisotropic structures of the KCl spectrum [74]; the theoretical results are in good agreement with the experimental data of Feher [59]. Adrian [75] pointed out the possibility of establishing a simple connection between the displacement of the g factor and the anisotropic hyperfine structure, since both these quantities are determined by the average value of $1/r^3$. Thus, for KCl, starting from the experimental value of the hyperfine structure anisotropy, theory yields $\Delta g = -0.0053$ while experiment gives $\Delta g = -0.007$. A good agreement with the experimental results of Feher was also obtained by Blumberg and Das [76], who used in their calculations of the hyperfine structure the g factor displacement and the wave function obtained under the following assumption: the vacancy is replaced by a potential well and the lattice by a system of corresponding point charges.

In developing the theory of paramagnetic resonance on F centers, we used the de Boer model [62], according to which the F center is an electron localized near a vacant lattice site. It is universally accepted that centers of this type are formed in alkali halide crystals. In silver halide crystals one might think that the F centers would be of the Hilsch and Pohl type [62], i.e., they would comprise metal atoms that have penetrated the interstices of the crystal lattice. Glinchuk and Deygen [77] calculated the hyperfine structure of the en-

ergy levels of an F center of this type, using the NaCl crystal as an example. Using the wave functions of both the continual and the orbital models, they obtained spin Hamiltonians with which they calculated the paramagnetic resonance spectrum, the line shapes, and the line widths. It turned out that the results differ qualitatively from those previously obtained for the de Boer model. Thus, a study of paramagnetic resonance uncovers a possibility of choosing between two existing F center models, something particularly valuable inasmuch as so far no other effective methods have been proposed for solving this problem.

Lord et al. [78] have found indirect proof for the existence of paramagnetic resonance absorption on an M center (a combination of an F center and a pair of vacant sites). It was established that the second moment of the resonance line increases appreciably whenever a LiF crystal is exposed to x-rays so as to be able to observe in it, by optical means, an increase in the number of M centers compared with the number of F centers.

Paramagnetic resonance was investigated in greater detail on V centers [79, 84]. In the studied alkali halide crystals, these centers were produced by means of x-rays at liquid nitrogen temperatures. Castner, Künzig, and Woodruff [82, 83], who have made the most complete study of this problem, interpret their experimental results with the aid of the following V center model: 1) the x-radiation causes an electron to break away from the halide ion, and the resultant electron hole is distributed among two neighboring ions oriented along the [110] axis of the crystal; 2) the molecular ion X_2^- produced in this fashion (where X stands for the halogen) is connected with neither the vacancy formation nor with the distortions of the crystal lattice.

Paramagnetic resonance was investigated in crystals of LiF, KCl,

KBr, and NaCl. The resonance lines had a hyperfine structure due to the interaction between the electron hole and the nuclei of both atoms, forming the X^{-1} molecule. The number and intensity of the hyperfine components in the LiF crystal agrees with a value $I = 1/2$ for the nuclear spin of fluorine, if one takes into account the selection rules for the singlet and triplet nuclear spin states; in precisely the same manner, the spectra of the remaining investigated crystals consisted of seven approximately equidistant components with intensity ratio 1:2:3:4:3:2:1, which corresponds to a nuclear spin $I = 3/2$ for the Cl or Br atoms. To interpret the paramagnetic resonance spectrum, starting with the X_2^{-1} molecular ion model, one can obtain a spin Hamiltonian of the type (6.31) by taking the [110] crystal axis to be the Z axis. The principal values of the g-tensor components are listed in Table 6.4, which shows also the absorption line widths.

TABLE 6.4

Вещество 1	g_x	g_y	g_z	Максималь-ная ошибка 2	Ширина, эрст 3
LiF	2,0227	2,0234	2,0031	± 0,0010	12,3 ±0,3
KCl	2,0428	2,0447	2,0010	± 0,0001	1,34 ±0,03
NaCl	2,0489	2,0425	2,0010	± 0,0001	4,5 ±0,1
KBr	2,179	2,175	1,980	± 0,0001	2,8 ±0,1

1) Substance; 2) maximum error;
3) width, oersted.

The main reason for the broadening of the resonance line are the hyperfine interactions between the electron hole and the nuclei surrounding the V center. The line shape is nearly Gaussian.

For Cl_2^-, calculations of the g factor were made by the molecular orbital method [85], and yielded values close to the experimental ones.

Känzig and Woodruff [86] observed paramagnetic resonance in the KCl crystal on H centers, which have a spectrum similar to that of V centers, but of more complicated nature. The latter is due to the fact

that in the case of the H centers the electron hole is shared by four chlorine ions arranged on a single line.

Kawamura and Ishiwatari [87] observed paramagnetic resonance on Z_1 centers in KCl crystals. The Z_1 centers are produced in alkali halide crystals in which divalent metals have been introduced. A possible model of the Z_1 center is that of a singly ionized divalent metal atom, which occupies the place of the alkali metal ion. The experiments involved crystals doped with Ca and Sr atoms in amounts of approximately 10^{17} cm^{-3}. Since the spins of the calcium and strontium nuclei are equal to zero, there is a deep analogy between paramagnetic resonance on Z_1 and on F centers. The essential difference lies in the fact that the broadening of the Z_1-center resonance line occurs primarily as a result of hyperfine interactions with the nuclei of the anions, whereas in F centers the principal role is assumed by the nuclear spins of the cations. Measurements have shown that the absorption line has a Gaussian form, a width $\Delta H = 79$ oersted, with $g = 1.999$.

§6.6. Irradiated Crystals with Covalent Bond

Paramagnetic resonance can serve as an effective method for investigating imperfections in crystals. This possibility is connected, first of all, with the fact that the occurrence of many types of imperfections in diamagnetic crystals is accompanied by formation of paramagnetic centers. Second, in paramagnetic crystals, imperfections of the dislocation type change the intercrystalline field and cause shifts in the paramagnetic resonance lines and a change in the spin-lattice interaction. In the last two sections we have considered paramagnetic resonance due to lattice defects of the inclusion, electron, or hole type. In the present section we discuss also a few examples and primarily the effect in neutron-bombarded diamond.

Griffiths, Owen, and Ward [88] carried out measurements at fre-

- 346 -

quencies $\nu \approx 9000$ and 25,000 megacycles in the temperature interval 20-280°K. The existence of two types of resonance lines was established:

a) Isotropic line with a spectroscopic splitting factor g = = 2.0028 ± 0.0006. The intensity and width of the line increase with increasing duration of irradiation. Heating to 1000°C causes the effect to disappear. An analogous change occurs in the coloring of the crystal. After prolonged neutron bombardment, the line width reaches 100 oersted at a temperature of 290°K; the width of the line is reduced to one half when the temperature is decreased to 90°K.

b) Family of 12 weak anisotropic lines, symmetrically situated relative to the central peak. The width of each of these lines is independent of the temperature and is approximately equal to 5 oersted. In this case the effect does not decrease upon heating to 1000°C. The paramagnetic absorption spectrum can be described with the aid of a spin Hamiltonian $\hat{H} = \beta_g \vec{H}_0 \hat{\vec{S}} + D\hat{S}_z^2$ if one admits the existence of paramagnetic centers with spin S = 1. It is necessary to assume here that the axis of the crystalline field is parallel to one of the edges of the tetrahedron made up of the carbon atoms. Thus, there exist six different orientations of paramagnetic centers, each of which has two absorption lines corresponding to the transitions $-1 \rightarrow 0$ and $0 \rightarrow 1$. The spin Hamiltonian constants have the following values: $D = 0.010$ cm^{-1}, average value of the g factor $\bar{g} = 2.0027 \pm 0.0005$ and $g_\perp/g_\parallel = 1.00035 \pm \pm 0.00005$.

The central isotropic line has apparently the following nature [89]. Let us consider an isolated vacancy, formed in the crystal lattice after the removal of one of the carbon atoms. Since diamond is not an ionic crystal, there are no grounds for expecting the vacancy to attract an electron or to contribute to its removal; it is more

likely that the vacancy is to be regarded as an electrically neutral stable formation. The vacancy is surrounded by four carbon atoms, in each of which one of the two covalent bonds is saturated and therefore each has an unpaired electron. It can be shown that one can apply to this four-electron system Hund's rule, according to which all electron spins are parallel to one another in the ground state, and consequently the spin of the entire system is $S = 2$. In this state, the orbital wave function is nondegenerate and consequently the paramagnetism will in first approximation be of pure spin nature.

The spin orbit coupling in the free carbon atom is very weak. Furthermore, owing to the high symmetry of the crystalline field, the spin level splitting due to the spin-orbit interaction becomes different from zero only in the fourth perturbation theory approximation. We can therefore conclude that this splitting should be negligibly small. An estimate shows that its order is 10^{-5} cm^{-1}. For the same reason, the deviation of the $\underline{g}$ factor from its value for the free electron should also be very small.

It is more difficult to present a theoretical interpretation of all the peculiarities of the anisotropic paramagnetic resonance spectrum. It is evidently connected with the carbon atoms which are situated in the interstices of the crystal lattice.

Let us proceed to an examination of paramagnetic resonance on color centers produced in quartz after exposure to x-rays; these centers disappear upon heating to $350°C$. Griffiths, Owen, and Ward [88] first observed this effect in quartz and established that the paramagnetic absorption is proportional to the optical absorption. Measurements of the paramagnetic resonance spectrum were made at temperatures of 90 and $20°K$; at higher temperatures, the lines broadened strongly. The existence of six types of paramagnetic centers was established,

with different magnetic-axis orientations. A complicated hyperfine structure of the lines was also observed, and could be resolved at 20°K. The spectrum can be described with the aid of a spin Hamiltonian with the following constants: $S = 1/2$, $I = 5/2$, $g_{\parallel} = 2.06 \pm 0.005$, $g_{\perp} = 2.00 \pm 0.005$, $A = 4.8 \cdot 10^{-4}$ cm^{-1}, $B = 5.6 \cdot 10^{-4}$ cm^{-1}, and $P = -0.4$ x x 10^{-4} cm^{-1}. The symmetry axes of $\underline{g}$ tensors of paramagnetic centers of different types are approximately parallel to the lines joining the pairs of silicon atoms within the crystal cell. The principal axes of the $\underline{g}$ tensor and of the hyperfine structure tensor do not coincide. The symmetry axes of the hyperfine structure tensor are parallel to the Si-O bonds.
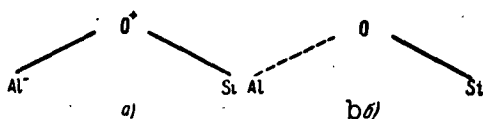
Fig. 6.5. Electronic structure of paramagnetism carriers in irradiated quartz.

The following interpretation can be offered for all these experimental facts [82]. The various impurities contained in the quartz include also aluminum, the atoms of which replace a small part of the silicon atoms. Before the quartz is irradiated, the aluminum atoms are Al$^-$ ions, which have the same number of electrons as the silicon atoms. Consequently, the crystal is not colored and there are no paramagnetic centers. The negative charge of the Al$^-$ ions is neutralized by the positive ions H$^+$, Li$^+$, and Na$^+$, which are located in the interstices of the crystal lattice. Irradiation with x-rays causes the atoms to be ionized and uncompensated electron spins appear. Calculations made by the electronic orbital method show [90] that the electron structure of the paramagnetism carriers has essentially the form shown in Fig. 6.5a. The nonzero spin belongs to the positive oxygen ion. Partially mixed

in with this structure is another one (Fig. 6.5b), containing neutral oxygen and aluminum atoms, and consequently, a hyperfine structure of the paramagnetic resonance lines is produced.

Paramagnetic resonance in single crystals of quartz was observed also by irradiation with fast neutrons [91, 92, 85a]. The observations were made at room temperature. The effect is apparently not connected with impurities and has an entirely different nature, as evidenced even by the absence of a hyperfine structure for the absorption lines. It is probable that the resonant absorption, as in the case of diamond, is due to broken bonds which result from the occurrence of the vacancies in the basic SiO_4 tetrahedron. An analogous effect was observed at $4.2°K$ in silicon bombarded by neutrons [93]. In explaining the effect in irradiated quartz crystals it must be borne in mind that a similar paramagnetic resonance spectrum occurs in silicate glasses [92, 94].

Paramagnetic resonance was observed at temperatures $4-225°K$ in γ-irradiated ice [95, 96]. The hyperfine structure of the line is connected with the protons in ordinary ice and the deuterons in D_2O. The nature of the paramagnetism carriers cannot be regarded as fully explained as yet.

§6.7. Metal-Ammonia Solutions. Paramagnetic Resonance on Polarons and Excitons

Alkali and alkali-earth metals are readily dissolved in ammonia. The solubility of sodium and potassium at the boiling temperature of ammonia (−33.35°C) is approximately 5.4 and 4.9 mole per liter, respectively; the solubility changes little with temperature. A distinguishing property of these solutions is their high electric conductivity, which approaches that of metals in order of magnitude. Measurements of the dependence of the static magnetic susceptibility on the

concentration of the solution have shown that at large concentrations the addition of metal is not accompanied by an increase in the susceptibility.

The first measurements of paramagnetic resonance in metal-ammonia solutions were made in the microwave band [97, 98, 99]. One exceedingly narrow absorption line, with a width not larger than 0.2 oersted, was established. Later experiments were made usually at lower frequencies [100, 101, 9], which called for the application of a static magnetic field with intensity of only a few oersteds; it was necessary besides to take account of the earth's field. The measurements were carried out at temperatures from −80 to 20°C. For potassium solutions, the spectroscopic splitting factor is $g = 2.0012 \pm 0.0002$. For other metals it deviates by less than 0.005. We see that the g factor is close to (but noticeably smaller than) the g factor of the free electron. Table 6.5 lists data for the resonance line widths, showing that the width decreases with increasing temperature and increases with increasing concentration. In addition to metal-ammonia solutions, solutions of lithium in methylamine [99, 9] and in ethylenediamine [99] were investigated. Galkin et al. [102] observed paramagnetic resonance in solutions of NaCl in ammonia after passing current through the solution. Apparently the current causes decomposition of the NaCl and thus results in an ordinary solution of Na.

Blume [103] measured the times of longitudinal and transverse relaxation (T_1 and T_2) at 17.4 megacycles by means of pulse techniques. The time T_2 was determined by measuring the time of fall-off of the free induction signal, which was followed at 90° by a pulse (see §8.4). It ranges from 3.2 to 0.7 microseconds when the sodium concentration in NH_3 increases from 0.03 to 0.75 mole/liter. The time T_1 was measured in solutions having concentrations from 0.24 to 0.5 mole/liter.

- 351 -

TABLE 6.5

1 Вещество	2 Ширина, эрст	3 Температура, °C	4 Концентрация, моль/л	5 Литература
Li—NH₃	0,1	—72	0,2	[9]
Na—NH₃	0,13	—75	0,1	[9]
K—NH₃	0,1	—70	0,08	[9]
K—NH₃	0,05	—33,45	0,08	[100]
K—NH₃	0,027	20	0,08	[100]
K—NH₃	0,08	20	0,43	[100]
Rb—NH₃	0,16	—70	0,1	[9]
Cs—NH₃	0,4	—70	0,5	[9]
Ca—NH₃	0,14	—70	0,05	[9]
Li—CH₃NH₂	0,6	—70	0,1	[9]
Li—NH₂CH₂NH₂	0,6	20	0,1	[99]

1) Substance; 2) width, oersted; 3) temperature, °C; 4) concentration, mole/liter; 5) literature.

It was found that $T_1 = T_2$ accurate to within 10%.

Kaplan and Kittel [104] explained the experimental fact by means of the Ogg model [105], which is based on the following assumptions: 1) the alkali metal atoms dissociate when dissolved; 2) the electrons separated from the metal atoms are localized in the cavities formed in the liquid, which have volumes equal to that of from 2 to 4 molecules of NH_3; 3) the wave function of the electron connected with the cavity is a linear combination of hydrogen functions pertaining to the protons of the NH_3 molecules located around the cavity; 4) the conduction band lies one electron volt below the energy level of the bound state of the electron; 5) some cavities contain one electron each (e centers) and some contain two electrons (e_2 centers); the distribution of the electrons among the e and e_2 centers is determined by the equilibrium conditions with respect to the reaction $e + e \rightleftarrows e_2 + 0.2$ ev.

Between the e centers and F centers considered in §6.5 there is a great similarity. Kaplan and Kittel therefore assume that the absorption line broadening has in both cases the same nature, namely the hy-

- 352 -

perfine interaction between the localized electron and the spins of the surrounding nuclei. An estimate of the width, made as in the case of §6.5 by the method of molecular orbitals, yields $\Delta \nu_0 \approx 7g\beta/h$. However, there exists an essential difference, which we did not take into consideration, between the $\underline{e}$ and F centers. The large mobility of the liquid is capable of appreciably decreasing the width of the resonance line. The correlation time (see §5.6) can be estimated with the aid of the Debye expression for the rotational dipole relaxation:

$$\tau_c \approx \frac{3\eta V}{kT},\qquad (6.43)$$

where V is the volume of the molecule. Hence $\tau_c \approx 10^{-11}$ sec. We see that the correlation time is much smaller than the transverse relaxation time $\sim 1/\Delta \nu_0$ and therefore the motion of the molecules should narrow down the resonance line appreciably. The width obtained as a result can be estimated by the formula $\Delta \nu \sim (\Delta \nu)^2 \tau_c$, from which it follows in our case that $\Delta H \approx 0.01$ oersted. So good an agreement with the experimental data is accidental, bearing in mind the crudeness of the theoretical estimate.

At large solution concentrations one can expect the dipole-dipole interactions between different localized electrons to start playing a role. The influence of dipole-dipole interactions on the resonance width can be estimated by means of Formula (5.14). Numerical calculation shows that this broadening mechanism can become significant at concentrations exceeding 0.1 mole/liter.

We know that if $\tau_c \ll 1/\Delta \nu_0$, we have $T_2 = T_1$, which, as we have seen, has been confirmed by direct measurements. We note that both mechanisms which we have considered for the broadening lead to a proportionality between the line width and the coefficient of viscosity. Experiment confirms this theoretical conclusion, too.

The Ogg e-center model, on which the theory of paramagnetic reso-
nance line broadening considered here is based, was seriously crit-
icized by Deygen [106], who developed a theory of optical, magnetic,
and other properties of metal-ammonia solutions by assuming that upon
dissociation of the metal atoms in the ammonia the electrons go over
into the polaron state. According to Deygen, it is the polarons and
not the local electron centers that cause the remarkable features of
solutions of metals in ammonia. Deygen and Pekar [107] have shown that,
in first approximation, the hyperfine interaction does not change the
polaron energy and consequently it cannot cause broadening of the
paramagnetic absorption line. The exceeding narrowness of the reso-
nance lines in metal-ammonia solutions was regarded as a direct proof
of the existence of polarons in these substances.

Deygen and Pekar considered also the possibility of producing ex-
citon concentrations high enough to permit observation of paramagnetic
resonance absorption of energy from a radiofrequency field by excitons.
The stationary exciton concentration N can obviously be determined
from the following formula

$$N = \frac{\tau \Pi \varkappa}{h\nu},$$
(6.44)

where τ is the exciton lifetime, Π the flux of light energy per square
centimeter per second, $\varkappa$ the coefficient of exciton absorption of
light in the crystal, and ν the frequency of absorbed light. If we as-
sume $\tau = 10^{-8}$ sec, $h\nu \approx 1$ ev, $\varkappa \approx 10^5$ cm^{-1}, $\Pi \approx 1$ w/cm^2, then we ob-
tain $N \approx 10^{16}$ cm^{-3}. Thus, observation of paramagnetic resonance with
the aid of modern technological means is fully feasible. In order to
reduce the nonradiative deexcitation of the excitons, it is desirable
to choose crystals free of impurities and to use low temperatures. It
must be borne in mind that, as in the case of polarons, there will be

no broadening of paramagnetic resonance line due to hyperfine interaction between the exciton and the spins of the surrounding nuclei.

REFERENCES TO CHAPTER 6

1. Griswold T.W., Kip A.F., Kittel C., Phys. Rev. 88, 951, 1950.

2. Kip A.F., Griswold T.W., Portis A.M., Phys. Rev. 92, 544, 1953.

3. Feher G., Griswold T.W., Phys. Rev. 93, 952, 1954.

4. Gutowsky S., Frank P.J., Phys. Rev. 94, 1067, 1954.

5. Schumacher R.T., Carver T.R., Slichter C.P., Phys. Rev. 95, 1089, 1954.

6. Feher G., Kip A.F., Phys. Rev. 95, 1343, 1954.

7. Kip A.F., Defects in crystalline solids, Bristol, 38, 1955.

8. Feher G., Kip A.F., Phys. Rev. 98, 337, 1955.

9. Levy R.A., Phys. Rev. 102, 31, 1956.

10. Garif'yanov N.S., ZhETF [J. Exp. Theor. Phys.], 32, 149, 1957.

11. Garif'yanov N.S., Starikov M.A., ZhETF 35, 798, 1958.

12. Jafet Y., Phys. Rev. 85, 478, 1952.

13. Bardeen J., J. Chem. Phys. 6, 367, 1938.

14. Brooks H., Phys. Rev. 94, 1411, 1954.

15. Argyres P., Kahn A., Phys. Rev. 98, 226, 1955.

16. Overhauser A.W., Phys. Rev. 89, 689, 1953.

17. Korringa J., Physica 16, 601, 1950.

18. Elliott R.J., Phys. Rev. 96, 266, 1954.

19. Andreyev V.V., Gerasimenko V.I., ZhETF 35, 1209, 1958.

20. Al'tshuler S.A., ZhETF 20, 1047, 1950.

21. Pines D., Phys. Rev. 95, 1090, 1954.

22. Dyson F.J., Phys. Rev. 98, 349, 1955.

23. Bloembergen N., J. Appl. Phys. 23, 1379, 1952.

24. Silin V.P., ZhETF 30, 421, 1956.

25. Azbel' N.Ya., Gerasimenko V.I., Lifshits I.M., ZhETF 31, 357, 1957;

32, 212, 1957; Azbel' M.Ya., ZhETF 32, 1259, 1957.

26. Azbel' M.Ya., Lifshits, I.M., ZhETF 33, 792, 1957.

27. Owen J., Browne M., Knight W.D., Kittel C., Phys. Rev. 102, 1501, 1956.

28. Owen J., Browne M., Kip A.F., J. Phys. Chem. Solids 2, 85, 1957.

29. Knight W.D., Phys. Rev. 76, 1259, 1949.

30. Kip A.F., Rev. Mod. Phys. 25, 229, 1953; Kip A.F., Kittel C., Portis A.M., Barton R., Spedding F.H., Phys. Rev. 89, 518, 1953.

31. Salikhov S.G., ZhETF 26, 447, 1954.

32. Al'tshuler S.A., ZhETF 26, 439, 1954.

33. Al'tshuler S.A., ZhETF 28, 49, 1955.

34. Portis A.M., Kip A.F., Kittel C., Bratain W.H., Phys. Rev. 90, 988, 1953.

35. Willenbroek F.K., Bloembergen N., Phys. Rev. 91, 1281, 1953.

36. Fletcher R.C., Yager W.A., Pearson G.L., Holden A.N., Read W.T., Merritt F.R., Phys. Rev. 94, 1392, 1954.

37. Fletcher R.C., Yager W.A., Pearson G.L., Merritt F.R., Phys. Rev. 95, 844, 1954.

38. Pearson G.L., Bardeen J., Phys. Rev. 75, 865, 1949.

39. Honig A., Kip A.F., Phys. Rev. 95, 1686, 1954.

40. Lüttinger J.M., Kohn W., Phys. Rev. 96, 802, 1954; 98, 883, 1955.

41. Slichter C.P., Phys. Rev. 99, 479, 1955.

42. Feher G., Fletcher R.C., Gere E.A., Phys. Rev. 100, 1784, 1955.

43. Honig A., Combrisson J., Phys. Rev. 102, 917, 1956.

44. Abragam A., Combrisson J., Compt. Rend. 243, 576, 1956.

45. Feher G., Fletcher R.C., Bull. Am. Phys. Soc., ser. II, 1, 125, 1956.

46. Pines D., Bardeen J., Slichter C.P., Phys. Rev. 106, 489, 1957.

47. Abrahams E., Phys. Rev. 107, 491, 1957.

48. Seitz F., Rev. Mod. Phys. 18, 384, 1946; 26, 7, 1954.

49. Hutchison C.A. Jr., Phys. Rev. 75, 1769, 1949.

50. Tinkham M., Kip A.F., Phys. Rev. 83, 657, 1951.

51. Schneider E.E., England T.S., Physica 17, 221, 1951.

52. Hutchison C.A., Jr., Noble G.A., Phys. Rev. 87, 1125, 1952.

53. Kip A.F., Kittel C., Levy R.A., Portis A.M., Phys. Rev. 91, 1066, 1953.

54. Jen C.K., Lord N.W., Phys. Rev. 96, 1150, 1954.

55. Lord N.W., Phys. Rev. 105, 756, 1957.

56. Wertz J.E., Weeks R.A., Auzins P., Silber R.H., Phys. Rev. 107, 1535, 1957.

57. Ard W.B., Jr., J. Chem. Phys. 23, 1967, 1955.

58. Portis A.M., Phys. Rev. 91, 1071, 1953; 100, 1219, 1955; Portis A.M., Shaltiel D., Phys. Rev. 98, 264, 1955.

59. Feher G., Phys. Rev. 105, 1122, 1957.

60. Lord N.W., Phys. Rev. Letters 1, 170, 1958.

61. Gordi V., Smit V., Trambarulo R., Radiospektroskopiya [Radio Spectroscopy], Gostekhizdat [State Unified Publishing House for Technical and Theoretical Literature], Moscow, 1955, p. 248.

62. Pekar S.I., Issledovaniye po elektronnoy teorii kristallov [Research in the electronic theory of crystals], Gostekhizdat, Moscow-Leningrad, 1951.

63. Muto T., Progr. Theor. Phys. 4, 243, 1949; Ynui T., Uemura I., Progr. Theor. Phys. 5, 252, 395, 1950.

64. Kahn A.H., Kittel C., Phys. Rev. 89, 315, 1953.

65. Dexter D.L., Phys. Rev. 93, 244, 1954.

66. Krumhansl J.A., Phys. Rev. 93, 245, 1954.

67. Deygen M.F., ZhETF 33, 773, 1957.

68. Fermi E., Z. Phys. 60, 320, 1930.

69. Pekar S.I., ZhETF 17, 868, 1947; Pekar S.I., Deygen M.F., ZhETF

18, 48, 1948.

70. Deygen M.F., Shul'man L.A., ZhOS [J. Optics and Spectroscopy] 3, 21, 1957.

71. Zevin V.Ya., ZhOS 3, 660, 1957.

72. Shul'man L.A., ZhOS 3, 684, 1957.

73. Gourary B.S., Adrian F.J., Phys. Rev. 105, 1180, 1957.

74. Adrian F.J., Phys. Rev. 106, 1356, 1957.

75. Adrian F.J., Phys. Rev. 107, 488, 1957.

76. Blumberg W.E., Das T.R., Phys. Rev. 110, 647, 1958.

77. Glinchuk M.D., Deygen M.F., ZhTF [J. Tech. Phys.] 28, 1981, 1958.

78. Lord N.W., Phys. Rev. 106, 1100, 1957.

79. Schneider E.E., Phys. Rev. 93, 919, 1954.

80. Känzig W., Phys. Rev. 99, 1890, 1955.

81. Cohen M.H., Phys. Rev. 101, 1432, 1956.

82. Castner T.G., Känzig W., J. Phys. Chem. Solids 3, 178, 1957.

83. Woodruff T.O., Känzig W., Rept. General Electr. Res. Lab. 39, No. 1827, 1957.

84. Suffczynski M., Postepy fiz. [Progress in Physics] 9, 27, 1958.

85. Inui T., Harasawa S., Obata Y., J. Phys. Soc. Japan 11, 612, 1956.

86. Känzig W., Woodruff T.O., Phys. Rev. 109, 220, 1958.

87. Kawamura H., Ishiwatari O., J. Phys. Soc. Japan 13, 574, 1958.

88. Griffiths J.H.E., Owen J., Ward I.M., Nature 173, 439, 1954; Defects in crystalline Solids 9 (Bristol), 81, 1954.

89. O'Brien M.C.M., Pryce M.H.L., Defects in crystalline Solids, Bristol, 88, 1954.

90. O'Brien M.C.M., Proc. Roy. Soc. A231, 404, 1955.

91. Weeks R.A., J. Appl. Phys. 27, 1376, 1956.

92. Molin Yu.N., Voyevodskiy V.V., ZhTF 28, 143, 1958.

93. Schulz-du Bois E., Nisenoff M., Fan H.Y., Lark-Horowitz K., Phys.

Rev. 98, 1561, 1955.

94. Weeks R.A., J. Appl. Phys. 27, 1376, 1956.

95. Smaller B., Matheson M.S., Yasaitis E.L., Phys. Rev. 94, 202, 1954.

96. Matheson M.S., Smaller B., J. Chem. Phys. 23, 521, 1955.

97. Hutchison C.A., Jr., Pastor R.C., Phys. Rev. 81, 282, 1951.

98. Garstens M.A., Ryan A.H., Phys. Rev. 81, 888, 1951.

99. Levinthal E.C., Rogers E.H., Ogg R.A., Jr., Phys. Rev. 83, 182, 1951.

100. Hutchison C.A., Jr., J. Phys. Chem. 57, 546, 1953.

101. Hutchison C.A., Jr., Pastor R.C., Rev. Modern Phys. 25, 285, 1953; J. Chem. Phys. 21, 1959, 1953.

102. Galkin A.A., Shamfarov Ya.A., Stefanishina A.V., ZhETF 32, 1581, 1957.

103. Blume R.J., Phys. Rev. 109, 1867, 1958.

104. Kaplan J., Kittel C., J. Chem. Phys. 21, 1429, 1953.

105. Ogg R.A., J. Chem. Phys. 14, 114, 295, 1946; J. Am. Chem. Soc. 68, 155, 1946.

106. Deygen M.F., ZhETF 26, 293, 300, 1954; Ukr. fizichn. zhurn. [Ukrainian Physics Journal] 1, 245, 1956.

107. Deygen M.F., Pekar S.I., ZhETF 34, 684, 1958.

108. Kim Y.W., Kaplan R., Bray P.J., Bull. Am. Phys. Soc. 3, 178, 1958.

109. Noble G.A., Bull. Am. Phys. Soc. 3, 178, 1958.

110. Watkins G.D., Bull. Am. Phys. Soc. Ser. II, 2, 345, 1957; Zudwig G.W., Woodbury H.H., Bull. Am. Phys. Soc. Ser. II, 3, 135, 1958; Phys. Rev. Letters 1, 16, 1958; J. Phys. Chem. Solids 8, 490, 1959; Phys. Rev. 113, 1014, 1959; Feher G., Wilson D.K., Gere E.A., Phys. Rev. Letters 3, 25, 1959; Koth L.M., Lax B., Phys. Rev. Letters 3, 217, 1959.

[Footnotes]

311   Levy [9], investigating the temperature dependence of the resonance line width of lithium, established the presence of a jump at approximately 80°K, this being apparently connected with the existence of a phase transition.

323   Gadolinium, the ions of which also have an odd number of electrons, will be considered separately.

326   A natural sample of silicon contains 4.68% of the isotope Si^{29}.

327   Recently, investigations of paramagnetic resonance in germanium have yielded positive results [110].

Chapter 7

FREE RADICALS

§7.1. Introduction. Hyperfine Structure of Paramagnetic Resonance Lines in Solutions of Free Radicals

The study of free radicals, i.e., molecules in which at least one electron has uncompensated spin, is one of the most important fields of application of paramagnetic resonance and attracts at present a very large number of investigators. It is sufficient to state that the total number of papers devoted to this problem already amount to several hundreds. We are therefore unable to give in our book an exhaustive exposition of all the results obtained. We refer the reader for details primarily to Ingram's book [1], and also to the reviews by Wertz [2] and by Blyumenfeld and Voyevodskiy [3].

The variety of substances that have to be considered in the present chapter is so great that their rigorous classification is very difficult.

Paramagnetic resonance in free radicals was first observed in 1947 by Kozyrev and Salikhov [4] with pentaphenylcyclopentadienyl $C_{35}H_{25}$ as an example. Solid $C_{35}H_{25}$ disclosed a single line with a g factor which, within the limits of the low measurement accuracy, differed little from two. It was therefore concluded that this free radical has essentially a spin magnetism, in accordance with the measurements of the static magnetic susceptibility of this substance.

In 1949, a systematic study of the paramagnetic spectra in free radical was initiated. By now numerous classes of these substances have

been investigated, for example organic derivatives of divalent nitrogen, radical ions of hydrocarbons, heptaquinones, compounds of the peroxide type, biradicals, etc.

An essential feature of paramagnetic resonance spectra in free radicals is the fact that the $\underline{g}$ factor is very close to its value for the free electron $g_{spin} = 2.0023$, i.e., pure spin magnetism. Thus, for ordinary organic free radicals containing only C, H, O, and N atoms, the difference $g - g_{spin} = \Delta g$ does not exceed 0.002-0.003. This practically complete lack of orbital magnetism is due to the fact that the molecules of the free radical have low symmetry, and consequently the orbital degeneracy is completely lifted; there is no doubt that in many of these cases the lowering of the symmetry is brought about by the Jahn-Teller effect. In connection with so strong a suppression of the orbit, the spin-orbit coupling in free radicals is small and the spin-lattice relaxation time is long (usually on the order of 10^{-7} sec).

A second feature characterizing practically all free radicals which in the condensed phase are in pure undiluted state is the exceeding naturalness of the paramagnetic resonance lines: their width as a rule is of the order of one or several oersted. This value is approximately 100 times smaller than that calculated from magnetic dipole interactions without account of exchange. Thus, in free radicals we have an example of a system with tremendous exchange forces. Accordingly, the absorption line shape in these radicals is close to Lorentzian, and the line width is determined by the spin lattice interactions [5].

It must be noted that in addition to exchange in free radicals, there exists still another important mechanism whereby the paramagnetic resonance lines become narrower; this mechanism was considered in [6]. It consists in a reduction in the effectiveness of the local magnetic fields, due to the motion of the strongly delocalized unpaired electron

within the molecule of the free radical. There are certain experimental confirmations of the reality of this mechanism.

The narrowness of the lines makes the height of the resonance peaks in free radicals very large, thus facilitating their detection. Thus, for the substance extensively used as the standard calibrating substance in research on paramagnetic resonance, $\alpha\alpha$-diphenyl-β-picrylhydrazyl (DPPH) this line can be observed with modern apparatus in the presence of only 10^{-13} mole of DPPH in the sample. Paramagnetic resonance is therefore the best of the existing methods for detecting free radicals (at least in condensed phases).

The significance of paramagnetic resonance to chemistry is not limited to this. An investigation of the spectra of paramagnetic resonance in solutions containing free radicals yields very valuable information with respect to the nature and properties of the latter. This information is obtained primarily by studying the hyperfine structure of paramagnetic resonance spectra. A well resolved hyperfine structure is observed only at sufficiently low concentration N of the free radical in the solution (usually with $N \leq 10^{-3}$ mole/liter), when the exchange interactions between the molecules of the free radicals turn out to be practically completely eliminated. In this case the number of hyperfine line components is frequently very large and their relative intensities vary. The occurrence of such a structure is explained by the considerable delocalization of the unpaired electron interacting with the summary spin I_{summ} of the several atomic nuclei contained in the molecule. Therefore an analysis of the observed hyperfine structure leads to conclusions both concerning the nature of the radical itself and concerning the character of the delocalization of the molecular orbit of the unpaired electron. We shall illustrate this using the simplest example of $\alpha\alpha$-diphenyl-β-picrylhydrazyl, the structure

- 363 -

of which is given by the formula
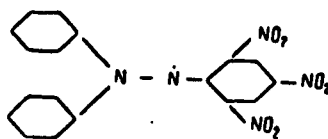
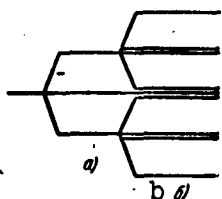The spectrum observed in dilute solutions of this radical consists of five lines with intensity ratio 1:2:3:2:1. It can be explained by assuming that the density of the unpaired electron cloud is equally distributed between the two central nitrogen atoms. Inasmuch as the spin of the ^{14}N nucleus is equal to one, we must have $2I_{summ} + 1 = 5$ hyperfine components. The ratio of the intensities of the individual components follows directly from an examination of Fig. 7.1, which shows first the hyperfine splittings of the ground level, due to the first ^{14}N nucleus, and then the splittings of equal magnitude, due to the second nucleus of ^{14}N, superimposed on the former splittings.

Fig. 7.1. Diagram of the hyperfine splittings produced: a) by the first atom of ^{14}N and b) by the second atom of ^{14}N, for $A_1 \approx A_2$.

A solution containing the negative p-benzoheptaquinone ion also displays five peaks, but with intensity ratio 1:4:6:4:1. Simple arguments analogous to the preceding ones show that in this case there are identical interactions between the electron spin and all four protons of the molecule, i.e., that the unpaired electron density is distributed over the entire ring (we recall that the spin of the nuclei ^{12}C and ^{16}O is equal to zero, and consequently these nuclei do not influence the hyperfine structure).
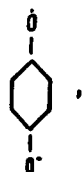
If the electron does not interact to the same degree with all the nuclear spins, the picture of the spectrum becomes more complicated. In particular, if the constant of hyperfine interaction with one group of nuclei, having a summary spin I_1, turns out to be much larger than the constant of interaction with another group with summary spin I_2, then each hyperfine structure peak resulting from the stronger interactions and consisting of $(2I_1 + 1)$ components breaks up into $(2I_2 + 1)$ close-situated peaks due to the weaker interaction. Finally, in the case when the constants for the interaction between the electron spin and each of the atomic nuclei a, b, c, ... of the molecule, enclosed by the delocalized orbit, turn out to be different and their ratios to one another are not whole numbers, we should have a spectrum consisting of $(2I_a + 1)(2I_b + 1)(2I_c + 1)...$ components.

We note that, strictly speaking, direct conclusions concerning the distribution of electron density can be drawn from data on paramagnetic resonance only if the atoms enclosed in the delocalized orbits are completely equivalent (as is the case, for example, in heptaquinone). For atoms that are not chemically equivalent (as are the nitrogen atoms in DPPH), such a treatment is only very approximate [3].

Let us proceed now to discuss the causes of the very possibility of occurrence of a hyperfine structure in paramagnetic resonance spectra of aromatic free radicals, such as, for example, the negative ions of aromatic hydrocarbons.

In order for hyperfine splitting different from zero to exist it is necessary that the electron density on the nuclei also be finite. Therefore, a direct interaction between an unpaired π-electron of an aromatic free radical with ring protons is impossible, for the latter are located in the plane of the ring, where the density of the π-electron cloud is equal to zero. Thus, it appears at first glance that the

hyperfine structure in paramagnetic resonance spectra of aromatic free radicals should be generally nonexistent. Yet experience shows the opposite to be true.

An attempt to explain the observed effect with the aid of an analysis of the proton vibrations normal to the plane of the ring has not led to any success. It was therefore assumed (in analogy with the assumption of the theory of hyperfine structure in ionic crystals, considered in Chapter 3), that the unpaired electron of the aromatic radicals actually has a small admixture of the excited σ state. A quantitative calculation of the configuration interaction for aromatic radicals was made by Weissman [7], McConnell [8], and others [9], [10].

According to [7], the ground state of the free aromatic radical is described as follows: (filled orbits) $\sigma_B^2\pi$, where σ_B is the molecular orbital binding C and H. A possible excited state that mixes with the ground state is: (filled orbits) $\sigma_B^1\pi(\sigma_A)^1$, where σ_A is the disintegrating orbit. Since one of the conditions of the configuration interaction is the requirement that both interacting states have the same symmetry with respect to reflection in the plane of the ring, an admixture of the state: (filled orbits) $\sigma_B^1\pi^2$ is impossible.

It follows from theory that the hyperfine splitting A', expressed in oersted, produced by the proton bound with the given carbon atom, is directly proportional to the density ρ_1 of the unpaired electron cloud on the nucleus:

$$A' = Q\rho_1. \qquad (7.1)$$

Here Q is a constant which is the same for all the aromatic free radicals, calculated to be approximately 28 oersted. This quantity is the distance between the peaks of the hyperfine structure under the condition that $\rho_1 = 1$, i.e., that the density of the electron cloud is entirely connected with a single C atom; on the other hand, if the den-

sity per one atom is < unity, then the constant A' should be accordingly smaller. Therefore, if the unpaired electron is delocalized over the entire ring, then the distance between the extreme peaks of the hyperfine structure should again be close to 28 oersted.

For the majority of the investigated aromatic free radicals, experience has yielded quite good agreement with theory (see Table 7.3). In some cases, however, for example in perinaphthene, the total hyperfine splitting turns out to be appreciably larger than 28 oersted. This was attributed to the possibility of "negative spin density" on certain carbon atoms. The "negative spin density" is the result of the perturbing action of the unpaired electron on the orbit of the paired electrons. This perturbation leads to a partial decompensation of the initially paired spins and thus again gives rise to a new unpaired electron density with a spin direction opposite that prevailing on the perturbing electron. The new density has therefore a negative sign. The initial, positive density in turn increases further, so that the algebraic sum of the densities on all the atoms of the ring remains equal to unity as before. For the hyperfine interactions, however, the sign of the spin density is immaterial, and therefore the total hyperfine splitting, which is proportional to the sum of the absolute values of the spin densities, should become larger than 28 oersted as a result of the perturbation [11].

The theory of configuration interaction does not explain, however, the hyperfine splittings that arise as the result of the protons in the groups that replace the ring hydrogen atoms, such as the CH_3, which replace the hydrogens of the ring in tetramethylbenzoheptaquinone

- 367 -
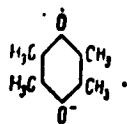
The mechanism that ensures the hyperfine interaction with the protons of the substitutes consists of direct overlap of the $2p_z$ orbit of the carbon atom of the ring with a linear combination of the orbits of the two protons of the methyl group. To the extent that the p_z orbit is a part of a system containing an unpaired electron, it becomes possible for spin density on the methyl group to appear. On the other hand, rotation of the methyl group relative to the ring causes the overlap of the electron clouds to become possible for all three hydrogen atoms of CH_3. This mechanism, due to the superconjugation phenomenon, is discussed in greater detail in [48, 49].

In the paramagnetic resonance spectra with which we dealt up to now and which are observed in liquid systems with low viscosity, containing free radicals, only the isotropic part of the hyperfine interactions plays an important role; the anisotropic part of these interactions is effectively averaged by the Brownian movement. In reference [12], which is devoted to paramagnetic resonance in the inorganic free radical ClO_2 (chlorine dioxide), it is shown that whereas in dilute liquid solutions of this radical one observes four hyperfine structure peaks (from $^{35,37}Cl$ with $I = 3/2$) with distance $A' = 17$ oersted between peaks and with each peak $\Delta H = 8$ oersted wide, after freezing the solutions A' becomes equal to 52 oersted with a corresponding increase in ΔH. The increase in both ΔH and in A' are due to the fact that freezing removes the averaging action of the motion.

An analogous result was obtained by Berthet [13], who investigated the hyperfine structure of the free radical $(CH_3OC_6H_4)_2NO$ in solid and liquid solutions. Whereas in the liquid solution we have for the constant $A' = 11$ oersted and the intensities of all three peaks (from the ^{14}N nucleus) are equal to one another, in solid solution we have $A' = 18$ oersted and the components have different intensities. Worthy of

notice is also the fact that the observed hyperfine structure appears in the solid solution at a 25% concentration of the free radical, whereas in liquid solutions it is observed only at 0.3% concentration. This difference may be evidence of the fact that in liquid solutions the free radicals are contained in the form of individual molecules only under appreciable dilutions.

§7.2. Free Radicals in the Pure State

Before we present the results obtained for different classes of pure free radicals, it is advantageous to dwell on the most investigated among these substances, $\alpha\alpha$-diphenyl-β-picrylhydrazyl, DPPH, as being one of the chemically most stable free radicals, widely used for an estimate of the sensitivity of magnetic spectroscopes, for an estimate of the number of paramagnetic centers in the investigated specimens, and finally, in some cases to determine the g factors.

Resonance in solid DPPH was first measured in 1950 [14]; the g factor in polycrystalline specimens was found to be 2.0036 ± 0.0003; the line width is $\Delta H = 2.7$ oersted. Later on it was observed in single crystals of DPPH that a slight anisotropy exists both in the values of g and in the values of ΔH [15, 77]. The saturation method was used to measure the longitudinal relaxation time T_1, which was found to be $6.3 \cdot 10^{-8}$ sec, which is close in magnitude to T_2, as should be the case for systems with strong exchange [5] (see §5.3). The theory of DPPH absorption lines in weak fields was developed in [16] and later on confirmed experimentally [17].

A characteristic, long-unexplained feature in paramagnetic resonance of solid DPPH was the great difference in the values of ΔH (from about 1 to about 7 oersted), obtained by different researchers.

The main reason for these discrepancies was explained in a paper by Arbuzov, Valitova, Garif'yanov, and Kozyrev [18], who investigated

TABLE 7.1

Width of Paramagnetic
Resonance Lines in
DPPH Specimens Ob-
tained with Different
Solvents

1 Растворитель	ΔH, эрст 2		$\nu = 9400$ Мгц 3
	$\nu = 300$ Мгц 3		
	295° K	90° K	295° K
4 Бензол	6,8	4,6	4,7
5 Толуол	2,9	2,6	2,6
6 Ксилол (смесь)	2,5	2,2	2,3
7 Пиридин	5,3	5,0	5,0
8 Бромоформ	2,2	2,5	2,5
9 Четыреххлори-стый углерод	1,9	2,7	2,3
10 Хлороформ	1,7	2,1	2,0
11 Сероуглерод	1,3	1,3	1,5

1) Solvent; 2) oe; 3)
Mcs; 4) benzene; 5)
toluol; 6) xylol (mix-
ture); 7) pyridine; 8)
bromoform; 9) carbon
tetrachloride; 10)
chloroform; 11) carbon
disulfide.

the influence exerted on ΔH by the solvent*
from which the DPPH is crystallized. The
results of their measurements, made in fine
crystalline powders in vacuum are listed in
Table 7.1.

It is seen from the table that the
nature of the solvent greatly influences the
line width; this is expected, incidentally,
since it has already been known that some
solvents enter into the crystalline lattice
of DPPH (it is not without interest to note
here that the chemical analyses show that
in no case is there a guarantee that the
solvent enters into the lattice in stoichio-
metric proportions).

The investigated specimens of DPPH are divided into two groups:
in the first (cyclic solvents) the lines narrow down upon cooling and
upon increase in the frequency; in the second (noncyclic solvents),
both relations are reversed. A slight narrowing down with increasing
frequency, observed in the first group, agrees qualitatively with the
theory of Kubo and Tomita for pure isotropic exchange (see Chapter 5)
and is probably the result of the vanishing of the nonsecular line
broadening in strong fields H_0. The narrowing down upon cooling can be
explained as being the result of the dependence of the nonsecular
broadening on the correlation time.

However, the dependence of the line narrowing in DPPH of the sec-
ond group on the frequency cannot be explained simply. One could as-
sume this dependence to be the consequence of the large anisotropy of
the g factor in the second group, but measurements made by Yablokov

[20] in single crystals of DPPH have shown that this anisotropy is approximately the same for a benzene specimen ($g_{||}$ = 2.0031 $\pm$ 0.0003; $g_{\perp}$ = 2.0039 $\pm$ 0.0003) and for a chloroform specimen ($g_{||}$ = 2.0030 $\pm$ $\pm$ 0.0002; $g_{\perp}$ = 2.0040 $\pm$ 0.0002). Thus, there is still no complete explanation of the line width in modifications of DPPH.

The nature of the solvent is not the only factor that influences ΔH in DPPH. As was established in [21, 18], a reversible line broadening, due to the adsorption of O_2 molecules from air, was observed in fine crystalline specimens pertaining to the second group. Pumping out the air narrows the line down to the value of ΔH corresponding approximately to the coarse crystalline specimen. This effect is analogous to one previously observed on carbons [22] and is due to shortening of the spin-lattice relaxation time in DPPH under the influence of the magnetic moments of the O_2 molecules. Indeed, it has been shown by the saturation method that along with broadening the lines, adsorption of oxygen causes also a shortening of T_1. The O_2 causes a particularly strong broadening of the narrowest line obtained in specimens that crystallize out of carbon bisulfide [18]. For specimens crystallized out of chloroform, the influence of oxygen is much greater at temperatures 90-273°K than at temperatures above 273°K [21].

It follows from all the foregoing that if DPPH is used as a standard, it is necessary to indicate the method by which it has been obtained, to know the chemical composition of the specimens, and to use specimens that have been isolated from the action of oxygen. Apparently the most suitable standard is DPPH crystallized out of benzene, where the adsorption of oxygen has a negligible influence.

It is necessary to take account of the fact that the dependence of ΔH on the fine points of its production technique and on the medium from which the specimen is crystallized is not confined to DPPH, but

TABLE 7.2

	1 Радикал	g	δ H, эрст 2	Литера-тура 3
4	Бензохингидрон, адсорб. на Ba(OH)₂·8H₂O	2,003	несколько	[28]
5	Бифенилентрифенилэтил	2,00	5	[30]
6	Вурстера голубой (перхлорат)	2,003	2,7	[32]
7	Вурстера голубой (пикрат)	2,0033	6	[33]
8	» » (феррициа-нид)	2,0028	2,7	[33][34]
9	Дипараанизилазота окись (мо-нокр.)	$g_\parallel = 2{,}0095$; $g_\perp = 2{,}0035$		
10	Дипараксенилметил	2,00	несколько	[32]
11	Дифенилентрифенилметил	—	5	[32]
12	Дифенилхиноксалина хлоро-станнит	2,0036		[33]
13	Кеньона — Банфилда радикал	2,0057	8,9	[32,33]
14	2-нитрофенантрофеназина хло-ростаннит	2,0032		[33]
15	Пентафенилциклопентадиенил	2,0025		[4, 23, 24]
16	Порфироксид	2,0065	17,0	[33, 35]
17	Порфириндин	2,0057	10,7	[32, 35]
18	Тетраметилбензидина формиат	2,00	3,4	[32]
19	Тетраметилбензидина перхлорат	2,00	—	[32]
20	Тетраметилстибонийпероксила-мина дисульфонат	2,00	100	[32]
21	Тимохингидрон, адсорб. на Ba(OH)₂·8H₂O			[28]
22	Три-р-ксенилметил	2,0031	5,7	[32]
23	Три-тетр.-бутилфеноксил	2,0052	7,7	[23]
24	Трифениламина перхлорат	2,003	2	[32]
25	Три-р-анизиламина перхлорат		0,68	[36]
26	Три-р-аминофениламина пер-хлорат		0,33	[36]
27	Три-р-нитрофенилметил	2,0037	0,7	[32]
28	Фенантрахингидрон, адсорб. на Ba(OH)₂·8H₂O			[28]
29	N-фенил-N-9-декалил-N-оксоа-минил	2,0036		[37]
30	Фенил (N-фенилового эфира оксима-2-метилпентанон-4-ила 2) нитроксид (монокрист.)	$g_x = 2{,}0042$ $g_y = 2{,}0064$ $g_z = 2{,}0083$		[34]
31	Хромоцен Cr(C₆H₆)₂|	1,975	38	[58]
	» Cr(C₆H₅—C₆H₅)₂|	1,987	28	[58]
	» Cr(C₆H₅—C₆H₅)₂OC₆H₅	1,993	26	[58]

1) Radical; 2) oe; 3) literature; 4) benzoquinhydrone adsorbed on Ba(OH)₂·8H₂O; 5) biphenylentriphenylethyl; 6) Wurster's blue (perchlorate); 7) Wurster's blue (picrate); 8) (ferricyanide); 9) nitrogen diparaanisyl oxide (monocrystalline); 10) diparaxenylmethyl; 11) diphenylenetriphenylmethyl; 12) diphenylquinooxaline chlorostannite; 13) Kenyon-Banfield radical; 14) 2-nitrophenanthrophenazine chlorostannite; 15) pentaphenylcyclopentadienyl; 16) porphyroxide; 17) porphyrindine; 18) tetramethylbenzidine formiate; 19) tetramethylbenzidine perchlorate; 20) tetramethylstiboniumperoxylamine disulfonate; 21) thymoquinhydrone, adsorbed on Ba(OH)₂·8H₂O; 22) tri-p-xenylmethyl; 23) tri-tetr. butyl-phenoxyl; 24) triphenylamine perchlorate; 25) tri-p-anisylamine perchlorate; 26) tri-p-aminophenylamine perchlorate; 27) tri-p-nitrophenylmethyl; 28) phenantraquinhydrone adsorbed on Ba(OH)₂·8H₂O; 29) N-phenyl-N-9-deoalyl-N-oxoaminyl; 30) phenyl (N-phenyl ether oxime-2-methylpentanone-4 or 2) nitroxide (monocryst.); 31) chromocene.

may occur also in many other radicals. Thus, for pentaphenylcyclopenta-dienyl, a value of ΔH amounting to several times ten oersteds was obtained in [4], 0.62 oersted was obtained in [23], and from 5 oersted upward was obtained in [24] (depending on the solvent).

Unfortunately, in most work on DPPH and its derivatives it is not indicated from which solvent the radical was crystallized.

In addition to DPPH, several polycrystalline free radicals of similar structure were investigated [25]; these were of the type

where X is Cl
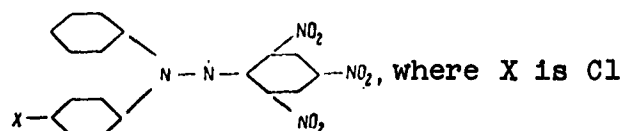
$(g = 2.0042;$ $\delta H = 1.2$ oe); Br $(g = 2.002;$ $\delta H = 2.2$ oe); OCH_3 $(g = 2.000;$ $\delta H = 2.6$ oe); F $(g = 2.000;$ $\delta H = 4.1$ oe). Here δH is the line width at the points of inflection. Also investigated was diphenyloxypicrylhy-drazyl powder, with the same value of g as in DPPH and $\delta H = 3$ oersted [26] and single crystals of N-picryl-9-aminocarbazyl, with $g = 2.0041$-2.0024; $\delta H = 0.5$ oersted [27, 28]. The last substance differs very little from DPPH, having a structural formula
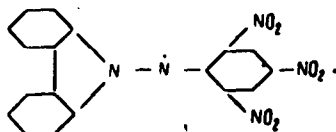
Nonetheless, its line width is considerably smaller than in any modification of DPPH.
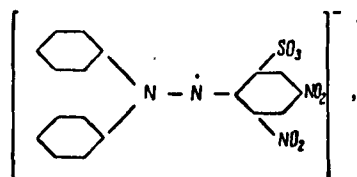
Certain results of measurements of paramagnetic resonance in solid organic free radicals of other types are listed in Table 7.2. They do not claim to be exhaustively complete.

§7.3. Free Radicals in Solutions

In §7.1 we pointed out that from the chemical point of view the most interesting is an investigation of the paramagnetic resonance line

hyperfine structure observed at sufficiently low free radical concentrations in solutions. We give here some results obtained in a study of solutions of free radicals.

We have seen that DPPH in solution yields five lines. N-picryl-9-aminocarbazyl, which is very close to it, yields seven lines, corresponding to a ratio of 2 between the constants A'_1 and A'_2 of interaction with the nuclei of the first and second atoms of the nitrogen. The maximum possible number of lines, namely nine, could be obtained in solutions of diphenyldinitrosulfophenylhydrazyl salt

$$\left[\begin{array}{c} \bigcirc \\ \bigcirc \end{array} \!\! N - \dot{N} - \bigcirc \!\! \begin{array}{c} SO_3 \\ NO_2 \\ NO_2 \end{array} \right]^{-} \cdot \; ,$$

where the constant of interaction with the first nitrogen atom is $A_1 =$ = 12 oersted, while $A_2 = 8$ oersted [38, 39]. We see from this example how sensitive the hyperfine structure is to the least changes in the distribution of the electron densities in the molecule.

In order to verify the hyperfine structure theory, great interest attaches to solutions containing ions of aromatic hydrocarbons. One of the first to be investigated [40] was the negative naphthalene ion

$$\left[\begin{array}{c} \alpha \;\; \alpha \\ \beta \bigcirc\bigcirc \beta \\ \beta \;\;\;\;\; \beta \\ \alpha \;\; \alpha \end{array} \right]^{-} \cdot \; ,$$
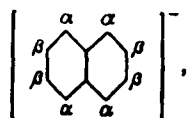
which is obtained when alkali metals act on solutions of naphthalene in tetrahydrofurane or dimethyoxyethane. The nature of the metal and solvent does not change the spectrum, which consists of 17 lines with intensities 1:1:1:2:2:1:2:2:1:2:2:1:2:2:1:1:1 and with a distance of 27.2 oersted between the outermost peaks ("total splitting"). This quantity is in very good agreement with the theoretical value of the total splitting (28 oersted). The number and intensity of the lines

- 374 -

were explained on the basis of an approximate calculation of the molecular orbitals, made as long ago as in 1931 by Hückel [41]. If the constants A_α and A_β of the hyperfine structure due to the α and β protons of the naphthalene ion are equal, we should have nine lines; if $A_\alpha \gg \gg A_\beta$ five groups of lines should be obtained, each containing five nearby-lying components. The number 17, on the other hand, corresponds to a ratio $A_\alpha/A_\beta = \rho_{1\alpha}/\rho_{1\beta} = 3:1$, which is obtained indeed from calculations made following Hückel. The most exact value of the ratio $A_\alpha : A_\beta$, obtained from a detailed analysis of the paramagnetic resonance spectrum, is 5.01:1.79.

Partial replacement of ^{12}C by ^{13}C has made it possible to obtain for the naphthalene ion the constant of the hyperfine structure due to the interaction between the electron spin and the spin of the ^{13}C nucleus ($I = 1/2$). It turned out to be equal to 7.1 oersted, from which the density of the electron cloud on the C nucleus was calculated. Several other negative aromatic ions were investigated in similar fashion (see Table 7.3), and the electron densities on the protons were calculated and found likewise to be in good agreement with the calculations based on [41]. In addition, experiments on paramagnetic resonance have made it possible to establish an electronegativity scale for the aromatic ions, and if it is assumed that the lifetime of the electron on the ion determines the line width, one can also determine the speed of electron transition between the aromatic molecule and the ion [42].

By treating aromatic hydrocarbons with concentrated H_2SO_4, it is possible to obtain positive ions of these hydrocarbons which are also, naturally, free radicals. Several such radicals were investigated by the paramagnetic resonance method [43, 44].

Treatment of several organic substances of other classes with sulfuric acid (for example, anthraquinone, thiophene, and many others),

also leads to the occurrence of paramagnetic resonance spectra [45, 46]. In these cases, however, one obtains not positive ions with the character of radicals, but radical oxidation products of the corresponding organic substances, as was convincingly shown in [47].

A large group of investigations was devoted to solutions containing various heptaquinones and their derivatives. The experimental values of the hyperfine structure constants were compared with those calculated on the basis of the superconjugation theory, developed in [48, 10] and gave good agreement [49].

The picture of the spectrum is frequently very complicated. Thus, for monomethyl-n-benzoheptaquinone it becomes necessary to assume that the hyperfine structure constant for the two ring protons is $A'_1 = A'_2 = 2.48$ oersted, while that for the third ring proton is $A'_3 = 1.73$ oersted, and for the methyl protons the same constant is $B' = 2.02$ oersted [50]. The spectrum becomes simpler if the substituents are chlorine atoms, inasmuch as the hyperfine splitting due to these atoms is small and does not produce resolved lines, since it participates only in the width of the components. Thus, in trichlorobenzoheptaquinone one observes only two components, due to the single ring proton [51]. On the contrary, fluorine- substituted heptaquinones disclose a hyperfine structure due both to the protons and to the ^{19}F nuclei, owing to the large magnetic moment and the small spin ($I = 1/2$) of the latter [1].

From among the numerous free radicals of other classes, investigated in solution, we shall discuss only a few and refer the reader for more details to Ingram's book [1]. Thus, we point out that the spectra in solutions of triphenylmethyl [52] and a few other radicals disclose anomalously large hyperfine splittings. Triphenylmethyl
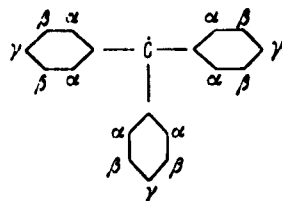
should yield, assuming that the corresponding H atoms in all three rings are equivalent, a total of $(2I_\alpha + 1)(2I_\beta + 1)(2I_\gamma + 1) = 196$ lines. These are not fully resolved, and the total splitting is 25 oersted. But an investigation of a specimen containing ^{13}C in the methyl position has shown the occurrence of a doublet due to the ^{13}C nucleus with a splitting of 22 oersted, which indicates that a considerable fraction of the density of the unpaired electron is concentrated precisely on the methyl carbon, and consequently, $\Sigma\rho_1$ on the remaining atoms should be considerably less than unity. An explanation of the spectrum of triphenylmethyl, which we shall not discuss, was given in [53. 54].

In the radicals considered so far, both in solid form and in solutions, the g factor is very close to 2.0023. More significant deviations from this value are observed in solutions of radicals containing sulfur, and also in radicals of the peroxide type [55]. This indicates a much stronger localization of the unpaired electron in the latter cases. Radicals containing sulfur were obtained by dissolving thiophenol, thiocresol, thionaphthol, and diphenyldisulfide in concentrated sulfuric acid [45, 46]. All give a paramagnetic resonance spectrum consisting of two groups of lines with $g_1 = 2.0151$ and $g_2 = 2.0081$ (the values of g are determined for the centers of the groups). These groups are due to two different radicals, since the second group turned out to be more stable in time, and remains when the first vanishes completely. A group of five lines with $g = 2.0081$ is produced by the thiatrene ring with four protons. The group with $g = 2.0151$ apparently is

due to the $(C_6H_5\overset{\bullet}{S})H^+$ radical with appreciable localization of the unpaired electron on the sulfur atom.

We note that along with organic sulfur derivatives with radical-like character, paramagnetic resonance was observed also in pure molten sulfur [56, 57]. It is observed at temperatures from 189 to $414^\circ C$. One line was noted (the spin of the ^{32}S nucleus is zero), with a near-Lorentzian shape and $g = 2.024$. Neither the line width nor $\underline{g}$ depend on the temperature. This resonance is due to a partial breaking of the bonds of the ring molecules S_6. A solution of sulfur in fuming sulfuric acid [1] also discloses two lines (at 20% SO_3) with $\underline{g}$ factors that fluctuate between 2.003 and 2.018 for one line and between 2.025 and 2.032 for the other. The latter is apparently due to the broken S_6 rings, and the former to some other radical containing sulfur.

Great interest is attached to an investigation, made by Voyevodskiy and his coworkers [58, 59], of solutions containing chromo-aromatic compounds of "sandwich" structure. Compounds of this type (metallocenes) have a structure $(C_6H_6)_2Me$ or $(C_5H_5)_2Me$, etc., where the metallic atom is situated between two parallel ring structures. The nature of the covalent bond of the metal with the addend in these compounds cannot be described within the framework of the theory of ordinary two-electron bonds. Quantum mechanical calculations on compounds of this type are developed in [60].

An investigation [58, 59] of paramagnetic resonance spectra in chromocene cations of the type

$$\begin{bmatrix} C_6H_6X \\ Cr \\ C_6H_6X \end{bmatrix}^+ ,$$
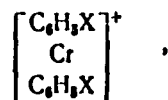
where $X = H$, C_6H_6, cyclo-C_6H_{11}, COOH, etc., have shown the presence of a hyperfine structure in which the number of components corresponds to the number of protons on the two rings; on the other hand, a binomial

distribution of the component intensities has led to the conclusion that all these protons are equivalent. The summary spin density on both rings amounts to 1.92. It follows from this that 0.92 of the density of the unpaired electron with opposite spin orientation is localized on the chromium atom.

It was shown in [61] that the width of the paramagnetic resonance spectrum components in chromocenes depends strongly not only on the substitutes, but also on the nature of the solvent and on the temperature.

In addition to the stable radicals, one can sometimes detect in liquid solutions radicals that are formed during the course of the reactions. Thus, for example, in [62] there was investigated the paramagnetic resonance of pyrogallol, which oxidizes in air, in aqueous and alcohol solutions. At room temperatures, the lifetime of the free radical turned out to be on the order of several minutes; g = 2.005; the spectrum consists of two triplets. In most cases, however, in solutions with low viscosity, the unstable radicals have so short a lifetime that their dynamic concentration lies on the borderline of the sensitivity of modern apparatus. Furthermore, the short lifetime causes broadening of the absorption lines, which makes their detection even more difficult. Unstable radicals are therefore investigated usually by rapidly freezing the solutions.

To conclude this section, we present Table 7.3, taken from [1]. It illustrates the experimental results obtained in the investigation of several types of stable free radicals in solutions.

§7.4. Irradiated Organic Substances. Radicals in Polymers and Carbons. Biradicals and Triplet States. Biological Objects

1. Irradiation of organic substances with ultraviolet, x-rays, and γ-rays frequently damages their molecular structure and leads to the

TABLE 7.3

Stable Free Radicals in Solutions [1]

1 Радикал	2 ΔH или расстояние между крайними пиками СТС, эрст	3 Число компонент СТС	4 Литература
А) Ароматические ионы			
антрацена	26	21	[63]
бензола	22,5	7	[64]
m-динитробензола	25	8	[65]
дифенила	21	9	[63]
нафталина	27	17	[66]
нафталина с ^{13}C	34,3	34	[67]
нафталина с D	29	15—16	[66], [63]
нитробензола	25	10	[66]
перинафтена	49	7×4	[68]
перилена	24	9	[44]
тетрацена	25	31	[44]
тринитробензола	25	8	[66]
Б) Семихиноны			
1) p-бензосемихинон	9,48	5	[69]
монометил-p-бензосемихинон	14	много линий	[70]
тетраметил »	23	13	[70]
монохлор »	6,0	4	[51]
трихлор »	2,11	2	[71]
тетрахлор »	0,4	1	[51]
2,5-ди-терт-бутил »	4,3	3×19	[71]
2) 1,4-нафтосемихинон	8	3×5	[72]
2,3-диметил-1,4-нафтосемихинон	12	7×5	[72]
3) o-бензосемихинон	10	3×3	[73]
4-терт-бутил-o-бензосемихинон	6	2×11	[73]
3-фенил »	8	7	[73]
окисленный 1, 2, 3-бензол-триол	7	2×3	[62]
В) Перхлораты триариламина			
трианизил	20	3	[74]
тридифенил	20	3	[74]
Г) Соли Вюрстера (положит. ионы)			
незамещенная соль Вюрстера	28	15	[75]
N-метилзамещенная соль	46	24	[75]
NN-диметил » »	73	27	[75]
NN'-диметил » »	76	9×3	[75]
NN-диметил-NN'-дейтеро »	51	7×3	[75]
тетраметилзамещенная соль	88	13×3	[75]
Д) Различные другие радикалы			
карбазил	60	7	[38]
дифторазот	9	10	[40]
димезитилметил	48	2×35	[76]
ди-p-анизилнитроксид	14	—	[65]
дифенилдинитросульфонил-гидразил	60	9	[38]
аз-дифенил-β-пикрил-гидразил	58	5	[77]
пероксиламина дисульфонат	26	3	[78]
феназин	60	5	[79]
натрий-тримезитил-бор	42	4	[40]
трифенилметил	25	21×4	[76]

1) Radical; 2) ΔH or distance between outermost hfs peaks, oe; 3) number of hfs components; 4) literature; 5) A) aromatic ions of; 6) anthracene; 7) benzene; 8) m-dinitrobenzene; 9) diphenyl; 10) naphthalene; 11) naphthalene with ^{13}C; 12) naphthalene with D; 13) nitrobenzene; 14) perinaphthene; 15) perilene; 16) tetracene; 17) trinitrobenzene; 18) B) heptaquinones; 19) 1) p-benzoheptaquinone; 20) monomethyl-p-benzoheptaquinone; 21) tetramethyl; 22) monochloro-;

23) trichloro-; 24) tetrachloro-;
25) 2,5-di-tert-butyl-; 26) 2) 1,4-
naphthoheptaquinone; 27) 2,3-dimethyl-
1,4-naphthoheptaquinone; 28) 3) o-
benzoheptaquinone; 29) 4-tert-butyl-
o-benzoheptaquinone; 30) 3-phenyl;
31) oxidized 1, 2, 3-benzenetriol;
C) perchlorates of triarylamine; 33)
trianisyl; 34) tridiphenyl; 35) D)
Wurster's salts (positive ions) non-
substituted Wurster's salt; 36) N-
methyl substituted salt; 37) NN-di-
methyl; 38) NN'-dimethyl; 39) NN-di-
methyl-NN'-deutero; 40) tetramethyl
substituted salt; 41) E) various
other radicals; 42) carbazyl; 43) di-
fluoronitrogen; 44) dimesitylmethyl;
45) di-p-anisylnitroxide: 46) diphen-
yldinitrosulfonylhydrazyl; 47) $\alpha\alpha$-
diphenyl-β-picryl-hydrazyl; 48) per-
oxylamine disulfonate; 49) phenazine;
50) sodium-trimesityl-boron; 51) tri-
phenylmethyl.

---

formation of free radicals. A study of such radicals by the paramag-

netic resonance method is of great scientific and practical interest;

by now a considerable literature has been devoted to this problem.

Usually the substances are investigated in the solid phase or in liquids

with high viscosity, for in this case it becomes possible to accumulate

the radicals that are obtained as a result of the irradiation.

An investigation of objects irradiated with ultraviolet has ad-

vantages over work with x-rays or γ-rays, for in the former case the

smaller size of the quantum makes the destruction of the molecules and

the formation of free radicals much more selective in character, and

therefore the observed spectra are simpler and easier to interpret. In

the case of x-rays, and particularly γ-rays, one obtains sometimes a

whole set of different free radicals; consequently the paramagnetic

resonance spectra becomes highly complicated.

The first work on the study of free radicals in irradiated sub-

stances was carried out in 1951 by Shneider and his coworkers [80], who investigated paramagnetic resonance in the polymer polymethylmethacrylate, which was exposed to x-rays. A large-scale study of irradiated substances began, however, only in 1955.

It was found that many substances (ethyl iodide, benzylamine, benzyl chloride, and others), dissolved in a suitable mixture of hydrocarbons (the most suitable one turns out to be a mixture consisting of 5 parts of ether, 5 parts of isopentane, and 2 parts of ethanol*) and vitrified by deep freezing, produce after exposure to ultraviolet a paramagnetic resonance spectrum [81]. An analogous effect was observed also in high-temperature organic glasses [82]. It turned out further that along with the primary radicals, arising as a result of direct action of the ultraviolet quantum, secondary radicals are produced as a result of interaction between the primary radicals and the solvent [83]. It thus turned out to be possible to obtain paramagnetic resonance spectra from radicals of substances on which ultraviolet does not act directly. A particularly successful converter for radicals was hydrogen peroxide, which produced the radicals $\overset{\bullet}{O}H$ upon irradiation with ultraviolet.

From the hyperfine structure of the spectrum it is possible to establish the nature of the secondary radicals. Thus, in the vitreous solution of hydrogen peroxide in alcohol $(CH_3)_2HCOH$, a spectrum of certain lines from six protons was observed after irradiation; it obviously belongs to the radical $(CH_3)_2\overset{\bullet}{C}OH$.

The widths of the lines in solid and vitreous systems containing free radicals is larger than in liquid solutions, in view of the absence of the narrowing due to the Brownian motion. However, the width observed in glasses is nonetheless smaller than that expected for the true solid-state arrangement of the atoms. This can be attributed to

the internal rotation of the protons in the molecules of the free radicals, which remain also at low temperatures [84].

In this connection, it is of interest to investigate the dependence of the secondary spectra on the temperature of the vitreous system. This investigation yields information on internal motion in the glass, and sometimes makes it possible to separate the effects due to individual radicals from the mixed spectrum, because the dependence of the line width on the temperature is not the same in different radicals. In particular, it was shown in [84] that the secondary radicals in a solution of H_2O_2 in methanol are $\overset{\bullet}{C}H_2OH$ and the biradical $\overset{\bullet}{C}H_2...H\overset{\bullet}{C}$.

Let us proceed to discuss the results obtained by irradiation with x-rays and γ-rays. The spectrum of polymethylmethacrylate obtained in 1951 [80] is so complicated that it took 7 years to interpret [85]. It turned out to be due to a radical of the type $R \cdot CH_2 -$ $- \overset{\bullet}{C}(CH_3)(COOCH_3)$. It is easier to interpret the spectra of x-irradiated amino acids. Thus, a triplet due to the radical $\overset{\bullet}{C}H_2$ [86] was observed in glycine. Anisotropy of the spectrum in an irradiated single crystal of glycine was reported in [87].

An investigation of γ-irradiated paraffin hydrocarbons [88, 89] has shown that in the case when the carbon chain does not contain too large a number of atoms, the spectrum has one central component of maximum intensity, and higher molecular radicals of this type have two components. This is evidence that in the former case the number of equivalent protons closest to free valency is even, and in the latter case it is odd. One can assume therefore that in hydrocarbons with a short chain one obtains essentially radicals of the type $\overset{\bullet}{C}H_2-CH_2-...$, while in high-molecular ones one obtains the type $...-CH_2-\overset{\bullet}{C}H-CH-...$. The simplest of the hydrocarbons, methane, produces at $20.4°K$ upon-γ-irradiation a paramagnetic resonance spectrum [90] consisting of four

- 383 -

components with intensity ratio 1:3:3:1, which agrees with expectation for the radical $\overset{\bullet}{C}H_3$.

Thus, paramagnetic resonance makes it possible to establish the nature of the radicals that form upon irradiation of solid organic substances. We mention here still other work on paramagnetic resonance in substances irradiated with x-rays and γ-rays. The following were investigated in [91]: methyl alcohol, which produces three hyperfine components; ethyl alcohol (five components); acetamide (three components); propionamide (five components); acetanilide (three components), and sodium methoxide (three components). Spectra of dimethyl-Hg (five components) and diethyl-Hg (three components) were obtained in [86]. Reference [94] reports an investigation of glycine (three components); alanine (five components); valine (complex spectrum); leucine (two groups of five or more lines); isoleucine (without resolved structure); cysteine (asymmetrical structure with four components); glycolic acid (two components); and glycocyanine (two components). There is no doubt that further systematic study of the influence of irradiation will continue [93]. It is of particular importance to the investigation of polymers, to the analysis of which we now proceed.

2. As is well known from chemical considerations, polymerization of molecules frequently proceeds via free radicals. However, a study of the kinetics itself of this process with the aid of paramagnetic resonance is difficult because of the low concentration of the free radicals. We therefore confine ourselves to a determination of the free radicals, which form on the ends of the growing polymer chains and which are fixed in the substance for steric reasons. This "freezing" takes place when the polymer has already become partially polymerized to form a gel or when the polymer is insoluble in the monomer and precipitates around the growing chains.

The first investigation of this type pertained to polyvinyl gels [94]. The spectrum observed in glycoldimethacrylate consisted of two partially overlapping groups, containing five and four lines; the spectrum turned out to be independent of the initiator of the polymerization and identical with the spectrum of irradiated polymethylmethacrylate. Both groups were recognized to belong to one radical

$$
\begin{array}{c}
\text{COOR} \\
| \\
-\text{CH}_2-\text{C}\cdot \\
| \\
\text{CH}_3
\end{array}
$$
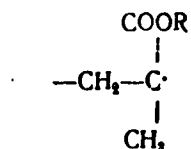
as a result of superconjugation of the p_π orbit of the C atom with 15 orbits of the protons from the CH_2 and CH_3 groups [85].

In addition to investigating free radicals "frozen" in gels or in polymer precipitates, the determination of radicals arising in ready polymers upon irradiation is used. An interesting example of such research is work on γ-irradiated frozen ($77^{\circ}K$) teflon [95]. After freezing with the access of air prevented, a spectrum of 11 lines was obtained; 10 of these form two partially overlapping groups of five lines each and are due to the radical $\ldots-CF_2-\overset{\bullet}{CF}-CF_2-\ldots$, in which the central ^{19}F nucleus produces the principal doublet splitting, and the four more remote fluorine nuclei split each line of the doublet into a quintuplet. The eleventh line is connected with the peroxide radical $-\overset{|}{\underset{|}{C}}-\overset{\bullet}{O}O$, inasmuch as action of the oxygen in the air on the irradiated teflon converts the entire spectrum into a single asymmetrical line which coincides in position with the eleventh line of the oxygen-free spectrum [95, 96]. The asymmetry of the line is connected with the great localization of the unpaired electron on the oxygen.

In addition to the foregoing case, irradiation was used to investigate the paramagnetic resonance spectra of the following polymers: polymethacrylic acid, polyethylmethacrylate [97], polymethylchloracryl-

ate, polyacrylic acid, polyvinyl alcohol, hydrolyzed polyvinyl acetate, polystyrol, polythene, nylon, and polyacrylonitrile [98].

The method of "freezing" in gels or in precipitates was used to investigate the free radicals obtained on polymerization of the following monomers: acrylonitrile, methacrylonitrile, vinyl bromide [85]; acrylic acid [1], methylmethacrylate [94], and a few other polymers.

The change in concentration of free radicals during the course of polymerization was investigated with copolymerization of methylmethacrylate and glycol dimethacrylate as an example [99]. The action of inhibitors on the polymerization process was investigated in [100].

3. A rather unexpected discovery was the large resonance effect in carbonized organic substances, discovered independently in [101-103].

In low-temperature pyrolysis products, the g factor of the only observed line is very close to 2.0023, and the line width fluctuates from 1 to 100 oersted. The intensity of the effect corresponds to between 0 and 10^{20} paramagnetic centers per gram of substance, and increases rapidly with increasing carbon content from 80 to 94% [104]. X-ray diffraction investigations have shown that it is precisely in this region of concentrations that the formation of large groups of carbon rings (from four rings upward) begins. It is noted that the spin-lattice relaxation time also shortens with increasing concentration of the free carbon [105]. The shortest times T_1, on the order of 10^{-7} sec, are found in coal of the anthracite type [106, 107], which gives rather narrow lines (δH from 0.7 to 0.3 oersted) and with strong exchange effect ($T_1 \approx T_2$).

The disorganized ring structure and the arbitrary arrangement of the carbon rings apparently weaken the exchange and lengthen the spin-lattice relaxation time in carbonlike substances with small contents of free carbon. The properties of the paramagnetic resonance line

change also with the temperature of the carbonization: the line inten-
sity increases with increasing temperature from approximately 350 to
approximately 550°C [108]. This is the temperature interval in which
the volatile pyrolysis products are removed and a ring carbon struc-
ture begins to arise. Above about 600°C, a sharp decrease in the inten-
sity of the effect begins. A decrease in intensity is observed also if
the concentration of the free carbon in the specimen is higher than
94%. The last two circumstances are apparently connected with the
graphitization of the specimens, on which multilayer three-dimensional
ring structures are produced, and this can lead to a partial pairing
of the free electrons and consequently to a weakening of the paramag-
netic resonance.

The intensity of the effect increases sharply upon removal of ox-
ygen of the air by pumping. The effect of the oxygen is reversible
[109, 110, 106]. One can propose two possible mechanisms for the ac-
tion of O_2 or other paramagnetic gases (in particular, for example,
NO_2 [106]), which influence the effect in complete analogy with oxygen.

The first type of mechanism is purely physical; it consists of
the perturbation of the energy of the unpaired electron by the motion
of the biradical molecule of the adsorbed O_2 relative to the electron,
or, to the contrary, by the motion of the electron relative to the sta-
tionary fixed O_2 molecule. As a result of this perturbation, the life-
time of the excited state of the electron should become shorter, that
is, the spin-lattice relaxation time T_1 becomes shorter. In this mech-
anism the number of paramagnetic centers in the irradiated substance,
and consequently the area under the resonance absorption curve, should
remain constant with increasing width δH.

The other possible explanation has a chemical character. One can
assume that some very weak "quasichemical" bonds [1] (weak because they

- 387 -

break when the oxygen is pumped out) are produced between the oxygen and the carbon, such that the spin of the uncompensated electron loses its effectiveness, becoming "paired" with one of the spins of the O_2 molecules. The remaining unpaired second electron of O_2 should be strongly localized on the oxygen atom and should therefore result in a strongly isotropic and broad line, which is consequently unobservable. In such a mechanism, the area under the resonance curve should decrease. It was shown in [111] that it is possible to select carbon specimens in which the action of the oxygen follows either the first or the second mechanism.

Many investigations devoted to the influence of the chemical processing of carbons has shown that in general paramagnetic resonance in carbon is not connected with any separate chemical group, and is due to the presence of uncompensated and strongly delocalized electrons in condensed carbon rings as a whole [1]. The paramagnetic centers are the result of a break in the bonds on the edges of the condensed rings, leading for the most part only to a growth in the ring structure, but which in individual cases can ensure also the appearance of uncompensated spins; another possibility of spin decompensation lies in imperfections of the ring structures: the presence of individual five-or seven-member rings should lead to the appearance of trivalent carbon atoms. The electron of the "broken bond" should have a π orbit (which guarantees the possibility of rather strong delocalization) with admixture of the σ state. The presence of very large exchange in the majority of the investigated carbons [106] shows that the electron clouds of the neighboring ring formations overlap in noticeable fashion.

In graphite and other high temperature carbons obtained at t > > 1400°C, paramagnetic resonance was also observed [112]. It is due not to the conduction electrons, as was initially assumed, but to de-
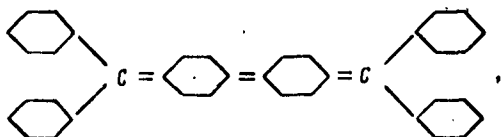
fects in the graphite lattice [113]. The unpaired electrons have in this case a much more strongly localized σ orbit. No resonance was observed in carbons obtained in the temperature interval 1000-1400°C.

A very important role can be played in future by research on paramagnetic resonance in various blacks.These apparently represent a mixture of high and low temperature carbons, since they are produced by very rapid heating at 1000-1700°C. Their spectrum, however, is near to low temperature carbons; in particular, it turns out to be quite sensitive to oxygen, whereas paramagnetic resonance in graphite is not affected by oxygen. The presence in blacks of unpaired electrons on delocalized π orbits should undoubtedly play a role in the reinforcing action of black introduced into rubber as a filler [1].

We note that paramagnetic resonance was observed in several tar-like substances (asphalt, carbolite, etc.) and in petroleum oil [106].

4. A unique type of organic paramagnet is a biradical, namely a molecule containing not one but two unpaired electrons. Among the biradicals one can distinguish a whole gamut of substances, starting with those in which the conditions brought about by the construction of the molecule cause the spins of both unpaired electrons to be separated from each other and not to add up to unity spin, and ending with such in which the spins interact quite strongly. The most reliable results on paramagnetic resonance were obtained for biradicals with noninteracting spins. These are, for example, 4,4'-polymethylene-bis-triphenylmethyl biradicals and para-substituted polyphenols, obtained in [114]. All g factors of these substances are very close to 2.0023, thus evidencing that the bond between the spins is practically nonexistent. The character of their spectrum, however, is the same as in monoradicals but naturally with twice the intensity per molecule.

Among the substances in which there are no grounds for assuming

- 389 -

the coupling between the molecule spins to be negligibly small, para-
magnetic resonance was observed in the so-called Chichibabin hydrocar-
bon [115]

which should have the following structure in the excited triplet state:
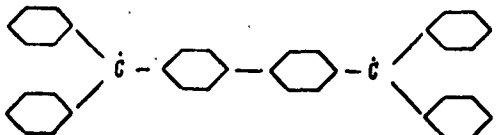
The observed resonance signal corresponded to 4% of the triplet
state. In Ingram's opinion [1], one has no firm assurance that this
signal was not due to some paramagnetic impurity. On the basis of sev-
eral negative results on paramagnetic resonance, obtained on optical
excitation of the molecule to the triplet state, he believes that
these molecules have a very powerful relaxation mechanism which leads
to so strong a line broadening that the lines become unobservable.

However, in addition to Chichibabin's hydrocarbon, there are many
other compounds in which one can assume the presence of excited trip-
let states and which display paramagnetic resonance. These, in particu-
lar, are the two highly conjugate systems: 1,9-bis(2 furyl)-5 oxo-
1,3,6,8-nonatetraene and 1,9-diphenyl-5 oxo-1,3,6,8-nonatetraene, in
which the weak resonance effect was noted in [116].

Further, many solid molecular compounds between various phenylene-
diamines and halide-substituted quinones, investigated by Biyl, Kainer,
and Rose-Innes [149], also displayed paramagnetic resonance. Its oc-
currence was interpreted as the result of the formation of biradical
ionic molecules due to the transfer of an electron from the donors
(phenylenediamine) to the acceptors (quinone). Finally, paramagnetic

resonance in such compounds as heated bianthrone (g = 2.0036; ΔH = 10 oersted) [29], violanthrene (g = 2.00; ΔH = 26 oersted) [31], and violanthrone (g = 2.00; ΔH = 30 oersted) [31] could hardly be assigned, without stretching the point, to any other factor except the presence in these compounds of a certain fraction of molecules in the triplet state.

5. To conclude this section, we mention investigations of paramagnetic resonance in biological objects, which undoubtedly have a great future and which already now have yielded interesting results. Thus, in [117] there were investigated three radicals which are the intermediate products in the oxidation-reduction processes that occur with adrenaline, vitamin K, and other biologically important substances. In [118] free radicals were observed in lyophilized tissues and liquids of animals and vegetables, belonging to the albumins. In [119] an investigation was made of the time dependence of the concentration of free radicals upon illumination of an aqueous suspension of chloroplasts and of the decrease in this concentration after turning off the illumination. Of great interest to biology are also investigations of iron in hemin, methemoglobin, and their derivatives, results of which are listed in the tables of Chapter 4 of the present book.

Particularly interesting are the investigations of Blyumenfel'd and his coworkers, devoted to questions of paramagnetic resonance in irradiated and nonirradiated albumins, and also in compounds of albumins with ribonucleic acids [120-123]. Since we cannot stop to detail these investigations, we must note that they uncover entirely new prospects with respect to many problems in theoretical biology, and particularly perhaps with respect to the question of the nature of inheritance.

We point out, finally, that an attempt was made [1] to establish

a correlation between the content of free radicals in tissues and the growth of cancerous cells. This attempt, however, has not led to any success.

§7.5. Inorganic Free Radicals. Paramagnetic Gases

So far we have considered organic substances with radical-like character. The class of inorganic radicals is much less rich, but in it we include , alongside with a small number of stable radicals, also several unstable ones, which are produced in discharges, upon irradiation, during the course of chemical reactions, etc. Among these radicals there are some that are very important from the chemical point of view. One can classify arbitrarily as free radicals various atomic substances. A class of free radicals which is unique in the character of its spectra is made up of paramagnetic gases. We shall consider briefly in this section first free inorganic radicals in condensed phases and then paramagnetic gases.

1. The spectrum of atomic hydrogen obtained upon γ-irradiation of the acids H_2SO_4, $HClO_4$, and H_3PO_4 frozen at $77^{\circ}K$ turned out to be a doublet with splitting $A' = 500$ oersted and with $g = 2.00$ [124, 125]. The maximum intensity of the effect in H_2SO_4 was observed at a ratio $H_2SO_4:H_2O = 1:5$; further dilution weakens the effect, which disappears in pure ice. These measurements were made in the centimeter wavelength band. At low frequencies (350 megacycles) an effect due to atomic hydrogen in pure ice was observed with $A' = 30$ oersted [126]. The appearance of this resonance in weak fields H only can be attributed apparently to the large anisotropy of the g factor for "atomic" hydrogen, observed in pure ice. The effects of atomic hydrogen and deuterium in frozen systems were observed in [127, 128].

The radical products produced upon discharge in water vapor and condensed at $77^{\circ}K$ were investigated in [129]. The authors observed one

- 392 -

line with $g = 2.0085$ and with weakly pronounced inflection corresponding to $g = 2.027$. Upon heating to $138°K$, the resonance disappeared. Analogous results were obtained with D_2O and H_2O_2. In [130], in an investigation of the products produced at low temperature from vapors of H_2O, H_2O_2, and D_2O dissociated in a glow discharge, one line was likewise obtained with a weak additional maximum on one of its skirts. This maximum was interpreted by the authors of [130] not as an indication of the presence of a second radical, but as a consequence of the anisotropy of the $\underline{g}$ factor. The observed effect was ascribed on the basis of chemical considerations to the radical $H\dot{O}_2$, and not $\dot{O}H$.

Irradiated nitrates of several salts gave a spectrum ascribed to NO_2 and consisting of a triplet with $A' = 50$ oersted [131, 132].

Among the stable inorganic radicals, mention should be made of the peroxides and ozonates of alkali metals (of the type MeO_2 and MeO_3, respectively). In the former the spectrum is due to the radical ion $\dot{O}_2^-$, and consists of one asymmetrical line with $g_{||} = 2.157$ and $g_{\perp} = 2.002$ [133]. In ozonates (NaO_3 and KO_3) the line turned out to be somewhat more symmetrical: $g_{||} = 2.003$, $g_{\perp} = 2.015$ [134]. Dithionate of sodium, in which the resonance is apparently due to the SO_2^- ions, gave a line with $g = 2.01$ and $\Delta H = 12$ oersted [135].

Investigations of chlorine dioxide (ClO_2) were already mentioned earlier (see page 368) [12].

Let us mention, finally, the inorganic radical ion $[(SO_3)_2NO]^{2-}$, the investigation of which in solution has been the subject of several papers. It gives a triplet picture, due to the interaction between the unpaired electron and the spin of the ^{14}N nucleus. The energy levels of the system, in investigations in weak fields, agree well with the Breit and Rabi formulas for the case $I = 1$, $S = 1/2$, as was shown in [135]. The mechanism of paramagnetic relaxation in solutions contain-

ing the $[(SO_3)_2NO]^{2-}$ ion was analyzed in detail by Lloyd and Pake [136].

2. Diatomic and polyatomic molecules of certain gases are, in accordance with the definition given at the beginning of this chapter, free radicals, inasmuch as they contain uncompensated electron spins. These gases include, in particular, O_2, NO, NO_2, ClO_2, and also vapors of some paramagnetic compounds. In addition to such stable gaseous free radicals, there is also a large number of unstable substances of radical-like nature, existing in a gaseous medium, for example $\overset{\bullet}{C}H_3$, $\overset{\bullet}{O}H$, etc., the investigation of which were discussed above for the case when they enter in the condensed phases.

Paramagnetic gases differ from the paramagnets considered above in the strong coupling between the magnetic moment of the unpaired electron and the moments of the rotational motions of the molecule. Consequently the system of levels observed in the investigation of paramagnetic resonance in gases turns out to be quite complicated.

The resolution of the spectral lines of paramagnetic resonance in gases can be observed only at reduced pressures p. When p > 20 mm Hg, the resolved lines are not observed in even a single case; actually, the pressure employed usually does not exceed 1 mm Hg. This brings about (considering the large number of spectral lines) difficulties in the experimental work with gases, which calls for installations of high sensitivity; the greater part of the research in this direction was carried out by Beringer and Castle.

From among the investigated gases, the one with the weakest coupling between electron spin and the rotation of the molecule is nitrogen dioxide NO_2. At a pressure p = 10 mm Hg, a triplet structure is observed, due to the nitrogen nucleus; at p = 1 mm Hg, it begins to be resolved into a large number of components; this was interpreted by

- 394 -

Beringer and Castle as the Paschen-Back effect of free magnetic moments of the molecule: the electron spin moment, the nuclear spin moment, and the moment due to the rotation of the molecule. The level system can be described by the expression

$$E_{M_S, M_I, M_J} = g\beta\, HM_S + AM_S M_I + BM_S M_J, \qquad (7.2)$$

where M_J is the rotational quantum number of the molecule. It was impossible to attain full resolution of the individual components [137, 138].

The NO molecule contains one unpaired electron and its ground state is $^2\Pi$. It is split by the spin-orbit coupling into two doublet levels with distance 120 cm^{-1} between them; of these, the lower level $^2\Pi_{1/2}$ is diamagnetic, since its projections of the spin and orbital momenta along the axis are equal and opposite; the upper level, $^2\Pi_{3/2}$, is paramagnetic. It splits further into several components because of the interaction with the rotation. The resultant states are characterized by the total angular momentum J. The momentum $J = 3/2$ corresponds to $g = 4/5$; this sublevel, split by the external magnetic field H into a fine structure triplet, was indeed observed in [139]. Each peak of the triplet has in turn a triplet hyperfine splitting due to the ^{14}N nucleus. The theory of the Zeeman effect in NO was presented in [140].

The O_2 molecule is a biradical; it contains two unpaired electrons with parallel spins, while its angular moment along the axis is zero. Its ground state is therefore $^3\Sigma$. Its orbital momentum combines with the spin momentum, producing levels corresponding to $J = K$, $K \pm 1$, where K is the quantum number of the total orbital angular momentum (molecular + electronic). The levels $K \pm 1$ are practically degenerate and are 2 cm^{-1} away from the level $J = K$. Therefore at a wavelength of approximately 5 mm one can observe absorption in the absence of an external magnetic field H. Superposition of the field H leads to a split-

ting of the J levels and to the possibility of observation of magnetic dipole transitions between the sublevels. In the region of fields H ≈ ≈ 3000 oersted, the coupling between the spin and orbital motion is disrupted, and this leads to the appearance of a large number (approximately 40) of resonance lines, due to the rotational levels. These lines were described in [141]. The theory of the spectrum was presented in [141-143].

In addition to stable paramagnetic gases, Beringer and his co-workers investigated also atomic hydrogen [144], oxygen [145], and nitrogen [146] in the gaseous phase. They used for this purpose a high-voltage gas discharge in a U-shaped discharge tube, in which they placed the corresponding molecular gases. This tube was directly connected to a vertical tube passing along the axis of a cylindrical cavity in the H_{011} mode. Recombination on glass was prevented as far as possible by using suitable anticatalysts.

Delmelt [147] proposed to add to the investigated gas (which had a partial pressure of about 0.01-0.1 mm Hg) inert gases at pressure 10-100 mm Hg. At such pressures it turns out to be possible to maintain a high arc temperature and thus dissociate by purely thermal means molecules of all types. In addition, the inert gas decreases the possibility of recombination, by slowing down the diffusion to the walls. They used this method to investigate atomic phosphorus $(^4S_{3/2})$. The line turned out to be a hyperfine doublet with A' = 20 oersted. Another method was used in [148] for the investigation of atomic iodine; for this purpose photodissociation induced by irradiation of I_2 vapor directly in a resonant cavity was employed.

REFERENCES TO CHAPTER 7

1. Ingram D.J.E., Free Radicals as Studied by Electron Spin Resonance, London, 1958.

2. Wertz J.E., Chem. Rev. 55, 829, 1955.

3. Blyumenfel'd L.A., Voyevodskiy V.V., UFN [Progress in the Physical Sciences] 68, 31, 1959.

4. Kozyrev B.M., Salikhov S.G., DAN SSSR [Proc. Acad. Sci. USSR] 68, 1023, 1947.

5. Bloembergen N., Wang S., Phys. Rev. 93, 72, 1954.

6. Walter R.I., Codrington R.S., D'Adamo A.F., Torrey H.C., J. Chem. Phys. 25, 319, 1956.

7. Weissman S.I., J. Chem. Phys. 25, 890, 1956.

8. McConnell H.M., J. Chem. Phys. 24, 764, 1956.

9. Jarrett H.S., J. Chem. Phys. 25, 1289, 1956.

10. Bersohn R., J. Chem. Phys. 24, 1066, 1956.

11. McConnell H.M., Chestnut D.B., J. Chem. Phys. 27, 384, 1957; 28, 107, 1958.

12. Bennett J.E., Ingram D.J.E., Schonland D., Proc. Phys. Soc. A69, 556, 1956.

13. Berthet G., Arch Sci. 10, 98, 1957.

14. Holden A.N., Kittel C., Merritt F.R., Yager W.A., Phys. Rev. 77, 147, 1950.

15. Livingston R., Zeldes H., J. Chem. Phys. 24, 170, 1956.

16. Garstens M.A., Singer L.S., Ryan A.H., Phys. Rev. 96, 53, 1954.

17. Becker S., Phys. Rev. 99, 1928, 1955.

18. Arbuzov A.Ye., Valitova F.G., Garif'yanov N.S., Kozyrev B.M., DAN SSSR 126, 774, 1959.

19. Lothe J.J., Eia G., Acta Chem. Scand. 12, 1535, 1958.

20. Yablokov Yu.V., Soveshchaniye po paramagnitnomu rezonansu [Conference on Paramagnetic Resonance], Kazan', 1959.

21. Garif'yanov N.S., Kozyrev B.M., DAN SSSR 118, 738, 1958.

22. Uebersfeld J., Compt. Rend. 241, 371, 1955.

23. Wertz J.E., Kolsch C.F., Vivo J.L., J. Chem. Phys. 23, 2194, 1955.

24. Arbuzov A.Ye., Valitova F.G., Garif'yanov N.S., Kozyrev B.M., Soveshchaniye po paramagnitnomu rezonansu, Kazan', 1959.

25. Chirkov A.K., Matevosyan R.O., ZhETF [J. Exp. Theor. Phys.] 33, 1053, 1957.

26. Berthe G., Arch. Sci. 9, 92, 1956.

27. Cohen V.W., Kikuchi C., Turkevich J., Phys. Rev. 85, 379, 1952.

28. Biyl D., Kainer H., Rose-Innes A.C., Nature, London, 174, 830, 1954.

29. Nielsen W.G., Fraenkel G.K., J. Chem. Phys. 21, 1619, 1953.

30. Meyer L.H., Saika A., Cutovsky H.S., J. Phys. Chem. 57, 481, 1953.

31. Yokozawa Y., Tatsuzaki L., J. Chem. Phys. 22, 2087, 1954.

32. Chu T.L., Pake G.E., Paul D.E., Townsend J., Weissman S.I., J. Phys. Chem. 57, 504, 1953.

33. Holden A.N., Yager W.A., Merritt F.R., J. Chem. Phys. 19, 1319, 1951.

34. Van Roggen A., van Roggen L., Gordy W., Phys. Rev. 105, 50, 1957.

35. McLean C., Rotgieser T., Kor G.Y.W., Appl. Sci. Res. 5, 469, 1956.

36. Codrington R.S., Olds J.D., Torrey H.C., Phys. Rev. 95, 607, 1954.

37. Trkal V., Cesksl. rasop. Fys. [Czech. Phys. Rev.] 7, 748, 1957.

38. Jarrett H.S., J. Chem. Phys. 21, 761, 1953.

39. Kicuchi C., Cohen V.W., Phys. Rev. 93, 394, 1954.

40. Weissman S.I., Townsend J., Paul D.E., Pake G.E., J. Chem. Phys. 21, 2227, 1953.

41. Hückel E., Z. Phys. [J. Phys.] 70, 204, 1931.

42. Ward R.L., Weissman S.I., J. Am. Chem. Soc. 76, 3612, 1954.

43. Yokozawa Y., Miyashita I., J. Chem. Phys. 25, 796, 1956.

44. Weissman S.I., de Boer E., Conradi J.J., J. Chem. Phys. 26, 963, 1957.

45. Hirshon J.M., Gardner D.M., Fraenkel G.K., J. Am. Chem. Soc. 75, 4115, 1953.

46. Wertz J.E., Vivo J.L., J. Chem. Phys. 23, 2193, 1955.

47. McLean C., van der Waals J.U., J. Chem. Phys. 27, 827, 1957.

48. McConnell H.M., J. Chem. Phys. 24, 632, 1956.

49. Tuttle T.R., Weissman S.I., J. Chem. Phys. 25, 189, 1956.

50. Venkataraman B., Fraenkel G.K., J. Chem. Phys. 24, 737, 1956.

51. Wertz J.E., Vivo J.L., J. Chem. Phys. 23, 2441, 1955.

52. Jarrett H.S., Sloan G.J., J. Chem. Phys. 22, 1783, 1954.

53. Brovetto P., Ferroni S., Nuovo Cimento 5, 142, 1957.

54. McConnell H.M., Chestnut D.B., J. Chem. Phys. 27, 984, 1957.

55. Bamford C.H., Jenkins A.D., Ingram D.J.E., Symons M.C.R., Nature, London, 175, 894, 1955.

56. Ingram D.J.E., Symons M.C.R., J. Chem. Soc., 2437, 1957.

57. Gardner D.M., Fraenkel G.K., J. Am. Chem. Soc. 78, 3279, 1956.

58. Tsvetkov Yu.D., Voyevodskiy V.V., Razuvayev G.A., Sorokin Yu.V., Domrachev G.A., DAN SSSR 115, 118, 1957.

59. Voyevodskiy V.V., Molin Yu.N., Chibrikin V.M., ZhOS [J. Optics and Spectroscopy] 5, 90, 1958.

60. Dyatkina M.Ye., Usp. khimii [Progress in Chemistry] 27, 57, 1958.

61. Chibrikin V.M., Burshteyn A.I., Solodovnikov S.P., cited from [3].

62. Hoskins R.H., Loy B.R., J. Chem. Phys. 23, 2461, 1955.

63. de Boer E., J. Chem. Phys. 25, 190, 1955.

64. Weissman S.I., Tuttle T.R., de Boer E., J. Phys. Chem. 61, 28, 1957.

65. Pake G.E., Weissman S.I., Townsend J., Disc. Faraday Soc. 19, 147, 1955.

66. Tuttle T.R., Ward R.L., Weissman S.I., J. Chem. Phys. 25, 189, 1956.

67. Tuttle T.R., Weissman S.I., J. Chem. Phys. 25, 190, 1957.

68. Sogo P.B., Nakazaki M., Calvin M., J. Chem. Phys. 26, 1943, 1957.

69. Venkataraman B., Fraenkel G.K., J. Am. Chem. Soc. 77, 2707, 1955.

70. Venkataraman B., Fraenkel G.K., J. Chem. Phys. 23, 588, 1955.

71. Fraenkel G.K., Ann. N.Y. Acad. Sci. 67, 553, 1957.

72. Wertz J.E., Vivo J.L., J. Chem. Phys. 24, 479, 1956.

73. Hoskins R.H., J. Chem. Phys. 23, 1975, 1955.

74. Gilliam O.R., Walter R.I., Cohen V.W., J. Chem. Phys. 23, 1540, 1955.

75. Weissman S.I., J. Chem. Phys. 22, 1135, 1954.

76. Jarrett H.S., Sloan G.J., J. Chem. Phys. 22, 1783, 1954.

77. Hutchison C.A., Pastor R.C., Kowalsky A.E., J. Chem. Phys. 20, 534, 1952.

78. Pake G.E., Townsend J., Weissman E.I., Phys. Rev. 85, 682, 1952.

79. Fellion Y., Uebersfeld J., Arch. Sci. 10, 95, 1957.

80. Shneider E.E., Day M.J., Stein G., Nature, London, 168, 645, 1951.

81. Ingram D.J.E., Hodgson W.S., Parker C.A., Rees W.T., Nature, London, 176, 1227, 1955.

82. Bijl D., Rose-Innes A.C., Nature, London, 175, 82, 1955.

83. Gibson J.F., Ingram D.J.E., Symons M.C.R., Townsend M.G., Trans. Faraday Soc. 53, 914, 1957.

84. Fujimoto M., Ingram D.J.E., Trans. Faraday Soc. 54, 1304, 1958.

85. Ingram D.J.E., Symons M.C.R., Townsend M.G., Trans. Faraday Soc. 54, 409, 1958.

86. Gordy W., Ard W.B., Shields H., Proc. Nat. Acad. Sci. 41, 983, 1955.

87. Uebersfeld J., Erb E., Compt. Rend. 242, 478, 1956.

88. Chernyak N.Ya., Bubnov N.N., Polak L.S., Tsvetkov Yu.D., Voyevodskiy V.V., ZhOS 6, 564, 1959.

89. Chernyak N.Ya., Bubnov N.N., Voyevodskiy V.V., Polak L.S., Tsvetkov N.D., DAN SSSR 120, 346, 1958.

90. Smaller B., Matheson M.S., J. Chem. Phys. 28, 1169, 1958.

91. Luck C.F., Gordy W., J. Am. Chem. Soc. 78, 3240, 1956.

92. Gordy W., McCormik C.G., J. Am. Chem. Soc. 78, 3243, 1956.

93. Rexroad H.N., Gordy W., Proc. Nat. Acad. Sci. 45, 256, 1959.

94. Fraenkel G.K., Hirshon J.M., Walling C., J. Am. Chem. Soc. 76, 3603, 1954.

95. Bubnov N.N., Tsvetkov Yu.D., Lazurkin Yu.S., Mokul'skiy M.I., Voyevodskiy V.V., DAN SSSR 122, 1053, 1958.

96. Ard W.B., Shields H., Gordy W., J. Am. Chem. Phys. 23, 1727, 1955.

97. Abraham R.J., Melville H.W., Ovenall D.M., Whiffen D.H., Trans. Faraday Soc. 54, 409, 1958.

98. Abraham R.J., Whiffen D.H. (cited from [1]).

99. Atherton N.M., Melville H.W., Whiffen D.H., Trans. Faraday Soc. (cited from [1]).

100. Harle O.L., Thomas J.R., J. Am. Chem. Soc. 79, 2973, 1957.

101. Ingram D.J.E., Bennett J.E., Phil. Mag. 45, 545, 1954.

102. Uebersfeld J., Etienne A., Combrisson J., Nature, London, 174, 614, 1954.

103. Winslow F.H., Baker W.O., Yager W.A., J. Am. Chem. Soc. 77, 4751, 1955.

104. Austen D.E.G., Ingram D.J.E., Tapley J.G., Trans. Faraday Soc. 54, 400, 1958.

105. Uebersfeld J., Erb E., Compt. Rend. [Proceedings] 243, 2043, 1956.

106. Garif'yanov N.S., Kozyrev B.M., ZhETF 30, 272, 1956.

107. Garif'yanov N.S., Kozyrev B.M., ZhETF 30, No. 6, 1956.

108. Ingram D.J.E., Tapley J.G., Jackson R., Bond R.L., Murnaghan A.R., Nature, London, 174, 797, 1954.

109. Singer L.S., Spry W.T., Bull. Am. Phys. Soc., 214, 1956.

110. Uebersfeld F., Erb E., J. Phys. Rad. 16, 340, 1955.

111. Austen D.E.G., Ingram D.J.E., Chem. and Ind. 981, 1956.

112. Castle J.G., Phys. Rev. 92, 1063, 1953; 94, 1410, 1954.

113. Ubbelohde A.R., Nature, London, 180, 380, 1957.

114. Jarrett H.S., Sloan G.F., Vanghan W.R., J. Chem. Phys. 25, 695, 1956.

115. Hutchison C.A., Kowalsky A., Pastor R.C., Wheland G.W., J. Chem. Phys. 20, 1485, 1952.

116. Kozyrev B.M., DAN SSSR 81, 427, 1951.

117. Blois S., Bioch. et. Biophys. Acta 18, 165, 1955.

118. Commoner B., Townsend J., Pake G., Nature, London, 174, 4432, 1954.

119. Commoner B., Heise J.J., Townsend J., Proc. Nat. Acad. Sci. 41, 983, 1955.

120. Blyumenfel'd L.A., Kalmanson A.Ye., DAN SSSR 117, 72, 1957.

121. Blyumenfel'd L.A., Kalmanson A.Ye., Biofizika [Biophysics] 2, 552, 1957.

122. Blyumenfel'd L.A., Kalmanson A.Ye., Biofizika 3, 87, 1958.

123. Blyumenfel'd L.A., Kalmanson A.Ye., Shen Pey-chen', DAN SSSR 129, 1144, 1959.

124. Livingston R., Zeldes H., Taylor E.H., Phys. Rev. 94, 725, 1954.

125. Livingston R., Zeldes H., Taylor E.H., Disc. Faraday Soc. 19, 166, 1955.

126. Smaller B., Matheson M.S., Yasaitis E.U., Phys. Rev. 94, 202, 1954.

127. Jen C.K., Foner S.N., Cochran E.L., Bowers V.A., Phys. Rev. 104, 846, 1956.

128. Matheson M.S., Smaller B., J. Chem. Phys. 23, 521, 1955.

129. Livingston R., Ghormeley Y., Zeldes H., J. Chem. Phys. 24, 483, 1956.

130. Gorbanev A.I., Kaytmazov S.D., Prokhorov A.M., Tsentsiper A.B., ZhFKh [J. Phys. Chem.] 31, No. 2, 1957.

131. Ard W.B., J. Chem. Phys. 23, 1967, 1955.

132. Bleaney B., Hayes W., Llewellyn P.M., Nature, London, 179, 140, 1957.

133. Bennett J.E., Ingram D.J.E., Symons M.C.R., George P., Griffith J.S., Phil. Mag. 46, 443, 1956.

134. Hodgson W.G., Neaves A., Parker C.A., Nature, London, 178, 489, 1956.

135. Townsend J., Weissman S.I., Pake G.E., Phys. Rev. 89, 609, 1953.

136. Lloyd J.P., Pake G.E., Phys. Rev. 94, 579, 1954.

137. Beringer R., Castle J.G., Phys. Rev. 78, 581, 1950.

138. Beringer R., Castle J.G., Phys. Rev. 80, 114, 1950.

139. Beringer R., Rawson E.B., Henry A.F., Phys. Rev. 94, 34, 1954.

140. Margenau H., Henry A., Phys. Rev. 78, 587, 1950.

141. Beringer R., Castle J.S., Phys. Rev. 81, 82, 1951.

142. Henry A.F., Phys. Rev. 80, 396, 1950.

143. Tinkham M., Strandberg M.W.P., Phys. Rev. 97, 937, 1955; 97, 951, 1955; 99, 537, 1955.

144. Beringer R., Heald H.A., Phys. Rev. 95, 1474, 1954.

145. Rawson E.B., Beringer R., Phys. Rev. 88, 677, 1952.

146. Heald M.A., Beringer R., Phys. Rev. 96, 645, 1954.

147. Dehmelt H.G., Phys. Rev. 99, 527, 1955.

148. Bowers K.D., Kamper R.A., Lustig C.D., Proc. Phys. Soc. B70, 1177, 1957.

149. Biyl D., Kainer H., Rose-Innes A.C., J. Chem. Phys. 30, 765, 1959.

Manu- script Page No.	[Footnotes]
370	For two solvents — benzene and carbon bisulfide — this influence was observed still earlier in [19].
382	Special experiments have shown that the ultraviolet does not act on the molecules of the solvent.

Manu- script Page No.	[List of Transliterated Symbols]
362	спин = spin = spin
363	сумм = summ = summarnyy = summary

Chapter 8

DOUBLE RESONANCE. CERTAIN APPLICATIONS

OF PARAMAGNETIC RESONANCE

§8.1. Introduction

So far we have considered resonant absorption of an alternating electromagnetic field of one fixed frequency. Yet double resonance, which consists of simultaneous resonant absorption of electromagnetic radiation at two different frequencies, has found a variety of uses. We consider the most important examples of double resonance: 1) the Overhauser effect and other dynamic methods of nuclear polarization; 2) paramagnetic amplifiers and 3) optical investigations of paramagnetic resonance.

In the Overhauser effect one investigates simultaneously electron and nuclear paramagnetic resonance. Therefore, one of the frequencies employed lies in the microwave range and the other at high radio frequencies. An interesting application of this effect is the polarization of atomic nuclei.

Paramagnetic resonance is used for technical purposes to build amplifiers with exceedingly low noise level. In these amplifiers one uses for the most part fields with two different frequencies, lying in the microwave band. Radiation at one frequency is used to supply energy to the working medium; the other frequency pertains to the signal to be amplified.

In many investigations, the medium studied was subjected to the simultaneous resonant action of radiation at optical and microwave

frequencies. The combination of optical and radio research methods turned out to be very fruitful and within a short time it yielded many interesting data both in the field of atomic spectroscopy and on the theory of atomic collisions.

§8.2. Dynamic Methods of Nuclear Polarization

I. Overhauser effect in metals and semiconductors

Let us assume that the substance contains, along with particles that have an electron magnetic moment, also particles that have a non-zero nuclear moment. In a particular case, the electron and nuclear moments can pertain to one and the same atom. In many cases the mechanisms of electronic and nuclear spin lattice relaxation are such that the saturation of the electron paramagnetic resonance leads to considerable polarization of the nuclei. This effect was first considered theoretically by Overhauser [1] for metals.

At first glance the increase in nuclear polarization upon saturation of electron resonance may appear paradoxical, since the equalization of the populations of the different energy sublevels of the spin system means an increase in its temperature. But an increase in temperature should cause a reduction in the differences in population of the different nuclear Zeeman sublevels. This paradox is resolved, as indicated in particular by Van Vleck [2], by the fact that in our case there is no single electron-nuclear spin system. In the processes of interest to us there are involved three weakly interacting systems: the K system, connected with the kinetic energy of the conduction electrons of the metal; the Z system, the energy of which is due to the interaction between the electrons and the external static magnetic field (the Zeeman energy of electrons), and finally the N system, which includes the Zeeman energy of the nuclei. These systems can have different temperatures: T_K, T_Z and T_N.

Overhauser [3] has shown that nuclear spin-lattice relaxation in metals is due essentially to the interaction between the moments of the nuclei and of the conduction electrons:

$$\mathscr{H}_{eN} = a\hat{I}\hat{S} = a(\hat{I}_z\hat{S}_z + \hat{I}_+\hat{S}_- + \hat{I}_-\hat{S}_+),$$ (8.1)

where

$$a = \frac{8\pi}{3}\beta\beta_N g g_N \delta(r).$$ (8.2)

Here $\underline{r}$ is the distance from the conduction electron to the nucleus and $\delta(r)$ is the delta function. The interaction (8.1) has a contact character and is isotropic, from which we see that the sum $S_z + I_z$ is the integral of the motion. Thus, it follows from the law of conservation of the angular momentum that under the influence of interaction (8.1) the following transitions are possible:

$$M, m \longleftrightarrow M - 1, m + 1.$$ (8.3)

Reorientation of the electron spin is accompanied by a reversal of the direction of the nuclear spin.

It must be kept in mind that the electron Zeeman energy $E_Z = g\beta H_0 M$ is approximately 10^3 times larger in absolute magnitude than the nuclear Zeeman energy $E_N = -g_N\beta_N H_0 m^*$. Consequently simultaneous reorientation of the electron and nuclear spins is possible if the K system, into which the excess of the energy released goes, participates in this process. Assume that the process (8.3) is accompanied by a change in the kinetic energy of the conduction electrons $E_K \longleftrightarrow E_{K'}$.

It then follows from the law of energy conservation that

$$E_{K'} - E_K - g\beta H_0 - g_N\beta_N H_0 = 0.$$ (8.4)

We denote by N_K, N_M, and N_m the number of particles per unit volume in the states K, M and $\underline{m}$ respectively. For each pair of interacting particles the probabilities of the direct and inverse transitions (8.3) are the same. Therefore the number of direct transitions will

be proportional to $N_K N_M N_m$, and the number of inverse transitions proportional to $N_{K'} N_{M-1} N_{m+1}$. Under stationary conditions we have

$$N_K N_M N_m = N_{K'} N_{M-1} N_{m+1}. \tag{8.5}$$

Since

$$\frac{N_K}{N_{K'}} = \exp\left(\frac{E_{K'} - E_K}{kT_K}\right) = \exp\left[\frac{(g\beta + g_N \beta_N) H_0}{kT_K}\right], \\ \frac{N_M}{N_{M-1}} = \exp\left(-\frac{g\beta H_0}{kT_Z}\right), \quad \frac{N_m}{N_{m+1}} = \exp\left(-\frac{g_N \beta_N H_0}{kT_N}\right), \tag{8.6}$$

it follows from (8.5) that

$$\frac{1}{T_N} = \frac{g\beta + g_N \beta_N}{g_N \beta_N T_K} - \frac{g\beta}{g_N \beta_N T_Z}. \tag{8.7}$$

Under electronic resonance saturation conditions we have $T_Z \to \infty$. If we recognize in addition that $g_N \beta_N \ll g\beta$, we get

$$T_N = T_K \frac{g_N \beta_N}{g\beta}. \tag{8.8}$$

Thus, saturation of electron resonance reduces the temperature of the nuclear Zeeman system by a factor $\frac{g\beta}{g_N \beta_N}$. Therefore, if we assume that $g\beta H_0 \ll kT_K$, we obtain

$$\frac{N_m}{N_{m+1}} = 1 - \frac{g\beta H_0}{kT_K}. \tag{8.9}$$

The polarization of the nuclei proceeds as if their magnetic moments were to increase by $\frac{g\beta}{g_N \beta_N}$ times. We note that the nuclear $\underline{g}$ factor can be both positive and negative. Accordingly, the temperature of the nuclear Zeeman system can assume both positive and negative values. For simplicity, a Boltzmann distribution was used in the derivation of (8.9). It is easy to verify that a Fermi distribution leads to the same result.

Under the influence of the radio frequency field that saturates the electron resonance, transitions are produced predominantly from the lower electronic Zeeman level to the upper one. The relaxation transitions of the electrons occur with large probability in the

opposite direction, and consequently a stationary mode is established. Among the various relaxation mechanisms, the one of importance to the Overhauser effect is that based on the electron-nuclear interaction (8.1). The electrons going from the upper Zeeman level to the lower one will continuously flip the nuclear spins in one direction or another. The nuclear polarization will grow until the number of transitions M, m → M − 1, m + 1, occurring under the influence of the given relaxation mechanism becomes equal to the number of inverse transitions. It is clear therefore that with increasing difference between T_N and T_K the number of transitions contributing to the equalization of these temperatures will also increase. The Overhauser effect is an irreversible process of continuous transition of the electron Zeeman energy into lattice vibrations. This effect can therefore be readily interpreted by methods of thermodynamics and statistical physics [4-9]; it can serve as a good illustration of the principal premises of these theories. For the general theory of the Overhauser effect it is important to consider the relaxation processes in two spin systems [10, 11], that is, in systems containing two sorts of particles having different magnetic moments.

In the derivation of (8.9) we have assumed that the mechanism based on the interaction (8.1) is the only relaxation mechanism for the nuclei. The relaxation time due to this mechanism will be denoted by T'_1. Yet there are also other spin-lattice coupling mechanisms. If we denote the total spin-lattice relaxation time by T_1 and, in addition, take into account the fact that the saturation factor q_{12} of electron resonance can differ from 0, we obtain in place of (8.9)

$$\frac{N_m}{N_{m+1}} = 1 - \frac{g\beta H_0}{kT_K}(1-q)\frac{T_1}{T'_1} - \frac{g_N \beta_N H_0}{kT_K}. \tag{8.10}$$

This formula can be used only for specimens whose linear dimensions

<u>d</u> are small compared with the skin layer depth δ. Azbel, Gerasimenko and Lifshits [12] have shown that the Overhauser method makes it possible to polarize nuclei in specimens for which d≫ δ. The point is that the mean free path of the electron in the metal is much shorter than the distance covered by the electron between two such collisions, which change the spin orientation. There exists therefore a unique "anomalous skin effect" for the magnetic moment. The polarization of nuclei in specimens of arbitrary thickness has been calculated in [12].
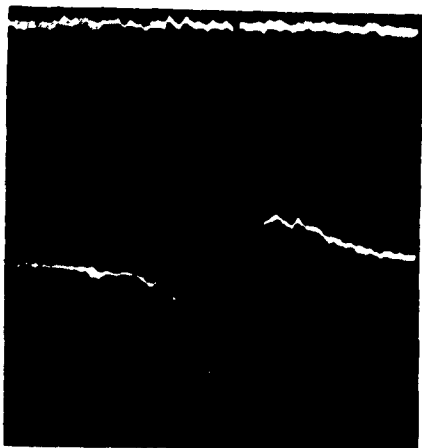
Fig. 8.1. Overhauser effect in lithium [14]. In the upper photograph, the nuclear resonance signal is lost in the noise. Below, the same signal is amplified by saturation of electron resonance.

The increased nuclear polarization resulting from saturation of the electron Zeeman levels should change the line shape of the electron paramagnetic resonance [13], since the field produced by the polarized nuclei will be superimposed on the external magnetic field.

The Overhauser effect was first investigated experimentally in lithium [14]. To avoid the difficulties connected with simultaneous utilization of a resonant cavity and a coil, the experiments were set up at relatively low frequencies, 13.4 megacycles and 7.96 kilocycles. Figure 8.1 shows a photograph in which it is seen how much the nuclear resonance signal is amplified as a result of the saturation of the electron resonance. The Overhauser effect was later on investigated in detail in sodium and lithium [15].

The use of the Overhauser effect to increase nuclear polarization was extended also to semiconductors, which offers the following advantages: 1) the poor conductivity eliminates the difficulties connected with the skin effect at microwave frequencies; 2) owing to the

small number of conduction electrons, the nuclear relaxation times are very large, so that the nuclear polarization effected with the aid of the high frequency field can be separated both in space and in time from the succeeding experiments on the observation of this polarization with the aid of a relatively low-frequency field.

The experiments were carried out with silicon crystals doped with phosphorus [16]. The polarization of the Si^{29} nuclei was retained for several minutes.

It must be noted that Honig [17] drew erroneous conclusions from his experiments on electron resonance in silicon containing arsenic impurities. Measurements have shown that the resonance absorption line has four hyperfine components in accordance with the value 3/2 of the nuclear spin of As^{75}. Upon repeated passage through one end of the same component, the absorption decreases exponentially as $1 - e^{-t/\tau}$ with $\tau = 16$ sec. If one goes in succession through two neighboring components within a time interval which is much shorter than 16 seconds, by varying the field H_0, then the intensity of the second peak will strongly increase. Honig assumed at first that he had discovered a method of 100 per cent polarization of nuclei at not too low temperatures. He thought that the transitions between the electron Zeeman sublevels, excited by the resonant radio frequency field, will rapidly align the nuclear spins as a result of the hyperfine $\overrightarrow{IS}$ interaction. The appropriate calculations were made by Kaplan [18]. However, later experiments made by Honig and Combrisson [19] have shown that the reason lies in the exceptionally long relaxation time.
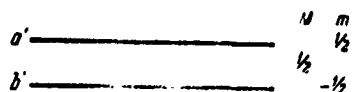
2. Overhauser effect in nonmetals

The Overhauser effect can occur in substances which are not metals or semiconductors [20-22]. Indeed, for the effect which we have been considering in metals, the following two circumstances are

- 411 -

significant: 1) one of the mechanisms whereby the electron spins are relaxed is based on their coupling with the nuclear moments, which calls for conservation of the total angular momentum; 2) this coupling plays a decisive role in the relaxation of the nuclear spins; 3) the possibility of conserving the energy during the time of these relaxation transitions is guaranteed by the continuity of the kinetic energy spectrum of the conduction electrons; 4) under saturation conditions, relaxation transitions from the upper Zeeman level to the lower one exceed in number the transitions in the opposite direction.

Perfectly analogous conditions exist in many nonmetals: 1) to increase nuclear polarization it is not essential to conserve the sum of the electron and nuclear spins; it is merely important that the probabilities of the nuclear spin flips $m \rightarrow m'$ and $m \rightarrow -m'$ be unequal; 2) the hyperfine interactions determine the nuclear relaxation not only in metals but in many other substances; 3) the conservation of energy during the time of simultaneous flip of electron and nuclear spins can be guaranteed by transfer of the excess energy to the lattice vibrations in solids or to the Brownian motion of the particles in liquids and gases; 4) if the lattice is in the state of thermodynamic equilibrium, then the a priori probabilities of the relaxation transitions from the upper Zeeman levels to the lower ones will always exceed the probabilities of the inverse transitions.

Abragam [23] considered in detail the question of the Overhauser effect in nonmetals for several important cases. He made the following assumptions: a) the nuclear spin is $I = 1/2$; b) the external magnetic field is strong, so that one can speak with good approximation of the quantum numbers of the projections of the electron and nuclear spins on the H_0 direction; c) there is no direct coupling between the nuclear moments and the lattice vibrations; nuclear relaxation is

a'——————————— M m ½ ½

b'——————————— ½ -½

a ——————————— -½ -½

b ——————————— -½ ½

Fig. 8.2. Energy
level scheme in the
case S = 1/2, I =
= 1/2.

realized by the magnetic interaction of the
nuclear and electron spins, which in general
case has the form

$$\mathscr{H}_1 = \hat{I} a \hat{S}, \qquad (8.11)$$

where $\underline{a}$ is a symmetrical tensor. The operator
$\hat{H}_1$ can be written in the form

$$\mathscr{H}_1 = -g_N \beta_N \hat{I} \hat{H}_e, \qquad (8.12)$$

where $\hat{H}_e = -(a/g_N \beta_N)\vec{S}$ can be called the mag-
netic field produced by the electron at the location of the nucleus.
The field H_e is a random function of the time because random changes
are possible both in the tensor $\underline{a}$ and in the direction of the spin S.
We shall speak of relaxation of the first type if it is due to changes
in the tensor $\underline{a}$, brought about by the lattice vibrations in solids or
by Brownian motion in liquids. Responsible for the relaxation of the
second type are electron spin flips resulting from the ordinary
mechanisms of electron spin-lattice interaction, independent of the
coupling with the nuclear moments.

We denote the states (M = 1/2, m = 1/2), (-1/2, 1/2), (1/2, -1/2),
(-1/2, -1/2) by a', a, b', b (Fig. 8.2), the summary population of the
levels $\underline{a}$ and a' by N_+, and that of levels $\underline{b}$ and b' by N_-. In addition,
we introduce the probabilities of the relaxation transitions between
the different electron sublevels:

$$\left.\begin{array}{l} A_{aa'} \approx A_{bb'} = A e^{-\epsilon} \approx A(1-\epsilon), \\ A_{a'a} \approx A_{b'b} = A(1+\epsilon), \quad \epsilon = \frac{g\beta H}{2kT}. \end{array}\right\} \qquad (8.13)$$

For the probabilities of the other relaxation transitions we assume

$$\left.\begin{array}{l} A_{a'b'} \approx A_{b'a'} \approx A_{ab} \approx A_{ba} = \lambda_1 A, \\ A_{b'a} \approx \lambda_2 A(1+\epsilon), \quad A_{ab'} \approx \lambda_2 A(1-\epsilon), \\ A_{a'b} \approx \lambda_3 A(1+\epsilon), \quad A_{b a'} \approx \lambda_3 A(1-\epsilon). \end{array}\right\} \qquad (8.14)$$

If the electron transitions a → a' and b → b' are saturated by a

radio frequency field, then, as shown by Abragam, the nuclear polari-
zation is determined by the following expression:

$$\frac{N_+}{N_-} = 1 - \frac{2\varepsilon\,(\lambda_\mathbf{s} - \lambda_\mathbf{t})}{2\lambda_\mathbf{t} + \lambda_\mathbf{s} + \lambda_\mathbf{t}}. \tag{8.15}$$

Let us consider the following particular cases.

1. In the metals which we considered above, relaxation of the
first type takes place, determined by the interaction (8.1); therefore
$\lambda_1 = \lambda_3 = 0$ and consequently

$$\frac{N_+}{N_-} = 1 + 2\varepsilon, \tag{8.16}$$

which agrees with formula (8.9).

2. In liquids, if we assume that the nuclear relaxation pertains
to the first type and is determined by the magnetic dipole interac-
tions between the nuclei and the paramagnetic impurities, the coef-
ficients λ_1, λ_2 and λ_3 are related as 3:2:12, that is, as the mean
values of the squares of the matrix elements of the operators $\hat{c}_{jk}$, $\hat{b}_{jk}$
and $\hat{e}_{jk}$ (5.9). For the nuclear polarization we obtain

$$\frac{N_+}{N_-} = 1 - \varepsilon. \tag{8.17}$$

3. In diamagnetic crystals containing paramagnetic impurities,
the relaxation is of the second type. In this case $\lambda_3 = \lambda_2$ and there
is no Overhauser effect.

This result can be explained in the following fashion. Let us
consider the transitions that lead to the nuclear spin flip $1/2 \rightarrow -1/2$,
namely a' $\rightarrow$ b $\rightarrow$ b' and a $\rightarrow$ b' $\rightarrow$ b. The transitions b $\rightarrow$ b' and b' $\rightarrow$ b
are realized under the influence of the saturating radio-frequency
field and are not accompanied by a change in the nuclear spin orienta-
tion. On the other hand, the transitions a' $\rightarrow$ b and a $\rightarrow$ b' are due to
the coupling with the lattice vibrations. Since the relaxation is of
the second type and is due to magnetic interactions of the electron

- 414 -

and nuclear spins, the probabilities of both processes turn out to be the same $(\lambda_2 = \lambda_3)$; as a result the lattice acquires no energy whatever, meaning that additional polarization of the nuclei due to electron resonance saturation is impossible.

4. For substances containing paramagnetic atoms with nonzero nuclear spin, the calculations have been carried out under the assumption that the hyperfine structure of the resonance line is resolved and has an isotropic character. In this case $\lambda_3 = 0$ and the polarization is

$$\frac{N_+}{N_-} = 1 + \frac{2\xi}{2 + \xi},$$ (8.18)

where $\xi = \lambda_2/\lambda_1$. If we saturate not both but one of the electron transitions, then

$$\frac{N_+}{N_-} = \frac{1 + \xi}{2 + \xi}.$$ (8.19)

The theory of relaxation transitions between hyperfine energy sublevels was developed by Valiyev [24], who calculated the values of $\lambda_1 A$ for typical ions of the iron and rare earth groups. The appropriate calculations for ions in the S states were made by Bashkirov [25]. The Overhauser effect was considered also theoretically for the case S = = 1/2, I = 1 with the ion ^{64}Cu as an example. It was shown there that simultaneous saturation of one electron and one nuclear resonance results in nuclear polarization of the same magnitude as in the saturation of all the electron transitions [26].

Khutsishvili [27] has considered the question of polarization of nuclei belonging to paramagnetic atoms in nonmetals, by saturating only one of the hyperfine structure components. It turned out that it is most convenient to saturate the m = 0 line if the nuclear spin I is even and the m = $\pm$ 1/2 if I is odd.

The Overhauser effect in nonmetals was investigated experimentally

in many cases: on the protons of the free radical diphenylpicrylhydra-zyl [28], on protons [29], on Li^7 and F^{19} nuclei [30] in solutions containing the free radical $(SO_3)_2NOK_2$, and on protons contained in benzene absorbed by carbon [31].

3. Method of adiabatic passage

The Overhauser method of nuclear polarization is applicable if the mechanism of nuclear spin-lattice relaxation obeys definite conditions.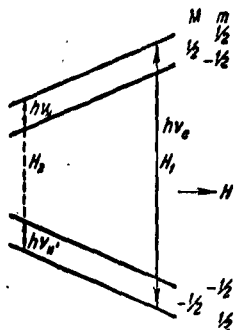 The method proposed by Feher [32], based on adiabatic rapid passage through the paramagnetic resonance lines (see §8.4) is suitable for substances that have a resolved hyperfine structure independently of the nature of the nuclear and electron spin-lattice relaxation mechanisms. The idea of the method will be illustrated with the aid of Fig. 8.3, which shows the Zeeman energy levels as functions of the applied magnetic field H_0 in the case $S = 1/2$, $I = 1/2$. By v_e and v_N we denote the frequencies of the microwave and radio frequency fields applied

Fig. 8.3. Diagram showing nuclear polarization by the adiabatic passage method.

perpendicular to H_0. By decreasing the field H_0 to a value H_1, we excite the electron transitions $M = -1/2$, $m = 1/2 \leftarrow \rightarrow M = 1/2$, $m = 1/2$. If this is done under conditions of adiabatic rapid passage, then the vector of electronic magnetization will turn through $180°$, and this will cause an inversion of the populations of the corresponding sublevels. The difference in populations of each pair of nuclear sublevels, pertaining to one and the same electron state, will now be determined not by the nuclear but by the electronic Boltzmann factor, something that can be readily observed by the nuclear resonance method. In this case, however, the population of both sublevels with $m = +1/2$ is equal to the population of the sublevels with $m = -1/2$,

and consequently on the whole there is no nuclear polarization. In order to obtain it, we pass adiabatically through nuclear resonance, to which the field H_2 corresponds. Since the energy interval $h\nu_N$ between one pair of nuclear sublevels is not equal to the interval between the other pair of sublevels, as a result we obtain nuclear polarization equal to

$$\frac{N_+}{N_-} = 1 - 2\epsilon. \tag{8.20}$$

This polarization vanishes after a time interval equal approximately to the nuclear relaxation time; the situation can be restored by repeated variation of the field H_0.

If we effect adiabatically the fast transition $\Delta m = 1$, $\Delta M = 0$, then the electron resonance will change strongly. Thus, we have a sensitive method of investigating nuclear resonance by observing the electron paramagnetic resonance absorption.

An experimental verification of the adiabatic passage method was carried out by Feher and Gere [33]. The experiments were set up with a silicon crystal containing phosphorus amounting to approximately $3 \cdot 10^{16}$ atoms of P^{31} per cubic centimeter. Earlier investigations (§6.3) have shown that it is possible to observe in this substance the hyperfine structure of paramagnetic resonance lines as a result of interaction between the donor electron and the magnetic moment of the P^{31}; the electron relaxation time was found to be quite long.

In the experiments of Feher and Gere, the external field at which the transitions were investigated was approximately 3130 oersted, and the specimen temperature was 1.25°K. The electron resonance line was observed by a superheterodyne method without the use of field modulation. The microwave cavity was made of pyrex coated on the inside surface with a thin layer of silver. This insured the penetration

into the cavity of the radio frequency field necessary for excitation of the transitions between the nuclear sublevels. The amplitudes of the microwave and radio frequency fields in the specimen were on the order of 0.001 oersted. The constant field H_0 changed within approximately four seconds from an initial value 3150 oersted to 3110 oersted, after which it again returned to 3150 oersted.

The results of the experiments confirmed Feher's calculations. In the absence of a radio frequency field, the amplitude of the electron resonance line changed little in the secondary passage through resonance; on the other hand, if a radio frequency field was applied during the interval between the first and second passages to induce the transition $h\nu_N$ (see Fig. 8.3), then the intensity of the electron resonance line decreased sharply during the second passage, thus evidencing the presence of nuclear polarization. An analogous method was used in [34].

4. Method of parallel fields

Jeffries [35] proposed to use for nuclear polarization the forbidden transitions that appear in the case when the alternating and static magnetic fields are oriented parallel to each other, as a result of the fact that the hyperfine interactions cause a slight overlapping of the states with different values of M and m. If the hyperfine interaction operator has the form $A\hat{I}_z\hat{S}_z + B(\hat{I}_x\hat{S}_x + \hat{I}_y\hat{S}_y)$ then the wave functions, which in the zero approximation are equal to $\psi(M,m)$, will assume in the next approximation the form $\psi(M,m) +$ $+ \alpha(B/H)\psi(M \pm 1, m \mp 1)$.

By way of illustration we consider the case $S = 1/2$, $I = 1/2$ (Fig. 8.4). The solid arrows denote the transitions that are possible in the usual mutually-perpendicular arrangement of the alternating and static magnetic fields ($\Delta M = 1$, $\Delta m = 0$). The dashed arrows show the
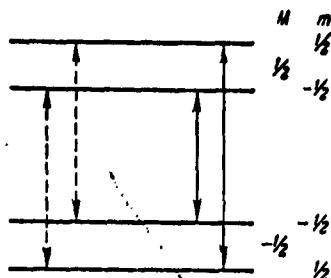
Fig. 8.4. Scheme of
nuclear polarization
by the parallel
field method.

"forbidden" transitions, which arise in the case when the fields are parallel. With this, from the form of the perturbed wave functions it follows that $\Delta(M + m) = 0$. If we saturate the transition $M = -1/2$, $m = + 1/2 \rightarrow M = 1/2$, $m = -1/2$, with a radio frequency field, polarization is immediately produced:

$$N_+/N_- = 1 - \varepsilon.$$

If the polarized nuclei are radioactive, then the polarization can be detected from the resultant anisotropy of the gamma radiation. The effect will in this case be proportional not to the number of atoms participating in the paramagnetic resonant absorption, but to the number of radioactive decays. This method is therefore particularly convenient for the study of short-lived nuclei.

The Jeffries method was used to polarize radioactive Co^{60} nuclei contained in the single crystal $La_2Mg_3(NO_3)_{12} \cdot 24D_2O$ [36]. The ratio of magnesium to its isomorphic cobalt-isotope substitutes was $Mg:Co^{59}$: $:Co^{60} = 10^4:50:1$. The measurements were carried out at a frequency of $9.3 \cdot 10^9$ cps at a temperature $1.6^\circ K$. The Z axis of the crystal was perpendicular to the static and the oscillating magnetic fields. The paramagnetic absorption in Co^{60} is very weak and cannot be measured directly. Paramagnetic resonance is detected by the anisotropy of the gamma radiation. The spectrum contained $2I = 10$ lines in accordance with the well known value of the spin of the Co^{60} nucleus. The following ratios were obtained for the line intensities: $83:100:83:52:18$ in good agreement with the predictions of the theory [37].

5. The method of Abragam and Proctor [38]

Let us assume that the substance contains electron and nuclear

paramagnetic centers. For simplicity we assume that the spins of the centers are S = 1/2, I = 1/2. Assume that some interaction exists between the electron and nuclear spins, say magnetic dipole coupling. This coupling causes an overlap of the electron and nuclear states, so that the wave functions assume the form $\psi(M,m) + \alpha\psi(M',m')$ where $\alpha \ll 1$.

Let us assume that an alternating field of frequency $\nu = \nu_e + \nu_N$ is applied perpendicular to the static field H_0. Then, with a certain probability P proportional to α^2, simultaneous reorientation of the electron and nuclear spins begins. We denote the time of the electron spin-lattice relaxation by T_{1e} and the corresponding time for the nucleus by T_{1N}. Let $1/T_{1N} < P < 1/T_{1e}$. Then obviously after the onset of dynamic equilibrium the ratio of the populations of the Zeeman levels of the nuclei will be the same as that of the electron levels.

A similar effect can be obtained by applying energy at the difference frequency $\nu_e - \nu_N$. In this case, obviously, the electron spin flip will be accompanied by a reorientation of the nuclear spin in the opposite direction.

Abragam and Proctor [38] verified experimentally their proposed method using a LiF single crystal. The experiments were carried out at a frequency $\nu = \nu_e \pm \nu_N$ = 9.4 megacycles. The attained increase in polarization of the Li^6 nuclei was approximately by $\gamma(F^{19}):\gamma(Li^6)$ = = 6.5 times.

The further development of this method is described in [120]. In particular, it became possible to polarize nuclei of aluminum in corundum with chromium impurity [121].

§8.3. Paramagnetic Amplifiers and Generators

Ordinary radio devices which use vacuum tubes, klystrons, magnetrons, etc. convert the kinetic energy of charged particles into energy of a radio frequency electromagnetic field. For many reasons,

the possibility of obtaining radio frequency electromagnetic energy by using the internal energy of atoms and molecules in an excited state is very attractive. This idea was first realized with the aid of molecular beams* [39-41]. Molecular generators have found many important applications because of their exceedingly high frequency stability, but cannot be used extensively for technical purposes owing to their unusually low power and limited range of operating frequencies. Such a device can be used in principle also as an amplifier with exclusively low noise level. However, such an amplifier has not found practical use because of the exceedingly narrow band of the frequencies amplified by it and the impossibility of tuning it.

It has recently become possible to use paramagnetic resonance in solids to produce amplifiers which have equally low noise, but have a much larger band width and can be readily tuned over a wide range. Along with paramagnetic amplifiers, it is possible that paramagnetic generators will also find technical applications, particularly in the range of millimeter and submillimeter wavelengths.

The operating principle of paramagnetic amplifiers and generators consists in the following. We have seen in §1.5 that unlike the optical range the probabilities of spontaneous transitions in the radio frequency band are exceedingly small. We can therefore speak here of the use of induced emission. In addition, whereas in optical light sources each atom radiates independently of the other and the radiation is therefore not coherent, in the radio band the radiation is coherent; there exist definite phase relationships between the induced emission and the radio frequency electromagnetic field that causes it.

We now consider a medium containing a large number of paramagnetic centers, each of which has a definite system of energy levels. Let E_m and $E_n (E_m > E_n)$ be a pair of levels, the interval between which lies

- 421 -

in the radio frequency band.* We denote by N_m and N_n the number of paramagnetic centers per unit volume at the levels E_m and E_n. We assume that the medium has in some manner been placed in such an equilibrium state, by which the number of centers in the upper level is larger than in the lower one. A discussion of different methods of exciting the medium will be presented in the following sections. We assume also that the relaxation mechanisms are of low efficiency and that therefore the transition of the paramagnet into equilibrium state resulting from internal interactions is relatively slow. Let now a weak radio signal of frequency $\nu_{mn} = E_m - E_n/h$ be incident on the medium. Under the influence of this signal, transitions $E_m \longleftrightarrow E_n$ occur, the probabilities of which are the same for both possible directions. But since $N_m > N_n$, the paramagnetic resonant absorption will be negative. In other words, radiation will take place, the power of which, according to (1.7) and (1.11), can be estimated with the formula

$$P_{\text{изл}} = \frac{\pi^2 (N_m - N_n)|< m\,|\,\mu_x\,|\,n >|^2\,\nu_{mn}\,q H_r^2}{h\Delta\nu}.$$

$$(8.21)$$

We note that the quantities $(N_m - N_n)$, $< m\,|\,\mu_x\,|\,n >$ and $\Delta\nu$ cannot, strictly speaking, be regarded as independent of one another. Indeed, the more appreciable the spin S of the paramagnetic centers, the larger will be the matrix elements of the magnetic moment. But an increase in S, that is, in the number of spin levels, brings about a decrease in N_n and N_m. At the same time, the increase in S can bring about an increase in the resonant width $\Delta\nu$. In speaking of the width of a resonance line it is necessary, as we already know (see §5.8), to distinguish between the "inhomogeneous broadening," due to the inhomogeneity of the fields acting on the different paramagnetic centers, and the "homogeneous broadening," which is a result of dipole-dipole and exchange interactions between like particles and due to other

- 422 -

factors. The sources of the inhomogeneous broadening — the spins of
the nuclei belonging to the diamagnetic atoms, the inhomogeneity of the
applied magnetic field, the inhomogeneity of the crystalline fields,
etc. — begin to play a lesser role with increasing concentration of
the paramagnetic centers. An increase in the concentration, and conse-
quently also in $(N_m - N_n)$ is accompanied, starting with a certain
minimum value, by an increase in the width $\Delta\nu$.

The simpliest amplifier, and at the same time the one having many
advantages, can be visualized as consisting of a wave guide filled with
an active paramagnetic substance. The traveling wave will increase in
power as it propagates, so that the power gain, neglecting losses in
the wave guide, turns out to be

$$g_a^i = \exp(\alpha, l),$$
(8.22)

where $\underline{l}$ is the length of the wave guide and $\alpha = AP_{1z1}/P_{pad}$, while A is
the area of the transverse cross-section of the wave guide. The power
of the incident wave is

$$P_{\text{max}} = \frac{1}{8\pi} AcH_r^2.$$
(8.23)

It follows from (8.21) and (8.23) that

$$\alpha = \frac{8\pi^3 (N_m - N_n) |<m|\mu_x|n>|^2 \nu_{mn} q}{ch\,\Delta\nu}.$$
(8.24)

Calculation shows that for real values of $(N_m - N_n)/\Delta\nu$ the length of
the wave guide must be very large, on the order of several meters, in
order to obtain noticeable amplification.

In order to reduce the amplifier dimensions one employs resonant
cavities in lieu of wave guides. If the nonmagnetic losses in the
medium and the losses in the cavity walls are smaller than the power
radiated by the paramagnet, then the energy stored in the cavity will
build up and in this case the induced emission of the paramagnetic
centers will occur not only under the influence of the weak radio

- 423 -

signal, but also under the influence of the radiation previously emitted by the paramagnet. Thus, a cavity filled with an active paramagnetic medium can be regarded as a resonant system with positive feedback.

This system can be characterized by means of a negative figure of merit Q_m, connected with the magnetic "losses," the figure of merit Q_0, determined by the nonmagnetic losses inside the cavity, and by the figure of merit Q_e, due to the external losses resulting from the coupling with the wave guide or with the coaxial line. According to (1.10) we have

$$-\frac{1}{Q_m} = \frac{4P_{\text{изл}}}{\nu(\overline{H_r^2})_V},$$

(8.25)

where $(\overline{H_r^2})_V$ is the value of H_r^2 averaged over the volume of the cavity. Our system will operate like a generator if the self-excitation condition

$$-\frac{1}{Q_m} > \frac{1}{Q_0} + \frac{1}{Q_e}.$$

(8.26)

is satisfied. The power of the generated oscillations will be limited by the saturation effect, for if the populations of the levels E_m and E_n start to become equalized, the increase in the power of the induced emission will stop. The saturation causes the self-oscillating system considered here to be nonlinear and thereby determines the amplitude of the steady-state oscillations in the cavity. The system will operate like an amplifier if

$$\frac{1}{Q_0} + \frac{1}{Q_e} > -\frac{1}{Q_m} > \frac{1}{Q_0}.$$

(8.27)

If we denote again the power gain by g_a^2, we can readily conclude that for a cavity type amplifier the following formula holds true*

$$g_a = \frac{Q_e^{-1} - Q_0^{-1} - Q_m^{-1}}{Q_e^{-1} + Q_0^{-1} + Q_m^{-1}}.$$

(8.28)

The amplifier bandwidth B can be defined as the ratio of the frequency ν to the Q of the apparatus:

$$B = \nu \left(\frac{1}{Q_e} + \frac{1}{Q_m} + \frac{1}{Q_0} \right).$$ (8.29)

Usually Q_0 is sufficiently large so that the last two formulas assume the simpler form

$$g_a = \frac{Q_m - Q_e}{Q_m + Q_e},$$ (8.28a)

$$B = \nu \left(\frac{1}{Q_e} + \frac{1}{Q_m} \right).$$ (8.29a)

Multiplying these expressions we obtain

$$g_a B = \nu \left(\frac{1}{Q_e} - \frac{1}{Q_m} \right).$$ (8.30)

If the gain is large, then Q_e and $|\, Q_m \,|$ should be practically the same. We therefore have

$$g_a B = \frac{2\nu}{Q_e} = \frac{2\nu}{|Q_m|}.$$ (8.31)

We see that the product of the square root of the gain and the band-width is a quantity that remains approximately constant for an amplifier in which the configuration of the resonant cavity and the volume of the paramagnetic medium remain constant. It is seen from (8.28) and (8.29a) that if the gain is large, then the power gain g_a^2 and the band width B are very sensitive to relatively small variations of Q_e and Q_m. However, no matter how large the variations of g_a and B may be, the product of these quantities remains almost constant.

Paramagnetic amplifiers and generators have important advantages. First, the amplifiers are rid of many noise sources that are inherent in electronic devices, and their noise temperature amounts to several degrees Kelvin. Second, paramagnetic generators and amplifiers have no upper frequency limits, since the frequencies of the generated and amplified oscillations are determined by the intervals between the spin energy levels. These intervals can be made sufficiently large

by a suitable choice of the medium and by increasing the static magnetic field within permissible limits.

No practical paramagnetic generators have been created to date. We shall therefore consider henceforth only amplifiers and only of the cavity type.

The main advantage of paramagnetic amplifiers, namely their high sensitivity, is connected with the low level of the intrinsic noise. Many special investigations have been devoted to this problem [43-45]. The low noise level in these devices is insured primarily by the fact that they, unlike devices using vacuum tubes and semiconductors, contain no free charges and therefore are not subject to the shot effect, nor are there any flicker noises, excess noises, etc. The lower noise limit of paramagnetic amplifiers is determined by the spontaneous emission. Noise in paramagnetic amplifiers can be characterized by an effective noise temperature T_n, the magnitude of which is approximately equal to the absolute value of the effective spin temperature T_s. The use of low (helium) temperatures, which is necessary for effective operation of the amplifier (so as to increase the difference in level populations and to lengthen the relaxation time T_1) contributes at the same time to a reduction in the noise levels.

Strandberg [45] calculated the noise figure K_{sh} of a paramagnetic amplifier.* The formula he obtained for a resonator type amplifier has the following form:

$$K_m = \left(\frac{g_a+1}{g_a}\right)^2 \frac{1}{t p_{\nu}(T_0)} \left\{ (1-t)p_{\nu}(T_i) + t p_{\nu}(T_a) + \right.$$
$$+ \frac{Q_e}{Q_0} \left[p_{\nu}(T_c) - p_{\nu}(T_m) \right] - \left(\frac{g_a-1}{g_a+1}\right) p_{\nu}(T_m) +$$
$$\left. + (g_a+1)^{-2} p_{\nu}(T_0) \right\}. \tag{8.32}$$

The values of many of the quantities contained in this formula can be understood by referring to the schematic diagram of the amplifier (Fig. 8.5). T_a, T_t, and T_c denote the temperatures of the antenna
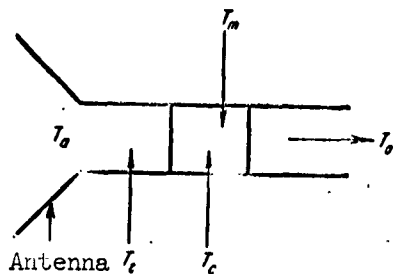
Fig. 8.5. Temperature parameters determining the noise figure of a paramagnetic amplifier.

(signal sources), transmission line, and the paramagnetic medium, respectively. T_0 is the temperature at the output of the cavity (load temperature), $\underline{t}$ is the power loss factor in the transmission line, that is, the ratio of the output power to the power at the input of the transmission line. The parameter T_m has the dimension of temperature and can be determined from the following formula:

$$\frac{N_m - N_n}{N_m + N_n} = \text{th}\left(\frac{h\nu_{mn}}{2kT_m}\right).$$

(8.33)

If η is the number of spin levels of one particle, then

$$N_m + N_n \approx \frac{2N_0}{\eta}.$$

(8.34)

From (8.33), (8.34), (8.21) and (8.25) it follows that

$$T_m = -\frac{h\nu_{mn}}{2k}\left[\text{Arth}\ \frac{\eta h \Delta\nu}{8\pi^3 q N_0 Q_m |(m|\mu_x|n)|^2}\right]^{-1}.$$

(8.35)

In accordance with Planck's formula, the mean oscillator energy at temperature T is

$$p_\nu(T) = \frac{h\nu}{\exp(h\nu/kT) - 1}.$$

(8.36)

Usually $h\nu \ll kT$ and therefore $p_\nu(T) = kT$. If we assume furthermore, first, that the losses in the transmission line are small and $t \approx 1$, and second that the gain is appreciable $g_a \gg 1$, then (8.32) assumes the simpler form

$$K_m = 1 - \frac{T_m}{T_a}\left(1 + \frac{Q_e}{Q_s}\right) + \frac{T_c}{T_a}\frac{Q_e}{Q_s},$$

(8.37)

and the noise temperature will accordingly be

$$T_n = (K_m - 1)T_a = -T_m\left(1 + \frac{Q_e}{Q_s}\right) + T_c\frac{Q_e}{Q_s} \ldots$$

(8.37a)

It is easy to see that by choosing the amplifier parameters we can

make the noise K_{sh} close to unity and $T_n \approx T_m$. An additional noise source is produced if the excitation of the working medium is carried out by the saturation method (see §8.5). Weber [46] has shown that the corrections to formula (8.32) brought about by this fact have no practical significance.

The most important problem arising in the construction of a paramagnetic amplifier is the choice of the working medium and the determination of the methods for its excitation. It is obvious that there is a great variety in the methods of exciting paramagnetic centers in the case of particles with effective spin $S' > 1/2$, that is, in the case when the number of spin levels exceeds two. We shall therefore consider in the following sections two- and three-level amplifiers separately.

§8.4. Two-level Paramagnetic Amplifier

All the methods proposed for the excitation of paramagnetic centers with effective spin $S' = 1/2$ consist in inverting the populations of the Zeeman energy sublevels. In the equilibrium state, the ratio of the populations of the lower [1] and upper [2] spin levels is

$$\frac{N_1}{N_2} = \exp\left(\frac{g'\beta H_0}{kT}\right) = \exp\left(\frac{h\nu_0}{kT}\right).$$
(8.38)

The problem consists of inverting this ratio for a more or less prolonged time interval. Let us stop to discuss three possible methods of inverting the populations of the spin levels.

a) Nonadiabatic change in direction of the static magnetic field

The simplest method of accomplishing the indicated purpose is by rapid (nonadiabatic) change in the sign of the applied static magnetic field H_0. The ratio N_1/N_2 is then reversed, the most populated lower level becomes the upper level, and vice versa. The reversal in the field H_0 must be so fast as to satisfy the nonadiabaticity condition

[47], which in our case has the form

$$\frac{1}{H_0}\frac{dH_0}{dt} > 2\pi \cdot \nu_0 . \tag{8.39}$$

The lower the precession frequency ν_0, that is, the smaller the field H_0, the easier it is to satisfy this condition. However, the field H_0 cannot be made as small as desired, for it must appreciably exceed the width of the resonance line: $H_{min} \gg \Delta H$.

It is therefore most advantageous to proceed in the following fashion: Reduce the field H_0 adiabatically and slowly to a value H_{min}, and then carry out nonadiabatically and rapidly the reversal $H_{min} \rightarrow$ $\rightarrow - H_{min}$ followed by an adiabatic and slow reduction of the field to $-H_0$. It is obvious that this entire procedure should be performed within a time much shorter than T_1. By way of an example let us assume that $\Delta H \approx 0.1$ oersted, $H_{min} \approx 0.5$ oersted; then, in order to change the field H_0 by 1 oersted, it is necessary in accord with (8.39) to have a time interval of about $5 \cdot 10^{-8}$ sec. Field changes of this type can be produced presently by modern pulse techniques. The method described by us has been used for the time being only in nuclear paramagnetism [48]. However, it has a great advantage over other methods of excitation of paramagnetic centers in that it does not need the application of an additional radio frequency field. One can therefore expect that nonadiabatic change of magnetic field direction will be used for the construction of microwave generators of very high frequencies.

b) Adiabatically rapid passage

Bloch [49] has shown that the spin level populations can be inverted by rapid but adiabatic passage through resonance, by changing the frequency of the alternating field or the intensity of the static field. Without dwelling on the calculations which lead to this result by a solution of (5.1) (see, for example, [50,51]), let us illustrate

- 429 -

this method with the classical model.

The behavior of a dipole in a magnetic field H is best investigated by changing over to a coordinate system rotating with a certain angular velocity ω. In the rotating coordinate system the motion of the dipole will be determined by the same equations of motion as in the inertial coordinate system, provided we assume that the dipole is acted upon not by the field H but by the effective field [52]

$$H_{\text{эфф}} = H - \frac{\omega}{\gamma}, \quad \gamma = \frac{g'\beta}{\hbar}. \qquad (8.40)$$

The magnetic moment of the dipole will precess in this case with circular frequency $\omega_{\text{eff}} = \gamma H_{\text{eff}}$. We now put, as usual. $\vec{H} = \vec{H}_0 + \vec{H}_1$, where $\vec{H}_0$ is the static field and $\vec{H}_1$ is a small field rotating uniformly with
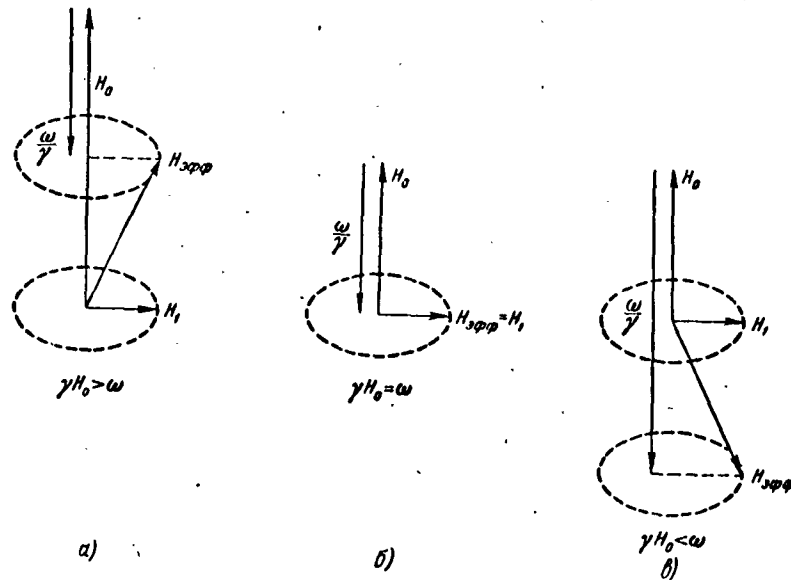

a)   б)   в)

Fig. 8.6. Effective magnetic field in a coordinate system rotating with angular velocity ω about the field H_0.

frequency ω in a plane perpendicular to $\vec{H}_0$. Figure 8.6 shows the three possible cases:

$$\gamma H_0 > \omega, \quad \gamma H_0 = \omega \quad \text{and} \quad \gamma H_0 < \omega.$$

We see that if the change in H_{eff} is adiabatically slow, then the sign of the magnetization vector reverses after passing through resonance,

- 430 -

and consequently the distribution of the particles over the spin levels is reversed: $N_2 > N_1$. The adiabatic change in H_{eff} denotes that the relative reduction in H_{eff} during the time $1/\omega_{eff}$ should be small. The smallest value of H_{eff} is H_1. Therefore the adiabaticity condition has in our case the form

$$(\gamma H_1)^{-1} \ll \Delta t; \qquad (8.41)$$

if we denote by Δt the time necessary to change the field H_0 by an amount equal to the half width ΔH of the resonance line. At the same time, passage through resonance should be rapid, for it is necessary to satisfy also the condition

$$\Delta t \ll T_1. \qquad (8.42)$$

The method of adiabatically rapid passage has the following advantages: 1) there is no need for good stabilization of the frequency ν of the field H_1; 2) the time of passage Δt can change over a wide range.

c) 180° pulse

Let us assume that the paramagnet is under resonance conditions. If we change over to a coordinate system rotating with resonant frequency, then $H_{eff} = H_1$. Consequently, the magnetic dipole is acted upon only by the constant magnetic field H_1 (Fig. 8.6b). The magnetization vector will precess about H_1 with angular frequency $\omega_1 = \gamma H_1$. If we use in place of a continuously acting alternating magnetic field only a pulse of duration

$$t_\pi = \frac{\pi}{\gamma H_1}, \qquad (8.43)$$

then the direction of the magnetization vector will change by 180° and the spin levels will be inverted. The inversion, however, will not be complete if, first, H_1 is not appreciably larger than the resonance width ΔH, and second if the condition (8.43) is not satisfied with great accuracy. It goes without saying that the duration of the pulse

- 431 -

t_π should be much shorter than the relaxation time T_1. The "180°" pulse" method is more convenient than the "rapid adiabatic passage" in that it consumes less alternating magnetic field power and a shorter time interval for the inversion of the spin levels [50].

The operation of a two-level amplifier can be visualized in the following fashion. At first the working medium is in the equilibrium state. Then the spin levels are inverted for a time t_1 by one of the methods considered above. Following this, for a time $t_2 \ll T_1$, the amplification process occurs. Then the thermal equilibrium is restored for a time t_3. We see that the two-level amplifier is an intermittently acting device. The time intervals t_2 of active operation are divided by "dead" intervals $t_3 + t_1$. If the thermal equilibrium occurs in a medium that is left alone, then the time t_3 will be very large, on the order of T_1. We propose here two methods for accelerating the transition to the equilibrium state.

The first method consists of illuminating the paramagnet. This method is suitable if the working medium is a doped semiconductor, such as silicon doped with elements of group V (P, As, Sb) or lithium. In these semiconductors, at heating temperatures and at concentrations $N_0 \approx 10^{17} - 10^{18}$ cm^{-3}, the time T_1 runs into many seconds (see §6.2). Under the influence of the illumination, the relaxation time is shortened to several microseconds. If we take account of the fact that the time t_1 amounts to in the worst case several milliseconds, we see that the "dead" time can be made negligibly small, and the amplifier operates almost continuously.

The second method of shortening t_3 consists in the following. We use as the working medium crystals containing paramagnetic particles of two types. Let the relaxation time T_1 of the particles of one type (A) be several orders of magnitude higher than that of particles of

the second type (B). These two sorts of particles, of course, have different spin level systems. The active paramagnetic centers of the amplifier are the particles A. After the end of the period t_2, the static field H_0 is changed such as to make the interval between the spin levels of particles A equal to the interval between any pair of spin levels of the particles B. Then, owing to the spin interaction, the energy will be transferred from particles A to particles B, and then very rapidly to the lattice. This type of decrease in relaxation time was experimentally investigated in several cases [53].

Let us determine the condition for the amplification, assuming that relaxation losses can be neglected. We denote by $(\overline{H_1^2})_S$ the square of the alternating magnetic field intensity averaged over the volume of the paramagnetic specimen. We assume that $| <m \, | \, \mu_x \, | \, n> | = \beta$, $N_m -$ $- N_n = N_0 h\nu / 2kT$. Then from (8.27), (8.25) and (8.21) it follows that amplification will take place if

$$N_0 > \frac{kT\Delta\nu}{2\pi^2 q\beta^2\nu Q_0} \frac{(\overline{H_1^2})_V}{(\overline{H_1^2})_S} .$$
(8.44)

The first attempt at constructing a paramagnetic amplifier was carried out using silicon doped with phosphorus under the following experimental conditions [54]: ν = 9000 megacycles, Q_0 = 10,000, T = 2°K, $\Delta\nu \approx 4 \cdot 10^6$, $(\overline{H_1^2})_S \approx (\overline{H_1^2})_V$. After substitution of these values, condition (8.44) assumes the form $N_0 > 10^{17}$ cm^{-3}. In the experiments described this condition was not fulfilled and therefore the sought effect was not observed. Positive results were obtained by Feher et al. [55], who replaced the natural silicon by isotopically pure $(99.88 \pm 0.08\%)$Si^{28}, as a result of which the paramagnetic resonance line was narrowed down from 2.7 to 0.22 oersted, since the inhomogeneous broadening due to the hyperfine interaction of the electron shell of the phosphorus with the Si^{29} nuclei disappeared. The

experiments were set up under the following conditions: $N_0 = 4 \cdot 10^{16}$ cm^{-3}, $T_1 \approx 1$ min at temperature $1.2^\circ K$, $\nu = 9000$ megacycles, $Q_0 \approx 20{,}000$. Excitation of paramagnetic centers was by the method of rapid adiabatic passage.

Working media successfully used for two-level amplifiers were quartz and magnesium oxide, the paramagnetic centers in which were produced by strong neutron bombardment [56]. The level inversion was by the method of adiabatic passage. The frequency of the amplified signal was $\nu = 9000$ megacycles, the Q of the loaded cavity was $Q \approx$ ≈ 6000, and the temperature was $4.2^\circ K$. In the experiments with quartz, the number of paramagnetic centers was $N_0 \approx 10^{18}$. The inverted state lasted about 2 milliseconds. If the signal is amplified 1.2 milliseconds after the level inversion, then $g_\alpha B \approx 5 \cdot 10^6$ sec^{-1} with the gain changing from 8 to 21 db. In experiments with MgO, the number was $N_0 \approx 10^{17}$. The inverted state lasted approximately 2.5 milliseconds. A gain of 20 db was observed 125 microseconds after the level inversion.

In conclusion, we note that continuously operating two-level amplifier designs were proposed [57], based on the use of mechanically rotating devices.

§8.5. Three-level Paramagnetic Amplifier

1. Operating principle

If the number of spin levels of paramagnetic centers exceeds two, then the excitation of the working medium can be effected by saturating the electron resonance. Let us assume that the particles have three spin levels (Fig. 8.7). We assume also that saturation has been produced with the aid of an oscillating field of frequency ν_{31} and of sufficient power, so that the populations of levels E_1 and E_3 have become equalized: $N_1 \approx N_3$. Then, obviously, either $N_2 < N_3$ and an ampli-
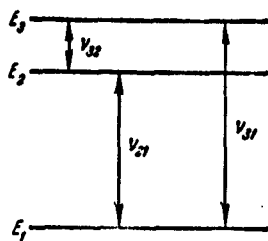
Fig. 8.7. Spin levels of para-magnetic centers of the working medium of a three-level amplifier.

fier can be produced for signals of frequency ν_{32}, or else $N_2 > N_1$ and signals of frequency ν_{21} can be amplified. The idea of the possibility of producing a molecular generator using this excitation method was first stated by Basov and Prokhorov [58]. The possibilities of constructing a three-level para-magnetic amplifier excited by the saturation method were considered by Bloembergen [59]. The advantages of an amplifier of this type are the continuous operation and the possibility of using media with relatively short relaxation times. These times should be sufficiently long to permit practical saturation of the paramagnetic resonance.

Let us find the conditions for the excitation of a three-level amplifier. Let A_{ik} be the per second probability for the transition of a particle from the level E_i to the level E_k under the influence of the lattice vibrations (see §5.3), and let p_{ik} be the probability of transition between the same levels under the influence of the radio frequency field, calculated in accordance with (1.3). If $h\nu_{ik} \ll kT_c$, then the populations of the individual levels will obey the equations

$$N_1 + N_2 + N_3 = N_0,$$

$$
\begin{aligned}
\frac{dN_2}{dt} &= A_{13}\left(N_1 - N_3 - \frac{N_3}{3}\frac{h\nu_{31}}{kT_c}\right) + \\
&\quad + A_{23}\left(N_3 - N_2 + \frac{N}{3}\frac{h\nu_{32}}{kT_c}\right) + p_{31}(N_1 - N_3) + p_{32}(N_3 - N_2), \\
\frac{dN_3}{dt} &= A_{23}\left(N_3 - N_2 + \frac{N}{3}\frac{h\nu_{32}}{kT_c}\right) + \\
&\quad + A_{31}\left(N_1 - N_3 - \frac{N}{3}\frac{h\nu_{31}}{kT_c}\right) + p_{32}(N_3 - N_2), \\
\frac{dN_1}{dt} &= A_{13}\left(N_3 - N_1 + \frac{N}{3}\frac{h\nu_{31}}{kT_c}\right) + \\
&\quad + A_{21}\left(N_2 - N_1 + \frac{N}{3}\frac{h\nu_{21}}{kT_c}\right) - p_{31}(N_1 - N_3).
\end{aligned}
$$

(8.45)

If it is assumed that $p_{31} \gg p_{32}$ and $p_{31} \gg A_{ik}$, we obtain

$$N_1 - N_3 = N_3 - N_2 = \frac{hN_0}{3kT_c}\frac{A_{21}\nu_{21} - A_{32}\nu_{32}}{A_{21} + A_{32}}.$$

(8.46)

This quantity will be positive, and consequently negative absorption

will take place at a frequency ν_{32} if

$$A_{31}\nu_{31} > A_{32}\nu_{32}.$$ (8.47)

If the opposite inequality holds true, then the negative absorption will take place at frequency ν_{21}. Substituting (8.46) in (8.21) and using (8.25) and (8.27) we obtain the following condition for the presence of amplification:

$$\frac{4\pi^2 q N_0 |\langle 2|\mu_x|3\rangle|^2}{3kT\Delta\nu}\frac{\overline{(H)}_S}{\overline{(H)}_V}\frac{A_{31}\nu_{31} - A_{32}\nu_{32}}{A_{13} + A_{23}} > \frac{1}{Q_\bullet}.$$ (8.48)

If the number of spin levels exceeds three, analogous calculations can be carried out, which, however, become quite cumbersome.

In the derivation of relation (8.47) we disregarded cross-correlation. Equation (8.45) would have to be replaced by equation (5.119), and we would then obtain in lieu of (8.47)

$$A_{31}\nu_{31} > (A_{32} + w + \frac{1}{3}\sum_i w_{ij})\nu_{32}.$$ (8.47a)

Since the probabilities of the cross-correlation transitions increase rapidly with increasing paramagnetic center concentration, it becomes understandable why appreciable increase in the center concentration causes the amplifier to stop operating.

The linear amplifier theory which we have presented can be regarded as correct if the "illumination" power of frequency ν_{31} is sufficient to overcome the spin-lattice relaxation and produce saturation, but is still not large enough to exceed the spin-spin interactions and bring about coherent ordered spin systems. In other words, the average time interval necessary for the spin reorientation under the influence of the saturating rate of frequency field must exceed the spin-spin relaxation time. If this condition is not satisfied, nonlinear effects arise [60] which result in a paramagnetic amplifier of the parametric type. Linearity can be readily maintained if the spin-lattice inter-

actions are much weaker than the spin-spin ones. The latter condition
is usually satisfied in most media at low temperatures and not too low
paramagnetic center concentrations.

It is interesting to note that the temperature T_m, which deter-
mines the minimum value of the noise figure, may turn out to be much
lower when the amplifier is excited by the saturation method than the
temperature T_c of the working medium. Indeed, if we assume $kT_m \gg h\nu_{32}$,
then it follows from (8.33), (8.34) and (8.46) that

$$T_m = T_c \frac{A_{12} + A_{23}}{\frac{\nu_{21}}{\nu_{32}} A_{31} - A_{23}}. \qquad (8.49)$$

If we can neglect A_{23} in this expression, we obtain $T_m \ll T_c$ by suitable
choice of the energy intervals.

2. Choice of medium

The first and principal problem that must be solved in the pro-
duction of a paramagnetic amplifier is the choice of a medium with
suitable properties. The working medium of a three-level amplifier
must satisfy the following main requirements: a) the number of spin
levels of the paramagnetic particle should exceed 2, and consequently
particles with effective spin $S' = 1/2$ are eliminated; b) the split-
tings of the spin levels in the crystal field in the absence of an
external magnetic field (initial splittings) should be of order $h\nu_{31}$,
in order to attain saturation readily at the frequency of the auxili-
ary radiation; if the initial splittings are small, then the only
magnetic dipole transitions that differ noticeably from zero are
those between neighboring spin levels; c) the probabilities of the
spin-lattice relaxation transitions should be sufficiently small so
that saturation sets in at attainable elimination powers; d) the re-
lation between the probabilities of the relaxation transitions should
satisfy for different spin level pairs the condition (8.47); e)

the number of magnetically nonequivalent ions per elementary crystal cell should be as small as possible; f) absence of hyperfine structure of the energy levels is the most favorable; g) the width of the individual spin levels due to the spin-spin interactions should be sufficiently small so that, first, the spin levels do not overlap and second, that saturation can be reached sufficiently readily; it is therefore necessary that the chosen medium be magnetically diluted in an isomorphous diamagnetic substance; h) finally, there are requirements that do not concern the magnetic properties of the medium: chemical stability, low dielectric losses, sufficient mechanical strength.

It must be noted that of great importance to the operation of a paramagnetic amplifier is the longitudinal relaxation mechanism. If the latter is defined as the rate of energy transfer from the system of effective lattice oscillators to the helium thermostat, then the resonance saturation due to transitions between levels E_1 and E_3 may influence the populations of other levels (see §5.4). Unfortunately, the available experimental data are incomplete and scanty and consequently the question of the nature of paramagnetic relaxation in different substances is still debatable. Bloembergen [61] states that the very existence of three-level amplifiers at temperatures below $4.2°K$ indicates that longitudinal relaxation in the employed paramagnetic crystals is not determined by the coupling between the effective lattice oscillators and the helium thermostat. However, he admits the possibility that the bottleneck of the energy transfer from the spin system to the lattice are the phonon-phonon interactions. Strandberg [62, 63], in an analysis of the results of experiments with three-level amplifiers, reached the conclusion that the phonon-phonon processes play an appreciable role. On the basis of subsequent investi-

gations Bloembergen [122] reached the conclusion that all the effects observed by Strandberg could be attributed to cross-correlation.

The only ones among the various paramagnets capable of satisfying the foregoing requirements are apparently crystals containing ions of the intermediate groups. The most investigated among these are the compounds of the iron group of elements. We know that in most crystals the iron group ions have a surrounding of octahedral symmetry; these are the compounds we shall consider primarily.

In this case ions with electron configuration d^1, d^2, d^6, d^7 have very short spin-lattice relaxation times (see §5.3). Therefore, naturally, we eliminate from consideration the compounds of Ti^{3+}, V^{4+}, V^{3+}, Cr^{2+} and Co^{2+}. The ions that remain suitable from this point of view are V^{2+}, Cr^{3+}, Cr^{2+}, Mn^{3+}, Mn^{2+}, Fe^{3+}, Ni^{2+} and Cu^{2+}. Among these ions, copper has a spin $S = 1/2$, so that its compounds are not suitable for three-level amplifiers; however, the presence of a hyperfine structure in the paramagnetic resonance line of copper apparently makes it possible to use its salts to produce an amplifier at frequencies $10^8 - 10^9$ cps [64]. Further, the ions of vanadium and manganese are little suitable because they have a large nuclear spin $(V^{51} : I = 7/2, Mn^{55} : I = 5/2)$. We are thus left for our primary choice ions of divalent and trivalent chromium, trivalent iron, and divalent nickel.

We have seen in §3.9 that it is necessary to distinguish between paramagnetic complexes with a small fraction of covalence and those with strong covalent bonds. The only compounds with strong covalent bonds suitable for our purposes are those containing Cr^{3+}; atoms with configuration d_ε^1 and d_ε^5 will have an effective spin $S = 1/2$. Atoms with configuration d_ε^2 and d_ε^4 have $S = 1$, but their initial spin level splittings are apparently too large. The atom Cr^{3+} has a d_ε^3 con-

figuration, and is in an effective S state with spin S = 3/2. It is analagous to the Fe^{3+} and Mn^{2+} ions in compounds with weak bond.

Let us dwell in somewhat greater detail on different compounds of the iron group ions selected by us.

Cr^{2+}. S = 2. Salts of divalent chromium are chemically less stable than all others. In addition, this ion in a cubic field has a double lower orbital level; the orbital degeneracy is lifted by a weak field of lower symmetry, and consequently we can expect the initial splittings of the spin levels in the crystalline field to be too large. This is confirmed by the only substance investigated to date, $CrSO_4 \cdot 5H_2O$, for which the spin Hamiltonian constant is D = 2.24 cm^{-1}, which would require the use of a wave four millimeters long for illumination.

Cr^{3+}. S = 3/2. Compounds of this ion have been well investigated; they have relatively long spin-lattice relaxation times; the zero level splittings of many lie in a convenient region of standard microwave frequencies. From among the compounds of this ion, the hexacyanide of chromium and corundum doped with Cr^{3+} are already used as working media for amplifiers.

Fe^{3+}. S = 5/2. The free ion is in the S state. The relaxation times are of the same order as in Cr^{3+}. The initial splittings of the spin levels are large in some cases. Fe^{3+} compounds may be of interest for the construction of an amplifier without the use of a constant magnetic field [65, 42] or with the use of weak magnetic fields, for the Fe^{3+} ions have three spin levels even in the absence of a magnetic field.

Ni^{2+}. S = 1. At first glance Ni^{2+} is the most suitable for use in working medium compounds, in view of the fact that this ion has only three spin levels. However, an attempt at creating an amplifier using

nickel fluorosilicate [68] was not successful because of the excessively short relaxation time T_1 and owing to internal stresses in the crystal, which have led to an excessive broadening of the paramagnetic resonance lines. There are many known paramagnetic salts of divalent nickel the only investigated magnetic property of which is the static susceptibility. It is possible that some of them, unlike nickel fluorosilicate, turn out to be suitable. We note that if the symmetry of the crystalline field surrounding the Ni^{2+} ion is so low that the spin Hamiltonian contains terms of the type $E(S_x^2 - S_y^2)$, then the spin degeneracy will be lifted even in the absence of an external magnetic field. Such compounds of Ni^{2+} may possibly turn out to be suitable for an amplifier without the use of a constant magnetic field [65].

So far we have considered octahedral paramagnetic complexes. An analysis of the structure of the energy levels of the iron group ions in a tetrahedral surrounding shows that for some reason or another (short spin-lattice relaxation time, large hyperfine structure, etc.) the only promising compounds of this type can be only the salts of divalent iron, which of course must be diluted by suitable diamagnets.

From among the group of rare earth elements, only compounds of Gd^{3+} and Eu^{2+} ions in the S state can be used, and in the remaining ions of this group the spin-lattice relaxation times are excessively short. Eu^{2+} is less suitable because of its appreciable hyperfine structure. The spin of Gd^{3+} is $S = 7/2$ and in the absence of an external magnetic field there are four spin levels, making compounds of Gd^{3+} promising for the construction of an amplifier without a magnetic field.

The magnetic complexes of compounds of the palladium and platinum group elements are characterized by a strong covalent bond. Therefore, in accordance with the considerations advanced with respect to com-

pounds of the iron group, the only complexes suitable for our purpose can be those with electron configuration d_ε^3, that is, complexes containing trivalent molybdenum, trivalent tungsten, and pentavalent ruthenium. Complexes containing Re^{4+} are not suitable since the nuclear spin of Re^{185} or Re^{187} is 5/2.

Most elements of the actinide group are radioactive. The uranium compounds have been little investigated. It is possible that some of the compounds of trivalent and tetravalent uranium will be found suitable.

Concluding the review of the substances that offer promise as being useful in three-level amplifiers, we note in addition the cubic lattice crystals of the type MgO, CaO, CaF_2, in which ions of Cr^{3+}, Fe^{3+}, Gd^{3+}, Mn^{2+}, etc., are introduced. The paramagnetic resonance absorption lines observed in these cases are very narrow (in Cr^{3+}, for example, the line width is merely 3 oersted). It is possible that these substances will find application in amplifiers at relatively low frequencies.

3. Choice of orientation of constant magnetic field

The orientation of the constant magnetic field relative to the crystal axes determines important characteristics of the working medium of a three-level amplifier, such as the position of the spin energy levels, the probabilities of transitions between them under the influence of the alternating magnetic field, and the probabilities of transitions under the influence of the lattice vibrations. The dependence of the probabilities of the relaxation transitions between the different spin levels on the constant magnetic field has hardly been investigated. The positions of the spin levels and the probabilities of the magnetic dipole transitions between them can, on the other hand, be calculated if we know the parameters of the spin

Hamiltonian (see Chapter III).

In choosing the direction of the magnetic field it is important to have not only suitable energy intervals, which give the required values of the frequencies v_{32} (or v_{21}) and v_{31}; it is also important to have the probabilities of the magnetic dipole transitions, p_{32} (or p_{21}) and p_{31} (1.3), sufficiently large. If p_{32} (or p_{21}) is small, then the gain will be small; if p_{31} is small, a large elimination power is necessary to obtain the saturation effect. Therefore, as already mentioned, the spin level splittings due to the application of an external static magnetic field should not exceed greatly the initial crystal splittings. If the external magnetic field is very large, then the spin levels will be practically equidistant, and transitions under the influence of the radio frequency field will be possible in practice only between neighboring levels, and consequently illumination will not be feasible.

In the case when $S \leq 3/2$ the spin Hamiltonian has a very simple form, since the part in it $\hat{H}_{kr}$ representing the action of the crystalline field contains only quadratic terms in the components of the spin vector $\vec{\hat{S}}$. If the field has trigonal or a tetragonal symmetry, then $\hat{H}_{kr} = D[\vec{\hat{S}}_z^2 - 1/3S(S + 1)]$; the symmetry axis coincides here with the Z direction. If the static magnetic field $\vec{H}_0 \parallel Z$, then the spin Hamiltonian represents a diagonal matrix and consequently the selection rule $\Delta M = \pm 1$ holds true for the magnetic dipole transitions. The possibilities for choosing suitable transitions for obtaining the required values of v_{32} (or v_{21}) and v_{31} are clear from Fig. 1.3. If the spin Hamiltonian contains also a rhombic term $E(\hat{S}_x^2 - \hat{S}_y^2) \equiv$ $\equiv 1/2E(\hat{S}_+^2 + \hat{S}_-^2)$ then the latter, obviously, causes an overlap of the states in which the quantum numbers of the spin projection on the Z axis differ by ± 2, that is, states with $M = -1$, $M = +1$ in the case

S = 1, states with M = -3/2, M = 1/2, M = -1/2, M = 3/2 in the case with S = 3/2. The number of level pairs between which transitions are allowed now increases.

We note that in the case of an even number of electrons, a rhombic field lifts the spin degeneracy completely, so that for ions with S = 1 we have three definite spin levels even in the absence of a magnetic field. As indicated, this opens up the possibility of using compounds of these ions as working media for the amplifier without the use of a magnetic field.

Assume now that the field $\vec{H}_0$ is perpendicular to the trigonal or tetragonal axis of the crystal. If as before we choose $\vec{H}_0 \parallel Z$, then the term $[\hat{S}_z^2 - 1/3 S(S+1)]$ becomes $1/2[\hat{S}_+^2 + \hat{S}_-^2]$ and causes overlapping of states with $\Delta M = \pm 2$ even without a rhombic field.

In the case S = 5/2 (and S = 7/2) the form of the spin Hamiltonian becomes appreciably more complicated, for it represents a fourth (sixth) degree polynomial in the components of the spin vector S. The position of the spin levels and the selection rules will depend essentially on the relationships between the values of the different spin Hamiltonian parameters.

Under certain orientations of the constant magnetic field, a symmetrical energy splitting is possible, making it possible to cause illumination at a single frequency to produce transitions between two pairs of spin levels. The use of such a symmetrical version increases the gain by several times.

We know that in the presence of initial crystalline splittings of the spin levels the resonant absorption is possible not only when the static and alternating magnetic fields are mutually perpendicular. To find the optimal conditions of amplifier operation it is necessary also to take into account the dependence of the absorbed power of

radio frequency field on its orientation relative to the constant magnetic field and to the crystal axes.

In conclusion we note that amplifiers operating without an externally applied magnetic field apparently assume great significance [42]. Such amplifiers would have many advantages: 1) no electromagnet is necessary; the difficulties involved in attaining high homogeneity of the magnetic field, current stabilization, and large working space are eliminated; 2) no single crystals are necessary; 3) all the ions of the crystal cell are used; 4) superconductors can be used in the construction of the microwave circuit; 5) the dimensions of the Dewar are not limited to the gap between poles; 6) there is no broadening due to the scatter of the angles between the crystal axes and the magnetic field.

TABLE 8.1

Initial Splittings of Spin Levels in Substances Containing Fe^{3+}, Ni^{2+}, and Gd^{3+}

1) Ион	2) Вещество	3) Начальные расщепления, см$^{-1}$		
		Δ_1	Δ_2	Δ_3
Fe³⁺	$RbFe(SO_4)_2 \cdot 12H_2O$	0,043	0,002	
	$NH_4Fe(SO_4)_2 \cdot 12H_2O$	0,085	0,014	
	$KFe(SO_4)_2 \cdot 12H_2O$	0,043	0,025	
	$Fe[(CH_3CO)_3CH]_3$	0,28	0,14	
	$BaTiO_3$	0,332	0,166	
	$SrTiO_3$	0,023	0,044	
	$(NH_2CH_3)Fe(SO_4)_2 \cdot 12H_2O$	0,134	0,48	
	Al_2O_3	0,38	0,63	
	$Al_2Be_3(SiO_3)_6$	0,05	0,06	
	$MgWO_4$	2,05	2,52	
Ni²⁺	$(NH_4)_2Ni(SO_4)_2 \cdot 6H_2O$	‾1,5	0,97	
	$(NH_4)_2Ni(SeO_4)_2 \cdot 6H_2O$	0,91	1,64	
	$Tl_2Ni(SeO_4)_2 \cdot 6H_2O$	2,5	0,2	
	$K_2Ni(SO_4)_2 \cdot 6H_2O$	2,95	1,1	
	$NiSO_4 \cdot 7H_2O$	2,0	3,0	
Gd³⁺	$Mg_3Gd_2(NO_3)_{12} \cdot 24H_2O$	0,0766	0,0479	0,0246
	$GdCl_3 \cdot 7H_2O$	0,0827	0,0504	0,0243
	$GdCl_3$	0,0087	0,00077	0,00065
	$Gd(C_2H_5SO_4)_3 \cdot 9H_2O$	0,131	0,085	0,0466
	$Gd_2(SO_4)_3 \cdot 8H_2O$	0,291	0,055	0,908

1) Ion; 2) substance; 3) initial splittings, cm^{-1}.

Table 8.1 gives the initial splittings of the spin levels of

paramagnetic centers for substances that can be used in amplifiers without field as of now.

4. Amplifier with gadolinium ethyl sulfate

The first three-level paramagnetic amplifier [66, 67] was constructed with diamagnetic lanthanum ethyl sulfate containing 0.5% gadolinium and 0.2% cerium. The role of the active paramagnetic centers was played by the Gd^{3+} ions. A static magnetic field of intensity 1800 oersted was placed perpendicular to the symmetry axis of the crystal. Of the eight spin levels of Gd^{3+}, which we shall designate in accordance with the value of the magnetic quantum number in a strong magnetic field, the following three neighboring ones were used: M = = -5/2, -3/2 and -1/2. The illumination frequency was $v(-1/2, -5/2)$ = = 11,500 megacycles, the signal frequency was $v(-3/2, -5/2)$ = 6000 megacycles, the magnetic field of signal and the magnetic field of the illumination were perpendicular and parallel to the static field H_0, respectively. The frequencies $v(-1/2, -3/2)$ and $v(-3/2, -5/2)$ were so close to each other that in order to invert the populations of the levels M = -5/2 and M = -3/2 it is necessary to have, in accordance with (8.43) $A(-1/2, -3/2) >> A(-3/2, -5/2)$. This requirement can be readily satisfied by using a small admixture of Ce. The described experimental conditions are such that the interval between the spin levels of Ce^{3+} is precisely equal to the interval (-1/2, -3/2) of the Id^{3+} ion. The spin-lattice relaxation time of Id^{3+} is about 10^{-4} sec at helium temperatures, and the relaxation time of Ge^{3+} is several orders of magnitude shorter. Because of the resonant spin interaction of gadolinium and cerium, the spin levels of Ce^{3+} are rapidly excited as a result of the transitions M = -1/2 → M = -3/2 of the Gd^{3+} ion. The excited Ce^{3+} ions transfer in turn their energy to the lattice vibrations very rapidly.

The illumination was effected by means of a radio-frequency field of 88 mW power. The resonant cavity had a $Q_0 \approx 6000$. The gain reached an order of 20 db at a band width of about 10^5 cps. The effective noise temperature of the entire installation, including the circulator and the control unit, was approximately $150°K$, but it can be greatly reduced in many ways.

Owing to the chemical instability of gadolinium ethyl sulfate, it is hardly likely that it will assume a practical significance as a working medium for paramagnetic amplifiers.

5. Amplifier with chromium hexacyanide

The exceedingly long longitudinal relaxation time, on the order of 0.2 sec at $1.25°K$, has attracted attention to chromium hexacyanide as a working medium for a paramagnetic amplifier [68]. The substance used in practice was the diamagnetic salt $K_3Co(CN)_6$, which contained 0.5% of chromium. In the complex $Cr(CN)_6$ there is a very strong covalent bond (see §3.8), owing to which the electron configuration $d\varepsilon^3$ gives a zero resultant orbital momentum and a resultant spin $S = 3/2$. The upper three of the four spin levels were used: $M = 3/2$, $1/2$, $-1/2$, the signal frequency was $\nu(3/2, 1/2) = 2800$ megacycles, the illumination frequency was $\nu(3/2, -1/2)$ megacycles. In this case there was no need to take any measures to satisfy the condition (8.47), since $\nu(1/2, -1/2) \gg \nu(3/2, 1/2)$. The central part of the amplifier, a resonant cavity, had to be specially constructed in order to be able to excite simultaneously oscillations at both the signal and illumination frequencies.

Figure 8.8 shows a block diagram of the installation, with the aid of which a gain of 37 db was obtained with a band width of $2.5 \cdot 10^4$ cps. It was possible to obtain saturation with 1 milliwatt of power. No change was noticed in the gain as the signal power was
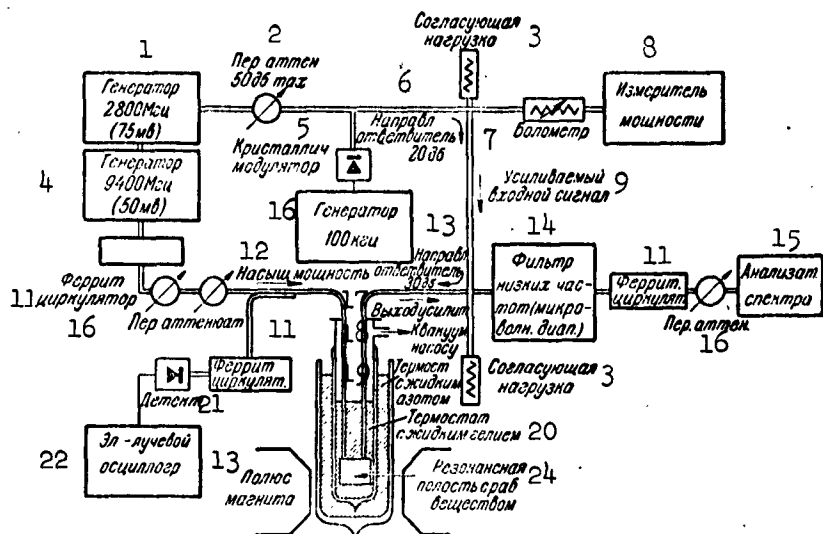
Fig. 8.8. Block diagram of microwave amplifier installation [68].
1) Generator 2800 megacycles (75 mv); 2) variable attenuator, 50 db maximum; 3) matching load; 4) generator 9400 megacycles (50 mv); 5) crystal modulator; 6) directional coupler; 7) bolometer, 8) power meter; 9) amplified input signal; 10) generator 100 kcs; 11) ferrite circulator; 12) saturated power; 13) directional coupler, 30 db; 14) low pass filter (microwave band; 15) spectrum analyzer; 16) variable attenuator; 17) output of amplifier; 18) to vacuum pump; 19) thermostat with liquid nitrogen; 20) thermostat with liquid helium; 21) detector; 22) cathode ray oscilloscope; 23) magnet pole piece; 24) resonant cavity with working medium.

Increased from 10^{-11} to 10^{-10} watt; a further increase in the power resulted in a decrease in the gain and an increase in the band width.

It was shown experimentally that the relation $g_\alpha B = $ const (8.31) holds true with great accuracy if the volume of the medium and the configuration of the resonant cavity remain unchanged. It was found in this case that $g_\alpha B = 1.8$ megacycles while theoretical calculations gave a close value of about 2.6 megacycles.

Chromium hexacyanide was used [69] also to produce an amplifier at a frequency of 1373 megacycles (the frequency of the interstellar hydrogen line). The illumination was at a frequency of 8000 megacycles.

With the aid of 9 milliwatts of illumination, the apparatus turned into a generator. Chromium hexacyanide was also used by others to build an amplifier [62, 70].

6. Ruby amplifier

Corundum with chromium added (ruby) is used to produce amplifiers for different frequencies [71, 72]. Ruby has the following favorable distinguishing properties: a) the initial crystalline splitting is of the order of the most widely used frequencies in practice; b) relatively long time of longitudinal relaxation, 0.1 sec at $4.2°K$; c) the crystal cell contains only 1 Cr^{3+} ion or the Al^{3+} ion which is isomorphous to it; d) low dielectric losses; e) high mechanical strength and chemical stability; f) good heat conductivity.

Makov et al. [71] constructed an amplifier for a signal frequency $v(-1/2, 1/2) = 9300$ megacycles; the illumination was at $v(-3/2, 1/2) = 24,000$ megacycles; the static magnetic field of intensity 4200 oersted was at an angle $54° 44'$ to the trigonal axis of the crystal. The chromium concentration in the specimen employed was 0.1%. The illumination was with the aid of a klystron with 120 milliwatts of power. The gain reached 20 db.

Prokhorov et al. [72] produced an amplifier at a frequency $v(-1/2, 1/2) \approx 3000$ megacycles with an illumination frequency $v(3/2, -1/2) = 15,000$ megacycles. When the temperature was reduced to $2°K$, the system became self excited and operated as a generator.

A recent communication [117] reports on a paramagnetic amplifier using a ruby with traveling wave (that is, of the wave guide type), having the following parameters: gain approximately 25 db, band width approximately 23 megacycles, noise temperature approximately $10°K$, working frequency tunable within several per cent near an operating point of approximately 6000 megacycles. Practical realization of such

an amplifier became possible by using slow-wave systems.

In the case of ruby, the dependence of the spin level splitting on the field $\vec{H}_0$ and on its inclination to the optical axis of the crystal were plotted [118] and investigations were made of the influence of the admixture of Co^{2+} ions and other ions on the probability of the relaxation transitions [119].

7. Amplifier using corundum with Fe^{3+} impurity

Kornienko and Prokhorov [34] constructed an amplifier for a frequency of about 10,000 megacycles with an illumination frequency of about 25,000 megacycles, using as the working medium corundum with iron ions added. The optical axis of the crystal made a small angle with the direction of the constant magnetic field. We shall denote the spin levels by the magnetic quantum numbers that can be ascribed to them in a strong field H_0. The levels with $M = -3/2$, $-1/2$ were used for the amplification and the levels $M = -5/2$, $-1/2$ for illumination. We note that since the spin Hamiltonian of the Fe^{3+} ions contains terms with not only axial but also cubic symmetry, transitions between any pair of the selected levels are allowed.

§8.6. Optical Methods of Investigating Paramagnetic Resonance

Many interesting results were obtained in recent years with the aid of experiments consisting of applying simultaneously to gases electromagnetic radiations at two different frequencies in the optical and in the radio bands. Investigations of this type were carried out both with atoms (or molecules) whose ground state is a singlet one and consequently nonmagnetic, and with atoms which are paramagnetic in the ground state. In the former case the radio frequency resonance occurs in the optically excited atoms, and in the latter it occurs on atoms in the ground state.

1. Resonance on optically excited atoms

The idea of paramagnetic resonance experiments on optically excited atoms was advanced in 1949 [73, 74] and consists of the following. Let us consider an assembly of diamagnetic atoms placed in a static magnetic field H_0 and subject to the action of polarized light of resonant frequency. The excitation of the atoms will obviously be selective. If the atoms are paramagnetic in the excited state, then only some of the Zeeman sublevels will be occupied. Consequently, the radiation produced upon the excitation of the atoms will be polarized. The radio frequency field, producing transitions between the Zeeman sublevels, changes the character of the polarization of the emitted light. Thus, measurements of the polarization of the emitted light make it possible to establish the occurrence of magnetic resonance.
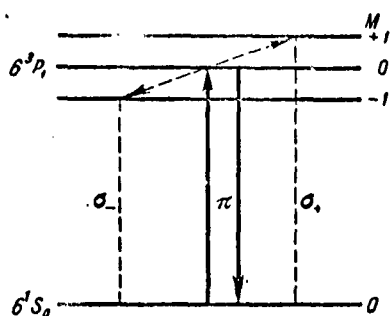

Fig. 8.9. Scheme of magnetic resonance on optically excited mercury atoms.

The investigation method which we have described was first experimentally realized by Brossel and Bitter [75], who applied it to even isotopes of mercury. Using linearly polarized light, they excited the 2537 angstrom ultraviolet resonance line $(6^1S_0 \rightarrow 6^3P_1)$. The field H_0 was applied parallel to the electric vector of the light wave. In this case, as is well known [76], only the Zeeman sublevel $M = 0$ is excited. The radiation therefore contains only the π components. Then an oscillating magnetic field of frequency $\nu = 2.9625 \cdot 10^{10}$ cps was applied perpendicular to the field H_0. By varying the intensity of H_0, the resonance condition $h\nu = g\beta_0 H^*_0$ was attained, where $g = 1.5$ is the Lande factor for the state $^3P_1$. Owing to the transitions $\Delta M = \pm 1$, produced by the radio frequency field, circularly polarized components appear in the optical
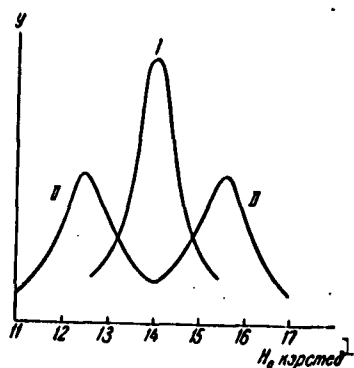
Fig. 8.10. Stark effect on the 2537 angstrom mercury resonance line.
I) Plot of the dependence of the σ components of radiation produced under magnetic resonance conditions on the field H_0; II) plot of the same dependence upon superposition of an electric field E = = 40 kv/cm.
1) Kilooersteds.

radiation. The dashed lines show the transitions arising as a result of the radio frequency field. In Fig. 8.10 curve I gives the dependence of the intensity of the σ components on the field H_0. The maximum intensity corresponds to a field intensity H^*_0 satisfying the resonance condition.

The method described makes it also possible to investigate the Stark effect with great accuracy. Blamont [77] produced parallel to H_0 an electric field E = 40 kv/cm. In the absence of the field E, the energy intervals $0 \rightarrow 1$ and $-1 \rightarrow 0$ are equal, and therefore only the resonance line I appears (Fig. 8.10). The levels M = 0 and M = $\pm$ 1 shift differently in the electric field E; this causes the appearance of two resonance lines (curve II in Fig. 8.10). Within the limits of the measurement accuracy, it was shown that the effect is quadratic. The interval between the resonance peaks is

$$\nu_2 - \nu_1 = 2KE^2, \qquad (8.50)$$

where the Stark constant is K = (2.13 $\pm$ 0.05) $\cdot$ 10^5 cps/kv $\cdot$ cm^{-1}.

2. Magnetic resonance line shape

If the gas is highly rarefied so that $N_0 < 10^{12}$ then the width of the optical resonance line $\Delta\nu = g\beta\Delta H$ is determined by the lifetime t_0 of the excited state. According to the uncertainty relation

$$t_0 \approx \frac{1}{\pi\Delta\nu} = \frac{h}{\pi g\beta\Delta H} . \qquad (8.51)$$

If the width ΔH is estimated from curve I of Fig. 8.10, we obtain for

the lifetime at the 6^3P_1 level $t_0 = 1.19 \cdot 10^{-7}$ sec, which is in good agreement with the pure optical data. The double resonance method was used [78] also to determine the much shorter lifetime at the excited level 7^3S_1.

It is easy to show [75] that the shape of the resonance line is given by the following expression:

$$y = \frac{1}{t_0} \int_0^\infty P(M, M', t)\, e^{-\frac{t}{t_0}} dt, \qquad (8.52)$$

where $\underline{y}$ is the relative intensity of the line and $P(M, M', t)$ is the probability that a transition $M \to M'$ will occur within a time t. This probability is calculated by means of the well known Majorana formula [79]. For the line $6^3P_1 \to 6^1S_0$ we obtain in this manner

$$y = \frac{\gamma^2 H_r^2 \left(\gamma^2 H_r^2 + \frac{4}{t_0^2} + 4\omega^2 \right)}{\left(\gamma^2 H_r^2 + \frac{1}{t_0^2} + \omega^2 \right)\left(\gamma^2 H_r^2 + \omega^2 + \frac{4}{t_0^2} \right)}. \qquad (8.53)$$

Here $\omega = 4\pi(\nu - \nu_0)$. Under resonance conditions $\omega = 0$ and consequently

$$y_{\text{pes}} = \frac{\gamma^2 H_r^2}{\frac{1}{t_0^2} + \gamma^2 H_r^2}. \qquad (8.54)$$

If the amplitude of the alternating field is small, then the width of the resonance curve can be determined from the following approximate formula:

$$(\Delta\nu)^2 = \frac{4}{t_0^2}\left[1 + 1.45\,(\gamma H_r t_0)^2 \right]. \qquad (8.55)$$

If the Zeeman levels are shifted by the Stark effect, then formulas (8.53) – (8.55) should, of course, be modified [80].

3. Multiple coherent photon scattering

Blamont [77] in an investigation of the dependence of the line width $y_\sigma(H)$ on the vapor density for the even isotopes of mercury, obtained the following unexpected result: an increase in density is accompanied by noticeable narrowing down of the resonance line. Thus,

for example, when the number of atoms per cubic centimeter is increased from 10^{11} to 10^{13}, the width is reduced to one-third. With increasing vapor density, the number of collisions between atoms increases. Under the conditions of this experiment it is evident that this cause of line broadening is insignificant. Detailed investigations undertaken by Brossel et al. [81] have shown that the narrowing down depends on the dimensions of the resonant cavity; it is determined by the concentration of the investigated isotope only and is not at all connected with the amount of other isotopes. All these facts have been explained by the circumstance that under the conditions of these experiments the multiple coherent scattering of the photons plays a major role [82].

The process of multiple photon scattering can be visualized in the following fashion: The photon is absorbed by atom A, which is de-excited after a time interval t_0; the photon is then absorbed by another atom B, etc. It is important that the scattering be coherent; then the resonance line width will be determined not by the lifetime t_0 but by the "duration of coherence" $t_k > t_0$. Theoretical analysis of multiple coherence scattering was carried out long ago by Weisskopf [83].

It should be noted that when $N_0 > 10^{14}$, collisions between atoms begin to exert a noticeable influence on the line width.

4. Investigation of hyperfine splittings

So far we have assumed that the investigated energy levels do not have hyperfine structure. If the nuclear spin is not equal to zero, then the double resonance method makes it possible to measure with great accuracy the hyperfine splittings. These measurements are particularly valuable when $J = 0$ or $1/2$ in the ground state, and consequently, only a study of the excited states makes it possible to

determine the quadrupole moments of the nuclei. This method was used for an analysis of the hyperfine structure of the $^3P_1$ level of the zinc atom [84] and the $^2P_{3/2}$ of the following alkaline metal atoms: sodium [85], potassium [86], rubidium [87] and cesium [88]. This method was used to determine the quadruple moments of the nuclei, for which the following values were obtained: Na^{23}, $Q = (0.11 \pm 0.01) \cdot 10^{-24}$ cm^2; K^{39}, $Q = (0.11 \pm 0.035) \cdot 10^{-24}$ cm^2; Rb^{85}, $Q = (0.29 \pm 0.02) \cdot 10^{-24}$ cm^2; Rb^{87}, $Q = (0.14 \pm 0.01) \cdot 10^{-24}$ cm^2; Cs^{133}, $Q = (-0.003 \pm 0.002) \cdot 10^{-24}$ cm^2. Related to this series of investigations is the work done on the Stark effect for the levels of the odd mercury isotopes, which, as is well known, have a hyperfine structure [89].

Rabi [90] supplemented his original beam method by optical excitation of the atoms. Measurements carried out in this way have yielded for the quadrupole moments of alkali element nuclei values that agreed with those mentioned above.

5. Orientation of atoms in the ground state

We proceed from a study of magnetic resonance on optically excited atoms to the effect on the ground atomic levels. We first stop to discuss the method of optical pumping, which makes it possible to orient atoms in the ground state. We shall illustrate the idea of the method using the $D_2(^2P_{3/2} \longleftrightarrow {}^2S_{1/2})$ lines of sodium. For simplicity we first neglect the hyperfine structure of the levels. Let the sodium atoms be in a static magnetic field H_0. The scheme of the Zeeman splittings arising thereby and of the possible electric dipole transitions is shown in Fig. 8.11. Let us assume that a circularly polarized light beam propagates along the field H_0 and gives rise to the σ^+ transitions indicated in Fig. 8.11 by the solid arrows. Upon de-excitation of the so excited atoms, the greater part of these atoms
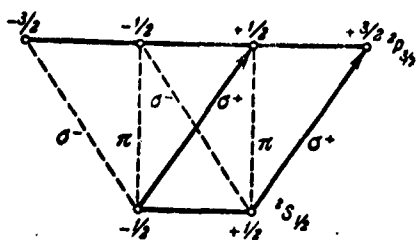
Fig. 8.11. Optical pumping by exciting with polarized light the σ^+ transition $^2P_{3/2} \leftrightarrow {}^2S_{1/2}$ in sodium atoms.

will go over into the state M = +1/2. After multiple repetition of this process, the level M = −1/2 becomes empty, and all the atoms gather at level M = = +1/2. Thus, as a result of the optical pumping all the atoms will be oriented against the field direction, and magnetization to saturation will set in. Actually the orientation of the atoms will never be complete, principally as a result of collisions with the walls of the vessel. Experiments show that it will nevertheless be appreciable. The extent to which the atoms are oriented can be evaluated from the character of the polarization of the radiation emitted by the optically excited atoms. In our example of the D_2 sodium line, the radiation will contain only the σ component if 100% atomic orientation is attained.

The idea of orienting atoms by optical pumping was advanced by Kastler [91]. The first experiments were carried out with atomic sodium beams [92, 93]. They were successfully repeated with sodium vapor, which greatly simplified the experimental technique [94]. In addition to the sodium atoms [95], other alkaline metals were later studied: K [96], Rb [97] and Cs [98]. Various modifications of the optical pumping method were proposed and realized [99, 100]. It was shown, in particular, that under the influence of natural light propagating along a magnetic field, the atoms become "aligned."*

6. Orientation of nuclei

If the nuclei have a nonzero spin, then the interaction between the electron and nuclear moments causes the orientation of the atoms to be accompanied by orientation of the nuclei. Attempts were made

- 456 -

to determine this orientation from anisotropy of the γ-radiation on the nuclei of alkali-metal atoms [102]. The result turned out to be negative, apparently because of adsorption of atoms on the vessel walls.

If the ground state is diamagnetic, then the method of optical pumping makes it possible to obtain a pure nuclear orientation. The first experiments with odd mercury isotopes were not successful because the light intensity was not sufficient [103]. Positive results were obtained [104] with mercury enriched to 90% with the ^{201}Hg isotope. The optical excitation was produced by natural light propagating in the direction of the magnetic field. Thus, alignment of the nuclei was obtained in these experiments.

7. Magnetic resonance on atoms in the ground state

Optical pumping causes the paramagnetic resonance absorption to increase appreciably. Usually, however, the detection of magnetic resonance is carried out by optical methods based on the depolarization of the resonant (optical) radiation resulting from transitions between the Zeeman levels under the influence of the radio frequency field. The first experiments, carried out with sodium atoms [105], have shown that in addition to the resonance peaks corresponding to the transitions $\Delta M = \pm 1$, other peaks appear if the intensity of the radio frequency field is sufficient and these are connected with the transitions $\Delta M = \pm 2$, ± 3,... The additional peaks appear as a result of absorption of 2, 3,... radio frequency quanta. A theoretical analysis has shown [106] that the intensity of the n-th order resonance is proportional to $(H_1/H_0)^{2n}$.

Winter [107] has predicted the possibility of resonance on multiple frequencies even when the atoms contain only two magnetic sublevels each. For this effect to appear it is necessary that the

radio frequency field not be polarized circularly, but that it contain photons of differing polarizations. The effect was observed experimentally on sodium atoms [108].

8. Effect of extraneous gases

The double resonance method which we have described is very convenient for the study of the influence of extraneous gases on the orientation of the investigated atoms. If the atoms are oriented and are an excited state, then it is well known that collisions with the molecules of the extraneous gas will cause depolarization of the resonant radiation [76], since the collisions mix up the states with different values of M.

Oriented atoms in the ground states are affected by the extraneous gases in two ways:

a) First, the extraneous gases produce disorientation, as in the case of excited atoms;

b) second, they play the role of a buffer preventing the atoms from colliding with the vessel walls.

If the density of the extraneous gases is relatively low, the buffer action plays the principal role and brings about an increase in the resonant absorption intensity by a factor 10-15 [99, 109]. If in the absence of impurities the straight line motion of the atoms is interrupted predominantly because of collisions with the vessel walls, then in the presence of extraneous gases the trajectory of the atoms becomes zigzaglike and therefore the orienting action of the incident light becomes more prolonged. This effect increases with increasing mass of the extraneous gas molecules. Atoms in the $^2S_1/2$ state are less sensitive to collisions. Dicke [110] has predicted that the collisions should give rise not only to an increase in the intensity but also to a narrowing of the resonance line. This was soon

observed in experiment [111].

In conclusion, let us dwell on several prospects in the development of the method of double optical-radio frequency resonance.

a) The measurement accuracy of ordinary optical spectroscopy is limited by the Doppler broadening of the lines. The double resonance method which we described is free of this shortcoming, making it valuable for measurement purposes.

b) Investigations made on vapors in the presence of extraneous gases yield valuable experimental material for the theory of collisions of oriented atoms. The weak influence of the collisions on the orientation of the atoms can be used to orient radioactive nuclei and to obtain polarized electrons [112].

c) In the experiments which we described, optical methods play a double role: 1) they are used for selective excitation of the atoms; 2) they are used to detect radio frequency resonance. Interesting results can be obtained by combining optical methods with other methods for either selective excitation of atoms or detection of magnetic resonance.

Let us point out some possible combinations which have yielded positive results:

1) Selective excitation of atoms can be carried out by the Frank and Hertz method of inelastic electron collisions, while detection of magnetic resonance can be carried out by the optical method; Dehmelt [113] investigated in this fashion magnetic resonance on the metastable mercury state 6^3P_2, and Pebay-Peyroula [114] made measurements for the 6^3P_1 level;

2) we have already mentioned that Rabi [90] combined optical excitation and resonance detection by the Stern and Gerlach beam method;

3) selective excitation can be carried out by optical means, and detection by ordinary methods of paramagnetic resonance [115].

d) Great interest attaches to the use of optical pumping in solids. The suitability of the substance for this purpose is determined by the following two conditions: 1) the spin-lattice relaxation time should be longer than the duration of one cycle of optical pumping; 2) optical transitions should exist in a practically convenient frequency region. A preliminary study [116] has shown that these conditions can be satisfied above all by salts of ions in the S state. Apparently the most suitable ones are salts of divalent europium.

We note that the changeover to solids is particularly important for experiments with oriented nuclei, since the use of gases is inconvenient, owing to the disorienting action of adsorption on the vessel walls.

3) It is possible to obtain by the optical pumping method a higher population for the upper Zeeman levels as compared with the lower ones. It follows therefore that this effect can be used to construct a low noise amplifier or generator [112]. The need for using rarefied gases so as to avoid multiple incoherent scattering of the photons greatly limits the practical applications of such devices. They may, however, turn out to be quite valuable as frequency standards.

REFERENCES TO CHAPTER 8

1. Overhauser A.W., Phys. Rev. 92, 411, 1953.
2. Van Vleck J.H., Nuovo cimento 6, suppl., 1081, 1957.
3. Overhauser A.W., Phys. Rev. 89, 689, 1953.
4. Brovetto P., Cini G., Nuovo cimento 11, 618, 1954.
5. Brovetto P., Ferroni S., Nuovo cimento 12, 90, 1954.

6. Kittel C., Phys. Rev. 95, 589, 1954.

7. Klein M.J., Phys. Rev. 98, 1736, 1955.

8. Slichter C.P., Phys. Rev. 99, 1822, 1955.

9. Barker W.A., Mencher A., Phys. Rev. 102, 1023, 1956.

10. Solomon I., Phys. Rev. 99, 559, 1955.

11. Little W.A, Proc. Phys. Soc. B70, 785, 1957.

12. Azbel' M.Ya., Gerasimenko V.I., Lifshits I.M., ZhETF [J.X.
    Theor. Phys.], 31, 357, 1956; 32, 1212, 1957.

13. Kaplan J.I., Phys. Rev. 99, 1322, 1955.

14. Carver T.R., Slichter C.P., Phys. Rev. 92, 212, 1953.

15. Carver T.R., Slichter C.P., Phys. Rev. 102, 975, 1956;
    Bekeshko, N.A., Kondorskiy, Ye.I., ZhETF, 32, 611, 1957.

16. Abragam A., Combrisson J., Solomon I., Compt. Rend. 245, 157,
    1957; 246, 1035, 1958.

17. Honig A., Phys. Rev. 96, 234, 1954.

18. Kaplan J.I., Phys. Rev. 96, 238, 1954.

19. Honig A., Combrisson J., Phys. Rev. 102, 917, 1956.

20. Bloch F., Phys. Rev. 93, 944, 1954.

21. Overhauser A., Phys. Rev. 94, 768, 1954.

22. Korringa J., Phys. Rev. 94, 1388, 1954.

23. Abragam A., Phys. Rev. 98, 1729, 1955.

24. Valiyev. K.A., Uch. Zap. KGU [Scientific Reports Kiev State
    University], 117, 145, 1957; FMM [Physics of Metals and Metal-
    ography], 6, 193, 1958.

25. Bashkirov Sh. Sh., Uch. Zap. KGU, 117, 154, 1957.

26. Bashkirov Sh. Sh., Valiyev K.A., ZhETF, 35, 678, 1958.

27. Khutsishvili G.R., ZhETF, 34, 63, 1958.

28. Beljers H.G., van der Kint I., van Wieringen J.S., Phys. Rev.
    95, 1683, 1954.

29. Allais E., Compt. Rend. [Proceedings], 246, 2123, 1958.

30. Landesman A., Compt. Rend. 246, 1538, 1958.

31. Motchane J.L., Erb E., Uebersfeld J., Compt. Rend. 246, 1833, 2121, 1958.

32. Feher G., Phys. Rev. 103, 500, 1956.

33. Feher G., Gere E.A., Phys. Rev. 103, 501, 1956.

34. Korniyenko L.S., Prokhorov A.M., ZhETF, 36, 919, 1959.

35. Jeffries C.D., Phys. Rev. 106, 164, 1957.

36. Abraham M., Kedzie R.W., Jeffries C.D., Phys. Rev. 106, 165, 1957.

37. Steenberg N.R., Proc. Phys. Soc. A65, 791, 1952.

38. Abragam A., Proctor W.G., Compt. Rend. 246, 2253, 1958.

39. Weber J., Trans. Inst. Radio Engin. Prof. Group on Electron Devices, PGED-3, June 1953.

40. Basov N.G., Prokhorov A.M., ZhETF, 27, 431, 1954; DAN SSSR [Proc. Acad. Skiy. USSR], 101, 47, 1954; Disc. Faraday Soc. 19, 99, 1955; UFN [Progress in the Physical Sciences], 57, 485, 1955; ZhETF, 30, 560, 1956.

41. Gordon J.P., Zeiger H.J., Townes C.H., Phys. Rev. 95, 282, 1954; 99, 1253, 1955.

42. Bogle S.S., Symmons H.F., Proc. Phys. Soc. 73, 531, 1959; Austr. J. Phys. 12, 1, 1959.

43. Shimoda K., Takahasi H., Townes C.H., J. Phys. Soc. Japan, 12, 686, 1957.

44. Pound R.V., Ann. Phys. 1, 24, 1957.

45. Strandberg M.W.P., Phys. Rev. 106, 617, 1957; 107, 1483, 1957.

46. Weber J., Phys. Rev. 108, 537, 1957.

47. Landau L., Lifshits Ye., Kvantovaya mekhanika [Quantum mechanics], File. 1, Moscow, Gostekhizdat [State Unified Publishing House for Scientific and Technical Literature], 1948.

48. Purcell E.M., Pound R.V., Phys. Rev. 81, 279, 1951.

49. Bloch F., Phys. Rev. 70, 460, 1946.

50. Endryu E., Yadernyy magnitnyy rezonans [Nuclear Magnetic Reso-
nance], IL [Foreign Literature Press], Moscow, 1957, page 150.

51. Loesche A., Kerninduktion [Nuclear Induction], VEB [People's
Own Publishers], Berlin, 1957, 62.

52. Rabil, Ramsey N.F., Schwinger J., Rev. Mod. Phys. 26, 167, 1954.

53. Feher G., Scovil H.E.D., Phys. Rev. 105, 760, 1957.

54. Combrisson J., Honig A., Townes C.H., Compt. Rend. 242, 2451,
1956.

55. Feher G., Gordon J.P., Buehler E., Gere A., Thurnmond C.D.,
Phys. Rev. 109, 221, 1958.

56. Chester, P.F., Wagner P.E., Castle J.G., Jr., Phys. Rev. 110,
281, 1958.

57. Bolef D.I., Chester P.F., IRE Trans. Microw. Theory a. Techn.
47, 1958.

58. Basov N.G., Prokhorov A.M., ZhETF, 28, 249, 1955.

59. Bloembergen N., Phys. Rev. 104, 324, 1956.

60. Javan A., Phys. Rev. 107, 1579, 1957; Clogston A.M., J. Phys.
Chem. Solids 4, 271, 1958; Prokhorov, A.M., URSI Meeting, Boulder,
Colo., IX, 1957.

61. Bloembergen N., Phys. Rev. 109, 2209, 1958.

62. Strandberg M.W.P., Davis C.F., Faughman B.W., Kyhl R.L., Wolga
G.J., Phys. Rev. 109, 1988, 1958.

63. Strandberg M.W.P , Phys. Rev. 110, 65, 1958.

64. Bashkirov Sh.Sh., Valiyev K.A., ZhETF, 35, 302, 1958.

65. Bowers K.D., Mims W.B., Conference Electronic Tube Research,
Berkeley, Calif., VI, 1957.

66. Scovil H.E.D., Feher G., Seidel H., Phys Rev. 105, 762, 1957.

67. Scovil H.E.D., Trans. Inst. Radio Engin. Prof. Group on Microwave Theory and Techniques 6, 29, 1958.

68. McWhorter A.L., Meyer J.M., Phys. Rev. 109, 312, 1958.

69. Artman J.O., Bloembergen N., Shapiro S., Phys. Rev. 109, 1392, 1958.

70. Autler S.H., McAvoy N., Phys. Rev. 110, 280, 1958.

71. Makhov G., Kikuchi C., Lambe J., Terhune R.W., Phys. Rev. 109, 1399, 1958.

72. Zverev G.M., Korniyenko L.S., Manenkov A.A., Prokhorov A.M., ZhETF, 34, 1660, 1958.

73. Brossel J., Kasler A., Compt. Rend. 229, 1213, 1949.

74. Pryce F., Phys. Rev. 77, 136, 1950.

75. Brossel J., Bitter F., Phys. Rev. 86, 311, 1952; Brossel J., Ann. Phys. 7, 622, 1952.

76. Mitchell A., Zemanskiy M., Rezonansnoye izlucheniye i vozbuzh-dennyye atomy [Resonance radiation and excitation of atoms], 1937, Chapter 5.

77. Blamont J.E., These (Paris, 1956); Blamont J., Brossel J., Compt. Rend. 238, 1487, 1954; Arch des. Sci. Geneve 9, fasc. special, 152, 1956; 243, 2038, 1956.

78. Brossel J., Julienne C., Compt. Rend. 242, 2127, 1956.

79. Majorana J.E., Nuovo cimento 9, 43, 1932.

80. Blamont J., Winter J., Compt. Rend. 244, 332, 1957.

81. Guichon M., Blamont J. E. Brossel J., J. Phys. Rad. 18, 99, 1957; Boutron F., Brossel J., Compt. Rend. 245, 2250, 1957; Barrat J., Brossel J., Compt. Rend. 246, 2744, 1958.

82. Rollet N., Brossel J., Kastler A., Compt. Rend. 242, 240, 1956.

83. Weisskopf V., Ann. Phys. 9, 23, 1931.

84. Bockmann K., Kruger H., Recknagel E., Nuovo cimento 6, suppl. ser. X, 1155, 1957.

85. Sagalyn P.L., Phys. Rev. 94, 885, 1954.

86. Ritter G.J., Series G.W., Proc. Phys. Soc. A68, 450, 1955; Proc. Roy. Soc. A238, 473, 1957; Series G.W., Phys. Rev. 105, 1128, 1957.

87. Meyer-Berkhout U., Zt. phys. [J. Phys.], 141, 185, 1955.

88. Althoff K.H., Z. Phys. 141, 33, 1955.

89. Blamont J.E., Brossel J., Compt. Rend. 243, 2038, 1956.

90. Perl M.L., Rabi I.I., Senitzky B., Phys. Rev. 98, 611, 1955; 103, 315, 1956; 104, 553, 1956.

91. Kastler A., J. Phys. Rad. 11, 255, 1950; Physica 17, 191, 1951.

92. Brossel J., Kastler A., Winter J., J. Phys. Rad. 13, 668, 1952.

93. Hawkins W.B., Dicke R.H., Phys. Rev. 91, 1008, 1953; 98, 478, 1956.

94. Barrat J., Brossel J., Kastler A., Compt. Rend. 239, 1196, 1954.

95. Kastler A., J. Opt. Soc. Amer. 47, 460, 1957.

96. Arditi M., Carver T.R., Phys. Rev. 109, 1012, 1958.

97. Skalinski T., Compt. Rend. 245, 1908, 1957.

98. Diamand F., Legendre J.M., Skalinski T., Compt. Rend. 246, 90, 1958.

99. Brossel J., Margerie J., Kastler A.J., Compt. Rend. 241, 865, 1955.

100. Dehmelt H.G., Phys. Rev. 105, 1487, 1957; Bell W.E., Bloom A.L., Phys. Rev. 107, 1559, 1957; 109, 219, 1958; Franzen W., Emslie A.G., Phys Rev. 108, 1453, 1957.

101. Margerie J., Brossel J., Kastler A., Compt. Rend. 241, 474, 1955; Hawkins W.B., Dicke R.H., Phys. Rev., 91, 1008, 1953; Hawkins W.B., Phys. Rev. 98, 478, 1955.

102. Brossel J., Mosser J.L., Winter J., J. Phys. Rad. 16, 814, 1955.

103. Bitter F., Brossel J., Phys. Rev. 85, 1051, 1952; Bitter F., Lacey R.F., Richter B., Rev. Mod. Phys. 25, 174, 1953.

104. Cagnac B., Brossel J., Kastler A., Compt. Rend. 246, 1827, 1958.

105. Brossel J., Cagnac B., Kastler A., Compt. Rend. 237, 984, 1953; J. Phys. Rad. 15, 6, 1954.

106. Besset C., Horowitz J., Messiah A. Winter J., J. Phys. Rad. 15, 251, 1954; Salwen H., Phys. Rev. 99, 1274, 1955; Hack M. N., Phys. Rev. 104, 84, 1956.

107. Winter, J., Compt. Rend. 241, 375, 600, 1955.

108. Margerie J., Brossel J., Compt. Rend. 241, 373, 566, 1955; Winter J., Brossel J., Arch. Sci. Geneve 9, fasc. spec., 148, 1956.

109. Bender P.L., Thesis, Princeton University, 1956; Cohen-Tannoudji C., Brossel J., Kastler A., Compt. Rend. 244, 1027; 1957; Hartman F., Rambosson M., Brossel J., Kastler A., Compt. Rend. 246, 1522, 1958.

110. Dicke R.H., Phys. Rev. 89, 472, 1953.

111. Wittke J.P., Dicke R.H., Phys. Rev. 96, 530, 1954; Wittke J.P., Thesis, Princeton University, 1954.

112. Kastler A., Holweck Lecture, Proc. Phys. Soc. A67, 853, 1954.

113. Dehmelt H.G., Phys. Rev. 103, 1125, 1956.

114. Pebay-Peyroula J.C., Brossel J., Kastler A., Compt. Rend. 244, 57, 1957.

115. Shimoda K., Nishikawa T., J. Phys. Soc. Japan 6, 512, 1951.

116. Series G.W., Taylor M.J., Colloque CNRS, No. 86, Paris, 1958.

117. De Grasse R.W., Schulz-du Bois E.O., Scovil H.E.D., Bell. Syst. Technic. Jorun. 38, 305, 1959.

118. Schulz-du Bois E.O., Bell. Syst. Technic. Journ. 38, 271, 1959.

119. Schulz-Du Bois E.O., Scovil H.E.D., De Grasse R.W., Bell. Syst.

Technic. Journ. 38, 335, 1959.

120.   Erb E., Motchane J.L., Uebersfeld J., Compt. Rend. 246, 3050, 1958; Uebersfeld J., Rev. univers. mines. 15, 594, 1959; Abraham M., McCausland M.A.H., Robinson F.N.H., Phys. Rev. Letters 2, 449, 1959.

121.   Cowen J.A., Schafer W.R., Spence R.D., Phys. Rev. Letters 3, 13, 1959.

122.   Bloembergen N., Shapiro S., Pershan P.S., Artman J.O., Phys. Rev. 114, 445, 1959.

BOOKS AND SURVEY PAPERS ON ELECTRONIC PARAMAGNETIC RESONANCE

1.   Gordi V., Smit V., Trambarullo R., Radiospektroskopiya [Radio Spectroscopy], GITTL [State Unified Publishing House for Technical and Theoretical Literature], Moscow, 1955.

2.   Bleaney B., Stevens K.W.H., Paramagnetic resonance, Rep. Progr. Phys. 16, 108, 1953.

3.   Bowers K.D., Owen J., Paramagnetic resonance II, Rep. Progr. Phys. 18, 304, 1955.

4.   Ingram D., Spektroskopiya na vysokikh i sverkhvysokikh chastotakh [Spectroscopy at high and superhigh frequencies], IL, Moscow, 1959.

5.   Ingram D.J.E., Free radicals as studied by electron spin resonance, London, 1958.

6.   Wertz J.E., Nuclear and electronic paramagnetic resonance, Chem. Rev. 55, 829, 1955.

7.   Pryce M.H.L., Paramagnetism in crystals, Nuovo cimento 6, suppl. No. 3, 817, 1957.

8.   Gorter C.J., Paramagnetic relaxation, Nuovo cimento 6, suppl. No. 3, 887, 1957.

9.   Van Vleck J.H., Line-Breadths and the theory of magnetism,

Nuovo cimento 6, suppl. No. 3, 993, 1957.

10.   Van Vleck J.H., The concept of temperature in magnetism, Nuovo
      cimento 6, suppl. No. 3, 1081, 1957.

11.   Low W., Paramagnetic resonance, New York – London, 1960.

12.   Khutsishvili G.R., Effekt Overkhauzera i rodstvennyye yavleniya,
      [The Overhauser effect and kindred phenomena], UFN [Progress in
      the physical sciences], 61, 9, 1960.

Manu-script Page No.	[Footnotes]
407	It should be remembered that g_N may be either positive or negative.
421	Such devices are customarily called masers abroad, which stands for "microwave amplification by stimulated emission of radiation."
422	We know that such splittings can be readily attained in magnetic fields of readily accessible intensities.
423	This formula pertains to an amplifier that is turned on with the aid of a ferrite circulator.
425	The misprints that have crept into the formulas [45] have been corrected in [46].
455	Alignment of atoms, unlike their polarization, denotes that levels with magnetic numbers M and —M have equal populations; levels with different M are unequally populated.

DISTRIBUTION LIST

DEPARTMENT OF DEFENSE	Nr. Copies	MAJOR AIR COMMANDS	Nr. Copies
		AFSC	
		SCFTR	1
		ASTIA	25
HEADQUARTERS USAF		TD-B1a	5
		TD-B1b	3
AFCIN-3D2	1	AEDC (AEY)	1
ARL (ARB)	1	SSD (SSF)	2
		APGC (PGF)	1
		ESD (ESY)	1
		RADC (RAY)	1
OTHER AGENCIES		AFSWC (SWF)	1
		AFMTC (MTW)	1
CIA	1	TD-B2	1
NSA	6		
AID	2		
OTS	2		
AEC	2		
PWS	1		
NASA	1		
RAND	1		
SPECTRUM	1		